APPLICATIONS OF INNOVATIVE TECHNOLOGIES IN GEOTECHNICAL WORKS

2 May 2008

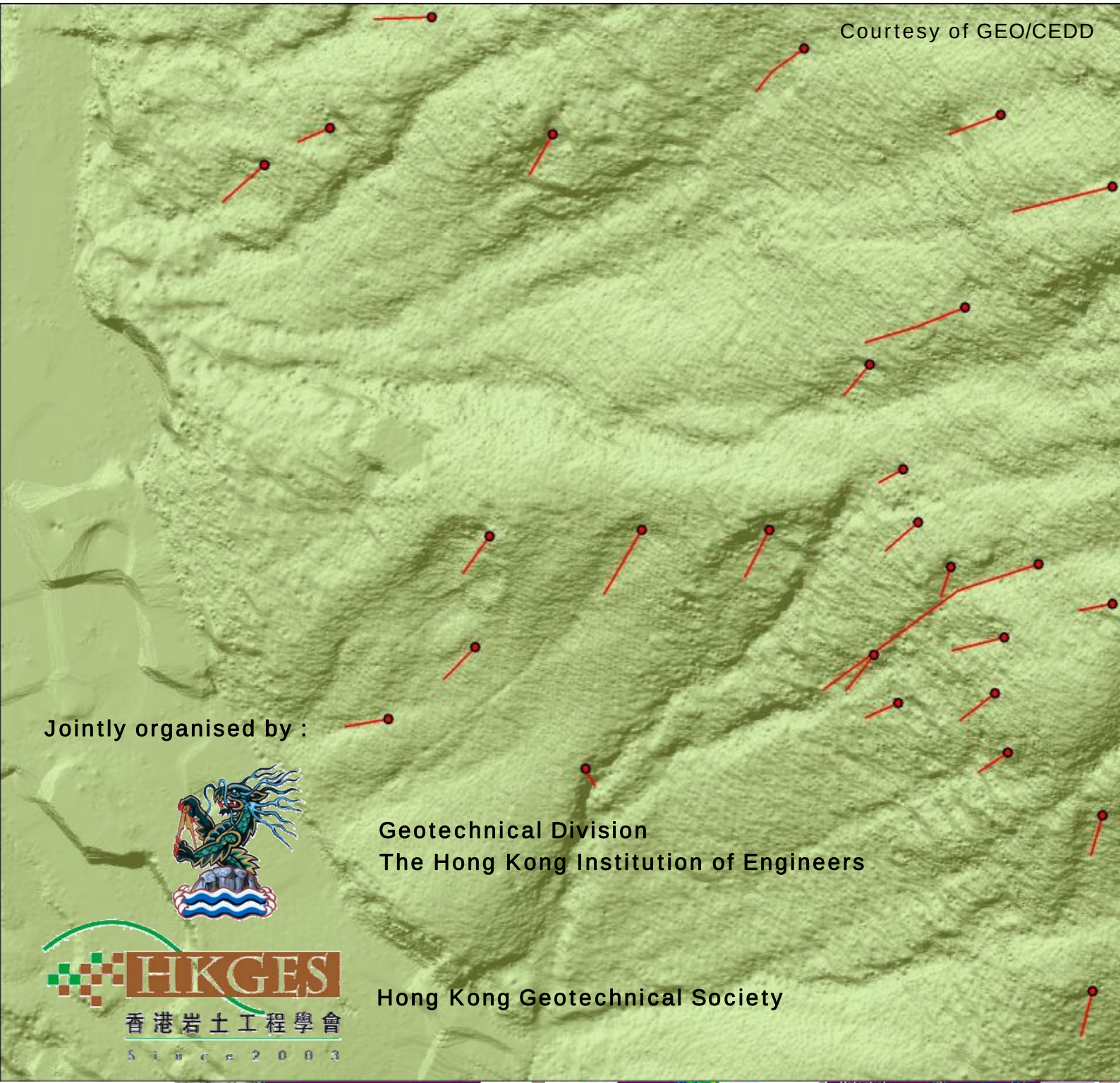

Courtesy of GEO/CEDD

Jointly organised by :

Geotechnical Division
The Hong Kong Institution of Engineers

HKGES
香港岩土工程學會
Since 2003

Hong Kong Geotechnical Society

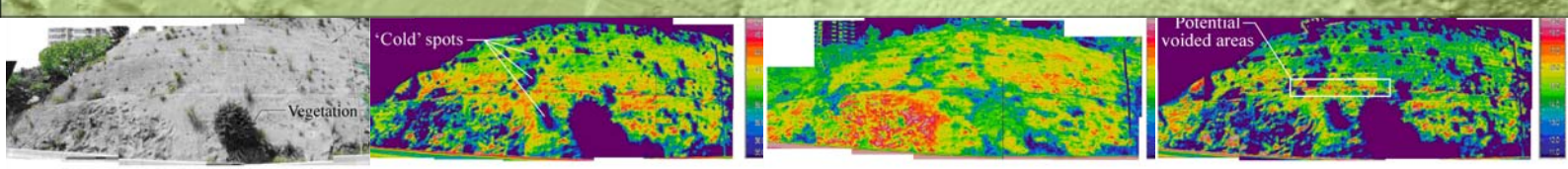

Proceedings of the 28th Annual Seminar
Geotechnical Division, The Hong Kong Institution of Engineers

Applications of Innovative Technologies in Geotechnical Works

2 May 2008
Hong Kong

Jointly organised by :
Geotechnical Division, The Hong Kong Institution of Engineers
Hong Kong Geotechnical Society

Captions of Figures on the Front Cover

Top figure:	The DEM, generated using LiDAR data, reveals the morphology of vegetated landslide scars identified by API (Courtesy of GEO/CEDD)
Bottom figures:	Daytime and night time infra-red images taken of a shotcreted slope in Hong Kong for use in thermal imaging analysis (Courtesy of GEO/CEDD)

Organising Committee

Chairman:
Ir Prof L G THAM

Members:
Ir Kenneth CHAN
Dr Johnny CHEUK
Ir Edwin CHUNG
Ir Albert HO
Ir S S KONG
Ir Joe LEUNG
Ir Dr Eric LI
Ir Neil NG
Ir Arthur SO
Ir Vincent TSE
Ir William WONG
Ir Ringo YU

Published by:
Geotechnical Division
The Hong Kong Institution of Engineers
9/F., Island Beverley, 1 Great George Street, Causeway Bay, Hong Kong
Tel : 2895 4446 Fax : 2577 7791

ISBN: 978-962-7619-32-1

Printed in Hong Kong

Foreword

Last year, the Geotechnical Division of the HKIE celebrated the twentieth anniversary of its establishment and organised the Annual Seminar titled "Geotechnical Advancements in Hong Kong Since 1970s". That was a timely reflection of the accomplishments made by the geotechnical practitioners in Hong Kong. It was also noted that considerable innovative developments and advancements have been achieved by Hong Kong engineers since geotechnical engineering works were formally recognised by the Hong Kong Government some 30 years ago.

The title of 2008 Geotechnical Division Annual Seminar is "Applications of Innovative Technologies in Geotechnical Works". This theme is selected by the Organising Committee to particularly address three issues, namely "Application", "Innovations" and "Geotechnical Works". We aim to provide a platform for geotechnical researchers and practitioners to showcase the innovative ideas they have developed. We also emphasis that the innovations must be practical and be applicable to construction works. With reference to the technical papers included in the Proceedings, we trust you will agree that the objectives have been successfully achieved.

In addition, for the first time, the Division has invited geotechnical experts in the Mainland, Taiwan and Macau to join our Annual Seminar and share with us the geotechnical engineering experience in their respective regions. This is also an innovative attempt with an aim to broaden Hong Kong engineers' horizon.

On behalf of the Geotechnical Division, I would like to thank our Guest-of-Honour, Mrs Carrie Lam, guests from outside Hong Kong, the Keynote Speakers, and the Authors of the papers to spend time in attending the Annual Seminar. The contributions made by our sponsors are also gratefully acknowledged. Lastly, I am grateful to the Organising Committee for their commitment and hard work throughout the past 12 months in making this Seminar possible.

Ir Dr Eric Li
Chairman, Geotechnical Division (2007/08 Session)
The Hong Kong Institution of Engineers

May 2008

Acknowledgements

The Organising Committee would like to express sincere thanks to the following sponsors for their generous support of the Seminar:

Barbican Construction Co. Ltd. / Vibro (H.K.) Ltd.

Earth Products China Ltd.

Excel Engineering Co. Ltd.

Fraser Construction Co. Ltd.

Fugro Geotechnical Services Ltd.

Gammon Construction Ltd. / Lambeth Associates Ltd.

Maunsell Geotechnical Services Ltd.

Ove Arup & Partners Hong Kong Ltd.

MAUNSELL | AECOM

Tunnel Works

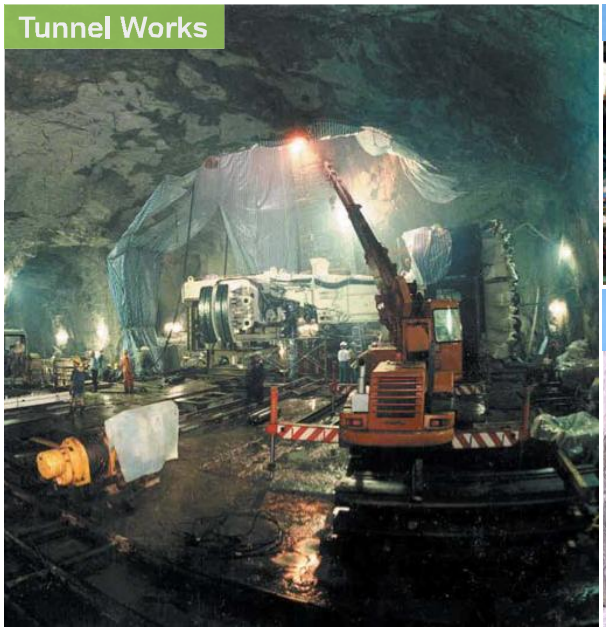

Innovation: Retractable TBM

Innovation: Installation of Sub-vertical Drains

Foundation

Innovation: Complex Foundation System and Associated Trial Pile Programme

Deep Excavation

Innovation:
Automatic Strut Load Compensation and Displacement Control System

Site Formation

Innovation:
Precise Installation of Tie-back System by Horizontal Directional Drilling

Landslide Investigation

Innovation:
Hydrogeology Model by GIS

Maunsell AECOM is part of AECOM, with businesses in Hong Kong, Mainland China and the rest of Asia. **AECOM** is a global provider of professional technical and management support services to a broad range of markets, including transportation, facilities, environmental and energy.

www.maunsell.aecom.com

Reclamation

Innovation: Mud Pool Treatment by Dynamic Replacement Method

When it's a question of monitoring or site investigation ....

... Ask Fugro

Fugro Geotechnical Services Ltd acquires the data that builds analytical models to describe the sub-surface of the earth, both onshore and offshore

Picture details (clockwise from above): Fugro 2" site investigation jack up in action off Zhejiang; satellite radar mapping (InSAR); aerial mapping (LIDAR and radar); real-time data acquisition and display of geotechnical monitoring data via internet and website

We are Hong Kong's leading specialist geotechnical contractor. Combining traditional and advanced technology with almost 30 years of local experience, we provide the insight to support construction projects in Hong Kong.

Fugro Geotechnical Services Ltd, Unit B-11, 10/F Worldwide Industrial Centre, 43-47 Shan Mei Street, Fo Tan, Sha Tin, NT
Tel: +852 2697 1126 Fax: +852 2694 0659 Web: www.fugro.com

NO OTHER COMPANY CAN PROVIDE THE SAME COMPREHENSIVE RANGE OF GEOTECHNICAL, SURVEY AND GEOSCIENCE SERVICES

FUGRO

Gammon

LAMBETH

Distinctly different

Queensway Subway
Hong Kong

Penny's Bay Reclamation, Stage 2
Hong Kong

Tsim Sha Tsui KCRC Extension
Hong Kong

KCRC Kowloon Southern Link
Hong Kong

Sheung Shing Street Redevelopment
Hong Kong

Removal of Underground Obstructions at Marina Bay Singapore

Route 8 Nam Wan Tunnel
Hong Kong

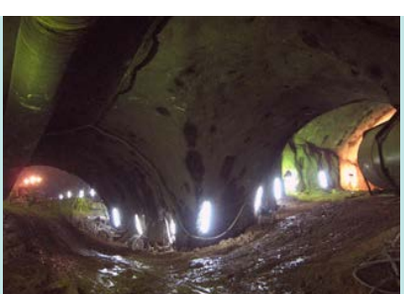

Centennial Campus of HKU
Hong Kong

Shenzhen Western Corridor Bridge
Hong Kong

Gammon is an Asian-based construction services group committed to finding innovative solutions for our customers. Jointly owned by Jardine Matheson and Balfour Beatty, and with quality as our watchword, Gammon combines local expertise with global resources to deliver a broad range of complex construction projects - staying ahead as we build Asia's infrastructure of tomorrow.

Lambeth Associates was established as the in-house engineering consultancy of Gammon Construction in 1976. Playing a critical and strategic design role in the operations of Gammon and its joint venture partners, Lambeth now has over 30 years of outstanding engineering achievements in Hong Kong, Singapore, Mainland China, Macau, Thailand and Vietnam.

www.gammonconstruction.com

www.lambeth.com.hk

VIBRO 惠保(香港)有限公司
VIBRO (H.K.) LIMITED
新創建集團成員 Member of NWS Holdings

百勤建築有限公司
BARBICAN CONSTRUCTION CO., LTD.
新創建集團成員 Member of NWS Holdings

香港柴灣常安街38號四樓
電話：(852)2137-5500　傳真：(852)2137-5599
電郵：email@vibro.com.hk | email@barbican.com.hk

Fraser Construction Co. Ltd.
科正建築有限公司

Slope Stabilization / Site Formation / Piling
Specialist Contractor

Managing Director : Mr. Ringo Yu
B.Eng(McGill) CEng MIStructE FHKIE
MICE Chartered Engineer
Registered Professional Engineer

Tel : 2770 0122 **Fax : 2580 0470**

Address : Rm. 823, 8/F., Pacific Link Tower (South Mark),
11 Yip Hing Street, Wong Chuk Hang,
Hong Kong.

Please contact us for free budgetary advisory and preliminary feasibility services.

EXCEL ENGINEERING COMPANY LTD.

怡 益 工 程 有 限 公 司

A member of Vantage International (HOldings) Limited

With the Compliments of

Tin Shui Wai Permanent Public Transport Terminus

Watermains Trenchless Rehabilitation Works

155 Waterloo Road, Kwoloon Tong, Kowloon, Hong Kong
Tel.: 2866 1022 Fax.: 2866 1019
Web Site: http://www.vantageholdings.com

TABLE OF CONTENTS

Innovation in Geotechnical Engineering in Hong Kong - A Personal View

J.W. Pappin
Ove Arup and Partners Hong Kong Limited

ABSTRACT

Hong Kong has a host of issues that require significant input from geotechnical engineers including very tall buildings with high foundation loads, deep excavations for basements and infrastructure projects, tunnels in a variety of ground conditions and of course slope stability problems. These opportunities should make it a perfect breeding ground for innovation. In addition, however, it also has a very onerous, somewhat rigid and formalised checking procedure. This paper explores the question of whether innovation is possible or encouraged in this environment? It does this by using a series of examples taken from the range of activities that geotechnical engineers become involved with that are largely drawn from continuing interesting personal experience gained in Hong Kong. They show that there are many instances where innovative design and construction practices have been used. While many times these are developed by contractors and designers in certain circumstances the GEO and Buildings Department of HKSAR have taken a leading role. Some times the checking authorities are wary of new methods. Given their remit this caution is often reasonable and all parties need to formulate strategies and approaches to be able to continue to innovate in a successful and assured manner.

1 INTRODUCTION

Hong Kong is a wonderland for geotechnical engineers. It has a host of engineering issues that require significant geotechnical expertise including very tall buildings with high foundation loads, deep excavations for basements and infrastructure projects, tunnels in a variety of ground conditions and of course slope stability problems. These opportunities should make it a perfect breeding ground for innovation. In addition, however, it also has a very onerous, somewhat rigid and formalised checking procedure. Many geotechnical practitioners would ask whether innovation is possible or encouraged in this environment? It is the author's opinion that it certainly is possible but sometimes it is more difficult than others. This paper addresses this dichotomy by using a series of examples. They are deliberately taken from the range of activities that geotechnical engineers become involved with in Hong Kong and are largely drawn from continuing interesting personal experience that has been gained over the past decade.

2 FOUNDATIONS

2.1 Interface coring of large diameter bored piles end bearing on rock

The geotechnical profession arrived at a crisis situation in Hong Kong in the late 1990's/early 2000's when it was discovered that a significant number of high rise buildings, both in the private and government sector, were already constructed, or about to be constructed on pile foundations that did not meet with the stated design requirements. Many of these were founded on large diameter bored piles supposed to be supported by end bearing on rock. They had been designed using the conventional Buildings Department recommendations of 7.5MPa on Grade II or better rock and 5MPa on Grade III or better rock (Buildings Department, 2004). Several projects required remedial works. The state of the defective piles was generally established by core holes drilled down the pile shaft that intercepted the pile base. While a completed building was demolished in one project, several other projects required remedial works that varied from replacement piles to augmenting

the capacities of dubious piles with additional pre-bored H piles within sockets into the underlying rock either by surrounding the existing piles or drilling down through the existing pile or a combination of both.

Clearly this situation was intolerable to the Buildings Department and industry and that contracting practices and site supervision must be improved. To achieve this for end bearing bored piles, in particular, the additional provision of interface coring was instituted for every pile. This entails casting a thin wall steel tube of about 150mm diameter into the pile such that it stops about 1m above the base of the reinforcement cage. After the pile is cast and the concrete hardened the remaining 1m of pile is cored and the interface onto the rock below and the condition of the rock itself examined. This process ensures that the toe level of the pile, the interface condition and the quality of the rock is established with confidence.

It is interesting to review the history of end bearing bored piles in Hong Kong. Up until the early 1990's many of the larger end bearing foundations were formed as hand dug caissons and the base or bearing area was individually inspected and approved prior to concreting. Safety concerns however lead to the demise of hand dug caissons and machine dug bored piles became the norm. A drawback of this system is that the quality of the base may be poor and this must raise questions as to the reliability of the pile load bearing performance. Perhaps the profession was lulled into a false sense of security as a small percentage of these bored piles were cored for their full length to prove the quality of the concrete in the pile shaft, the concrete rock interface and also the quality of the rock immediately beneath the pile.

The introduction of interface coring has brought about a significant improvement in the quality control of this piling process. After it was first introduced it was realised that in many instances debris in the form of soil inclusions or concrete aggregate formed at the pile base. Concreting procedures were improved by introducing cement rich material on the first pour and other methods were used. The quality has generally since improved and studies have been carried out (e.g. Arup, 2001) to show that a small inclusion of aggregate or even soil at the interface is not significant and that the piles have a capacity that is basically controlled by the confidence in the strength of the reinforced concrete shaft. The upshot of the use of comprehensive interface coring has been that the reliability of large diameter piles is now significantly improved.

It is the author's opinion however that this proof of the piles construction quality is not being taken full advantage of and that revised guidelines on allowable bearing pressures should be instituted. We know that the existing guidelines are conservative (West Rail test piles, see Hill et al., 2000) and interface coring removes the doubt about quality of the concrete rock interface. Continued effort should be made in this issue.

2.2 Shaft grouted piles and barrettes

The use of shaft grouting has long been recognised as a method of tightening the ground after the bored pile or barrette has been excavated probably to restore insitu soil lateral stresses to be at least as high as that existing before the piles or barrette are excavated. The procedure is particularly suited to barrettes as they both maximise the shaft area presented to soil to enhance the skin friction capacity and the process of forming a barrette can lead to significant soil disturbance as evidenced by the settlement of the ground if a line of barrettes is formed to create a diaphragm wall.

Shaft grouted barrettes have been used on several projects in Hong Kong (e.g. Plumbridge et al., 2000). The International Commerce Centre to the south of the Kowloon Airport Express MTR Station, is a particular example. This project, comprises 240 shaft grouted barrettes formed on a regular pattern within a 75m diameter perimeter diaphragm wall as shown in Figure 1. The spacing between the 2.8 by 1.5m barrettes was maintained at 2m as described by Chan et al., 2004. The project was located at a fault and the depth to rockhead was extremely deep at over 100m and in places rock was not proven even at 130m depth. Consequently conventional end bearing piles could not be used and shaft friction needed to be relied upon.

The shaft grouting comprised attaching 6 tube-a-manchette grout pipes to the outside of the reinforcement cage and then after the barrette concrete had hardened, using a thick cement grout to compact the soil by forming a grout layer between the barrette concrete and the soil. It is intended that there is a minimum amount of grout injected at each metre down the pile or that a minimum grout pressure is achieved. The design and quality control methods for construction were developed by a joint venture between Bachy Soletanche and Intrafor with assistance from Arup. The design relied on an enhanced skin friction as a function of SPT N value for the alluvium and CDG layers. These values were verified and refined based on a test barrette program. The working load on each barrette was about 40MN which is about the maximum load that can be applied by a kentledge test and therefore preliminary test barrettes could not be completed to verify the total

capacity with any factor of safety. Four preliminary test barrettes that used slip coats and varying length such that only the friction from one part of the soil profile was tested within each test, were therefore adopted.

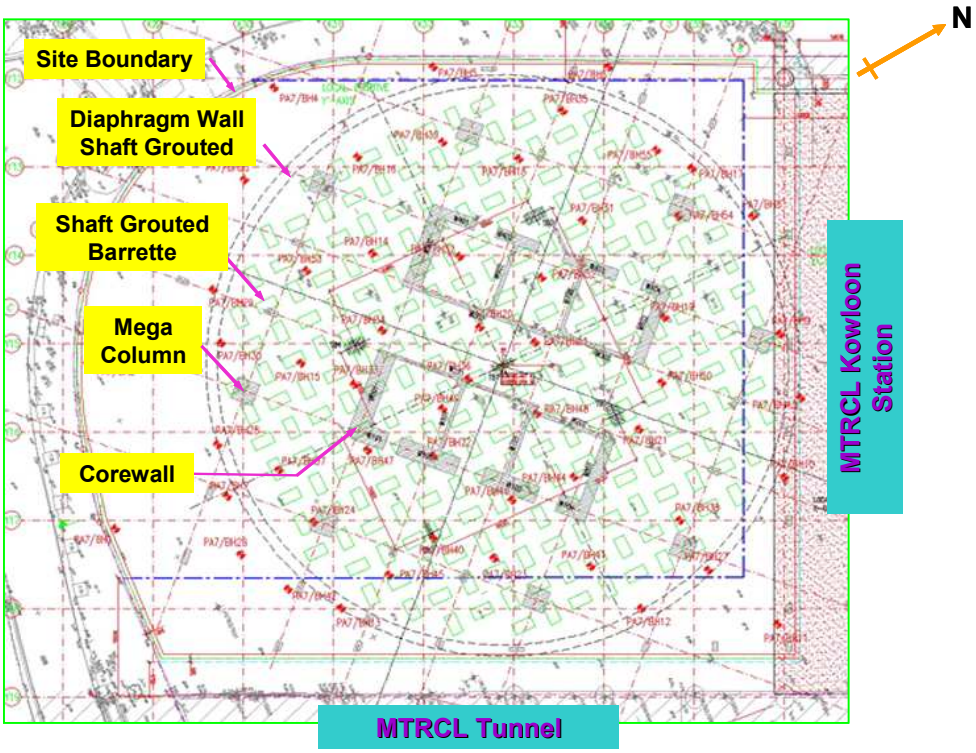

Figure 1: Plan of the barrettes and circular diaphragm wall at the ICC, Kowloon

The design and testing procedure was agreed with the Buildings Department. They had a reasonable concern about the quality control of the grouting works and a detailed real time monitoring system was developed by the contractors based on their previous experience from the West Rail pile testing programme and other projects. A continuously recorded real time monitoring system was setup to measure the grout volume and pressure at each injection point. If the grout volume is exceeded without sufficient pressure being developed or if insufficient grout volume is achieved over part of the barrette a further sequences of grouting was carried out. This procedure was refined in the preliminary test barrettes and subsequently applied to the working barrettes.

2.3 H piles to augment large diameter bored pile capacity

A companion paper in these proceedings (Pappin et al., 2008) describes the use of pre-bored concreted H piles used to enhance the capacity of large diameter bored piles founded in rock. Up to 9 H piles were arranged in a circle around the central bored pile at a radius of about 3.5m. This was necessary to increase the combined capacity such that a top down construction sequence for the 4 level basement could be used. By the time the basement reaches the deepest level about 40% of the superstructure load has been applied. Therefore by the time the pile cap is cast the bored pile is quite significantly stressed and considerations of elastic shortening indicate that it the allowable working bearing stress will be exceeded when the full load is applied. This potential problem is overcome by using jacks to pre-load the H piles and to therefore partially unload the central bored pile. When the full load subsequently is applied both the H piles and the central bored pile are all at about their design working capacity. Figure 2 illustrates this process for the situation where 3 H piles are used.

While this procedure appears to be logical and has received approval by the Buildings Department there is an argument that it is unnecessarily conservative in that the pre-loading is not necessary if it can be shown that the central pile has an adequate margin against compression failure of the reinforced concrete section under the final load if the pre-loading is not used. This is further discussed later in Section 5.2.

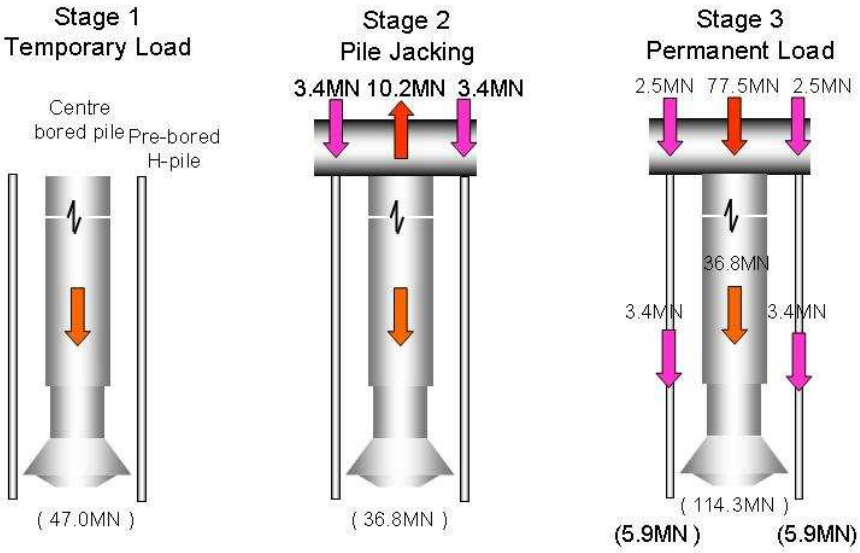

Figure 2: Illustration of load transfer with pile jacking for 3 H piles

3 DEEP EXCAVATIONS

3.1 Pre-trenched props and the observational method

This example of innovation was published in the 2001 HKIE Geotechnical Seminar (Ho et al. & Pan et al. 2001). The project was the 18m deep excavation for the Tseung Kwan O MTR station and the ground comprised 15 to 18m of fill over 8m of under-consolidated soft marine clay over variable thicknesses of alluvium and CDG. A conventional excavation sequence with several levels of temporary props lead to too much wall movement and alternative excavation sequences were required. Having decided that a jet grout slab within the clay was too expensive the original design concept had been to prop near the surface, excavate to the final formation level under water, tremie in the concrete base slab and then pump out the water. The diaphragm wall was constructed using reinforcement designed for this sequence. Eventually it was decided that the quality control of the permanent base slab was too difficult and an alternative of excavating part way and then digging trenches across the site, lowering in dumbbell shaped precast concrete props and using tremie concrete to structurally connect them in compression to the diaphragm walls. These precast props were located just under the lowest basement permanent slab and became part of the permanent works. This excavation sequence did not overstress the, by then existing, diaphragm walls and there were no major issues in obtaining approval from Buildings Department and GEO for this construction method.

During the progress of the works it became clear that the marine clay was gaining in strength with time and also that the diaphragm walls were moving less than predicted. These observations allowed a revised set of design calculations to be prepared using FREW and it was able to be demonstrated that the pre-trenched props could be avoided without exceeding the bending capacity of the walls. This is one of the few cases the author is aware of where the observational method has been used in Hong Kong and again it was subject to approval by the Buildings Department and GEO.

3.21 Circular excavations

The development of excavations supported by circular diaphragm wall excavations has been progressively developed in Hong Kong with projects at the Stonecutters Sewage Treatment works and IFC2 have excavations exceeding 50m diameter. The largest has been the 26m deep excavation at the International Commerce Centre having an excavated diameter of 75m and supported by a 1.5m thick diaphragm wall (see Figure 1). These walls have a relatively substantial capping beam and support the soil by their own hoop compression capacity. Usually concrete ring beams are cast against the wall at about 7m spacing but all these

achieve is to rectify any lack of alignment or local defect in the wall. They are not stiff enough in bending to contribute to the overall stability significantly.

The movement of these walls is observed to be very small at the time of excavation and consequently they need to be designed to support the full at rest horizontal pressure (σ_X) within the soil. The peak compression stress in the walls occurs at the excavation level and is equal to σ_X times the excavation radius divided by the wall thickness. Allowances need to be made for construction tolerances between adjacent panels. It can be calculated that the peak stress in the ICC wall is at least 13MPa and is approaching the maximum compression capacity of conventional concrete.

A major advantage of using this wall at this particular location was the low lateral deflection associated with the excavation. As shown in Figure 1 the existing Airport Express MTR line is only about 5m to the east of the wall and limiting the lateral movement of this tunnel was a major concern. Again it needs to be emphasised that this design was approved by the Buildings Department and GEO.

4 SLOPE ENGINEERING

Slope engineering is somewhat different to the previous examples in that GEO are the major client in Hong Kong and, in that role, they have continued to prove to be innovative and progressive (for example see Ho, 2004). Indeed in these proceedings the author is aware of two papers, Ho et al and Lau et al. that respectively present innovation in the use of real time drilling monitoring of soil nail installation and the use of innovative real time monitoring of selected slopes in Hong Kong. There have been many significant innovations in the prediction and modelling of debris flows, quantitative risk assessment of natural terrain and the use of non-destructive testing to check lengths of soil nails and many others. To attempt to address the range of innovations in slope engineering in Hong Kong is considered to be beyond the scope of this paper however.

5 DESIGN METHODS

5.1 The use of partial factors for the design of retaining walls

The use of partial factors in design in geotechnical engineering has had a long and relatively tortuous history. It appears to be relatively obvious that partial factors on loads that allow for their variability, by increasing them for more onerous situations and by reducing them if they are beneficial, leads to safe design. The situation is less clear for soil loads however. The situation becomes particularly difficult for retaining walls where the same soil body can both be applying disturbing lateral load to one side of the wall and also providing restoring lateral load on the other. It has now become quite well understood that the only consistent and rational way to deal with this is to factor the soil strength and not the soil unit weight as has been proposed on some occasions in the past. Factoring soil strength has merit in guarding against failures of retaining walls in that, if a failure mechanism is to form within a retaining wall system, it must involve the strength of the soil and also, sometimes, the strength of the wall.

In Hong Kong the GEO lead the way on this topic by the introduction of partial factors in the 2nd Edition of Geoguide 1, 'Design of retaining walls', in 1994. A drawback with it, however, is that it is limited to gravity walls and excavations with singly propped excavations. It specifically excludes multiply propped retaining walls. In 2003 however CIRIA published C580 entitled 'Embedded retaining walls – guidance for economic design' (Gaba et al., 2003). It contains much useful advice on the design and construction of retaining walls and also contains a partial factor on soil strength method for the design all typed of walls including multiply propped retaining walls. It require a stability calculation check with factored soil strength and, if displacement is of concern, requires a serviceability calculation with unfactored or characteristic soil strength to enable the displacement to be estimated. For a sheet pile or diaphragm wall usually a certain wall capacity is required for stability and it requires that the ultimate wall capacity be sufficient to withstand the factored soil strength forces. If displacement is important the ultimate strength of the wall must also be at least 1.35 times that calculated in the serviceability calculation. This method is inherently more robust than the traditional design method that only checks the serviceability condition for wall capacity. The C580 method also ensures that the wall is robust even in the condition where the soil strength is less than the characteristic strength due to some local weaker deposit.

In consultation with industry GEO have again taken the lead here and have come to an agreement with the Buildings Department that a design in accordance with C580, modified slightly such that factors are in line with Geoguide 1, can be approved. There has been little take up in its use here however, partly due to recent lack of deep basement projects and partly due to unfamiliarity and a concern that GEO, while being supportive, are being excessively cautious in its application requiring extensive sensitivity checks of many parameters etc. While it is true that C580 recommends that sensitivity analyses be carried out they are no more necessary with this method than the traditional methods. The use of partial factors is explicitly forcing the sensitivity of the design to study the occurrence of weaker soil than expected in a much more robust way than traditional lumped factor of safety methods.

5.2 Design of pile groups

The design of pile groups appears to be developing into a more complex task partly due to the improved accessibility to more complex computer programs. Take, for example, a 4 by 4 group of piles to support a single central load. If a rigid pile cap is assumed and if all the piles are the same length and extend to rock each pile would take $1/16^{th}$ of the load and the design would be complete. If, however, a flexible cap is used, and the piles assigned a uniform vertical spring stiffness the inner piles would attract more load. If on the other hand the piles are friction piles and a rigid cap is used, most computer programs (e.g. PIGLET) would show that the outer piles attract more load. If a flexible is used with friction piles the result could go either way depending on the relative stiffness between the cap and the soil.

It seems to be becoming standard practice that the piles are analysed using either a program like PIGLET or a flexible cap analysis with uniform pile stiffnesses. It is clear that neither method is reliable if a flexible cap is used in conjunction with friction piles. Nevertheless, usually the pile distribution is taken as predicted and each pile designed accordingly. The author suggests however that a more reliable procedure can be used to address this problem that will be more resilient to the limitations of the analysis method and produce a safe result. It is largely based on the design philosophy embodied in C580 in that both an ultimate and a serviceability analysis are to be carried out. The ultimate calculation would ensure that there is sufficient pile capacity to balance the factored applied load (e.g. 1.4∗dead load + 1.6∗live load). The pile capacity must be the minimum assured capacity which would be about 1.5 times the current working capacity (this may be a function of the number of test piles and further guidance is given in Eurocode 7 on this). The piles and the pile cap must also have ultimate strengths sufficient to withstand the derived pile reactions. In addition it is necessary to carry out a serviceability calculation, based on an appropriate soil structure interaction analysis, to derive the probable forces in the pile caps and the reactions in the piles. These should then be factored up by about 1.4 to check that the ultimate capacities of the structural elements (the piles and the pile cap) are sufficient.

If the example described previously in Section 2.3 followed these principles it may well be possible to remove the use of the preloading jacks. This would only be possible however if the structural capacity of the central bored pile is sufficient to take the increased load and also if the superstructure could tolerate about 5mm additional settlement. It is clear that the central pile will attempt to carry more load than that conventionally used at present. This is still a safe situation however in that if the central pile can support this additional load then all is well. If however due to this additional load the pile geotechnical capacity is reached and tends to yield then load will be transferred to the surrounding H piles causing them to settle a little, but this is still safe situation. It must be noted that this procedure is based on the premise that if the geotechnical capacity is reached the pile will yield in a ductile manner. Load tests consistently show this is the case.

The author has attempted to use this design approach on several occasions and has had mixed reaction from the approving authorities.

6 CONCLUSIONS

The preceding examples show that there are many instances where innovative design and construction practices have been used in geotechnical engineering in Hong Kong. While many times these are developed by contractors and designers, in certain circumstances the GEO and Buildings Department of HKSAR have taken a leading role. Other times the conservative nature of these checking authorities and their distrust of new methods has slowed progress but rarely prevents it. Given their remit this caution is often reasonable and all

parties need to formulate strategies and approaches to be able to innovate in a successful and assured manner. Rarely does the axiom 'there is no need to change as it has worked before' successfully withstand detailed scrutiny if there is a logical and more efficient alternative to be followed. In this current age where sustainability is becoming the driving force for all human activities we need to work together to achieve appropriate innovation.

REFERENCES

Arup, (2001). Study of Bored Pile Interface Acceptance Criteria. Report for the Hong Kong Construction Association Ltd., Piling Contractors Committee, 35 p.

Arup, (2002). QRA of Collapses and Excessive Displacements of Deep Excavations. GEO Report No. 124, Geotechnical Engineering Office, Government of the Hong Kong Special Administrative Region, 109 p.

Buildings Department, (2004). Code of Practice for Foundations. Government of the Hong Kong Special Administrative Region, 57 p.

Chan, G., Lui, J.Y.H., Lam, K., Yin, K.K., Law, C.W., Lau, R., Chan, A., & Hasle, R. (2004), "Shaft Grouted Friction Barrette Piles For A Super High-rise Building," Proceedings of the New Perspectives in the Design and Construction of Foundation Structures, HKIE: 83-98.

Gaba, A.R., Simpson, B., Powrie, W. & Beadman, D.R., (2003). Embedded retaining walls – guidance for economic design. CIRIA report C580.

Geoguide 1, (2000). Guide to retaining wall design. Geotechnical Engineering Office, CEDD, Government of the Hong Kong Special Administrative Region.

Hill, S.J., Littlechild, B.D, Plumbridge, G.D. & Lee, S.C. (2000), "End Bearing & Socket Design for Foundations in Hong Kong". 19th Annual Seminar, Geotechnical Division, HKIE.

Ho, K.K.S. (2004). Recent Advances in Geotechnology for Slope Stabilization and Landslide Mitigation - Perspective from Hong Kong. Proceedings of the Ninth International Symposium on Landslides, Rio de Janeiro, Brazil, Vol. 2, pp 1507-1560.

Ho, J., Pappin, J.W., Hope, S & Blair, C. (2001). Buried concrete prop design and construction of Tseung Kwan O Station and Tunnels. 20th Annual Seminar, Geotechnical Division, HKIE.

Ho, N.L., Yau K.M., Wright, M.J. & Wong, K.L. (2008). Application of real-time process monitoring during soil nailing works. 27th Annual Seminar, Geotechnical Division. HKIE.

Lau, K.W.K., Sun, H.W., Millis, S.W., Chan, E.K.K. & Ho. A.N.L. (2008). Application of Innovative Monitoring Techniques at Four Selected Natural Hillsides in Hong Kong. 27th Annual Seminar, Geotechnical Division, HKIE.

Pan, J.K.L., Pappin, J.W., Cowan, S. & Lam, L.W.Y. (2001) Diaphragm wall propping optimisation using the observational approach. 20th Annual Seminar, Geotechnical Division, HKIE.

Pappin, J.W., Lam, A.K.M., Sze, J.W.C. & Chan, K.M. (2008). A Special Combined Deep Foundation System for a Residential Complex. 27th Annual Seminar, Geotechnical Division, HKIE.

Plumbridge, G.D., Littlechild, B.D., Hill, S.J. & Pratt, M. (2000). Full scale shaft grouted piles and barrettes in Hong Kong – A first. 19th Annual Seminar, Geotechnical Division, HKIE.

Design and Analysis of a Large-scale and Deep Cylindrical Structure in Soft Soils

W.D. Wang
East China Architectural Design & Research Institute Co.,Ltd., Shanghai

ABSTRACT

The Shanghai 500kV World Expo Underground Transmission and Substation, situated in the central district of Shanghai city, is an important attached project of the 2010 Shanghai World Expo. The project involved the construction of a four level cylindrical underground structure with a diameter of 130 m. The excavation depth for the project was 34 m and it was constructed in difficult soft soil conditions. It is one of the most difficult recent underground construction jobs in Shanghai. This paper serves to provide a summary of the design and key techniques of the project.

1 INTRODUCTION

The Shanghai 500 kV World Expo Underground Transmission and Substation (SWEUTS) project is located in the central district of Shanghai city. It is an important attached project of the 2010 Shanghai World Expo. It is expected to contribute significantly in alleviating power supply pressure on the downtown area of the city. In addition, the SWEUTS is expected to provide guaranteed power supply for the success of the 2010 World Expo. The project, constructed to a depth of 34 m below the ground surface, has a diameter of 130 m. The SWEUTS is the first multi-voltage 500kV grade underground terminal substation in China. Completion of the project will make it one of the largest and most advanced underground substations in the world.

The project is an unusual one. It is a large-scale and deep cylindrical underground structure constructed by top-down method in difficult soft soil conditions. Though a large number of case histories of deep excavations has been reported in the literature, there is a very limited number of case histories available for cylindrical excavations. Bruce et al. (1991) introduced the design, construction, and performance of the new Richmond Avenue Pump Station in Staten Island NY. This project was constructed to a depth of 27 m below existing grade within a 16.5m circular, 50 m deep slurry wall cofferdam. Kuwagai et al. (1999) investigated the behavior of a 500 kV large-scale underground substation in Tokyo. The excavation, 144 m in diameter and 29.2m in depth, was retained by 2.2 m (upper portion) and 1.0 m (lower portion) thick diaphragm walls. Kim and Lee (2003) investigated a deep excavation for a 56 m deep cylindrical in-ground LNG storage tank with a diameter of 8 m in a coastal area of Korea. Chu et al. (2005) analyzed the monitored data of the excavation of the tower part of the Shanghai World Financial Center. The excavation, with a diameter of about 100 m and depth of about 18 m, was retained by 1.0 m thick cylindrical diaphragm walls. Liu (2005) studied the structural performance of a deep cylindrical excavation with a diameter of 73 m and depth of 45.5 m in stiff soil condition. The excavation was supported by 1.5 m thick diaphragm walls. Chen et al. (2006) introduced a cylindrical excavation (33 m deep) with a diameter of 30 m. It was retained by 0.8 m thick diaphragm walls without internal strutting

All the cylindrical excavations mentioned above were retained by diaphragm walls without internal strutting. This was quite different to the SWEUTS project which was supported by cylindrical diaphragm walls and four levels of permanent horizontal slabs. Moreover, the SWEUTS project was constructed in a congested urban environment and in difficult soft soil conditions. Thus design and construction of the SWEUTS project was a challenging task as no similar project could be used as a reference. A series of problems were encountered

during the design and construction of the project. Presented herein are some key techniques used during the design of the project.

2 PROJECT DESCRIPTION

The SWEUTS project was bounded by North Chengdu Road on the east side, West Beijing Road on the south side, Shanhaiguan Road on the north side, and Datian Road on the west side. Figure 1 presents a plan view of the project site including the relative locations of adjacent roads, buildings and services. The nearest existing building was about 26 m away from the project on the north side. The minimum distance between the project and an adjacent pipeline was about 17 m.

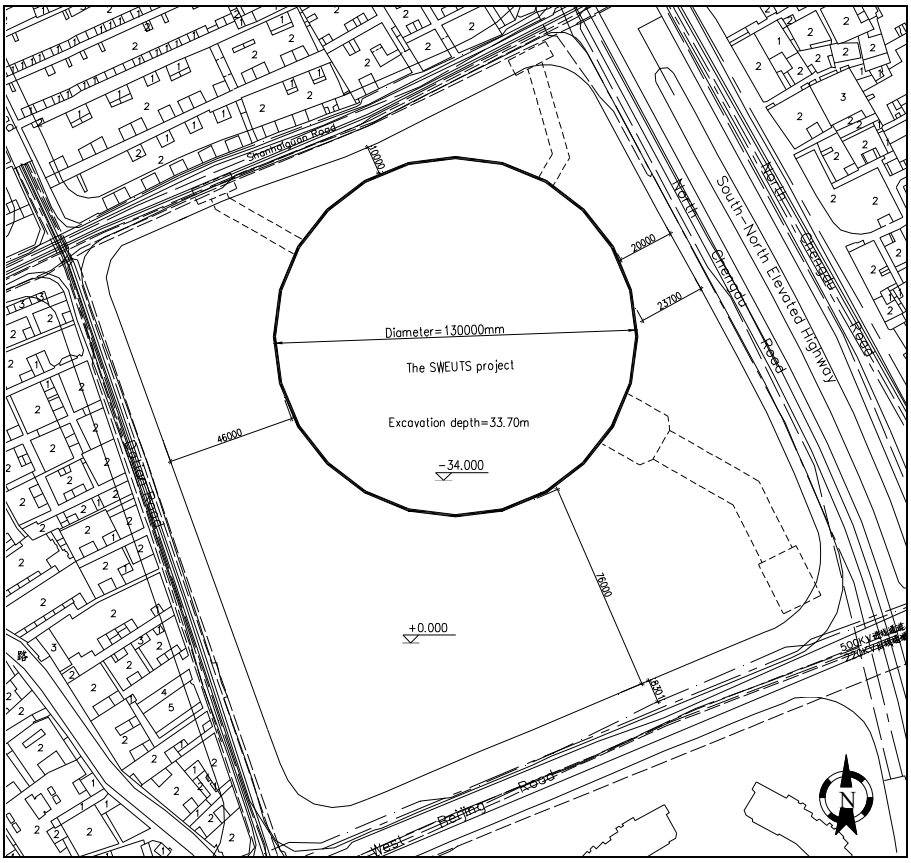

Figure 1: Plan view of the SWEUTS project site

The permanent structure of the substation is a four-level cylindrical underground structure with a diameter of 130 m and a depth of 34 m. According to the functions design, the first-level basement is used for installing electrical and cooling equipment. The second-level basement houses power cables. The third-level basement is used for accommodating large power transformers. Large power transformers are supported by special equipment foundations, which in turn are installed on the bottom slab of the underground structure. Figure 2 shows a perspective view of the SWEUTS underground structures. On completion, there will be a sculpture garden on the roof of the underground structure providing public facilities such as sitting-out areas, sculpture works exhibition and plantings.

According to the geotechnical investigation report (ECEPDGE, 2005), the underlying ground could be subdivided into 15 sub-horizontal layers. Table 1 details the sub-horizontal layers and the main physical

Figure 2: Perspective view of the SWEUTS showing the functions of the basement

(including voids ratio, e, and natural water content, w_n) and mechanical (including cohesion and friction angles obtained from direct shear test, SPT blowcounts, and specific penetration resistance and tip resistance of CPT) properties. Starting from ground level and moving downwards to a depth of about 30 m, the typical subsoil profile (including layers ①, ②, ③, ④, $⑤_{1\text{-}1}$, and $⑤_{1\text{-}2}$) consisted of made ground, silty clay and dominantly soft clay. These soils generally had large voids ratio and compressibility, with low shear strength and coefficient of permeability. These weak soils brought great difficulties to the design and construction of the excavation. From a depth of about 30 m to a depth of about 90 m, the typical subsoil profile (including layers $⑥_1$, $⑦_1$, $⑦_2$, $⑧_1$, $⑧_2$, $⑧_3$, $⑨_1$, and $⑨_2$) mainly consists of clay, silt and sand. These soils had much lager SPT blowcounts compared with to the upper weaker soils.

Table 1: Soil layers and geotechnical parameters at the construction site

Number of layers	Soil layer	Average thickness (m)	e	w_n (%)	c (kPa)	φ (^{O})	SPT (N)	p_s (MPa)	q_c (MPa)
①	Fill	4.25	---	---	---	---	---	---	---
②	Silty clay	1.67	0.958	34.4	15.7	15.8	---	0.72	0.66
③	Very soft silty caly	1.51	1.317	46.6	7.4	14.7	3.4	0.71	0.55
④	Very soft caly	7.01	1.358	48.1	7.2	17.2	2.6	0.65	0.53
$⑤_{1\text{-}1}$	Clay	6.93	1.091	38.3	12.3	12.3	4.3	0.94	0.72
$⑤_{1\text{-}2}$	Silty clay	4.25	1.032	35.4	6.8	13.9	6.5	1.30	0.98
$⑥_1$	Silty clay	5.38	0.753	26.1	30.7	13.5	14.6	2.78	1.94
$⑦_1$	Sandy silt	3.94	0.852	30.5	7.9	29.8	28.1	12.19	9.71
$⑦_2$	Silty sand	6.51	0.772	27.5	3.6	31.7	50.1	23.23	19.28
$⑧_1$	Silty clay	8.32	1.052	37.2	13.9	23.2	9.7	2.38	1.41
$⑧_2$	Silty clay and silty sand interbedded strata	14.76	0.992	34.6	12.3	23.8	15.5	3.45	2.35
$⑧_3$	Silty clay and silty sand interbedded strata	13.08	0.902	30.7	14.1	24.4	---	5.98	6.00
$⑨_1$	Medium sand	3.99	0.582	18.6	4.5	30.8	62.0	---	---
$⑨_2$	Coarse sand	4.90	0.544	16.7	5.3	33.0	83.4	---	---

Note: e＝voids ratio; w_n=natural water content; c＝cohesion obtained from direct shear test; φ＝angle of internal friction obtained from direct shear test; SPT=standard penetration test; p_s=specific penetration resistance of CPT; q_c=tip resistance of CPT.

The groundwater table was generally 0.3 m to 1.5 m below the ground surface. The ⑦$_1$ and ⑦$_2$ layers were the primary confined aquifer and the ⑧$_2$ and ⑧$_3$ layers were the second confined aquifer. Hydrogeological investigation revealed that the artesian head of the confined groundwater was about 3 m to 8 m below ground surface. It was found that there might be some connection between the primary confined aquifer and the second confined aquifer.

3 STRUCTURAL DESIGN

3.1 Structural system

The structural system of the SWEUTS consisted of reinforced concrete frame, shear walls and the cylindrical outer walls of the basement. Adoption of this kind of structure was due to some special factors, including the requirements for electrical installations, large excavation depth, high groundwater level, weak soil conditions in the shallow depth (from ground level to a depth of about 30 m) at the construction site, and huge lateral earth pressure acting on the structure.

Cylindrical diaphragm walls were adopted as retaining walls during the construction stage. Reinforced concrete lining walls with a thickness of 0.8 m were successively constructed in accordance with excavation progress to form a second barrier against water and at the same time prepare for unexpected cases such as non-uniform lateral pressures. A lining wall was connected with the diaphragm wall with pre-embedded bars in the diaphragm wall. The composite structure of the diaphragm wall and the lining wall formed the permanent cylindrical outer wall of the basement. The cylindrical structure was adopted due to its structural superiority where self horizontal stability can be achieved by virtue of hoop-compression stresses on the circular wall.

An in-situ RC frame was used as the inner structure of the basement. Flat slab supported by beams was a major part of the horizontal stiffening member in the inner framed structure the majority of the inner structure ranged between 6 m to 17m span in regular grids. Large span of the frame provides benefits such as providing enough space to accommodate large equipment and will be convenient for maintaining the equipment at the service stage.

3.2 Tension piles

The bottom of the underground structure was about 34 m deep. As the groundwater table in the construction site was generally 0.3 m to 1.5 m below the ground surface, the characteristic value of the uplift force of the whole underground structure was about 440,000kN. However, the characteristic value of the sum of the self-weight of the whole underground structure and down force exerted on the roof of the underground structure was about 290,000kN. Uplift force was far greater than the down force. Therefore, a large number of uplift (tension) piles were adopted to counter-balance the uplift effect due to groundwater pressure acting on the bottom slab of the underground structure.

A total of 665 bored piles were installed as tension piles by reverse circulation drilling methods. The diameter of the piles was 0.8 m. The piles penetrated through the stiff sandy soil layers (layers ⑦$_1$ and ⑦$_2$) and the thick silty clay layers (layers ⑧$_1$, ⑧$_2$, and ⑧$_3$). The medium sand layer (layer ⑨$_1$) was used as the founding layer for the piles. Pile tips went down to a depth of about 82 m below ground surface and the effective length of the piles was 48.6m. The design value of tension capacity of a single pile was 3000 kN. Post grouting of the pile shaft was used for the first time in Shanghai to improve the tension capacity of the

piles. Five injection points were distributed along each pile shaft, as can be seen in Figure 3. A total amount of 0.4 ton cement was used at each injection point.

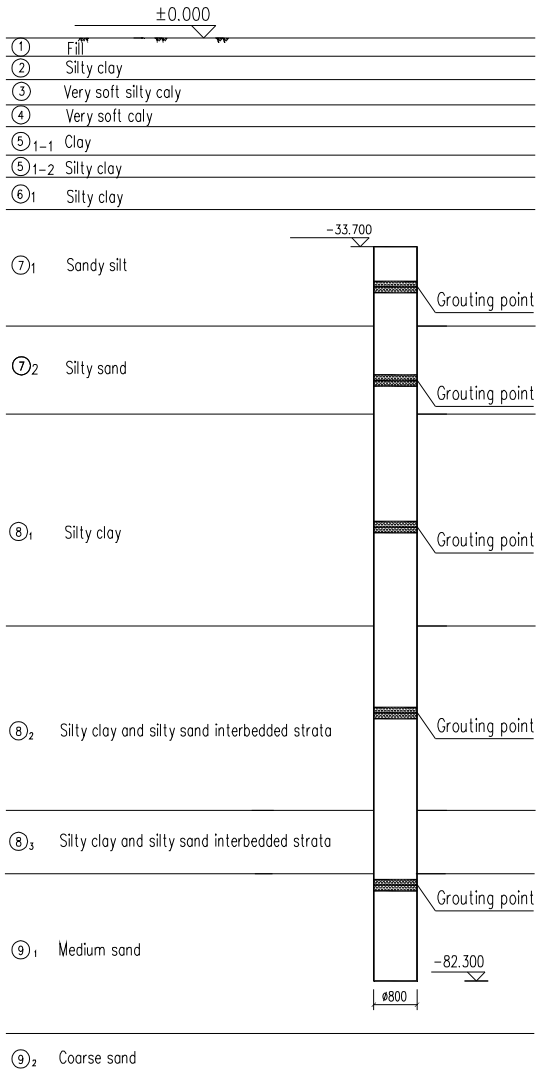

Figure 3: Distribution of injection points along pile shaft

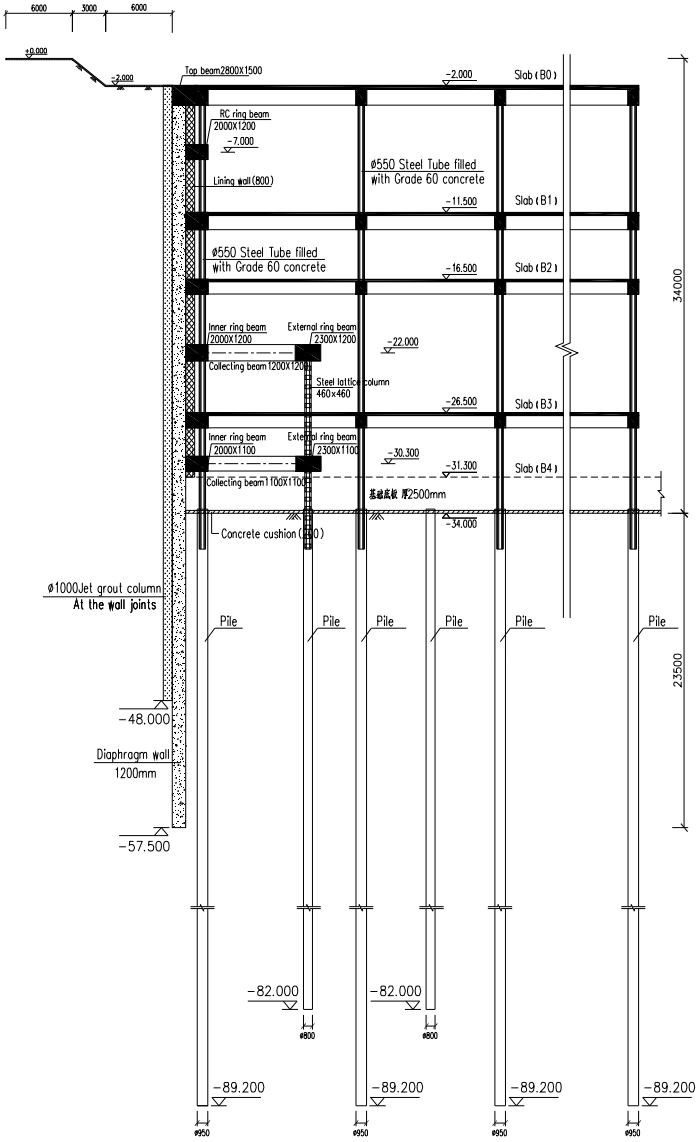

Figure 4: Sectional view of the supporting system

4 DEEP EXCAVATION

4.1 Diaphragm wall

The 13,200 sq m, four-level underground structure was constructed using a top-down method. The SWEUTS project involved a total of about 449,000 cu m of excavation. The excavation was retained by 1.2 m thick concrete diaphragm walls. At the excavation stage, the diaphragm walls were retaining and waterproofing structures. At the service stage, the diaphragm walls form part of the permanent wall of the basement. It was decided to embed the retaining wall toe in the ⑧$_2$ layer (see Figure 4). The embedded length was 23.8 m, making the retaining wall as deep as 57.5 m. The widths of the panels were 4 m and 6 m. The simple rigid steel I-beam joints (see Figure 5), which had effective water sealing performance, were adopted to join the panels of the diaphragm wall. Jet grout columns with diameter of 1.0 m were installed at the outside of the

joints of the diaphragm wall to form a second barrier against water. The walls were made of Grade 35 reinforced concrete. Toe grouting was carried out on all panels.

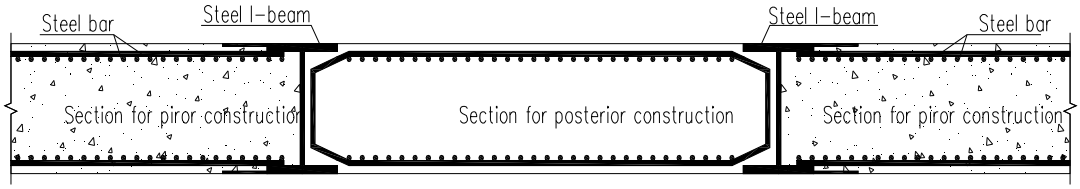

Figure 5: Sketch map of the joints between diaphragm wall panels

4.2 Lateral supporting system

The retaining walls were braced at the floor levels by the four basement slabs. The roof slab was also used as a platform for soil excavators, dump trucks and other construction machines. Big access openings were distributed in the slabs to facilitate the removal of the excavated materials and delivery of building materials. This improved the working environment underneath the roof slab and increased the construction speed. The height of the first, second and fourth level basement were 9.5 m, 10.0 m, and 7.5 m, respectively. In order to reduce the spacing of the lateral struts and further restrict wall movements, temporary ring RC strut frame systems were installed between the slabs in the first, second and fourth level basement (see Figure 4). Figure 6 shows the plan view of the roof slab showing the locations of access openings. Figure 7 shows the plan view of the temporary ring RC strut frame system.

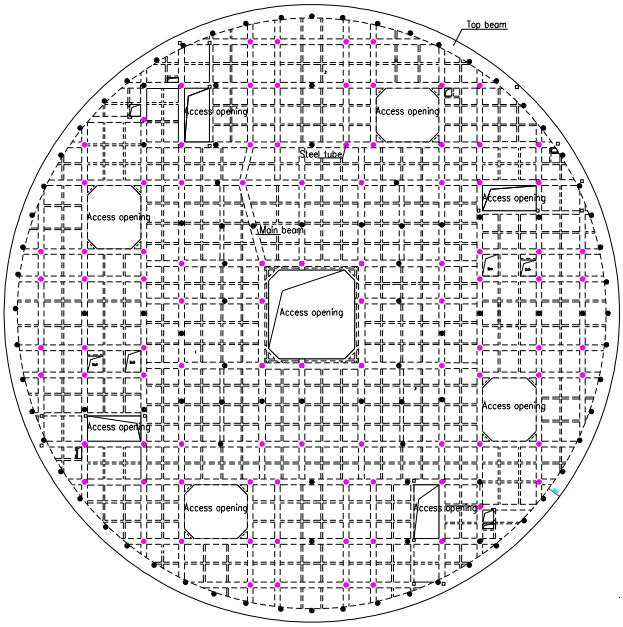

Figure 6: Plan view of the roof slab showing the locations of access openings

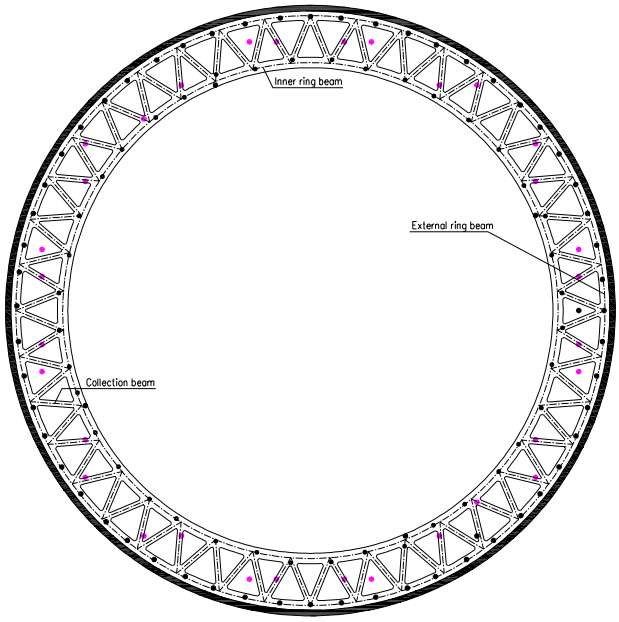

Figure 7: Plan view of the temporary ring RC strut frame system

4.3 Vertical supporting system

Temporary columns at the same position as the permanent columns were erected in the bored piles to support the underground structure that was constructed from the top level downward at the excavation stage. The design value of load acting on a single temporary column was 9500 kN. Bearing capacity and stability of a

regular steel lattice column, which is commonly used in top-down method in Shanghai, could not satisfy the design requirements in this project. Hence, steel tubes with diameter of 550 mm and wall thickness of 16 mm, filled with Grade 60 concrete, were used as temporary columns. A verticality of 1/600 was required for the installation precision of these columns. The steel tubes would finally be encased in concrete to be transferred into permanent columns. Figure 8 shows an elevation view of the temporary steel tube showing connections with the slabs.

A total of 201 bored piles were installed to support the temporary steel tubes at the excavation stage. After the construction of the bottom slab and the recovery of groundwater, these piles would be subjected to uplift load caused by groundwater pressure acting on the bottom slab. This meant that these piles would be compressed at the excavation stage and tensioned at the service stage. Design of these piles thus should meet the requirements at both the excavation stage and the service stage. The diameter of these piles was 950 mm. The coarse sand layer (layer ⑨$_2$) was selected as bearing layer for these piles. Pile tips went down to a depth of about 89.2 m below ground surface and the effective length of the piles was 55.8m (see Figure 9). The design value of bearing capacity of a single pile was 9500 kN. These piles were made of Grade 35 reinforced concrete. A verticality of 1/300 was required for the installation precision of these piles.

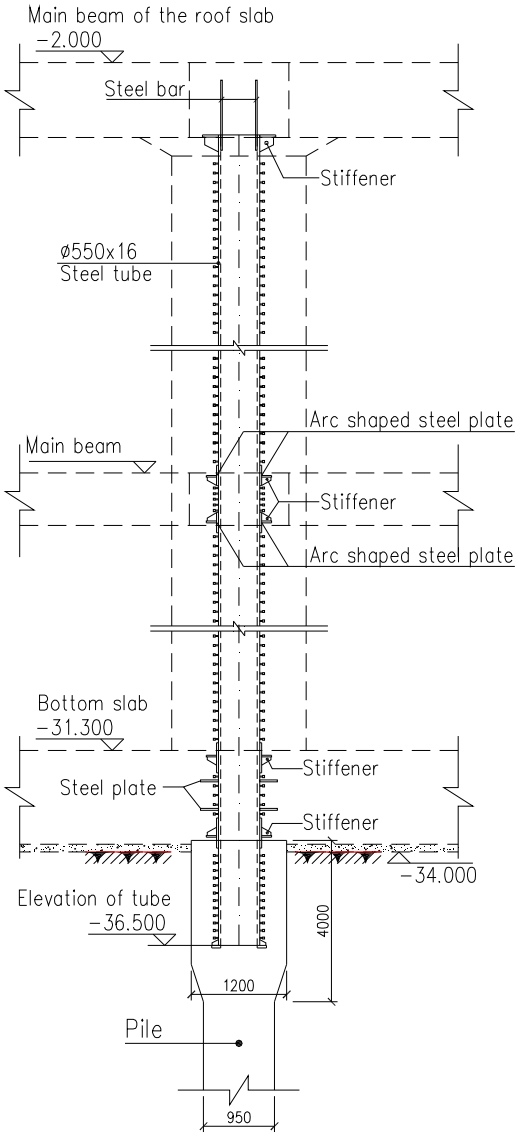

Figure 8: Elevation view of the temporary steel tube

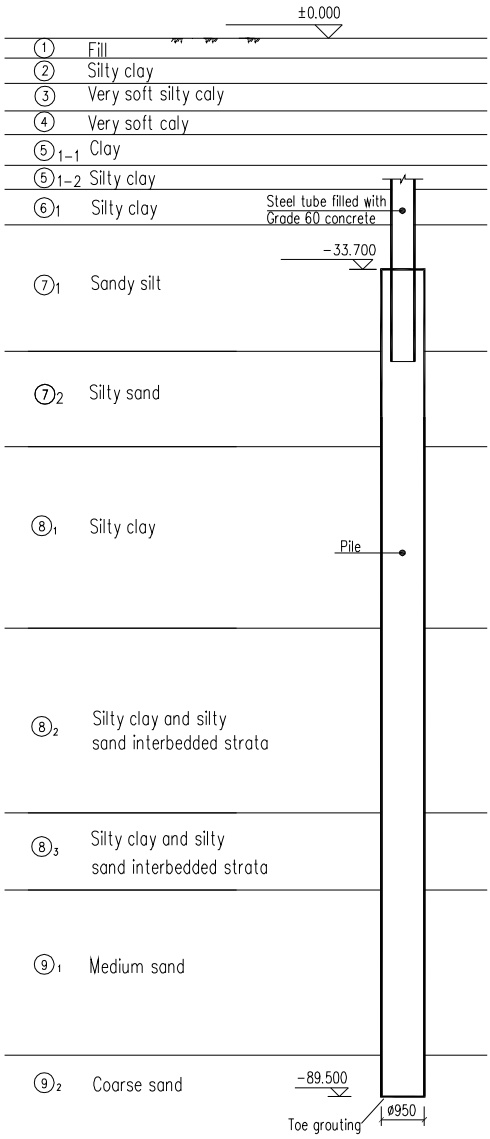

Figure 9: Elevation view of a bored pile used to support steel tube

5 KEY TECHNIQUES

5.1 Excavation supported by permanent structure

Construction of the SWEUTS project was quite difficult. The overall design scheme of the excavation should consider not only the safety of the supporting system and adjacent structures and facilities, but also the cost of the construction. The top-down method was finally adopted with consideration of the scale of excavation, ground conditions, and the cylindrical shape of the project.

In the top-down method, diaphragm walls were used as a retaining and waterproofing structure at the excavation stage and also used as the permanent wall of the basement at the service stage by efficient connection with the permanent beams and slabs of the underground structure. Permanent slabs were simultaneously used as lateral support of the retaining wall. Steel tubes were used to support the underground structure at the excavation stage and would be encased in concrete to form permanent columns. At the design stage, a series of key technique problems were solved. These included the design of diaphragm walls and slabs at different stages (excavation stage and service stage), connections between diaphragm walls and permanent beams and slabs, design of roof slab used as platform for vehicles and construction machines, connection between vertical steel tubes and horizontal slabs, and control of the verticality of steel tubes installation.

5.2 Design analysis of the cylindrical structure

Analysis methods include slab-spring approach and three dimensional continuum finite element method were adopted to model the construction processes. In the slab-spring approach, the cylindrical diaphragm wall and horizontal slabs were modeled by shell elements, horizontal beams and vertical supporting system were modeled by beam elements, ground reaction effects on the excavation side were modeled by spring elements, and the effects of the soil at the back of the diaphragm wall were modeled as loads acting on the wall. Figure 10 shows the analysis model using slab-spring approach. Internal forces and deformation of the underground structure were analyzed. Figure 11 shows the contour plots of the displacement of the diaphragm wall in radial direction after the final excavation. The wall bulged in toward the pit and the maximum distortion of the diaphragm wall was about 32 mm. Figure 12 shows the distribution of circumferential axial forces in the wall along the depth. It can be seen that circumferential axial forces were not uniform along the wall depth. The magnitudes of circumferential axial forces are closely related to the magnitude of wall distortion. Larger distortion would result in larger magnitudes of circumferential axial forces.

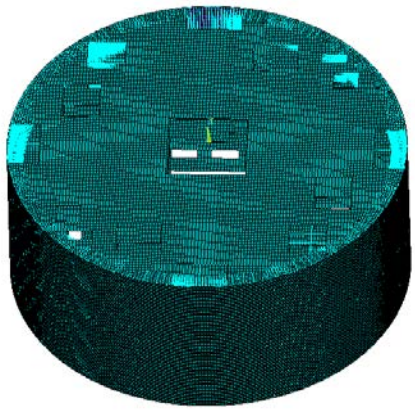

Figure 10: Analysis model using slab-spring approach

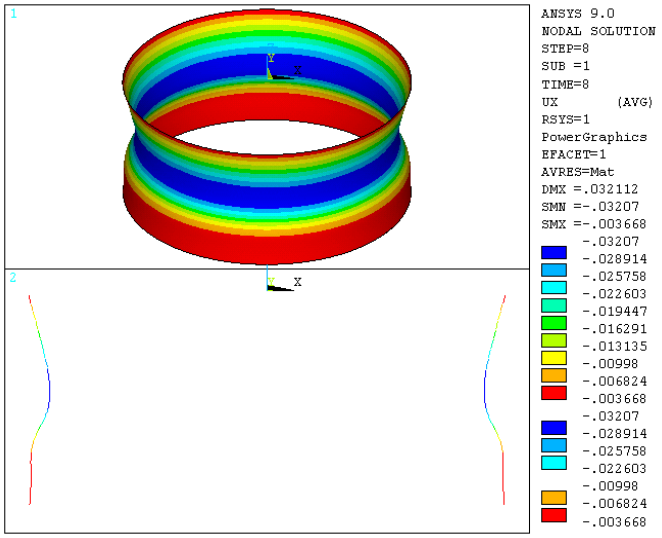

Figure 11: Contour plots of the displacement of the diaphragm wall in radial direction

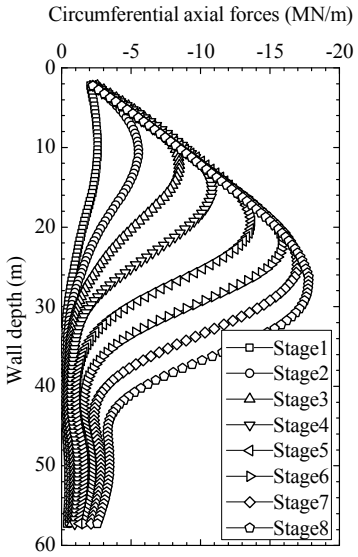

Figure 12: Distribution of circumferential axial forces in the wall along depth at different stage

In the three dimensional continuum finite element method, soils were modeled by 3D solid elements and the structural components were modeled as the same as that in the slab-spring approach. This method could model the deformation of the soil around the excavation, which could be indirectly used to evaluate the effects of excavation on the adjacent structures and facilities. Figure 13 shows the overall three dimensional analysis model using continuum finite element method. Figure 14 shows the contour plots of soil displacement in radial direction after the final excavation.

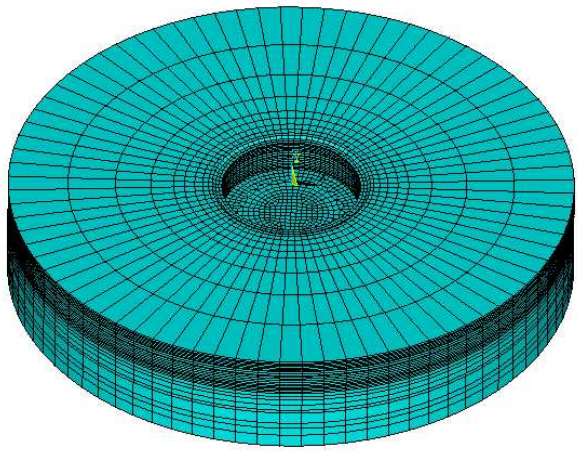

Figure 13: 3D finite element model of the excavation

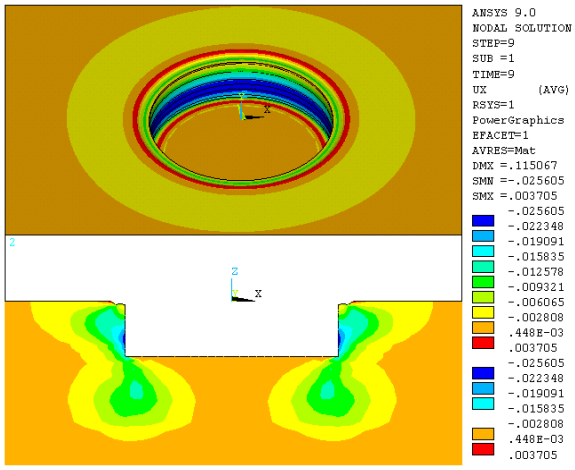

Figure 14: Contour plots of soil displacement in radial direction

Many design codes (e.g. ACECS 1997, CABR 1999) suggest using classical earth pressure theories such as Coulomb's earth pressure theory or Rankine's earth pressure theory to calculate earth pressure of excavations. These theories were based on limit equilibrium methods under plane strain conditions. However, these theories are not suitable for cylindrical excavations as the plane strain condition assumption is not satisfied. There is little literature discussing the calculation method of earth pressure of cylindrical excavations. Research on active earth pressure in this project was carried out. It was found that the magnitude of active

earth pressure at limit state under axisymmetric conditions was much smaller than that under plane strain conditions. Smaller diameter of the cylindrical excavation would result in smaller magnitudes of active earth pressure. It was concluded that the magnitude of real active earth pressure of cylindrical excavation might be between the magnitude of active earth pressure at limit state and that at rest. Earth pressure at rest was used as active earth pressure in the SWEUTS project as the deformations of the cylindrical diaphragm walls were considered to be very small.

5.3 Deep diaphragm wall

The 57.5-meter deep diaphragm walls were installed to the ⑧$_2$ layer through the firm sandy soil layers (layer ⑦$_1$ and ⑦$_2$) with SPT blowcounts of 28 to 50 and specific penetration resistance of 12 to 23 MPa. The firm sandy soil layers presented great difficulties to the installation of the diaphragm walls. To ensure quality and speed of diaphragm wall installation, special construction methods were employed. The sectors of wall trenches in soft soils (above the ⑦$_1$ layer) were excavated by conventional clamshell grabs while the deep sectors in the firm sandy soil layers (layers ⑦$_1$ and ⑦$_2$) and the silty clay layers (layers ⑧$_1$ and ⑧$_2$) were formed by trench cutting machines. This combined method was used for the first time in Shanghai district. Figure 15 shows the excavation methods of the diaphragm wall trench.

Diaphragm wall panels were joined by rigid steel I-beam joints. The steel I-beams were connected to the steel reinforcement cages by wielding. This kind of joint effectively improved the integrity of the diaphragm wall structure and water-proofing performance.

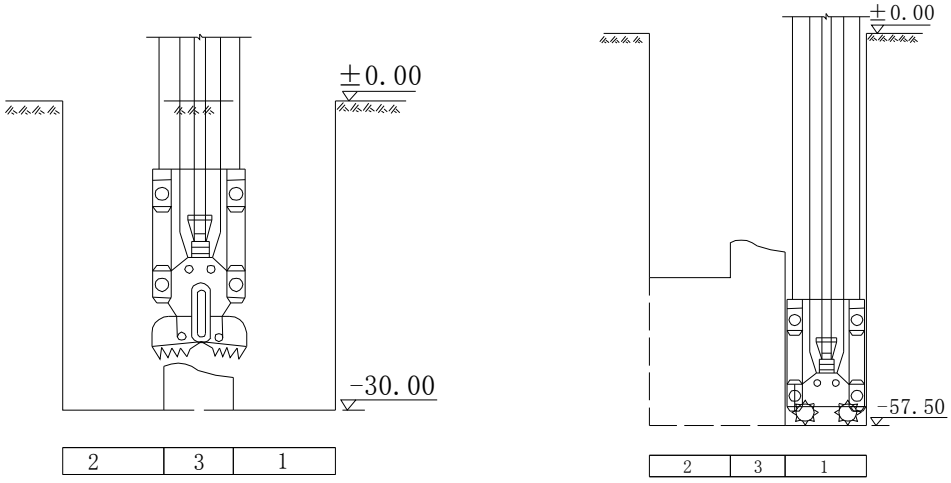

(a) Using clamshell grabs in soft soils (b) Using trench cutting machine in hard soils

Figure 15: Excavation methods of the diaphragm wall trench

5.4 Post-shaft-grouting of tension piles

Design of the tension piles was a key design issue for the anti-floating design of the overall underground structure. In order to select the most suitable pile type, static load tests were carried out to test the performance of two types of piles (pile with bell-out and post-shaft-grouting pile). The test results showed that both bell-out method and post grouting method could significantly improve the capacities of the piles. However, the vertical displacement of the pile top of the pile with bell-out was much larger than that of the post-grouted pile when the two types of piles were subjected to the same uplift load, as shown in Figure 16. Moreover,

quality control and post construction testing of piles with bell-out were quite difficult as the pile tips had penetrated into the hard sandy soil layer (layer ⑨$_2$). As a result, post-shaft-grouted piles were finally selected for the SWEUTS project.

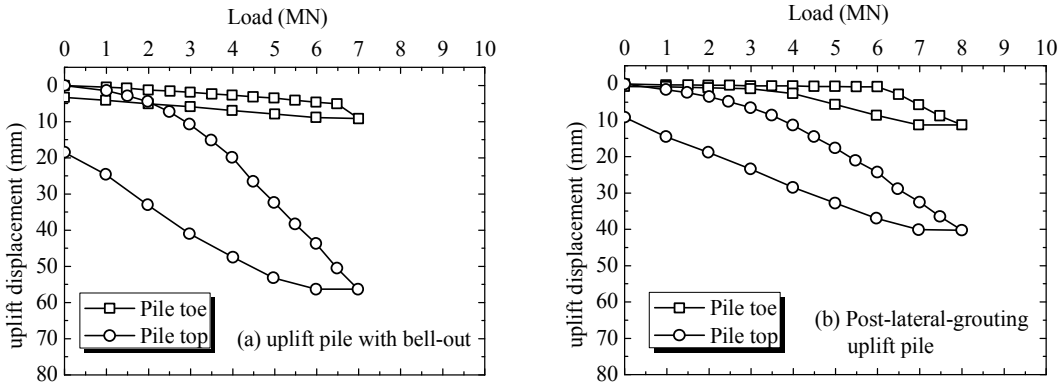

Figure 16: Load-displacement curves for uplift load tests

5.5 Design of tension piles under deep excavation

The area and depth of the excavation for the SWEUTS project were extremely large. Numerical analyses and centrifuge tests were carried out to study the effects of unloading due to deep excavation on the bearing behavior of piles. It was found that the bearing capacities of the uplift piles were reduced and tension stresses appeared in the middle and lower part of the pile shafts due to unloading. A discount of the bearing capacities of the uplift piles was adopted in the design stage considering the decrease of bearing capacities of uplift piles due to unloading. The quantity of reinforcement of the uplift pile was checked by the sum of the axial force caused by the uplift load at the service stage and that caused by unloading at the excavation stage. Research in the SWEUTS project showed that design of pile under deep excavations should take the effect of unloading into consideration.

6 CONSTRUCTION PROGRESS OF THE SWEUTS PROJECT

The project dates back to September 2005 when pile load tests commenced. The installation of diaphragm walls and piles commenced in December 2005 and took roughly 10 months to complete. Excavation started in December 2006. Up to present, the structure of the first, second, and third level basements has been constructed. The last excavation will commence soon. The construction of the bottom slab is expected to be completed in June 2008. Figures 17, 18, 19 and 20 show some photos of the construction progresses of the project. A lot of instrumentation was installed to monitor the performance of the excavation and the impact on surrounding structures and facilities. Monitored data showed that the maximum lateral displacement of the diaphragm wall was less than 35 mm. This agrees quite well with the analyzed results obtained by the slab-spring approach and three dimensional continuum finite element method.

7 CONCLUSIONS

Development of large scale and deep underground space has highlighted problems which are seldom encountered in regular underground engineering. Significant design issues of large-scale and deep

Figure 17: Pouring concrete of the central part of the roof slab

Figure 18: An aerial view of the project showing the completion of the roof slab

Figure 19: An interior view of the excavation showing steel tubes used as vertical support

Figure 20: A view into an access opening showing the underground structure

underground engineering include aspects such as design and analysis of the underground structure system under heavy horizontal loads, anti-floating design of the overall underground structure, high risk of deep excavation and its rational design, impact of unloading on bearing capacities of uplift piles and analysis of cylindrical structures. This paper introduces the design of the SWEUTS project which is a special large and deep cylindrical underground structure in soft ground. A series of advanced design concepts, new methods, and new techniques were adopted in this project. Due to the successful completion of this project, valuable experience has been gained which can be used as reference for other large scale and deep underground projects.

REFERENCES

Association of Civil Engineering Consultants in Shanghai (ACECS). (1997). Shanghai Standard Code for Design of Excavation Engineering-DBJ08-61-97, Shanghai. (in Chinese)

Bruce D.A., Chan H.C., and Tamaro G.J. (1991). Design, construction and performance of a deep circular diaphragm wall. Slurry Walls: Design, Construction and Quality Control, ASTM STP 1129, International Symposium on Slurry Walls, Atlantic City, NJ, June 1991

Chen Y.F., Zhang Q.H., Zhou J., and Wang Y. (2006). Half-inverted construction and supervision on circular special deep foundation excavation. Chinese Journal of Geotechnical Engineering, 28(S): 1865-1869 (in Chinese)

China Academy of Building Research (CABR). (1999). Technical Specification for Retaining and Protection of Building Foundation Excavations-JGJ-120-99, Beijing. (in Chinese)

Chu W.H., Huan Y.J., and Zhang X.H. (2005). Case study on construction monitoring for tower part of Shanghai World Financial Centre. Chinese Journal of Underground Space and Engineering, 1(4): 627-633 (in Chinese)

East China Electric Power Design Geotechnical Engineering CO., Ltd. (ECEPDGE) (2005). Geotechnical investigation report for the Shanghai 500 kV World Expo Underground Transmission and Substation, Shanghai. (in Chinese)

Kim D.S. and Lee B.C. (2003). Cylindrical diaphragm wall movement during deep excavation for in-ground LNG Storage Tank in coastal area. International Journal of Offshore and Polar Engineering, 13(4): 285-292

Kuwagai T., Ariizumi K., and Kashiwagi A. (1999). Behaviour and analysis of a large-scale cylindrical earth retaining structure. Journal of the Japanese Geotechnical Society of Soils and Foundations, 39(3):13-26

Liu M.H. (2005). Structural performance of the deep foundation pit bracing with circular diaphragm wall. Journal of Highway and Transportation Research and Development, 22(11): 96-99 (in Chinese)

Applications of Geophysics Methods in Underground Construction

W. F. Lee
Taiwan Geotechnical Society
National Taiwan University of Science and Technology
K. Ishihara
Chou University, Japan

ABSTRACT

Resistivity imagine profiling method has recently become one of the popular tools in soil exploration. It was mostly used in investigating geological structures before. In current urban geotechnical work, resistivity imagine profiling method was modified to examine performance of underground geotechnical works, or to verify ground conditions. In this paper, the author will introduce the basic theoretical background RIP methods. Two case histories are then presented to illustrate the promising applications of the resistivity imagine profiling method in verifying performance of soil improvement work and investigating ground condition. Progress presented in this paper is hoped to promote applications of advanced technologies such as RIP methods in engineering practice, and to provide alternative resolutions to similar geotechnical problems.

1 INTRODUCTION

Resistivity Imagine Profiling (RIP) method is one of traditional geophysical surveying technology, which has been developed for many years. It has recently become one of the popular tools in soil exploration. The RIP method has advantages in investigating ground water distribution, geological structures and soil profile over large area because of high sensitivity for water and different geo-materials. The RIP method was mostly used in investigating geological structures in the past. Applications of RIP method on investigating specific soil conditions or underground structures were not yet well developed. In an effort to develop a reliable soil exploration method for urban geotechnical work of which levels of complications and scales has greatly increased recently, the RIP method was modified to examine complicated ground conditions or manmade underground structures. In the presented paper, the authors will first introduce the basics of RIP methods. Theories and typical installation layouts of both 2D and 3D crosshole RIP methods are depicted in detail. Two case histories are then utilized to illustrate the applications of RIP methods. In the first case, the 3D crosshole RIP method was used to verify effectiveness of different soil improvement works that were adopted to retrofit defected diaphragm walls of a deep excavation site. Results of the 3D RIP method were found to be able to identify different soil improvement works and to exhibit quality condition of inspected diaphragm walls. In the second case, the surface 2D RIP method was planned to cover a construction failure site. Results of the RIP imagines were used to interpret the ground condition and possible failure causes of the accident. Applications of the RIP method to the urban geotechnical works were validated via the presented case histories. Information presented in this paper is hoped to promote applications of advanced technologies such as RIP methods in engineering practice, and to provide alternative resolutions to similar geotechnical problems.

2 RESISTIVITY IMAGINE PROFILING METHOD

2.1 Basics of Resistivity Imagine Profiling Method

The RIP method is one of traditional geophysical surveying technologies, which has developed for many years. Its applications have been further extended because of recent advances in electronic equipments and computer technology. The RIP method has advantages in investigating ground water distribution, geological structures and soil profiles over large area by measuring electrical resistivity distribution over the target soil deposits or underground space. Table 1 shows the typical values of resistivities of different geomaterials. As can be noted, the resistivities of cemented material such as concrete or grout vary from 10,000 ~ 40,000 ohm-m, while those of porous and moisture material such as saturated sands, silts and clay vary from 15 to 1,000 ohm-m. Also indicated in Table 1, the resistivity of sea water is as low as 1 to 5 ohm-m. Because the RIP method has high sensitivity to water content of various geomaterials and grout materials, it is therefore possible to identify different soil deposits, to detect defects of underground structures, to tell ground condition with different level of treatments, and to locate possible water leaking paths accordingly.

Usually, electrical currents are introduced into the target area by setting up layers of electrical circuits. Resistivity values at specific locations could be measured by specially arranged probing posts or sensors. Recorded values of resistivities are then input into analytical models to calculate the resistivity field of the target area. Key factors of the RIP method include optimization of sensor layout designs and resolution of the inverse models used to calculate the resistivity field.

Table 1 Resistivities of different material

Material	Typical Resistivity _(Ω-m)
Sea water	1 ~ 5
Clay (saturated)	15 ~ 30
Silt (saturated)	30 ~ 200
Sandstone	100~ 800
Sand (saturated)	200 ~ 1,000
Gavel (saturated)	1,000 ~ 5,000
Sand (dry)	5,000 ~ 20,000
Concrete Cemented Grout	10,000 ~ 40,000

2.2 Inverse Programs

In this study, two kinds of inverse programs: 1) The inverse program, RES2DINV ver. 3.54 by Loke(2005) and 2) the 3-D program, EarthImager 3D by AGI(2006) were used in the studied cases for calculating electrical resistivity fields.

RES2DINV Software The inversion routine used by the program is based on the smoothness constrained least-squares method (De Groot-Hedlin and Constable 1990). A new implementation of the least-squares method based on a quasi-Newton optimization technique (Loke 2001) was also used. This technique can be more than 10 times faster than the conventional least-squares method for large data sets and requires less computation effort. The smoothness constrained least-squares method is based on the following equation

$$(\mathbf{J}^T\mathbf{J} + u\mathbf{F})\mathbf{d} = \mathbf{J}^T\mathbf{g} \quad (1)$$

Where $\mathbf{F} = \mathbf{f_x}\mathbf{f_x}^T + \mathbf{f_z}\mathbf{f_z}^T$,

fx, **fz**, are the horizontal flatness filter and vertical flatness filter respectively,
J is the matrix of partial derivatives, $\mathbf{J}^T$ is transpose of **J**
u is the damping factor, and
d is the model perturbation vector and **g** is the discrepancy vector.

The 2D model used by this program divides the subsurface into a number of rectangular blocks (shown in Figure 1(a)). The purpose of this program is to determine the resistivity of the rectangular blocks that will produce an apparent resistivity pseudo-section in agreements with the actual measurements.

EarthImager 3D Software In this program, the underdetermined and ill-posed nature of 3D resistivity inverse problems makes the inverse solution inherently non-unique. Additional constraints, or regularization, must be imposed on the model to single out one optimal solution. The smooth model inversion, also known as Occam's inversion, could find the smoothest possible model whose response fits the data to a-priori Chi-squared statistics. The true model must be at least as, but never less complex than, the smooth model obtained through smooth model inversion. Smooth model inversion is based on the assumption of Gaussian distribution of data errors. The smooth model inversion algorithm was originally described in DeGroot-Hedlin and Constable (1990). The mesh of the program is shown in Figure 1(b). The objective function of smooth model inversion is given by

$$\mathbf{S(m)} = (\mathbf{d_{obs}}-\mathbf{g(m)})^{T}\mathbf{W}_{d}(\mathbf{d}_{obs}-\mathbf{g(m)})+ \alpha \quad \mathbf{m}^{T}\mathbf{Rm} \qquad (2)$$

Where α is a Lagrange multiplier and a stabilizing factor. It determines the amount of model roughness imposed on the model during the inversion, and
R is a roughness operator.

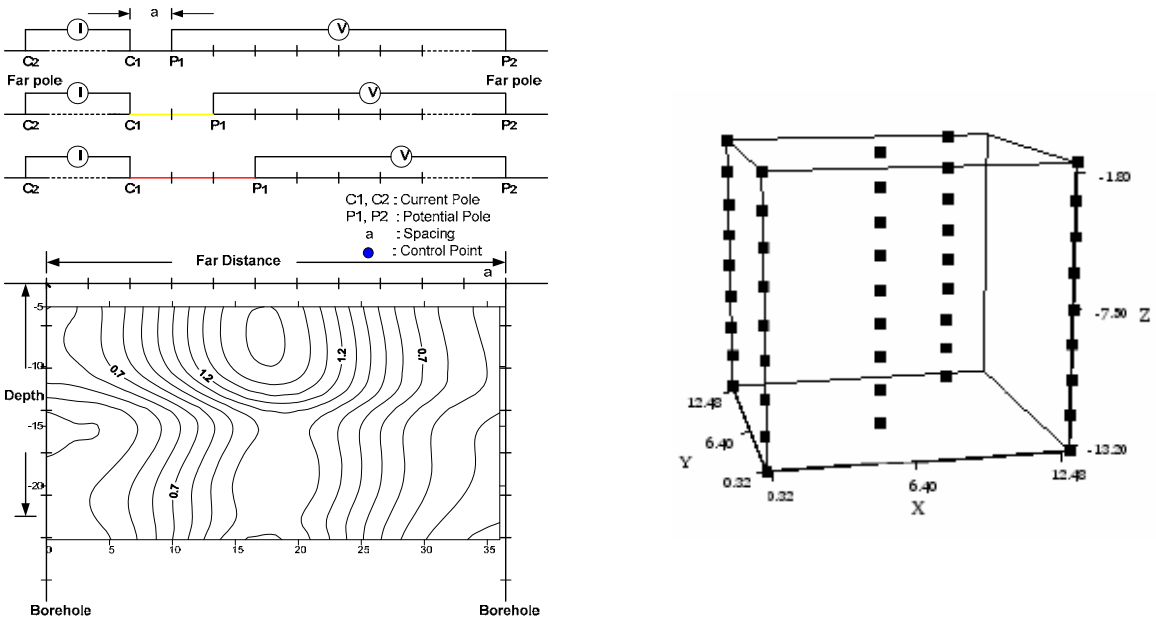

(a) (b)

Figure 1 (a) 2D mesh of borehole measurement and (b) 3D Electrode Geometry of EarthImger 3D (AGI, 2006).

3 CASE STUDY I

3.1 Site Information

O1 Station of Kaohsiung Mass Rapid Transit (KMRT) system is an underground terminal station at the western end of the KMRT Orange line (Figure 2). Excavation for the station was carried out to a depth of 20m by using diaphragm walls as the retaining structures. Two types of diaphragm walls were designed in this excavation work. Walls of 800mm in thickness were designed to a depth of 39m and those of 1000mm in thickness were designed to a depth of 37.5m. The studied site was a salt pan used for fish farming till the completion of the Kaohsiung Harbor in the beginning of the 20th century. The area was reclaimed by using the soil dredged from the harbor. Subsoils on site are the typical silty sand and sandy silt interlayers. These deposits are young sediments with high water contents and low plasticity. Such soils can easily be softened

once disturbed or liquefied when subjected to steep hydraulic gradients. Figure 3 shows the soil profile summarized using numbers of boreholes collected before and after the failure event (Ho et al, 2005). Soil properties adopted in designs are listed in Table 2. Ground water table is 1 to 3m below the ground surface. On account of the formation of subsoils as well as special site location as shown in Figure 2, ingression of sea water increased the high chloride content in groundwater. It has been suspected that the quality of diaphragm walls may deteriorate as a result of chloride attack. In many cases, jet grouting piles were installed to prevent guiding trench of diaphragm walls from collapsing; however, necking that reduced the sectional areas of diaphragm walls as well as sludge pockets inside the diaphragm walls that provided leakage paths are still frequently occurred.

Figure 2 Location of O1 station of KMRT.

Table 2 Basic soil properties adopted in design of diaphragm walls.

	Unit weight KN/m^3	C' kPa	Φ' degrees	Su kPa
SF	20.1	0	28	
CL	18.9	0	27	18
SM	20.2	0	32	
CL/SM	19.5	0	29	85
CL	19.5	0	28	113

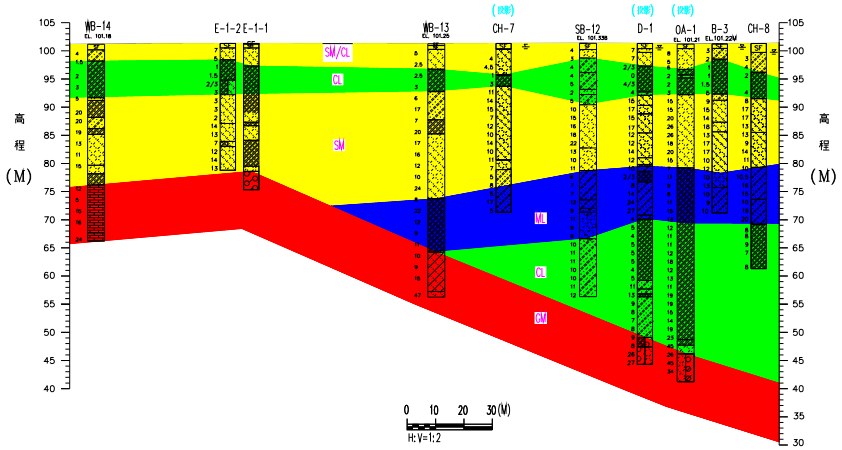

Figure 3 Soil profile of O1 station.

On 9 August 2004, a large sinkhole was quickly formed behind central wall panels on the south side of excavation area. It was caused by uncontrolled leakage of the diaphragm walls when excavation already reached a depth of 15m. This ground failure has resulted in served ground subsidence and building damages. Excavation work was stopped right after the incident. Countermeasures were soon taken to improve the watertightness of diaphragm walls. The 3D cross-hole RIP method was adopted to verify the effectiveness of the ground treatments, and to examine the condition of the defected diaphragm walls.

3.2 Test Plan

In this case, RIP tests were carried out in order to identify effectiveness of different ground treatments that were applied after the excavation failure, and to inspect the integrity of diaphragm walls. Diaphragm wall panels S72MF to S74MF were selected as the test wall panels because they were concluded by pumping test as the potential defected wall units. The test wall panels were first treated by Super Jet Grouting (JSG) columns. After the JSG treatment, Jet Grout Pile (CCP) was again added at panel connection to enhance watertightness. RIP tests were performed before and after the CCP treatment. Figure 4 shows the schematics of layouts of RIP testing in stereo and plane views.

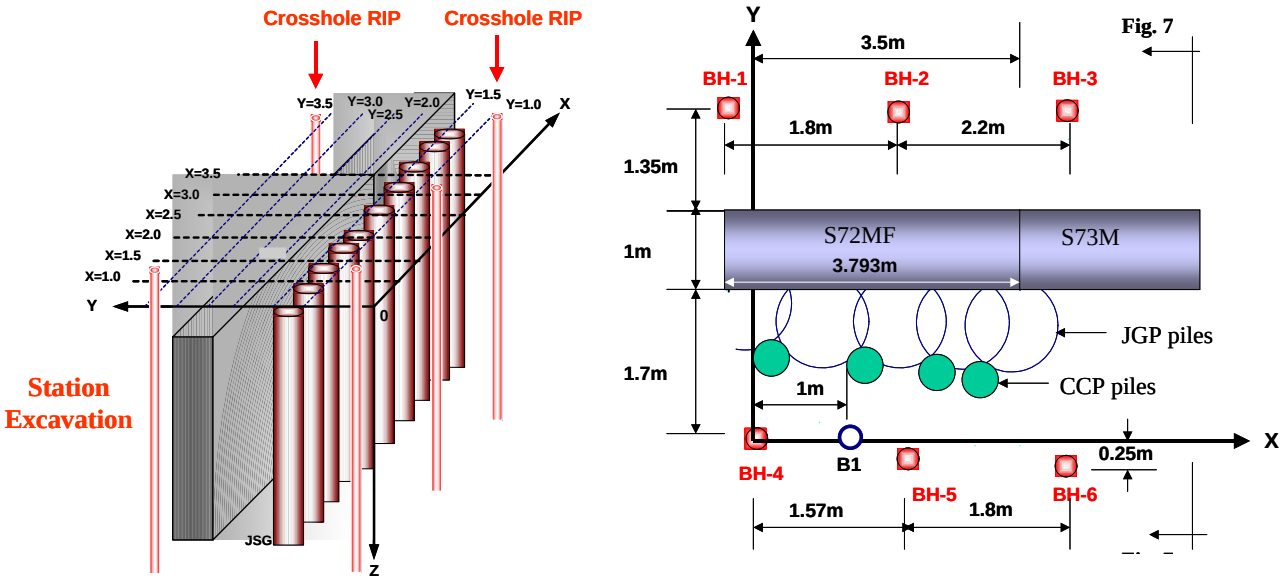

Figure 4 Stereo and plane view of RIP layouts.

To perform the RIP test, electrodes were installed on both sides of target wall units to a depth of 40m in order to cover full wall depth and treated ground. Total six boreholes were drilled to install electrodes so that a 4mX4mX40m column of ground condition could be "visualized". Potential electrodes were installed at 1m intervals in vertical direction. Electrical current was applied to the ground through two current electrodes and electrical fields were then generated within the probing area. The resulting voltage difference between two potential electrodes was measured to determine the resistance of the ground. Resistivity measurements were then input into commercial computer software to produce 2D and 3D imagines of resistivity distribution of tested ground (Hwang et al, 2007).

3.3 Test Results

Figure 5 shows the RIP image columns before the after the CCP treatment. The imagines were presented in colored contour. Cold colors, from green to deep blue, represent low resistivity materials like saturated sand or clay. On the contrary, warm colors, from yellow to red, represent high resistivity material such as grout or cemented soil. As shown in the figure, location and condition of diaphragm wall panels could be clearly identified in the 3D imagines. Before the CCP treatment, it could be seen that wall panel had a permeable fragment below the depth of GL-30.33m. It also found that CCP treatment had in fact improve the watertightness of the diaphragm wall with apparently increased volume coverage of high resistivity zone. The

permeable fragment that showed before CCP treatment was also found to be improved in the post-CCP treatment 3D imagine. The 3D RIP imagine columns were further sliced into 2D imagines at different locations to have closer views of the quality of wall panels and effectiveness of ground treatments. Figures 6 and 7 show the 2D imagine slices those were prepared parallel (XZ sections) and vertically crossing (YZ sections) the tested wall panels accordingly. As illustrated in Figure 4, XZ sections at location where Y=2.0 to 2.5 represent the body of the examined diaphragm wall panels. X=3.5 of YZ sections represent the joint between wall panels where leakage is most likely to occur. As shown in figure 6, the 2D RIP slices of Y=2m and Y=2.5 clearly indicate scattered permeable portions at depth of 30m before CCP treatment. Nevertheless, the post-treatment RIP slices show that the possible defects had effectively improved. Similar result could be also shown in Figure 7. The 2D slices of X=3.5 show distinguished difference of water permeability at adjacent location of panel joint. In summary, effectiveness of different ground treatments for diaphragm wall defect mitigation could be clearly verified through the 3D RIP method. Test results show that the inspected diaphragm wall units had a possible sludge pocket below the depth of GL-30.33m that might lead to potential leakage. Test results also indicate that CCP method had better performance in improving watertightness and ground voids of treated ground than JSG method. However, this outcome might be a consequence of accumulated grouting.

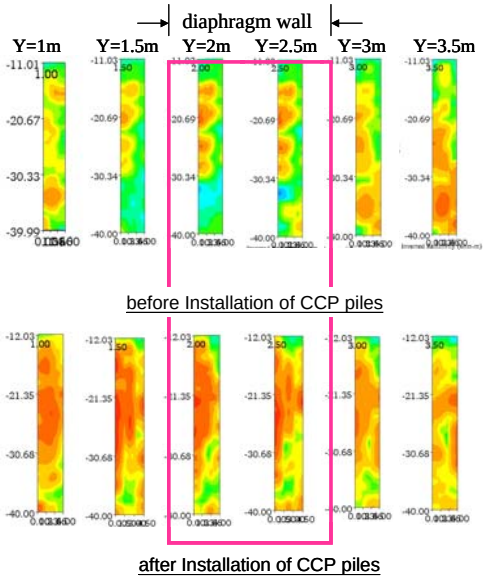

Figure 6 RIP imagine slices in YZ direction.

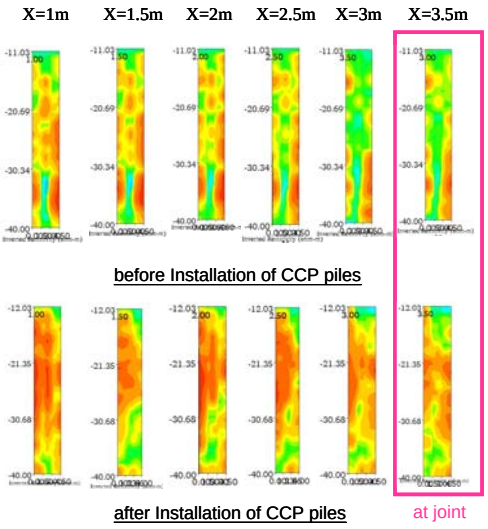

Figure 7 RIP imagine slices in XZ direction.

4 CASE STUDY II

4.1 Site Information

The corridor connecting the up-line and down-line subway tunnels between O7 and O8 stations of KMRT had collapsed during excavation on December 4th, 2005. The corridor was constructed by means of the NATM method. A vertical shaft 3.3m in diameter was designed to provide a sump for water collection in the middle of the corridor. The accident happened when the shaft excavation reached a depth of 4.95m from the floor of the corridor, at the very last stage of the excavation. The collapse was followed by steadily increased outflow of mud water. This breakage led to undermining the already built-up tunnels, accompanied by an inflow of soil and water from the rips opened at the junction on the ceiling between the corridor and tunnel. This breakage culminated eventually in a large scale collapse of the tunnel structure involving formation of two cave-ins on the ground surface (Ishihara & Lee, 2008). Figure 8 shows the location of the collapse and the feature of the cave-in on the ground surface. The cross section and side views of the tunnel are shown in Figure 9. It is to be noted that there was an underground roadway called Chung Cheng underpath just above the subway tunnel (Ishihara & Lee, 2008).

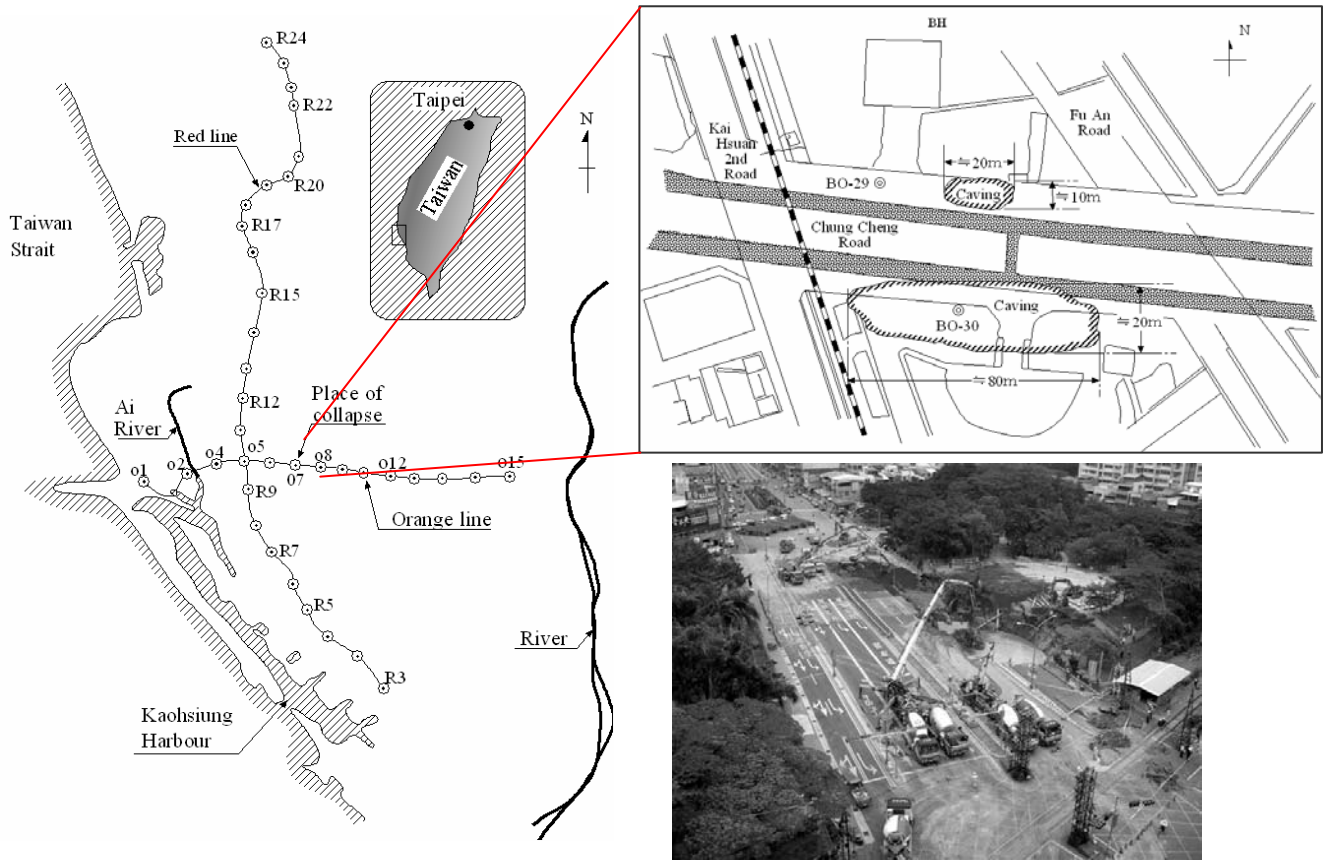

Figure 8 Location of the collapse and the feature of the cave-in on the ground surface (after Ishihara & Lee, 2008).

Soil condition of the studied case is comprised predominantly of silty sand deposit with occasional layers of low-plasticity clay to a depth of 40m. Figure 10 shows the typical soil profile at the location of collapse. The blow count, N-value, is shown to increase with depth and to have a value of 20 to 30 at the depth where the sump for water collection was excavated (Ishihara & Lee, 2008).

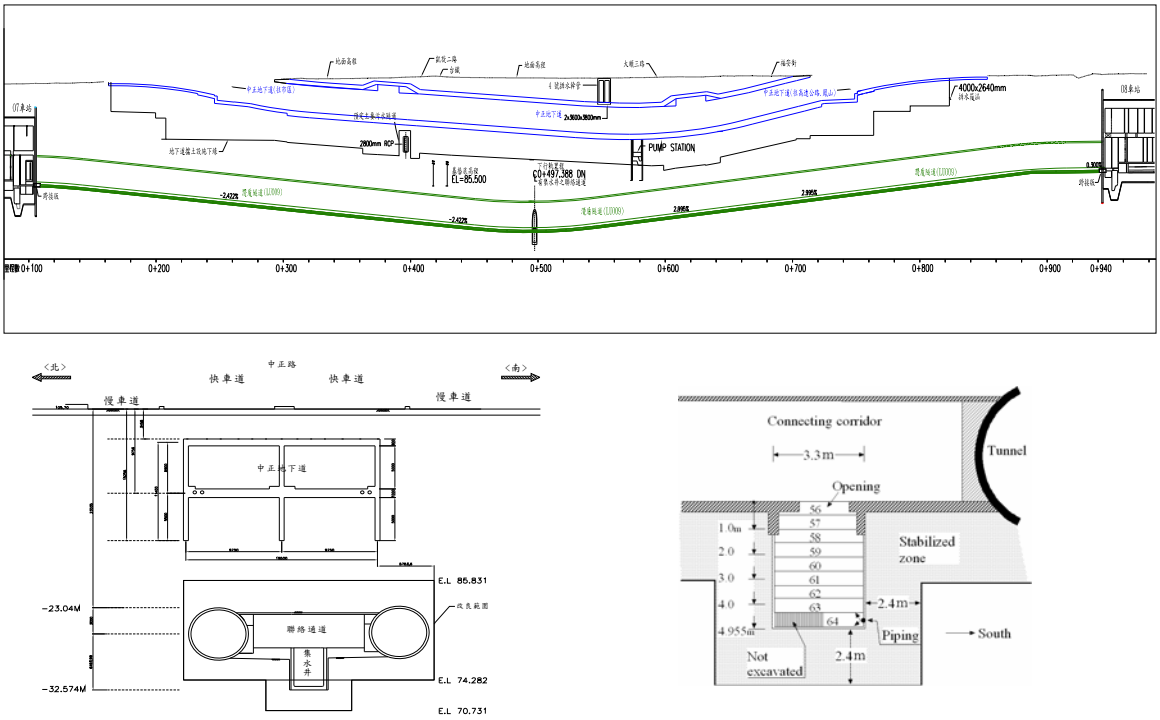

Figure 9 Cross section and side views of the collapsed tunnel site (after TCRI, 2006, Ishihara and Lee, 2008).

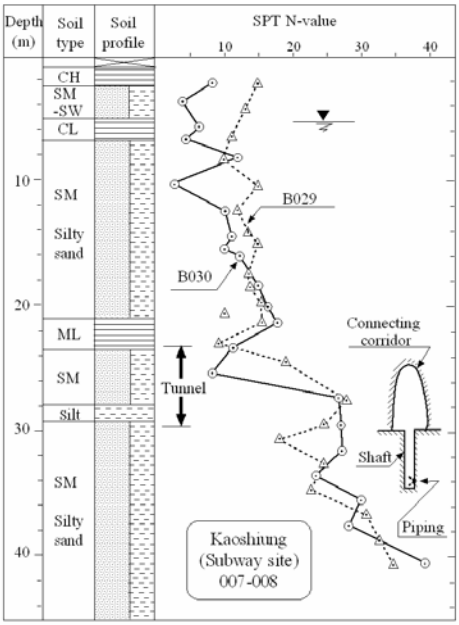

Figure 10 Soil profile at the site of collapse (Ishihara & Lee, 2008).

4.2 Test Plan

Right after the accident, surface 2D RIP testing was conducted to probe ground condition, and to check the effectiveness of remediation grouting. Figure 11 shows the layout of the 2D RIP testing. As depicted in Figure 11, six survey lines in north-south direction and one in east-west direction were installed in an attempt to cover the damaged area; and hopefully to identify different soil conditions and underground structures. The corridor was surrounded by grout material which was installed to stabilize the ground prior to excavation. Large numbers of sand bags and backfill material were dumped into the surface sinkholes to stabilize the disturbed ground after the event. Ground conditions was fairly complicated when the 2D RIP survey was conducted.

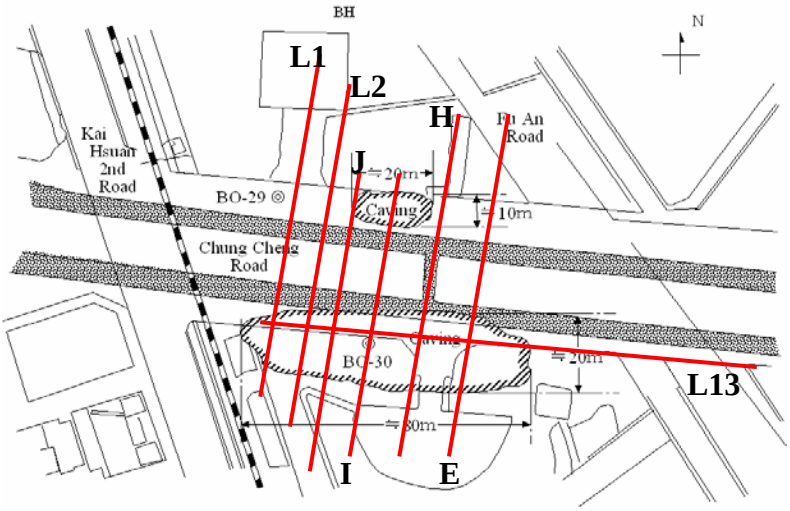

Figure 11 2D RIP layout of the studied site.

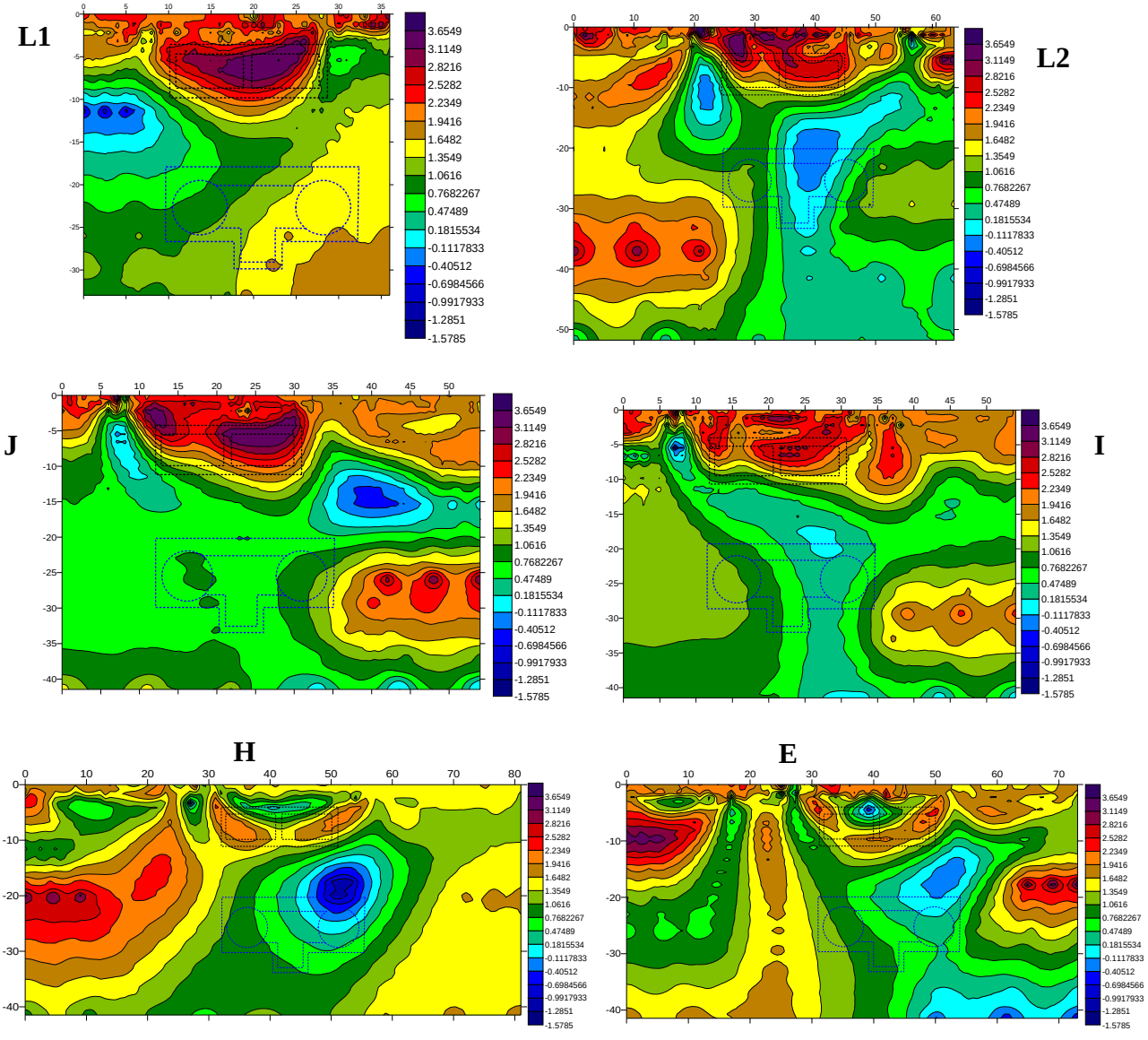

Figure 12 2D RIP results of survey lines in north-south direction.

4.3 Test Results

Figure 12 shows the results of 2D RIP in cross sectional profiles. Similar to the display mode of 3D RIP imagines presented in previous case study, the 2D RIP imagines were presented in colored contour. Cold colors, from green to deep blue, represent low resistivity materials as the disturbed ground with larger volume of ground water content. On the contrary, warm colors, from yellow to red and brown, represent high resistivity material such as grout materials or cemented backfill. Inverse analysis of the 2D RIP is basically similar to reflection and refraction laws of wave propagation. Underground structures shown in imagines of 2D RIP tend to be distorted from rectangular shapes into upward shell shapes. As depicted in Figure 12, despite the imagine distortion, area in between the underground carpass and the subway corridor were identified as in seriously disturbed condition. Moreover, distribution of the weak ground also indicates that both surface sinkholes were extended from 30m below ground surface where the subway tunnels located as results of deep soil piping. At locations of Line L2 and Line E, which are the east and west boundaries of the soil improvement block of the damaged corridor, soil beneath the subway tunnels was also found to be severely agitated by the piping failures. This observation implied that the subway tunnels outside the grouted area might subside and resulted in dislocations of tunnel ring segments. Imagines shown in Figure 12 also indicate that immediate remediation grout treatments have effectively reached both sides of the corridor as displayed in warm color. Figure 13 shows the 2D RIP imagine of survey line L13. Imagine shown in this figure has a good agreement to those obtained in cross sectional views. Longitudinal scale of the weak ground were further identified by means of this imagine. Effectiveness of immediate remediation grout treatments at east and west end of sinkholes were also verified in this imagine profile.

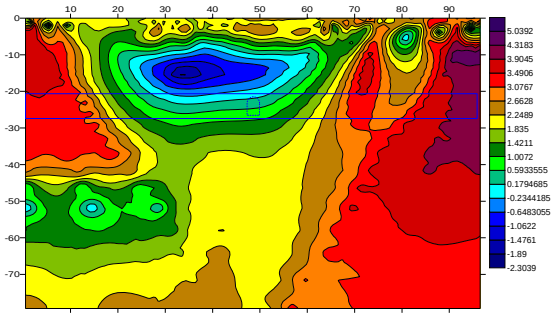

Figure 13 2D RIP imagine of survey line L13.

4.4 Describing the Failure

2D RIP results presented above was the most important information that provided visual imagines of the failed ground. Figure 14 shows the possible failure schema predicted based on the RIP results and other forensic investigation works (Ishihara and Lee, 2008). As shown in the figure, after triggering the piping, the blackish mud water continued to come out in the sump with increasing volume. It is believed that the mud water flowed into the sump from the bottom. This assumption would hold true in the light of the fact that the zone stabilized by the jet grouting could not so easily broken down in the horizontal direction, and a weak zone might have existed in the form of vertical pipe. The aggressive piping extended from the bottom of the sump had resulted in underscouring of the soil below the corridor and tunnel segments, and had caused the corridor block and tunnel lining segments to subside and possibly breakdown as shown in Figure 14. Mud water then started to cascade from the ripped joints of ring lining segments into the tunnels. Because large amount of debris continuously flooded into the tunnels, the fall-off of the soil had spread upward form the depth of the corridor and the tunnels up to ground surface, and had created two large sinkholes on the surface.

In an effort to validate the scale of the damaged tunnel portion, borehole probing was also conducted at the same time when 2D RIP survey was performed. Figure 15 shows the results of the borehole probing. It has good agreement to the 2D RIP results of survey lines L2, E, and L13 shown previously. Tunnel lining segments outside the corridor block had subsided seriously as a result of sever soil collapse underneath.

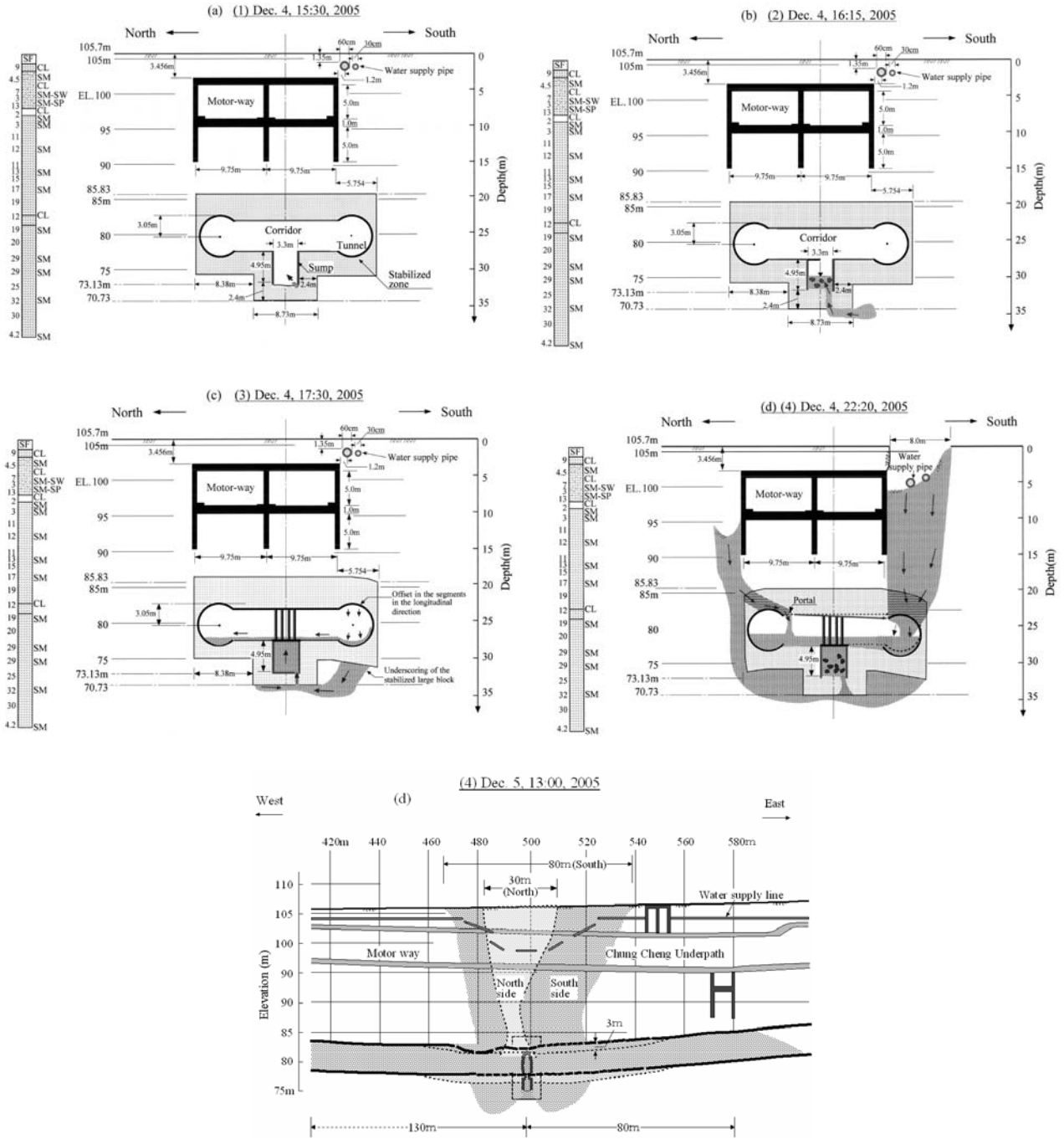

Figure 14 Possible failure schema of the accident based on the RIP results (after Ishihara and Lee, 2008).

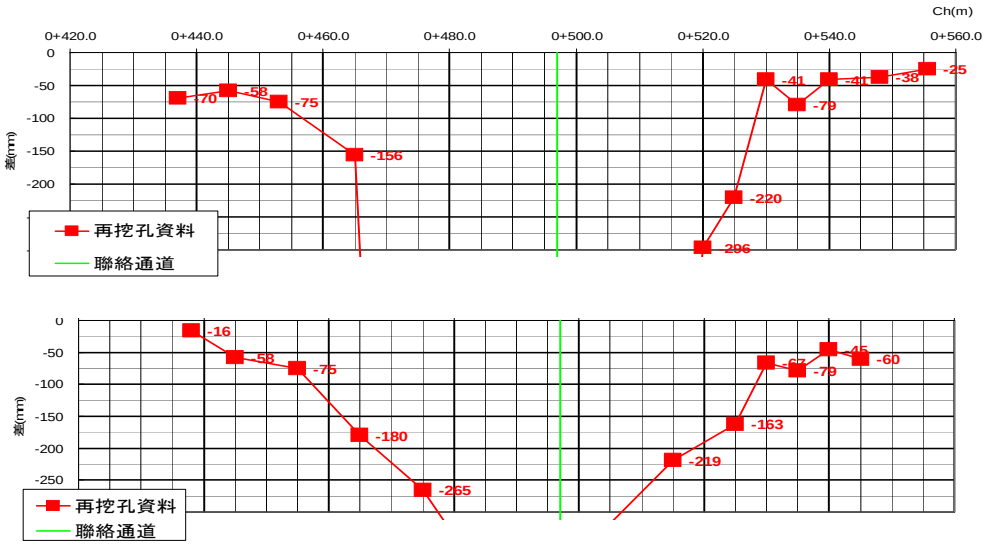

Figure 15 borehole probing result for settlement of damaged tunnel.

5 CONCLUSIONS

Both 2D and 3D crosshole RIP technologies were concluded to be capable of identifying various ground conditions and performance of underground structures. Promising results and applications presented in this paper prove that RIP technology could be adapted in underground constructions with adequate planning and design. It has great advantages of providing visual imagines and decoding different objects than present soil exploration methods used for underground construction. Studied cases presented in this paper is hoped to promote applications of advanced geophysics technologies such as RIP method in engineering practice, and to provide alternative resolutions to similar geotechnical problems.

ACKNOWLEDGEMENTS

The authors are grateful to Kaohsiung Mass Rapid Transit Company, Da-Cin/Shimizu Joint Venture, and Maeda Company for the authorization to publish the data presented herein.

REFERENCES

Advanced Geosciences, Inc.(2006) “Instruction mamual of EarthImager 3D ver. 1.2.7”

Chen, C.H. and Lee, W. (2007), “Forensic Investigation of a Disastrous Failure at the Arrival End of a Station of the Kaohsiung Mass Rapid Transit System”, Proceeding of the International Conference on Forensic Engineering, Mumbai, India

DeGroot-Hedlin, C. and Constable, S., (1990).”Occam’s inversion to generate smooth, two-dimensional models from magnetotelluric data,” Geophysics 55, pp.1613-1624.

Ho, S. K., Chou, C. C., Chen, D., Chung, L-J, Liao, Z-B, Chen, Y-Y (2007), The pumping tests at KMRT O1 Station, Proc., 2007 Cross-Strait Symposium on Geotechnical Engineering, April 15~17 (in Chinese)

Hwang, N.H., Ishihara, K. and Lee, W. (2007), “Forensic studies for failure at an underground station”, Proceedings of the Thirteenth Asian Regional Conference on Soil Mechanics and Geotechnical Engineering, Calcutta, India.

Ishihara, K. and Lee W. F. (2008), “Forensic diagnosis for site-specific ground conditions in deep excavations of subway constructions,” *Geotechnical and Geophysical Site Characterization*, Proceeding of the 3rd International Conference on Site Characterization, Taipei, Taiwan.

TCRI (2006). “Applications of Resistively Image Profiling Technique for Evaluating Integrity of Diaphragm Walls and Effectiveness of Ground Treatment”, Taiwan Construction Research Institute. (in Chinese)

Loke M. H. (2001), “Tuorial： 2-D and 3-D electrical imaging surveys”

Load Tests for Jet Grouting at Macau

T.M.H. Lok, H.S. Leong, Y.L. Wong, I.C. Chan & W.M. Yan
Macau Association for Geotechnical Engineering, Macau SAR, China

ABSTRACT

A construction project involved ground improvement for a mat foundation with high pressure jet grouting is described. The mat foundation is about 1700 m^2 in area. The soil profile consists of 12 m of soft soil below the ground surface, which was improved by jet grout piles at 1.5 m spacing. There were two tests on individual jet grout piles and two plate load tests on the composite foundation. Observations of the foundation settlements during and after construction showed satisfactory performance of the ground improvement.

1 INTRODUCTION

This paper describes a project of ground improvement for a mat foundation by jet grouting at Macau (Tai Ah Co., 2006). The project is for the extension of police station which covers an area of about 1700 m^2, approximately in L shape with maximum dimension of about 39m × 70m. As shown in Figure 1, the center to center spacing of jet grout columns is 150 cm. There are about 780 jet grout columns with depth from GL-1.1 to 12.0 m and diameter of about 30 cm.

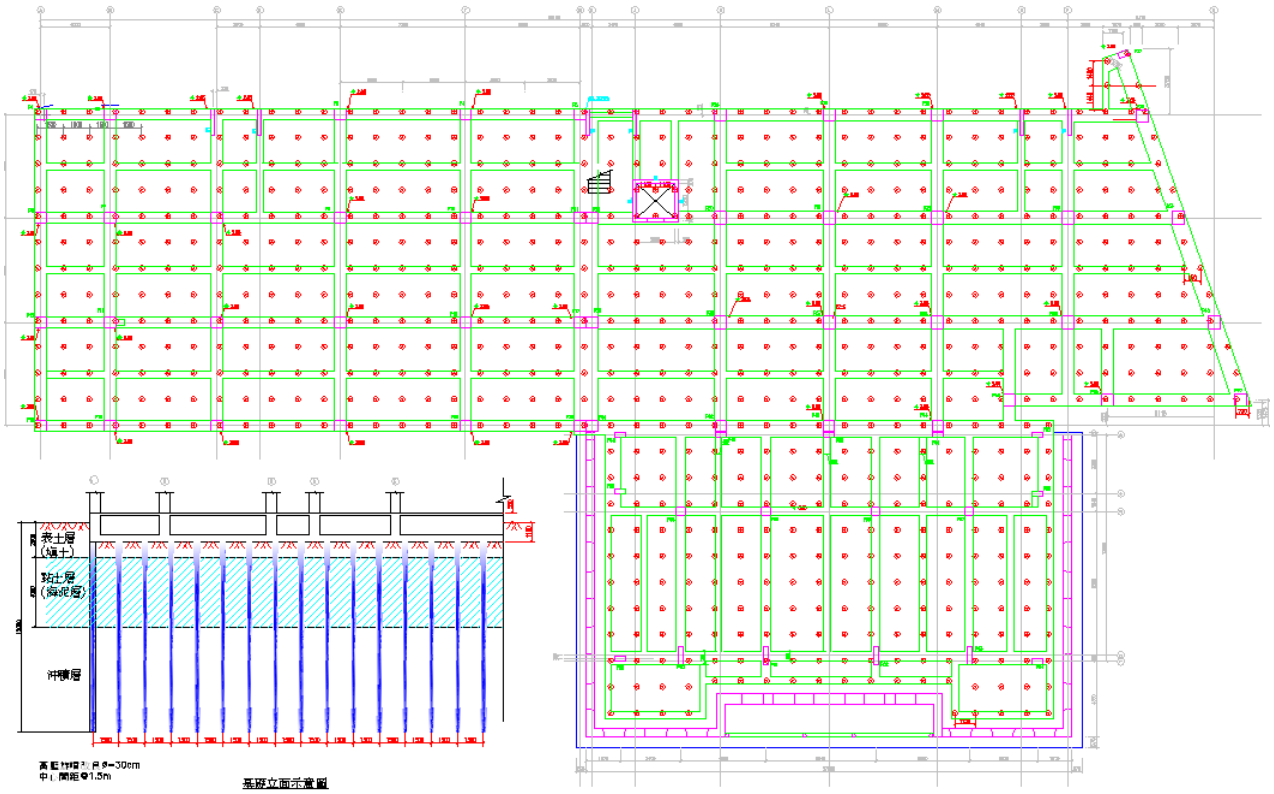

Figure 1: Plan of jet grouting (jet grout piles shown in dots)

2 SITE INVESTIGATION

According to the site investigation, a layer of fill of about 2 m is found at the ground surface, underlain by soft clay followed by alluvium and decomposed soils. The variation of SPT N values is shown in Figure 2. N values are generally less than 12 from depth of 0 to 12 m, where jet grouting was applied. Below 12 m, N

values are generally over 25 where soil improvement was not planned. Average ground water table is at about GL-2.0 m.

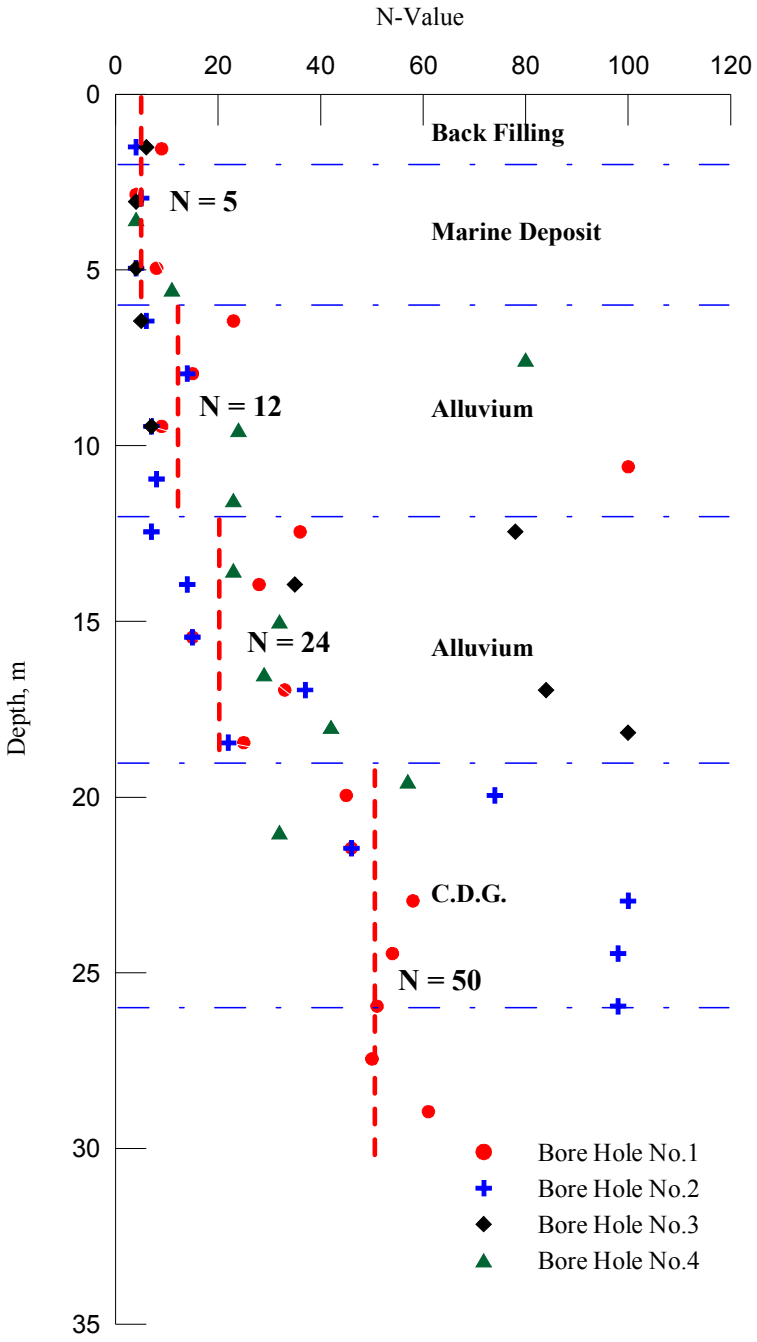

Figure 2: SPT N values vs. depth

Table 1 shows the simplified soil parameters for design purpose. Undrained shear strength was determined from consolidated undrained triaxial tests. Undrained shear strength (S_u) was correlated with preconsolidation pressure (p_c), and the Young modulus was estimated based on Bjerrum (1972), where $E_s = 1000S_u$ for cohesive soils, or as $E_s = 4000 \times \log N$ for cohesionless soils.

Table 1 Simplified soil parameters for design

Soil Layer	Description	Depth (m)	γ_t (kN/m^3)	SPT (N_{avg})	p_c (kN/m^2)	S_u (kN/m^2)	E_s (kN/m^2)
Back filling	silty sand	2.0	19.6	5	—	—	29,430
Marine deposit	sandy silty clay	6.0	16.7	5	92.2	106.0	106,050
Alluvium	fine to coarse clayey sand /sand Silt	12.0	19.8	12	136.0	156.4	156,370
Alluvium	medium to coarse clayey sand /sand silt	19.0	19.6	24	200.3	230.3	230,340
Completely Discomposed Granite (C.D.G)	fine to medium sand /sandy silt	26.0	20.6	>50	267.0	307.1	307,050

3 FIELD LOADING TESTS

3.1 Jet grout pile tests

There are two tests performed on individual jet grout piles, No. N25 and No. Q22, as shown in Figure 3. Loading was applied with a hydraulic jack under a weight platform (kentledge). Three cycles of loading were applied up to 70, 120 and 165kN, corresponding to 100%, 170%, and 235% of the design load. At each loading stage, the load was maintained until the pile head settlement rate was less than 0.004 mm/min. The maximum loading was maintained for 24 hours for studying long term settlement. The load vs. settlement curves are shown in Figure 4a and 4b.

As shown in Figure 4a, for pile No. N25, the maximum pile head settlement was 3.17 mm under the maximum load of 165 kN including the 0.7 mm due to creeping from 24 hours of maintained load, while for pile No. Q22, the maximum pile head settlement was 5.88 mm under the maximum load of 165 kN including the 0.9 mm due to creeping from 24 hours of maintained load as shown in Figure 4b. The settlements observed for the individual jet grout piles are relatively small compared with those from the plate load tests as described below, implying probably the loading for the jet grout piles were well below the ultimate condition.

3.2 Plate load tests

There are two plate load tests performed at the locations shown in Figure 3. The plates were made of 30 cm thick reinforced concrete with an area of 3 m by 3 m. The pressure vs. settlement curves are shown in Figure 5a and 5b. The design load of the foundation was estimated to be 86.6 kPa, 2.5 times of which was planned as the applied loading, for plate load tests. However, as shown in Figure 5a for test A, settlement quickly increased upon 139 kPa, and the test was terminated. This was probably due to adverse site condition after heavy rainstorm on the testing day. For test B, the maximum load of 224 kPa was achieved before unloading as shown in Figure 5b. The corresponding average settlement at maximum load was about 16 mm.

Also shown in Figure 5a and 5b are the reading from different dial gauges located at the four corners of the plate. As the applied loading approached the maximum load, the readings from different dial gauges started to deviate from each other, implying possible rotational failure of the foundation.

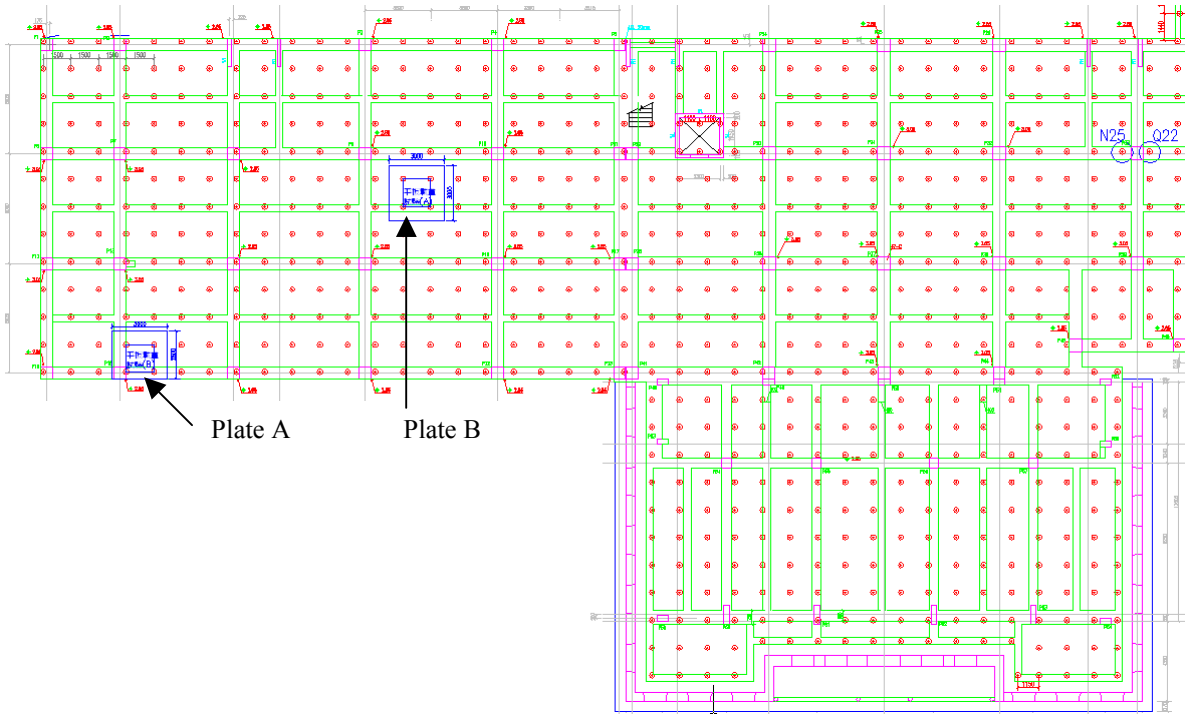

Figure 3: Location of jet grout pile and plate load tests

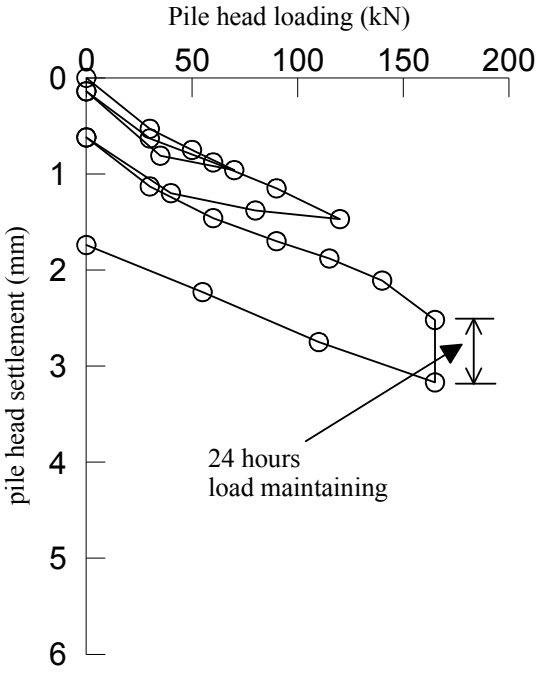

Figure 4a: Load test curve for jet grout pile No. N25

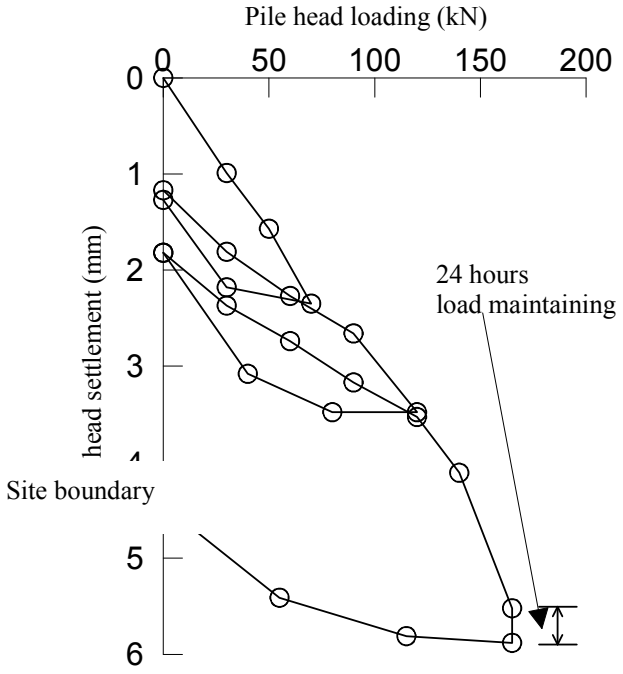

Figure 4b: Load test curve for jet grout pile No. Q22

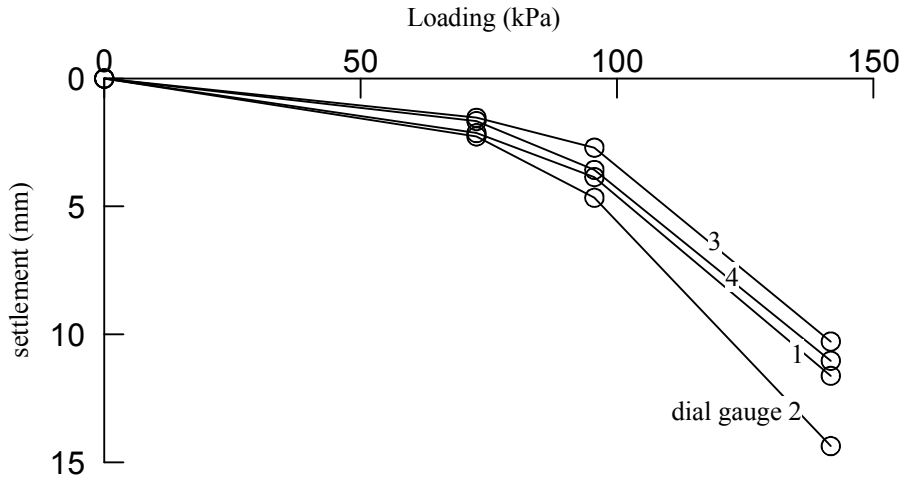

Figure 5a: Load settlement curve for plate load test A

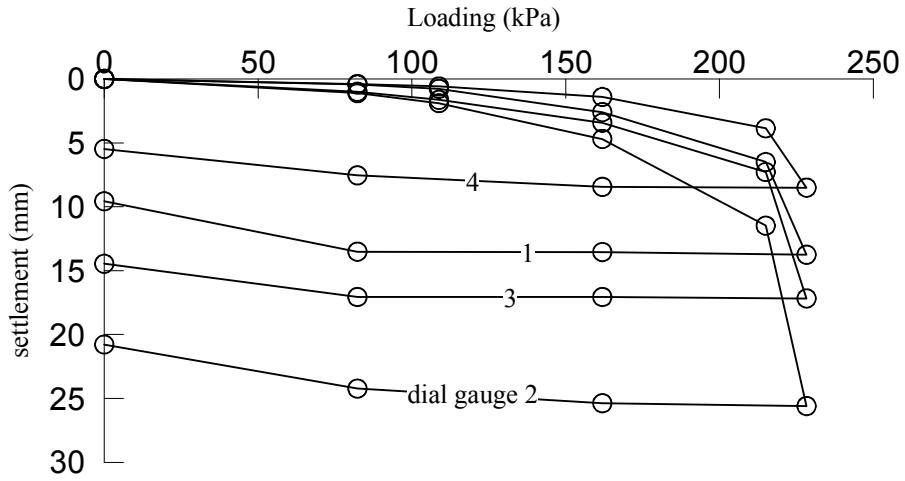

Figure 5b: Load settlement curve for plate load test B

4 ESTIMATED AND OBSERVED SETTLEMENT

The settlement was estimated by considering elastic settlement and consolidation settlement for the treated and untreated soil layers, respectively. Young's modulus of the jet grout treated soil was estimated to be 144,800 kN/m^2, based on the area ratio of the jet grout to the untreated soil. The following properties were obtained for the alluvium and the weathered soil:

Table 2 Consolidation properties of untreated soils

Soil	e_o	C_c	C_r
Alluvium	0.63	0.0975	0.0139
Weathered soil	0.54	0.030	0.0043

The distributed loading from the superstructure is shown in Figure 6. Most of the foundation will be loaded with 63.8 kPa (6.5 t/m^2) except the lower rectangular part will be loaded with 25.5 kPa (2.6 t/m^2). The estimated settlements of the mat foundation are within 1.4 cm as shown is Figure 7. A monitoring program of the settlement after the completion of the superstructure was carried out for a period of about 8 months. As shown in Figure 8a, 8b and 8c; the observed settlement at the end of the monitoring were in the range of 5 to 8 mm, which were generally less than the predicted final settlement except at a few locations.

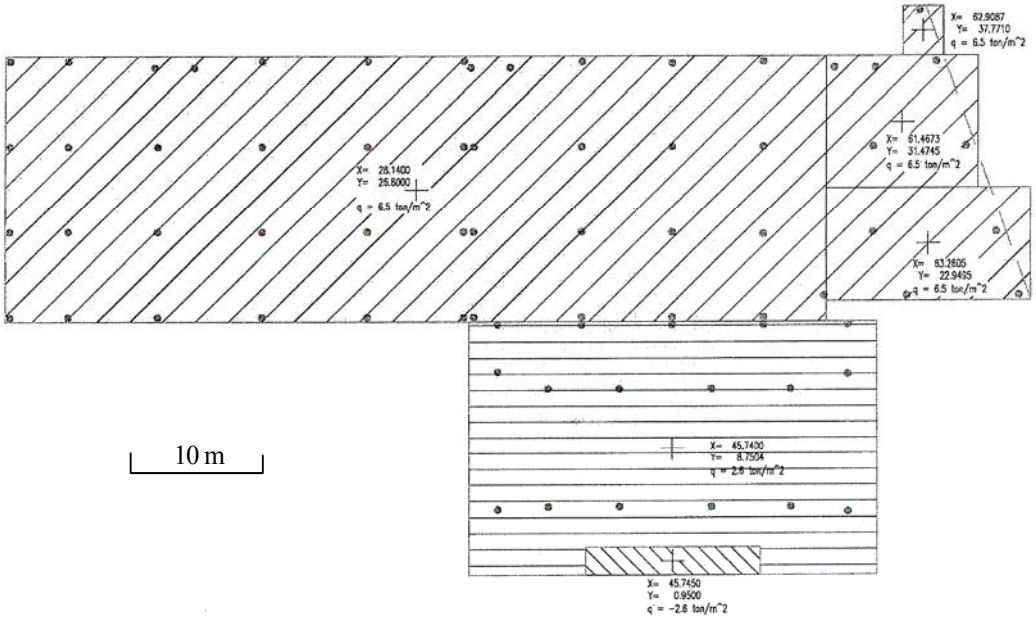

Figure 6: Distributed load on mat foundation

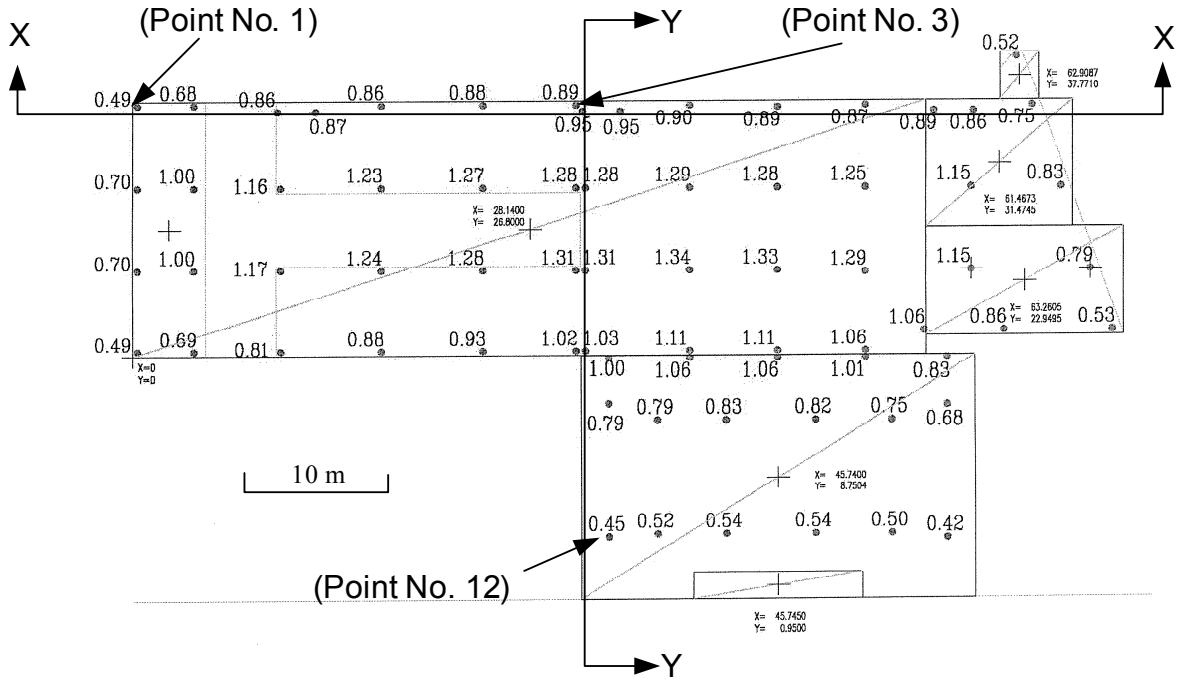

Figure 7: Estimated settlement for the mat foundation (values in cm)

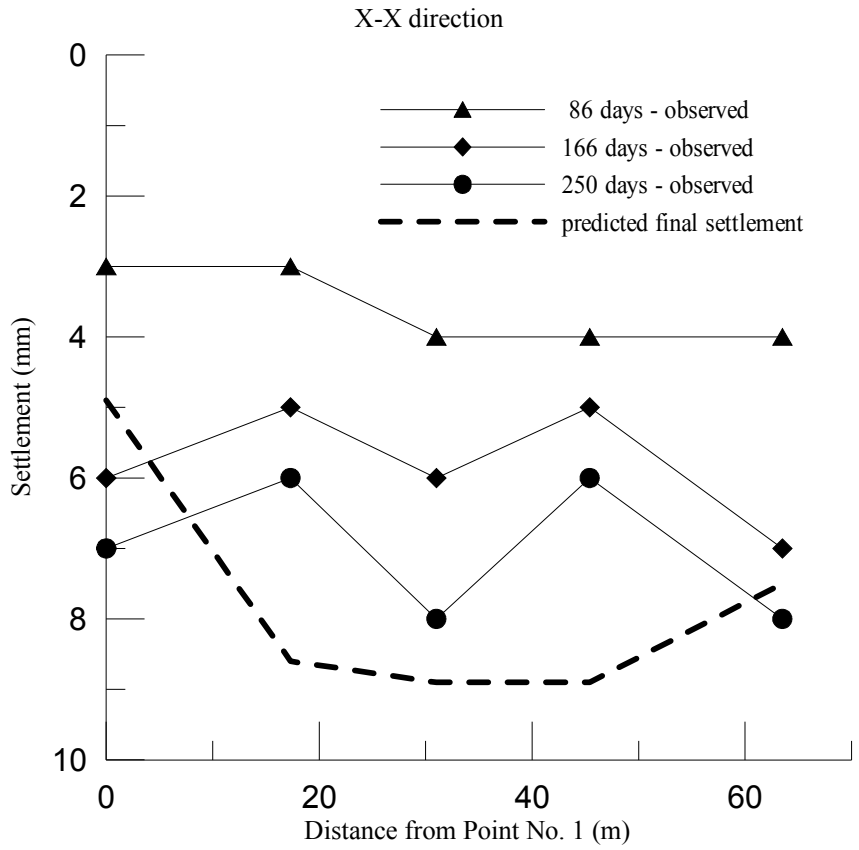

Figure 8a: Settlement profile along X-X section

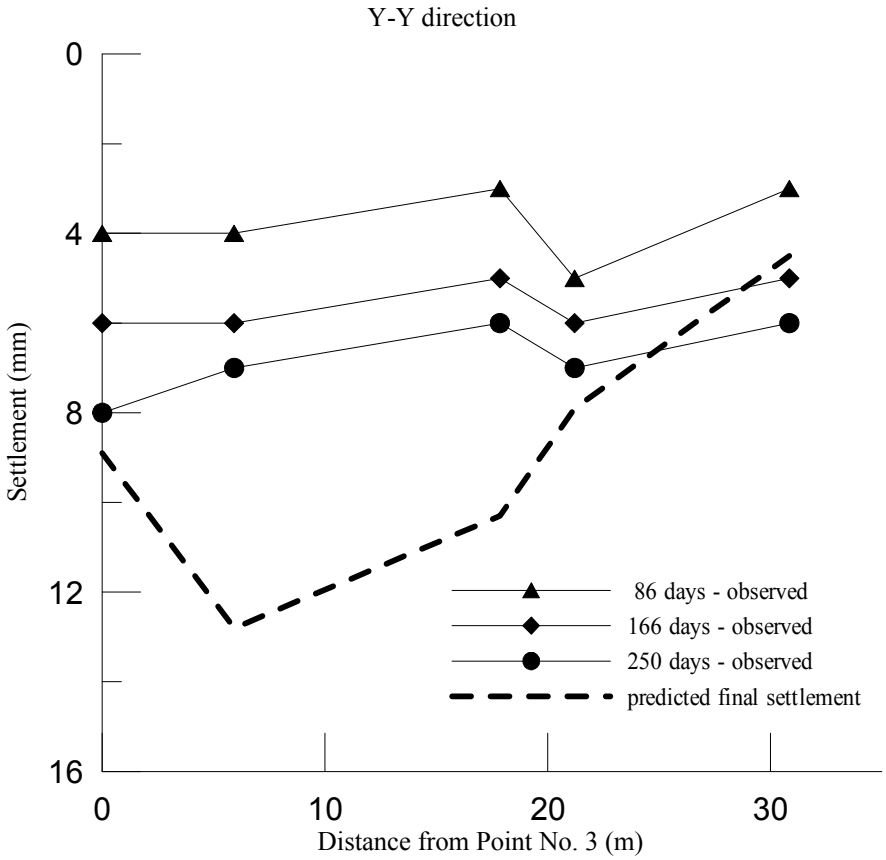

Figure 8b: Settlement profile along Y-Y section

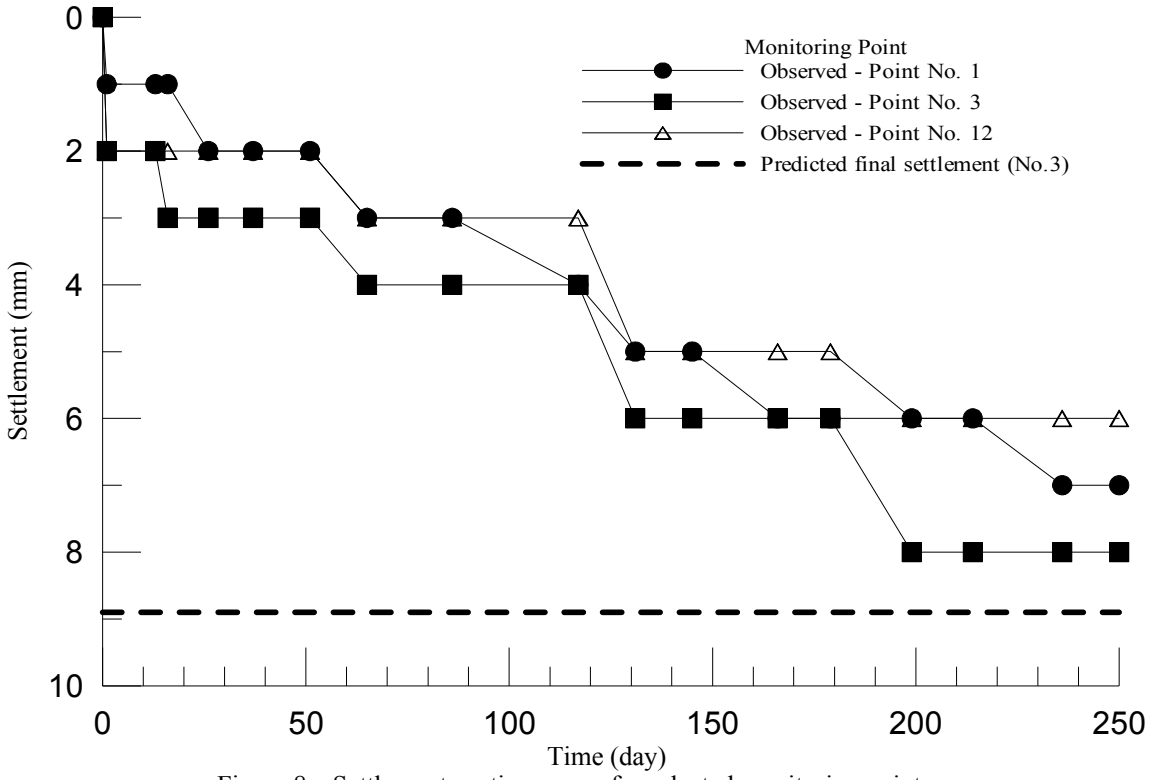

Figure 8c: Settlement vs. time curve for selected monitoring points

5 CONCLUDING REMARKS

A case history of load tests for jet grouting at Macau was presented. The project involves ground improvement of an area of about 1700 m^2. Two tests on individual jet grout piles and two plate load tests on the composite foundation were carried out according to the local requirements. The monitoring of the settlement during construction of the superstructure indicated that the improved foundation performed satisfactory.

As driven piles are commonly recommended for such scale of construction projects in Macau, jet grouting provides an economical alternative. The case history presented here is just one of the few cases using ground improvement in Macau. Further utilization and improvement of the technique in Macau is foreseen for the future.

ACKNOWLEDGEMENTS

The information of this paper is provided by Tai Ah Construction and LECM. The assistance of relevant personnel is greatly appreciated. The responsibility of the correctness of the presentation, however, is borne by the authors.

REFERENCES

Bjerrum, L. (1972) "Embankments on Soft Ground," 5th PSC, ASCE, vol. 2, pp. 1-54.

Tai Ah Construction (2006) "Police Station 2 Extension: Ground Improvement for Foundation - Construction Plan for High Pressure Jet Grouting." (in Chinese)

Asphalt Heaving at the Hong Kong International Airport – Investigation and Design of Remedial Works

A.R. Pickles & S.W. Lee
Geotechnical Consulting Group (Asia) Limited, Hong Kong
D.C.H. Li
Airport Authority, Hong Kong

ABSTRACT

The second (northern) runway at the new Hong Kong International Airport began operating in July 1999. Shortly after this runway was opened, during periods of very wet weather the asphalt wearing course on the shoulders of the pavements was observed to occasionally heave in the form of domes with various sizes. Pavement damage in the form of cracking and localised bulging of the wearing course was observed at various locations, particularly on the taxiway shoulders. In the later part of the year a heave dome occurred at one of the rapid exit taxiways and caused the closure of the captioned taxiway for an emergency repair. The heaving was found to be associated with air being displaced by the rising water level in the rock fill below the runway caused by tidal effects. The air pressure developed beneath the asphalt was found to significantly increase when the surface of the asphalt and the adjacent ground was very wet. This paper describes the investigation carried out to identify the cause of the heaving and to define the extent of the problem area. The results of the investigation were used to predict the potential for future heaving and the particular conditions required to cause heaving. The paper also describes the technical background to the design of the temporary measures taken to mitigate the problem as well as the development and implementation of a long-term solution.

1 BACKGROUND

1.1 Pavement structures

The runways and taxiways of the Hong Kong International Airport (HKIA) are constructed on reclaimed land. To cater for the ground settlement, a flexible pavement design was adopted. The flexible pavement layers comprise a Marshall Asphalt Wearing Course and a Base Course (MAWC & MABC) on a compacted Crushed Aggregate Base Course (CABC) and a Crushed Aggregates Sub-Base (CASB). The total thickness of the MAWC and MABC varies from 130 mm on the runway to 50 mm on the shoulders of the runway and taxiways. A typical cross section of the runway / taxiway pavement is shown on Figure 1.

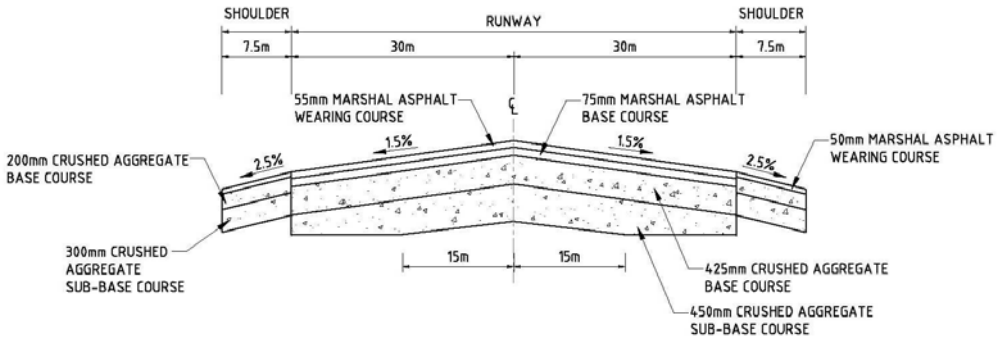

Figure 1: Cross section of runway/taxiway pavement

1.2 Subgrade and fill

Prior to the reclamation, the soft marine clay, which blankets most of the seabed, was removed by dredging. The reclamation in the area of the runway and taxiways is comprised of a 2-4 m thick marine sand capping layer overlying 13 m rock fill which in turn is underlain by 5-10 m of marine sand to dredge level. A horizontal geotextile filter fabric was installed between the marine capping sand and rock fill to prevent the wash out of the capping sand into the underlying rock fill. The subgrade sand fill below the CASB was compacted to 95% to 98% of maximum dry density.

2 PROBLEM OF PAVEMENT HEAVING

Pavement damage associated with the heave of the wearing course was first observed on the taxiway shoulders within the North Runway Area between July and September 1999. At some of these locations the wearing course was observed to be temporarily lifted away from the underlying crushed aggregate base course forming a dome with height of up to 400 mm and a diameter up to approximately 10 m, see Figure 2. At the remaining locations the damage was observed in the form of cracking and localised bulging of the wearing course. Detailed investigations demonstrated that the cracking and bulging was caused when a heave dome subsided back onto the underlying aggregate base course.

Figure 2: Heaving of pavement at the taxiway shoulder

It was noticed that the heaving phenomena occurred only after prolonged heavy rainfall during the summer months. Air bubbles were also observed at the locations of the damaged pavement surfaces during the heaving occurrence. The duration of each heaving occurrence was also very short, about one or two hours, after which, the dome disappeared.

During the summer months of 2000, the heaving at the shoulder area continued. In 2001, the heaving problem extended to the aircraft traffic area at a taxiway. On 7 June 2001, after 5 days of heavy rainfall, an area of taxiway pavement at Rapid Exit Taxiway (RET) A5 heaved and fractured the pavement asphalt along a construction joint.

3 POTENTIAL CAUSE OF HEAVING

Following the initial heaving problem in 1999, a task force was set up to undertake a thorough investigation of the phenomena. The investigation included a review of the as-built drawings of the reclamation, construction and the underground utilities and correlation of heave occurrences with rainfall events, ambient temperature, tide level and sunshine hours. Leung et al. (2007) discuss the potential causes of the heave investigated by the task force.

The most obvious correlation of the heaving damage phenomenon was with rainfall but it was apparent that the rainfall acted as a trigger for the heave damage rather than being directly responsible. A detailed review of the tidal record indicated that all of the heaving incidents occurred during a rapidly rising "Spring" tide and after continuous heavy rainfall for a few days. Spring tides are associated with either a full moon or new moon and are the highest tides of the monthly cycle. A high tide is associated with a rapid rate of tide rise approximately 3 hours before the actual high tide.

The tidal water level varies between approximately 0.0 and 2.6 mPD and the ground level at the runway and taxiways is typically approximately 6.5 mPD. The heaving caused by direct tidal water force was ruled out and it was considered that the pavement heaving was caused by the build-up of air pressure underneath the pavement due to the rising tide and blockage of free air flow in the saturated capping sand layer and the wet asphalt. Under dry weather, a rising tide would push the air in the voids in the rock fill (30% by volume) below the geotextile up through the relatively permeable sand capping and this air would escape slowly through the pavement layers and asphalt or through the landscaped areas.

Calculations indicated that a pressure of only 1.2 kPa would lift a 50 mm asphalt layer such as either the asphalt on the shoulders on the runway and taxiways or potentially a 55 mm thick layer of MAWC which had debonded from the underlying MABC. A pressure of 3 kPa would lift the 130 mm full thickness asphalt pavement (MAWC and MABC).

4 MEASUREMENT OF AIR PRESSURE

In order to confirm the hypothesis that air pressure caused by a rising tide was the cause of the heave, a number of pressure sensors were installed close to the centreline of the runway and taxiways. The pressure sensors were small diameter vibrating wire piezometers, 120 mm long and 12 mm in diameter. The piezometers were inserted into small diameter holes drilled in the asphalt surfacing with their tip set at the level of the underside of the asphalt. The cables from the piezometers were laid across the pavement surface in 6 mm wide by 30 mm deep saw cut grooves backfilled with asphalt sealant. The cables were connected to dataloggers which were buried in waterproof boxes in the landscaped area directly adjacent to the pavements.

A typical pressure monitoring result over a three day period of dry weather is shown in Figure 3, which also shows the variation of tidal water level in the rockfill beneath the pavement. Figure 4 presents the same data but this time compares the air pressure beneath the asphalt with the rate of rise of tide. This figure shows that the maximum pressure occurs when the rate of rise of the tide is at its greatest, approximately 3 hours before high tide.

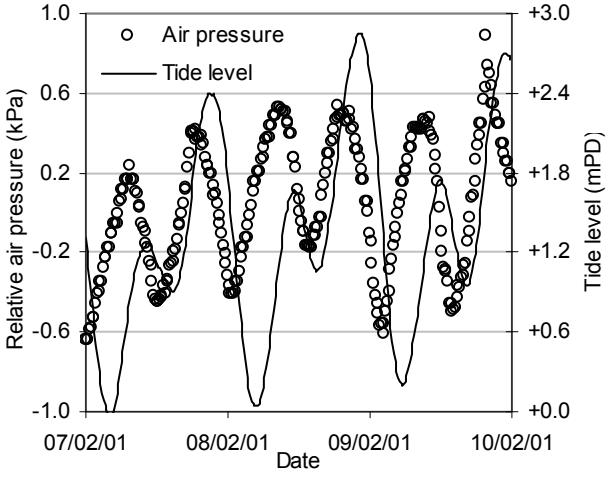

Figure 3: Measured air pressure and tide level

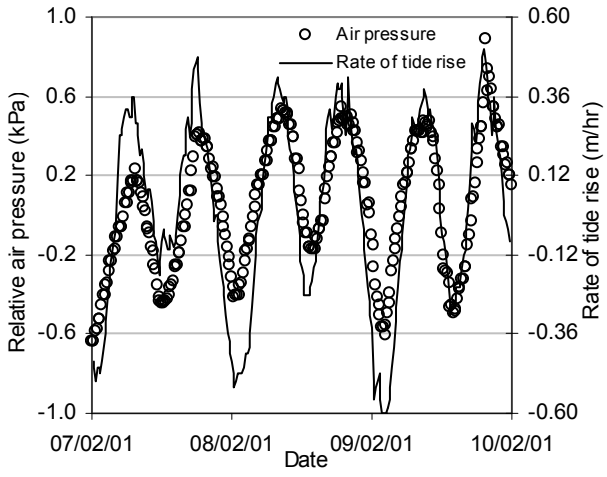

Figure 4: Measured air pressure and rate of tide rise

Subsequent monitoring of vibrating pressure gauges installed in the asphalt demonstrated that the peak pressure increased significantly during wet weather events. Figure 5 shows the pressure monitoring results from one of these pressure gauges during the 2002 wet season. The highest peak pressures were measured during wet weather which occurred around 11 June, 27 July and 10 August 2002.

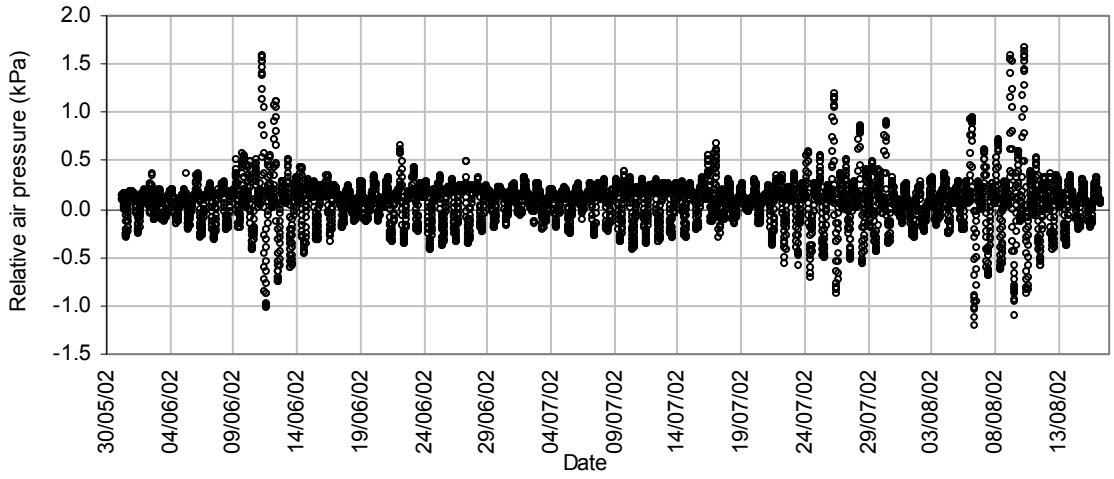

Figure 5: Measured air pressure during the 2002 wet season

The monitoring data confirmed that the rising tide was the most probable cause of the heave. The next problem was to define the extent of the runway and taxiways which was being affected by the pressure, requiring a measurement of the pressure at many locations.

It was considered that it might be possible to drill a small diameter hole through the asphalt and then insert a small pressure probe into the hole and temporarily seal the hole. A simple water filled manometer tube equipped with a rubber bung to seal the hole was constructed and a small number of holes were drilled through the asphalt. Figure 6 shows the manometer being used to measure the air pressure below the asphalt. During one of the regular overnight runway closures which coincided with a rapidly rising tide the system was tested and it was demonstrated that a reliable pressure measurement could be obtained within approximately 10 seconds.

Figure 6: Manometer measured air pressure beneath asphalt

Once it had been confirmed that this simple system worked, pressure monitoring holes were drilled at approximately 20 m centres along the length of the runway and taxiways. In total approximately 600 pressure monitoring holes were drilled in the asphalt surfacing

During a subsequent night closure, which coincided with a rapidly rising tide, four sets of monitoring equipment were used to measure the pressure at all 600 points during a 3 hour period. The exercise was repeated on two further occasions when a rapidly rising tide coincided with a night closure. In order to allow the data measured at different times and on different days to be compared, the data was normalised by adjusting the measured pressure by a factor which related to the measured rate of rise of tide and this could also be correlated with the pressure monitoring data measured using the vibrating wire piezometers.

The pressure data obtained through this process was used to zone the pavements into three pressure categories, high, medium and low, allowing remedial work to be prioritised and optimised. A plan showing the pressure zones on the runway and taxiways determined from the pressure monitoring and the pressure measured beneath the runway is shown in Figure 7.

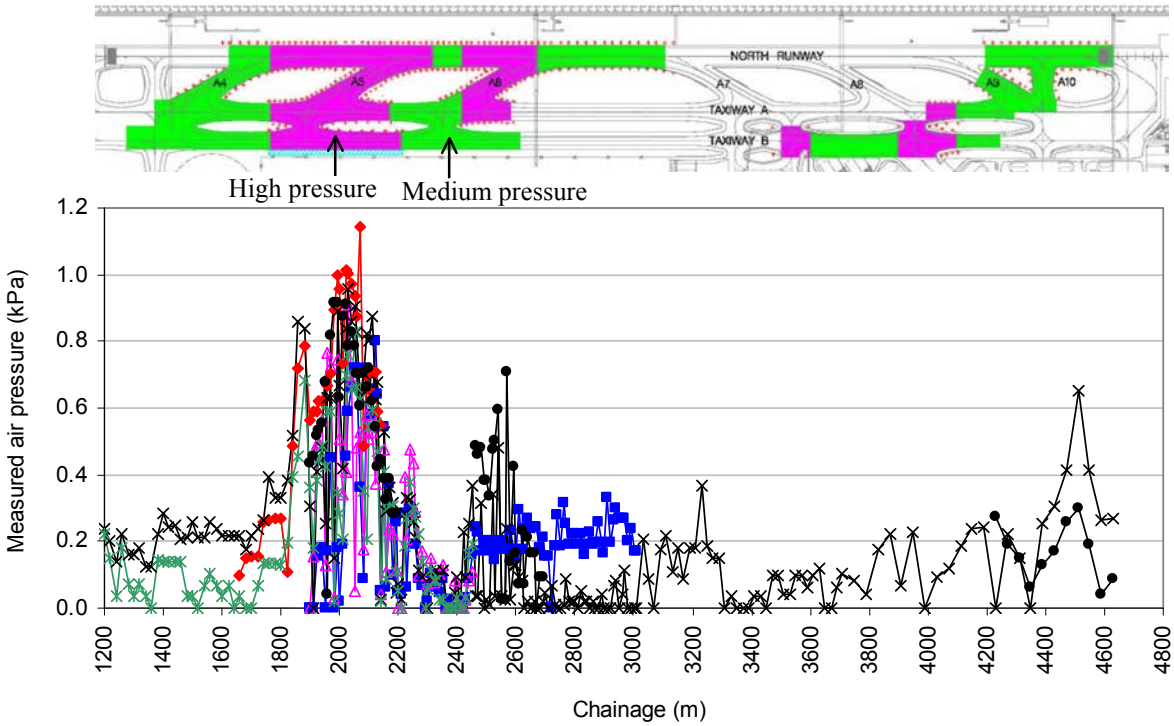

Figure 7: Measured air pressures along Northern Runway and taxiways

5 MEASURING THE AIR PERMEABILITY OF ASPHALT

It was apparent from the piezometer monitoring data that the rising tide caused an increase in the pressure below the asphalt and it was also apparent that the magnitude of this pressure was influenced by rainfall, although it was not obvious why the rainfall caused an increase in the pressure. At this time it was thought that the very dense asphalt used for airport pavements would be virtually impermeable to airflow but this was not consistent with the observed heaving and its link to rainfall. It was therefore decided to investigate the permeability of the asphalt to airflow.

A novel piece of apparatus was constructed to measure the permeability of the asphalt as illustrated in Figure 8. The apparatus consisted of a 200 mm diameter cylinder in which a cored sample of asphalt could be inserted and a seal formed around the perimeter of the sample using silicone sealant. The chamber below the sample could be pressurised to create a pressure difference across the asphalt sample, allowing the permeability to be measured. A pressure gauge connected to the lower chamber allowed the air pressure to be monitored.

The test routine adopted to determine the air permeability was similar to a falling head permeability test. The air pressure in the sealed chamber below the sample was raised to approximately 5 kPa and then allowed to fall as a result of leakage through the asphalt. Readings of air pressure against time were made until the air pressure in the chamber returned to atmospheric. Because the volume of the chamber below the sample was known, the change in air pressure could be equated to a volume flow rate in order to determine permeability.

Because the edge of the test cylinder was higher than the asphalt sample it was possible to cover the asphalt surface with water in order to test the air permeability of the asphalt either with the surface dry or with the asphalt surface wet. The wet surface typically had a water depth of 1 to 2 mm. Figure 9 presents the results of an air permeability test carried out on a sample of asphalt with both a dry surface and wet surface. It can be seen in Figure 9 that the air pressure beneath the dry sample falls to atmospheric after approximately 15

seconds. However the air pressure below the wet asphalt initially falls in a similar but slower manner to the dry test but then stabilises with a locked in pressure of 0.6 kPa.

Figure 8: Custom-made apparatus for measuring the permeability of asphalt

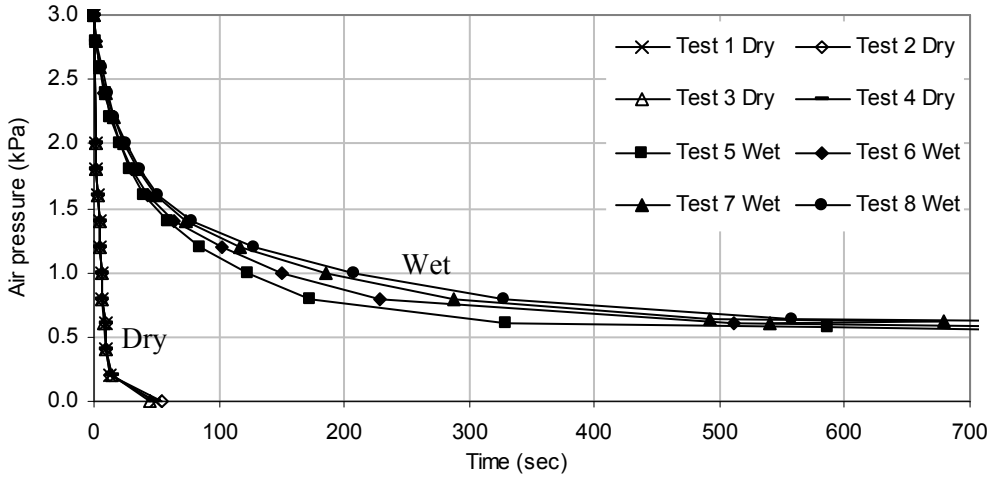

Figure 9: Results of air permeability tests for dry and wet asphalt surface

The lock in pressure of the wet sample is referred to as the air entry value, which is the pressure required to overcome the surface tension of the water which forms a meniscus over the small voids in the asphalt. The air entry value is controlled by the size of the voids in the asphalt, being higher where the voids are smaller.

The slower rate at which the air pressure drops when the sample is wet indicates a lower effective permeability and demonstrates why the pressure would be greater beneath wet asphalt in comparison to dry asphalt assuming the same rate of airflow through the asphalt. Back analysis of the asphalt permeability test results based on the airflow rate caused by a rising tide indicated that on average an air pressure of 0.6 kPa would be expected beneath dry asphalt and 2.6 kPa would be expected beneath wet asphalt during a rising tide. This finding was consistent with the observed phenomenon that the air pressure was capable of lifting the asphalt on the shoulders (50 mm) but not sufficient to lift the full thickness of asphalt (130 mm)

This finding indicated that the heave problem was very unlikely to occur for the full asphalt thickness. However, because the asphalt was constructed in two layers, there was a possibility that the upper layer may heave if it became debonded from the underlying layer. This is thought to have been the cause of the one heave related damage incident on the pavement of a rapid exit taxiways, where only the upper layer was damaged.

6 DESIGN OF EMERGENCY REMEDIAL SCHEME

Based on the results of both the air pressure monitoring and the asphalt permeability testing the mechanism causing the asphalt heaving was understood and the extent of the problem had also been identified. It was clear that it would not be possible to design and install a permanent solution prior to the wet season in 2002, however because of concern that heave domes could form on the runway if debonding between the asphalt layers occurred, it was decided that a short term measure to prevent the heave problem should be implemented.

The short term scheme comprised drilling small holes through the asphalt to relieve the air pressure build up directly below the asphalt. Numerical modelling of the air flow through the sand capping and exiting through a small vent hole in the asphalt was carried out to investigate the pressure distribution. The result of a flow model is presented in Figure 10, where it can be seen that the extent of the influence on air pressure is confined to a relatively small radius of approximately 50 mm around the vent hole.

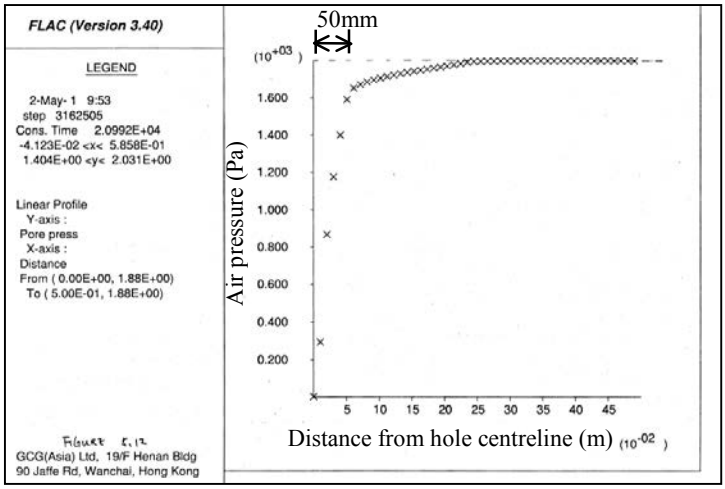

Figure 10: Predicted reduction in air pressure by a 14 mm diameter small hole

It was determined from this analysis that the small holes could not eliminate pressure build up below the asphalt. However, should a heave dome start to develop, the asphalt would lift from the underlying base course forming an air void directly under the asphalt. The air void would form a direct path for the air to the vent, thereby assisting the quick relief of pressure. In essence the vent holes act as a way of pre-popping heave domes before they form. Drilling holes through domes as they developed had previously been used as a remedial measure so it was known that this system would work.

The spacing at which the holes were drilled through the asphalt was based on a combination of the pressure zoning determined from the pressure monitoring and the sensitivity of the location to the development of heave zones. In the high priority areas, such as within the wheel paths on the runway in high pressure areas, a hole spacing of 1 m was adopted. Elsewhere the spacing was increased to either 2 m or 4 m. A total of 160,000 holes were drilled through the asphalt during overnight closures of the runway.

In addition to the small diameter vent holes a number of pressure sensors were installed in the high pressure areas in order to allow continuous monitoring of the air pressure throughout the following wet season.

Although the Airport Authority was confident that the small diameter vents would prevent heave problems, as an additional precaution during the high risk periods, when there was a potential for heave domes to form, a number of maintenance teams were deployed to continuously inspect the runway and taxiways. The high risk periods were defined as periods when the tide was rising at a rate faster than 0.3 m per hour combined with a period when more than 50 mm of rain had fallen in the preceding 24 hours and the asphalt surface was wet.

7 DEVELOPMENT OF A LONG TERM SOLUTION

The short term pressure relief measures were successful in preventing any further heave domes occurring subsequent to the 2001 wet season. However, as expected based on the result obtained from the pressure monitoring, the small holes could not relieve the pressure, instead they ensured that when pressure built up it was vented. The small holes were considered to be a short term measure for two reasons, first there was concern that the holes could become blocked and second the holes would allow water to penetrate into the underlying base course, which is not ideal for pavement life. A long term solution to the problem was needed.

A number of options were considered including the following:

- Building a water cut-off structure, for example a diaphragm wall, around the perimeter of the runway and taxiways to prevent tidal fluctuation of the water level.
- Adding an additional layer of asphalt to the surface to provide extra weight to resist the pressure.
- Anchoring the asphalt down to the underlying base course using short steel or glass fibre rods.
- Providing an air venting system to vent air directly from the underlying rock fill.

A workshop was held to discuss the various solutions and it was determined that the air venting system would be the most cost effective system if it could be proved to work. The air vent system was based on the concept of constructing vertical vents in the landscaped areas adjacent to the runways and taxiways which would penetrate through the sand fill capping and into the underlying rock fill.

8 PRELIMINARY DESIGN OF A VERTICAL VENT SYSTEM

Following the workshop, numerical modelling of the air flow to a vent was used to develop a design for the venting system and in particular to determine the necessary vent spacing and vent size. The initial numerical models were based on axisymmetric modelling of the vent with the controlling parameters being the air permeability of the rock fill, sand capping and asphalt, the volume air flow rate to be vented and the spacing of the vents.

The volume of air to be vented could be determined from the maximum rate of rise of tide and the porosity of the rock fill. The porosity of the rock fill was known to be approximately 0.3 based on the construction records of the rock fill reclamation (i.e. volume of rock from the quarrying to volume as placed). The maximum rate of rise of tide was based on the data from two tide gauges established at the airport site and was determined to be 0.45 m/hour.

The air permeability of the asphalt had already been measured. The apparatus manufactured to measure the air permeability of the asphalt was modified by the addition of a larger air cylinder to enable air permeability testing of compacted samples of the CABC, CASB and Sand Capping to be carried out. Figure 11 presents a schematic representation of the modified apparatus. Tests were carried out to establish the variation of the air permeability of these materials as a function of both relative density and relative saturation. In addition, tests were carried out in the field to measure the in situ relative compaction and relative saturation of these layers.

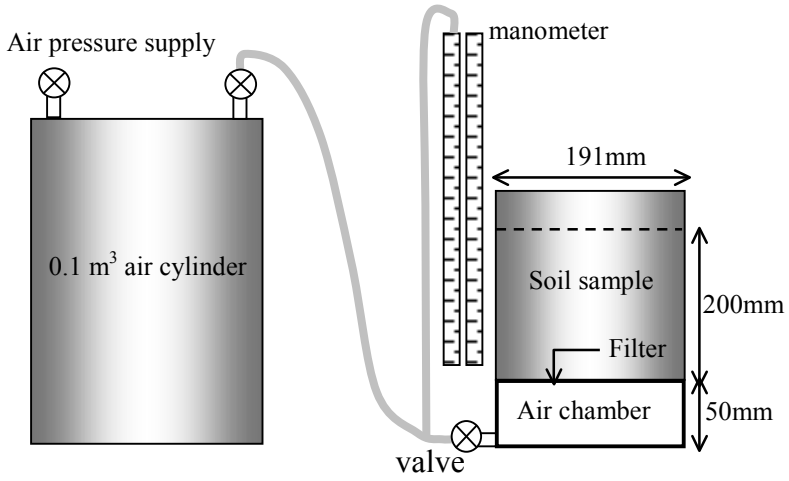

Figure 11: Modified apparatus for measuring permeability of CABC, CASB and Sand Capping

Although the water permeability of the rock fill had not been measured it was known to be very high. For example it is impossible to dewater even small excavations in the rock fill. It was assumed that the air permeability of the rock fill would be very high and would not influence the analysis results.

Based on the results of the numerical analyses of air flow to the vents, it was determined that vertical vents installed along both sides of the runway at a spacing of approximately 20 m and with a vent diameter of approximately 1 m could successfully limit the build up of air pressure beneath the asphalt.

9 DESIGN OF THE VERTICAL VENT

The design of the vertical vent was controlled by the requirement to install the vent during the night-time closures of the runway. The final design for each vent comprised five 150 mm diameter plastic pipes installed from ground surface to a depth of 2 m below the lowest tide level, a total depth from ground level of approximately 8 m. Figure 12 shows a schematic detail of the vent pipe system and the completed installation adjacent to the runway. The plastic pipes were slotted below the base of the sand capping and protrude only approximately 100 mm above ground level. Leung et al. (2007) describe in detail the construction sequence which was adopted to install the vents during overnight closures of the runway.

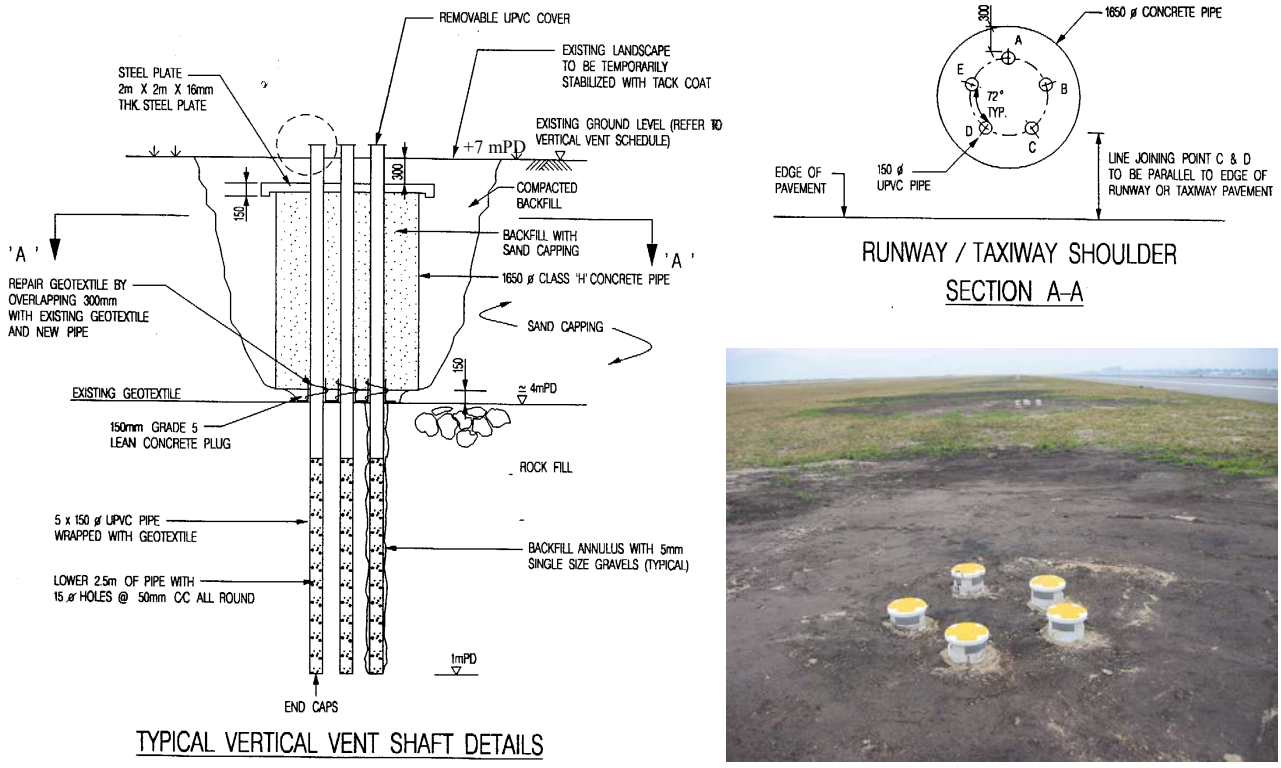

Figure 12: Schematic details of vent shafts and installed shafts along Northern Runway

10 SITE TRIAL OF THE VERTICAL VENT SYSTEM

Because the short term pressure relief system was known to be working it was decided that prior to installing the long term vertical venting system a site trial would be carried out. The site trial was used to confirm that the vent design was appropriate, to obtain data to optimise the final layout and to confirm that the proposed installation system was possible during the night-time closures. Accordingly eight vertical vents were installed adjacent to the runway in the highest pressure area. The vents were spaced at 30 m, with four vents on either side of the runway. Additional pressure monitoring sensors were installed to monitor the pressure below the asphalt in the trial area.

The performance of the vents was monitored during the 2002 wet season. In addition to the pressure monitoring, the air flow rate from the vents was measured during both dry weather and also during a very wet

period. During the monitoring period there were a number of high risk periods when the rate of rise of tide was in excess of 0.3 m per hour and heavy rainfall occurred.

The air flow monitoring confirmed that the air vents were displacing a volume flow rate of 3500 m^3 per hour from the 8 vents. Based on the known rate of rise of tide it was determined that the vent pipes were venting the air from an area of approximately 5 times greater than the area enclosed by the venting trial.

11 MODELLING OF THE VENTING TRIAL

The data obtained from the venting trial was back analysed in order to determine the performance of the final system. A numerical model of the flow was developed assuming that the airflow was concentrated within the rock fill and as such a horizontal slice through the rock fill could be adopted for the model. The numerical model made use of symmetry effects such that only 2 vents (i.e. one quarter of the trial area) was included in the model. Figure 13 presents the pressure contours predicted by the model.

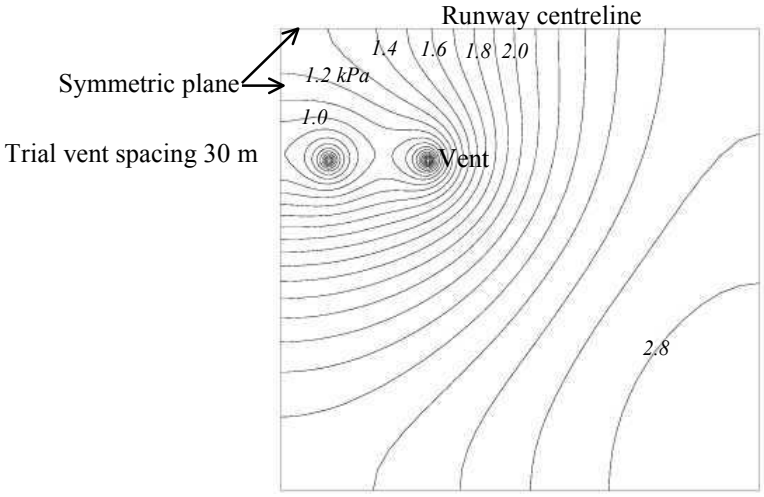

Figure 13: Predicted contours of air pressure for the venting trial

The numerical model of the vent trial indicated that the maximum pressure generated below the asphalt could be limited to approximately 1.6 kPa, which was in line with the pressure measurements. The results obtained from the numerical model of the vent trial were used to calibrate a numerical model of the full venting system with vertical vents constructed along the length of the runway and this allowed the spacing of the vents along the runway to be optimised. Figure 14 presents the predicted maximum pressure beneath the runway during a wet weather event as a function of the vertical vent spacing.

The overall design criteria for the venting system was to limit the maximum rise in pressure to less than 1.0 kPa, which is less than the weight of a 50 mm layer of asphalt. A total of 282 vertical vents were installed at a spacing of 20 m along both sides of the runway in the high pressure zones, increasing to 30 m spacing in the medium pressure zones.

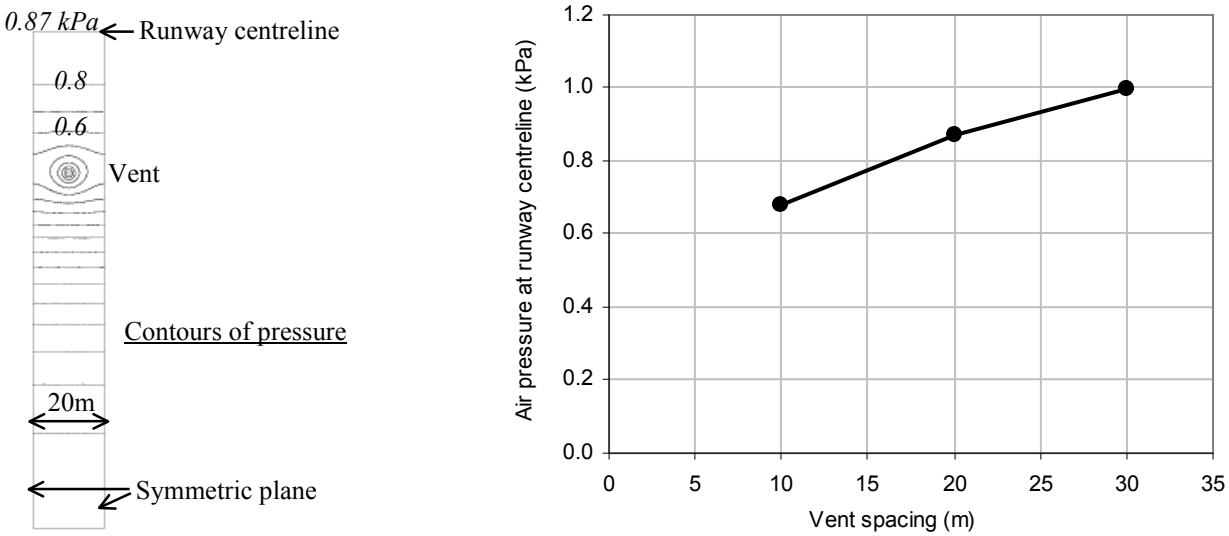

Figure 14: Predicted air pressure build-up beneath runway centreline for different spacing of vertical vents.

12 OBSERVATION AFTER INSTALLING VERTICAL VENTS

The vertical vents were installed during the 2002/3 dry season. In order to ensure the effectiveness of the entire venting system, an online monitoring system was also installed including 47 sub-pavement sensors along the centreline of the runway and taxiways to measure the build up of air pressure under the pavement. All these devices were linked and connected to a computer in the Maintenance Service Control Centre. Special software was developed to analyse the collected data and generate a warning alarm if the preset safety threshold pressure was exceeded.

The development of a cost effective solution to the unique problem of asphalt heaving was achieved by following a logical sequence of site investigation, laboratory testing, numerical modeling of the problem and potential solutions, implementation of a site trial, numerical modeling of the result of the site trial and development of the final solution, installation of the remedial scheme and development of a monitoring system to confirm that the scheme is working. A number of innovative test methods, design and construction approaches were developed to ensure the success of each step.

The air venting system has been operational now for 4 years and to date there have been no further instances of heave dome formation and the measured pressures have been within the predictions. The vertical venting system has allowed the temporary small diameter drill holes through the asphalt to be sealed to prevent water ingress into the CABC and CASB layers.

ACKNOWLEDGEMENT

The authors would like to thank the Airport Authority (Hong Kong) for their kind permission to publish this paper and also to thank their many colleagues working for the Airport Authority whose hard work contributed to finding a solution to this unique problem.

REFERENCE

Leung, R.W.K., Li, D.C.H. & Pickles, A.R. 2007. Heaving of airfield pavement at Hong Kong International Airport. *Proc of 2007 FAA Worldwide Airport Technology Transfer Conference*, New Jersey, April, paper P07033.

Non-Explosive Drill-And-Split Tunnelling Technology of Hong Kong Electric Lamma Island Cable Tunnel

H. Chan
Hong Kong Electric Co. Ltd.
J. Lo
Maunsell AECOM – Maunsell Geotechnical Services Ltd.
R. Cheung
Formerly Maunsell AECOM – Maunsell Geotechnical Services Ltd

ABSTRACT

In year 2004, The Hong Kong Electric Co. Ltd. (HKE) constructed two cable tunnels in Lamma Island to facilitate an additional 275kV Power transmission system. The tunnels were excavated by using non-explosive Drill-and-Split rock fracturing methods which adopted chemical expanding agent and hydraulic splitting for the cable tunnel excavation. In this paper, we overview the excavation for one of the cable tunnels between Lamma Power Station and Yung Shue Wan South which is 220m long with tunnel span of 2.5m. The tunnel was excavated at first by the chemical expanding agent method which was later changed to the hydraulic splitting method. The rates of progress of tunnel advancement were increased substantially. The mechanism involved in the chemical expansion and hydraulic splitting methods is similar, by providing expanding tensile forces in the pre-drilled pattern holes to fracture the rock mass. However, the excavation progress rates in the hard rock tunnel were very different. This paper provides an overview of both the tunnelling technologies and the excavation progress rates of hard rock tunnelling using different plants and equipments.

1 INTRODUCTION

The Hong Kong Electric Co. Ltd (HKE) has completed construction of an additional high-voltage (275kV) power transmission system from Lamma Power Station (LPS) new extension to Cyber Port via a 220m long tunnel between Yung Shue Wan South Cable Landing Point and Lamma Power Station which forms one of the major elements of the project. The tunnel excavation commenced in November 2004 and broke through in September 2005. In order to comply with the Environmental Permit, the drill and blast conventional tunnelling method was prohibited in order to avoid noise impact to nearby residents, and also to prevent any damage to equipment at the adjacent LPS which was very sensitive to vibration. Therefore, two alternative methods were proposed for the cable tunnel excavation using non-explosive Drill-and-Split rock fracturing methods. This paper will provide an overview of both tunnelling methods in terms of mechanism, production cycle, manpower and equipment. It also compares the weekly tunnelling progress rates of both the chemical expansion method and hydraulic splitting method.

2 SITE DESCRIPTION & GEOLOGY

The cable tunnel is located between the Yung Shue Wan South shoreline and the Northwestern corner of Lamma Power Station. The total tunnel length was about 220m with a constant gradient between tunnel axis levels from +7.9mPD to +6.5mPD (see FIGURE 1). The tunnel was excavated as an inverted U or horseshoe shape with a lined internal span of 2.5m (see FIGURE 2). The ground encountered in the tunnel was strong slightly decomposed medium grained granite with closely to medium spaced joints. The rock mass classification and tunnel support class was determined by the NGI Q system. The geological mapping records revealed that the tunnel was excavated through good rock conditions with Tunnel Support Class 1 which is self supporting with spot dowel support for local potentially unstable rock features. The Q values varied between 1.02 and 25.0 with an average Q of 7.28. The observed groundwater inflows during tunnelling were found to be minor and were limited to observations of drips and localised minor ponding. The groundwater influence on the tunnel excavation rate was therefore considered to be insignificant.

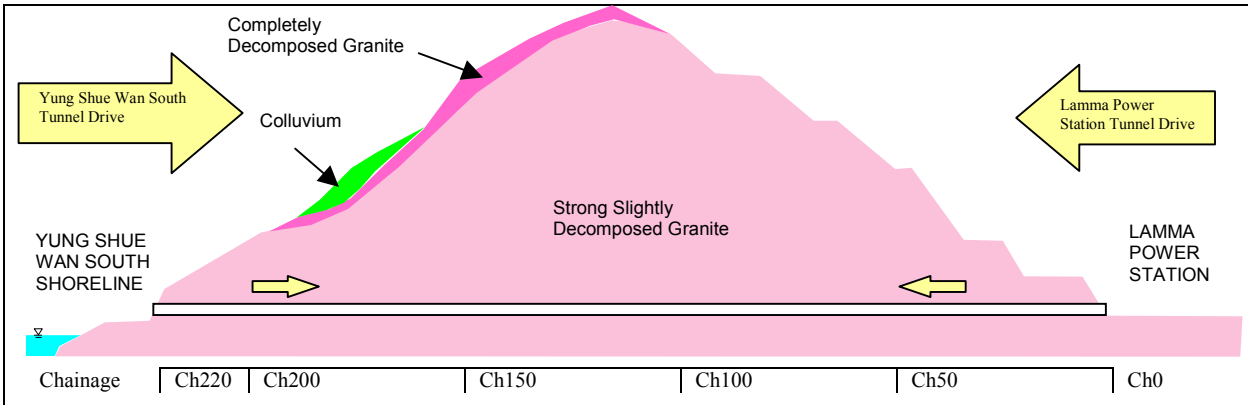

FIGURE 1 - Longitudinal Section of the 275kV Cable Tunnel

General View of Cable Tunnel Excavation

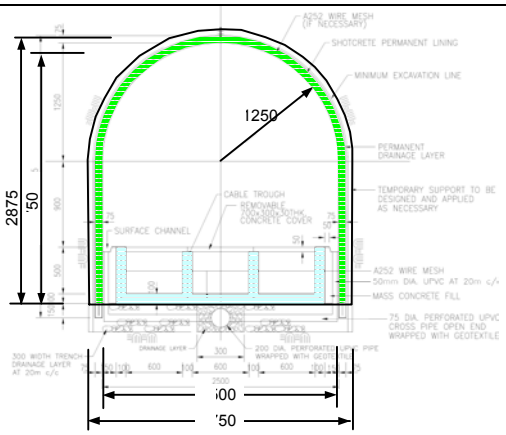

FIGURE 2 - Typical Cable Tunnel Cross Section

3 SITE CONSTRAINTS AND TUNNELLING METHOD

The south tunnel portal is very close to the existing Lamma Power Station and Yung Shue Wan South. The Environmental Permit did not allow using the blasting method in order to avoid any noise impact to nearby residents and also to prevent any damage to adjacent equipment at LPS which was identified as being very sensitive to vibration. With the conventional drill and blast tunnelling method prohibited and other tunnelling methods such as using TBM and roadheader machinery considered not to be cost effective because of the short tunnel length to be excavated and difficulties with plant mobilization into Yung Shue Wan South seashore, other alternative excavation methods were considered.

4 TUNNEL EXCAVATION BY CHEMICAL EXPANDING METHOD

Considering the constraints, the selected method of tunnel excavation was by chemical expanding agent for the initial works stage. The expanding agent is a dry powder consisting of an inorganic compound made mainly of a special kind of silicate and an organic compound. 1.5 to 1.7 litres (water ratio of 30% to 34%) of clean water is poured into container and the powder gradually mixes well until it has a good fluidity. The mixing time by hand-mixer is about 2-3 minutes. This is then poured into drillholes in the tunnel face, and allowed to 'cure', during which the mixture will expand thus inducing stress in the rock mass, leading to cracking and loosening. The normal excavation cycle by chemical expansion was as follows:-

Excavation cycle for Yung Shue Wan Tunnel Drive

(i) Pattern hole drilling Pattern holes were drilled into the excavation face by horizontal leg hammer drill. The holes were 44mm in diameter and were formed with spacing from 250mm to 300mm with depth varying from 1m to 1.8m. A full face tunnel excavation required about 200 numbers of holes.	
(ii) Slot formation Two rows of pilot holes of 44mm diameter were drilled at the middle third points of the tunnel height. Further reaming by a 150mm diameter drill bit formed two horizontal continuous slots in the tunnel face with depth varying from 1.2m to 1.8m. The slots were formed to act as stress relief zones to induce the rock fracturing.	
(iii) Mixing and injection of the chemical expanding agent The dry chemical powder was mixed with clean water (i.e. free from oil and organic substances) at a designed water ratio for between 2 and 3 minutes with an electric handheld mixer. The pattern holes were filled with the expanding agent which were mixed by a pump. The hole was plugged with a polyethylene seal to prevent leakage.	

(iv) Curing The chemical agent set and expanded over a period up to 20 hours at the designed temperature such that the additional stress fractured the rock mass and cracks were formed on the tunnel excavation surface.	
(v) Crack development In a normal operational mode, the time required for crack formation in the rock was between 10 to 20 hours. The cracks usually developed from the edges of the slots.	
(vi) Rock Breaking, scaling and mucking out After crack development, secondary breaking was carried out with a hydraulic breaker mounted on backhoe loader. Loose blocks from the tunnel crown and wall were also scaled off. The removal of the excacated rock mass was carried out by a front bucket of loader.	
(vii) Geological Mapping, temporary support installation and setting out After a completed excavation cycle, the rock mass classification and tunnel support assessment was determined by the engineering geologist. Based on the NGI system, temporary supports were installed subsequently if necessary. Survey and setting out works for the next excavation cycle were then carried out.	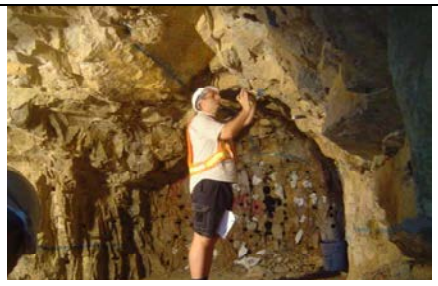

A normal excavation cycle by chemical expanding agent method took an average of five to six days with average pull length varying between 1m and 1.8m. However, the performance of the chemical curing reaction for splitting and cracking of the rock was found to be unreliable and resulted in slow excavation progress. The average tunnel excavation advance rates were 2.04m per week at the Lamma Power Station Drive and 1.06m per at Yung Shue Wan South Drive using a 24 hours shift cycle for both tunnel faces. There were several factors observed that affected the performance of the tunnelling method using chemical expanding agent.

(a) Temperature –Temperature was the more significant factor affecting the performance of the chemical agent. (the lower the ambient temperature was, the longer the time for the chemical curing reaction to take place and the more uncertain of the development of the crack formation.)
(b) Performance of rock fracturing in confined rock condition was unreliable – the magnitude of the additional stress caused by the chemical expansion cannot be controlled. The additional stresses may enhance the arching effect and reduce the rock fracturing between rock blocks.

(c) Water cleanness (free from oil and grease in the water, mixing equipment)
(d) Pattern and width of relief slot free surface
(e) Power of hydraulic breaker
(f) Mix proportion and time control on the chemical expanding agent
(g) Rock strength, joint spacing, contact and orientation

Due to the slow progress being made and in order to expedite the tunnel excavation rate, the method of rock fracturing was changed to the hydraulic splitting method. Other improvement included the use of separated benches of excavation being carried out in the Lamma Power Station Drive while a mini-jumbo was imported for the Yung Shue Wan Tunnel Drive.

5 TUNNEL EXCAVATION BY HYDRAULIC SPLITTING METHOD

Mechanism of hydraulic splitting method

The hydraulic splitter was powered by a hydraulic pressure pump. The cylinder contains a control valve and a piston that moves a plug between two feathers (called wedge and counter-wedges respectively). The wedge and counter-wedge end was placed into the drilled hole. The wedge is pushed down between the two counter-wedges forcing them against the rock sides within the hole. When the tension stresses increase beyond the tensile strength of the rock, a crack is formed through the rock mass. The entire operation of the cylinder is controlled by a single lever on top of the tool which advances and retracts the wedge.

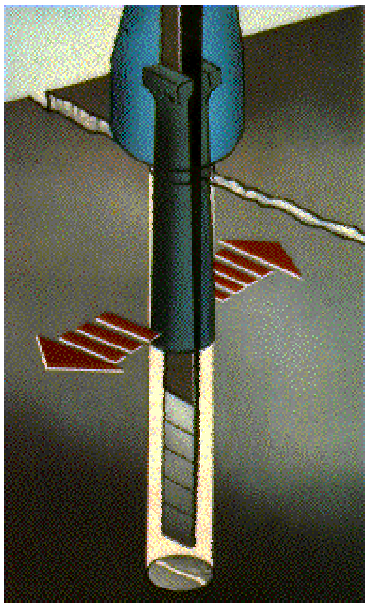

Yung Shue Wan Tunnel Drive with Mini-Jumbo

A mini-jumbo with double booms was imported to Yung Shue Wan South tunnel drive in order to increase the pattern drilling rate. The use of a mini-jumbo rig effectively shortened the pattern hole drilling time and increased the drillhole depths to 3m. The average excavation rate was increased from 1.06m per week to 2.67m per week for the 24 hour shift cycle.

Excavation cycle for Yung Shue Wan Tunnel Drive

(i) Pattern hole drilling The pattern holes were drilled into the excavation face by the double boom mini-jumbo. The hole spacing was formed at a 300mm spacing with a depth of about 3m. The hole diameter was maintained at 46mm to 48mm.	
(ii) Hydraulic Splitting The wedge and counter-wedges were inserted into the drill hole. Rock was split from the upper centre face of the tunnel to the lower part of the tunnel in order to keep a suitable height for equipment handling. (iii) Geological mapping, Temporary support and Setting out After a completed excavation cycle, the rock mass classification and tunnel support assessment was determined by the engineering geologist. Based on the NGI system, temporary supports were installed subsequently if necessary. Survey and setting out works for the next excavation cycle were carried out next.	

Lamma Power Station Tunnel Drive with Separated Bench Excavation

As for the Lamma Power Station tunnel drive, Upper and lower bench excavation was used in lieu of full face excavation. Two tunnelling teams were allocated to excavate the upper bench and lower bench separately. The average excavation rate was expedited from 2.04m per week to 2.94m per week.

Typical Excavation Cycle at Lamma Power Station

(i) Pattern hole drilling The pattern holes were drilled into the excavation face by a horizontal leg hammer drill. The hole spacing was formed at about 300mm spacing to depth varying from 1m to 1.8m. The hole diameter was between 46mm and 48mm.	

(ii-a) Upper bench excavation by Hydraulic Splitting The wedge and counter wedges were inserted into the drill hole. Rock was split from the centre of upper bench to form a 'burn cut' of stress relief free surface for the subsequent rock fracturing around the tunnel profile.	
(ii-b) Lower bench excavation The lower bench was either excavated by the chemical expanding agent or hydraulic splitting method. The mucking out process was also carried out continuously during the bench excavation process.	
(iii) Geological Mapping, temporary support installation and setting out After a completed excavation cycle, the rock mass classification and tunnel support assessment was determined by the engineering geologist. Based on the NGI system, temporary supports were installed subsequently if necessary. Survey and setting out works for the next excavation cycle were carried out next.	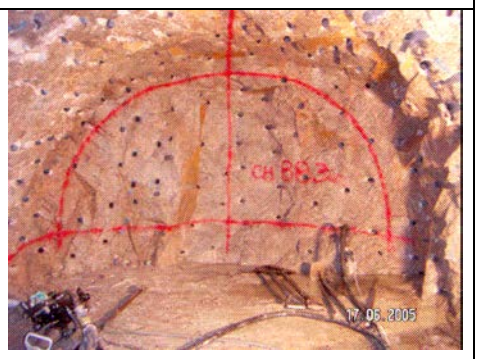

The application of heading and bench excavation would create more working space and excavation rate was effectively increased with the additional resources and effort. The use of Jumbo also shortened the time of pattern hole drilling. The use of hydraulic splitting method required, a very tight control on the drillhole size of 46mm to 48mm as the splitting operation could not be performed in holes larger or smaller than this range. Because of the hardness of the rock, a large number of drill bits and wedge and counter-wedge parts were consumed. During the learning period, wear and tear of the parts were high due to insufficient hole depth and uncontrolled 'swing angle' of the cylinder with respect to the tunnel face. This had reduced the excavation progress. The hydraulic splitting method required more skilled labour including both drillers and hydraulic splitter operators than the chemical expansive agent method.

6 COMPARISON OF TUNNELLING ADVANCE RATES OF DRILL AND SPLIT ROCK FRACTURING METHODS BY CHEMICAL EXPANSION AND HYDRAULIC SPLITING

The average tunnelling excavation rates by hydraulic splitting method increased from 2.04m to 2.94m advance per week in Lamma Power Station tunnel drive (see FIGURE 3). For Yung Shue Wan tunnel drive, the excavation rate increased from 1.06m to 2.67m advance per week (see FIGURE 4). The estimated results are summarized in TABLE 1 below.

TABLE 1 – Comparison of Tunnel Advance Rates

	Lamma Power Station Tunnel Drive	**Yung Shue Wan South Tunnel Drive**	**Overall Tunnel Excavation rate of Two tunnel drives**
Tunnel Length Excavated by Chemical Expanding (m)	31.7	17.5	49.2
Tunnel Length Excavated by Hydraulic Splitting (m)	85.4	85.2	170.6
Average Excavation rate by Chemical Expanding (m per week)	2.04	1.06	3.10
Average Excavation rate by Hydraulic Splitting (m per week)	2.94 (by Separated Benches Excavation)	2.67 (with Mini-Jumbo)	5.61
Percentage increase in excavation rate after change of tunnelling method	44%	152%	81%

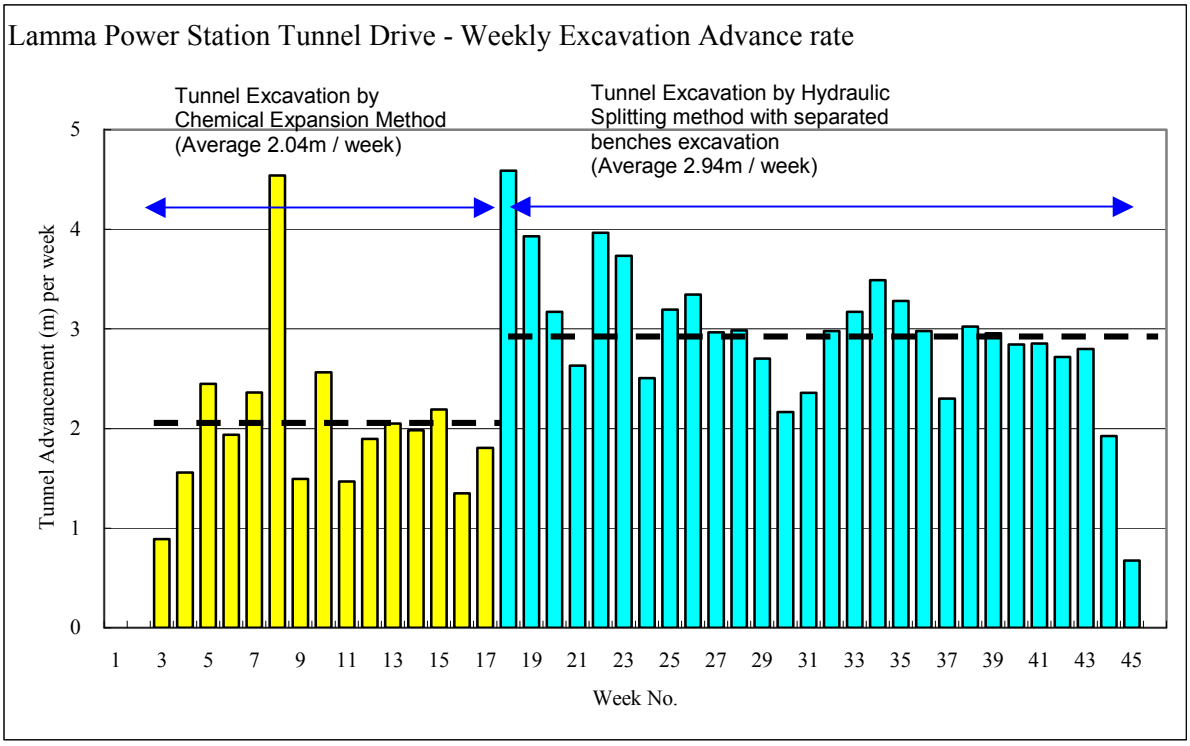

Figure 3 – Lamma Power Station Tunnel Drive – Weekly Excavation Advance Rate

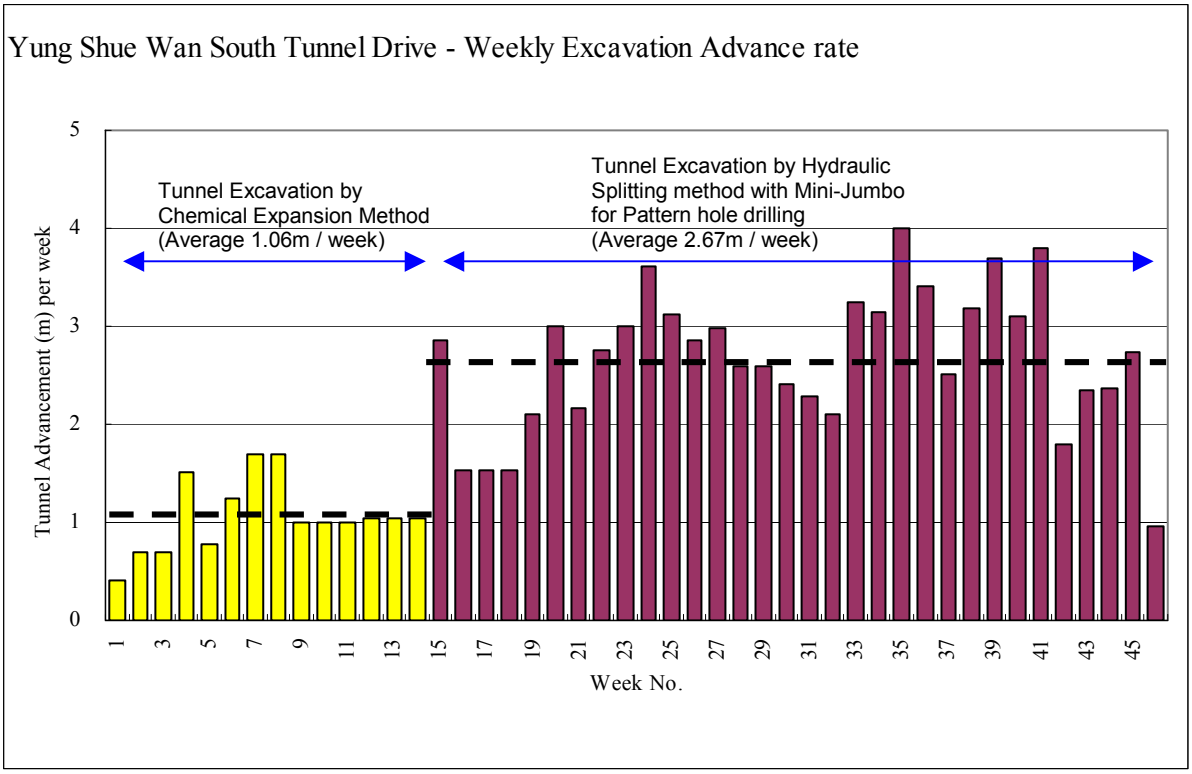

Figure 4 – Yung Shue Wan South Tunnel Drive – Weekly Excavation Advance Rate

Based on the estimated tunnel excavation rates for the Lamma Power Station and Yung Shue Wan South tunnel drives, the projected break through day should have been in late January 2006. In this project, the change of tunnelling method, use of jumbo and application of heading and bench excavation had effectively increased the excavation rate for about 81%, and the tunnel was holed through about 5 months earlier (FIGURE 5).

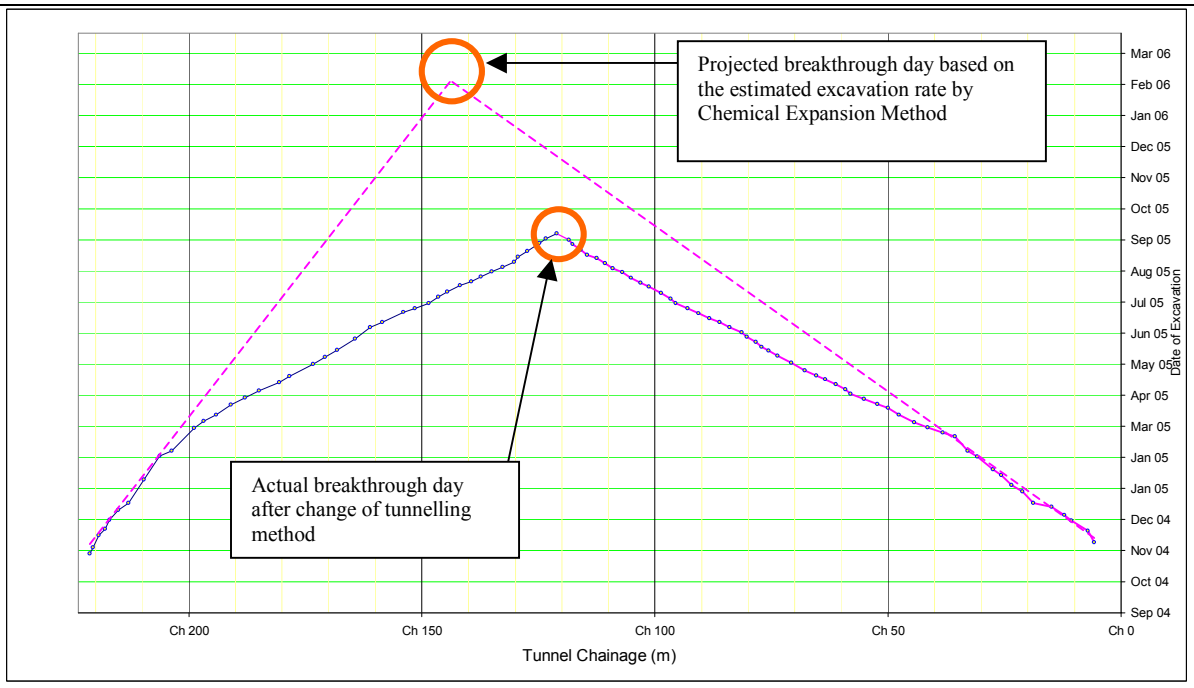

Figure 5 – Comparison of projected and actual breakthrough

7 CONCLUSIONS

The mechanism of both the chemical expansion and hydraulic splitting methods is similar by providing a large expanding force in the pattern holes to fracture and split the rock mass by inducing tensile stresses in the tunnel face. Both excavation methods used were found to be feasible for rock tunnel excavation with excessive over-break and vibration be well controlled. The chemical expansion method is dependent on several factors, particularly the long duration of the chemical curing reaction. The curing reaction will also be affected by temperature fluctuation and the advance rate of the tunnel excavation cannot be guaranteed. The hydraulic splitting method in comparison, which required a larger pool of skilled labour, very tight controlling measures during the pattern hole drilling, constant drill bit and hydraulic wedge splitting equipment replacement, led to a well maintained and acceptable tunnel excavation advance rate.

ACKNOWLEDGEMENTS

The writers gratefully acknowledge the permissions given by The Hong Kong Electric Co. Ltd. and Kaden Construction Ltd. to publish this paper.

REFERENCES

Tatsuya Noma, Toshiro Tsuchiya (2003). “Development of low noise and vibration tunnelling methods using slots by single hole continuous drilling”. Tunnelling and Underground Space Technology 18 (2003), 263-270.

Caldwell T. “A comparison of Non-Explosive Rock Breaking Techniques”.

James D Broomfield. “Long Distance pipejacking in hard rock”.

Ian McFeat-Smith and H H Ichiawa (1993). “Construction of Hong Kong’s First TBM Drive Tunnels”. Options for Tunnelling 1993.

M. Shimizu (1993). “Construction of tunnel without Blasting in Densely Built-up Residential Area”, Options for Tunnelling 1993.

Environmental Initiative in 'Tree Recycling' in Castle Peak Cable Tunnel Project

P.C.F. Chan & A.S.M. Chu
Engineering Projects Department, CLP Power Hong Kong Limited, Hong Kong
M.W. Cheng
Generation/Generation Integrated Services Department, CLP Power Hong Kong Limited, Hong Kong

ABSTRACT

Removing existing trees is sometimes inevitable for civil engineering projects especially for the works in rural area. The current government policy on this issue is stated in the Development Bureau Technical Circular No. 03/2006 where tree felling should only be considered as a last resort if there is no other practical alternative or the concerned trees have unrecoverable health problem. Problems arising from those trees with low survival rate where felling is not allowed, but unlikely to survive after transplantation. It is not uncommon that efforts and resources were spent to preserve those trees but its fate cannot be changed at the end of the day. Although felling of a tree means the end of its life, it does not represent the end of its contribution to the environment. This paper describes the environmental initiative taken during the site formation of the CLP Castle Peak Cable Tunnel (CPT) Project where the felled trees, those with unrecoverable health problem and low survival rate, were further chipped into recycle materials for the use mulching and composting. The author appreciates the importance of tree preservation and it is not the intention of this paper to encourage civil/ geotechnical engineering practitioners to act indiscriminately on felling trees but to exercise our commitment on social responsibility to save our precious landfill sites and on the re-use of natural materials.

1 INTRODUCTION

1.1 The Project

CLP Power Hong Kong Limited (CLPP) has planned to construct a cable tunnel, to secure the power supply of the existing network in Tuen Mun, Yuen Long and the Airport and to develop the future outlets from Black Point and Castle Peak Power Stations. The 4.5km long Cable Tunnel, which is presented in Plate 1 below, will bored through the mountainous area of Castle Peak with 4.5m internal diameter to contain eight 132kV cable circuits. The method of construction was chosen to reduce visual and environmental impacts associated with these power cables, avoid interface with Castle Peak Firing Range and nearby landfill and site of special scientific interest, and increase the reliability of the electricity supply system by protecting the cables from the natural elements and accidental damages.

1.2 Background

Throughout the history, the project owner has been at the forefront in Hong Kong of operating in respect for the betterment to the project, environment and the quality of societal life as a whole. With this founding principle of the project owner the concept of tree recycling was envisaged and implemented. Before the actual site work a detailed environmental study was undertaken and to facilitate the site formation works for the Castle Peak Portal and the vertical shaft at Tuen Mun, unavoidably a considerable numbers of existing trees, which were not indigenous species but were artificially planted as part of the power station development, were needed to be either transplanted or fell, for trees with low value to be preserved. After a series of environmental initiative meetings amongst the project team, options to turn the felled trees to useful products of compressed timber boards, paper, bio-charcoal and planting products – composed and mulched materials

rather than disposal to the landfill site for the felled trees have been considered. Having considered the availability of plants and economic viability locally for re-processing timber, paper and bio-charcoal, the option of recycling the felled trees to composted and mulched material for planting purpose was finally taken on-broad. Whole trees and tree stumps arising from site formation works can be processed into a variety of useful products. These include compost for soil improvement, mulch for weed control, sawdust for animal bedding, and wood flour for cleaning up spills.

Plate 1: Aerial photo showing the Cable Tunnel alignment

2 TREE PRESERVATION

2.1 Current Hong Kong Government Policy and Social Responsibility

The current government policy on this issue is stated in the Development Bureau Technical Circular No. 03/2006 where tree felling should only be considered as a last resort if there is no other practical alternative or the concerned trees have unrecoverable health problem. Problems arising from those trees with low survival rate where felling is not allowed, but unlikely to survive after transplantation. It is not uncommon that efforts and resources were spent to preserve those trees but its fate cannot be changed at the end of the day. Although felling of a tree means the end of its life, it does not represent the end of its contribution to the environment. As stated in Steiner & Steiner (2006, 459) that the ideal level of regulation to the environment can be presented by using Cost-Benefit Analysis (Chilton, 1999). As illustrated in Figure 1 when government restriction is substituted into the model, the optimize level is to maximize the gap between benefits and costs at point R. When more benefits are achieved, more philanthropy would return to the society. As a result, the society and stakeholders would benefit the most from the extent of regulation and pay the least cost.

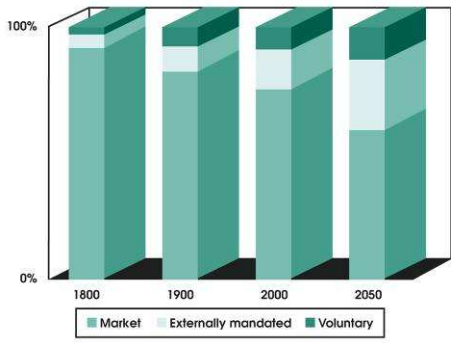

Figure 2: Principal elements of social responsibility and their evolving magnitudes (Steiner, G. & Steiner, J. (2006), p124).

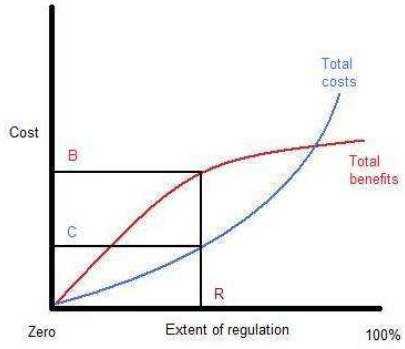

Figure 1 - Relationship between Extent of Regulation, Costs, and Benefits in Environmental Regulation (Chilton 1999, 8; Steiner & Steiner, 2006, 459).

The key factor to drive this environmental initiative is that the project owner is committed to the responsible use of resources and management of the impact of his operations and business on the environment. According to (Steiner & Steiner (2006), there is a trend of principal elements of social

responsibility and their evolving magnitude (Figure 2). The general trend tells us that the elements of voluntary social responsibility increase from Year 1800 to present and will continuously show an uptrend to Year 2050. This trend can truly reflect the situation within the client company and more voluntary events and actions are taken place and one of the voluntary areas is the promotion of environmental awareness within the operations. Hence, in this cable tunnel project one of the environmental initiatives/ voluntary is tree recycling for the felled trees.

2.3 Tree Preservation

To facilitate the site formation works for the Castle Peak Portal (Plate 1) and the vertical shaft at Tuen Mun, unavoidably, the CPT requires the tree felling and transplanting of a considerable number of trees, in which the selection of felling and transplanting is based on their invasiveness, ecological significance, healthiness, and survival rate. The Landscape Consultant who prepared the Tree Felling Report, however, raised concerns about the suitability of the trees for transplanting. Taking into account of her concerns, it is proposed that these trees be recycled in the same manner as the felled trees.

A taskforce was set up by CLPP / Power Systems Business Group (PSBG) in May 2007 to plan the tree recycling works for the trees to be felled within Lot No. TMTL220. The taskforce decided that the trees to be felled would be recycled to produce wood chips for mulch and fine material for composting. The quantity of materials that would be available for recycling was tabulated in Table 1 through a detailed inspection of the trees that were to be felled.

Recycled Material	**Estimated Quantity (m^3)**
Wood Chips for Mulch	24 m^3
Fine Material for Composting	2 m^3

Table 1: Estimated Quantity of Recycled Material

Plate 1: Felling of Trees at Castle Peak Tunnel

3 TREE RECYCLING

Wood waste is the portion of the wood waste stream that can include sawn lumber, stumps and whole trees from site formation of this project. The disposal of wastes generated from the tree felling activities represents a significant portion of operating expenses in landfill space. Wood waste from this tunneling site and such wood waste can be used in its original form or can be processed into a variety of products. In this project 2 major products were generated from this wood waste, which were mulched materials and composted materials. The tree felling works commenced on this site in June 2007. The felled trees were transferred to a temporary storage area on site (Plates 2 & 3) for recycling. Recycling was carried out using a Gravity Feed Wood Chipping Machine with adjustable chipping blades to permit the production of variable sized recycled material. Whole trees and tree stumps arising from site formation works can be processed into a variety of useful products. These include compost for soil improvement, mulch for weed control, sawdust for animal bedding, and wood flour for cleaning up spills.

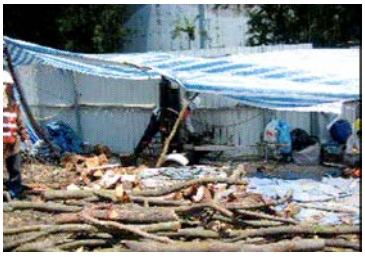

Plates 2 & 3: Temporary Storage of Materials within Work Site

3.1 Wood Chipping

Recycling was carried out using a Gravity Feed Wood Chipping Machine (Plates 4 & 5) to produce variable sized recycled material. The recycled material was delivered to the pre-determined organisations, throughout July 2007. The large size of wood chip was used as mulching material, on the other hand the leaves, sawdust and relatively smaller sizes of wood chip with less time for decomposition rate were used as composting materials.

Plates 4 & 5: Chopping of Tree Trunks and Chipping of Tree

3.2 Composting

As stated in (Clarence G. (1972),p13) "Composting is a biological process for converting organic solid wastes into a stable, humus-like product whose chief use in as a soil conditioner." Having considering the scale and complication of the set up of the tree recycling, in this project the method of aerobic composting was adopted and a storage area of 6 nos. of 1m (H) x 3m (W) x 3.5m (D) compartment was used for the process of composting as illustrated in Plates 6 & 7. As stated in Compost - Wikipedia, the free encyclopedia (2008) "In a properly operated compost system, pile temperatures are sufficient to stabilize the raw material, and the oxygen-rich conditions within the core of the pile eliminate offensive odors. High temperatures also destroy fly larvae and weed seeds, yielding a safe, high-quality finished product." The critical factors for the application of composted material are carbon and nitrogen. It is suggested in (Mackinnon, J. E. R. a. H. C. (1997), p143) "Compost with wide ratios of C:N may not be suitable for incorporation into soil." and in (p145), the C:N ratio for the composted material of dead hulls, leaves, straw and sawdust are generally be 120:150, 100:180, 120:180 and 300:500. Hence, this implies that the materials generated from felled tree are good composted materials for such application. Technical benefits recommended in (Compost - Wikipedia, the free encyclopedia (2008)) "It is used in landscaping, horticulture and agriculture as a soil conditioner and fertiliser. It is also useful for erosion control, land and stream reclamation, wetland construction, and as landfill cover." and in (Rechcigl, J. E. (2000), p283) "Compost applications have significantly positive effects on plant disease suppression, especially soil-borne root pathogens." The saw dust generated from the wood chipping process was then mixed up with other green wastes such a grass clippings and fallen leaves generated from the landscape maintenance in Power Stations as the composting materials. The end product free of plant pathogens and weed seeds with fresh earthy aroma is ready for use after 3 months composting process. In fact, the compost is used as planting medium for landscape planting, landscape maintenance and potting soil mix for seasonal and indoor plants for CLP's Power Stations.

Plates 6 & 7: Composting Process at CLP / Generation Business Group Nursery

3.3 Mulch

"In agriculture and gardening, mulch is a protective cover placed over the soil, primarily to modify the effects of the local climate." (Mulch - Wikipedia, the free encyclopedia (2008)). It is a widely used method to maintain the plants healthiness. The mulching material should apply as a top layer of the planting area with thickness of 2 to 4 inch depth. "Properly composted wood chips can be used as a long lasting mulch that weathers to a silver-gray color." (Mulching Tree and Shrubs (2000)) In this project the relatively larger size wood chips from the felled trees have been used as mulching material and this material was delivered and applied to 4 planting areas managed by Hong Kong Housing Society (HKHS) - Plates 8 & 9 refers. According to Mulch - Wikipedia, the free encyclopedia (2008), "Mulch is used for various purposes:

(1) to adjust temperature by helping soil retain more heat in spring and fall, and by keeping soil cool and even out temperature swings during hot and variable summer conditions; (2) to control weeds by blocking the sunlight; (3) to retain water by slowing evaporation; (4) to add organic matter and nutrients to the soil through the gradual breakdown of the mulch material; (5) to repel insects; (6) to incrementally improve growing conditions by reflecting sunlight upwards to the plants, and by providing a clean, dry surface for ground-lying fruit such as squash and melons; (7) for erosion control - protects soil from rain and preserves moisture; and (8) for sediment control - slows runoff velocity ".

4 REVIEW

4.1 Application

Given the quantities of recycled materials produced the taskforce considered a numbers of potential organisations that could be used these materials. The recycled materials were delivered to the following organizations throughout July 2007.

Facility	**Date of Delivery**	**Quantity of Material Delivered**
Jat Min Chuen, HKHS	9 July 2007 / 10 July 2007	$12m^3$
Clauge Garden Estate, HKHS	10 July 2007	$6m^3$
Lok Man Sun Chuen, HKHS	11 July 2007	$6m^3$
CLP/Generation Business Group Nursery	20 July 2007	$2m^3$

Table 3: Delivery of Recycled Materials

The material of wood chips was delivered to HKHS for mulching purpose, see Plates 9 & 10. There was a positive feedback of the recycled material with an appreciation letter from HKHS.

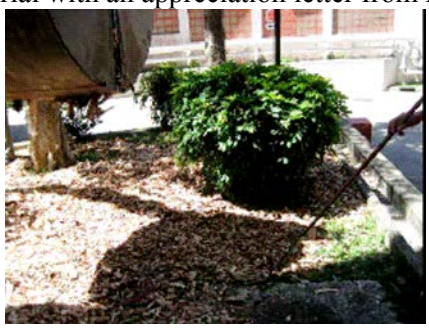

Plates 8 & 9: Mulching at Hong Kong Housing Society Planting Areas

The composted material was delivered to Generation Business Group of CLPP (GBG) used for the planting within the power station. The composted material was applied to replace the peat moss, which was used to import from European countries. The application of the composted materials to the garden in Black Point Power Station of GBG was presented in Plates 10 and 11.

In addition, a trial has also undertaken to test the effectiveness of the composted material. It is noted that there was a better growth of vegetation at the area where the material has been applied. Although there is no quantifiable figure to support, with the results show in Plates 12 to 14, it appears that the composted material not only can serve the purpose of soil conditioner but also has some sort of fertilizing power.

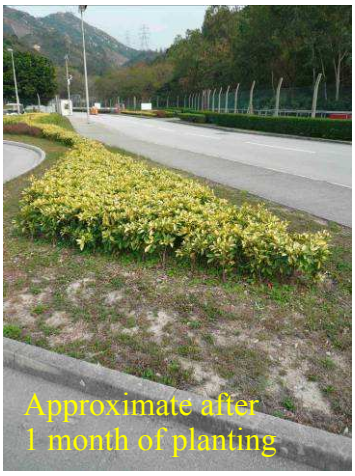

Plates 10 & 11: Application of Composting at Black Point Power Station of Generation Business Group of CLPP

Plates 12, 13 & 14: Application of Composting at Generation Business Group of CLPP

4.2 Benefit Vs Cost

These recycling products of mulching and composting have technical as well economical benefits. The technical benefits on applying the composted material and mulched material for planting have been discussed in earlier Sections of 3.2 and 3.3. Economically their applications can (1) reduce the waste of felled trees that go to the landfill area, the handling fee for each 9 cubic metres industrial waste skip is about HK$300; (2) reduce the environmental pollution of burning the felled trees; (3) serve the purpose of the replacing the sphagnum peat moss imported from foreign countries, around HK$250 per 250 litres per bale imported from Germany; (4) reduce landscape maintenance; (5) the processes of composting and mulching have low sensitivity problem, hence much more easy to control.

Although there are economic benefits as discussed about, there are also varies costs in association with the composting process. These costs include the cost of temporary storage, chipping, labouring and transportation. In addition, as discussed in earlier Section of 2.1 there is other factor such as social responsibility to be considered. Because the scale of this tree recycling initiative in this cable tunnel project, the cost and benefit analysis can not be undertaken to reflect the full scale application. Apart from the cost implication, whether we should apply such environmental initiative depends on how much we appreciate the project sustainability and our responsibility to the society as a professional engineer.

5 CONCLUSIONS

In this paper, re-use the recycling material from felled trees for composting and mulching are discussed. Using the products from the tree recycling has both technical and economical benefits and the project team of this cable tunnel project appreciates the importance of tree preservation. It is not the intention of this paper to encourage civil/ geotechnical engineering practitioners to act indiscriminately on felling trees but to exercise our commitment on social responsibility to save our precious landfill sites and on the re-use of natural materials.

ACKNOWLEDGEMENT

The authors would like to express their gratitude to the project team of Castle Peak Tunnel; CLP Hong Kong Power Limited; Atkins China Ltd.; and Dragages Hong Kong Limited.

REFERENCES

ACLA in Association with Mott Connell Limited (2007). "Tree Felling Report." *Mott Connell Limited.*
Atkins China Ltd. (2007). "Castle Peak Cable Tunnel Project, Tree Recycling Proposal." *Atkins China Ltd.*
Clarence G. (1972). "Composting, A Study of the Process and Its Principles" *Rodale Press, Inc.*
Conservationist, T. (1994). "Recycling and innovative gardening." *Albany* 48(5): 4.
Chilton, K. (1999) Enhancing environmental protection while fostering economic growth, *Policy Study No. 151 (St. Louis: Washington University, Center for the Study of American Business, March 1999)*, p. 8.
Emerson, D. (2004). "Transforming Lumber Scraps into Compost, Mulch and Fuel." *BioCycle* 45(12): 2.
Ennis, K. (2003). "Evolution of a mulch marketer Kent Ennis." *BioCycle* 44(7): 1.
Glenn, J. (1997). "A nursery moves big time into organics recycling." *BioCycle* 38(7): 3.
Kempter, G. (1994). "Tree care industry seeks recycling partners." *BioCycle* 35(10): 3.
Logsdon, G. (1993). "A green model from Decatur." *BioCycle* 34(9): 1.
Rechcigl, J. E. (2000). "Soil Amendments and Environmental Quality." *Lewis Publishers.*
Spencer, R. L. (1993). "Composting expands Disney recycling program." *BioCycle* 34(10): 4.
Steuteville, R. (1993). "Bringing out the best in waste wood." *BioCycle* 34(2): 1.
Stuart C Buckner, F. C. M. J. (2002). "Controlling odors during grass composting." *BioCycle* 43(9): 6.
Steiner, G. & Steiner, J. (2006). "Business, Government & Society. A Managerial Perspective, Text and Cases, Eleventh Edition." *Irwin McGraw-Hill, Boston*.
Mackinnon, J. E. R. a. H. C. (1997). "Agricultural Uses of By-Products and Wastes." *ACS Symposium Series 668.*
Mulch - Wikipedia, the free encyclopedia (2008). http://en.wikipedia.org/wiki/Mulch
Compost - Wikipedia, the free encyclopedia (2008). http://en.wikipedia.org/wiki/Compost
Composting - Wikipedia, the free encyclopedia (2008). http://en.wikipedia.org/wiki/Composting
Mulching Tree and Shrubs (2000) http://www.ces.ncsu.edu/depts/hort/consumer/factsheets/trees-new/text/muching.html

A Glimpse of the New Technology Applications in the Landslip Preventive Measures Programme

T.C.F. Chan & D.C. Chan
Geotechnical Engineering Office, Civil Engineering and Development Department, The Government of the Hong Kong Special Administration Region

ABSTRACT

In the quest for improvements in the design and construction of slope upgrading works under the Landslip Preventive Measures (LPM) Programme, the Geotechnical Engineering Office (GEO) continuously strives to develop innovative technology applications and explore new products to enhance the programme efficiency, improve quality of works, and better protect the environment. In recent years, trials of a number of new technologies and products have been carried out, and some have found successful applications in LPM works. This paper will present the outcome of the trials, the potential applications in LPM works and their limitations.

1 INTRODUCTION

The government has since 1977 embarked on the Landslip Preventive Measures Programme to systematically retrofit sub-standard man-made slopes to progressively reduce landslide risk to the public. In response to the advancement in the slope engineering practice, new technologies and products were explored during the implementation of the LPM Programme as a continuous drive to enhance efficiency, improve quality of works, and better protect the environment. In recent years, a number of new technologies and products have been studied and tried in the LPM works. Some of these trials have found successful applications while others require further study. In this paper, the new technology applications tried or actually put into practice in LPM works in recent years will be presented.

2 NEW TECHNOLOGY APPLICATIONS IN THE LPM PROGRAMME

2.1 Concrete grillage/soil nail system in upgrading loose fill slope

In the past, many of the old fill slopes were formed by end-tipped method without compaction. These fill slopes are in loose state and are liable to failure by liquefaction. Up to the early 2000's, sub-standard loose fill slopes were upgraded by the conventional method of excavating and re-compacting the top 3m of the fill. This method very often faces a number of construction constraints, such as access and stockpiling problems, stability of the temporary excavation and the need to fell the existing trees on the slopes. Particularly on the issue of tree removal, the method is not an environmentally friendly solution readily accepted by the public in some cases. Recent work by the Hong Kong Institution of Engineers (HKIE) (2003) has developed a new method using soil nails in conjunction with a grid of grillage beams to stabilise loose fill slopes.

Concrete grids are constructed on the slope surface to restrain the sliding potential of the soil mass at steady state and in turn restrained by soil nails bonded into a competent sub-surface stratum. Existing trees are preserved within the grillage openings. During construction, the layout of the grids is adjusted on site to accommodate the existing trees. To minimize the effect on tree roots which tend to be at shallow depth, grid beams are normally buried shallow on the slope surface, say 100mm. Typical soil nail spacing is about 2m horizontal and 1.5m vertical. However, this design method is applicable only to loose fill with a relative compaction not lower than 75%, and usually costs about 30-50% more than the fill re-compaction method. Since early 2000's, this method has been used in about 50 cases under the LPM Programme to upgrade loose fill slopes with existing mature trees. Figure 1 displays the typical design grid arrangement and Plate 1 shows a completed project where trees are preserved satisfactorily within the grids.

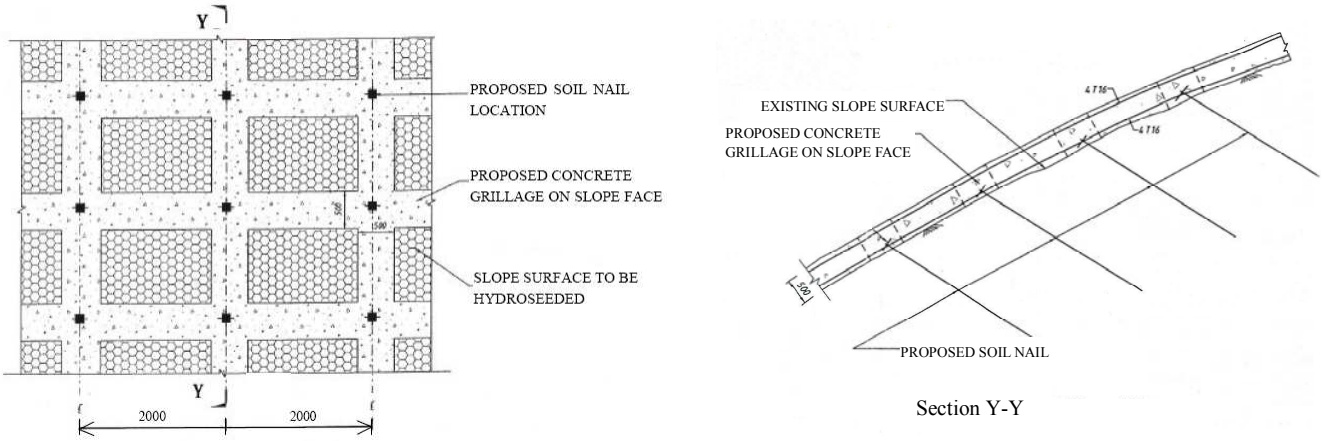

Figure 1: Typical grid arrangement and the section

Plate 1: Completed LPM project taken in 2003 & 2007 using the concrete grillage/soil nail system

2.2 Pit-by-Pit Re-compaction Method

Pit-by-Pit re-compaction method is used as an alternative option for upgrading loose fill slopes to cope with the situation where trees and restrictive site constraints exist. Close proximity of the slope to private lot and too loose a state for the fill (degree of compaction less than 75%) preclude the use of the grillage-nailing method. Difficult site access, inadequate working space for excavation and stockpiling, and adverse environmental impact to the nearby developments make re-compaction in bulk impracticable. Under such circumstances, the loose fill between trees can be excavated in small pits adjoining one another measuring 1.5 to 2 metres on plan to avoid the trees and their roots, leaving behind the volume of fill at the tree locations. The liquefaction potential of the loose fill left in place is adequately reduced due to its small quantity and the presence of tree-root action. The common backfill materials are soil-cement, mass concrete, lightweight concrete or no-fines concrete. The Pit-by-Pit excavation will result in stepped profile of the backfill and it is difficult to construct continuous drainage blanket underneath the backfill. The liquefaction potential of any loose fill left in place underneath the backfill will need to be considered by the designer in adopting this option. Mitigation measures may include raking drains tapped into the loose fill, or an impermeable cap on slope surface in case no-fines concrete backfill is used. Usually a layer of topsoil is placed on the top of the concrete backfill for vegetation growth. The method is more suitable for small fill slope as the construction is normally more time consuming.

2.3 Rubber soil

Rubber soil is a construction material normally comprising shredded rubber tires mixed with cementitious material. The application allows reuse of waste and saves landfill space. Trial use of the material as an alternative backfilling material for re-compaction of two small loose fill slopes was carried out under the LPM Programme in around 2002 and 2005 taking advantage of its free draining property, high cemented strength, and different densities for different mixes.

Plate 2: Slope with loose fill replaced by rubber soil

In the original design of the two features, conventional fill replacement of the top 3m was planned using compacted fill and no-fines concrete respectively. The rubber soil backfill was proposed as an alternative by the respective contractors. The slurry mixture which was composed of rubber crumbs/chips, cementitious materials as the binding agent, and water was delivered to site pre-mixed. The backfill was placed in horizontal layers of 800mm to 900mm employing wooden formwork as required and compacted by means of a lightweight roller. A rubber soil primer layer was applied on the temporary excavated face acting as a 1-way drainage layer, according to the designer, for intercepting the rain water from penetrating into the remaining loose fill below the porous rubber soil. An interlocking surface protection grids were placed on the final slope surface and filled with 150mm of planting soil for hydroseeding and some light planting. The layer also served as a protective surface against fire hazard. Plate 2 shows the finished slope in one of the trials.

The performance of the completed features was monitored for more than a year using field instrumentations. The results showed that all the measurements were well below the alert levels during the monitoring period. However, there are a few issues to be considered for wider use of rubber soil in re-compaction of loose fill slopes. The effectiveness of the primer layer in preventing saturation of the underlying loose fill needs further study. The cost of the material is relatively high in comparison with the normal soil backfill and no-fines concrete. Similar to the conventional re-compaction, the application requires the removal of existing fill and hence the removal of existing trees, and is generally not an environmentally acceptable solution.

2.4 Stabilisation of loose fill by grouting

The use of grouting as an alternative upgrading method to stabilize loose fill slope was investigated. Two ground improvement techniques, namely compaction grouting and permeation grouting, were studied by site trials. The adopted compaction grouting involved capsulated grouting using the tube-a-manchette (TAM) method to densify the surrounding soil. The grout holes along the grout pipe served as the injection points in the formation of a series of expanded grout capsules lined by fabric at different depths, thus achieving the compacting effect. Whereas for the permeation grouting, grout was pressurized through the grout points of the TAM to permeate into the voids to increase the inherent strength of the soil and to reduce its contractive tendency when sheared. In both cases, as grouting was carried out within the top 3m of the loose fill, the grout pressure was carefully controlled to guard against the risk of heaving. The limiting grouting pressure was set at 5 bars. In the trials, a layer of shotcrete was applied on the slope surface to act as a reaction boundary. The

spacing of the grout holes were 1.2m c/c and 1.5m c/c for the compaction and permeation grouting respectively. Figures 2 and 3 show the diagrammatic details of the grouting methods respectively.

The results of the trials were not satisfactory. The fabric bags in the capsulated grouting cracked along the connecting seams at low grout pressure and grout escaped into the surrounding through preferential paths in the soil matrix instead of forming capsules to compact the soil. The average diameter of the grouted capsules was found to have expanded to about 220mm, only slightly larger than the grout hole diameter of 150mm. For the permeation grouting, the grout travels along preferential paths instead of permeating into the voids. Verification tests on the soil properties before and after the trials did not lend positive and affirmative results confirming achievement of the design effects, that is densifying the soil to 95% relative compaction or an improvement in the strength. Effective means of controlling heaving, hence improving the efficiency of soil densification near the slope surface has to be reviewed. Improvement in the choice of liner fabric has to be studied. In general, the heterogeneity of the fill body, which is common in loose fill slopes in Hong Kong formed by uncontrolled dumping, renders both grouting methods less promising. Further research and trials on other ground improvement methods are being undertaken by the GEO.

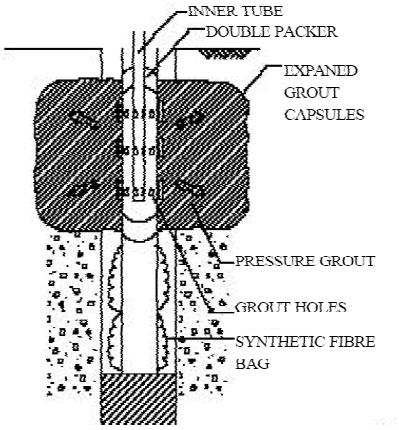

Figure 2: Details of capsulated grouting

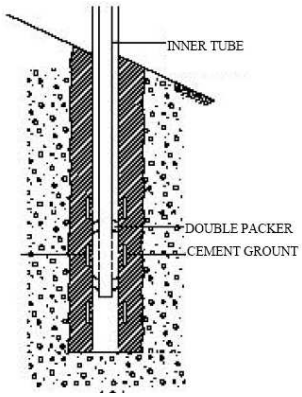

Figure 3: Details of permeation grouting

2.5 Fibre reinforced polymer soil nail

Fibre Reinforced Polymer (FRP) reinforcement because of its high tensile strength, durability, light weight and flexibility was studied for its potential as alternative to steel bar in soil nailing works. The fibres commonly used in composite include carbon FRP (CFRP), glass FRP (GFRP) and aramid FRP (AFRP). The high corrosion resistance can eliminate the need of sacrificial thickness, zinc coating or corrugated plastic sheath. Different FRP bars were tried under the LPM Programme.

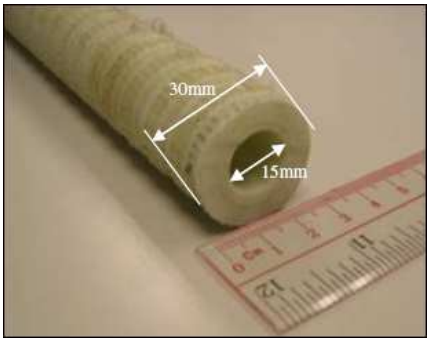

Plate 3: View of the CSDN hollow bar

Ho et al. (2007) investigated two types of FPR nail, namely the Composite Self-drilling nails (CSDN) and the actively stressed soil nails (ASN). The CSDN used a hollow FRP bar equipped with an end drill bit as the drill rod. Grout was pumped through the central bore of the rod which was then left in place in the grouted

hole as the nail. Pull-out tests on the nails concluded that they were capable of resisting the design ultimate load. The shortcoming of the CSDN nail was that it could not penetrate rock efficiently and it would be difficult to maintain the hole alignment in soil with boulders. For the actively stressed nails (ASN), two FRP bars were installed in the same hole with one of them actively stressed and debonded in the active zone, while the second member passively tied the active zone to the resistant ground zone. The installation would reduce or eliminate ground movement needed to mobilize the nail strength. Two such nail assemblies were pull-out tested. In both cases, the plastic nuts that transferred the loads from the jack to the bars fractured prematurely.

Cheung & Lo (2005) presented the study on the use of CFRP in soil nail application. Pull-out tests were performed on seven CFRP soil nails covering both flat strips and round bars. To accommodate the conventional pull-out equipment, factory fabricated head adapters were fixed onto the bars. For the pull-out tests, pre-mature failure of some of the CFRP reinforcements behind the adapters was observed, mostly found on the flat strip type. The probable cause was the stress concentration behind the adapter during transportation. However this was not observed for the round reinforcement. The conclusion of the study indicated that CFRP reinforcement is a potential alternative to steel bars in soil nail application. However its brittle behaviour, low shear and bending capacity are concerns relevant to the use of the material. To gain insight and experience, a set of interim design and construction guidelines has been promulgated for the trial use of the reinforcement in the LPM Programme.

2.6 Stainless steel soil nail

The use of stainless steel bar in soil nail application was investigated because of its corrosion resistant property. Based on a review of the published literature and the test information, Grade 304 and Grade 316 (Austenitic type stainless steel) and the more superior grades are considered potentially feasible. Both the solid stainless steel bar, and the stainless steel clad bar were considered. The latter type makes use of a stainless steel clad metallurgically bonded onto a carbon steel core to provide the corrosion resistant characteristic thus reducing the material cost. The study is still in the process. An initial assessment indicated that the construction cost of soil nailing using solid and cladded stainless steel bars are about 41% and 28% more costly than the usual double corrosion protected carbon steel nails. Some physical property tests have been arranged to verify some of the manufacturing information on the cladded bar.

Plate 4 (left): solid stainless steel bar
Plate 5 (top): stainless steel clad bar

2.7 Non-destructive test for steel soil nails

A number of non-destructive testing (NDT) techniques were investigated in GEO (2003) & GEO (2006b) for determining the length of grouted soil nails. The Time Domain Reflectometry (TDR) was identified as a suitable method because it is cost effective and the simplest. The TDR test assembly involves pre-installing an electric wire parallel to the steel soil nail. In the test, an electrical pulse is sent through the steel nail and by determining the time for the pulses to travel from the pulse generator and get reflected from the point of discontinuity or mismatch, that is the end of the nail, the pulse propagation velocity is determined and hence the length of the nail. The method can also assist in identifying defects in the grout sleeve based on the

displayed waveform and the short TDR-deduced bar length. Since 2004, the method has been routinely used in LPM projects as a tool to supplement site supervision in the quality control of soil nailing works. The TDR tests provide additional assurance on construction quality and a deterrent against mal-practice.

2.8 Drilling Process Monitoring system

The Drilling Process Monitoring (DPM) technique can be employed to continuously monitor and record a series of parameters in real time sequence for ground characterization during drilling. The device equipped with sensors collects data from the various components of the drilling process and determines the penetration rates that are used in the ground characterization. The assembly was developed by the Civil Engineering Department of the University of Hong Kong (HKU). Trial of the equipment in LPM soil nail drilling works was described in GEO (2006a) & GEO (2007a). Also tested was the RT-DPM, which incorporated the real-time capability, capable of automatically retrieving, processing and sending the DPM data via wireless channels to a site server for analysis. The records provide real time information on the position of the drill bit inside the drill hole, the drilled length and the penetration rates.

The trial suggests that the RT-DPM is quick and reliable in providing real-time drilling data on site in estimating the depth of the hole based on the collected data and could be used as a driller's log for record purpose. There is a general correlation between the penetration rates derived from the DPM system and the actual site conditions. However, the relationship is dependent on factors such as the skill of the operator, the condition and state of wear of the drill bits. Therefore calibration of the DPM data with known ground conditions is important for meaningful interpretation.

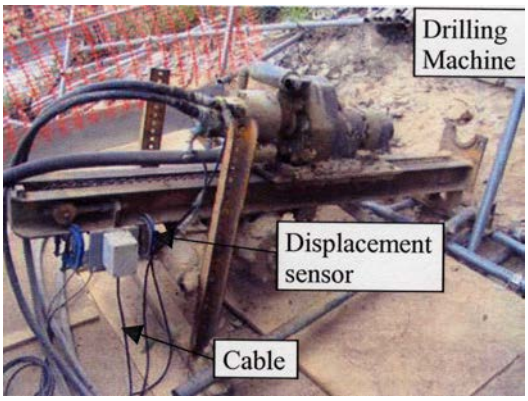

Plate 6: Drilling rig equipped with DPM

2.9 Inflatable packer for soil nail pull-out test

When using the conventional sponge packer in forming the grout length in the pull-out test, there is reasonable concern regarding the accuracy of the formed length as grout may leak into the free length, and therefore affect the confidence level of the test data. To improve the performance of the packer, two types of inflatable packers shown in Plates 7 and 8 were developed and the performance tested in LPM projects. Details of the studies were described in Cheung et al. (2005) and Swann et al. (2007).

Both packers are inflatable by compressed air, and are made of rubber membrane for the HK Packer and rubber tube for the inflatable rubber tube packer. In both studies, measures were incoroporated to verify the effectiveness of the packers in forming and isolating the bond length. These included the real time monitoring by video camera placed in the drillhole in front of the packer and instrumentation on the nails with strain gauges on the bonded section. The test results concluded that both inflatable packers perform well allowing reliable and practical control of the grout length. The use of the new inflatable packers is encouraged in future pull-out tests.

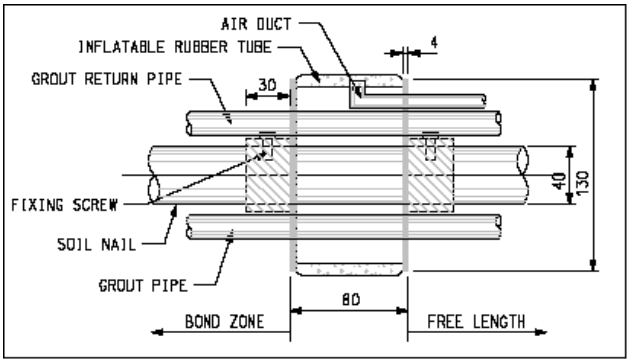

Figure 4: Diagrammatic view of the rubber tube inflatable packer

Plate 7: HK Packer

Plate 8: Rubber tube inflatable packer

2.10 Pre-fabricated formwork system for concrete grillage construction

The conventional method of constructing grillage beams involves erecting temporary formworks for the construction. Trial was carried out using frame of steel net pre-fabricated in the factory. The frame, a proprietary product, was first unfolded on site and placed at the design location. The longitudinal main bars and the upper stirrups were then installed. Sprayed concrete was applied to form the beams.

It was concluded that the framing system requires less time to install. However it is more difficult to install on undulating ground and the proprietary system is more expensive than the conventional formwork method for the wider application.

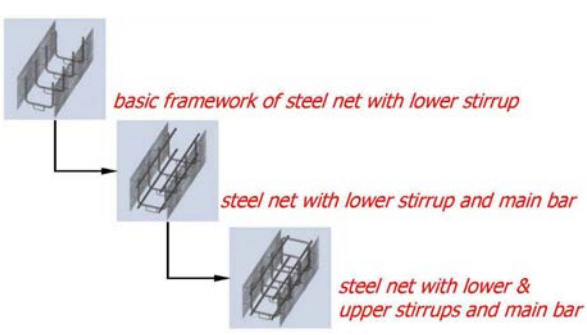

Plate 9: Pre-fabricated formwork system for concrete grillage construction

3 CONCLUSIONS

In recent years, a number of new technologies and products were investigated for application in the LPM Programme in the quest to improve construction efficiency, cost-effectiveness and quality of works, and to better protect the environment. Some have found successful applications in the Programme such as the concrete grillage/soil nail system, Pit-by-Pit re-compaction, non-destructive testing of steel soil nails, and inflatable packer. More feasible applications may evolve from the studies at hand. Under the continuous improvement initiatives of the Programme, new technologies and products will continuously be studied and investigated to identify their potential for application in the slope upgrading works.

ACKNOWLEDGEMENTS

Valuable assistance is given by Ms Yvonne Lo of LPM Division 2 in compiling the background information for the preparation of this paper. This paper is published with the permission of the Head of the Geotechnical Engineering Office, and the Director of Civil Engineering and Development Department, the Government of the Hong Kong Special Administration Region.

REFERENCES

Cheung, Tony D. T., Chan, Terence C. F., Chiu, S. L. and Tang, Charles K. L. (2005). Behaviour of Two Soil Nails under Pull-out Test. The HKIE Geotechnical Division 25th Annual Seminar.

Cheung, W. M., and Lo, D. O. K. (2005), Use of Carbon Fibre Reinforced Polymer Reinforcement in Soil Nailing Works. The HKIE Geotechnical Division 25th Annual Seminar.

Cheung, W. M., Lo, D. O. K., Cheng, P. F. K., Chan, T. C. F. (2007). Use of the Time Domain Reflectometry to Check The Quality of Steel Soil Nails with Pre-installed Wires. Proceedings of the Geotechnical Advancements in Hong Kong since 1970s, Hong Kong.

ETI (2006a). Site Equipment Calibration Guide on Real-time Digital Drilling Process Monitoring & Management System. E-business Technology Institute, the University of Hong Kong, 2p.

ETI (2006b). Site Operation Guide on Real-time Digital Drilling Process Monitoring & Management System. E-business Technology Institute, the University of Hong Kong, 19p.

GEO (2003). Non-destructive tests for Determining the Lengths of Installed Steel Soil Nails, GEO Report No. 133. Geotechnical Engineering Office, Civil Engineering and Development Department, HKSAR Government.

GEO (2005a). Information Note on Rubber Soil (GEO Information Note 1/2005). Geotechnical Engineering Office, Civil Engineering and Development Department, HKSAR Government.

GEO (2005b). Interim Report on Non-Destructive Tests for Checking the Integrity of Cement Grout Sleeve of Installed Soil Nails, GEO Report No. 176. Geotechnical Engineering Office, Civil Engineering and Development Department, HKSAR Government.

GEO (2005c). Pull-out Test of Soil Nails in Hong Kong. Design Division Technical Guideline No. 11. Geotechnical Engineering Office, Civil Engineering and Development Department, HKSAR Government.

GEO (2006a). Evaluation of Application of Drilling Process Monitoring (DPM) Technique for Soil Nailing Works, GEO Report No. 189. Geotechnical Engineering Office, Civil Engineering and Development Department, HKSAR Government.

GEO (2006b) Use of Time Domain Reflectometry to Determine the Length of Steel Soil Nails with Pre-installed Wires, GEO Report No. 198. Geotechnical Engineering Office, Civil Engineering and Development Department, HKSAR Government.

GEO (2007a). Trial of Real-Time Drilling Process Monitoring System, Technical Notes TN/2007. Geotechnical Engineering Office, Civil Engineering and Development Department, HKSAR Government.

GEO (2007b). Good Practice in Design of Steel Soil Nails for Soil Cut Slopes. GEO Technical Guidance Note No. 23. Geotechnical Engineering Office, Civil Engineering and Development Department, HKSAR Government.

HKIE (2003). Soil Nails in Loose Fill Slopes, Final Report, Hong Kong Institution of Engineers.

Ho, N.L., Yau, K.M., Wright, M.J. & Wong, C.W., and Wong, P.C. (2007). Trial of Innovative Soil Nails for Slope Upgrading Works in Hong Kong. 13th Asian Regional Conference.

Schlosser F. & Guilloux A (1981). Le Forttement dan lews sols. Revue Francaise de Geotechnique, No. 16: 65-77.

Shen, J. M. & Kung, Dickson (2005). A trial on the Use of Steel Strands for the Construction of Soil Nails. The HKIE Geotechnical Division 25th Annual Seminar.

Smith, Martyn J., Li, Ronald P. M., Swann, Leslie H. (2005). An alternative Method of Soil Nail Design in Hong Kong. The HKIE Geotechnical Division 25th Annual Seminar.

Swann, L. H., Lorimer, M. J. & Li, R. P. M., Chan, T. C. F. & Leung, F. W. K. (2007). Instrumented Soil Nail Pull-out Tests in Decomposed Tuff and Working Bond Study. The HKIE Geotechnical Division Annual Seminar 2007.

Tang, M.C., Ho, K.K. S., Chan, T.C.F., Chan, C.F. (2007). The Landslip Preventive Measures Programme of the Hong Kong SAR Government – Reflections on Achievement, Advancement and Lessons Learnt in the Past 30 Years. Development, Advancement and Achievements of Geotechnical Engineering in Southeast Asia, The 40th Anniversary Commemorative Volume of the Southeast Asian Geotechnical Society.

Yeung, Albert T., Cheng, Y.M., Lau, C.K., Mak, L.M. (2005). Innovative Korean System of Presssure-Grouted Soil Nailing as a Slope Stabilisation Measures. The HKIE Geotechnical Division 25th Annual Seminar.

Yeung, Albert T. (2008). Collaboration between Hong Kong and Korea on The Development of a Soil Nailing Technique. Seminar on "The State-of-the-art Technology and Experience on Geotechnical Engineering in Korea and Hong Kong". The HKIE Geotechnical Division.

Yue, Z. Q., Lee, C. F., Law, K. T. & Tham, L. G. (2004). Automatic Monitoring of Rotary-percussion Drilling for Ground Characterization – Illustrated by a Case Example in Hong Kong. International Journal of Rock Mechanics and Mining Science. Vol 41, pp 573-612.

Development of Some New Pile Types for Foundation Works in Hong Kong

H.T. Cheung & S. Yuen
Lap Kai Engineering Co. Ltd.
V. Li
Victor Li & Associates Ltd.

ABSTRACT

This paper presents a piling system named Rock Penetration Composite Pile (RPCP) recently accepted by the Buildings Department as a recognized foundation type. The new piling system is a rock socketed pile involving the use of precast prestressed concrete pile (or Spun pile) as the main load-carrying structural element of the pile above the rock socket and reinforcing bars encased in cement grout as the structural element within the rock socket. The paper presents details, load transfer mechanism and results of a full-scale loading test of RPCP. Discussions on developing variations to this new piling system are also presented in the paper.

1 INTRODUCTION

The common foundation types currently used in Hong Kong include bored piles, barrettes, socketed H-piles, driven piles, mini-piles and auger piles. They can be classified in terms of pile capacity as follows:

Pile type	Pile capacity	Examples
Bored pile and barrettes founding on rock	High	A maximum geotechnical pile capacity of 119,105 kN can be attained, for instance, for a bored pile with a shaft diameter of 3m, a socket length of 6m and a bellout diameter of 4.5m designed to be founded on moderately decomposed rock.
Rock-socketed and driven steel H-piles	Medium	Pile capacities of 5900 kN and 3500 kN can be achieved with rock socketed piles and driven piles respectively using Grade S460 305x305x223kg/m H-piles
Mini-piles and auger pile	Low	A pile capacity of 1400 kN can be achieved with mini-piles comprising four 50mm diameter high-yield steel bars and a pile capacity of 3500 can be achieved using a 610mm diameter auger pile constructed.

The cost of steel H-piles has escalated sharply in recent years and nearby doubled in the past twelve months. Rock-socketed H-piles and driven steel H-piles have therefore become increasingly less competitive compared with the traditionally more expensive bored piles. To tackle this problem, a new pile type has recently been developed with an aim to achieve medium pile capacity comparable to conventional rock-socketed H-piles at a lower cost. Details of the new pile type will be discussed in this paper.

2 THE NEW PILING SYSTEM

Figure 1 shows the typical details of the patented pile type recently developed in Hong Kong. The new pile type, which is named Rock Penetration Composite Pile (RPCP), has been accepted by the Buildings Department (BD) as a recognized pile type in 2006 and is given a BD reference number of BD-RP017.

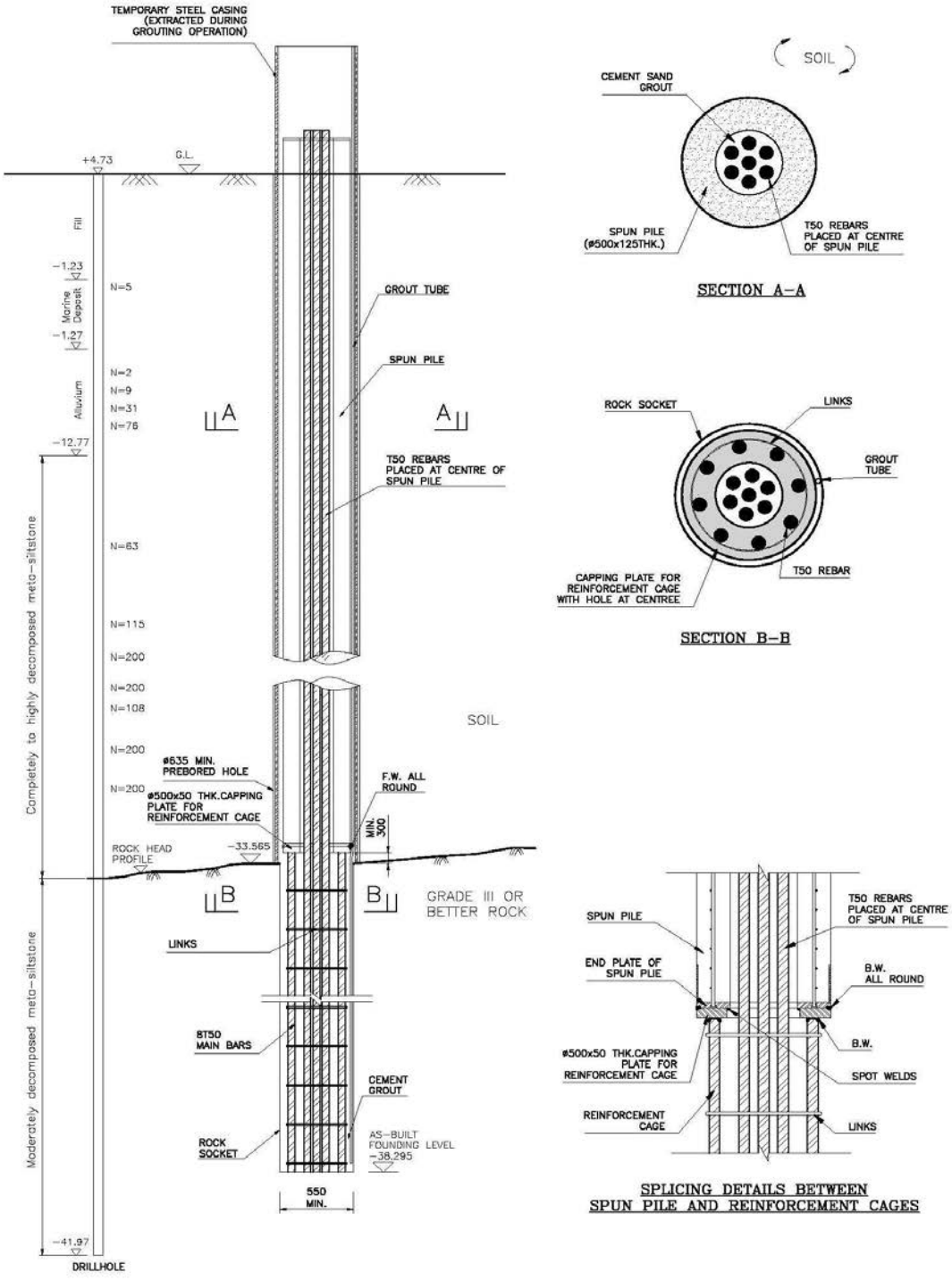

Figure 1: Details of a RPCP (based on an actual test pile)

2.1 Features of a RPCP

RPCPs are rock socketed piles. The salient features of a RPCP are:

a. The structural elements of a RPCP can be divided into two portions. The upper portion is located above the rock socket and is constructed using spliced segments of precast prestressed concrete pile (also commonly known as Spun pile in the literature). The rock socket portion of a RPCP is a pre-fabricated reinforcement cage welded onto a steel capping plate. A RPCP is then formed by welding the steel capping plate of the pre-fabricated reinforcement cage onto the cast-in steel end plate at the lowest end of the Spun pile. A RPCP can be designed to attain a design capacity up to 5104 kN which is comparable to a conventional rock-socketed Grade S460 305x305x223 kg/m steel H-pile
b. Spun piles are not new in Hong Kong. The "Daido piles" commonly used as driven piles in Hong Kong in the past are one type of Spun piles produced by a local manufacturer in Hong Kong. Spun piles are now available from manufacturers in the Mainland China at lower costs. Spun piles are manufactured in standard segments, typically of 12m in length and with steel plates provided at both ends of the pile. Splicing of individual Spun piles can simply be effected by welding the steel end plates together on site.
c. A Spun pile is circular in shape and has a circular hollow at the centre of the pile. Spun piles used in Hong Kong are commonly supplied in standard size of 500mm in outer diameter and with concrete thickness of either 100mm or 125mm. A 100mm thick Spun pile itself can achieve a design pile capacity of 2300 kN while a 125mm thick Spun pile can give a design capacity of 2700 kN. To attain a high axial load capacity for a RPCP, a bundle of 50mm diameter high-yield reinforcing bars are inserted in the central hollow of the Spun pile to the full length of a RPCP down to the bottom of the rock socket. The maximum number of reinforcing bars that can be inserted in the central hollow are 8 and 7 for 100m thick and 125mm thick Spun pile respectively. In essence, the bundle of reinforcing bars and the Spun pile forms a composite reinforced concrete section to enhance the structural capacity of the pile above the rock socket. The central bundle of reinforcing bars also serves to increase the structural capacity of pile within the rock socket.
d. The reinforcement cage at the rock-socketed portion of a RPCP is fabricated from 50mm diameter high yield deformed steel bars. It can be pre-fabricated in a workshop or fabricated on site. As deformed steel bars have a higher bond strength with cement grout than steel H-piles with planar surfaces, the required rock socket length of a RPCP will be smaller in comparison.

2.2 Installation procedures

A RPCP is installed in procedures similar to that of a rock-socketed steel H-pile. The procedures are:

- A pile bore with a diameter sufficient to accommodate a RPCP (usually 635mm) is formed using the Odex method to the required depth. A temporary steel casing is to be sunk to the rockhead level in phase with drilling and to be extracted later during the subsequent grouting process of pile installation.
- The pile bore is cleaned by air-lifting.
- The reinforcement cage can either be welded in advance onto the Spun pile and inserted into the pile bore in a single operation as shown in Figure 2(a). Alternatively, the reinforcement cage can be lowered into the pile bore first and the Spun pile is then connected to the capping plate of the reinforcement cage by welding on site.
- A RPCP can be lengthened if necessary by welding a new segment of Spun pile onto the segment of Spun pile already inserted inside the pile bore. The process can be continued until the entire RPCP has been installed.
- A bundle of reinforcing bars is then inserted into the circular hollow of the Spun pile to the bottom of the pile bore.
- The space in the rock socket, the remaining space in the central hollow of the Spun pile and space left in the pile bore outside the Spun pile are then filled up by cement grout.

Figure 2 shows some photographs taken during installation of a RPCP.

(a) (b)

Figure 2: (a) Reinforcement cage and Spun pile being placed in pile bore
(b) A bundle of reinforcing bars installed inside a Spun pile

2.3 Load transfer mechanism

The load transfer mechanism of a RPCP is similar to that of a conventional rock-socketed steel H-pile. When a RPCP is loaded axially, the loading will firstly be transferred to the composite reinforced concrete section formed by the Spun pile and the bundle of reinforcing bars installed inside the central hollow of the Spun pile. The loading will then be transferred to reinforcement cage below the Spun pile in the rock socket. The loading sustained by the reinforcing cage in the rock socket will ultimately be transferred to the bedrock through interface shear stresses developing between reinforcing bars and cement grout and between cement grout and rock.

3 LOAD TEST RESULTS

To verify the design capacity of RPC piles, a full-scale loading test was carried out in 2006 on a test pile designed to its full capacity at working load of 5104 kN. Details of the test piles and the ground profile at the test pile location are actually presented in Figure 1. The test pile was 43m in length with a 4.73m rock socket in moderately decomposed meta-siltstone. Figure 3 shows a photograph of rock cores taken at a location close to the test pile and at depths equal to the rock socket depth of the test pile. It can be observed that the meta-siltstone at the location of the rock socket was highly fractured and closely jointed.

A RPCP is designed as a rock-socketed pile deriving its geotechnical capacity mainly from the strength of the rock socket. It was considered desirable to construct the test pile such that the test load can be transferred to the rock socket as much as possible during a loading test. An effort was therefore made to reduce the frictional resistance along the Spun pile by coating it with bituminous paint and then wrapping the coated Spun pile by plastic sheets before installation.

The test pile was load-tested to twice the design pile capacity (i.e.10208 kN) in accordance with test procedures specified in the Code of Practice for Foundations (BD, 2004).

Figure 3: Rock quality at rock socket location of test pile

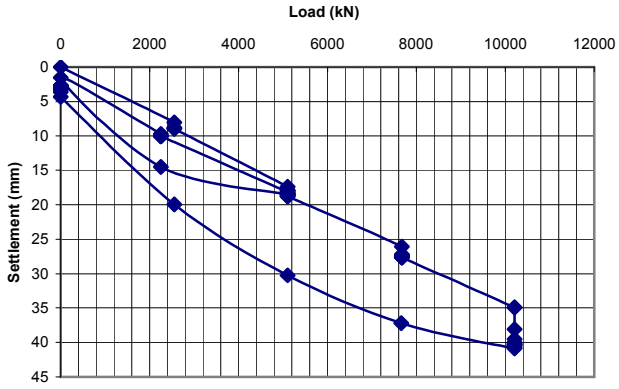

Figure 4: Load-settlement curve of test pile

Figure 4 shows the load-settlement curve of the test pile. The load-settlement response is largely linear throughout the entire range of virgin loading. About 6mm of delayed or creep settlement occurred during the 72 hours of maintained loading at maximum test load. Upon full unloading from peak test load, the residual settlement was only 2.68mm. This suggested that over 50% of the settlement occurring within the 72 hours of maintained loading at maximum test load were recoverable.

The small residual settlement indicated that the pile response was essentially elastic. The ultimate load of the test pile is expected to be significantly higher than the maximum test load of 10208 kN. This indicated that significant pile resistance had developed even if the pile was socketed in highly fractured rock. The test pile demonstrated the adequacy of the new piling system.

4 FURTHER DEVELOPMENTS

There are variations to the above new piling system which are covered by the same patent. Such variations are also covered by the same new pile type recognized by the BD. They differ in the design of structural elements in the rock socket. A steel H-pile can be used in lieu of the reinforcement cage as shown in Figure 5(a) and the bundle of reinforcing bars within the Spun piles will not be extended into the rock socket. As another variation, more reinforcing bars can be used in fabricating the reinforcement cage to achieve the same structural capacity and the bundle of reinforcing bars within the Spun pile will be terminated at the bottom o the Spun pile. The adequacy of RPCP with the design variations shown in Figure 5 has also been confirmed by loading tests, although the test results are not presented in this paper due to lack of space.

5 DISCUSSIONS AND CONCLUSIONS

A new piling system is developed to take advantage of the lower material costs of Spun piles. Different variations and pile capacities of the same piling system can be developed by varying the structural details of the pile within the rock socket and changing the number of reinforcing bars to be provided within the central hollow of the Spun pile and in the rock socket. The piling system is proven to be viable by full scale loading tests. It is recognized by the Buildings Department as a safe piling system.

The maximum capacity of RPCP currently approved by the BD is limited to 10208 kN. Although RPCPs tend to be more economical than conventional rock-socketed steel H-piles, considerations are given to develop rock penetration composite piles with a higher pile capacity in future using steel bars with an even higher design yield strength such that the new piling system can outperform conventional rock-socketed H-piles both in terms of costs and pile capacity.

REFERENCES

Buildings Department (BD). 2004. Code of Practice for Foundations.

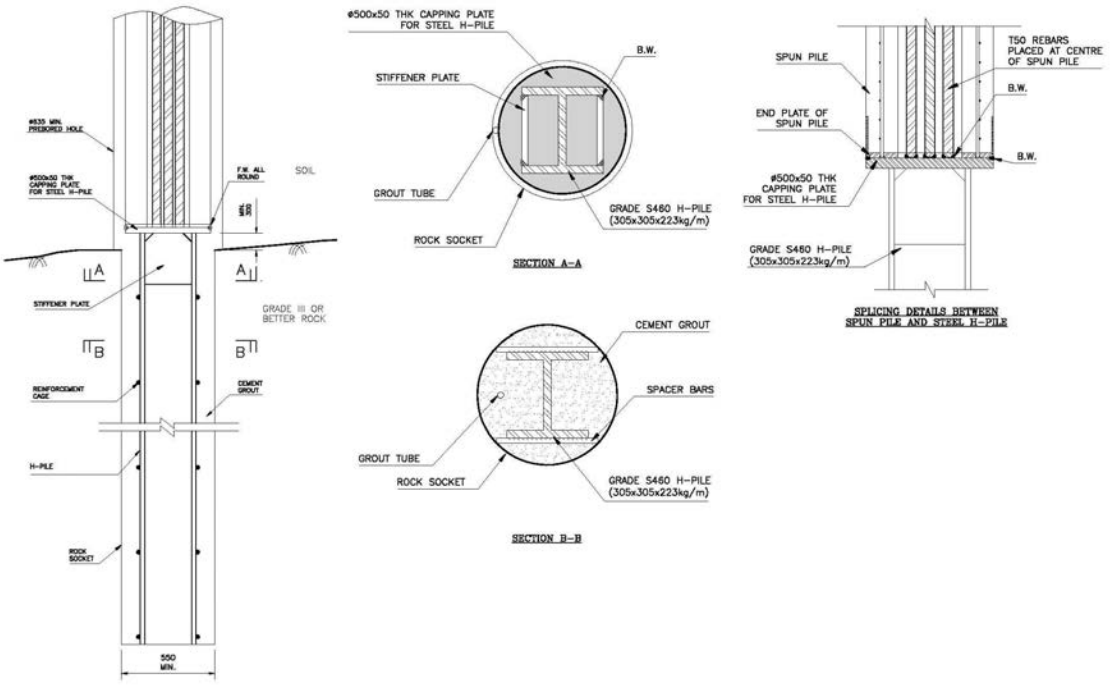

(a)

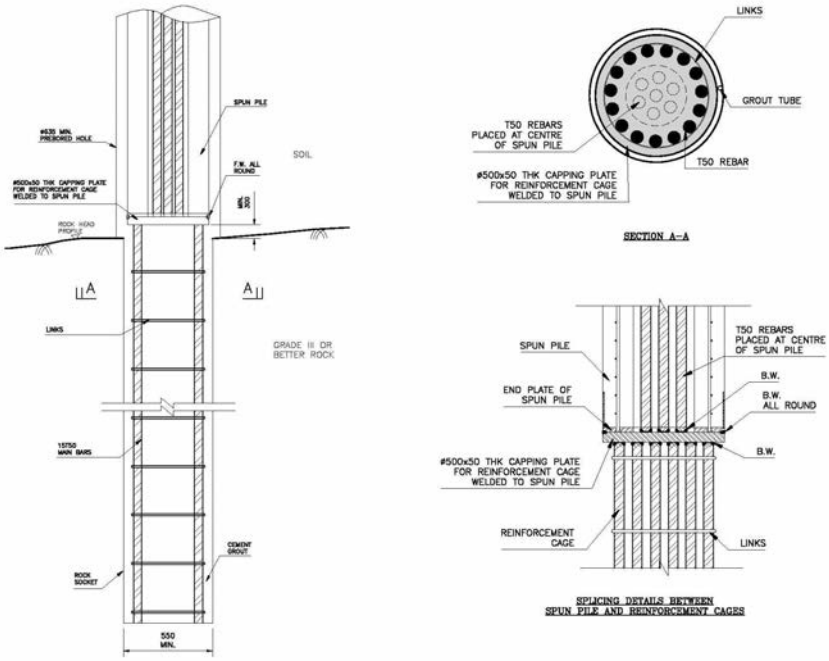

(b)

Figure 5 : Variations of design details of RPCP

Use of Time Domain Reflectometry in Soil Nailing Works

W.M. Cheung, D.O.K. Lo and W.K. Pun

Geotechnical Engineering Office, Civil Engineering and Development Department
The Government of the Hong Kong Special Administrative Region

ABSTRACT

Time domain reflectometry (TDR) technique is conventionally applied in geotechnical engineering for the detection of slip planes and groundwater levels in slopes, and determination of soil moisture content. Since 2004, the Geotechnical Engineering Office of the Civil Engineering and Development Department has adopted TDR technique as part of its quality control measures on soil nailing works. While development work on this subject is being further pursued, an innovative idea of using TDR technique as an alternative to the use of packers to control the designated grouted length of soil nails in pullout tests has recently evolved. This paper presents the principle and the findings of field trials of using TDR technique to determine the grouted length of soil nails in pullout tests. The working procedure that has been developed, and the merits and limitations of the technique are also described.

1 INTRODUCTION

Soil nailing technique was introduced to Hong Kong in the 1980s. Nowadays, it is the most popular slope stabilizing method in Hong Kong. Each year, more than 10,000 soil nails are installed to stabilise slopes under the Landslip Preventive Measures (LPM) Programme administrated by the Geotechnical Engineering Office (GEO) of the Civil Engineering and Development Department (CEDD). In order to enhance the quality control of soil nailing works, the GEO strengthens site supervision and introduces an independent site audit on soil nail construction works, and in 2001 began to identify and try out potential non-destructive testing (NDT) methods that could be carried out on installed soil nails to infer their as-built quality. Among the potential NDT methods that have been examined, TDR was the simplest and least expensive (Cheung, 2003; Cheung et al, 2007). While development work on this subject is being further pursued, an innovative idea of using TDR as an alternative to the use of packers to control the designated grouted length of soil nails in pullout tests has recently evolved. This paper describes the principle and findings of the field trials of using TDR technique in the determination of the grouted length of soil nails in pullout tests. The working procedure that has been developed together with the merits and limitations of the technique are also presented.

2 PRINCIPLE

The principle of TDR technique was derived in the 1950s from that of radar. Instead of transmitting a 3-D wave front in radar, the electromagnetic wave in the TDR technique is confined in a waveguide (O'Connor & Dowding, 1999). TDR is commonly used in the telecommunications industry for the identification of discontinuities in transmission lines. In the 1980s, the application of the technique was extended to other areas such as geotechnology, hydrology, material testing, etc (Dowding & Huang, 1994; Siddiqui et al, 2000; Liu et al, 2002; Lin & Tang, 2005). TDR is based on transmitting electromagnetic pulses through a transmission line, which is in the form of coaxial or twin-conductor configuration, and receiving reflections at the locations of discontinuities. Whenever there is a change in the impedance of the transmission line, a signal will be reflected from the point of change.

If a wire is pre-installed alongside a soil-nail reinforcement, which is generally a steel bar, the configuration becomes analogous to a twin-conductor transmission line and the end of the reinforcement-wire pair becomes a discontinuity (Cheung, 2003; Cheung & Lo, 2005). If the wire and the reinforcement at the soil nail end are not connected electrically (i.e. an open circuit), a positive signal will be reflected from the

end of the pair as shown in Figure 1(a), otherwise a negative reflection as shown in Figure 1(b) will be obtained. If the wire and the reinforcement are of different lengths, a signal will be reflected at the end of the shorter one.

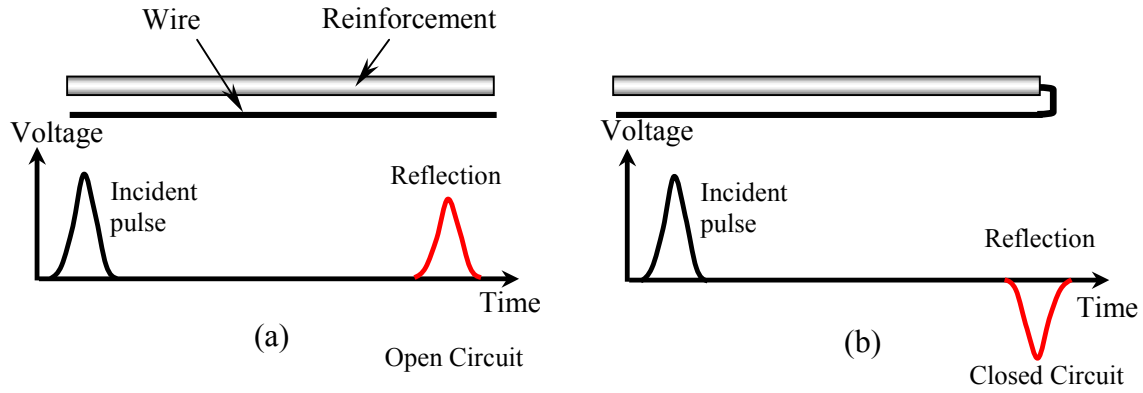

Figure 1 – Theoretical TDR waveform of a soil nail with and without an electrical contact at the end

3 DETERMINATION OF GROUTED LENGTH USING TDR TECHNIQUE

It is common practice to carry out field pullout tests of soil nails to verify the design assumptions of the bond strength at the interface between the ground and the cement grout sleeve. The credibility of the verification depends on, among various factors, the accuracy of the as-built grouted length. Conventionally, the as-built grouted length is controlled by placing a packer between the grouted and the free length sections of the soil nails for pullout tests.

As an alternative to the use of packer, one can in principle use TDR technique to detect the grouting front and stop injection of grout into the drillhole when the grout just fills up the intended grouted portion. This involves the installation of a wire with a length that equals the free length of the soil nail, L_U ($L_U = L - L_G$) (see Figure 2). Following the principle described in Section 2, a positive reflection will be returned at the end of reinforcement-wire pair (i.e. end of the wire) prior to grouting (see Figure 2a). When the level of grout touches the end of the wire, the wire and the reinforcement will be electrically in contact via the fluid grout. Consequently, the polarity of the reflected pulse will switch from positive to negative (see Figure 2b). At this incidence, the grouting operation can be stopped. The as-built grouted portion will have a shape and length similar to that shown in Figure 2(b).

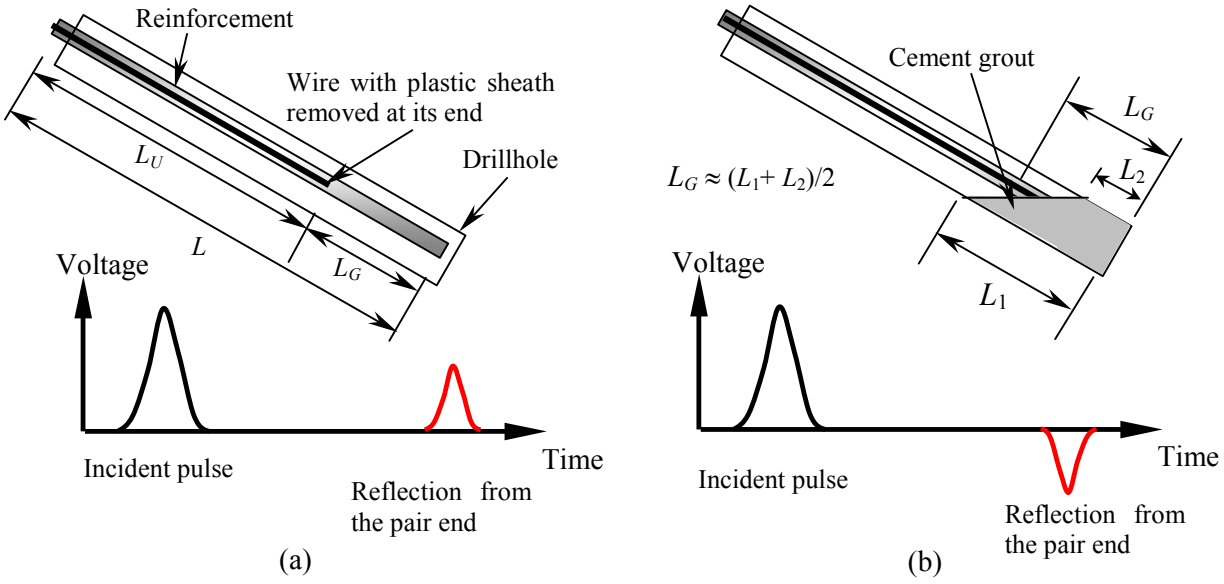

Figure 2 – Theoretical TDR waveforms of a soil nail before and after grouting

In practice, even if one stops the grouting operation at the incidence when the reflected pulse switched polarity, the grouted length will continue to increase due to extra grouting during the time lapsed between the first observation of reverse polarity of reflected pulse and the actual cessation of grouting and the surplus grout from the grout tube. A number of refinements to the operation can be made to reduce the difference between the design grouted length (L_G) and the as-built average grouted length (L_A), and to improve the accuracy of the measurements:

(a) the length of the wire is made longer than the free length of the soil nail, say by 100 mm,
(b) the wire is to be placed inside a perforated tube installed alongside the steel reinforcement and is free to move along the tube, and
(c) the head of the wire is graduated to facilitate the determination of the exact length of wire inside the tube when the wire is withdrawn from or pushed into the tube.

This technique evolves the following working procedure:

(d) Pre-install a plastic tube with a copper wire as shown in Figure 3.
(e) Connect the TDR instrument to the pullout nail (one clip to steel reinforcement and the other to the wire).
(f) Identify the positive pulse reflected from the end of the reinforcement-wire configuration (i.e. the end of the wire) as shown in Figure 4(a).
(g) Record the marking on the wire.
(h) Start grouting works.
(i) Stop grouting works when there is a change in the polarity (i.e. from positive to negative) of the reflected pulse as identified in Step (c) (see Figure 4(b)).
(j) If the reflected pulse remains negative, withdraw the wire slowly until the pulse changes to positive again.
(k) Record the marking on the wire.
(l) Estimate the as-built grouted length based on the readings recorded in Steps (d) and (h).

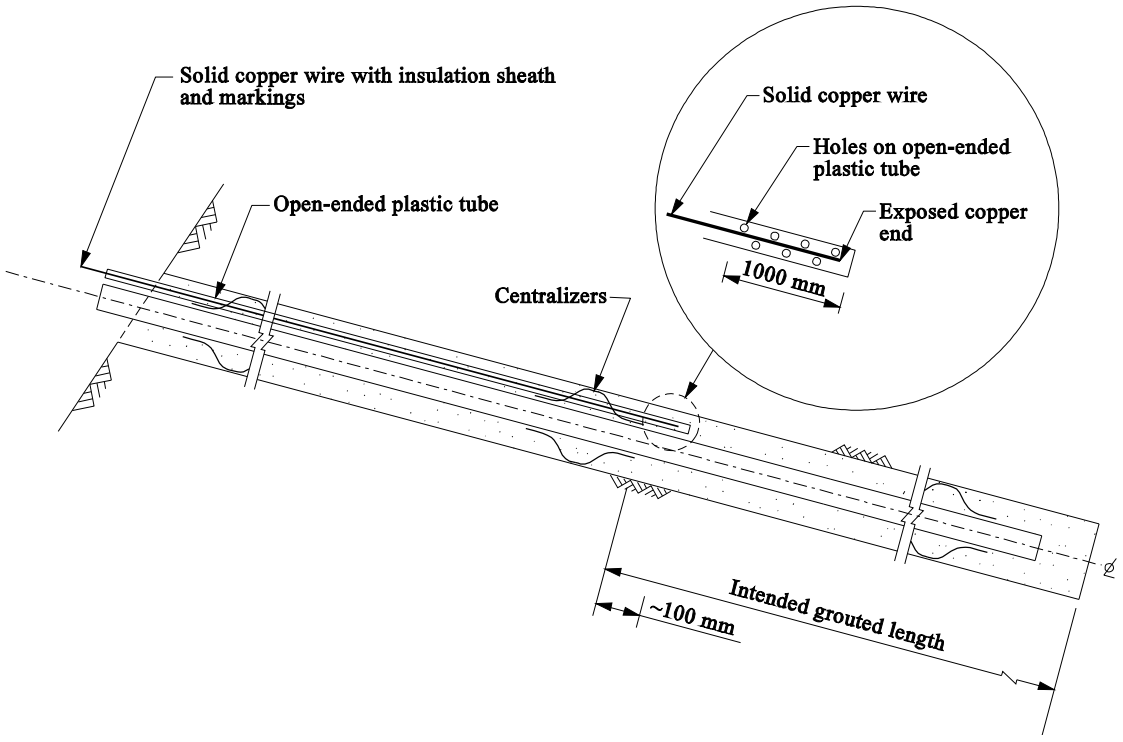

Figure 3 – Details of soil nail in pullout test

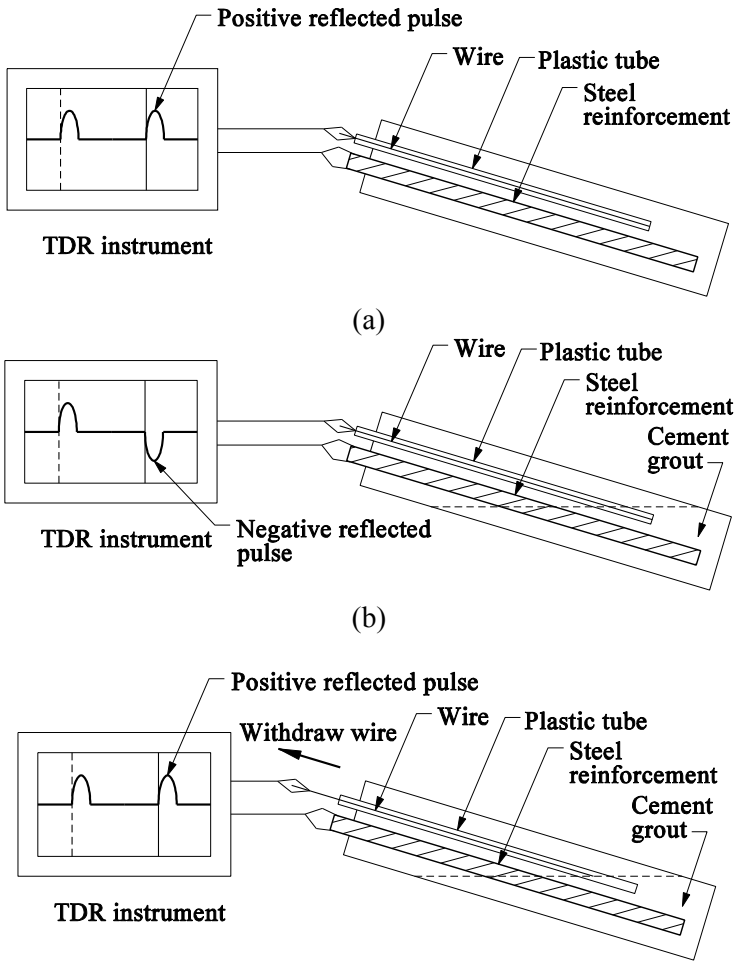

Figure 4 – Procedure of using TDR to determine the grouted length of soil nails in pullout test

4 FIELD TRIAL

In order to investigate the practicability and accuracy of this technique, an experiment was carried out. In the experiment, a 10 m long reinforcement was installed inside a 100 mm diameter transparent plastic pipe, which was inclined at an angle of 10^{o} below horizontal (Plate 1). The intended grouted length was 1.5 m.

(a) Overview (b) Close-up

Plate 1: Set-up of the field demonstration

Plate 2a shows the positive reflection prior to the grout font contacting the copper wire. When the grout front reached the wire end, a negative reflection, as shown in Plate 2b, was observed and the grouting works was stopped. The wire was then withdrawn slowly until the point of change in polarity was identified. Based on the markings on the wire, the grouted length was estimated to be 1.57 m. The actual grouted length was measured by tape to be 1.55 m.

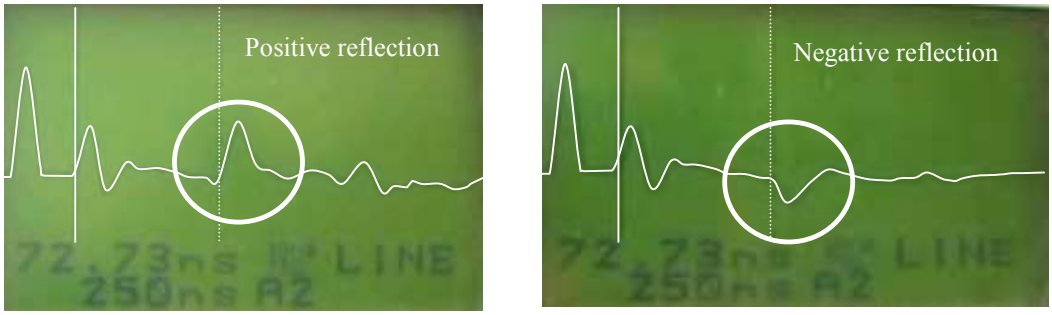

(a) TDR waveform before the grout front touching the wire

(b) TDR waveform after the grout front touching the wire

Plate 2: The change in TDR waveform before and after the touching of grout front to the wire

The experiment demonstrated the accuracy of the method. Field trial was carried out at an LPM site to assess its feasibility under working conditions. The field trial indicates that the installation of the set-up was quick and simple. The working procedure was easy to follow. The measured and the intended grouted lengths are shown in Table 1.

Table 1: Results of field trial

Pullout soil nail	Intended grouted length (m)	Measured grouted length (m)
P2	2.0	1.9
P3	2.0	2.2
P4	2.0	2.2

5 DISCUSSION

The field trials indicate that the TDR technique can be used to determine the as-built grouted length of soil nails in pullout test with a fairly high accuracy. The test was simple, efficient (completed in a few minutes) and no packer is necessary. Most of the set-up can be reused except the perforated plastic tube. However, because of the absence of packer, only the average grouted length can be measured (see Figure 2(b)). Unlike the use of packers, which control the as-built grouted length to the intended grouted length, this technique only measures the as-built grouted length. Nevertheless, since the as-built grouted length is known, the pullout test results can be properly interpreted for assessing whether the design requirements are met.

A limitation of the technique is that it may not be feasible if the grouted zone is submerged in groundwater, in particular when the groundwater contains high minerals content, where a close circuit will be formed regardless of the presence of cement grout.

Apart from TDR instrument, the feasibility of using other commercial instrument to determine the grouted length has been explored. Field tests indicate that a multi-meter, which is commonly used to detect a close circuit and to measure electrical properties such as voltage and resistance, can be used as an alternative to TDR instrument for grouted length measurement.

6 CONCLUSION

By using the TDR technique, the process of the grouting can be monitored and the actual grouted length for a pullout test can be measured. This provides an alternative to using a packer for controlling the grouted length of the test nail. Field trial demonstrated that the technique is feasible and reliable.

ACKNOWLEDGEMENTS

This paper is published with the permission of the Head of the Geotechnical Engineering Office and the Director of Civil Engineering and Development of the Government of the Hong Kong Special Administrative Region. Valuable assistance was given by Ms Alice C.S. Lai of the Geotechnical Engineering Office and Mr Ringo L.Y. Cheong of Halcrow China Ltd in arranging the site trial. All contributions are gratefully acknowledged.

REFERENCES

Cheung, W.M. 2003. *Non-Destructive Tests for Determining the Lengths of Installed Steel Soil Nails (GEO Report No. 133)*. Geotechnical Engineering Office, Hong Kong, 54 p.

Cheung, W.M. & Lo, D.O.K. 2005. *Interim Report on Non-Destructive Tests for Checking the Integrity of Cement Grout Sleeve of Installed Soil Nails (GEO Report No. 176)*. Geotechnical Engineering Office, Hong Kong, 43 p.

Cheung, W.M., Lo, D.O.K., Cheng, P.F.K. & Chan, T.C.F. 2007. Use of time domain reflectometry to check the quality of steel soil nails with pre-installed wires. *Proceedings of the HKIE Geotechnical Division 27th Annual Seminar*, HKIE, Hong Kong, pp. 233-239.

Dowding, C.H. & Huang, F.C. 1994. Early detection of rock movement with time domain reflectometry. *Journal of Geotechnical Engineering*, ASCE, Vol. 120, pp. 1413-1427.

Lin, C.P. & Tang, S.H. 2005. Development and calibration of a TDR extensometer for geotechnical monitoring. *Geotechnical Testing Journal*, ASTM, Vol. 28, No. 5, pp. 464-471.

Liu, W., Hunsperger, R., Chajes, M., Folliard, K. & Kunz, E. 2002. Corrosion detection of steel cables using time domain reflectometry. *Journal of Materials in Civil Engineering*, ASCE, Vol. 14, No. 3, pp 217-223.

O'Connor, K.M. & Dowding, C.H. 1999. GeoMeasurements by Pulsing TDR Cables and Probes. CRC Press, 394 p.

Siddiqui, S.I., Drnevich, V.P. & Deschamps, R. 2000. Time domain reflectometry development for use in geotechnical engineering, *Geotechnical Testing Journal*, ASTM, Vol. 23, No. 1, pp. 9-20.

Review of the Approach for Estimation of Pullout Resistance of Soil Nails

W.M. Cheung, K.W. Shum & W.K. Pun
Geotechnical Engineering Office, Civil Engineering and Development Department
The Government of the Hong Kong Special Administrative Region

ABSTRACT

Pullout resistance is one of the key parameters for the design of soil nails. At present, methods for estimating pullout resistance are not unified as reflected by the many approaches used in different technical standards and codes of practice. As part of a series of soil nail related studies initiated by the Geotechnical Engineering Office (GEO), Civil Engineering and Development Department of the HKSAR Government in developing a new guidance document on soil nailing, a review of the design methods and safety factors adopted by Hong Kong and overseas, including the US, Japan and some European countries (the UK, France, and Nordic countries), for estimation of pullout resistance of soil nails has been conducted. Field pullout test data have also been collected from local construction sites for analysis. Potential areas for improvement are identified. This paper presents and discusses the findings of the review as well as the new design approach.

1 INTRODUCTION

Nowadays, soil nailing is the most common slope stabilising method in Hong Kong. It offers an effective, robust and economic reinforcing system for a variety of ground and groundwater conditions, and more than 200 man-made slopes are upgraded using soil nails each year under the Landslip Preventive Measures (LPM) Programme. The soil nailing technique improves the stability of slopes principally through the mobilisation of tension in the soil nails. The tensile forces in the soil nails reinforce the ground by directly supporting some of the applied shear loadings and by increasing the normal stresses in the soil on the potential failure surface, thereby allowing higher shearing resistance to be mobilised. The resistance against pullout failure of the soil nails is provided by the part of soil nails that is embedded into the ground behind the potential failure surface. Hence, pullout resistance is one of the key parameters for the design of soil nails.

In 2008, GEO published a new guidance document on soil nailing, entitled Geoguide 7 : Guide to Soil Nail Design and Construction (GEO, 2008). Modifications have been made to the previous pullout resistance design guidelines given in GEO Technical Guidance Note No. 23 Issue No. 1 (TGN23) (GEO, 2005). The changes were made based on the findings of a review of the approach for estimation of pullout resistance, which was part of a series of soil nail related studies initiated by GEO in developing Geoguide 7. In the review, the design methods and safety factors adopted in Hong Kong and overseas for estimation of pullout resistance of soil nails have been examined, and about a thousand of field pullout test data collected from the LPM contracts since 2004 have been analysed. This paper presents and discusses the findings of the review as well as the new pullout resistance design guidelines given in Geoguide 7.

2 DESIGN APPROACH OF PULLOUT RESISTANCE OF SOIL NAILS

2.1 Design approach in TGN23

The previous design approach of pullout resistance of soil nails given in TGN23 basically followed that proposed by Watkins & Powell (1992). The effective stress method (see Section 2.2.1) was used to estimate the pullout resistance of the soil nails. A safety factor against pullout failure of 2.0 is applied to the estimated pullout resistance to obtain the allowable pullout resistance. The safety factor accounts for the uncertainty on the surface area of grout sleeve, contact stress at the interface between grout and soil, grout surface roughness, reduction in bond resistance over time, etc.

2.2 Design approaches in overseas countries

Soil nailing design guidelines adopted overseas, including the US, the UK, France, Japan and Nordic countries (i.e., Norway, Sweden, Denmark, Finland and Iceland), have been reviewed. Different design methods and different safety factors are used in these countries to estimate the pullout resistance of soil nails.

2.2.1 Design methods

The pullout resistance of a soil nail is affected by factors including soil type, shear strength, surface roughness of grout sleeve, drilling and grouting technique, the presence of groundwater, etc. According to literature (CIRIA, 2005; Clouterre, 1991; FHWA, 1998 & 2003; HA, 1994; JHPC, 1998; NGS, 2005), there are four practical methods for estimation of pullout resistance of soil nails. The methods are briefly described below.

(a) Empirical correlations. Empirical correlations of the bond stress of soil nail in soil with various soil types and various construction methods have been developed overseas. This method is adopted in the US (correlated with soil type), Japan (correlated with SPT-N values) and France (correlated with limit pressure from pressuremeter tests) for design of soil nails. Typical values of soil-nail bond stress are also given in the overseas design guides (e.g., Clouterre, 1991; FHWA, 1998 & 2003; JHPC, 1998).

(b) Field pullout tests. This method requires the carrying out of site-specific pullout tests. Appropriate characteristic pullout resistance for design of soil nails can be determined from the measured values. This method is adopted in France and such provision is also given in other European countries and the US (BSI, 2002; FHWA, 2003).

(c) Undrained shear strength method. The pullout resistance of soil nails in cohesive soils can be estimated using the undrained shear strength and an adhesion factor, in a way similar to piles in clay.

(d) Effective stress method. The pullout resistance of soil nails in granular soils, and in cohesive soils under long-term conditions, can be calculated by considering the effective stress acting on the soil nail and the coefficient of interface friction. This method is adopted in the UK and Hong Kong.

2.2.2 Safety factor against pullout failure

A summary of safety factor against pullout failure adopted in various design guides is given in Table 1.

Table 1 : Safety factor against pullout failure adopted in different soil nail design guides

Design guide	UK (HA 68/94)	UK (CIRIA C637)	Nordic countries (NGS)	France (Clouterre)	US (FHWA)	Japan (JHPC)	HK (TGN23)
Safety factor	1.0 (ϕ_{cv}') 1.5 (ϕ_{peak}')	1.5	1.5	1.4 (pullout test) 1.8 (chart)	2.0	2.0	2.0

As the UK, France and Nordic countries adopt the limit state design approach, it would be difficult to make a direct comparison between the global safety factor of Hong Kong and the partial safety factors of these countries. Among these design guides, HA 68/94 (HA, 1994) and CIRIA C637 (CIRIA, 2005) adopt the effective stress method to estimate the pullout resistance of soil nails, but they have a slight difference from TGN23 in the effective stress equations used, which is basically related to the assumption on reinforcement shape and radial stress distribution.

3 ANALYSIS OF FIELD PULLOUT TEST DATA

Field pullout test data have been collected from LPM contracts since 2004. Improved test set-up and procedures (GEO, 2004) were adopted. The improvement helps to minimise friction loss along a test soil nail, achieve better control of the length of the grouted portion and increase the test load by using larger bar size. A total of 914 test results were collected. About 84% of the tests were conducted in weathered granite and volcanic rocks. The rest were conducted in other types of materials such as fill, colluvium and moderately decomposed rock.

Most of the pullout tests were only tested to 90% of the yield strength of steel (T_p), i.e., not reaching the

ultimate pullout resistance (T_{ult}). Figure 1 shows the plot of the ratio of the field pullout resistance (T_{field}) to the estimated pullout resistance ($T_{estimated}$) (using TGN23) against the overburden pressure. Some of the field pullout tests (26 nos.) were carried out under saturated condition, and the results do not show particularly low pullout resistance when compared with other pullout tests carried out under dry condition of the same overburden pressure.

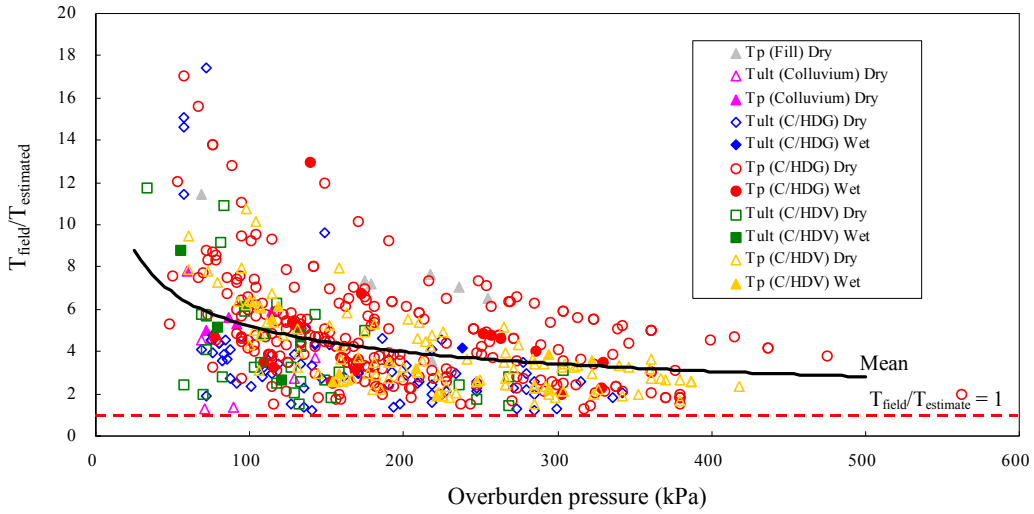

Figure 1 : Plot of field ($T_p + T_{ult}$) to estimated pullout resistance against overburden pressure

5 DISCUSSION

5.1 Design method

There are four practical methods for the estimation of pullout resistance of soil nails. The merits and limitations of the methods are summarised in Table 2.

Table 2 : Merits and limitations of the methods for estimation of pullout resistance of soil nails

Method	Merits	Limitations
Empirical correlations	Related to field performance data; can better account for influencing factors.	Need a large number of field data and take a long time to establish a reasonable correlation; a general correlation may not be applicable to all sites.
Field pullout tests	Related to site-specific performance data.	Need to carry out a considerable number of field pullout tests during the design stage; not feasible for small-scale project; time consuming.
Undrained shear strength method	Based on soil mechanics principles; easy to apply.	Generally not suitable for Hong Kong; many factors that affect the pullout resistance are not accounted for.
Effective stress method	Based on soil mechanics principles; easy to apply.	Many factors that affect the pullout resistance are not accounted for.

Many design guidelines recommend the use of empirical correlation. However, the overseas experience may not be applicable to Hong Kong because of difference in ground condition. To develop a correlation specific to a site in Hong Kong, sufficient good quality data have to be collected. Although the effective stress method has limitations, local designers are familiar with the method and it gives a safe solution for soil nail design in Hong Kong.

5.2 Safety factor against pullout failure

Many factors that affect the pullout resistance of a soil nail are difficult to be quantified in a design. The effective stress method does not account for factors including soil arching, restrained soil dilatancy, soil

suction, roughness of drillhole surface, over-break, etc. All these factors except soil arching tend to result in higher pullout resistance than the design value. Field pullout test data support this hypothesis in that the actual pullout resistance is generally much higher than that estimated in design.

A statistical approach has been adopted to analyse the safety factor against pullout failure using the field pullout test data. The probabilities of failure in pullout with safety factor of 2.0 and 1.5 are estimated by comparing the field pullout resistance with the allowable pullout resistance, where allowable pullout resistance is equal to the estimated pullout resistance divided by the safety factor against pullout failure. Frequency distribution and probability density function plots of the safety margin ($T_{field}/T_{allowable}$) for safety factors equal to 2.0 and 1.5 are given in Figures 2 and 3.

By fitting the field test results with log-normal model as in Figures 2 and 3, nearly all of the modelled field pullout resistance is larger than the allowable pullout resistance, with mean ratios (field vs allowable) of 7.6 and 5.7 if the factor of safety equals to 2.0 and 1.5 respectively. This gives comfort on the use of the effective stress method and the recommended minimum factor of safety in Geoguide 7 : Guide to Soil Nail Design and Construction (GEO, 2008).

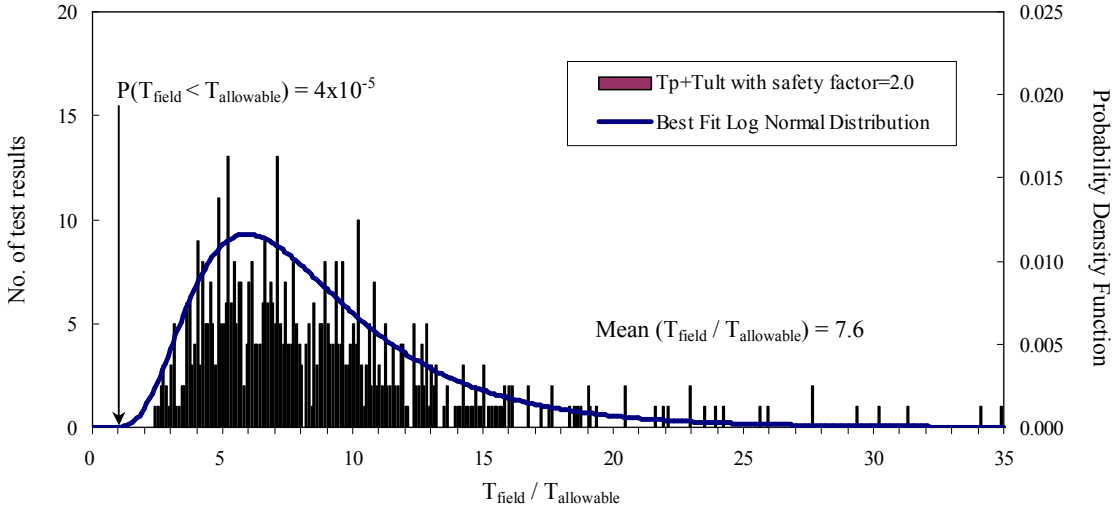

Figure 2 : Plot of frequency distribution and probability density function of field to allowable pullout resistance with safety factor against pullout failure = 2.0

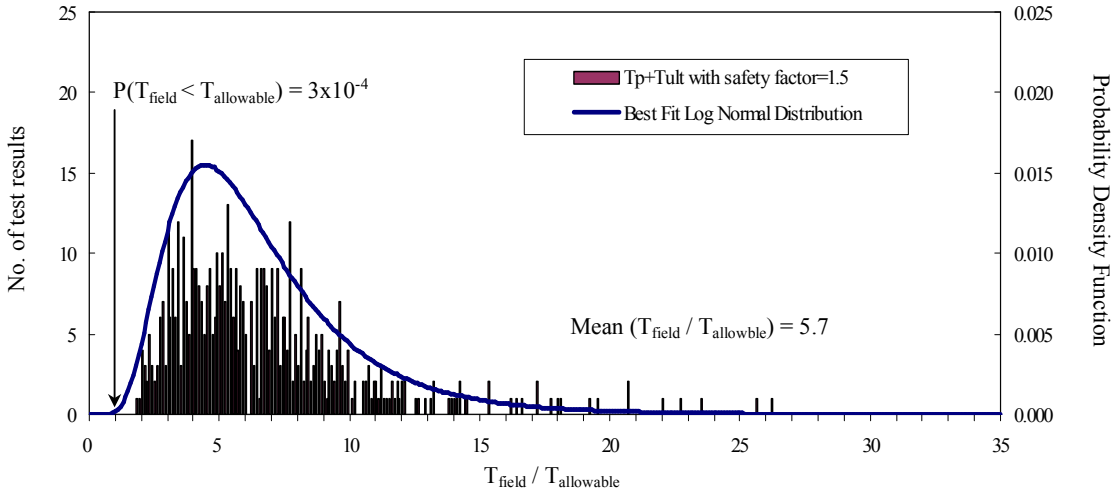

Figure 3 : Plot of frequency distribution and probability density function of field to allowable pullout resistance with safety factor against pullout failure = 1.5

5.3 Effect of Soil Arching

The process of drilling in soil nail construction introduces soil arching around the grout sleeve of a soil nail. The grouting process during construction and any disruption to the soil surrounding a soil nail in the long term, e.g., wetting and drying, will reduce the amount of soil arching along time. The presence of soil arching significantly reduces the radial stress acting on the soil nail. This will theoretically result in a low pullout resistance. However, field pullout test results show the contrary, i.e., the pullout resistance is high. This reflects the limitation of the effective stress method which does not account for surface roughness, soil dilatancy, etc., as noted in Section 5.2 above. Strictly speaking, the effective stress method is a semi-empirical method which involves large uncertainty in the pertinent factors particularly where no field data are available for evaluation of arching, surface roughness, soil dilatancy, etc. Although a factor of safety of 1.5 or 2.0 seems to be on the high side, given that there may be a limit on the "positive effect" attributed by factors like soil dilatancy, it is necessary to limit the overburden pressure for the calculation of pullout resistance to account for this uncertainty.

6 CONCLUSIONS

A review of the approach to the estimation of pullout resistance of soil nails in Hong Kong and overseas has been conducted. Based on literature review and field pullout test data analysis, potential areas for improvement in the design method and safety factor as given in TGN23 have been identified. Modifications have been made to the pullout resistance design guidelines, which are promulgated in the new guidance document Geoguide 7 : Guide to Soil Nail Design and Construction. While the effective stress method may continue to be adopted for estimating the pullout resistance of soil nails, one should caution the limitations of the method. It may be treated as a semi-empirical design tool, which has been applied in Hong Kong with successful performance for over 15 years. Nevertheless, Geoguide 7 does not preclude the use of other methods to establish site-specific empirical correlation or design parameters for pullout resistance provided that due consideration is given to the adequacy and quality of the field data, representativeness of the test results, the reliability of the empirical correlation, and the safety margin needed.

ACKNOWLEDGEMENTS

This paper is published with the permission of the Head of the Geotechnical Engineering Office and the Director of Civil Engineering and Development, The Government of the Hong Kong Special Administrative Region. The assistance of LPM Division 2 of the Geotechnical Engineering Office in collecting the field pullout test data is gratefully acknowledged.

REFERENCES

BSI. 2002. *Execution of Special Geotechnical Work – Soil Nailing (prEN 14490 : 2002) (Draft)*. British Standard Institution, London, UK.

Clouterre. 1991. *French National Research Project Clouterre - Recommendations Clouterre (English Translation 1993)*. Federal Highway Administration, FHWA-SA-93-026, Washington, USA.

CIRIA. 2005. *Soil Nailing – Best Practice Guidance (CIRIA C637)*. Construction Industry Research and Information Association, UK.

FHWA. 1998. *Manual for Design and Construction Monitoring of Soil Nail Walls, Report No. FHWA-SA-96-069R*. Federal Highway Administration, US Department of Transportation, Washington D.C., USA.

FHWA. 2003. *Geotechnical Circular No. 7, Soil Nail Walls, Report No. FHWA0-IF-03-017*. Federal Highway Administration, US Department of Transportation, Washington D.C., USA.

GEO. 2004. *Design Technical Guidance No. 11 – Pullout Tests of Soil Nails in Hong Kong*. Geotechnical Engineering Office, Civil Engineering and Development Department, Hong Kong.

GEO. 2005. *Technical Guidance Note No. 23 – Good Practice in Design of Steel Soil Nails for Soil Cut Slopes. Issue No.1 (TGN 23)*. Geotechnical Engineering Office, Civil Engineering and Development Department, Hong Kong.

GEO. 2008. *Guide to Soil Nail Design and Construction (Geoguide 7).* Geotechnical Engineering Office, Civil Engineering and Development Department, Hong Kong.

HA. 1994. *Design Methods of the Reinforcement of Highway Slopes by Reinforced Soil and Soil Nailing Technique (HA 68/94)*. Highway Agency, UK.

JHPC. 1998. *Guide for Design and Construction on Soil-Nailed Cut Slopes (In Japanese)*. Japan Highway Public Corporation, Japan.

NGS. 2005. *Nordic Guidelines for Reinforced Soils and Fills*. The Geosynthetic Group, The Nordic Geotechnical Societies.

Watkins, A.T. & Powell, G.E. 1992. Soil nailing to existing slopes as landslip preventive works. *Hong Kong Engineer*, March, Hong Kong, pp. 20-27.

Application of Computed Tomography Technology for Exploration of Underground Cavities and Solution Features

S.L. Chiu & D.K.C. Yu

Maunsell Geotechnical Services Limited, Hong Kong

ABSTRACT

The Computed Tomography (CT) technology has been used widely in medical science for years. CT scanning has nowadays become a very important tool for disease diagnosis in medical examinations and diagnoses of hidden anomalies in numerous engineering applications. CT technology has been applied to civil engineering works and particularly gained its popularity in recent years in geological and geo-environmental investigations. There are not many cases reported on its application on foundation construction in ground of solution features and cavities. This paper presents a case of its application on detection of underground solution features and cavities for a property development site in Dalian PRC, where two buildings, each 5 to 6 storeys high and 240 m by 140 m in plan. Preliminary ground investigation revealed that underlying the top 20 m of soil mantle and in the top 20 m of the bedrock of highly to moderately decomposed limestone, there are solution features and cavities of different shapes and sizes that are vulnerable and prone to collapse when subjected to the imposed building loads. In the subsequent detailed ground investigation programme, three geophysical survey methods, namely resistivity method, seismic reflection method, and seismic wave method, were included in order to delineate the spatial locations and sizes of these solution features and cavities probably present in bedrock under the footprints of the proposed buildings. With the aid of computed tomography technology, the large amount of spatial survey data can be woven together to make images of these underground anomalies and provide valuable information on their locations and sizes for foundation design engineer to get over the complex foundation problems.

1 INTRODUCTION

CT technology has been applied to civil engineering works and particularly gained its popularity in recent years in geological and geo-environmental investigations (Lee, et al, 2000; Fonseca et al, 2005). There are not many cases reported on its application on foundation construction in ground of solution features and cavities. In Hong Kong, Lee et al (2000) was probably the first paper that addresses the use of borehole geophysics in the foundation Design in cavernous rock where natural gamma and induction probe were employed. Spatial data collected were displayed in tomograms. Fonseca et al (2005) conducted an investigation programme making use of geophysical borehole and surface methods including seismic refraction, reflection and electrical resistivity, to explore the characteristics of a residual (saprolitic) soil at University of Porto in Portugal.

This paper presents a case of the application of geophysical survey with the aid of CT technology on the detection of underground solution features and cavities for a property development site in Dalian PRC, where two buildings, each 5 to 6 storeys high and 240 m by 140 m in plan. Preliminary ground investigation revealed that underlying the top 20 m of soil mantle and in the top 20 m of the bedrock of highly to moderately decomposed limestone, there are solution features and cavities of different shapes and sizes that are vulnerable and prone to collapse when subjected to the imposed building loads. In the subsequent detailed ground investigation programme, three geophysical survey methods, namely resistivity method, surface seismic reflection method, and borehole seismic reflection method, were included in order to delineate the spatial locations and sizes of these solution features and cavities probably present in bedrock under the footprints of the proposed buildings. Since application of CT on the three geophysical survey methods was basically on the same principle and only the borehole seismic reflection method will be discussed in this paper for brevity.

The site was a newly reclaimed land for about 2 years of time. The site area is about 135710 m2. During site investigation total 744 boreholes have been sunk down to investigate the sub-surface geology of the site for foundation design. The boreholes were spaced at the nodes of a 9m x 9m grid, following the layout of columns.

The bedrock of the site comprises carbonate rocks in the age of Sinian Period (震旦纪). According to Chinese Academy of Sciences (1992), the underground karstic cavities at the region of the site are evident down to 70m to 120m below the seabed level.

Quaternary deposits are overlying the bedrock. The lowest Quaternary deposit unit is onshore lateritic soil in the age of early mid-Pleistocene. It was noted from the regional geological information made available for the project that the landmass together with the lateritic soil had been submerged under water during late mid-Pleistocene to late upper-Holocene; thus alluvium might have deposited on top of the lateritic soil. Sea-level rose to about the present day's level at the start of Holocene, about 11,000 years ago. The Holocene marine mud formed the uppermost Quaternary deposit layer overlying the alluvium deposit and lateritic soil.

The lateritic soil overlying carbonate rocks is classified as "Red Clay" according to the Chinese code for Investigation of Geotechnical Engineering (GB 50021 - 94).

The ground investigation results revealed that solution features and cavities of different sizes and shapes were recorded within the highly and moderately decomposed Limestone (H/MDL). The subsoil geological stratigraphy of the subject site with depths is as follows:

- Fill comprised of granular material in the top 10m deep
- Localized marine deposit / alluvium of thickness up to 3m
- A layer of lateritic soil of thickness up to 7m
- Highly Decomposed Limestone (HDL) of thickness varied in the range of 5m to 50m
- Moderately Decomposed Limstone (MDL) underlying the HDL.

The solution features and cavities found in the borehole investigation works were presented in a 3-dimensional view in Figures 1 and 2.

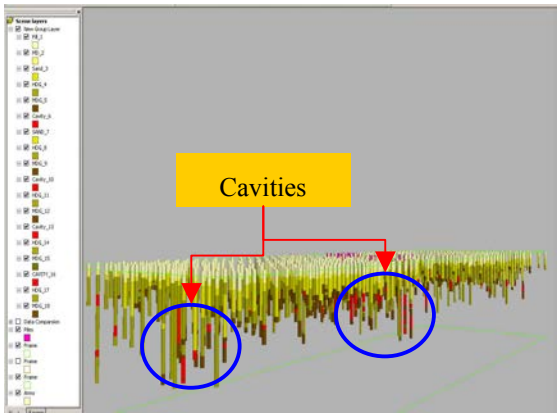

Figure 1

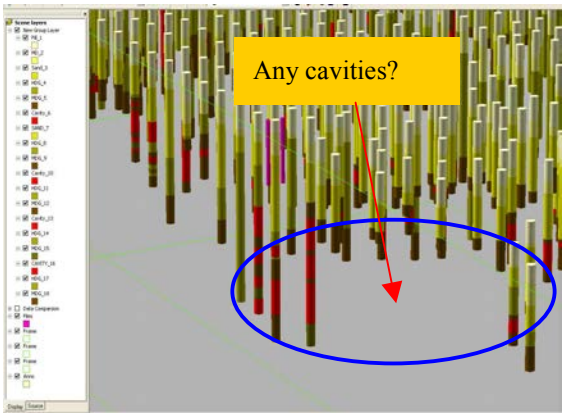

Figure 2

The presence of solution features and cavities in boreholes were discrete and local; the situations of the solution features and cavities between boreholes were unclear (Figure 2). In order to clarify the spatial distribution of the solution features and cavities for the foundation design, geophysics investigation in aid of Computed Tomography (CT) technology was conducted to investigate the patterns, shapes, sizes and continuity of the solution features and cavities.

2 COMPUTED TOMOGRAPHY

Computed Tomography (CT) is a technique in which an incident beam of signal, such as seismic or acoustic wave, electricity current, electromagnetic radiation (x-rays or gamma rays) passes thought an object and is collected with an array of detectors (Alshibli et al, 2000). The object is rotated such that the beam probes from several angles to collect attenuation data and produce the equivalent of a "slice" through the region of interest. The attenuation information collected during the rotation is then read by a computer program to reconstruct a slice image of the internal structure of objects. Three-dimensional reconstructions can be made by stacking the CT slices and attenuation is measured on individual planes whereas conventional radiographs comprise attenuation data from all planes within an object superimposed onto one plane."

Dines et al (1979) carried out an experiment on an urban mass-transit site for testing the attenuation reconstruction of data for electromagnetic and seismic wave in straight-wave cross-borehole probing. It was concluded that data from both electromagnetic and seismic wave could also be used to reconstruct the structure of the object being passed through.

Fonseca et al (2005) made use of P and S-wave seismic refraction and reflection data in cross-holes or down-hole method in an experimental site to form tomography section to investigate /characterize the sub-soil profile and formulate the preliminary geological interpretation model for determination of the relevant geotechnical properties of the sub-soil profile.

Lee et al (2000) also carried out borehole geophysics in ground investigation for foundation design in limestone rock area. A combined natural gamma and induction probe was used to obtain information on the karst features whereas ground penetration radar was used in cross-hole for further exploration in the areas within complex karst features. The results revealed that it was a useful tool for foundation design in karstic environment and hence significantly reduce total number of deep holes for the design of deep foundation in cavernous bedrock.

2.1 Method of Geophysics Investigation - Borehole Seismic Reflection Method

Preliminary GI work results inferred that the solution features and cavities mostly were encountered in shallow ground at levels between 20m and 40m deep below ground. Surface seismic wave method was adopted. The signals were generated from the existing ground level and were received by a series of signal receiver phones pre-installed in boreholes sunk to a maximum depth of about 60m. The signal was generated at a series of excitation points spread radiating from the borehole as shown in Figure 3 below. A typical vertical section through the borehole and the excitation points on ground at various distances from the borehole is given in Figure 4. The signals collected were woven together to form tomography sections for establishing image of object passed through by the seismic wave.

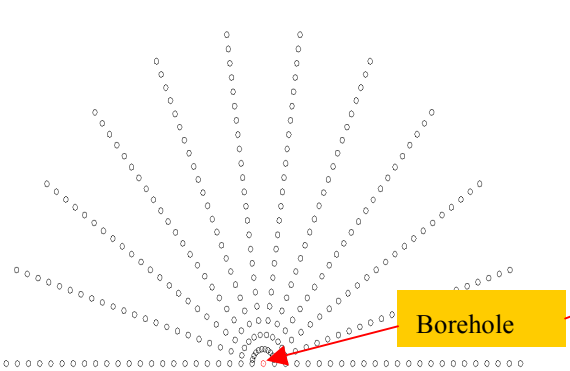

Figure 3 – Layout and pattern of signal being generated

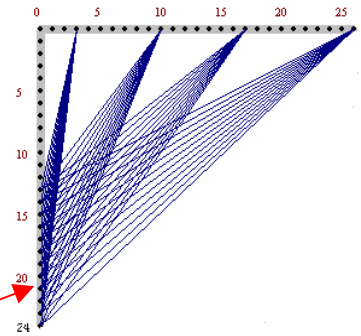

Figure 4 – Section showing the scan lines of seismic wave

2.2 Result of the seismic wave data

Seismic wave signals were generated and received by an automated data logger hooked to a display for real time monitoring of the survey. The data were analysed and transformed into a graphical output format for interpretation. Typical survey results in graphical form are shown in Figures 5 and 6 below.

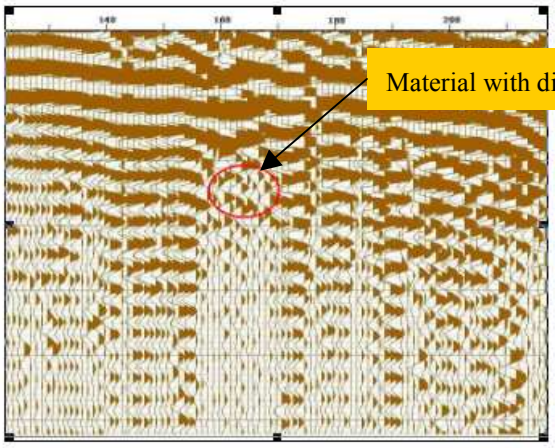

Figure 5

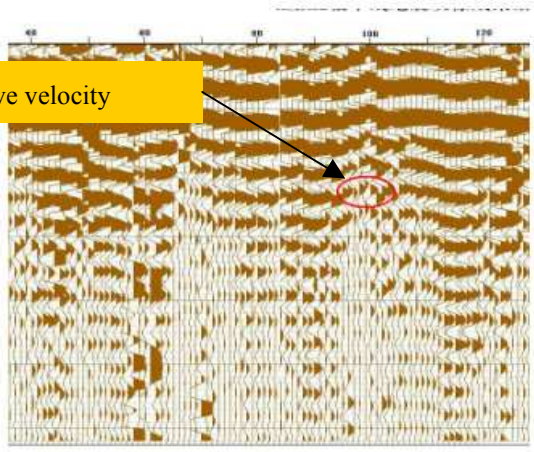

Figure 6

3 TOMOGRAPHY IMAGING

Although the data shown in Figures 5 and 6 were in graphical format, it still needs experienced professional to decode the results into valuable information ready for use by foundation engineers. By tomographic inversion the data were further transformed to images which with different colours show the characteristics of attenuation of wave passing through ground with anomalies (Figures7 and 8)

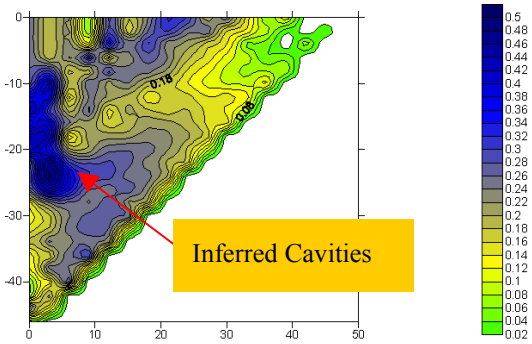

Figure 7

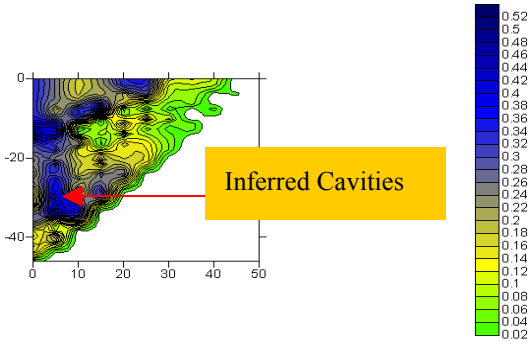

Figure 8

Besides, wave data could also be transformed into a plan section at a required depth to show the spatial distribution of different type of materials as illustrated in Figures 9 to 12

It is noted from the above figures that the sizes and locations of the inferred cavities are changed with depths of borehole. The cavities at depth of 20m were getting larger in size towards depth of 22m and then getting smaller and discrete at depth of 24m. However, the cavities re-developed at depth 26m.

The extent and development of cavities at depth of borehole could thus be identified. Making use of these CT images, the foundation design engineer established the sub-surface geological model for a safe and cost effective foundation design.

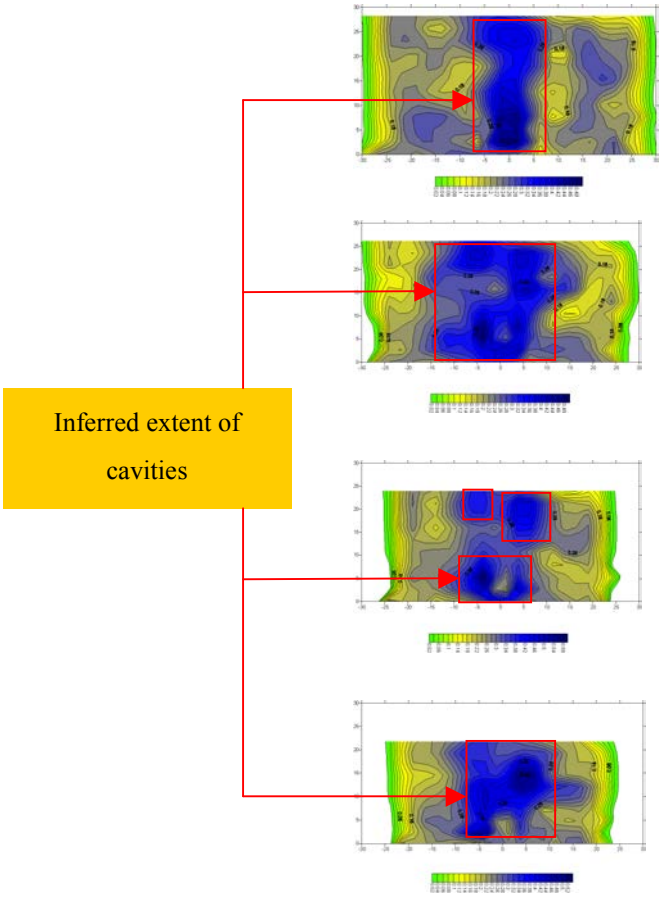

Figure 9
Plan section at 20m deep of borehole

Figure 10
Plan section at 22m deep of borehole

Figure 11
Plan section at 24m deep of borehole

Figure 12
Plan section at 26m deep of borehole

4 CONCLUSIONS

Following on the fast development of computer techniques, computed tomography is now widely used not only in the medical treatment but also in ground investigation. By making use of the images generated by CT method of computed tomography, the subsurface conditions of ground could become visible that helps foundation engineers to depict anomalies hidden in complex and non-homogenous in natural soil and rock. It was also noted that computing software for transforming wave data onto a three dimensional image was working in progress and in very near future the underground geological model for any given site would be easily established so that risk of unforeseen ground conditions would be further reduced in forthcoming foundation design.

ACKNOWLEDGEMENT

The authors would like to express their thanks to Nan Fung China Development Company for their kind permission to the publication of this paper.

REFERENCES

Chinese Academy of Sciences (Year 1992), Proceedings No 6 of Institute of Geology 中国科学院地质研究所集刊第6号

GB 50021 - 94 (1994), Code of investigation of geotechnical engineering, National Standard of People Republic of China promulgated on 1994-08-09.

Lee, D.M., Pascall, D., Lui, Y.H., Chan, Y.W. 2000. “The use of borehole geophysics in the foundation design in cavernous Marble”, pp.17- 26, Proceedings of HKIE GD Annual Seminar on Foundation, May 2000.

Fonseca, A.V.D., Carvalho, J.M., Ferreira, C. 2005 "Combining geophysical and mechanical testing techniques for the investigation and characterization of ISC'2 residual soil profile" Vol. 2, pp.765 - 768, Proceedings of the 16th ICSMGE, 2005 Osaka.

Alshibli, K.A., Batiste, S.N., Swanson, R.A., Sture, S., Costes, N.C., Lankton, M.R., "Quantifying Void Ratio Variation in Sand Using Computed Tomography", Marr, W.A. (eds), Geotechnical Measurements Lab and Field: pp.30-43. ASCE.

Dines, K.A., Lytle,R.J. 1979. "Computerized Geophysical Tomography", pp.1065 – 1073, Proceedings of the IEEE, 67(7)

Innovative Design in Po Shan Tunnel Project

J. Ho
GEO, CEDD
Y.C. Lam & J.Y.C. Lo
Maunsell Geotechnical Services Ltd.

The Po Shan hillside of the Mid-Levels is affected by high groundwater levels and unfavourable geological conditions. Maunsell Geotechnical Services Ltd. (MGSL) has been appointed by the Geotechnical Engineering Office (GEO) of the Civil Engineering and Development Department (CEDD) in 2005 to design a more robust landslide preventive works to control the groundwater levels for guarding against large-scale slope instability. With consideration of site constraints, technical requirements, long-term performance and cost-effectiveness, an innovative scheme comprising two drainage adits with some 200 sub-vertical drains has been adopted.

There are other innovations and value adding features adopted in the project such as excavation of adits by Tunnel Boring Machine (TBM) with retractable mode, installation of sub-vertical drains upwards from the drainage adits, controllable inflow of sub-vertical drains, and collaboration with the Hong Kong Observatory (HKO) for setting up a new underground seismograph station.

1 INTRODUCTION

Maunsell Geotechnical Services Ltd. (MGSL) has been appointed by the Geotechnical Engineering Office (GEO) of the Civil Engineering and Development Department (CEDD) in 2005 to design a more robust landslide preventive works to control the groundwater levels for guarding against large-scale slope instability.

Key design elements of this Project include 2 nos. of 3.5m outer diameter underground drainage adits, some 200 nos. of sub-vertical drains with various lengths up to 104m from the drainage adits, a 5m high, approximately 130m long flexible barrier, soil nailing on the natural terrain and an automatic groundwater surveillance system. Only innovative design elements of sub-vertical drains, TBM tunnel and the value adding feature of collaboration with the Hong Kong Observatory (HKO) for a new seismograph station will be discussed in detail under this paper.

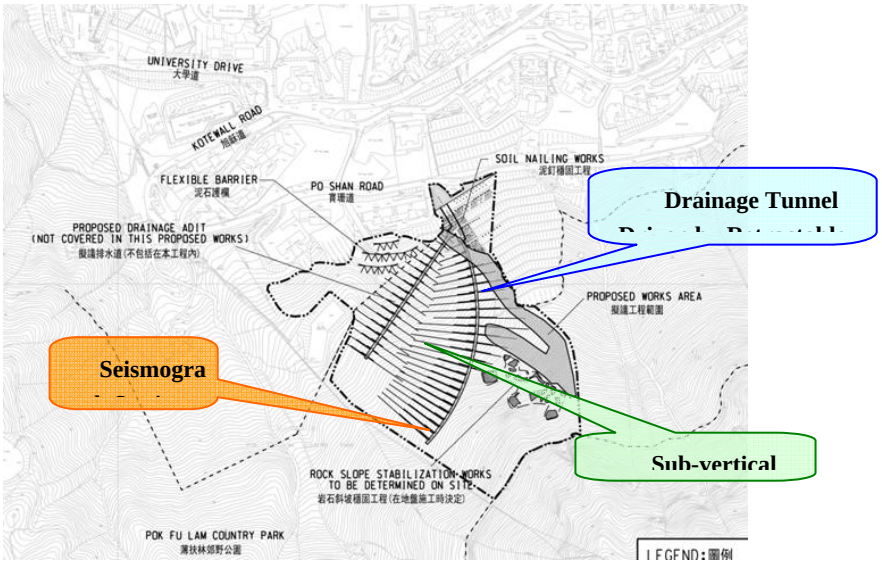

General Layout showing key design elements

2 SITE DESCRIPTION

The site is located at NW flank of Victoria Peak and south of Po Shan Road. The project area can be broadly defined as encompassing the mostly undeveloped hillsides above No. 4 Po Shan Road in the west to No. 20 Po Shan Road in the east, beyond the man-made cut slope, 11SW-A/CR175, at the site of the catastrophic 1972 Po Shan Road failure.

The project area falls largely within the Pok Fu Lam Country Park and is mainly covered by dense vegetation comprising grasses, shrubs and trees. It is about 210m high, with crest and toe level around at +390mPD and +180mPD respectively. The maximum span of the site is approximately 730m in length. Generally, the site is mainly natural terrain with an average gradient of 25^{o}. Lugard Road is located at the crest whilst residential buildings are located along the toe of the project area.

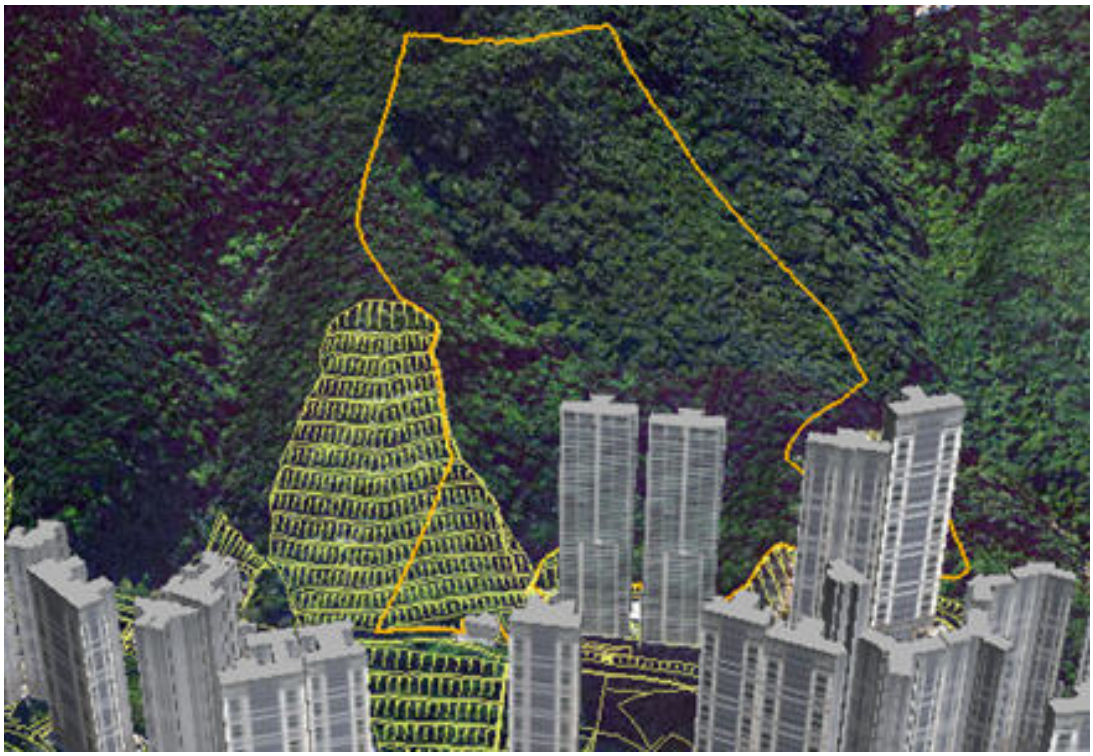

Perspective View of the Project Area

3 INNOVATIVE SCHEME FOR THE LANDSLIDE PREVENTIVE WORKS

The followings are the key requirements of this project:

- The function of the existing horizontal drains should be maintained during construction period.
- The new groundwater drainage system should not be affected by shallow landslides.
- The new system should have reliable long-term performance.
- The Po Shan hillside falls within the Pok Fu Lam Country Park and there are many plants of conservation interest on the hillside.
- There is limited works space.
- Adjacent old buildings are sensitive to settlement, which may occur if the groundwater drawdown is excessive.
- Earthwork should be minimized due to regional stability and environmental concerns.

To meet the challenging requirements of the project, various design schemes were considered. After detailed evaluation of different alternatives, an innovative scheme comprising two drainage adits with some 200 sub-vertical drains to be installed upward from the adits was adopted for the project. This design also

permits the control of the amount of groundwater drain into the adits through the operation of the valves provided at each sub-vertical drain.

4 DESIGN APPROACH AND SPECIAL CONSIDERATIONS

Sub-vertical Drains

Hydrogeological modelling was carried out using SEEP/W software, which employs a 2-dimensional finite-element continuum model adopting Darcy's principle of flow through granular media.

Models initially simulated the steady stage of highest natural groundwater condition recorded in 1983 before any drain installed in the system, which was a benchmark for subsequent modeling.

Sub-vertical drains were then set in the models to draw the water table down to the design groundwater level. The tunnels were assumed to be lined and contribute negligible effects to the models. The groundwater was assumed to be drained out through the soil portion of the sub-vertical drains but not in rock portion of the drains. The model therefore simulated the steady state groundwater condition dropping from 1983 highest groundwater level to the design groundwater level after installation of sub-vertical drains. The discharge seeping into the sub-vertical drains was determined in this analysis.

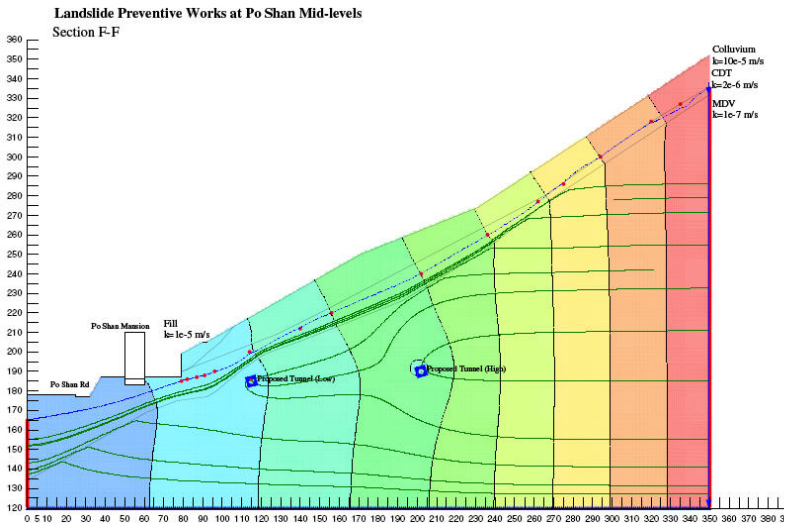

Seepage model to simulate the drainage effect by sub-vertical drains

Based on the analytical results, it is estimated that the total discharge of the entire area through the sub-vertical drains is about 400 m³/day. Therefore, it is considered that this discharge capacity is adequate in replacing the existing discharge by horizontal drains installed in 1984/85 with maximum flow rate of about 300m³/day.

Drainage Adits Excavated by Tunnel Boring Machine (TBM)

The project is categorised as a designated project as part of the works area encroaches into the Pok Fu Lam Country Park. An Environmental Permit (EP) has been issued by the Environmental Protection Department with conditions to be strictly followed. One of the key requirements is that non-explosive method of tunnelling must be adopted. During the detailed design stage, mechanical excavation method by means of hydraulic splitting and tunnelling by TBM were assessed.

Comparing with the mechanical breaking method, there are many inherent advantages to TBM method. Some of these are:

- Good structural stability at the face
- Better rock integrity with less temporary support requirements
- More pleasant working environment and less disturbance to nearby residents

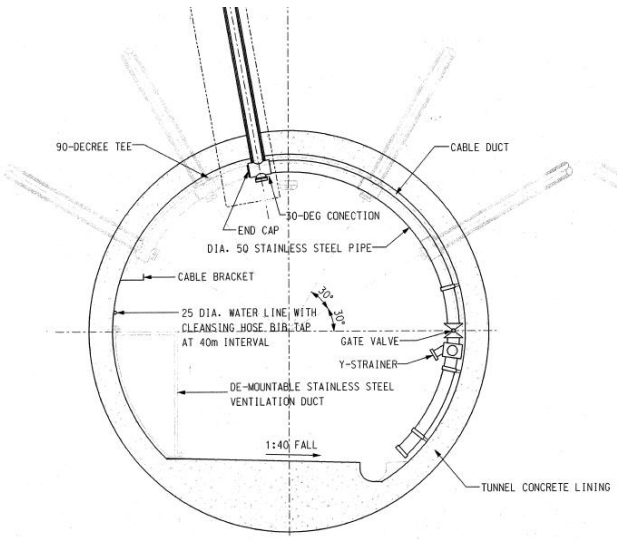

Typical 3m span Tunnel Section

- Higher excavation rates
- Less overbreak

With appreciation of the special requirement stipulated under the EP and those inherent advantages, TBM was adopted as the major tunnelling method of this Project. In order to enhance the overall cost-effectiveness, both tunnels were designed to be excavated by one TBM. Hence, an innovative approach by retracting the TBM from the completed High Tunnel and re-orientating it for the excavation of the Low Tunnel was adopted. The tunnel size has also been optimized so that refurbished TBM could be adopted with less cost and shorter procurement period.

For the permanent support, unreinforced concrete lining was designed for the circular tunnels with thickness of 300mm. Minimal temporary support by means of rock dowels and steel fibre reinforced concrete were designed with reference to the ground conditions.

5 OTHER INNOVATIONS AND VALUE ADDING FEATURES OF THE PROJECT

Sub-vertical Drains

Horizontal drains have been widely used in Hong Kong for lowering groundwater table. However, clogging and deterioration inevitably affect the long-term performance of this common type of drains. In order to replace the existing system of horizontal drains with a more robust network, we made use of the self-cleansing advantages under the effect of gravity by installing the drains at steep angles from the crown of the drainage adits. The sub-vertical drains are also fanned out at different orientation to maximize the effective drainage area served by each adit.

Even though the conventional way to drill holes is by rotary method, we decided to use percussive drilling due to the tight construction programme. It has been demonstrated that percussive drilling has a much faster penetration rate than the conventional rotary drilling. In fact, it is the first time in Hong Kong that drains are driven upwards by “Up-the-hole” hammer.

Drilling of the first sub-vertical drain of this project was commenced on 3 January 2008 after some site trials carried out in advance. Although the drilling and installation works are still being carried out on site, the longest drain drilled so far is about 102m. The highest outflow intercepted to date reaches as high as 26 litre / minute. However, each drain will be regulated mechanically by valve with pre-determined flow to be determined by a performance review at the post-construction stage.

Water Hammer for percussive drilling

Drilling rig providing torque and support

Retractable TBM

Although tunnelling by TBM has been commonly adopted in Hong Kong, the operation is usually carried out with both launching and receiving shafts. However, due to constraints at the site, no receiving shaft will be available in this Project. In other words, the TBM will be retracted after completion of the first tunnel and re-orientated to drive the second bore. This "Blind Boring" technique which is seldom used by tunneling projects, was adopted in this project.

TBM operation for the curved High Tunnel with the radius of curvature of 225m was commenced on 19 September 2007. With an average advance rate of 3m to 4m / day, the "Blind Boring" of the High Tunnel was completed on 8 December 2008. The machine was then pulled back to the portal chamber in about 2 weeks.

Refurbishment of the TBM was carried out at the portal chamber before re-orientating towards the Low Tunnel. TBM excavation at the straight Low Tunnel was started on 26 February 2008. The average advance rate is about 12m / day and the excavation was completed on 17 March 2008.

TBM Fabrication Yard in Shanghai


TBM Retracted to the Portal Chamber from Low Tunnel

New Seismograph Station at the end of High Tunnel

The HKO has been looking for a suitable site to establish a new Broadband Seismograph Station for enhancing the detection of earthquake in the South China Sea. The solid rock conditions and the quiet environment of the drainage adits were considered suitable for the new Seismograph Station. Upon request by the HKO, a review was carried out to study the feasibility. The study concluded that it was feasible to collaborate with HKO to establish the Seismograph Station at the last 6 m of the High Tunnel.

A design review of the effect on the structural lining due to the provision of four circular holes with diameter up to 600mm on the invert for the seismograph has been assessed. Upon the analytical results, recommendations have been made for the locations and arrangements of these holes. Minor adjustments of the locations of a few of the sub-vertical drains were also made to avoid conflict with the Seismograph Station. With close liaison between the

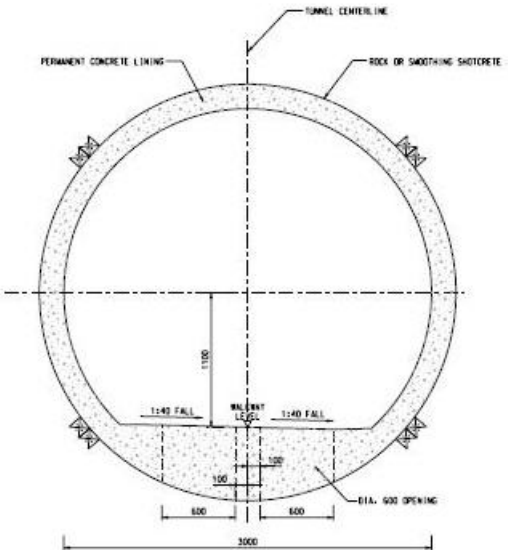

Special modification at tunnel invert

Engineer, HKO and GEO, such modifications can be arranged for construction under the same Works Contract.

6 INVALUABLE MERITS OF THE PROJECT

Values to the Project

Since the commencement of this challenging project, all possible ways to enhance the outcomes economically, socially and environmentally have been identified and assessed.

Sub-vertical Drains

Although the initial setup cost for the sub-vertical drain system is higher as compared with the horizontal drain installation, this sub-vertical drain system provides a practical, accessible and inexpensive way for future upgrade and maintenance. More sub-vertical drains may still be installed from the tunnels in the future economically if it is considered necessary. Furthermore, unlike the conventional horizontal drain system, no ground surface works are required and it is definitely more environmental and socially friendly.

Retractable TBM

With the aid of the retractable TBM, the construction is anticipated to be completed within 2 years instead of 4 years if drill and break method is adopted. This time / cost saving is not just economically beneficial to the Client, it is also socially welcome by the public because residents in the area will be protected by the comparatively early completed system. Furthermore, any nuisance to the public can be substantially reduced with a shorter construction programme. In addition to the economical and social benefits, the retractable TBM approach also provides us environmental advantage because no receiving shafts are required to take back the machine. Therefore, no earthworks at the ground surface area, which is within the Pok Fu Lam Country Park, are required at all. In other words, the ecological settings in the area can be conserved with this innovative approach.

Seismograph Station

In order to get precise measurements of seismic activities, a seismograph station need to be in solid bedrock with sufficient rock cover, it would be costly to build a deep rock cavern for setting up a new broadband seismograph station. However, enhanced tunnel design was carried out to make provision (i.e. 6m at the end of High Tunnel) to the HKO to set up an equipment room for the seismograph station. This arrangement provides value added to the project and facilitates substantial benefits in term of cost and time for the community.

Values to the Communities

The project team is committed to share the practical experience on adopting these innovations with the practitioners. Technical visits have been arranged to learned societies including the technical visit for HKIE in late August 2007 to demonstrate the use of retractable TBM. Similar site visits were also organised for other societies such as IMMM and AGS(HK).

With the implementation of these innovations, potential social impact has been minimized to the possibly lowest. In fact, this “green” system is constructed underground. Hence, disturbance to

Technical visit organized by HKIE

vegetation is minimized and no tree felling is required under this Project. The Project had been presented to the public through numbers of district council meetings and discussions with nearby residents. In fact, the Project received overwhelming support from the public including the Green Group and residents at Po Shan because of our "green" approach and reasonably short construction programme yielded by using the innovative sub-vertical drain installation method.

7 CONCLUSIONS

With the implementation of innovations, values can be added to the project. Although it is challenging to bring in advance techniques not previously applied in Hong Kong, designers should be innovative and demonstrate the practicality and effectiveness on using them. With the full support from the Client, cooperation from the Contractor, quality supervision from the resident team, and acceptance from the public, smooth implementation of this challenging Project was achieved.

Experience sharing through technical seminars and visits has been carrying out to demonstrate the successful applications of the state-of-the-art technology, which may help to broaden one's knowledge and eventually strengthen our engineering industry. The experience of successful applications of the innovations has effectively passed on to other practitioners so that further applications can be implemented even more successfully and efficiently.

ACKNOWLEDEMENTS

This paper is published with the permission of the Head of the Geotechnical Engineering Office and the Director of Civil Engineering and Development Department, the Government of the Hong Kong Special Administrative Region.

REFERENCES

Barton, N. (2000). "Rock Mass Classification for choosing between TBM and Drill-and-Blast or a Hybrid Solution." Tunnels and Underground Structures, Zhao, Shirlaw & Krishnan (eds), Balkema, Rotterdam, pp. 35-50.

Barton, N., and Grimstad, E. (1994). "The Q-System following Twenty Years of Application in NMT Support Selection." Felsbau 12 (1994) Nr. 6, pp. 428-436.

Barton, N., and Grimstad, E. (1993). "Updating of the Q-System for NMT." Proceedings of the International Symposium on Sprayed Concrete – Modern Use of Wet Mix Sprayed Concrete for Underground Support, Fagemes, 1993, (Eds Kompen, Opsahl and Berg. Norwegian Concrete Association, Oslo).

Barton, N., Lien, R., and Lunde, J. (1977). "Estimation of Support Requirements for Underground Excavations." Proceedings of 16th Symposium on Design Methods in Rock Mechanics, Minnesota, 1975. Published by ASCE, N.Y. 1977, pp. 163-177. Discussion pp. 234-241.

GEO Geoguide 4 (1992), "Guide to Cavern Engineering", Geotechnical Engineering Office, Civil Engineering Department, Hong Kong SAR Government.

Hoek, E. and Brown, E. T. (1980). "Underground Excavations in Rock". Institution of Mining and Metallurgy, London.

Lam, Y. C., Tam, K. W. and Lo, Y. C. (2008). "Ground Investigation for Tunnel Works", Proceeding of HKIE (2008).

Lo, Y. C., Cheuk, C. Y. and Chau, S. F. (2008). "Prediction of Water Inflow during Tunnel Construction", Proceeding of HKIE (2008).

Pang, K.K. and Au S.W.C. (1988). Review of the Po Shan Drainage Works. GCO Report No. MLR 1/88, Vol 1 & 2, 242p.

Peter J. Tarkoy and James E Byram (1991). "The advantages of tunnel boring : a qualitative / quantitative comparison of D&B and TBM excavation." Hong Kong Engineer, 1991

Application of Real-time Drilling Process Monitoring during Soil Nailing Works

N.L. Ho, K.M. Yau, M.J. Wright & K.L. Wong
Ove Arup & Partners Hong Kong Ltd, Hong Kong Special Administrative Region, China

ABSTRACT

An innovative technology called Drilling Process Monitoring (DPM) has been developed by the Department of Civil Engineering of the University of Hong Kong (HKU) to monitor the drilling process of soil nailing works (Yue et al, 2004). With sensors for movement and pressure mounted onto the drilling rig and control panel, a series of parameters representing the full drilling process for soil nailing is recorded automatically and continuously. Real-time DPM raw data together with the calculated penetration rate can be viewed on a designated website. Two slope sites identified to have potential ground related problems were selected for a real-time DPM production trial during drilling for soil nails under a Landslip Preventive Measures (LPM) Contract. CCTV survey was also conducted at selected drillholes with suspected cavities and joints. This paper presents the results of DPM carried out and correlation with the CCTV surveys and soil nail grouting records.

1 INTRODUCTION

1.1 Background

Ove Arup & Partners Hong Kong Ltd was commissioned by the Geotechnical Engineering Office (GEO) of the Civil Engineering and Development Department (CEDD) of the Government of the Hong Kong Special Administrative Region to undertake the investigation, design and construction of Landslip Preventive Works for 60 substandard man-made slopes maintained by the Government.

Soil nailing is a commonly adopted technique to stabilize and upgrade soil slopes in Hong Kong. Studies and research have been supported by the Government to improve the effectiveness of soil nailing works. One of the innovative technologies called Drilling Process Monitor (DPM) has been developed by the Department of Civil Engineering of the University of Hong Kong (HKU) to monitor the drilling process of soil nailing works (Yue et al, 2004).

Studies have been carried out on the application of DPM. Evaluations of the application of DPM and field trials of the whole system have been conducted at various slope sites by HKU and GEO (Lam & Siu, 2004; Lai & Lo, 2007). Studies were mainly carried out in weathered rock strata such as decomposed Granite and Tuff. Studies have also confirmed that the drilling penetration rate changes within different types of ground conditions (Ho et al, 2007).

The latest production trial is to confirm the application to different ground conditions including Fill and Colluvium and that application of real-time DPM can be an instant and accurate means of estimating the depth of the hole and remote monitoring of ground conditions within the drillholes and drilling process.

1.2 Real-time DPM Equipment

The real-time DPM equipment mainly consists of 1 displacement and 5 pressure sensors. The displacement sensor is mounted onto the drilling rig "mast" and engages the steel loop chain of the drilling rig to record forward and backward movement of the drill string. The pressure sensors measure the required hydraulic pressure for percussion of the down-the-hole hammer, upward and downward thrust of the drilling bit, and clockwise and anti-clockwise rotation of the drill (Lai & Lo, 2007; ETI, 2006a & 2006b). All of the pressure sensors are mounted onto the control panel of the drilling machine. Calibration for each drilling rig is required

to ensure that appropriate parameters are adopted for data processing. A photograph showing the typical setup of the sensors is given in Plate 1.

Data is recorded at 0.5-second intervals and transmitted to the control box and sensor box wirelessly. The processed drilling data, which is uploaded to a remote server through the General Packet Radio Services (GPRS) mobile network, can be viewed in real time on a secure website of HKU (Lai & Lo, 2007).

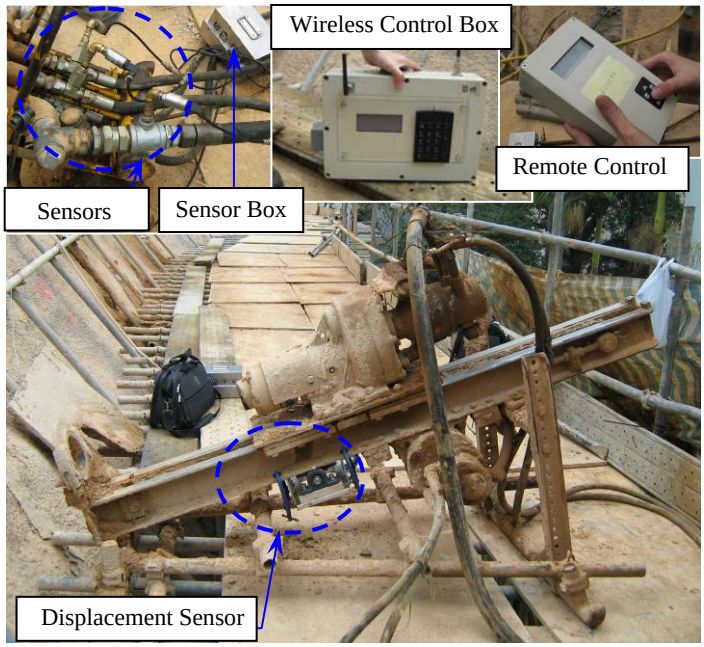

Plate 1: Setup of DPM sensors on a typical rotary percussion drilling rig

1.3 Closed-circuit Television (CCTV) Survey

CCTV survey was carried out at selected drillholes, which allowed inspection of the ground conditions within the drillholes and correlation with the DPM results and subsequent soil nail grouting operation. Features such as local drillhole collapse, voids and joints were easily identified and recorded.

1.4 Details of Selected Sites

Two sites were selected to carry out real-time DPM. Feature No. 11SW-A/CR34 is located in Mid-levels on Hong Kong Island. The feature is a 16m high cut slope with a 3m high reinforced concrete retaining wall along the toe. Based on the previous studies, geotechnical investigation, aerial photographs interpretation as well as previous and recent ground investigation (Arup, 2007a), the soil strata of the feature is a succession of Fill and Colluvium. Colluvium mainly comprises firm, yellowish red, sandy, clayey silt with sub-angular to sub-rounded fine to coarse gravel, cobble and boulder sized rock fragments (Arup, 2007a). Shear strength parameters of $c' = 3kPa$ and $\phi' = 38°$ were adopted for Colluvium in the slope stability analysis. The DPM was selected to be carried out within the Colluvium with voids and cavities, and excessive cement grout loss were anticipated to be encountered at some of the drillholes. The geological model of the feature is shown in Figure 1.

The other site, Feature No. 11SW-D/FR71, is a 6m high fill slope with a 7m high concrete retaining wall at the toe. According to the ground investigation and geotechnical study report (Arup, 2007b) carried out in April 2007, the soil strata of the feature are interpreted as a succession of up to 8.0m of Fill underlain by Completely Decomposed Granite (CDG). The DPM was carried out within the Fill and CDG. The Fill comprises loose to dense, silty fine to coarse sand with some angular to sub-angular fine gravel sized quartz fragments and occasional angular to sub-angular fine to coarse gravel sized highly decomposed Granite fragments while CDG comprises extremely weak, moist, completely decomposed medium grained Granite (Arup, 2007b). In-situ relative compaction tests carried out in trial pits within the Fill found results varying between 72.6% and 95.3% of the maximum dry density. SPT-N values of 9 to 79 were obtained within the

CDG (GCE, 2007). Shear strength parameters of c' = 0kPa and ϕ' = 33° and c' = 5kPa and ϕ' = 37° were adopted for Fill and CDG respectively in the slope stability analysis. The geological model of the feature is shown in Figure 2.

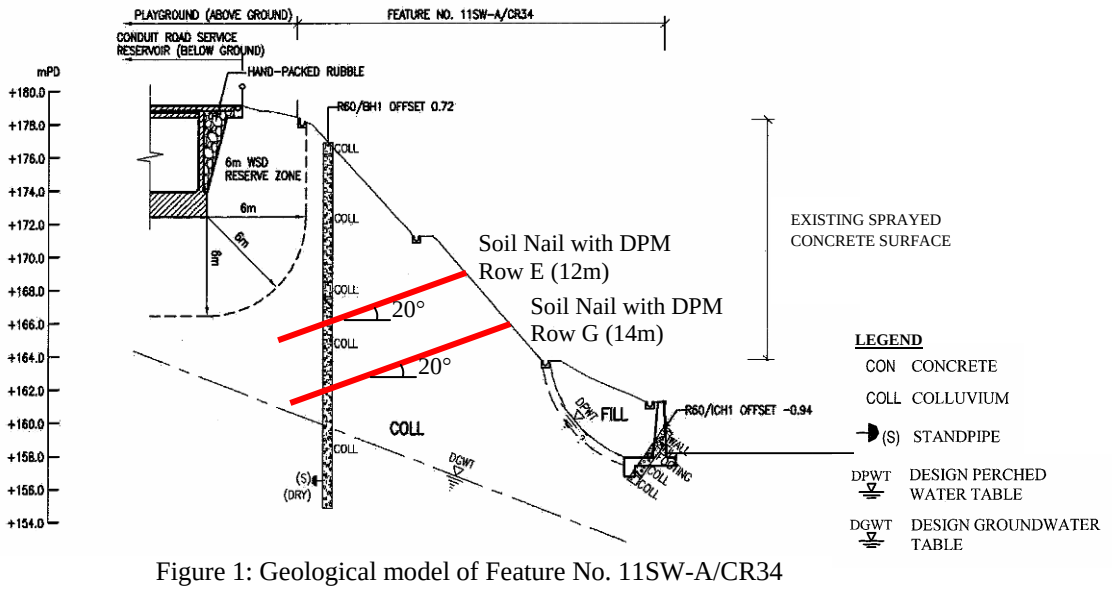

Figure 1: Geological model of Feature No. 11SW-A/CR34

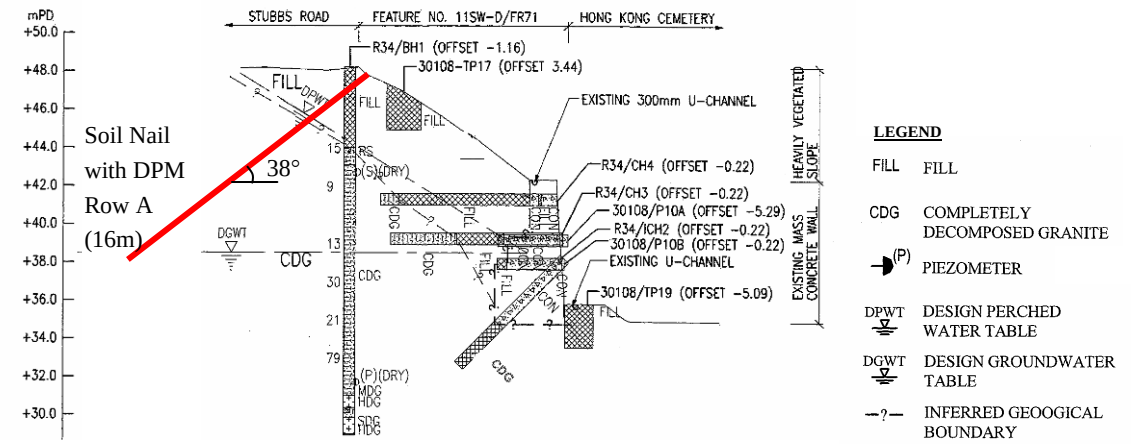

Figure 2: Geological model of Feature No. 11SW-D/FR71

2 DPM RESULTS AND ANALYSIS

2.1 DPM Data Collected at Feature No. 11SW-A/CR34

The DPM was carried out at 4 numbers of 12m long drillholes (nos. E27 to E29 and E34) and 11 numbers of 14m long drillholes (nos. G24 to G29, G32, G34 and G36 to G38). Diameter of drillholes was 100mm with drillholes inclined at 20° to the horizontal with a 1.5m horizontal spacing. A geological section of the feature is shown in Figure 1.

The depth of drillholes was manually measured after drilling and compared with depth from the DPM results. It is found that the difference of the manually measured and drillhole depth from DPM ranges from -0.4m to 0.6m which is within ±5% of the measured depth.

Drilling rate graphs (depth vs time graphs) were downloaded from HKU's website and retrieved. Average drilling rates ranging from 0.43 m/minute to 2.73 m/minute were obtained from DPM results at the above drillholes. CCTV survey was conducted at drillholes nos. E27 to E29, E34 and G29 to G31. The drilling rate graph for the DPM of 4 drillholes (nos. E27 to E29 and E34) is extracted and illustrated with some photographs recorded during CCTV survey which are shown in Figure 3.

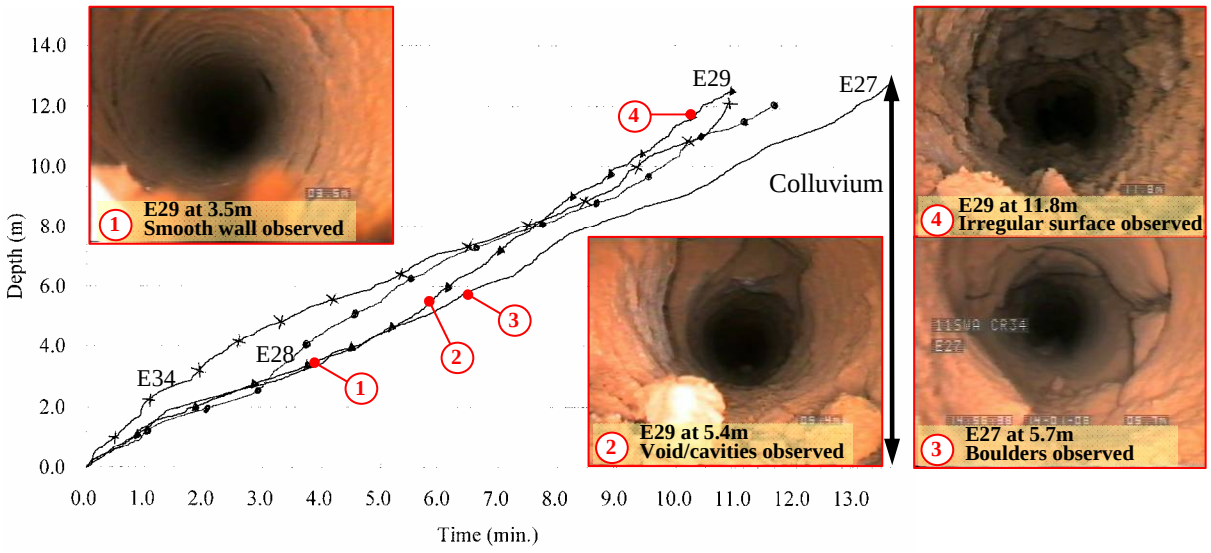

Figure 3: Depth vs Time Graph of DPM Results for Feature No. 11SW-A/CR34 (Row E)

From the drilling rate graph of Rows E and G drillholes of Feature No. 11SW-A/CR34 (Figures 3 and 4), the average drilling rate ranged from 0.43 m/minute to 2.73 m/minute. The relatively fast drilling rate (i.e. 2.73 m/minute) indicates that the drill bit was drilling through relatively soft materials while the slow drilling rate (i.e. 0.43m/minute) indicates that the drill bit was drilling through relatively hard materials such as boulder. The drilling rate from the DPM result for rock such as moderately and slightly decomposed rock tends to be less than 1 m/minute while the drilling rate for soil varies from 1 m/minute to over 2 m/minute as inferred from the previous studies (Lai & Lo, 2007).

In Figure 3, the graph gives consistent drilling rate of 1.07 to 1.30 m/minute at first 2m of drillholes nos. E27 to E29. From the depth of 2 to 4m, the drilling rate is about 0.64 to 0.83 m/minute. The relatively slow drilling rate indicates that the ground from 2 to 4m comprises relatively hard materials. From the depth of 4m onwards, the penetration rate become irregular and voids or cavities were probably encountered which are correlated with the CCTV survey. Some photographs of the CCTV survey were captured and shown in Figure 3.

The drilling rate graph for the DPM of the remaining 11 drillholes (nos. G24 to G29, G32, G34, and G36 to G38) is extracted and shown in Figure 4. The overall average drilling rate ranges from 0.76 m/minute to 1.30 m/minute as shown in Figure 4. In general, the drilling rate gradually increased from drillhole nos. G25 to G38, which was probably due to changes of soil strength along the slope. A significant variation of drilling rate is observed from of 9 to 12.5m depth in some drillholes (nos. G24, G25, G26 and G29). Penetration rates ranged from 0.56 m/minute to 5.6 m/minute. This indicates significant changes of ground conditions. High penetration rates of 2.07 m/minute and 5.6 m/minute were observed at the depth of about 10.6 to 12.1m and 9.2 to 9.8m of drillhole nos. G26 and G29, respectively, which indicates the presence of very soft soil and/or cavities. Excessive cement grout loss greater than 10 times of the theoretical volume of the drillhole was encountered at drillhole nos. G24, G26 and G27 and pre-grouting operation was adopted for drillhole nos. G28 and G29 to solve the grout loss problem.

2.2 DPM Data Collected at Feature No. 11SW-D/FR71

The DPM was carried out at 10 numbers of 16m long drillholes (nos. A8 to A11, A14 to A16, and A18 to A20). Diameter of drillholes was 100mm with drillholes inclined at 38° to the horizontal with a 1.5m horizontal spacing. A geological section of the feature is shown in Figure 2.

The depth of drillholes was manually measured after drilling and compared with the drillhole depth from the DPM results. It is found that the difference of the manually measured and drillhole depth from DPM is ranged from -0.4m to 0.3m which is within ±3% of the measured depth.

Drilling rates ranging from 1.38 to 4.68 m/minute were obtained for the Fill layer from DPM results at the above drillholes. The depth vs time graph for the DPM of 6 selected drillholes is extracted for illustration and shown in Figure 5.

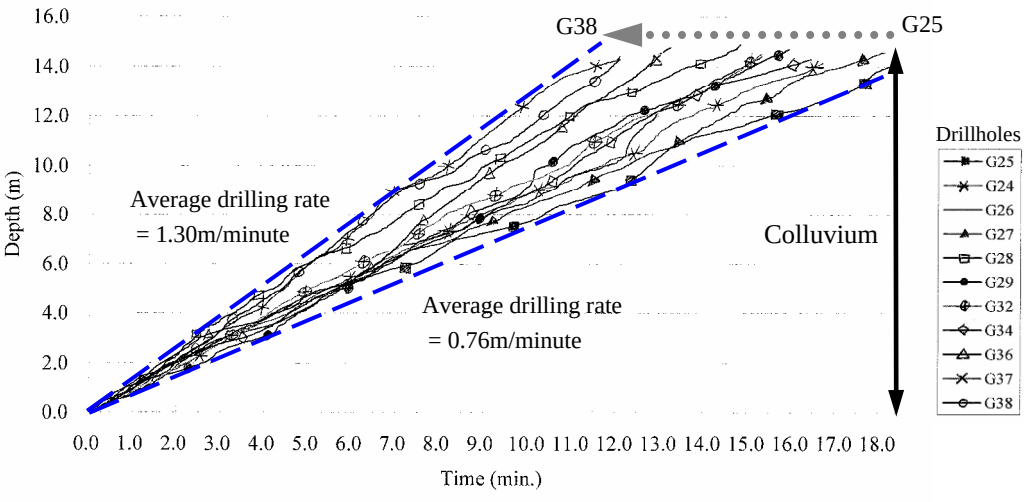

Figure 4: Depth vs Time Graph of DPM Results for Feature No. 11SW-A/CR34 (Row G)

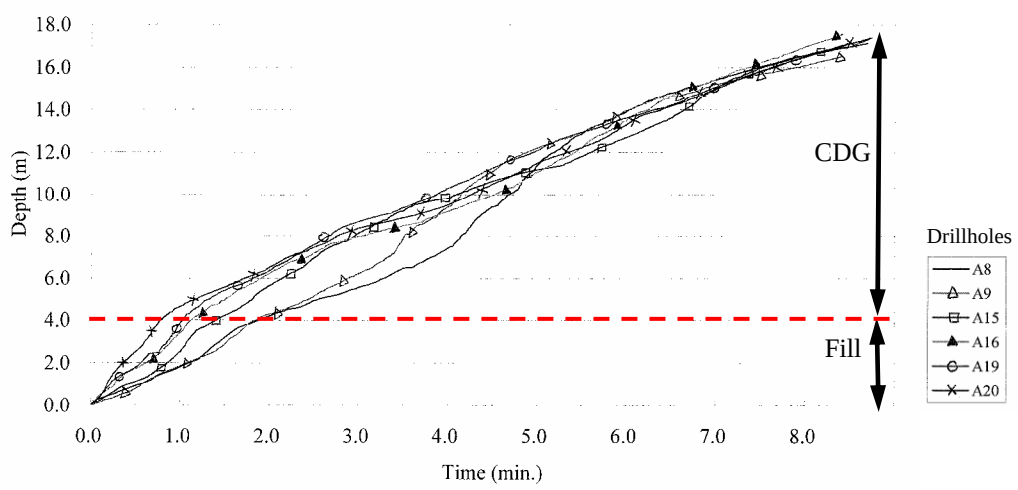

Figure 5: Depth vs Time Graph of DPM Results for Feature No. 11SW-D/FR71 (Row A)

A significant change in drilling rate from an average of 2.73 m/minute to an average of 2.02 m/minute is observed at the depth of about 4m as shown in Figure 5. This change of drilling rate indicates a change in soil strength. With reference to the geological section of the slope in Figure 2, the Fill/CDG interface is about 4m below the slope surface at soil nail Row A which coincides with the change in drilling rate measured by the DPM. There was no large variation of drilling rate and excessive grout loss was not encountered at the drillholes at Feature No. 11SW-D/FR71.

3 CONCLUSIONS

Application of real-time DPM was confirmed to be an instant and accurate means of measuring the depth of the drillholes and monitoring the drilling process and ground conditions. Change in character of strata was observed in the drilling rate graphs and correlated with the ground investigation information and geological model. Potential difficulties such as excessive grout and drillhole collapse were identified at an early stage. It offered the project team an opportunity for a better planning or arrangement of site works and gave the

designer an early review of the geological model, and hence minimize risks of construction delay and cost overrun for the subsequent upgrading works due to excessive grout loss, re-design and/or subsequent claims.

Using DPM equipment, drilling process monitoring could be incorporated as part of the normal requirements for test nails which are currently required to be installed and tested to verify the design prior to the installation of permanent soil nails.

ACKNOWLEDGEMENTS

The authors wish to thank the research group of The University of Hong Kong. This work owes to the DPM advice of Dr Quentin Z Q Yue and Professor Leslie George Tham of the Department of Civil Engineering of HKU. We also thank Dr Frank Tong, Edward Wong and their project team at the E-business Technology Institute, under the Innovation and Technology Fund of the HKSAR Government, for their development and transfer of the know-how of the real-time digital DPM system. Lastly, we thank ETI Consulting Ltd for the endless discussions with their engineers and their helpful assistance in the DPM experiments. This paper is published with the permission of the Head of the Geotechnical Engineering Office and the Director of the Civil Engineering and Development Department of the Government of the Hong Kong Special Administrative Region.

REFERENCES

E-business Technology Institute [ETI]. 2006a. *Site Equipment Installation Guide on Real-time Digital Drilling Process Monitoring & Management System.* E-business Technology Institute, the University of Hong Kong, 15p.

E-business Technology Institute [ETI]. 2006b. *Site Operation Guide on Real-time Digital Drilling Process Monitoring & Management System. E-business Technology Institute, the University of Hong Kong,* 19p.

Geotechnics & Concrete Engineering (Hong Kong) Ltd. [GCE]. 2007. *Final Field Work Report for Feature No. 11SW-D/FR71 adjacent Lamp Post 24314 Srubbs Road.*

Ho, N.L., Yau, K.M., Wong, C.W. & Wong, P.C. (2007). Special Field Tests and Surveys for Trial Soil Nails at Ground Investigation Stage in Hong Kong. *Proceeding of the 16th Southeast Asian Geotechnical Conference, 8-11 May 2007.*

Lam, J.S. & Siu, C.K. 2004. *Evaluation of Application of Drilling Process Monitoring (DPM) Technique for Soil Nailing Works (GEO Report No. 189).* Geotechnical Engineering Office of Civil Engineering and Development Department, Hong Kong, 42p.

Lai, A.C.S. & Lo, D.O.K. 2007. *Trial of Real-time Drilling Process Monitoring System (Technical Note No. TN 1/2007).* Geotechnical Engineering Office of Civil Engineering and Development Department, Hong Kong, 32p.

Ove Arup & Partners Hong Kong Ltd [Arup]. 2007a. *Stage 3 Study Report for Feature No. 11SW-A/CR34, At the Rear of Chater Hall, No. 1 Conduit Road (Stage 3 Study Report No. S3R 119/2006).* Report prepared for Geotechnical Engineering Office of Civil Engineering and Development Department, Hong Kong.

Ove Arup & Partners Hong Kong Ltd [Arup]. 2007b. *Stage 3 Study Report for Feature No. 11SW-D/FR71, Adjacent Lamp Post 24314 Stubbs Road (Stage 3 Study Report No. S3R 262/2006).* Report prepared for Geotechnical Engineering Office of Civil Engineering and Development Department, Hong Kong.

Yue, Z.Q., Lee, C.F., Law, K.T. & Tham, L.G. (2004). Automatic Monitoring of Rotary-percussive Drilling for Ground Characterization – Illustrated by a Case Example in Hong Kong. *International Journal of Rock Mechanics and Mining Sciences.* Vol 41, pp 573-612.

Mobility Assessment of Debris Floods – Recent Advancement

J.S.H. Kwan & F.W.Y. Ko
Geotechnical Engineering Office, Civil Engineering and Development Department,
Government of the Hong Kong Special Administrative Region

ABSTRACT

There have been increasing concerns for landslide hazard arising from debris floods in Hong Kong given the adverse consequences caused by a number of recent debris flood incidents. Amid the rapid advancement of various modelling approaches and rheologies for debris mobility assessments in the past decade, the Geotechnical Engineering Office (GEO) has recently undertaken a series of mobility assessments for debris flood events using the numerical algorithm, FLO-2D, to test the novel technology in mobility modelling of debris floods and to investigate its potential applications. This paper outlines the basic principles associated with the modelling approach and rheology of mobility assessment for debris floods, and illustrates how the advancement in the technology enhances the engineering capability in assessing mobility of debris floods and their potential consequences.

1 INTRODUCTION

In Hong Kong, natural terrain landslides are mostly shallow failures on open hillsides, some of which may find their paths to drainage lines and develop into channelised debris flows. Occasionally, debris floods may occur due to overflow or overtop from catchwaters being blocked by landslide debris. While open hillside failures and channelised debris flows are relatively common in Hong Kong, there have been increasing concerns for debris floods, in view of the adverse consequences caused by a number of recent incidents of which the extent of the affected areas were often large as compared with typical landslide cases.

Amid the rapid advancement of various modelling approaches and rheologies for debris mobility assessments in the past decade, the Geotechnical Engineering Office (GEO) has recently undertaken a series of mobility assessments for debris flood events using the numerical algorithm, FLO-2D, to test the novel technology in mobility modelling of debris floods and to investigate its potential applications. This paper outlines the basic principles associated with the modelling approach and rheology of mobility assessment for debris floods, and illustrates, with two recent case studies, how the advancement in the technology enhances the engineering capability in assessing mobility of debris floods and their potential consequences.

2 NUMERICAL MODELLING OF DEBRIS FLOODS

2.1 Basic characteristics

Debris flood is a hyper-concentrated sediment flow. It is a mixture of sediments and water, sharing the characteristics of fluid in terms of the fluidity, and solid in terms of the internal modulus. The high fluidity and modulus of the sediment-fluid matrix often supports transportation of sizeable materials, e.g. cobbles and boulders.

The high water content of the sediment-fluid matrix results in small or even no effective stress among the soil particles, which are suspended in the matrix. This marks one of the major differences between debris floods and other types of landslides and geo-dynamic mass flows, in which the physical interaction among the soil particles, and between the soil particles and the basal ground surface, plays a more significant role.

Debris flood is viscous in nature. Its resistance to flow is governed by yield stress, laminar flow friction and turbulent stress. Their relative significance varies with flow velocity. At very low velocity close to deposition, flow behaviour is largely not velocity dependent. But as velocity gradually increases, yield stress starts to take a role in controlling the resistance to flow, which behaves as a Bingham fluid (Julien & Lan

1991), followed by laminar flow friction at high velocity. As velocity continues to increase, turbulence at the basal layer is set up and energy loss as a result of the turbulence becomes critical.

2.2 Numerical simulation

Many of the numerical simulations of debris floods assume that the sediment-fluid matrix is a homogenous fluid, using continuum formulations. The simulation requires input of an appropriate rheological model that is described by a number of mathematical terms to simulate resistance to flow, e.g. Jin & Fread (1999).

In this study, the numerical algorithm, FLO-2D, developed by O'Brien et al. (1993) was adopted to study the flow behaviours of debris floods and to investigate its potential applications. The fluid mechanics involved are described by the following shallow-water equations, which are solved using finite difference formulations in an Eulerian grid comprising square cells:

Continuity Equation
$$\frac{\partial h}{\partial t} + \frac{\partial h V_x}{\partial x} + \frac{\partial h V_y}{\partial y} = i \tag{1}$$

Momentum Equation in x-direction
$$S_{fx} = S_{ox} - \frac{\partial h}{\partial x} - \frac{V_x}{g}\frac{\partial V_x}{\partial x} - \frac{V_y}{g}\frac{\partial V_x}{\partial y} - \frac{1}{g}\frac{\partial V_x}{\partial t} \tag{2}$$

Momentum Equation in y-direction
$$S_{fy} = S_{oy} - \frac{\partial h}{\partial y} - \frac{V_y}{g}\frac{\partial V_y}{\partial y} - \frac{V_x}{g}\frac{\partial V_y}{\partial x} - \frac{1}{g}\frac{\partial V_y}{\partial t} \tag{3}$$

where h, V_x and V_y are the flow depth and velocities in the x and y directions. i denotes the inflow into the computational domain. In the above momentum equations, the friction slope components S_{fx} and S_{fy} are expressed in terms of bed slope S_{ox} and S_{oy}, pressure gradient (with hydrostatic condition assumed) and convective and local acceleration terms.

Resistance to flow as exemplified in the friction slope components is simulated by a quadratic rheological model that considers yield stress, laminar flow friction and turbulent stress as follows:

$$S_f = \frac{\tau}{\rho g h} + \frac{K\eta}{8\rho}\frac{V}{h^2} + \frac{n^2 V^2}{h^{4/3}} \tag{4}$$

where τ = Bingham yield stress, ρ = sediment flow density, g = gravitational acceleration, η = viscosity, K = laminar flow resistance coefficient, and n = Manning's n-value. The Bingham yield stress term, τ, and the viscosity, η, are defined as an exponential function of sediment concentration.

3 CASE STUDIES

3.1 Tong Fuk debris flood

The Tong Fuk debris flood occurred on 5 November 1993. A landslide occurred above a catchwater at Tong Fuk, Lantau, during a heavy rainstorm and blocked the downstream flow of surface water. The backwater overflowed and undermined the portion of the hillside immediately below the catchwater, resulting in another landslide of an estimated source volume of about 3000 m^3. The surface water, mixed with the landslide debris, flowed along the streamcourse and developed into a debris flood (Figure 1). On reaching the gentler ground, the debris spread and deposited across the village. No casualty and no severe damage of the village houses were reported. Based on the size of the catchment and the available rainfall record, it was estimated that the rate of overflow was about 10 to 20 m^3/s. The average depth of the debris deposit was about 0.75 m (Figure 2).

Similar to other typical landslides in Hong Kong, the process of mass detachment for the landslide that occurred immediately below the catchwater could have been completed within a very short duration. This was estimated to be about 3 minutes with a sediment concentration by volume of 60% for input to the inflow hydrograph of the simulation model. The flow continued after the complete detachment of the landslide mass.

Figure 1: The Tong Fuk debris flood

Figure 2: Landslide debris deposited within Tong Fuk village

The exact period of time of the overflow was not reported and therefore, an inflow of water at the landslide location was specified with sufficiently long period of time in order to obtain a steady flow pattern at the deposition zone.

The model parameters were optimised based on the extent of the influence zone, the surge height, and the deposition depth observed within the village. The overflow was assumed to be 20 m^3/s that ran on a 3 m-grid digital elevation model (DEM). The rheological parameters adopted are shown in Table 1. Figure 3 shows the results at different simulation times, which exhibit reasonable agreement with the site observations.

Table 1: Rheological parameters for simulation of Tong Fuk and Lo Wai debris floods (FLO-2D 2006)

Cases	Sediment Concentration by Volume *Cv*	Yield Stress τ (Pa) = $\alpha e^{\beta Cv}$		Laminar Flow Resistance *K*	Viscosity η (Pa·s) = $\alpha e^{\beta Cv}$		Manning's *n* Roughness *n* ($m^{-1/3}s$)
		α	β		α	β	
Tong Fuk debris flood	0.6	0.00283	23	30	0.0345	20.1	0.4
Lo Wai debris flood	0.3	0.00283	23	Automatically computed from Manning's n-value	0.0345	20.1	0.3

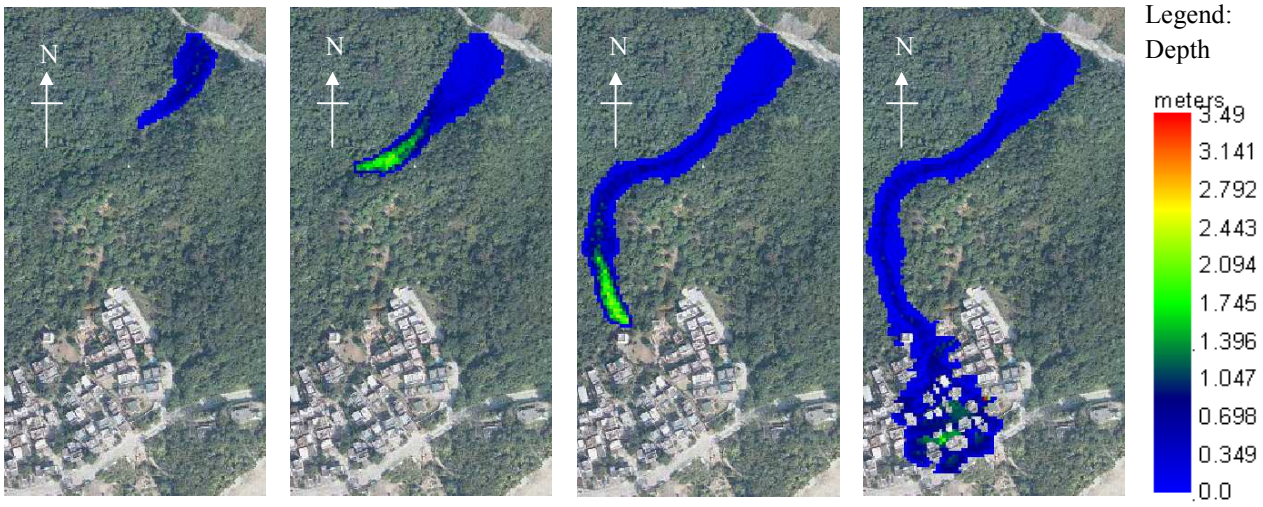

t = 108 s t = 216 s t = 288 s t = 324 s

Figure 3: Simulated debris depths at different simulation times

3.2 Lo Wai debris flood

A catchwater at Lo Wai, Tsuen Wan was blocked by landslide debris in a rainstorm on 20 August 2005, which resulted in overflow of a large amount of surface water at its overflow weirs immediate upstream of the blockage location (Figure 4). The overflowed surface water rushed down and entrained the loose materials along the streamcourse, forming a debris flood and affecting a village along Lo Wai Road.

The landslide investigation (MGSL 2006) revealed that during the incident, the depth of water in the streamcourse rose to as high as 2 m to 3 m at the upper trail of the debris flood and the entrainment of the bases of the streamcourse at this section extended to a maximum depth of about 3 m. The maximum thickness of debris deposited at Lo Wai Road at the end of the debris trail was about 0.3 m.

The debris flood event was back-analysed with a 5 m-grid DEM and an overflow rate of 7 m^3/s at each of the overflow weirs. Input of the rheological parameters is shown in Table 1. Specific features observed along the flow path of the debris flood on site, e.g. boundary walls of buildings and roadside fences, were also modelled. The simulation results are shown in terms of debris depth and velocity in Figure 5, which match reasonably well with the site observations.

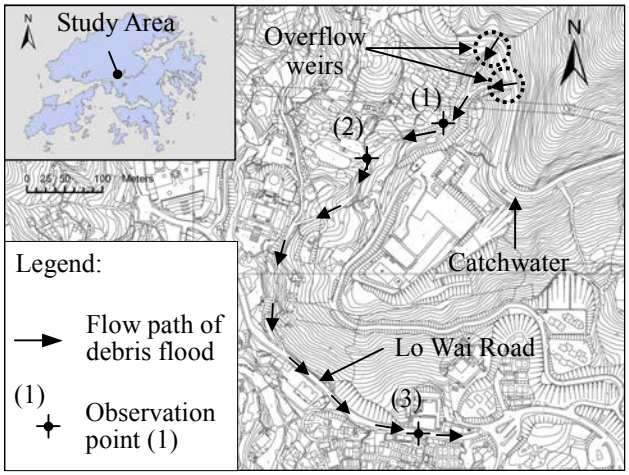

Figure 4: Layout of Lo Wai debris flood

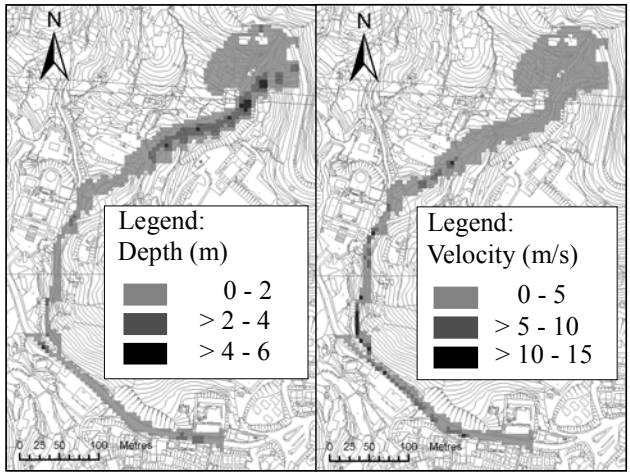

Figure 5: Simulation results

4 DISCUSSION

4.1 Digital elevation model

Given the same set of topographic data, a fine resolution DEM usually allows for a closer simulation of the observed flow patterns than a coarse DEM, in particular at locations of local variation in gradient. From the Lo Wai case, the fine DEM has greater capability in mapping out the actual land profiles in that the debris of the simulated debris flood was not trapped in the local depression, which matches well with the site observations (Figure 6). The 5 m-grid DEM, nevertheless, aggravates the extent of the local depression, resulting in excessive trapping of debris.

Despite the above, the appropriate resolution of a DEM should always depend on the resolution of input terrain data, the complexity of hillside/ land profiles, and the required output resolution. A more complicated model does not necessarily mean more accurate results, as all models involve idealisations and the uncertainties in some of the input parameters may not be easy to allow for, e.g. variability in local slope gradients which may not be reflected by conventional topographical maps, especially in a heavily vegetated hillside. Appropriate field mapping and investigation, together with use of appropriate tools, such as airborne LiDAR (Wong 2007), would help to enhance the resolution of the input data and hence the mobility assessment.

4.2 Sensitivity of parameters

Notwithstanding the simulation capability of FLO-2D, one of the key factors leading to best-fit simulation is whether the controlling parameters are adequately incorporated and realistically modelled in the simulation

model. Parameter uncertainty is nevertheless inevitable. It is therefore important to appreciate the sensitivity of the controlling parameters and the possible range of uncertainties that may be encountered in order to evaluate the reliability of the simulation results.

A study on the sensitivity of inflow rate to the simulated results was carried out for the Tong Fuk case. Using the same rheological parameters (Table 1), analyses were repeated for three different inflow rates (Q) of 5, 10 and 20 m^3/s. Although the inflow rates vary up to 400%, only about 30% change in the average debris flood velocity is noted. This could be related to the basic function of the quadratic rheological model that allows mutual control between resistance to flow and flow velocity in order to maintain sufficient stability in motion. Meanwhile, the maximum debris depth when Q = 20 m^3/s is about two-fold of that when Q = 5 m^3/s. This suggests that debris depth, when compared with flow velocity, is more sensitive to a change in inflow rate.

Another sensitivity analysis was carried out for the Lo Wai case to evaluate the sensitivity of two key rheological parameters, i.e. Manning's n roughness and sediment concentration, to the simulated results. Sediment concentration is one of the controlling factors of yield stress and viscosity. The findings are shown in Figure 7 with reference to three observation points, one at the upper section of the streamcourse (observation point (1)) while the other two along the concrete-paved road (observation points (2) and (3) (Figure 4). It can be seen that the simulation output is highly sensitive to changes in sediment concentration. A ±30% deviation in sediment concentration results in exponential changes in debris depth and velocity, owing possibly to the couple effect of yield stress and viscosity, particularly at high velocity. The variations in the rate of change indicate the relative contribution of yield stress, laminar flow friction and turbulence stress in the rheological model at different velocities. Changes in Manning's n roughness was tested at observation point (1) only as the uncertainty involved in the selection of Manning's n-value for the concrete-paved road, i.e. observation points (2) and (3), is small. It is noted that the greater the Manning's n-value, the greater the debris depth and smaller the velocity, in particular at zones of high velocity. The variations are as much as ±100% for debris depth and velocity. Despite this, the changes made to the Manning's n roughness at upstream of the debris flood seems to have negligible effects on the simulated results at downstream, possibly because of the extremely low Manning's n-value adopted at the downstream section, resulting in negligible changes in flow behaviours.

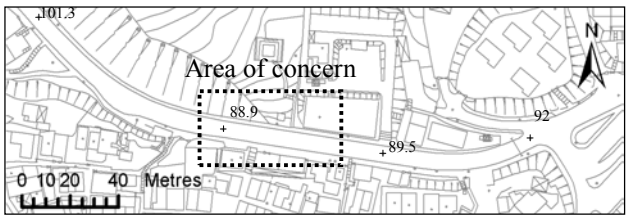

(a) Location plan showing area of concern

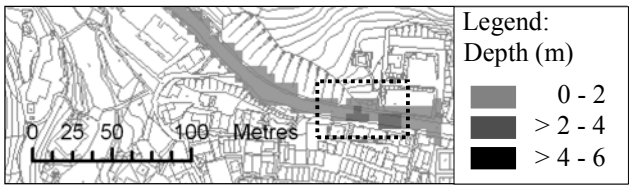

(b) Simulated debris depth using 5 m-grid DEM

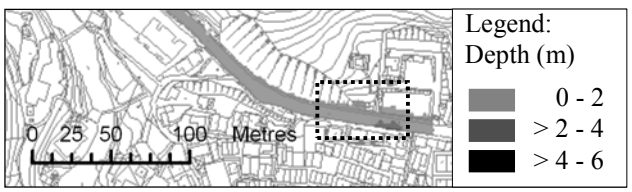

(c) Simulated debris depth using 1 m-grid DEM

Figure 6: Comparison of output between 5 m-grid and 1 m-grid DEM

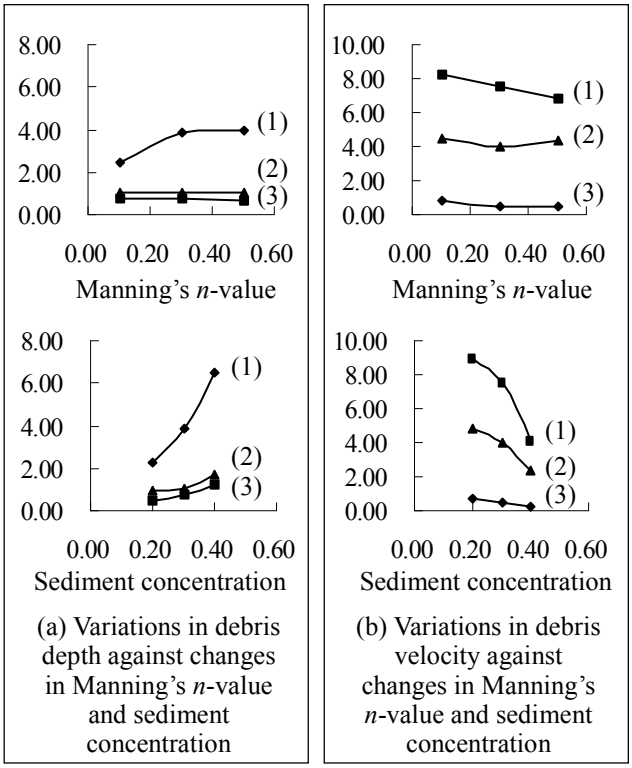

(a) Variations in debris depth against changes in Manning's n-value and sediment concentration

(b) Variations in debris velocity against changes in Manning's n-value and sediment concentration

Figure 7: Sensitivity analysis for rheological parameters at the three observation points

4.3 Obstructions

Flow direction of a debris flood is particularly sensitive to partial or full obstruction, given its high fluidity and flow mobility. Modelling these obstructions is important in order to reflect the actual site situations and the eventual flow path and pattern of the landslide debris. Otherwise, the simulated debris flood may simply flow along gradients on the DEM (Figure 8).

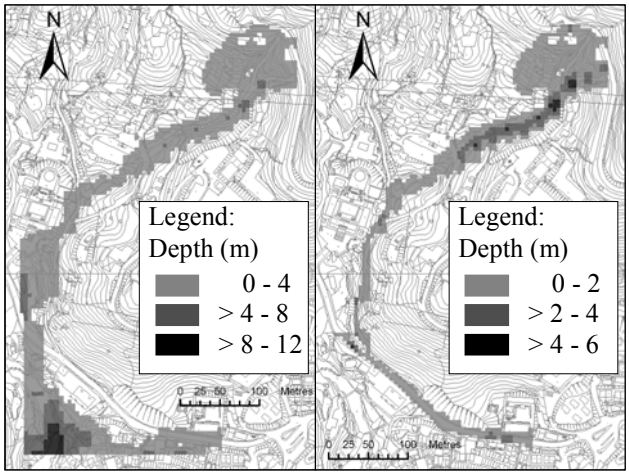

(a) Obstructions not modelled (b) Obstructions modelled

Figure 8: Effect of obstructions to simulated flow of debris flood

However, modelling these features at such fine resolution is often difficult, as they are narrow in plan and their interactions with landslide debris is complex. In many cases, they can be modelled either using DEM of very fine resolution or with specific modelling techniques, e.g. assigning certain percentage of blockage of flow at cells. The former would produce DEM of unnecessarily fine resolution at the expense of modelling effort and simulation time. It is estimated that the modelling effort required for setting up a 1 m-grid DEM with site features modelled is two times as much as that required for a 5 m-grid DEM while the simulation time is 10 times as much. The latter is therefore usually preferable provided that the simulation algorithms are sufficiently robust to take into consideration the various features and their interactions with watery flow. FLO-2D is one of these simulation algorithms incorporating a variety of modules for simulating different flow-structure interactions when the debris flood hits obstructions, e.g. levees.

5 CONCLUSIONS

It is demonstrated from the case studies that the numerical algorithm provided by FLO-2D is one of the credible tools for mobility assessment of debris floods. It enables an assessment of the probable effects of debris floods on elements at risk, in terms of influence zone, debris depth and debris velocity. Nevertheless, the associated model and parameter uncertainties should be carefully examined and evaluated. In any case, the possible range and effects of variations should be fully appreciated. It is advisable not to over-emphasis on model and output accuracy at the expense of modelling efforts and simulation time. There is a need to carry out more back-analyses of well-documented cases, to gain further insight into the possible values of the governing rheological parameters of typical debris flood events in Hong Kong and the sensitivity of the modelling results to the assumptions made.

ACKNOWLEDGEMENTS

This paper is published with the permission of the Head of the Geotechnical Engineering Office and the Director of Civil Engineering and Development, Government of the Hong Kong Special Administrative Region.

REFERENCES

FLO-2D Software Inc. 2006. *FLO-2D Users Manual Version 2006.01*.

Jin, M. & Fread, D. L. 1999. 1D Modeling of Mud/Debris Unsteady Flows. *J. of Hyd. Engg*., 125(8): 827-834.

Julien, P.Y. & Lan, Y. 1991. Rheology of hyperconcentrations. *J. of Hyd. Engg.*, 117(3): 346-353.

O'Brien, J.S., Julien, P.Y. & Fullerton, W. T. 1993. Two-dimensional water flood and mudflow simulation. *J. of Hyd. Engg.*, 119(2): 244-261.

Wong, H.N. 2007. Digital technology in geotechnical engineering. *Proc. HKIE Geotechnical Division Annual Seminar 2007 on Geotechnical Advancements in Hong Kong Since 1970s*, Hong Kong, 15 May 2007.

MGSL 2006. *Review of the 20 August 2005 Debris Flood at Lo Wai*, *Tsuen Wan*. Landslide Study Report LSR 5/2006, Geotechnical Engineering Office, Hong Kong, 100.

Methodology to Measure Roughness of Hong Kong Granite Using 3D Laser Scanning Technique

A.K.L. Kwong, C.C.Y. Tam & P.K.K. Lee
The University of Hong Kong, Hong Kong

ABSTRACT

In rock slope design, the mobilized frictional angle of rock joint roughness depends on basic frictional angle, small-scale roughness and large-scale waviness. If the shearing surface is wavy and the unstable block size is large, it would greatly affect the adoption of representative parameters for the design of the overall stability of a rock slope.

Automatic 3D laser scanning unit is now available that can be used to record 3D coordinates of closely spaced points representing the rock surface. After the rock surface is 3D scanned, it can be transformed into a triangulated irregular network representing the continuous wavy surface of the rock. Dimensionally accurate surface profile and pictorially correct images can then be generated and the asperities height and angle can be assessed at different sample sizes. The use of automatic 3D laser scanning technique with the incorporation of photo images would allow fast and accurate determination of representative roughness profile of different sizes of rock surface, thus the effect of small-scale roughness and large-scale waviness can be differentiated and determined. This paper describes the use of 3D laser scanning technique and direct shear test to measure the local roughness of laboratory-size joint plane and large undulating Granite sheeting joint in Hong Kong, with particular emphasis on sampling-effect and scale-dependency.

This paper describes the use of 3D laser scanning technique and direct shear test to measure the local roughness of laboratory-size joint plane and large undulating Granite sheeting joint in Hong Kong, with particular emphasis on scale-effect.

1 INTRODUCTION

Stability problem involving sliding mode of failure may be induced during an excavation of a rock slope. Improper use of design frictional angles may give rise to serious consequences resulting in casualties and loss of life, damage to the natural and/or built environment, as well as economic losses (Dai, 2002). Proper determination of shearing resistance for rock joint design has been studied over the past 30 years but still remained as a challenging problem due to the complexity of the irregular surface characteristics and the empiricism of the existing formulae. Errors and uncertainties also arise during the process of investigation and interpretation of results because of the limited quantity and quality of available data.

The estimation of shearing resistance of a rock joint can be arrived from at least 3 components: basic frictional angle (ϕ_{basic}), asperities angle (i) and sample size (geometrical). When shearing occurs under a low normal stress, the edges of the asperities will tend to move up along the inclined surface causing dilation to the sample. Dilation angle can be defined as the change of vertical distance over the change of horizontal distance at the instant when a pronounced peak of shear stress is achieved.

Barton and Bandis (1990) observed that such dilative behavior is found only for those strong, rough and unfilled surfaces and it is dependent on the size and roughness of the individual sample. They further correlated a design parameter called Joint Roughness Coefficient (JRC) from the back-calculation of some laboratory tests or empirically assigned with respect to ten standard profiles of 100 mm long via visual approximation (Barton, 1977). However, the latter exercise is very subjective and variable, not only from the designer's point of view, but also that it is scale dependent. For example, the appearance of the wavy surface is very lengthy and wavy when the unstable block size is relatively large in a slope-engineering problem; however, such estimation of JRC values may vary when its size is reduced to a standard of 100 mm. Hence there is a practical need to quantify the effect of joint roughness in small and large scales in a more scientific manner.

To overcome the problem, a number of researchers had recently adopted the technology of 3D laser scanning onto a variety of applications in the field of surveying and engineering, such as the monitoring of tunnels and natural slopes as well as rock joint roughness (Hong, 2006; Lichti et al., 2002, Schulz, 2005). They concluded that the 3D laser scanning technique is a very promising approach that can systematically and quickly digitize a given region directly at the scene without contact and damage to the object. The generated huge amount of data is presented in an x-y-z coordinate system (so-called point clouds), which are dimensionally accurate and precise with respect to the overall size of the object. Different dedicated reverse engineering software are available that would allow modeling of 3D images, editing and analysis.

This study investigates the methodology and develops a framework in the use of automatic 3D laser scanners to quantify, without human judgment, the roughness angles of rock joints in small and large scales. Rock cores of different standard sizes (60 mm, 83 mm and 90 mm), and surface profile of over 8 m long have been digitally laser scanned (3D) and then transformed into a triangulated irregular network representing the continuous wavy surface of the rock. A 2D surface profile can then be generated and the roughness angles can be quantified consistently at different sample sizes. Direct shear test in the laboratory have also been conducted on the rock joint samples in order to calibrate the results analyzed from the 3D laser scanning techniques.

2 3D LASER SCANNING

2.1 Field scanning at Shek O, Hong Kong

The Leica Cyrax and Scan Station (Leica Geosystem, 2007) were employed to characterize three exposed rock fracture planes on May and October 2006. The three exposed sheeting joints are pinkish brown, highly eroded, smooth to undulating GRANITE with narrow cracks parallel to the scanning direction. Each specific area of interest is about 4 m × 8 m and one of the joint planes is photographed and shown in Figure 1(a).

The Leica 3D laser scanners are terrestrial and based on the time-of-flight (TOF) concept. Each machine consists of a laser head that emits a narrow laser beam through two special rotating mirrors that can rapidly and systematically sweep over the predefined target. It computes the distance between the transmitter and the reflecting surface from the angular deflection angle of the mirrors and also the travel time that the signal has taken between the transmission and reception.

The two days of scanning were both conducted under good weather condition. The scanner was set at a location identified by a Global Positioning System (GPS) device that tied into the coordinate system of Hong Kong and within a distance around 20 m to 30 m away from the scan surface. A scanning density of 10 mm (0.01 m) was originally selected such that each scan took about 1-2 hours of operation and output a total of over 60,000 coordinate points for each surface. Using the Cyclone software for editing, registration was taken to integrate the scan areas into a single coordinate system to transform and align the objects. For two of the joint planes, rescanning was carried out to refine the obtained data.

Based on the generated point clouds, an example of the TIN model after scanning of one of the joint planes is shown in Figure 1(b). It can be seen that the 3D image looks very realistic that well represent the characteristics of the joint. It even allows identification of detail geological features such as the distinctive joint and major cracks on the joint face.

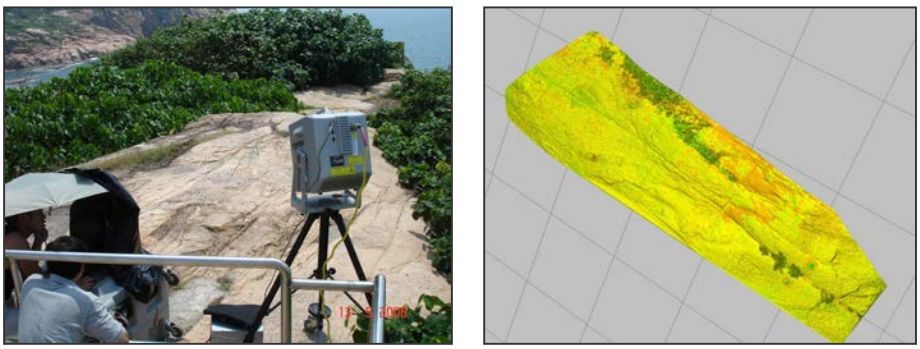

Figure 1. (a) Joint plane at Shek O, Hong Kong, and (b) 3D image of the joint plane

Along the direction of movement, two to three 2D cross sectional profiles are selected from the point clouds which are exported into an Excel spreadsheet program for plotting of the joint surface profile. In Figure 2(a), the scatter points are densely spaced and clearly depict the rolling downhill direction of the joint plane. The cross section in Figure 2(a) can be zoomed-in and presented with an exaggerated scale on the y-axis in Figure 2.(b) for illustration purpose. The latter diagram illustrates the unevenness of the surface in a small window. This shows that relatively small delegates of the profile roughness are well captured by the Leica scanners in full scale.

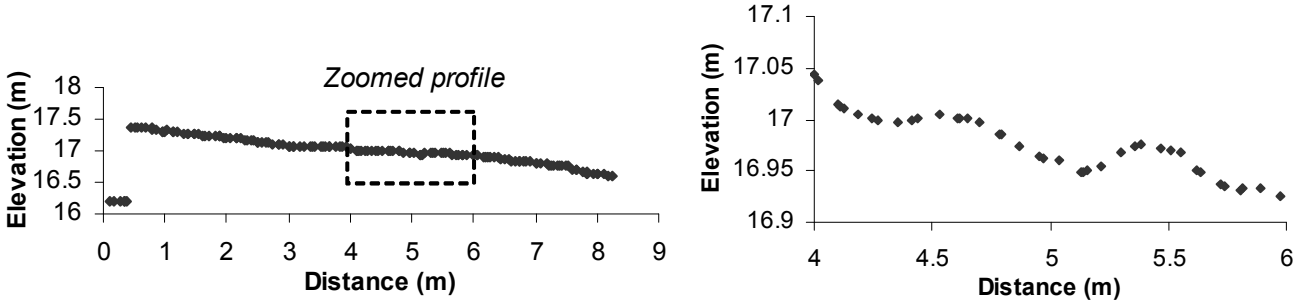

Figure 2. (a) Selected cross sectional profile of a sheeting joint, and (b) zoomed-in cross sectional profile of Figure 2(a)

It is interesting to note that the scan density was originally assigned to be 10 mm during the field operation. However, the resulting data in Surface 1 ended with an average density of 40 to 50 mm over the length of 8 m in the selected cross sections. This loss of resolution is likely due to the existence of blind spots hidden under the trough of the surface. It is expected that an accuracy of a single measurement could deviate about ±6 mm according to the specification of the machine. On the other hand, a trial of rescanning was performed on Surface 2 and Surface 3 with equipment set up at different locations. The two sets of data of each surface are orientated with the same reference point hence they are integrated together into a universal system. They show that rescanning can improve the scan density to 30 to 40 mm for the 6 m surface profiles, and has avoided some of the blind spots. This further suggests that the degree of accuracy on illustrating a joint plane in 3D relies on the amount of effort and time devoted in the scanning process.

2.2 Laboratory scanning

A desktop laser scanner (Roland LPX-60) is available in the Rock Research Centre at The University of Hong Kong and it was used to capture the surface roughness of granitic rock cores between 60 mm to 90 mm in diameter (Figure 3(a) and (b)). The rock cores were recovered in Hong Kong and they were fractured surfaces of GRANITE that are rough, undulating and clean.

The Roland LPX-60 is an automatic non-contact 3D laser scanner that adopts the spot-beam triangulation method. It consits of a spot beam laser that emits light at a defined angle onto the interested object and a CCD camera would detect the reflected light. The object is mounted on a base plate which rotates at a small interval of a predetermined angle, then the laser beam moves from bottom to top after a layer is completely scanned. It includes a modelling software, Dr. Piza3, for operation, editing and modeling.

Each set of core consists of two natural joint plane surfaces, and a total of five core sets in 60 mm diameter, six core sets in 83 mm diameter, and three core sets in 90 mm were prepared for scanning (and later shear testing). A gypsum mould was prepared that would hold and align the joint faces and leveled horizontally by using a leveling-bubble indicator prior to molding.

A scan density of 0.4 mm in the x- and y- directions was specified and scanning was performed automatically for about 1 hour for each of the joint face. Although scanning noise and blind spots (areas that are hidden or beams not reflected back to the camera) were observed in all of the specimens, the densely spaced data points adequately generated a colorless 3D model (see Figure 4) that well represents the actual object. Selective cross sectional profiles from these cores were also created and exported to an Excel program for plotting of the surface profile (see Figure 5).

Figure 3 (a) Roland LPX-60 laser scanner, and (b) specimens prepared before scanning

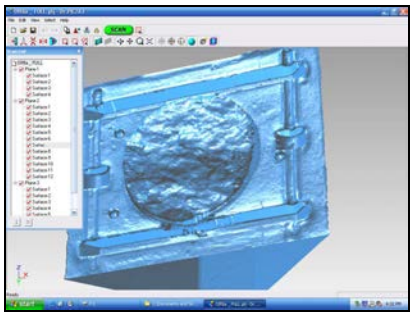

Figure 4. Typical example of a 3D model of a rock core specimen after scanning

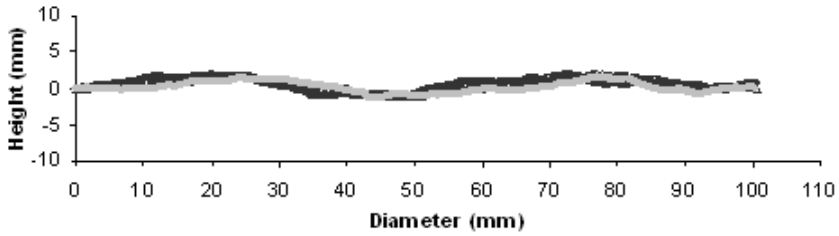

Figure 5. Selected cross sectional profiles of a rock core surface scaled to 100 mm

As an example, Figure 5 shows a scatter-point plotting which clearly depict the overall undulations of the two different surface profiles obtained at different locations of the same joint. It implies that small-scale roughness of rock cores can be efficiently and accurately digitized and captured by the Roland scanner, and the retrieved data are further calibrated against the roughness properties in the following Section 4.

3 DIRECT SHEAR TESTS IN LABORATORY

Direct shear tests have been carried out using a Roberson shear box. Pressure gauges and displacement transducers are connected to an automatic data logger for recording purpose. Tests were carried out with procedure following the specification of the ISRM suggested method (1981).

After a series of direct shear tests were conducted, the measured dilation angles were 47° for the 60 mm core group and 40° for the 83 mm core group respectively. Peak strengths were generally reached at a horizontal displacement of 1-6 mm and it is equivalent to approximately 1-2 % of the core diameter. It implies that the contribution of asperities roughness upon shearing is very sensitive and occurs at a relatively short distance (Tam, 2008).

4 ANALYSIS, RESULTS AND DISCUSSION

4.1 Methodology of analysis and results

To make use of the scanned data, roughness angles were mathematically calculated by measuring a change in elevations over a change in length between two scanned points along a linear profile. Using the illustration in Figure 6, the asperities angle (i) is dependent on the length of the sampling intervals such that a shorter sampling length would generally measure a steeper angle. Sampling length is defined as the total distance between the specified numbers of scanned points. An Excel program is coded to perform systematic trials of each point that connect to the next point as per the assigned sampling unit hence to calculate the change of slope and the resultant angle. Any linking between the two scanned points which has obstacle of other asperities in between is considered as invalid and rejected because it is not physically possible to measure nor it exists. Only positive value of generated angle is recorded since it indicates an inclination of the joint profile that can provide shearing resistance against the direction of shear. 1 unit is equivalent to a sampling length between 2 data points.

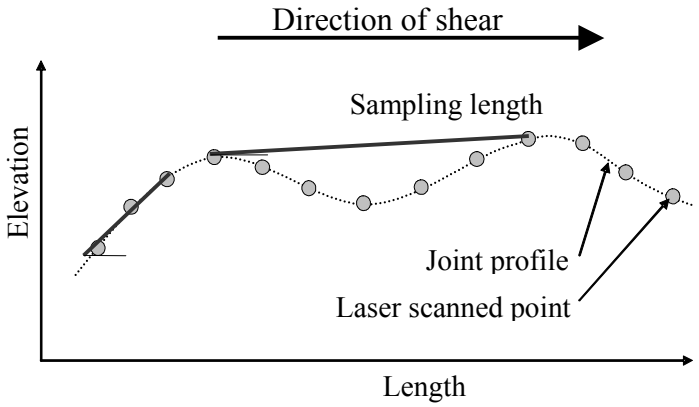

Figure 6. Measurement of roughness angle using different sampling intervals between scanned points

For the assessment of the laboratory rock cores, a sampling length between 1-50 units, equivalent to 0.4-20 mm was adopted. To measure the large-scale waviness angles of the Shek O joint planes, a sampling length between 1-9 units sampling, equivalent to 40-360 mm was adopted. The simulated angles are summarized in Figure 7 and Figure 8.

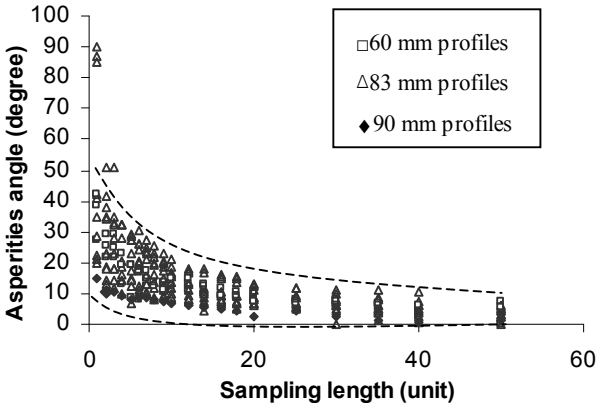

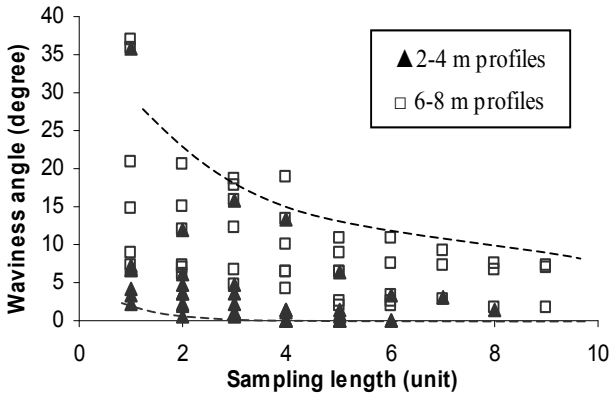

Figure 7. Scanned asperities angles for 60, 83, and 90 mm cores, Figure 8. Scanned waviness angle for Shek O joint planes

4.2 Effect of sampling length

Figure 7 and Figure 8 demonstrate that the generated angles are highly sensitive to the change of sampling length. When the joint surface is small, the asperities angles change from 85° to 1° when sampled by 1 to 50 units respectively in Figure 7. When the joint surface is large, the waviness angles vary from 36° to 1° when sampled by 1 to 9 units as shown in Figure 8. Generally, the shorter sampling length measures a higher roughness angles than that of a longer sampling length and it converges in an exponential manner with a decrease in angles against an increase in sampling lengths. In addition, when sampling unit is small, the roughness angles vary in a wider range than that measured by a longer sampling unit. This is consistent and is an expected outcome as illustrated in Figure 6.

4.3 Determination of asperities angle and waviness angle

Since the dilation behavior is sensitive to a small change of displacement in a direct shear tests, a relatively small sampling length should be adopted to capture the roughness that causes dilation. A sampling length of 1 % of the core diameter, equivalent to 2 units, is selected to determine the average asperities angle of the rock cores. Based on Figure 7, the average asperities angles are equal to 39°, 34° and 18° for the 60 mm, 83 mm and 90 mm cores. These angles are relatively close but lower than the dilation angles obtained from the laboratory tests with a few degree of deviation. It suggests that a sampling length of 1 % core diameter may be sufficient to capture the dilation effect in a small-scale sample.

Similarly, the idea of 1 % joint length is adopted to measure the waviness angle of the large rock joint planes and it is equivalent to about 1 to 2 units sampling length for the joint planes at Shek O in Figure 8. The average waviness angle is measured to be around 10° for the three 6-8 m joint faces. Each profile surface is then reduced to 2-4 m by only taking the first section of each joint in order to mimic a shorter cross section. The average waviness angle for the 2-4 m profiles is also around 11°.

4.4 Effect of scale

A comparison between Figure 7 and Figure 8 indicates that a smaller core generates a much higher angle than that of a long profile. Based on the sampling of 2 units (equivalent to 1 % of the joint length), the predicted frictional angles in Figure 5 (60-90 mm) could be reduced by 2-3 times when the profile length is increased by 2 orders of magnitudes in Figure 6 (2-8 m). However, such reduction becomes progressively less apparent when the waviness angles tend to converge to a stationary value. This demonstrates that the influence of scale effect is very significant when the representative core sizes are smaller than that to the field scale. The importance of scale effect to shearing resistance is clearly shown by both the laboratory testing and through the analyses of the scanned data.

5 CONCLUSIONS

An application of 3D laser scanning technique was carried out in this study and the methodology adopted has shown that the technique has proven to be feasible and efficient in the investigation of joint roughness. Two different types of scanners were adopted to generate a high resolution of scanned data. They provided detailed information in a quantitative manner for rendering of realistic 3D images and selection of 2D cross sectional profiles for numerical analysis. They also calculated the asperities angles of small-scale rock cores and the waviness angles of large-scale rock planes. The predictions based on the scanning technique were in close agreement with that measurement in the laboratory given that an appropriate sampling length is chosen. The significance of the effect of sampling length and scale-dependency of joint roughness are further demonstrated through a series of numerical calculation and assessment.

Therefore, the roughness characteristics of a rock joint can be captured accurately in a quantitative manner without empiricism. It can quickly digitize an object without direct contact and human judgment, in different sizes from millimeter to meters.

This study has presented an initial prototype and framework on the potential use of 3D laser scanners to investigate joint roughness. Future works are being carried out to calibrate the asperities angles obtained from the scanners with those measured in the laboratory for practical engineering uses.

ACKNOWLEDGEMENTS

The work described in this paper is supported by the Research Grants Council of the Hong Kong Special Administrative Region, China (RGC Ref No.714705).

REFERENCES

Barton, N. and Bandis, S. 1990. *Review* of predictive capabilities of JRC-JCS model in engineering practice, In Rock joints, N. Barton and O. Stephansson (eds.), *Proc. Int. Symp. On Rock Joints*, pp. 603-610. Loen, Norway. Balkema.

Barton, N. and Choubey, V. 1977. The Shear Strength of Rock Joints in Theory and Practice, *Rock Mechanics*, (10), 1-54.

Dai, F.C. and Lee, C.F. 2002. Landslide characteristics and slope instability modeling using GIS, Lantau Island, Hong Kong. *Geomorphology,* Vol. 42, pp. 213-228

Franklin, J.A. et al. 1981. Part 2. In E.T. Brown (eds), *Rock Characterization Testing and Monitoring, ISRM*: 129-140. Pergamon Press.

Hong, E. S., Lee, I. M. and Lee, J. S. 2006. Measurement of rock joint roughness by 3D scanner, *Geotechnical Testing Journal*. 29(6). Paper ID GTJ100169.

Leica Geosystem. 2007. Leica Scan Station Product Specification. Switzerland.

Lichti, D. D., Gordon, S. J. and Stewart, M. P. 2002. Ground-based laser scanners: operation, systems and applications. *Geomatica,* 56 (1), pp. 21-33.

Roland LPX-60 User's Manual. 2006. Roland DG Corporation. Japan.

Schulz, T., Lemy, F. and Yong, S. 2005. Laser scanning technology for rock engineering applications. *The 7th Conference on Optical 3-D Measurement Techniques*. Vienna, Austria.

Tam, C. C. Y. 2008. Study of rock joint roughness using 3D laser scanning technique. The University of Hong Kong. MPhil dissertation *(in preparation)*

Ground Investigation for Tunnel Works

Y.C. Lam, J.K.W. Tam & J.Y.C. Lo
Maunsell Geotechnical Services Limited, Hong Kong

ABSTRACT

A comprehensive ground investigation (GI) plan is essential to identifying potentially problematic ground and groundwater conditions before the commencement of major construction activities, in particular, for tunnel projects. Comprehensive ground information with high degree of certainty could help to optimize the engineering design, plan for an effective construction programme, and mobilize appropriate resources for the works. There is always a need to interpolate the conditions of the ground between investigation stations, e.g. vertical or inclined drillholes. It is commonly difficult to ascertain the area of uncertainty in the ground with conventional GI methods.

With the availability of new technologies, continuous ground information can be obtained along the proposed alignment of a tunnel more effectively in terms of cost and time. This paper has focused on some GI methods such as Horizontal Directional Coring (HDC), groundwater inflow tests and geophysics that have been adopted for investigating the ground and groundwater conditions of the drainage tunnels for the landslide preventive works at Po Shan.

1 INTRODUCTION

An appropriate design of the GI programme ensures that sufficient and reliable information can be obtained for a capital project. Guidelines published by Geotechnical Engineering Office (GEO) such as the Geoguide 2, Geoguide 4, Technical Guidance Note No.24, and the Ground Investigation Guidelines issued by AGS(HK) demonstrate that many useful GI techniques can provide valuable GI information for defining a safe and economical construction design. GI programme can also be proposed for assessing specific problems or checking of existing works. In order to achieve an effective GI programme, a clear understanding of the project objectives is required.

Unforeseen ground conditions are always inherent for tunnel works prior to construction. It is important to minimize the potential risks, which may have significant impact on the design, construction, and most importantly on public safety. At different stages of a tunnel project, a good planning of GI programme with various techniques can serve for different purposes. At the planning stage, desk study limited GI works are required to provide general picture of ground conditions; consequently to propose some alternative routes and estimate the order of cost for the project. At the preliminary design stage, GI works shall focus on the preferred route in order to develop the hydrogeological models for the preferred alignment. However, the extent of GI works shall cover a wider area in the proximity of the preferred alignment to enable the flexibility to further modify the alignment at the later stage. Investigation methods including sampling, insitu testing and instrument installation shall be utilized. The presence of geohazards (e.g. fault zone) shall be identified by other specific investigation methods at this stage. At the detailed design stage, the extent of the additional GI works shall provide the information for the cost estimation of the overall construction works. This information is used by tenderers in assuming risks of the project and helps to provide more competitive tender prices. The aim of this paper is to briefly discuss on those GI techniques effectively chosen during the detailed design stage of the Po Shan groundwater drainage tunnel project.

2 EFFECTIVE GROUND INVESTIGATION TECHNIQUES

An effective GI programme shall provide reliable information along the tunnel alignment such as the geological model, hydrogeological profile, presence of adverse geological features and groundwater flow. Specific laboratory tests are proposed to examine the engineering properties of subsurface geology. The

laboratory results are used to determine the design parameters and facilitate the detailed design. Instruments installations are required for monitoring of groundwater levels and ground movement.

Seismic survey is a commonly adopted geophysical GI technique to explore the sub-surface geological structures along the proposed tunnel alignment. Seismic methods can provide profile images with quantitative depth to bedrock, rock quality indication and identification of potential weak zones.

Insitu Tests

Groundwater inflow measurements under atmospheric condition indicate the natural inflow rate into the drillhole. The testing sections can generally cover 50 m to 100 m along the proposed tunnel alignment. It can provide information to visualize a more realistic hydrogeolgical condition than using the water absorption test. The inflow measurements can be used to predict the water inflow into the tunnel during excavation. By analyzing these results, the tunnel design can be more effectively with a more realistic hydrogeological model.

The water absorption test measures the water acceptance by insitu rock under pressure. The measurement represents the volume of water that can escape from an uncased section of borehole, in a given time and under a given pressure (GEO, 1987). The water absorption test provides the approximate permeability of insitu rock, which can be considered as an indirect measurement of groundwater inflow and served as the guidance for the grouting design.

Borehole discontinuity survey can be conducted by carrying out the impression packer test or acoustic borehole televiewer. The discontinuity data can be processed to determine the rock wedge and design the tunnel temporary support. The data can also be correlated empirically to determine the insitu loading acting on the tunnel wall.

Laboratory Tests

Depending on the tunnelling methods, specific laboratory tests can be used to evaluate the hydrogeological conditions, determine the sequence of works, and facilitate the detailed design. Typical tests for soil include triaxial compression tests, oedometer tests, dispersion tests, chemical tests and fundamental index tests. Major tests for rock include Unconfined Compressive Strength (UCS) tests, Brazilian tests, Point Load tests, tests to determine Young Modulus, Poisson's Ratio. Rock hardness, dilatancy of joint and joint characteristics are also common parameters to be determined from laboratory tests. Possible swelling minerals and swelling capacity of clay infilling can be identified by testing the joint infill materials. Typical tests for facilitating the use of Tunnel Boring Machine (TBM) include Punch tests, Cerchar Scratch tests, thin section petrography, and testing for Drilling Rate Index (DRI), Bit Wear Index (BWI) and Cutter Life Index (CLI).

Geophysical Survey

Seismic methods can be used to identify the rockhead level and adverse areas for tunneling. The depths of the underlying layers can be determined by analyzing of the travel-time curve for reflected or refracted rays. The two types of seismic methods, which are commonly used for ground investigation, include the reflection survey and the refraction survey. A successful application of geophysical survey was carried out for the Po Shan Drainage tunnel project, which will be discussed in the following section of "Project Experience".

Ian *et al.* (1986) suggested some seismic explorations for the GI of rock tunnels. Namely, the determination of rockhead and identification of discontinuity zones using seismic refraction survey; tomographic acoustic measurements to study the area that is too complex for refraction survey and too far below ground. It can be applied with the "crosshole" method or "borehole to surface" method. Table 1 shows some typical applications of the geophysical surveys, suggested by Kearey & Brooks (1991).

Reflection Survey	Refraction Survey
Hydrocarbon Exploration	Determination of rockhead level
Vertical Seismic Profiling – to reveal subsurface detail	Determination of in-situ elastic rock properties
Geological Mapping – including the structural and stratigraphic information	Determination of groundwater level & overall hydrogeology (in conjunction with resistivity survey)

Table 1 – Applications of the seismic reflection and refraction surveys, (Kearey & Brooks, 1991).

Horizontal Directional Coring

Horizontal Directional Coring (HDC) can provide continuous core sample along the tunnel alignment, which can serve as a pilot tunnel. Hence, the unforeseen tunneling conditions by just using only the vertical & inclined boreholes can be avoided. The continuous geological information is valuable for the determinations of construction programme, grouting works and excavation method, such as the use of tunnel boring machine or drill & blast method. The areas of problematic rock condition can be located using the HDC, and a specific excavation scheme for these areas can be proposed before tunneling. HDC also enables the measurement of groundwater inflow in different sections of a tunnel. It is valuable data for the grouting design that directly affects the programme and cost estimation of tunnel construction.

The two main components of a HDC programme include the borehole drilling and the borehole surveying. The steerable drilling is performed by using the steerable directional core barrel, and the borehole profile is surveyed by using the electronic multishot (EMS) instrument.

Steerable Directional Core Barrel

Steerable directional core barrel is made as 5.4 m in length. It provides deviated rock core when drilling in a controlled direction at a control rate. The maximum length of the rock samples is 3 m per core-run, and the core diameter is 31.5 mm for both the B-size (60 mm) and N-size (76 mm) barrels. The steerable barrel is available in both conventional and wireline core barrel configurations. It requires only the normal setup for a conventional or wireline diamond-drilling programme, without additional equipment is necessary. It can be driven by the conventional drill string as normal drilling. The two main components of a steerable barrel consist of a stationary outer barrel and a rotating inner barrel. The functionality of this device will be demonstrated in the next section.

Steerable Directional Core Barrel

Stationary Outer Barrel

The non-rotating, stationary outer barrel controls the directional setting; by maintaining the toolface angle for the required "dogleg" and stabling the set location during the drilling. It comprises three main components, which are the locking piston, packer assembly and the adjustable eccentric housing.

Locking Piston

a) Locking Piston

When the locking piston is in a locked position, both the non-rotating section of the outer barrel and the rotating section of the outer barrel are locked together. Hence, the toolface position can be adjusted and ascertained by rotating the outer barrel. When the locking piston is in an unlocked position, the inner rotating barrel and the drill string can rotate independently to the outer barrel.

b) Packer Assembly

The packer assembly maintains the toolface position during the drilling process. The rubber packer inflates when drilling fluids/water passes through it. The inflated rubber packer gives pressure on the expanding pads, which push the harden guide bars to indent the borehole wall. The indentation of the harden guide bars onto the borehole wall prevents rotation of the outer casing in drilling. The hydraulic feed pressure causes the outer casing to slide forwards along the drillhole wall.

Packer Assembly

c) Adjustable Eccentric Housing

The eccentric housing is located in the lower portion of the non-rotating outer barrel. It is used to adjust the angle of "dogleg", with maximum "dogleg" for N-size core sample about 12°/30 m.

Eccentric Housing

Rotating Inner Barrel

The rotating inner barrel comprises an outer casing and an inner tube for core collection. The casing of the outer barrel is the driveshaft of the barrel, and is attached to a reaming shell and diamond bit coupling.

Electronic Mutishot (EMS) Instrument for Borehole Survey

Electronic Mutishot (EMS) Instrument belongs to a family of magnetic and non-magnetic instruments for borehole surveying. The tri-axis accelerometer and magnetometer measure the gravity and the magnetic field from the earth respectively. It provides the survey data of borehole including the azimuth, inclination, gravity toolface, magnetic toolface and temperature. It records data at given time intervals and stores the data in an internal flash memory. The two types of EMS to be discussed in this paper include the Standard probe and PeeWee probe. Both tools are operated by a hand held terminal or PC. The survey data can be exported to the software package for calculation and analyses.

Standard EMS in the steerable barrel

Standard EMS

The Standard EMS is a probe of electronic multishot and designed for serving the steerable barrel. It has a diameter of 30 mm and a length of 0.83 m.

PeeWee EMS

The PeeWee EMS is a miniature electronic multishot that is used for surveying of borehole profile. It has a diameter of 30 mm and a length of 0.975 m. It is an integrated pressure barrel that can resist a pressure of 300 bars. It has an internal memory that stores multiple readings at pre-set intervals.

PeeWee EMS & Hand Held Terminal

3 PROJECT EXPERIENCE

Seismic Refraction Surveys in Po Shan

Seismic refraction surveys were conducted as part of the GI works for Landslide Preventive Works at Po Shan, Mid-Levels – Agreement No. CE28/2004(GE), under works orders GE/2003/18.56 & GE/2003/18.64. A total of eight seismic traverses were carried out for the captioned works orders. Equipments used for the survey include the Geometrics Model S-24 Smartseis, cables, geophones (14 Hz), hammer switch, hammer trigger cable, sledgehammer and metal plate.

Geometrics Model S-24 Smartseis

Geophone installed on ground & connected to a cable

Setting Up and Surveying

Six seismic traverses were carried out by 12-channel traverses, and two were conducted by 24-channel traverses. The seismic source was positioned at the end of traverse (End shot), middle of traverse (Centre shot) and at 20 m from the nearest geophone (Off-end shot). It was produced by striking a sledgehammer onto a metal plate. Hammer blows were stacked at each point in order to reduce the signal to noise ratio. The used geophone spacing was 10 m, which enabled the traverse lengths of 110 m and 230 m. The record length and the sampling interval of the seismograph were set to 128 ms and 125 ms respectively, and a delay time of zero millisecond was used. Results were previewed before stacking and only valuable seismic signals were used in the stacking process. The seismic data was digitally recorded, and hard copies of the data were also printed on site.

Analysis and Findings

The first arrival times of seismic trace at the geophones, were determined from seismograms. The time-distance graphs of all traverses were plotted using the obtained arrival times versus distance travel. Results were then analyzed using the Hagedoorn 'Plus-Minus' method. Interpretation of the results suggested that a 3-layer model composed the sub-surface geology of the study area, and the depth of resolution reached 12 m to

15 m. The 3-layer model has comprised of the top "residual soil/colluvium" layer, the middle "colluvium/CD tuff" layer and the bottom "CD/HD/MD tuff". The thicknesses of the top and middle layers were inferred to be 1 m – 4 m (with a seismic velocity of 0.4 m/ms – 0.5 m/ms) and 8 m – 12 m (with a seismic velocity of 0.9 m/ms – 1.2 m/ms) respectively. The upper boundary of the bottom layer varies from 12 m to 15 m below ground level, with a seismic velocity of 2.6 m/ms – 3.2 m/ms. However, the seismic velocities were correlated to the different material layers, and the effect of groundwater table had not been filtered out from the model. For studying the seismic velocities of materials in particular to the groundwater regime, further analysis of piezometric data in conjunction with the seismic data shall be required.

The results of the captioned seismic survey have provided the stratigraphy of the study area, reaching a depth of 15 m below ground level. The bedrock level could not be determined using these captioned surveys, and is suggested to be more than 15 m below ground.

Horizontal Directional Coring (HDC) in Po Shan

Two horizontal directional coreholes were drilled under the works order (GE/2005/03.401) for the Po Shan Tunnel Project. The entry points of the two horizontal directional drillholes, namely PS-HDD/01 and PS-HDD/02, are located at the toe of Feature 11SW-A/CR175 adjacent to the No 16 Po Shan Road. The captioned G.I. works, including drilling and insitu tests, started on the 01 Nov. 05 and completed in about two months. The layout plan of two horizontal directional drillholes is showed below.

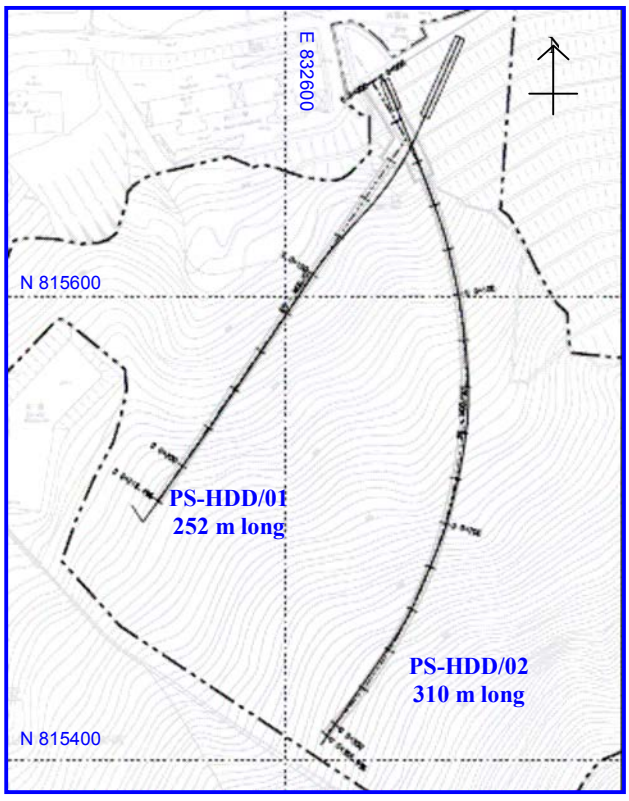

Layout Plan of PS-HDD/01 & PS-HDD/01

Drillhole Survey

The "PeeWee" EMS was used for surveying the profiles of drillholes with intervals of 6 m to 10 m. The corehole profiles were correlated to the given control points (namely CPT/01-01 to CPT/01-07 for PS-HDD/01 and CPT/02-01 to CPT/02-10 for PS-HDD/02), to ensure the coreholes were in line with the proposed alignments. The full coreholes directionally driven for PS-HDD/01 and PS-HDD/02 were attempted with a tolerance of 2 m radius in all directions to the proposed alignments. The proposed alignment of PS-HDD/01 was a straight line, while the proposed alignment of PS-HDD/02 was under a curvature with a 225 m radius.

The used "dogleg" angle for the two horizontal directional coreholes was generally 0.2 to 0.3 per 1 m, and occasionally 0.5 per 1 meter. PS-HDD/01 had an upwards gradient of 3 to 4, and PS-HDD/02 had a downwards and then upwards gradients of ±2. Referring to the drillhole survey, PS-HDD01 profile was steered with offsets of 4.7 m and 2.6 m offset at the control points CPT/01-01 and CPT/01-02 respectively. It deviated initially and trended back to align with the proposed alignment at the control point CPT/01-03. It positioned within the tolerance envelope from the control points CPT/01-03 to the end of drillhole (252.16 m in length). The setting up of the PS-HDD/01 drilling rig was 10 offset from the proposed position due to the site limitation. Hence, the first 50 m of the corehole PS-HDD/01 was offset from the proposed alignment. The complete profile of PS-HDD/02 has adequately aligned with the proposed alignment. It positioned within the tolerance envelope from the control points CPT/02-01 to the end of corehole (310.44 m in length).

Insitu tests in the horizontal directional drillholes

Insitu tests under the same works order included impression packer tests, water absorption tests and groundwater inflow measurements along the two horizontal directional coreholes.

Impression Packer Tests in sub-horizontal holes

It is necessary to determine the azimuth, inclination and toolface of the sub-horizontal testing section. Under the GI works for the Po Shan Drainage Tunnel project, a Reflex EzShot instrument was used to obtain these geometrical measurements. It was placed in a casing that was attached to the lower end of the packer device. Before the packer was inserted into the drillhole, a reference line pointing to the zero toolface (i.e. 12 o'clock position) was drawn on the parafilm. The zero toolface of the Reflex EzShot was also calibrated with the reference line marked on the packer. The orientation measurements were recorded after the inflation when the packer was placed at the specified testing section.

The joint data of the rock cores was obtained in the following steps:

1. Adjust the direction & dip angle of the Goniomenter according to the measurements captured by the Reflex EzShot at the testing section.
2. Mark a zero toolface reference line on the rock core, using the joint impressions and the previously marked reference line on the parafilm.
3. Place the rock core with the reference line on the Goniometer. Then, rotate the rock core to an angle same as the toolface captured by the Reflex Ezshot.
4. Measure the oriented joints by compass.

Packer Device

Reflex EzShot Instrument

Rock core placed on the Goniometer

Water Absorption Tests

For the Po Shan Drainage Tunnel project, water absorption tests were also conducted using the conventional and wireline methods. The wireline system was used for the testing sections located at a long distance.

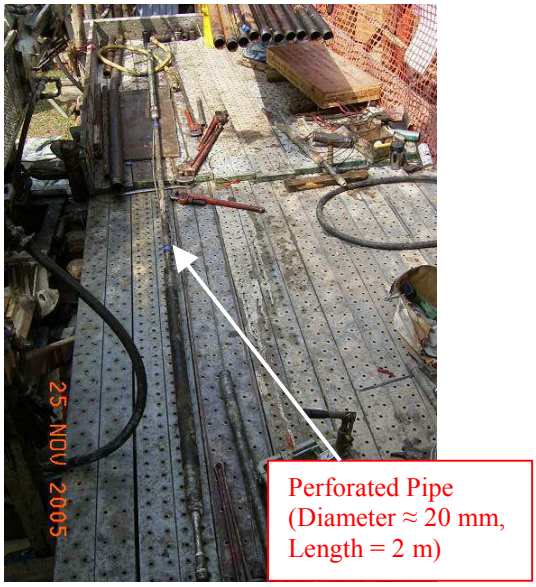

Water absorption tests by conventional metho method

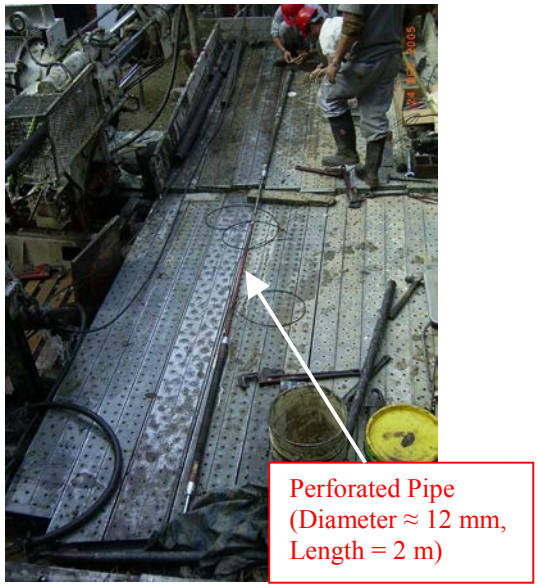

Water absorption tests by wireline

Groundwater Inflow Monitoring

Groundwater inflow was measured during the drilling process and after the completion of drilling. The groundwater inflow monitoring was conducted to determine the sectional inflow and the inflow of the full drillhole. In addition to the conventional indirect measurement of groundwater inflow by packer test (i.e. injection test), groundwater inflow test (i.e. production test) can be carried out to simulate the residual groundwater inflow during tunnel excavation. The inflow measurements have been analyzed in the detailed design stage for the estimations of grouting condition, construction programme and risks.

4 CONCLUSIONS

An effective GI programme of tunnel works may consist of HDC, geophysical explorations and specific laboratory tests. The HDC provides continuous geological data and engineering properties of the ground along

the tunnel alignment and is invaluable for minimizing the risk of unforeseen ground conditions. In additional, conventional boreholes are used to identify the rockhead level and determine the rock cover. The use of geophysics helps to identify the variation of structural geology in a broader extent. A continuous rockhead profile can be provided by seismic methods, where correlation of the geological loggings of conventional boreholes and seismic survey data are required. These fieldworks should be implemented in conjunction with the specific insitu tests, appropriate laboratory tests and field instrumentations.

Interpretations of GI information include, but not limited to, the use of groundwater inflow data as guidance for the grouting design of the tunnel. Fault and weak zone can then be inferred for developing the construction programme. The rock hardness and abrasiveness test data can be used to estimate the cutter life of TBM. Results of oedometer test and standard penetration test can be adopted for the analysis of ground settlement.

An appropriate design of the GI programme can provide reliable information along the tunnel alignment and minimize uncertainties in the geological model, hydrogeological profile, areas of adverse geological features and high groundwater flow. Comprehensive reliable GI information is essential to arrive at a safe and economical construction design, and the timely completion of construction within budget for a tunnel project.

ACKNOWLEDGEMENTS

This paper is published with the permission of the Head of the Geotechnical Engineering Office and the Director of Civil Engineering and Development Department, Government of the Hong Kong Special Administrative Region.

REFERENCES

AGS-HK (2003), "Ground Investigation Guidelines", Association of Geotechnical & Geoenvironmental Specialists (HK).

GEO Geoguide 2 (1987), "Guide to Site Investigation", Geotechnical Engineering Office, Civil Engineering Department, Hong Kong SAR Government. (reprinted)

GEO Geoguide 4 (1992), "Guide to Cavern Engineering", Geotechnical Engineering Office, Civil Engineering Department, Hong Kong SAR Government.

GEO Technical Guidance Note No. 24 (2005), "Site Investigation for Tunnel Works" , Geotechnical Engineering Office, Civil Engineering Department, Hong Kong SAR Government.

Ho, J., Lam, Y.C. and Lo, Y.C. (2008). "Innovative Design in Po Shan Tunnel Project", Proceeding of HKIE (2008).

Hoek, E. and Brown, E. T. (1980). "Underground Excavations in Rock". Institution of Mining and Metallurgy, London.

Ian, M. S., Nieuwenhuif, G.K. and Lai, W. C. (1986). "Application of seismic surveying, orientated drilling and rock tunnels'. Rock engineering and excavation in an urban environment. The Institution of Mining and metallurgy, pp. 249-261.

Kearey, P. and Brooks, M. (1984). "An Introduction to Geophysical Exploration" 2nd edition, 1991 (reprinted)

Lo, Y. C., Cheuk, C. Y. and Chau, S. F. (2008). "Estimation of Water Inflow during Tunnel Construction", Proceeding of HKIE (2008).

Milne, D., Hadjigeorgiou J., and Pakalnis R. (1998). "Rock Mass Characterization for Underground Hard Rock Mines."

Proctor, R. V., and White, T. L. (1968). "Rock Tunnelling with Steel Supports." Commercial Shearing and Stamping Co., Youngstown, Ohio, 1946. (reprinted)

Deep Basement Construction near Metro Tunnel in Shanghai

C.S. Lau
Shanghai Wheelock Square Development Ltd., Shanghai
S.L. Chiu
Maunsell | AECOM, Hong Kong
K. Ha
Maunsell | AECOM, Shanghai

ABSTRACT

This paper describes techniques adopted for construction of a deep basement (18.0m ~ 26.0m) located at a distance of 5.4m from an existing metro tunnel in Shanghai. To minimize the excavation effect to the tunnel, a number of precautionary measures have been applied to the ELS design and works, such as soil strengthening works by SMW for diaphragm wall construction. Struts were designed to be preloaded with hydraulic jacks left in place, under real-time monitoring and controlled by a computer-hooked hydraulic pump for strut load compensation. The excavation works were carried out under real time monitoring and accomplished on time without interruption to the services of the metro line.

1 INTRODUCTION

With the rapid development of Shanghai Metro Railway system, there are 8 lines in operation up to now. Everyday, these metro railway lines run though the densely populated downtown area. As well known, Shanghai is situated at the mouth of Yangtze River, a soft ground region covered with thick alluvial deposit overlying the bedrock at approximately 300m below ground level. The top 30m depth of soil stratum consists alternately of clay, sand and silt materials. Most of the metro tunnels are built in these soft layers.

In recent years, many high-rise buildings are located in close proximity to metro lines. It is not uncommon that these buildings have deep basements, normally 3-4 levels; about 20m below ground. This paper presents a case of such building works where the external boundary wall of the building lies at 5.4m away from an existing metro tunnel. Innovative techniques to ELS construction have been employed for minimizing the excavation effect to the metro tunnel.

2 THE SITE CHARACTERISTICS

Located in the CBD of Shanghai, the proposed development was to build a high rise commercial complex of 55-storey high above ground with a 4-level basement underneath. Typical subsoil geology can be divided into 12 layers (Shenyuan, 2002). The top 5 layers where excavation was carried out are as follows:

- General Fill, around 2m thick, moist, loose, compose of construction debris, such as crashed concrete blocks and brick crumbles
- Silty Clay, brown yellow, 1.5m thick, moist, intermediate plasticity, medium compressible, uniform
- Silty Clay, very soft grey clay, 3.6m thick, saturation, high plasticity, highly compressible
- Clay, 8.5m thick, grey, very soft, with occasional shell fragments, very moist, saturation, uniform, high plasticity
- Clay, grey, 22.0m thick, very moist, high plasticity, uniform, occasion with shell fragments and interbedded with silt and sand

Figures 1a and 1b show the layout plan and a typical profile of the excavation works. The subsoil geology is shown in Figure 2. An existing tunnel is situated about 5.4 m away from the north boundary of the site

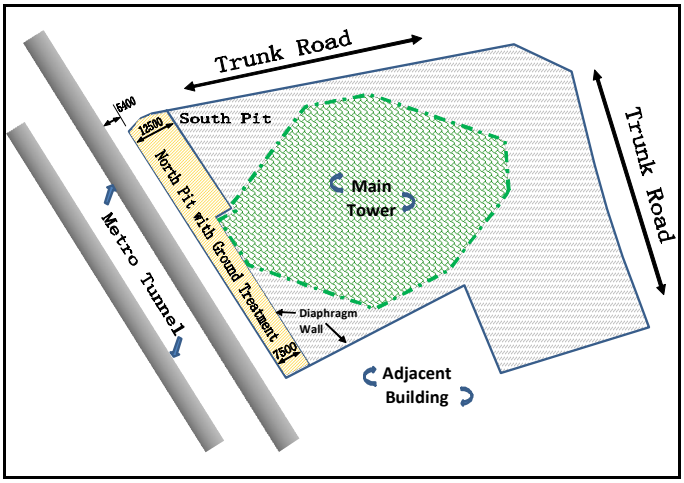

Figure 1a: Site Plan

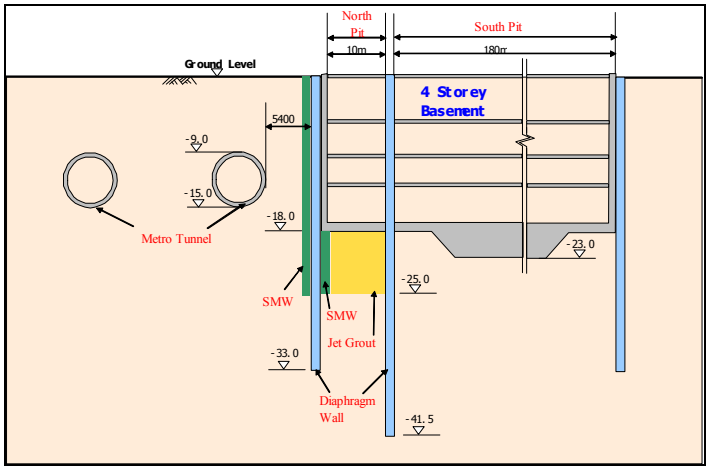

Figure 1b : Typical Section of the Site

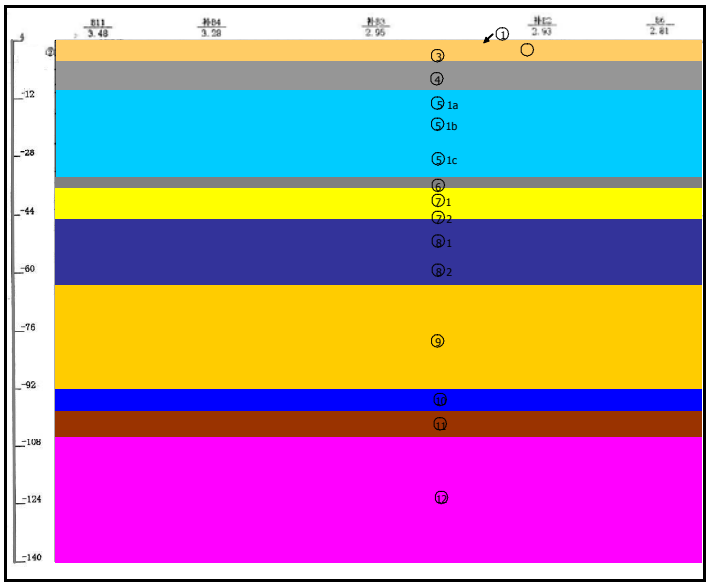

Figure 2 : Typical Geological Profiles

3 DESIGN CONSIDERATIONS

Shanghai Code for Protection of Metro Tunnels and Structures specifies the following limits that should not be exceeded in regard to construction works taking place within the protection zone:

- The induced vertical settlement and horizontal settlement of tunnel shall not exceed 20mm;
- Deformation curvature shall not be less than 15000m in radius;
- Differential settlement shall not exceed 1 in 2500;
- Imposed pressure on the tunnel shall not exceed 20kPa.

Besides, any horizontal movement at the crest of retaining wall shall not be greater than 0.1% of the retaining height, the maximum wall deflection shall not be greater than 0.14% of the retaining height, and the maximum settlement of the adjacent ground shall not be greater than 0.1% of the retaining height (Shanghai, 1999).

3.1 Planning Scheme

In order to minimize disturbance to the tunnel, the deep basement excavation was divided into two, namely South Pit and North Pit (Figure 1a).

3.1.1 South Pit

A diaphragm wall, 1m thick by 41m deep was installed separating the South and North Pits. The strategy of excavation work was that two diaphragm walls (north boundary wall and the additional wall that separated the site into 2 pits) sandwiched with 10m grout-strengthened soil formed a very stiff and rigid barrier to protect the metro tunnel from the potential lateral movement during excavation works in the south pit. This arrangement was also aimed to minimize the time duration for exposure of the northern wall, thus to minimize the tunnel movement due to potential time dependent deflection of diaphragm wall during bulk excavation. This could also minimize the settlement of the tunnel that might have been caused by ground heave due to unloading of soil during excavation.

3.1.2 North Pit

Soils on both sides of the boundary wall to the north were strengthened with Soil Mixing Wall (SMW) of North Pit; as such soil movement was significantly reduced in the course of diaphragm wall construction as well as during excavation at the later stage.

For the excavation works in North Pit, a new automated strut force adjustment system was introduced. The purpose of application of the system was to ensure that no excessive deformation of the north boundary wall would take place. The details about the system are given in the following section.

3.2 Automated Strut Force Adjustment System

For the North Pit, there were a total of 5 levels of struts. The 1st layer was RC strut at -0.5 m below ground. The 2nd layer (at about -4.6 m) and 3rd layer (at about -7.85 m) were steel struts preloaded manually with jacks and stress-locked with wedges. The strut loads were monitored with strain gauges installed on the web of the struts near northern ends.

The 4th layer (at -11.595 m), and 5th layer (at -15.02 m), were located approximately at and below levels of the metro tunnel (-9 m to -15m). The required preloading forces are given in Table 1.

Table 1: Preloading value

Layer of Strut	Preload (kN)
2	1400
3	1700
4	2200
5	1800

An automatic control system was introduced to the 4th and 5th layers of struts. This system was for the first time applied to excavation project in Shanghai. One hydraulic jack was installed at one end of each strut. All jacks were linked to the central unit of a pressure chamber where pressure monitoring and automated adjustment to the strut force were controlled by computer.

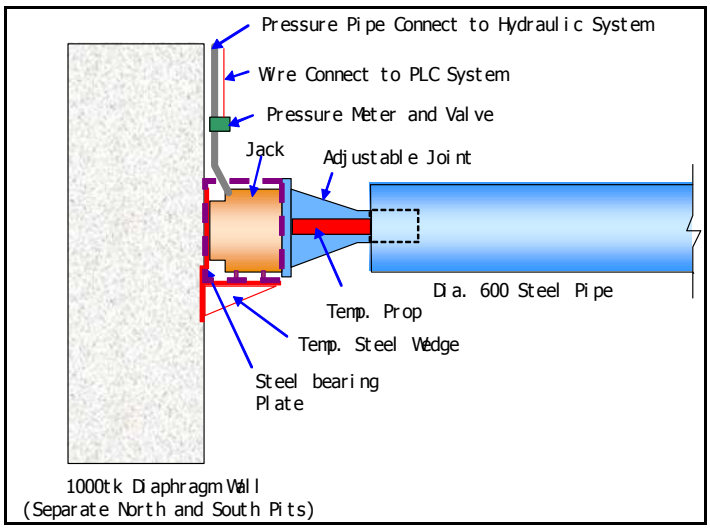

Figure 3: Connection Detail for Steel Strut and Jack

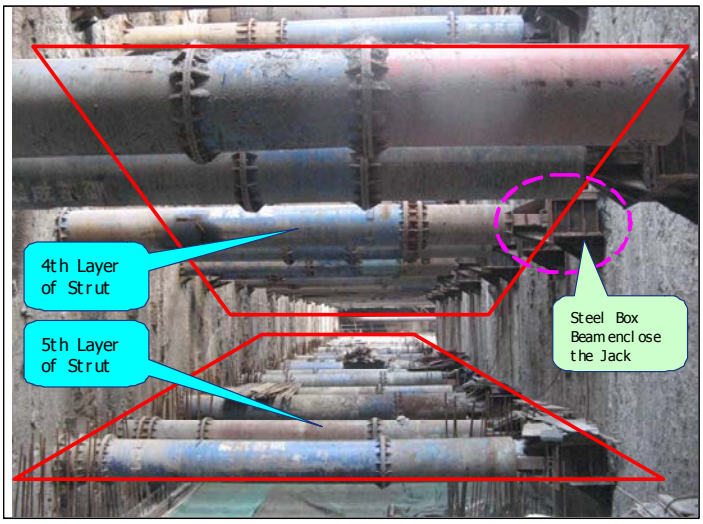

Plate 1: View of 4th and 5th Layers of Struts

4 CONSTRUCTION ISSUES

The implementation of ground improvement methods successfully reduced lateral movement to the metro tunnel during construction.

4.1 SMW for Construction of Diaphragm Wall

In general practice for diaphragm wall construction in Shanghai, bentonite slurry is in use as temporary support medium for diaphragm trenching, but over breaks and trench collapses may sometimes occur due to excessive ground disturbance by the construction machinery or surcharges exerted by other underground facilities or structures including building foundations. To minimize ground disturbance to the nearby tunnel, two rows of SMW piles, each 32.5 m in depth, 0.85 m in diameter centered at 0.6 m intervals, of 28-day unconfined compressive strength of 1.5MPa, were installed along two sides of the proposed diaphragm wall prior to the trenching works. Trenching in the SMW with the support of bentonite slurry efficiently stabilized the trench formation. Inspection of the excavated profile by sonic checking afterwards confirmed that the trench formation was straight without any over breaks. Good water tightness between wall panels was also observed during bulk excavation.

4.2 Automatic Control System

The Automatic Control System was composed of two components: a hydraulic power supply, and automated control system (China State, 2008). A schematic diagram of the system is shown in Figure 4.

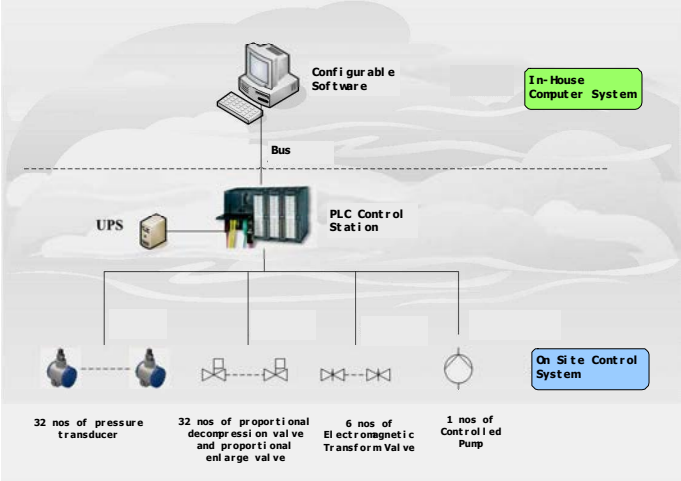

Figure 4: Topological Diagram of the Whole System

The system was operated by a Siemens S7-300 Series PLC system as shown in Figure 5.

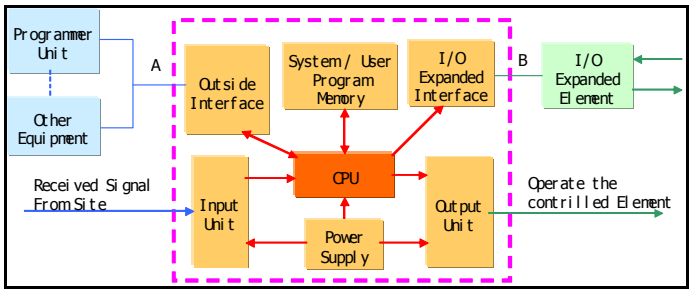

Figure 5: PLC Systematic Diagram

In total, 52 jacks were in use. They were divided into 32 groups driven by separated pressure controls. Each jack was housed in a steel box welded to the end of the strut (Plate 1 and Figure 3).

Hydraulic pipes and pressure meters were connected to the jacks. Each strut was preloaded to a lock-off load at 200 kN greater than the designed preload. The target pre-loading to each strut was set to be maintained automatically to an accuracy of ±100kN.

Strut loads measured by pressure transducer mounted on the respective struts were transmitted at a certain frequency to the computer for comparison with the required strut forces. Should any out of range (i.e., ±100kN) strut force be detected, the system would send alarm to the operator on duty. The computer would take necessary action automatically unless otherwise overridden by the operator. With this system in place, the strut force adjustment could be much more efficient and time saving as compared to the efforts that were required to carry out manually for those struts at upper levels. Readings were also stored into a database for further analysis and graph plotting.

Report was generated by the system regularly and uploaded to the web site accessible to the client and engineers at their office off-site.

Figure 6: Control and Monitoring Panel for 4th and 5th Layers of Strut

5 DISCUSSION

5.1 Effect of SMW as soil strengthening measure

SMW was applied to soil alongside the northern diaphragm wall where the metro tunnel stood at about 5.4 m away floating in the soft alluvial deposit. At all other sides encompassing the site, no SMW was carried out. Comparison of wall deflection due to excavation could be made for the diaphragm walls on eastern and northern boundaries for the effectiveness of SMW as a soil strengthening measure.

Inclinometer Q4 was installed in the diaphragm wall panel mid-way along the northern boundary in North Pit while Q11 was in the corresponding diaphragm wall panel on eastern boundary in South Pit. Upon completion of the excavation works at the south pit, a maximum lateral deflection of 86mm was recorded by Q11, which is approximately 0.48% of the excavation height (H). Only 8mm wall deflection was recorded at Q4, or 0.045% H as the excavation was carried out down to the bottom of the formation at about -18m in the North Pit. The maximum wall deflections for both cases were significantly less than the rule-of-thumb figure of 1% H for braced excavation as indicated in GCO Publication No.1/90 (GCO 1999), Review of Design Methods for Excavations. The smaller than usual deflection of diaphragm wall observed in the present excavation is believed to be attributable to the SMW and effective control of the strut forces by close monitoring of the variation and timely adjustment of the strut forces.

5.2 SMW Pile for Diaphragm Wall Construction

SCJ21 on the tunnel shield was a settlement check point closest to the northern diaphragm wall. SCJ21 could therefore reflect the effect of works taking place on site in its vicinity. At the time of SMW works, the tunnel was observed to have been raised for 3.5 mm due to soil displacement by the SMW. After installation of SMW, it was evident that soil movements were significantly reduced throughout the excavation works in comparison with those experienced in excavation for the south pit as mentioned in the previous section.

The potential hazard of excessive movement to the metro tunnel could thus be significantly mitigated. The tunnel settlement induced by diaphragm wall construction and bulk excavation for the north pit was about 5mm, a figure that enabled the works to carry on without cessation or interruption to the operation of the metro line throughout the period of basement excavation.

5.3 The Struts and Preloading System

The 2nd layer and the 3rd layer of struts at North Pit were preloaded and then monitored manually. The strut was tubular in shape, 609 mm in diameter, 16mm thick, rested on brackets bolted to the diaphragm wall panels (Plate 1). At one end of it where the jack was seated, there was an adjustable joint made of a pair of channel sections inserted into the tubular section of the strut (Figure 3). The adjustable joint and the tubular section were fixed tight together by a wedge applied in between as the strut was preloaded to the required force. The wedging was found unable to maintain the strut force due to its slippage effect. The slippage problem was then fixed by welding the wedge to the tubular section. The wall deflection could have been intolerably increased if the problem had not been fixed in time.

The problem of loss in strut force did not occur in struts at 4^{th} layer and 5^{th} layer because of the different set up where a jack was placed at each strut against the wall. The maximum daily variation of strut force was in the range from 100 kN to 300 kN as the excavation was carried out down to the designed formation depth, namely about -18m. The variation of strut forces was believed attributable to a maximum daily temperature change of about 10ºC in winter time in Shanghai. With the presence of the automated force adjustment system, the strut forces could be adjusted in controllable manner which was particularly important for carrying out deep excavation in soft clay. This system successfully limited the wall deflection thus the lateral movement of the metro tunnel in the course of deep excavation works in its proximity.

Figure 7 shows a typical deflection profile of the diaphragm wall and the tunnel in relation to the excavation. The inclinometer (C19) was installed in the corresponding diaphragm wall panel to show the effect of excavation to the tunnel and its adjacent ground as the excavation was carried out at the north pit. It can be seen that ground movement developed with the depth of excavation. 5.5 mm movement was resulted from excavation to about -8m for the 3^{rd} layer of struts whereas there was only 2.5 mm movement was developed for further excavation for remaining 10 m to the formation level. The advantage of automated force adjustment system applied to the lower two levels of struts was evident and obvious.

Figure 8 shows the cumulative movement of the diaphragm wall resulting from excavation for the north pit, which was 11.5 mm, and the induced settlement and lateral movement of the metro tunnel were only 2.67mm and 3.5mm respectively.

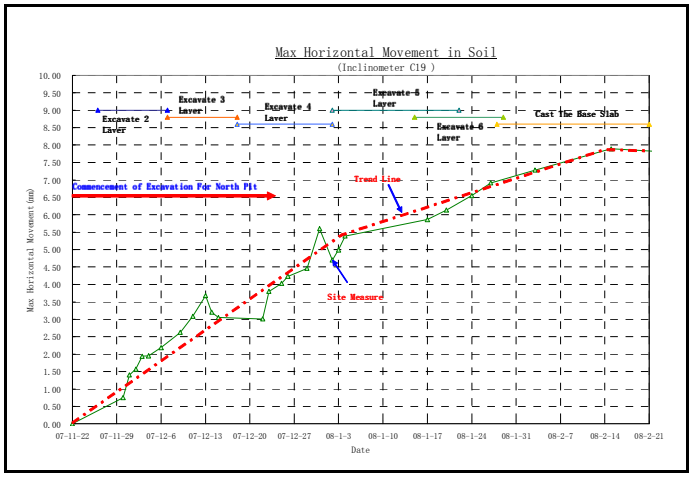

Figure 7: Max Horizontal Movement in Soil at Inclinometer C19

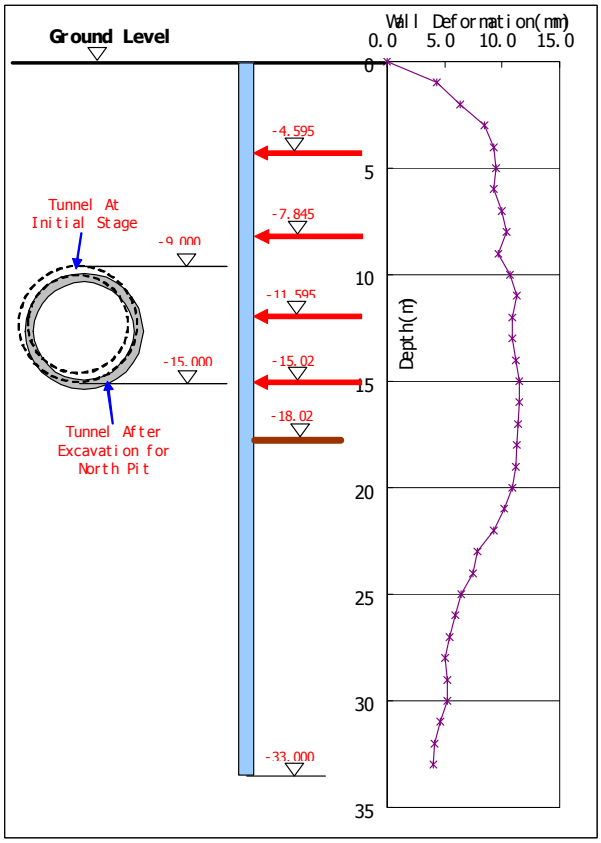

Figure 8 Wall Deformation Shape at Q3

6. CONCLUSIONS

6.1 The excavation strategy adopted was to minimize the time dependent deflection of diaphragm wall in order to mitigate the potential tunnel movement due to the excavation works in its proximity.

6.2 The pre-installed SMW at both sides of the diaphragm wall before trench excavation effectively increased the strength of the soil and minimized the risk of over breaking and collapse of soil during diaphragm wall trenching; thus minimized the risk of excessive movement of the metro tunnel.

6.3 An automated strut monitoring and timely force-adjustment system was proven to be effective in reducing the development of deflection of diaphragm wall with depth of excavation; thus the risk of excessive movement of the metro line could be properly minimized.

ACKNOWLEDGEMENT

The authors express their gratitude to cast their vote of thanks to Client, Shanghai Wheelock Square Development Limited, Shanghai for their kind permission to the publication of the project data in this paper

REFERENCES

China State (2008), China State International Construction Company, Research and Application of "Automatic restoring and displacement control system for supported excavation at soft ground region" 2008.2.

Shenyuan (2002), Shenyuan Geotechnical engineering Investigation Ltd., Supplemental Geotechnical engineering Investigation Report 2002.7

Shanghai (1999), Shanghai Modern Architectural Design (Group) Ltd, Foundation Design Code (DGJ08-11-1999), 1999.12.

GCO (1990), GCO Publication No.1/90 Review of Design Methods for Excavations, 1990.3.

Trial Application of Thermal Infra-red Imaging and Seismic Sympathetic Vibration Techniques for Slope Investigation

J.W.C. Lau, T.M.F. Lau & K.K.S. Ho
Geotechnical Engineering Office, Civil Engineering and Development Department
Government of the Hong Kong SAR, China

ABSTRACT

Thermal Infra-red Imaging Analysis (TIIA) and Seismic Sympathetic Vibration Analysis (SSVA) have reportedly been used in Japan for some time to detect the presence of voids beneath the hard surface cover to a slope. To assess the potential applicability of these relatively new technologies for landslide studies and/or slope investigations in Hong Kong, a series of field trials has been conducted on typical soil cut slopes with a hard surface cover. Invasive ground investigations, comprising coreholes and surface stripping, were subsequently undertaken to check and verify the interpreted results of TIIA and SSVA. These highlighted the potential capability of TIIA in identifying the approximate locations of possible voids beneath the hard surface cover in a rapid manner. However, its resolution is subject to certain limitations. SSVA has shown to be capable of identifying areas with very minor loss of contact, although its reliability is not fully proven in the field trial because of some inconsistent results in local areas. Through the pilot field trials, useful insight was gained in respect of the practicality and applicability of these innovative technologies. The trials have reinforced the need to exercise due rigour in the verification of the resolution of new technologies, especially in local conditions, before proceeding with the technology transfer.

1 INTRODUCTION

Thermal Infra-red Imaging Analysis (TIIA) and Seismic Sympathetic Vibration Analysis (SSVA) have been developed and used in Japan for the detection of voided areas beneath the hard surface cover to a slope, or loss of contact between the hard cover and the underlying ground mass. According to Nakamura (2004), Japan has more than 10 years of experience in using the above technologies as investigation tools, reportedly with considerable success. Experience in Japan suggested that the early detection of voids beneath hard surface covers has proved to be useful in identifying possible signs of slope deterioration and the need for follow-up actions before the situation deteriorates further to give rise to problems (e.g. local detachments or large-scale failures).

To assess the potential applicability and effectiveness of the above non-invasive techniques for landslide studies and/or slope investigations, pilot field trials comprising the application of TIIA to two soil cut slopes and the use of TIIA/SSVA on another soil cut slope in Hong Kong were arranged by the Geotechnical Engineering Office (GEO). Confirmatory ground investigations, comprising coreholes and surface stripping, were subsequently carried out to check and verify the interpreted results of TIIA and SSVA. This paper presents some of the key observations of the pilot field trials.

2 OPERATIONAL PRINCIPLES

2.1 Thermal Infra-red Imaging Analysis

TIIA is a remote sensing technique that is capable of detecting thermal radiation emitted from an object and providing an image of the temperature profile over the surface of the object. The principles and practical application of infra-red thermography in Japan are described by Nakamura (2004). The use of this technique in identifying the possible presence of voids below the hard surface cover to a slope (e.g. shotcrete) operates

on the basis that the thermal conductivity between a hard cover and the underlying ground mass is a function of the continuity of their contact.

During daytime, the hard cover is heated up by sunlight and the heat energy will be transmitted to the ground below. At night time, the ambient air temperature is likely to be lower than that of the slope-forming material and therefore heat energy will be transmitted out of the slope. The transmission rate depends on the thermal conductivity of the transmission medium. Any air voids that are present beneath the hard surface cover would act as an insulator, which reduces the thermal conductivity locally. As a result, the heat energy transmission will be reduced. Hence, during daytime, areas of the hard cover with voids below would have a higher temperature than that with a good contact (Figure 1(a)). Conversely, during night time, the temperature of areas of the hard cover with voids below would be comparatively lower than that with a good contact (Figure 1(b)).

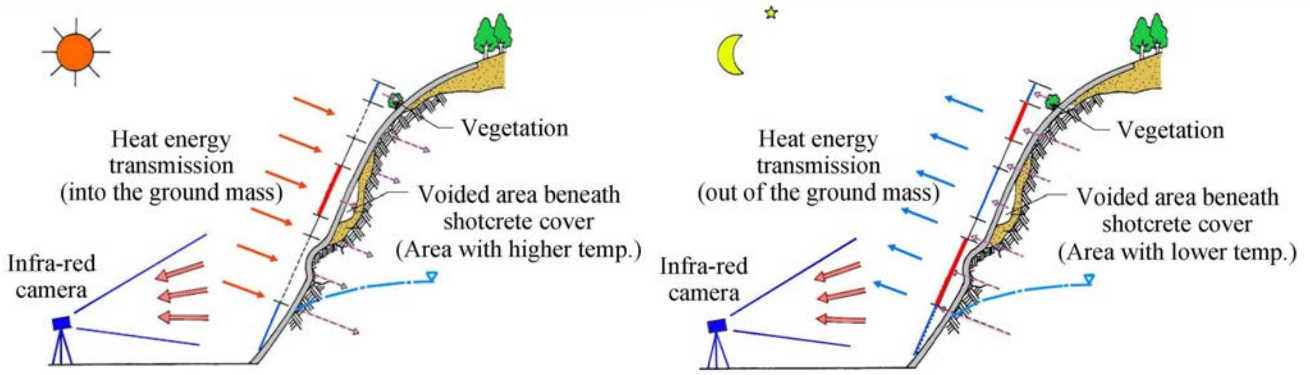

(a) During daytime (b) During night time

Figure 1: Principles of Thermal Infra-red Imaging Analysis

The temperature profile of a hard cover can be established remotely through taking infra-red images of the slope surface (Figure 1). TIIA involves the use of 'smart' sensors comprising light quantum detectors and thermal detectors to provide good quality infra-red images. These images are generally taken in early afternoon as well as in early morning before sunrise, in order to capture the maximum thermal differential of the hard cover and enhance data resolution for the subsequent analysis. The pair of infra-red images, viz. the high-temperature and low-temperature images, can then be analysed to produce a plot that depicts the distribution of thermal differential of the hard cover. According to theory, those areas with voids beneath the hard cover will manifest themselves through a display of a greater thermal differential.

2.2 Seismic Sympathetic Vibration Analysis

SSVA is generally reserved for a detailed assessment of the extent and significance of the potential voided areas beneath the hard surface cover. The technique involves measuring the intensity of a sympathetic vibration signal emitted from the hard cover. The system comprises a transmitter and a receiver of resonance signals, together with a data logger and an oscilloscope for instant display of the received signals.

Resonance, or so-called sympathetic vibration, occurs when the frequency of the transmission signal coincides with the natural frequency of the hard cover. The natural frequency of the hard cover such as shotcrete generally ranges from about 600 Hz to 800 Hz. An air void beneath a hard cover act as a separator which minimises the loss of resonance signal into the ground below. As a result, a relatively high intensity of resonance signal can be detected at the ground surface. On the other hand, the intensity of the detected resonance signal will greatly reduce if the hard cover is in good contact with the underlying ground. Hence, the possible presence of voids beneath the hard cover can be identified from a contour plot of the signal strength to be in those areas that show a relatively high intensity of resonance signal.

SSVA is generally conducted on a grid pattern, typically at 1 m spacing, in order to achieve the necessary data resolution.

3 KEY OBSERVATIONS OF THE FIELD TRIALS IN HONG KONG

The field trials of TIIA and SSVA were conducted with the assistance of a specialist Japanese contractor that has much experience with the use and interpretation of these technologies. TIIA was applied to three cut slopes, one of which was also subjected to SSVA. The equipment used and the testing methodology were the same as that used in Japan. Details of the field trials are documented by Hui & Sun (2007). The key observations are summarized below.

3.1 Slope A above Castle Peak Road

The subject slope comprises a soil/rock cut, which is 210 m long, up to 32 m high and inclined at an angle of about 60°. It was formed prior to 1949. In 1997, a minor landslide (7 m³) occurred in the central portion of the slope. Following this incident, the entire soil portion of the slope was covered with shotcrete. The thickness of the shotcrete cover was not known before the field trial. The slope was also subjected to a landslide study under the GEO's systematic landslide investigation programme following a rockfall that occurred in June 2001.

The thermal differential plot (Figure 2(d)) shows that a horizontal strip in the vicinity of the lowermost berm exhibited a large temperature difference between daytime and night time. As this part of the slope is under the maintenance responsibility of a private owner, no follow-up invasive investigations were carried out. However, it is noted that the cold spots shown on the high-temperature image (Figure 2(b)) coincide with areas covered by the shadows of the slope vegetation whereas other areas that are at a higher temperature are not subject to such external influence. This highlights the potential constraints of TIIA and emphasizes the need for exercising caution and engineering judgement in the judicious interpretation of the results which may be subject to uncertainty.

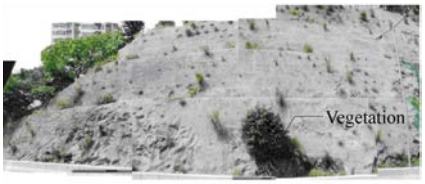

(a) General view of the slope

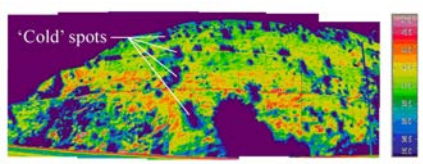

(b) High-temperature infra-red image

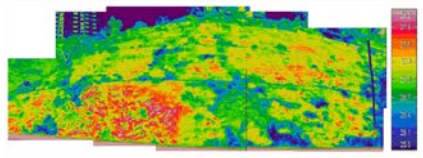

(c) Low-temperature infra-red image

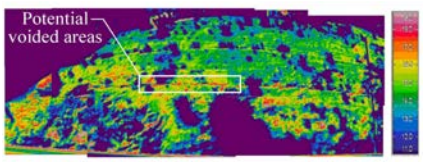

(d) Thermal differential plot

Figure 2: TIIA results for Slope A

(a) General view of the slope

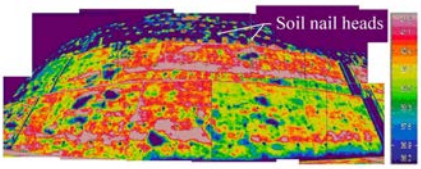

(b) High-temperature infra-red image

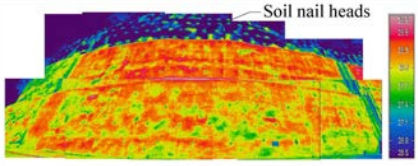

(c) Low-temperature infra-red image

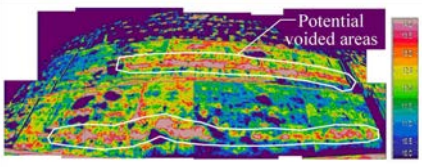

(d) Thermal differential plot

Figure 3: TIIA results for Slope B

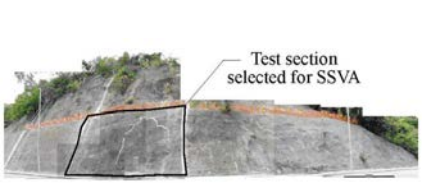

(a) General view of the slope

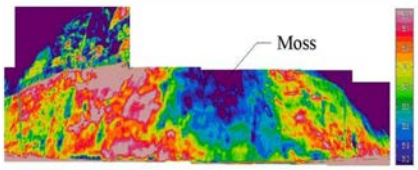

(b) High-temperature infra-red image

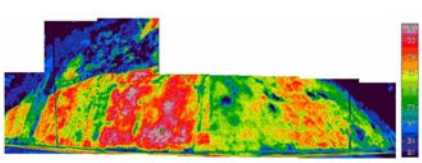

(c) Low-temperature infra-red image

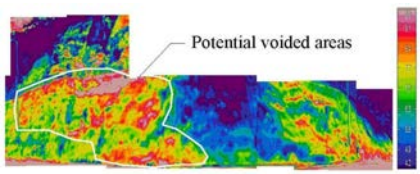

(d) Thermal differential plot

Figure 4: TIIA results for Slope C

3.2 Slope B in Ho Man Tin

The subject slope is a soil/rock cut (Figure 3(a)), which is 150 m long, up to 32 m high and inclined at an angle of about 60°. The shotcreted slope comprises four batters. It was upgraded in 1998 under the Landslip Preventive Measures (LPM) Programme of the GEO. The upgrading works comprised soil nails at 2 m centres, together with the provision of a layer of 75 mm thick shotcrete cover to the bottom two batters on top of the pre-existing shotcrete cover which was not removed. The thickness of the previous shotcrete cover was not known before the field trial.

The extent of two horizontal strips interpreted to have possible voids beneath the hard cover is delineated on the thermal differential plot (Figure 3(d)). Seepage stains from weepholes can be observed within these two strips (see Figure 3(a)). Based on the TIIA, the contractor surmised that localised subsurface seepage may have occurred behind the shotcrete cover, leading to the formation of voids through seepage erosion, which are concealed by the hard cover.

The uppermost batter was found to be relatively 'cold', as reflected by a darker colour in both the high-temperature and low-temperature images (Figure 3(b) and 3(c)), in comparison with the bottom two batters where an additional shotcrete cover was provided. In the above two thermal images, a local 'cold' area was also detected at a location that was under the shadow of large corestones on the slope. Furthermore, possible subsurface seepage behind the shotcrete (based on its darker colour in the high-temperature image) was interpreted by the contractor on the second batter from the slope toe.

On the uppermost batter, spots of a brighter colour in a staggered arrangement can be observed on the temperature profile of the hard cover. These coincide with the locations of the concrete soil nail heads beneath the hard cover (Figure 3(b)). However, the corresponding soil nail heads on the bottom two batters could not be similarly identified on the thermal plots, which may be due to the presence of an additional shotcrete cover as explained above.

3.3 Slope C in Tai Po

The subject slope is again a soil/rock cut (Figure 4(a)). It is 85 m long, up to 25 m high and inclined at an angle of about 50°. The shotcreted slope was formed prior to 1968. The thickness of the shotcrete cover was not known before the field trial.

Some 'hot' spots (i.e. areas where possible presence of voids) at the lowermost batter were apparent in the high-temperature image (Figure 4(b)). The thermal differential plot (Figure 4(d)) also shows an area within the middle portion of the lowermost batter exhibiting a relatively high temperature differential, which could be interpreted as potential voids beneath the shotcrete cover. A local low-temperature zone in Figure 4(b) was interpreted by the contractor as being the result of the presence of moss on the slope surface.

Based on the TIIA results, it is suspected that some local voids may be present within the middle portion of the lowermost batter. Hence, the slope portion of concern, which measured about 15 m wide by 9 m high, was also subjected to SSVA (Figure 4(a)). The sensors were set up at an 1 m grid over the area of concern. Based on past experience, the specialist contractor determined that the resonance frequency of the shotcrete cover was about 760 Hz prior to the SSVA trial and assumed this in the interpretation of the tests.

The contour plot of the vibration data (Figure 5) suggests that possible voids are present within the middle and upper portions of the slope batter under investigation. The darker colour on the plot is interpreted as reflecting a higher likelihood of good contact between the hard cover and the ground.

4 CONFIRMATORY GROUND INVESTIGATION OF SLOPE IN TAI PO

Confirmatory ground investigation comprising 120 coreholes through the shotcrete cover and one surface stripping was undertaken at the middle portion of the cut slope in Tai Po where possible voids were interpreted beneath the hard cover based on TIIA and SSVA (Figures 4(d) and 5). The objective of the ground investigation was to check for voided areas beneath the hard cover and determine the physical dimensions of the voids as appropriate. A small hand-held coring machine of about 100 mm in diameter was used, with a view to minimising the possible disturbance that might be generated during the coring operation (e.g. the possibility of some small voids being filled up with dust or soil debris during the coring operation). Apart from the above, hammer tapping was also conducted on the shotcrete cover.

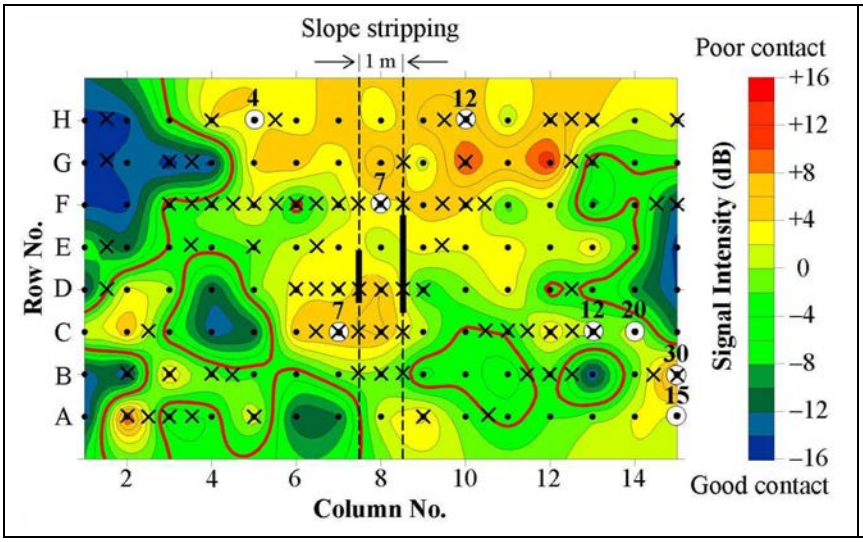

Legend:

- Sympathetic vibration data point / corehole location
- × Hollow sound when shotcrete cover struck with a hammer
- 12 ○ Corehole indicating void (12 mm) beneath shotcrete cover
- ▬ 5 mm gap between shotcrete cover and the ground below as identified along surface stripping

Note: A general view of the test section is shown in Figure 4(a).

Figure 5: Results of seismic sympathetic vibration and confirmatory ground investigation for Slope C

The coreholes revealed that the thickness of the shotcrete cover ranged from 20 mm to 50 mm, with a maximum of 120 mm locally. Eight of the 120 coreholes identified voids of varied thicknesses ranging from 4 mm to 30 mm. All these eight coreholes were located within or in close proximity to the possible voided areas as identified by SSVA (Figure 5). Over 70% of the coreholes show consistent results with the interpretation based on SSVA, viz. the coreholes did not identify any voids at locations where the sympathetic vibration signals are weak (which are indicative of good contact), or the coreholes revealed the presence of voids at locations where the sympathetic vibration signals are strong (which are indicative of voids). The remaining 30% of the coreholes are not consistent with the findings of SSVA in that the coreholes did not identify any voids at the locations with strong sympathetic vibration signals. However, it is noteworthy that none of the coreholes revealed the presence of voids at locations where a good contact was interpreted by SSVA.

Voids of about 5 mm deep were exposed along two short sections of the slope surface stripping (Figure 5), which were predominantly located at about 4 m to 6 m below the slope crest where there is a change in slope angle from about 40° to 60°. Along the length of the surface stripping, over two-thirds of the strip show a good contact between the hard surface cover and the ground below, although the interpreted SSVA results had suggested a relatively poor contact.

The approximate extent of possible voided areas as revealed by the hammer tapping survey is comparable with that interpreted by SSVA. However, the findings of these two tests are not consistent at some isolated spots, such as the top left corner and the bottom part of the surveyed area (Figure 5).

5 DISCUSSION

Based on the results of the field trials, it would appear that TIIA shows some promise as being capable of screening out the approximate locations of possible voided areas behind a hard surface cover in a rapid and non-invasive manner. However, some inconsistencies were noted in certain local areas (e.g. near the top left hand corner and the bottom right hand corner of the test area for SSVA), where a relatively weak vibration signal was detected in SSVA whereas TIIA showed a high temperature differential. The dimensions and the precise locations of the voids, if present, will require further confirmatory investigations. The field trials have also highlighted the potential application of TIIA in identifying areas with concentrated subsurface water flows or areas with a locally high groundwater table concealed by the hard cover. In addition, the trials have shown that the locations of the covered soil nail heads can be detected as a by-product, so long as the hard cover is not of an excessive thickness.

Apart from the need to engage experienced personnel for conducting the tests and interpreting the results, it is important to have a good appreciation of the areas of uncertainties so that the results can be viewed in context. As TIIA relies on the thermal differential of the hard cover in the diagnosis of the possible presence of voids, factors that may affect the temperature of the surface cover or the corresponding thermal conductivity may potentially influence the test results. For example, a shotcrete with a variable mix and

thickness may give rise to different thermal conductivities and is therefore liable to affect the resolution of the results. Such possibilities need to be borne in mind, although they have not been systematically investigated in the present pilot trials.

Based on the experience from the field trials, TIIA appears to be subject to some limitations. This technology has shown to be more effective on slopes with a smooth surface with no major undulations. Irregularities such as corestones or dense vegetation (e.g. mature trees) on the slope surface can form shadows on the slope surface locally where the temperature differential might be reduced. This could in turn affect the reliability of TIIA results interpretation. Seepage and the presence of cracks on the slope surface will also have a cooling effect on the hard cover and are liable to further complicate data interpretation.

As for SSVA, the field trial has indicated that the technique is generally capable of determining the likely extent of air voids. However, the depth of a void cannot be deduced from the SSVA results. Invasive investigations, such as carefully conducted coring, are required to determine the actual dimension of a void. It would appear that the resolution of SSVA tests is generally capable of identifying areas with very minor loss of contact (e.g. depth of void of less than 5 mm), as verified by the coreholes and slope surface stripping. However, the consistency and reliability of interpreted SSVA results are not fully proven as some results did not correlate well with the coring in local areas, as explained above. It is not certain whether the discrepancies are due to poor quality data, inappropriate interpretation or other factors in respect of the local site setting that were not taken into account in the interpretation. In principle, the resolution of SSVA could be a function of a range of factors. These may include, for example, the material density and the thickness of the hard cover, the continuity of contact between the cover and the underlying material, the characteristics of the near-surface slope-forming material, etc.

All in all, the field trials have emphasized the need to exercise rigour in assessing the applicability of new technologies that have reportedly a good track record in other countries. It is of the essence to appreciate and confirm the capabilities as well as the potential limitations in different site conditions so that the reliability of the results, particularly those of non-invasive techniques that require a high degree of interpretation based on simplifying theories and assumptions of simple boundary conditions. Technology transfer can serve to quickly advance the technological skill base and add to the engineer's tool-box, but the potential risk of having a black box without an adequate understanding of the physics involved and the corresponding limitations needs to be borne in mind.

6 CONCLUSIONS

The pilot field trials examined the application of TIIA and SSVA to a number of typical cut slopes in Hong Kong. Useful experience was obtained in respect of the practicality and applicability of these novel technologies, which have reportedly been used successfully in Japan for some time. Based on collaborative studies and a careful review of factors that can influence the test results, some useful insights were gained regarding the resolution and potential limitations of these techniques. The application of these techniques needs to be tempered with the use of engineering judgement.

ACKNOWLEDGEMENTS

This paper is published with the permission of the Head of the Geotechnical Engineering Office and the Director of Civil Engineering and Development, Government of the Hong Kong Special Administrative Region. The assistance provided by Halcrow China Limited, Hong Kong Construction (Civil Engineering) Limited and Nittoc Construction Limited from Japan in the field trials is gratefully acknowledged. Thanks are also due to Ir Dr H.W. Sun and Ir T.H.H. Hui for their input in this project.

REFERENCES

Hui, T.H.H. & Sun, H.W. 2007. *Trial Application of Thermal Infra-red Image and Seismic Sympathetic Vibration Techniques for Slope Investigation.* GEO Report No. 199, Geotechnical Engineering Office, Hong Kong, 52 p.

Nakamura, H. 2004. Field instrumentation and laboratory investigation (Keynote Paper). *Proceedings of the Ninth International Symposium on Landslides: Evaluation and Stabilization,* Rio de Janeiro, Brazil, 1: 541-548.

Application of Innovative Monitoring Techniques at Four Selected Natural Hillsides in Hong Kong

K.W.K. Lau & H.W. Sun
Geotechnical Engineering Office, Civil Engineering and Development Department, Hong Kong
S.W. Millis, E.K.K. Chan & A.N.L. Ho
Ove Arup & Partners Hong Kong Limited, Hong Kong

ABSTRACT

With the continuous improvement of instrumentation techniques and better understanding of slope behaviour, it is anticipated that instrumentation for long-term performance monitoring of landslide development at individual sites will become more frequently used in Hong Kong. To prepare for this trend, a project is being undertaken to carry out real-time monitoring of four selected hillsides in Hong Kong and to assess the conditions of the hillsides with respect to ground movements and hydrogeological conditions. All field instrumentation works at the four hillsides have now been completed and real-time monitoring has been ongoing since late 2007. A wide range of conventional and state-of-the-art geotechnical instruments, real-time automatic data communication and geotechnical data processing system have been installed. This paper presents the background, relevant technical details of the instrumentation scheme (including highlights of the basic principles of the some of the innovative instruments adopted), data collected and interim findings.

1 INTRODUCTION

Geotechnical instrumentation has been adopted in many countries for assessment of the likelihood of landslide occurrence and the need for further mitigation measures (NCR, 2004). This practice has not been widely adopted in Hong Kong because of its urban setting and the potentially severe consequences of most local landslides (Wong et al, 2006). With the close proximity of densely used facilities to slopes in Hong Kong, it is more technically and economically viable to stabilise slopes showing signs of distress. Moreover, the sudden occurrences of small-scale, brittle landslides, most common in Hong Kong, often exhibit few signs of distress.

The geotechnical profession in Hong Kong is familiar with the use of geotechnical instrumentation as a ground investigation tool for stability assessment of slopes and design of slope stabilisation measures. Geotechnical instrumentation has also helped collection of field data for research and development projects that further our understanding of slope behaviour in Hong Kong. In structural and bridge engineering, performance monitoring is gaining importance as an asset management tool to assess, verify and monitor the performance of a given structure. As instrumentation techniques continue to improve and the profession continue to gain a better understanding of slope behaviour, it is anticipated that instrumentation for long-term performance monitoring of landslide development at individual sites will become more frequently used in Hong Kong (Wong et al, 2006).

To prepare for this trend, the Geotechnical Engineering Office (GEO) is undertaking relevant technical development work to test the performance of new monitoring and instrumentation techniques and arranging pilot instrumentation schemes to set up a prototype real-time instrumentation network in Hong Kong. The first of these pilot schemes was initiated in June 2005 when the GEO engaged the services of Ove Arup & Partners Hong Kong Limited (Arup) to undertake detailed engineering geological and hydrogeological studies of four landslide prone areas across Hong Kong, and plan site specific instrumentation and monitoring schemes applicable to the predicted types of ground movements and groundwater conditions present at each site.

A wide range of conventional and state-of-the-art geotechnical instruments were installed since late 2007 (Table 1) and a Instrumentation Database Monitoring System (IDMS) has been recently set up in the Civil Engineering and Development Department (CEDD) for real-time collection, transmission, processing and

dissemination of the monitoring data. The following sections present the ground movements and hydrogeological conditions of the four selected hillsides, and the applications of the innovative instruments installed with highlights of the basic principles and preliminary findings.

Table 1: Geotechnical Instruments Installed at the Four Selected Hillsides

Conventional Geotechnical Instruments		State-of-the-art Geotechnical Instruments
• Surface Markers • Crack Meters • Manual Inclinometers • In-place Inclinometers • Earth Pressures Cells	• Rain Gauges • Automatic Piezometers • Evaporimeter • Jet Fill Tensiometers • Flowmeter	• Differential Global Positioning Systems • Translation, Rotation & Settlement Sensors • Displacement Time Domain Reflectometry • Water Content Time Domain Reflectomery • Thermal Conductivity Suction Sensors

2 THE FOUR SELECTED NATURAL HILLSIDES

The four natural hillsides were selected on the basis of various geological/hydrogeological conditions and landslide mechanisms anticipated, none of which presented an immediate hazard to the general public. The differing nature of the four sites meant that a variety of instrument types and monitoring scenarios could be tested with little risk to public safety and with a view to applying the findings to other slopes where potentially more hazardous conditions may exist.

2.1 Tsing Shan Foothills, North West New Territories

The Tsing Shan Foothills site comprises an active, elongate, very slow-moving translational earth slide with a basal shear surface typically at 4 – 6 m depth (Figure 1). The landslide is occurring along shallow dipping foliations within Completely Decomposed Andesite and it has been estimated that the volume of material experiencing long-term deformation is in the order of 45,000 m^3. Further details of the geological setting and landslide processes operating at the site have been reported by Parry & Campbell (2003). Initial monitoring of landslide movement by means of an inclinometer was carried out between 2002 and mid-2006, when excessive deformation in the order of 200 mm cause damage to the inclinometer tubing and precluded further readings from being obtained. Given the active nature of the landslide at this site and its known history of slope deformation, especially during Hong Kong's rainy season, this site was selected for instrumentation using a variety of different geotechnical instruments.

(a) (b)

Figure 1: Landslide Study Area at (a) Tsing Shan and (b) the Landslide Basal Shear Surface

2.2 Tung Chung Foothills, Lantau Island

This site comprises a shallow slump failure that appears to have reactivated during the wet season, with small seasonal down slope movements observed. The landslide mass, estimated at about 1,500 m^3 in volume and 45 m across, moves along poorly defined rupture surfaces at 2 – 4 m depth. A notable back scarp has formed at the head of the landslide with lateral tension cracks (Figure 2) and small thrust features evident along the landslide flanks and at its toe. Detailed ground investigation works within the landslide area, including drillholes, trial trenches and electrical resistivity profile surveys, indicated that the movement was occurring just beneath the colluvium/saprolite boundary and was likely resulted from short term loss of soil suction due to transient development of high pore water pressures during rainstorms.

(a) (b)

Figure 2: Landslide Study Area at (a) Tung Chung and (b) the Landslide Back Scarp

2.3 Pa Mei, Lantau Island

This site was selected due to the high frequency of relatively small-scale shallow open hillside failures. These failures, the locations of which are presented on Figure 3, typically comprised shallow open hillslope landslides with volumes less than 100 m^3 and varying degrees of mobility. Nearly all of the open hillslope landslides appear to have failed in a brittle manner, with little or no obvious signs of distress.

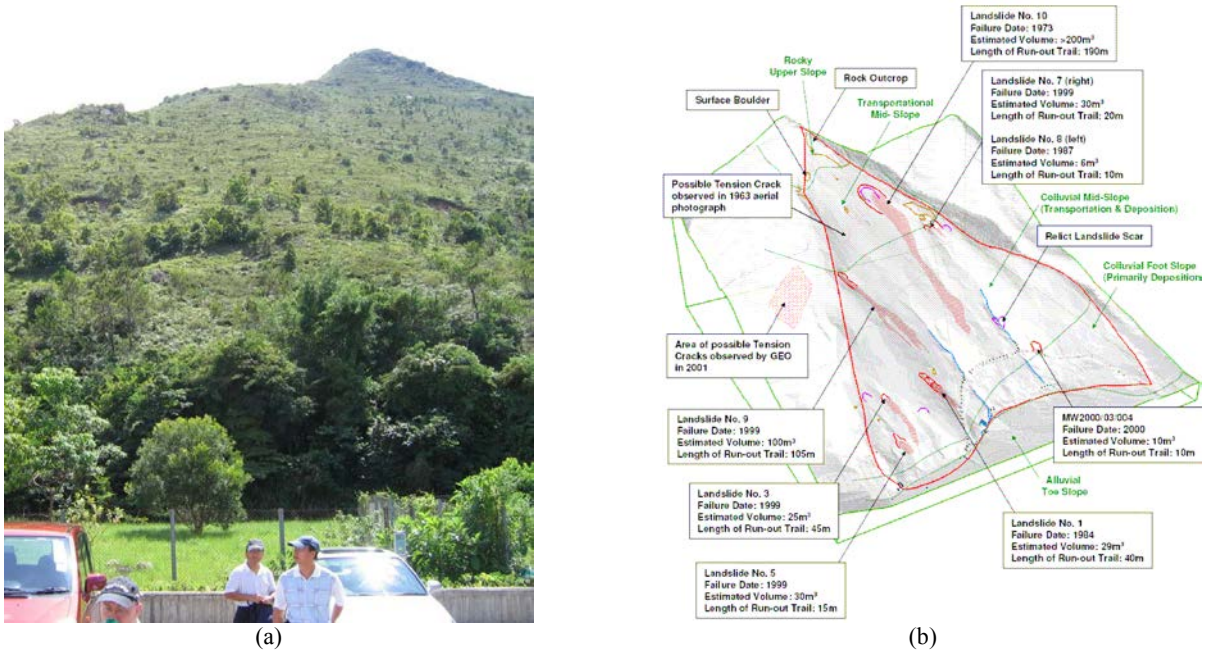

(a) (b)

Figure 3: Landslide Study Area at (a) Pa Mei and (b) Block Model of Geomorphological Setting and Past Landslides

In addition to the high frequency of open hillslope landslides, field mapping of the site also identified an area of distressed ground close to the slope toe. This area comprised tension cracks, with up to 0.5 m vertical displacements, which extend across the slope from the head of a small retrogressive landslide located close to the toe of the hillside (Landslide No. 5 as indicated in Figure 3). Small discontinuous thrust features were also identified approximately 20 m below the tension cracks.

2.4 Ching Cheung Road, Kowloon

This site comprised a series of cut slopes and a thin strip of natural terrain overlooking Ching Cheung Road. A number of large landslides had occurred on those cut slopes in 1972, 1982 and 1997, with notable delay between major rain storms and failures. The most notable of these, which occurred in 3 stages between 7 July 1997 to 3 August 1997, resulted in closure of the road, Figure 4. Details of the landslides together with a review of the past landslide history of the area and an account of the extensive slope stabilisation works, including a large rock fill buttress at the slope toe and over 1,000 soil nails within the surrounding cuttings, are discussed in Halcrow (1998).

The consistent delay between storm events and landslide initiations at this site is suggestive of a complex hydrogeological regime. Indeed, the landslide study postulated that subsurface groundwater flow within the hillside was controlled by a series of natural 'tanks and pipes' with soil erosion pipes acting as preferential flow paths and less permeable dyke materials damming/ tanking of the groundwater flow, (Okunshi and Okimura, 1987). In view of the above observations, the instrumentation proposal thus focussed primarily on monitoring of groundwater conditions at various levels within the slope profile.

Figure 4: Images of the July/August 1997 landslide within the Ching Cheung Road Study Area (Halcrow, 1998)

3 DIFFERENTIAL GLOBAL POSITIONING SYSTEM

Global Positioning System (GPS) is the only fully functional Global Navigation Satellite System (GNSS). It utilises a network of 24 United States satellites orbiting the earth and transmitting microwave signals back to the ground surface. Other systems include the Russian GLONASS and the Chinese BEIDOU, each with 8 and 4 operational satellites respectively. The time taken for these signals to reach a single GPS receiver can be used to calculate the satellite–receiver distance. By comparison of the time lags received from four or more satellites, a GPS unit is able to determine its longitude, latitude and altitude with accuracy in terms of meters.

The accuracy of the GPS readings can be improved by reducing the satellite navigation signal errors. This is achieved by comparing the differences between GPS signals received from its receiver and those signals broadcasted from a local reference base station of known fixed coordinates, thus commonly referred to as Differential Global Positioning System (DGPS). The positioning accuracy of a DGPS can be further improved by using receivers with dual frequency tracking capability to apply a precision correction to measure the difference delays between the L1 and L2 bands. Current high-grade DGPS receivers can achieve real-time positioning with 10 mm horizontal accuracy and 20 mm vertical accuracy.

Two types of DGPS were planned for the Tsing Shan site, Figure 5. The first system was installed in early March 2008, Figure 5(a) and (b). It comprises a GPS receiver and a single antenna to track the signals from

both the US GPS and the Russian GLONASS satellites, with the differential GPS signals broadcasted from a local reference base station operated by the Lands Department. Post-processing of the preliminary real-time DGPS data indicate that the horizontal and vertical accuracies can be improved to 5 mm and 10 mm respectively. The second system is a multi-antenna system with a GPS receiver custom-made by the Hong Kong Polytechnic University (HKPU) to receive sequential signals from several antennae (Ding et al, 2002), Figure 5(c). This system is currently under construction in research collaboration with the HKPU to receive GPS signals from a network of 5 antennae placed within the landslide body and differential GPS signals from a reference antenna placed just outside the landslide body.

(a) (b) (c)

Figure 5: Single Antenna DGPS (a) Lightning Protection System & Solar Power System, (b) GPS Receiver, GPRS Modem and Back-up Power System, and (c) Schematic Design of Multi-antenna DGPS (Ding et al, 2002)

Both DGPSs were placed within chain link fence enclosures with lightning protection system to avoid theft or damage due to lightning strikes. Through collection and transmission of monitoring data at regular intervals, the movement path of the DGPS receivers can be plotted on plan and both the rate and direction of slope movement can be detected. The current set up allows the long-term performance of the two DGPS to be assessed and compared with each other and other conventional movement sensors like in-placed inclinometers installed at this site.

4 TRANSLATION, ROTATION AND SETTLEMENT SENSOR

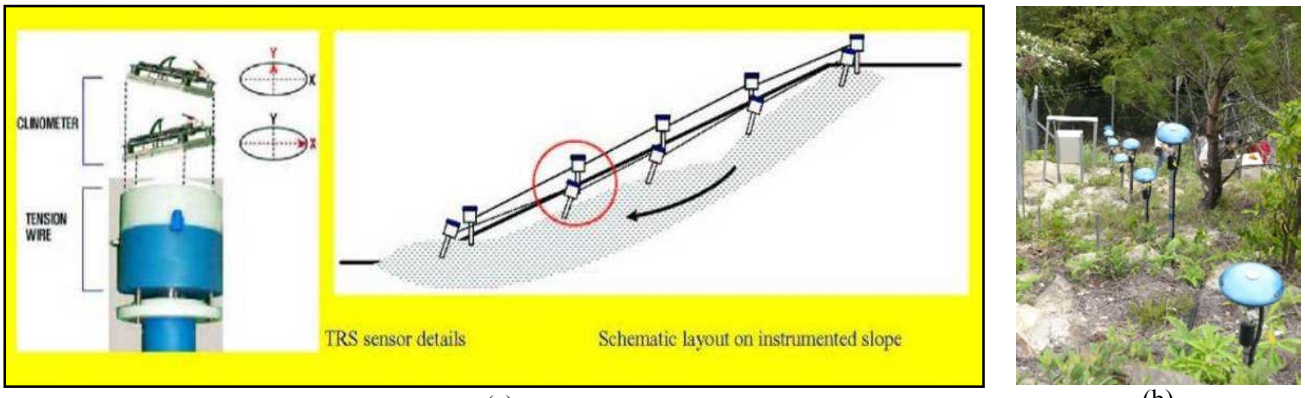

(a) (b)

Figure 6: Multi-point TRS System (a) Schematic Layout & (b) TRS Sensors installed at Pa Mei Site

Developed in South Korea and discussed in detail by Chang et al (2006), this system comprises a series of translation, rotation and settlement (TRS) sensors, which are interconnected with tension steel wires and installed at designated points along the profile of a slope, Figure 6(a). Each TRS sensor consists of a precision potentiometer for measurement of linear displacement up to a range of 200 mm and a pair of orthogonally

arranged inclinometers to measure vertical tilt in directions parallel and perpendicular to the slope profile, with ranges of 20° and 10° respectively. Movements of a slope installed with TRS sensors will thus be recorded in terms of the displacements, rotations and settlements measured by the TRS sensors.

A single array of 8 TRS sensors has been installed within the distressed area at the slope toe of the Pa Mei site, making it the first application of this technique outside South Korea. A variety of other instruments have also been provided in this area to allow direct comparison of the recorded data and assessment of the effectiveness of this method.

5 DISPLACEMENT TIME DOMAIN REFLECTOMETRY

The Time Domain Reflectometry (TDR) technique has been employed by the power and communications industries to locate cable faults and breaks in an electrical co-axial cable. In recent years, this technique has been adopted in geotechnical applications to enable the depth to shear planes or zones of deformation within the ground to be detected.

The TDR technique passes a timed electronic pulse along a coaxial cable and can detect whether or not the cable has become damaged based on the reflected signal received. In order to monitor any movement within a slope, a coaxial cable is grouted in place within a borehole and its integrity continually checked using a reflectometer, which generates the electrical signal passed through the cable. As the electrical pulse passed through the cable is timed, both the location and magnitude of any faults within the cable can be determined, Figure 7. The characteristics of the test results are stored and, when plotted over time, will reveal any changes should the slope be moving.

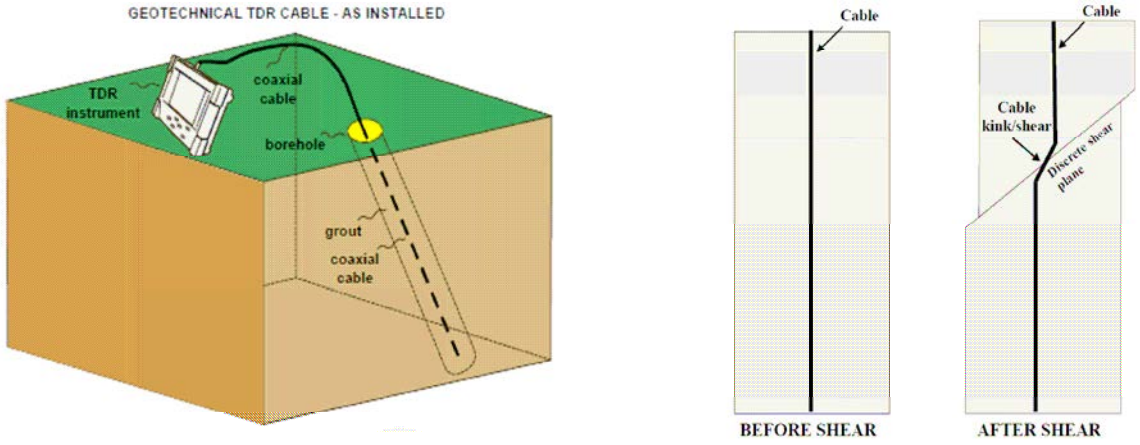

Figure 7: Schematic of Vertical TDR Monitoring System (Kane, 2000)

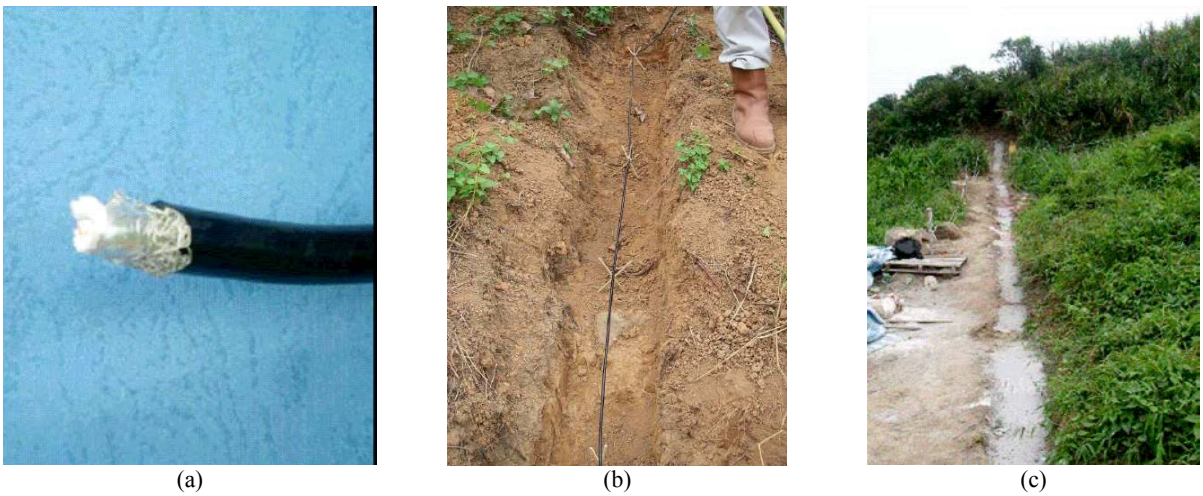

(a) (b) (c)

Figure 8: Trial Installation of a TDR Monitoring System at the Tsing Shan Site: (a) RG 58 Co-axial Cable; (b) Pre-grouting and (c) Post-grouting of Horizontal TDR Installation

Whilst this technique of slope monitoring has been implemented overseas for several years, mostly within the United States (Kane, 2000), it has not previously been adopted in Hong Kong. A trial installation was thus adopted at the Tsing Shan study site, with electrical co-axial cables grouted in drillholes adjacent to in-place inclinometers such that any indicated depths of movement could be verified. Instrument specific reflectometers were installed at the site and used for the cable testing. A cable was also grouted in-place within a 150 mm wide by 150 mm deep horizontal trench running across the site in order to test the effectiveness of delineating the extent of deformation using this technique (Figure 8). The strength of the grout was kept sufficiently low that the backfilled trench has no anticipated reinforcing effect on the surrounding soil and will freely crack and deform, thus inducing kinks in the installed cable.

6 THERMAL CONDUCTIVITY SUCTION SENSOR

The degree of soil suction in the shallow ground profile has significant impact on the stability of soil slopes and a number of past studies have been conducted on this effect (Shen, 1998; Sun et al, 1998; Sun & Ho, 2003; Ng & Chen, 2008). Initial consideration of a number of potential devices for monitoring soil suction, included Soil Psychrometers, Time Domain Transmission, Gypsum Blocks etc. Ultimately, Jet-Fill Tensiometers (JFT) was adopted mainly as a result of their ready availability and knowledge acquired through their past applications in Hong Kong. As a further development to the use of JFTs, which have been successfully used in Hong Kong for a number of years but require a high degree of manual maintenance, an array of 3 Thermal Conductivity Suction (TCS) sensors was also installed at the Tung Chung site, with depths at 0.2 – 0.6 m.

(a)

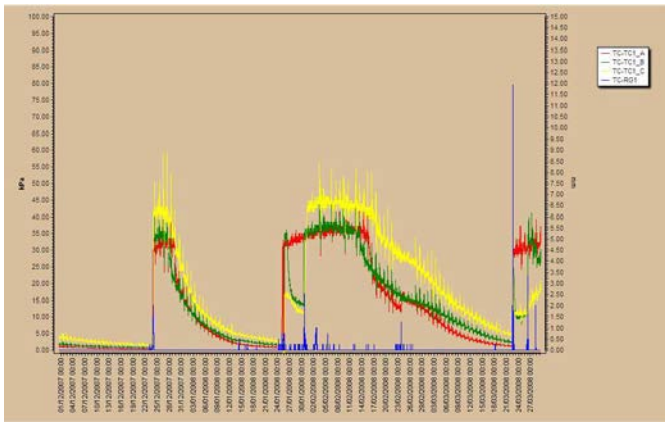

(b)

Figure 9: TCS Sensor (a) Porous Ceramic Tip and (b) Preliminary Monitoring Results

A TCS sensor consists of a heating element and a thermocouple embedded in the middle of the porous ceramic part of the probe, Figure 10(a). To calculate the soil suction, a 50 mA current is excited to the heating element for about 30 – 90 seconds and the thermocouple measures the rise of the temperature. The magnitude of the temperature rise varies in accordance with water content of the porous ceramic matrix, which changes as the surrounding soil wets and dries. Soil suction is inferred from previously determined calibration coefficients between the heat dissipation and soil suction. The calibration of the TCS sensors was carried out in research collaboration with the Hong Kong University of Science and Technology (Ng & Chen, 2008). Preliminary data showing the response of soil suction with respect to rainfall is quite promising, Figure 10(b), although more meaningful interpretation will require data of longer monitoring period.

7 WATER CONTENT TIME DOMAIN REFLECTOMETRY

A Water Content Time Domain Reflectometry (WTDR) probe comprises two 30 cm long stainless steel rods connected to a circuit board which is linked to a data logger by a shielded four conductor cable to supply power, enable probe, monitor the output and grounding, Figure 9(a). The principle of WTDR is that an electromagnetic (EM) pulse will be triggered from the circuit board to propagate along a pair of stainless steel rods to their ends where the pulse will be reflected back. The circuit board then detects the reflected EM pulse and triggers the next one. The velocity of the EM pulse depends on the dielectric permittivity of the

surrounding soil in such a manner that as the water content increases, the propagation velocity will decrease because it will take time for the water molecules in the soil to get polarized. Hence, the return period of the two-way wave propagation time is empirically related to water content using a calibration equation, with the lower and upper bounds of return period of 14 μs and 42 μs for the probe rods in air and completely immersed in tap water.

The probe can be inserted to the required depth at the bottom of a hole formed by hand auger or buried at any orientation to the ground surface. The installation method can affect the accuracy of the measurement as the probe rods should be kept as close to parallel as possible to reduce interference of wave propagation along the rods. For vertical installation in very dense soils, a probe insertion guide can be used to maintain the parallel orientation of the rods during insertion.

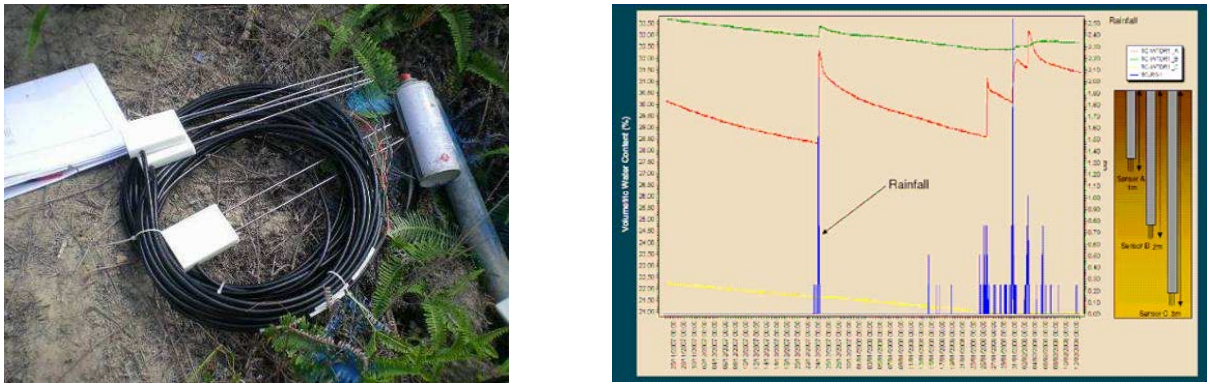

(a) (b)

Figure 10: WTDR (a) Stainless Steel Rods, Circuit Board and Four Conductor Cable and (b) Preliminary Monitoring Results

Monitoring arrays, including 3 number of WTDR probes and conventional jet-fill tensiometers (JFT) were installed at a number of locations in order to monitor how changes in matric suction and volumetric water content within the shallow soil profile during periods of intense rainfall. Preliminary data indicating good correlation between the response of the water content and rainfall is shown in Figure 9(b). In addition, the results of adjacent WTDR probes and JFTs will also allow the Soil Water Characteristic Curves (SWCC) to be determined under the in-situ conditions and compared with those measured in the laboratory. SWCC is a plot of the relationship between volumetric water content and soil suction under several cycles of wetting and drying. The method of testing to determine these relationships was discussed in detail by Ng & Pang (2000).

8 INSTRUMENTATION MONITORING DATABASE SYSTEM

One of the key component of the monitoring project is the Instrumentation Monitoring Database System (IMDS) which was designed with the necessary computer hardware and software to collect, store, analyse and present the real-time monitoring data automatically. The total storage capacity of the IMDS is such that it can handle monitoring data from an additional 6 monitoring sites (i.e. 10 sites in total), each with an average number of 60 instruments installed. The IMDS normally collects data at 15-minute intervals but is capable of retrieving data at a maximum frequency of 5 minutes, although the instruments themselves have far higher frequency capabilities should this be required. The IMDS performs validation checks on the monitoring data within 96 hours of data collection.

The user interface for the database server of the IMDS is of critical importance as this forms the main access portal through which the data is retrieved and visualised. To this end, the database server facilitates internet accessibility and combines Geographical Information System (GIS) compatible platforms to allow the data to be visualised in a user specified manner. Monitoring data for the various sites can be accessed through site specific home pages that present both the site setting, in terms of digital ortho-photographs, topographic survey plans, landslide features etc., as well as the as-built surveyed locations of all sensors installed at the sites (Figure 11). Use of a simple layering structure facilitates the availability of any desired combination of viewing options. The IMDS also allows the monitoring data to be exported in a variety of formats, from instrument-specific Excel tables to automatically generated PDF reports for each site covering a predefined time period. Such automated protocols greatly ease the efficiency with which the data can be handled.

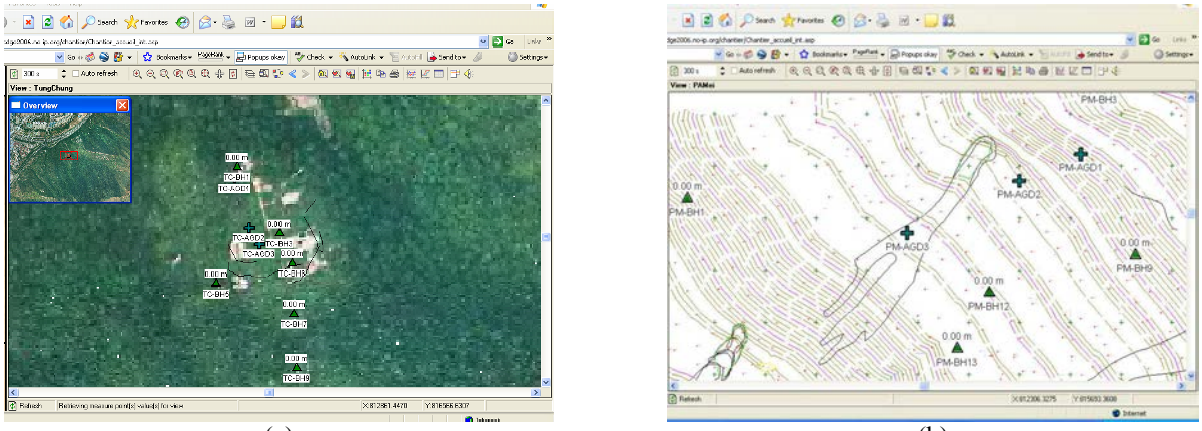

(a) (b)

Figure 11: Example of the User Interface for the IMDS (a) Digital Ortho-photo Background and (b) Topographic Survey Background (both with landslide features overlain)

The primary control mechanism for the collection, initial storage and transmission of the monitoring data was achieved by a number of dataloggers each of which is connected to a cluster of instruments in accordance with the technical specification of this instrumentation project. Wireless data transmission was used as far as practicable in this project to reduce the use of cables, which are vulnerable to lightning strikes (Shoup, 1992) and damage from other factors such as human activities, roaming animals and hill fires. The monitoring data are transmitted from the monitoring sites back to the IMDS typically by means of GPRS (General Packet Radio Service) modems, Figure 12(a).

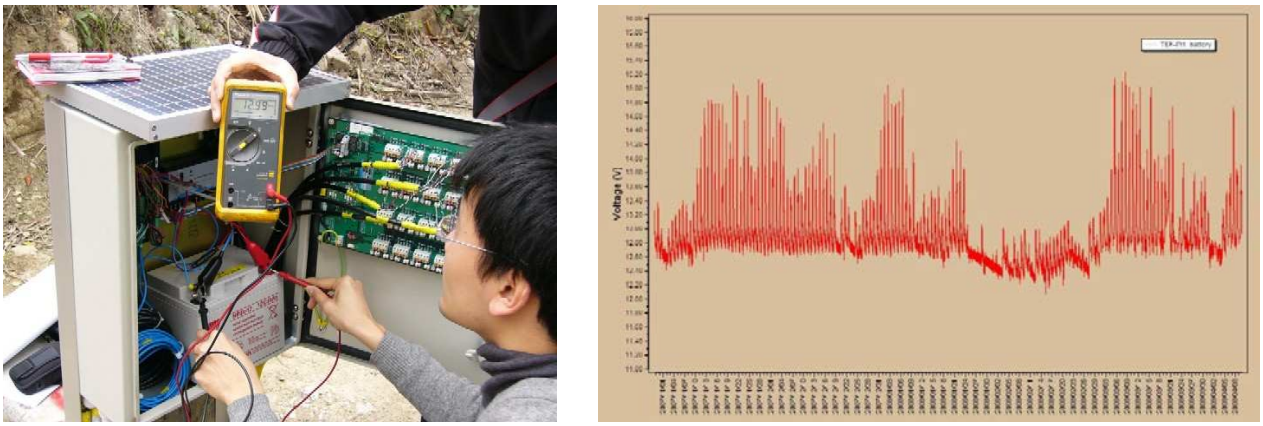

(a) (b)

Figure 12: Typical Setup of Datalogger (a) A4-sized Solar Panel, 12V Backup Battery & GPRS Modem & (b) Voltage Status of a 12V Backup Battery Including the Effect of the Long Cold Spells in early 2008

All the dataloggers are capable of collecting, storing, and transmitting the monitoring data at 5-minute intervals for a period of 7 days in accordance with the particular specification of this instrumentation project. Thus, the dataloggers are powered by solar panels with provision of secondary battery backup of at least 168 hours capacity, assuming that the data are collected and transmitted at 5-minute intervals. Recent site inspections after the long cold spells in early 2008 confirmed that all the backup batteries had been adequately charged by the A4-sized solar panels (Figure 12).

9 FUTURE WORK

As the installation of all the instruments was completed in late March 2008, only limited results are currently available for review and the content of this paper has largely been confined to the purpose and intent of the instrumentation carried out.

Given that the instrumentation project has a monitoring period of 24-months after installation, the data currently being obtained will provide a reliable set of baseline conditions that can be used for comparison against those fluctuations and movements recorded during the 2008 and 2009 rainy seasons that occur during Hong Kong's summer time. The performance of the state-of-the-art instruments installed, the technical knowledge on slope instrumentation, the results of the future monitoring works, and interpretation thereof, will therefore be analysed and assessed at the end of the monitoring period.

The experience gained from the technical specification of this instrumentation project and the procurement of the instrumentation contract will be beneficial for planning and designing future instrumentation and monitoring projects. The knowledge and experience of the IMDS of this project will also help providing a basis for further enhancement of our capability in setting up a prototype real-time instrumentation network in Hong Kong.

ACKNOWLEDGEMENTS

This paper is published with the permission of the Head of the Geotechnical Engineering Office and the Director of Civil Engineering and Development of the Government of the Hong Kong Special Administrative Region. Thanks are due to Ir H.N. Wong who has been instrumental in steering the project.

REFERENCES

Chang, K.T., Mothersille, D., Barley, T., Ho, A., & Wang, J.F. 2006. Predicting Slope Failure Using Real-Time Monitoring Technology and the TRS Sensor. *Proc. of the Intl. Conf. on Slopes, Kuala Lumpur, Malaysia, 6-9 Aug 2006*: 173-180.

Ding, X.L., Huang, D.F., Yin, J.H., Chen, Y.Q., Lau, C.K, Yang, Y.W., Sun, Y.R., Chen, W., & He, X.F. 2002. Development and Field Testing of a Multi-Antenna GPS System for Deformation Monitoring. *Proc. of the 9th Intl. Symp. on GPS/GNSS (CD Rom), Wuhan, China, 7-8 Nov 2002*.

Halcrow Asia Partnership. 1998. Report on the Ching Cheung Road Landslide of 3 August 1997. *GEO Report No. 78*: 142p. Geotechnical Engineering Office, Hong Kong.

Kane, W.F. 2000. Monitoring Slope Movement with Time Domain Reflectometry. *Geotechnical Field Instrumentation: Applications for Engineers and Geologists*, ASCE Geotechnical Group Spring Seminar, Seattle, USA, 1 April 2000.

National Research Council. 2004. *Partnership for Reducing Landslide Risk – Assessment of the National Landslide Hazards Mitigation Strategy*. National Academies Press, Washington, D.C., USA.

Ng, C.W.W. & Chen, R. 2008. (Draft). Recompacted, Natural and In-situ Properties of Unsaturated Decomposed Geomaterials.

Ng, C.W.W. & Pang, Y.W. 2000. Experimental Investigation of Soil-Water Characteristics of a Volcanic Soil. *Canadian Geotechnical Journal*, *37(6)*: 1252-1264.

Okunshi, K. & Okimura, T. 1987. Groundwater Models for Mountain Slopes. *Geomorphology*: 265-285. John Wiley and Sons, New York, USA.

Parry, S. & Campbell, S.D.G. 2003. A Large Scale Very Slow Moving Natural Terrain Landslide in the Leung King Valley. *GEO Geological Report GR2/2003*. Geotechnical Engineering Office, Hong Kong.

Shen, J.M. 1998. Soil Suction in Relation to Slope Stability: A Summary of Research Carried out in Hong Kong in 1978-1997. *Proc. of the 1997 HKIE Annual Geotechnical Seminar on Slope Engineering in Hong Kong, 2 May 1997*: 93-99.

Shoup D. 1992. Protecting Geotechnical Sensors and Cable from Lightning Damage. *Sensors in the Real World*. Slope Indicator, USA.

Sun, H.W., Wong, H.N. & Ho, K.K.S. 1998. Analysis of Infiltration in Unsaturated Ground. *Proc. of the 1997 HKIE Annual Geotechnical Seminar on Slope Engineering in Hong Kong, 2 May 1997*: 101-109.

Sun, H.W. & Ho, K.K.S. 2003. Influence of Surface Infiltration on the Stability of Partially Saturated Slopes. *Proc. of the 2nd Asian Conf. on Unsaturated Soils, Osaka, Japan, 15-17 April 2003*: 457-462.

Wong, H.N., Ho, K.K.S. & Sun, H.W. 2006. The Role of Instrumentation in Landslide Risk Management: Hong Kong Experience. *Proc. of the Conf. on Landslide*, *Sinkhole, Structure Failure: Myth or Science*, *Ipoh, Malaysia, 6-7 March 2006*.

3D Modelling of Deep Excavation in Decomposed Granite: Influence of Small Strain Stiffness and Presence of Individual Piles

S.W. Lee, A.R. Pickles, T.O. Henderson & E.S.F. Li
Geotechnical Consulting Group (Asia) Limited, Hong Kong
W.W.L. Cheang
Plaxis (Asia) Limited, Singapore

ABSTRACT

This paper uses the Hardening Soil-Small model to represent the non-linear stiffness of decomposed granite from small strain. The use of the HSsmall model only introduces two additional input parameters G_0 and $\gamma_{0.7}$ to model the variation of small strain stiffness. A three-dimensional analysis models the deep excavation at the Dragon Centre. The prediction of the wall deflection is reasonably good, whereas that of the ground surface settlement is less good. The study also investigates the potential pitfalls of modelling individual piles in 3D as an equivalent pile-wall in 2D both adjacent to and within a deep excavation. For a row of piles located behind the wall, as the distance between the piles and the wall increases the 2D pile-wall analysis under predicts the pile deflection by up to 50%. As the piles get closer to the wall the 2D pile-wall analysis over predicts the pile bending moment by up to 40%. For piles located within the cofferdam, the 2D pile-wall analysis predicts a pile tension force which is 4 times larger than the 3D analysis. The paper highlights the potential significance of adopting non-linear stiffness models and the difficulties associated with modelling individual piles when using 2D numerical models.

1 INTRODUCTION

Hong Kong will experience an increase in construction activity in the coming years due to the commencement of several major infrastructure projects. A number of these projects will involve underground construction within and/or under built-up areas including excavations associated with cut-and-cover tunnel. These excavations will induce ground movements in the surrounding ground and potentially on existing structures. It is therefore important to estimate the potential ground movement with some degree of confidence, leading to a realistic assessment of the effect on the existing structures.

Design for deep excavations in Hong Kong is usually carried out using boundary element methods or finite element/difference methods. In the calculation the stiffness of soils is usually related to Standard Penetration Test (SPT) N values. Chan (2003) has recommended an empirical relationship, Young's modulus, E = 2N (MPa), for FREW analysis associated with deep excavations in completely decomposed granite (CDG). In the finite element/difference method, the linear elastic perfectly plastic Mohr Coulomb model is usually used with constant E values.

In the finite element/difference analysis, the use of a constant soil stiffness is unlikely to give a good prediction of wall deflection and ground settlement generated for all excavation stages. This is because the soil stiffness will degrade non-linearly with shear strain as the excavation progresses. In addition, the Mohr Coulomb model has limitations in modelling the stress path and loading/unloading stiffness experienced in the soil. These deficiencies warrant a more advanced constitutive model to better represent the soil behaviour under different shear strains and stress levels. This is particularly critical when analysing excavations adjacent to sensitive structures where the control of the building response may have a significant influence on the design or construction process.

This paper investigates the use of a non-linear stiffness from small strain constitutive model to model a deep excavation in Hong Kong. The study also investigates the predicted behaviour of individual piles located both adjacent to and within the excavation cofferdam, as these will influence the distribution of strain and

resulting ground movements. This exercise has used 2-dimensional (2D) and 3D analyses. The objectives of the paper are twofold:

1. To investigate the applicability of a non-linear stiffness from small strain model with relatively simple input parameters for routine geotechnical design; and
2. To identify the shortcomings of modelling individual piles as an equivalent pile-wall in 2D analysis.

2 DEEP EXCAVATION FOR DRAGON CENTRE

Lui and Yau (1995) presented details of the deep excavation carried out for the Dragon Centre at the West Kowloon Peninsula. Figure 1 shows a cross-section of the deep excavation. The Dragon Centre is a 9-storey reinforced concrete building built on top of a five-level basement and has a plan area of 107 m by 67 m. The ground conditions are loose granular fill underlain successively by sandy Marine Deposits, CDG, highly decomposed granite (HDG) and granite bedrock. The groundwater table is at about 1.5 m below ground level.

The top-down excavation was 27 m deep and supported by 1.2 m thick concrete diaphragm walls. The walls were installed down to the rockhead and toe grouted to achieve groundwater cut-off. Prior to excavation a pumping test was carried out which showed negligible groundwater drawdown outside the walls. The groundwater table inside the walls was allowed to recover completely and thereafter excavation was carried out.

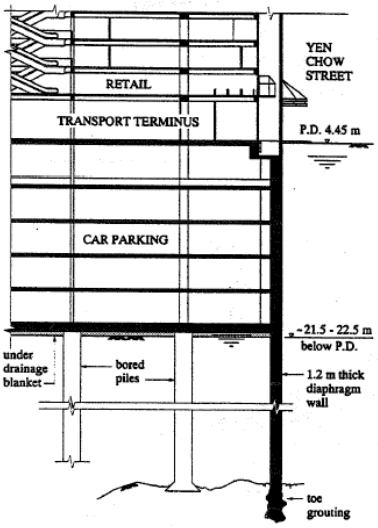

Figure 1: Dragon Centre excavation (Malone et al. 1997)

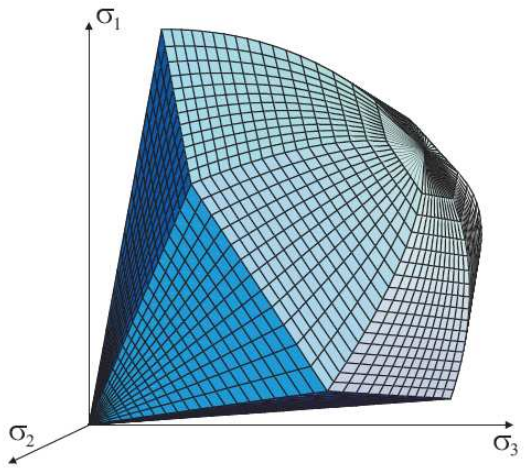

Figure 2: Yield surface of the HSsmall model (Benz 2007)

This study has used the Dragon Centre case history due to the following reasons:

1. It is a well documented case history with field measurements of wall and ground movements;
2. The availability of high quality field and laboratory test data which are relevant to this site; and
3. The availability of documented 2D analyses using the standard Mohr Coulomb model and more sophisticated 'Brick' model (Simpson 1992) with outputs in terms of wall and ground movements.

3 THE HARDENING SOIL-SMALL MODEL

Benz (2007) has developed a Hardening Soil-Small (HSsmall). The HSsmall model is a combination of the Hardening Soil (HS) model (Plaxis 2006) and the Small-Strain Overlay model which makes the soil stiffness dependent on strain history. Figure 2 shows the yield surface of the HSsmall model with the Mohr Coulomb failure criterion. The HSsmall model only introduces two additional parameters to describe the variation of soil stiffness from small strain:

1. The initial or very small strain shear stiffness (G_0); and
2. The shear strain ($\gamma_{0.7}$) at which the secant shear stiffness G is reduced to 72% of G_0.

Malone et al. (1997) and Ng et al. (1998) carried out pressuremeter tests and drained triaxial tests with small strain measurement on CDG samples obtained from a site in Kowloon Bay. Figure 3 shows the modulus

decay curves measured from the tests, plotted as secant shear stiffness normalised by mean effective stress (G_{sec}/p') versus shear strain.

The results of the Ng et al.'s triaxial tests have been used to calibrate the HSsmall model using single element (triaxial) modelling. Table 1 shows the selected input parameters for the HSsmall model. The profiles Upper and Lower refer to the parameters selected to match the upper bound and lower bound of the Ng's triaxial results respectively. The profile Baseline refers to the parameters used in the deep excavation analysis. The single element modelling models the constant p′ stress path of 200 kPa adopted in the triaxial tests.

Table 1: Selected input parameters for the HSsmall model

Profile	E_{50}^{ref} (MPa)	E_{oed}^{ref} (MPa)	E_{ur}^{ref} (MPa)	m -	$\gamma_{0.7}$ -	G_0^{ref} (MPa)	p^{ref} (kPa)	υ_{ur} -	K_0^{nc} -	c′ (kPa)	ϕ (°)
Upper	50	50	150	0.5	5E-5	250	200	0.2	0.43	5	35
Lower	20	20	60	0.5	5E-5	100	200	0.2	0.43	5	35
Baseline	39	39	117	0.5	5E-5	200	200	0.2	0.43	5	35

The definitions for the input parameters of the HSsmall model are:
E_{50}^{ref}: reference secant stiffness in drained triaxial test
E_{oed}^{ref}: reference tangent stiffness for primary oedometer loading
E_{ur}^{ref}: unloading/reloading stiffness at engineering strains of 10^{-3} to 10^{-2}
m: power for stress dependency stiffness
$\gamma_{0.7}$: shear strain at which $G=0.72G_0$
G_0^{ref}: reference shear modulus at very small strains, i.e. less than 10^{-6}
p^{ref}: reference stress for stiffness
υ_{ur}: unloading/reloading Poisson's ratio
K_0^{nc}: coefficient of earth pressure at-rest for normal consolidation
c′: cohesion
ϕ: friction angle.

Figure 4 compares the modulus decay curves between the Ng et al.'s triaxial results and the HSsmall model predictions. The data points represent the upper and lower bounds of the triaxial results. The HSsmall model predicts reasonably well the magnitude and pattern of the degradation of shear stiffness from small strain. In the deep excavation analysis that forms the remainder of this paper, the input parameters for the Baseline profile are used to represent the CDG behaviour.

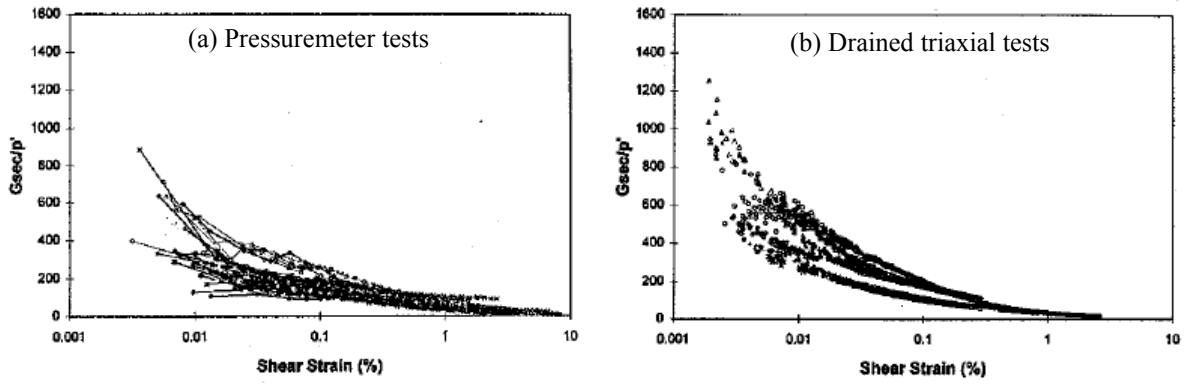

Figure 3: Modulus decay curves for CDG (Malone et al. 1997 and Ng et al. 1998)

4 3D MODELLING OF DEEP EXCAVATION

At the Dragon Centre the cofferdam was 107 m by 67 m in plan, giving a dimension ratio of 1.6. A 2D analysis may not be reliable particularly towards the corners of the excavation. The study has modelled the deep excavation in 3D using the finite element programme Plaxis 3D Foundation Version 2.

Figure 5 shows the 3D model set up for the Dragon Centre. The 3D model simulates one-quarter of the deep excavation, taking advantage of symmetry about the mid plane in both the longitudinal and transverse directions of the cofferdam. The number of 15-node wedge elements is 31,000. Table 2 sets out the input parameters for the soils modelled in the analysis. The input parameters for the CDG are based on the calibration against the Ng et al's triaxial results. The input parameters for other soils are based on the Authors' experience on other deep excavation projects which have similar ground conditions.

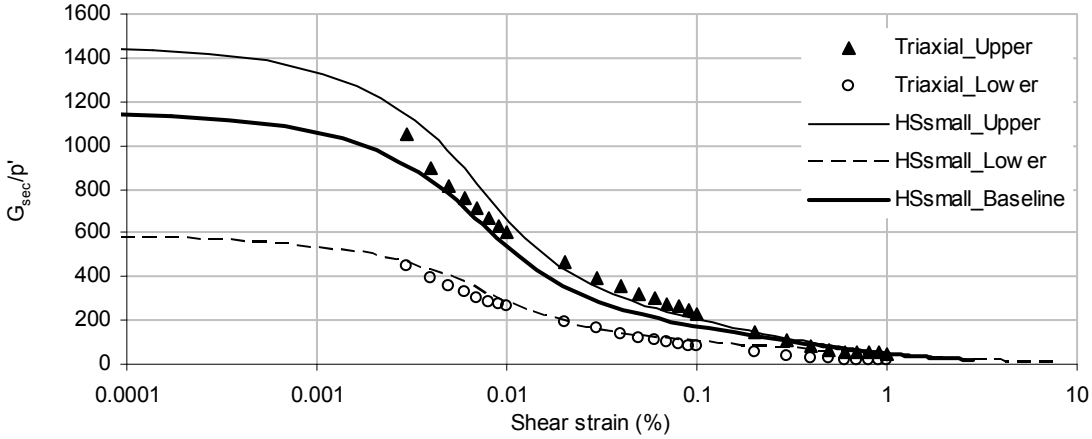

Figure 4: Calibration of the HSsmall model against the measured CDG small strain stiffness in triaxial tests

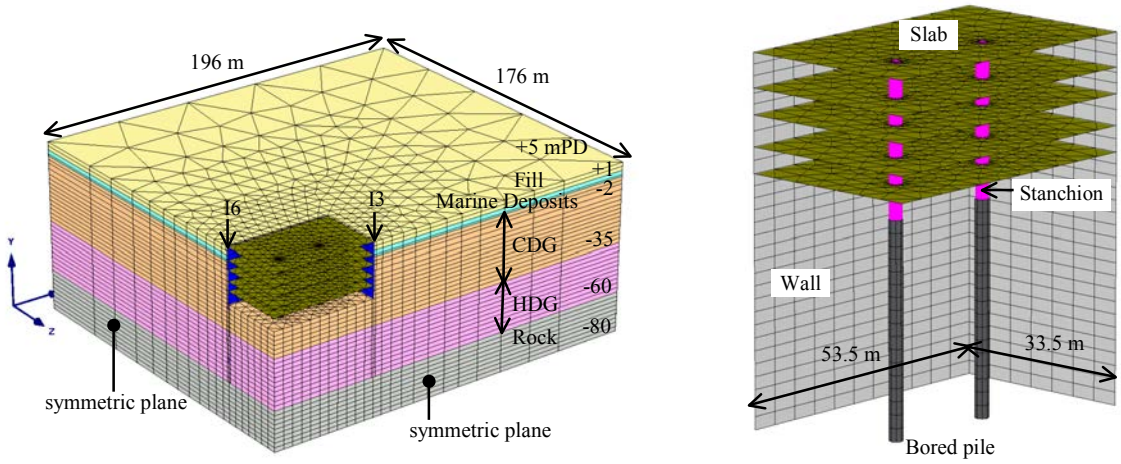

Figure 5: 3D model for deep excavation at the Dragon Centre

Table 2: Input parameters for the soils

Soil	Level (mPD)	Model	γ_{sat} (kN/m^3)	E_{50}^{ref} (MPa)	E_{oed}^{ref} (MPa)	E_{ur}^{ref} (MPa)	m -	$\gamma_{0.7}$ -	G_0^{ref} (MPa)	p^{ref} (kPa)	υ_{ur} -	K_0^{nc} -	c′ (kPa)	ϕ (°)
Fill	+5 to +1	HS	20	10	10	30	0.5	-	-	100	0.2	0.5	0.1	30
Marine Deposits	+1 to -2	HS	16	3	3	9	1	-	-	100	0.2	0.58	0.1	25
CDG	-2 to -35	HSsmall	20	39	39	117	0.5	5E-5	200	200	0.2	0.43	5	35
HDG	-35 to -60	HSsmall	20	195	195	585	0.5	5E-5	988	200	0.2	0.36	5	40
Rock	-60 to -80	Elastic	22	1000	-	-	-	-	-	-	0.2	1	-	-

The 3D analysis models the pumping test, groundwater recovery and 5 stages of excavation to 27 m depth. The analysis models an average drawdown of 11 m caused by the pumping test, taking into account the proportion of the observed localised drawdown area and the hydrostatic area. During excavation, the water table inside the cofferdam is taken at the excavation level.

The 1.2 m thick diaphragm walls and the 0.45 m thick basement slabs are modelled using the 'Wall' and

'Floor' structural elements respectively. They are modelled as a linear elastic material with an E of 28 GPa and a Poisson's ratio of 0.15. Interface elements are modelled on the faces of the walls. The coefficient of wall/soil interface (R_{inter}) for the sandy Marine Clay is specified as 0.5, whereas the other soils have a R_{inter} of 0.67.

5 RESULT OF ANALYSIS

Malone et al. (1997) carried out 2D analyses to model the deep excavation at the Dragon Centre. They used both the Mohr Coulomb and Brick models to represent the CDG behaviour and concluded that the Brick model predictions gave better agreement with the field measurements than the Mohr Coulomb model. The predictions made by the 3D analysis with the HSsmall model are compared to the field measurements and to the Malone et al.'s Brick predictions.

Figures 6 and 7 compare the measurements and the predictions of the cumulative wall deflections at inclinometers I3 and I6 respectively. Inclinometers I3 and I6 were located at the mid-span of the short and long side wall respectively (see Figure 5). For the pumping test the HSsmall model slightly under predicts the wall deflections, comparing the maximum predicted 36 mm and 48 mm to the measured 55 mm. The Brick model predicts 75 mm maximum deflection. For the groundwater recovery the HSsmall reasonably predicts the profile of the reduced wall deflections, although slightly over predicting the magnitude of the deflections. The Brick model does not have a similar prediction for comparison. For the final excavation to 27 m depth the HSsmall model predicts reasonably well the wall deflections at inclinometer I3 above level +18. Below this level the deflections are over predicted. The Brick model over predicts the wall deflections at I3. At inclinometer I6 both the HSsmall and Brick models give slightly different deflection profiles from the measurement, although the measured maximum deflection of 85 mm is reasonably well predicted.

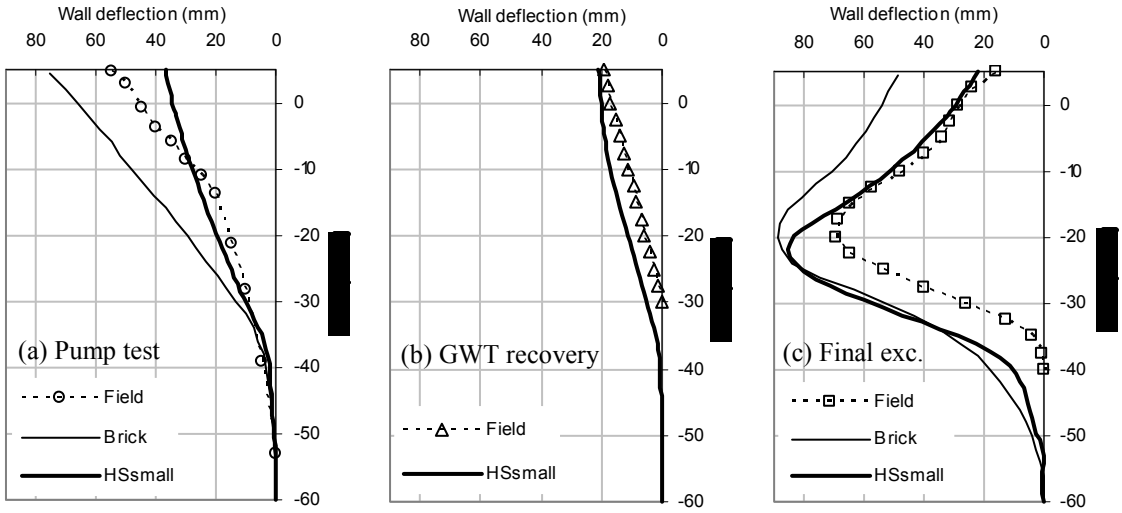

Figure 6: Comparison of cumulative wall deflections at inclinometer I3

Figure 8 shows the predicted wall deformations at completion of the 27 m deep excavation. The stiffening effect provided by the corner of the walls is evident, with the deflections at the mid spans of the walls being larger than those near the corner.

Figures 9 and 10 compare the measurements and the predictions of the ground surface settlements behind inclinometers I3 and I6 respectively. For the pumping test the HSsmall model predicts the maximum settlements of 29 mm and 34 mm, compared to the measured 8 mm and 15 mm. The width of the settlement trough is also over predicted. The Brick model predicts 65 mm maximum settlement. For the final excavation the settlements presented are the incremental settlements due only to the 27 m deep excavation. Although the HSsmall model reasonably predicts the maximum measured settlement of about 40 mm, the pattern of the surface settlement trough is not well predicted. The Brick model predicts 50 mm maximum settlement. In comparison to the prediction of the wall deflection, the HSsmall prediction of the ground surface settlement is less good.

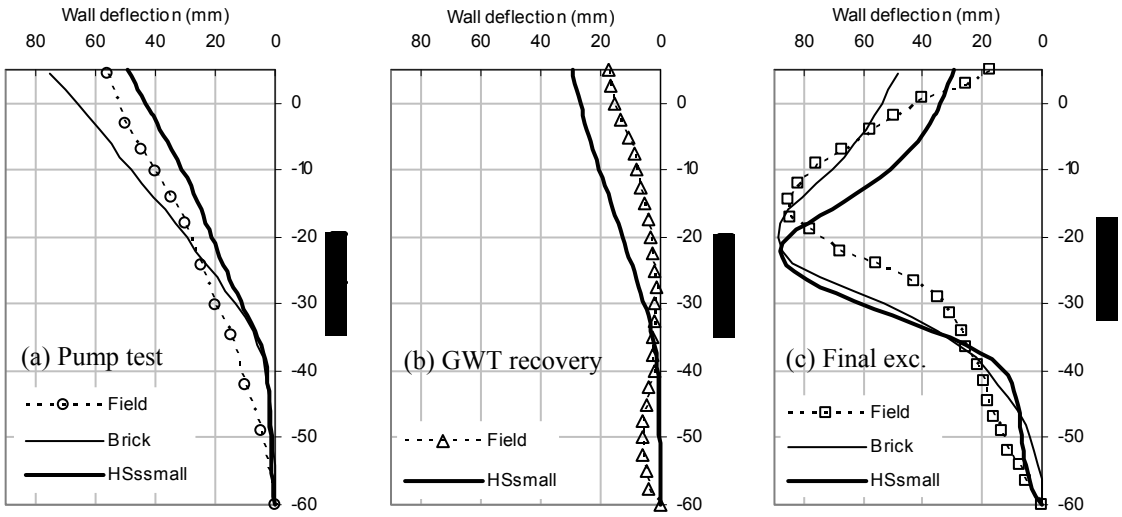

Figure 7: Comparison of cumulative wall deflections at inclinometer I6

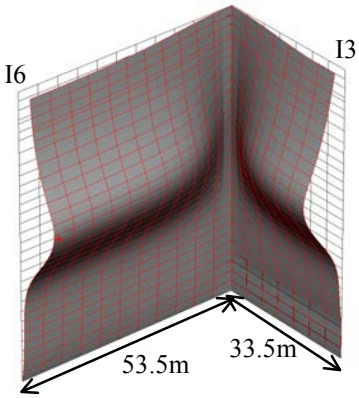

Figure 8: Predicted wall deformations (exaggeration scale 120).

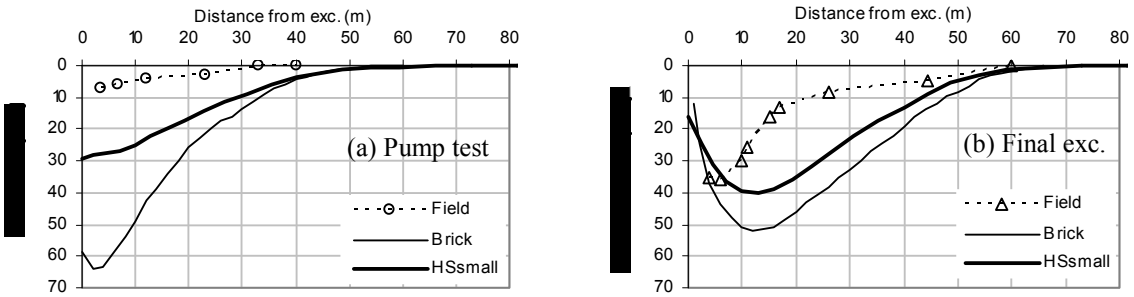

Figure 9: Comparison of ground surface settlements behind inclinometer I3

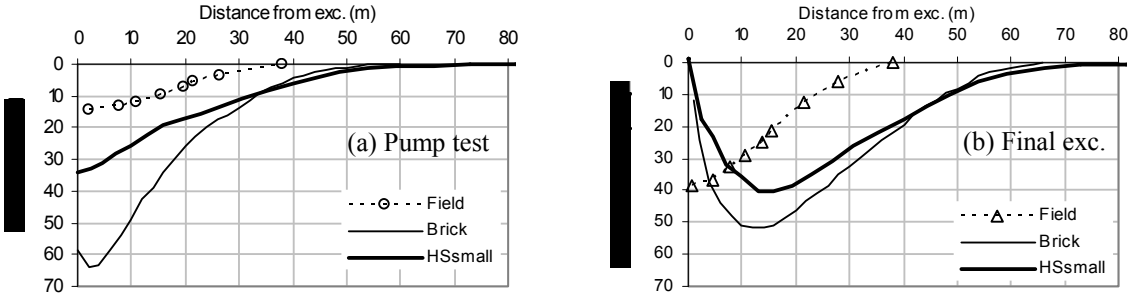

Figure 10: Comparison of ground surface settlements behind inclinometer I6

6 INDIVIDUAL PILES BEHIND WALL

This section investigates the appropriateness of modelling a row of individual piles in 3D as an equivalent pile-wall in 2D adjacent to a deep excavation. The pile-wall approach in 2D is usually used in routine geotechnical design, because engineers are relatively new to 3D modelling.

2D analysis cannot physically model a row of individual piles spaced at a distance into-the-plane. The individual piles are usually modelled as an equivalent pile-wall into-the-plane in 2D. The flexural stiffness (EI) and axial stiffness (EA) of the pile are divided by a 'reduction' factor, which is usually taken as the pile spacing into-the-plane, to give the equivalent EI and EA of the pile-wall used in 2D models. The predicted pile bending moment and axial force from the 2D analysis are multiplied by the 'reduction' factor to give the moment and force of the individual pile. In certain circumstances the 2D analysis is not appropriate because the equivalent pile-wall does not allow the surrounding soil to flow past the piles.

A series of 3D and 2D analyses has been carried out using the Dragon Centre example. The 3D analysis models a row of piles sized 1.5 m diameter (d) and spaced at 7.5m centres (5d) along the long side of the excavation. Figure 11 shows an example of the 3D model. The distance between the centre of the piles and the retaining wall (S) is specified as 3 m (2d), 7.5 m (5d) and 15 m (10d). There are nine piles in the one-quarter model, with the last two piles located outside the corner of the cofferdam. The piles are assumed to be founded on the rockhead at level -60 mPD and installed before the pumping test. Interface elements are modelled down the piles which have a Young's modulus of 28 GPa and a Poisson's ratio of 0.15.

Figure 12 shows an example of the corresponding 2D model using the programme Plaxis 2D Professional. The 'Plate' elements with interfaces (equivalent pile-wall) model the individual piles with an equivalent EI and EA of 9.3×10^5 kNm^2/m (=EI_{pile}/7.5 m) and 6.6×10^6 kN/m (=EA_{pile}/7.5 m) respectively. The 2D analysis models an infinitely long excavation into-the-plane along the long side of the cofferdam. Both the 2D and 3D analyses model the construction sequences implemented at the Dragon Centre.

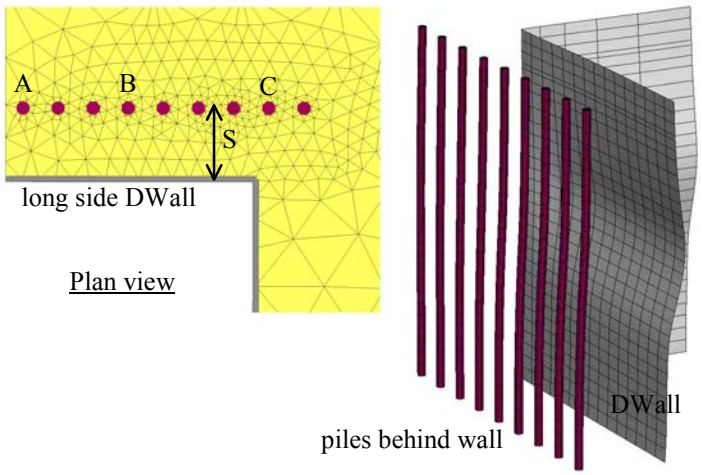

Figure 11: 3D model for individual piles behind DWall

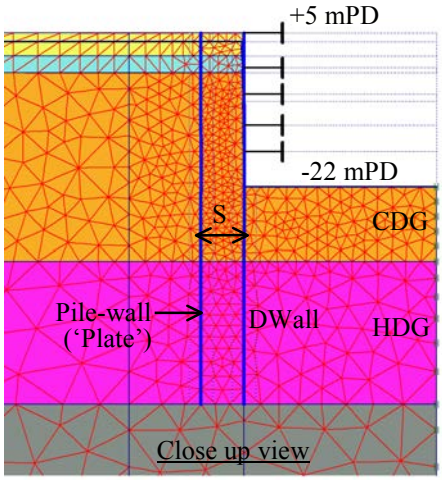

Figure 12: 2D model for pile-wall behind DWall

Figure 13 compares the predicted pile deflections between the 3D and 2D analyses. For the 3D analysis Piles A (near the mid-span of the long wall), B (at one-quarter location of the long wall) and C (slightly outside the cofferdam) are selected for the comparison, see Figure 11. For S=3 m (distance between the pile centre and the wall), the 2D analysis predicts the pile deflections comparable to Piles A and B from the 3D analysis. The 2D predicts the maximum pile deflection (δ_{max}) of 53 mm, compared to 54 mm and 60 mm at Piles A and B respectively. However, the 2D prediction obviously cannot be applied to Pile C. Due to the corner effect where the wall flexural stiffness is increased, Pile C shows a small deflection of less than 7 mm. As distance 'S' increases, the 2D analysis predicts smaller pile deflections than the 3D analysis. Figure 13(b) shows that for S=7.5m, the 2D analysis predicts the δ_{max} of 34 mm, compared to 47 mm and 54 mm at Piles A and B respectively. For S=15 m, the 2D analysis predicts only 40% to 50% of the deflections predicted at Piles A and B.

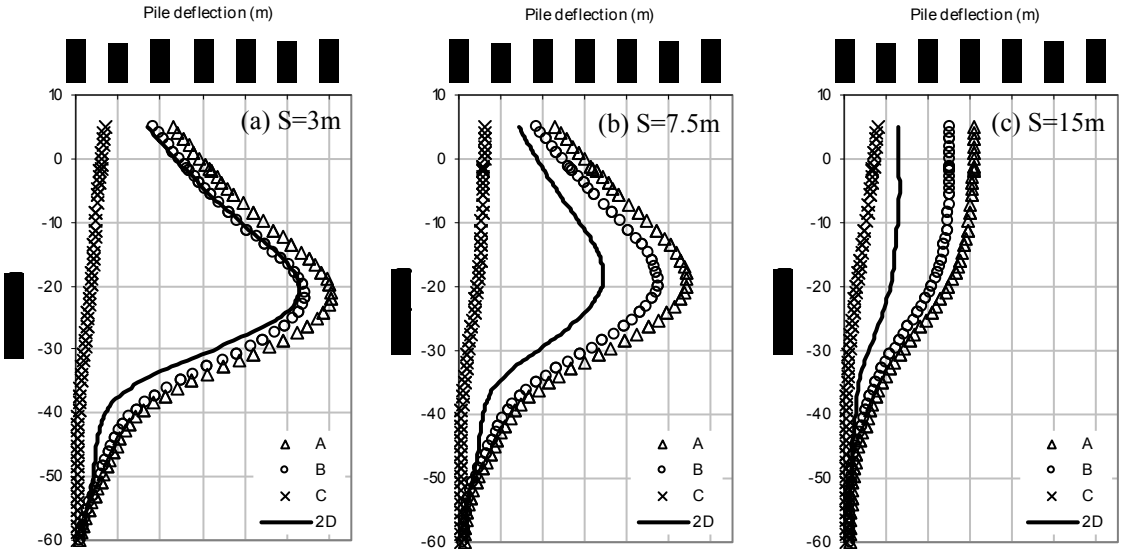

Figure 13: Comparison of pile deflections between the 3D (Piles A, B and C) and 2D analyses

Figure 14 compares the predicted pile bending moments between the 3D and 2D analyses. The pile bending moment is a function of curvature of the deflection profile. For S=3 m and 7.5m the 2D analyses predict the maximum moments of 3400 and 2100 kNm respectively, which are larger than the 3D predictions of 2500 and 1500 kNm respectively. The predicted profiles of the bending moments are however very similar between the 3D and 2D analyses. Pile C has bending moments of less than 100 kNm, because the predicted pile deflection curvature is small due to its proximity to the cofferdam corner. For S=15 m both the 2D and 3D analyses predict moments of less than 500 kNm, and the difference in the predicted moments between the two analyses is not significant considering the relatively small magnitude of the bending moments.

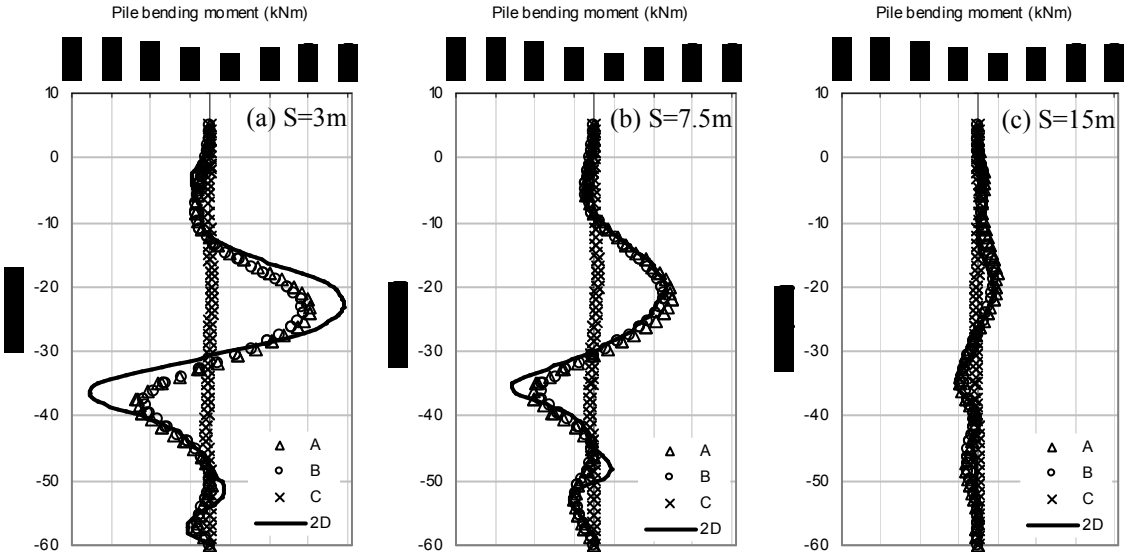

Figure 14: Comparison of pile bending moments between the 3D (Piles A, B and C) and 2D analyses

7 INDIVIDUAL PILES WITHIN COFFERDAM

Piles installed within a cofferdam are subject to upward displacement arising from excavation of the cofferdam. The upward soil displacement relative to the piles will generate tension force in the piles. A study has been carried out to investigate the appropriateness of 2D analysis using an equivalent pile-wall to predict the tension force of individual piles in 3D. Figure 15 shows the 3D model with a row of piles sized 1.5 m

diameter and spaced at 7.5m centres installed at centreline of the cofferdam down to the rockhead. Interface elements are modelled down the piles. Figure 16 show the corresponding 2D analysis. The equivalent pile-wall is specified with the equivalent EI and EA values for modelling the individual piles. Details of the 2D and 3D analyses are similar to those presented in Sections 4 and 6. When excavating downward to a new level the pile heads are cut to the new excavation level. The axial force predicted from the 2D analysis is multiplied by the pile spacing of 7.5 m to give the individual pile axial force.

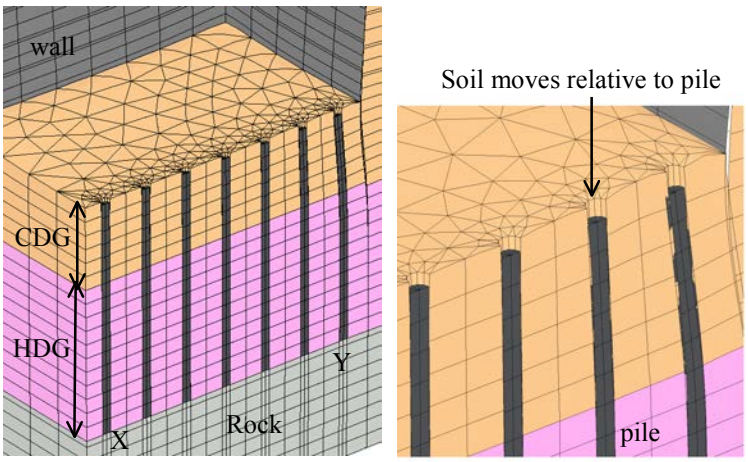

Figure 15: 3D model for piles within cofferdam

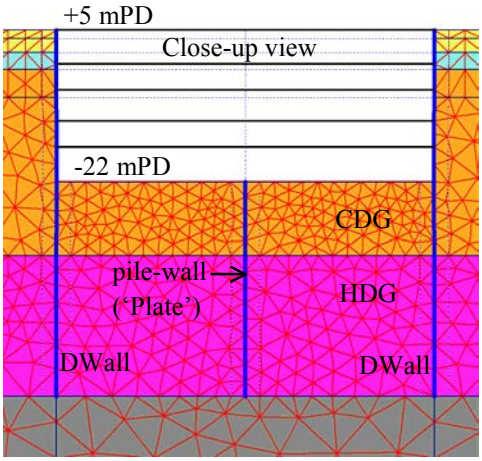

Figure 16: 2D model for pile-wall within cofferdam

Figure 17 compares the predicted axial forces at completion of the 27 m deep excavation between the 3D and 2D analyses. The 3D predictions are plotted for Piles X and Y (see Figure 15) which represent the lower and upper bounds of the predicted axial forces. The 2D analysis predicts the maximum pile axial force of 4600 kN, which is about 4 times larger than the 3D prediction of 1250 kN. The over-prediction of the pile axial force occurs because in 2D the equivalent pile-wall provides an unrealistically large surface area for mobilisation of shaft friction when the soil moves upward relative to the pile-wall. The pile-wall provides a surface area of 2 m^2/m into-the-plane/m depth, whereas the individual pile provides a surface area of 0.63 m^2/m into-the-plane/m depth. The 'reduction' factor applied to the equivalent EI and EA values cannot reduce the surface area of the pile-wall, which is an inherent geometrical problem in 2D.

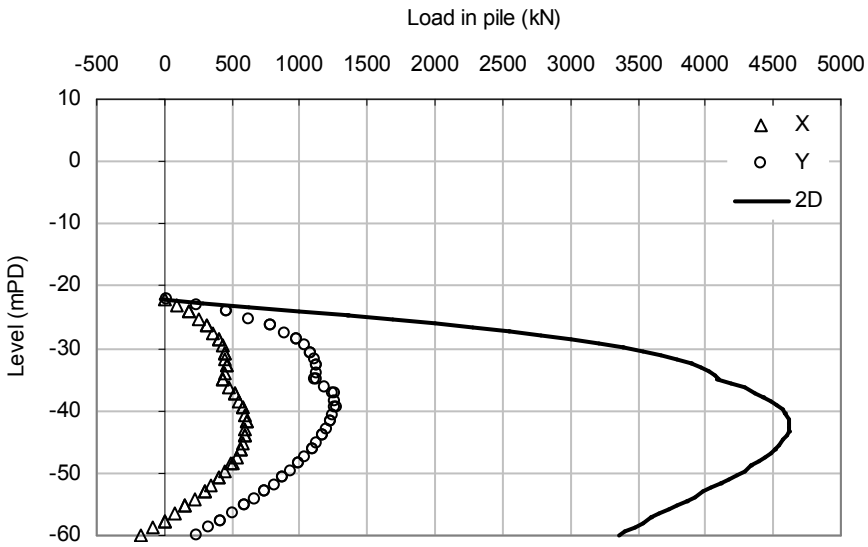

Figure 17: Comparison of tension force (+ve) in piles between the 3D (Piles X and Y) and 2D analyses

8 SUMMARY

This paper uses the Hardening Soil-Small model to represent the non-linear stiffness of decomposed granite from small strain. The HSsmall model only introduces two additional input parameters G_0 and $\gamma_{0.7}$ to model the variation of small strain stiffness. The model is calibrated against the modulus decay curves measured from pressuremeter and triaxial tests on completely decomposed granite (CDG).

A 3D analysis has been carried out to model the deep excavation at the Dragon Centre, in which the CDG and HDG are represented using the HSsmall model. The predictions of the measured wall deflections are reasonably good for the construction stages representing the pumping test, groundwater recovery and final excavation of 27 m depth. The predictions of the ground surface settlements are however less good.

A series of 3D and 2D analyses has been carried out to investigate the potential pitfalls of modelling individual piles in 3D as an equivalent pile-wall in 2D both adjacent to and within a deep excavation. This is an important issue, because in routine geotechnical design the equivalent 2D pile-wall approach is usually used.

For the particular condition analysed, as the distance between the piles and the back of the wall increases the 2D pile-wall analysis under predicts the pile deflection by up to 50%. On the contrary, as the piles get closer to the wall the 2D pile-wall analysis over predicts the pile bending moment by up to 40%. For piles located within the cofferdam, the 2D pile-wall analysis predicts a pile tension force which is 4 times larger than the 3D analysis.

The 2D pile-wall analyses produce different predictions to the 3D individual piles analyses mainly because

1. The pile-wall does not allow the surrounding soil to flow past the piles; and
2. The pile-wall provides an unrealistically large pile surface area for mobilisation of shaft friction.

The analyses presented in this paper demonstrate the importance of understanding some of the external factors and constraints associated with modelling deep excavations. The paper highlights two important factors. First, the potential significance of adopting non-linear stiffness models in place of the more commonly adopted constant stiffness models. Second, the difficulties associated with modelling isolated structural elements such as individual piles when using 2D numerical models. Understanding the influence of these factors can be critical when assessing ground and structure movements adjacent to excavations, particularly in the vicinity of sensitive structures. A failure to examine the extent of their influence may lead to unrealistic predictions of ground and building response.

REFERENCES

Benz, T. 2006. *Small strain stiffness of soils and its numerical consequences*. PhD thesis, University of Stuttgart.

Chan, A.K.C. 2003. Observation from excavations – a reflection. *Proc. 23rd Annual Seminar*, Geotech. Div., HKIE, 83-102.

Lui, J.Y.H. & Yau, P.K.F. 1995. The performance of the deep basement for Dragon Centre. *Proc. Seminar on Instrumentation in Geotechnical Engineering*, Geotech. Div., HKIE, 183-201.

Malone, A., Ng, C.W.W. & Pappin, J. 1997. The prediction and the control of displacements around deep excavations in completely decomposed granite. *Proc. 14th Int. Conf. Soil Mech. and Found. Engrg.*, Vol. 4, Balkema, 2325-2328.

Ng, C.W.W., Sun, Y.F. & Lee, K.M. 1998. Laboratory measurements of small strain stiffness of granitic saprolites. *Geotechnical Engineering*, Southeast Asian Geotechnical Society, 29(2): 233-248.

Plaxis 2006. *Plaxis version 8: material model manual*. Plaxis BV, the Netherlands.

Simpson, B. 1992. The thirty-second Rankine Lecture: retaining structures: displacement and design. *Geotechnique*, 42(4): 541-576.

Analysis of the Impact of Deep Excavations on Adjacent Properties in Soft Soil District

J.J. Li, Z.H. Xu, & W.D. Wang
East China Architectural Design & Research Institute Co., Ltd., Shanghai

ABSTRACT

The predictions of impact on adjacent properties induced by excavation are the most important aspects that must be considered in the design of deep excavations. Finite element method is used to analyze the impact on adjacent structures. It was recommended to use the Plaxis Hardening Soil (HS) model to simulate the constitutive responses of soils in Shanghai soft soil. The appropriate calculation parameters of the HS models are obtained by using back-analysis. Lateral displacement of the retaining wall calculated by the beam on elastic foundation method (BEF) is used to calibrate the inverse analysis. Other aspects such as appropriate modelling the initial condition, the interface between soil and structure, and modelling the procedure of the excavation are also important. Cases study shows that the calculated results using finite element method agreed well with the in-situ monitored data in deep excavations adjacent to properties in Shanghai urban area.

1 INTRODUCTION

In recent years, a large number of deep excavations have been constructed in Shanghai urban area to meet the demands of mass transportation and use of underground space (including basements of buildings, underground car parks, underground metro stations, underpasses for roads, and so on). At the same time, more and more deep excavations have been constructed in close proximity to existing properties including buildings, subway stations, metro tunnels, embankments and underground pipelines. Figure 1 shows the typical situations of excavations adjacent to these properties.

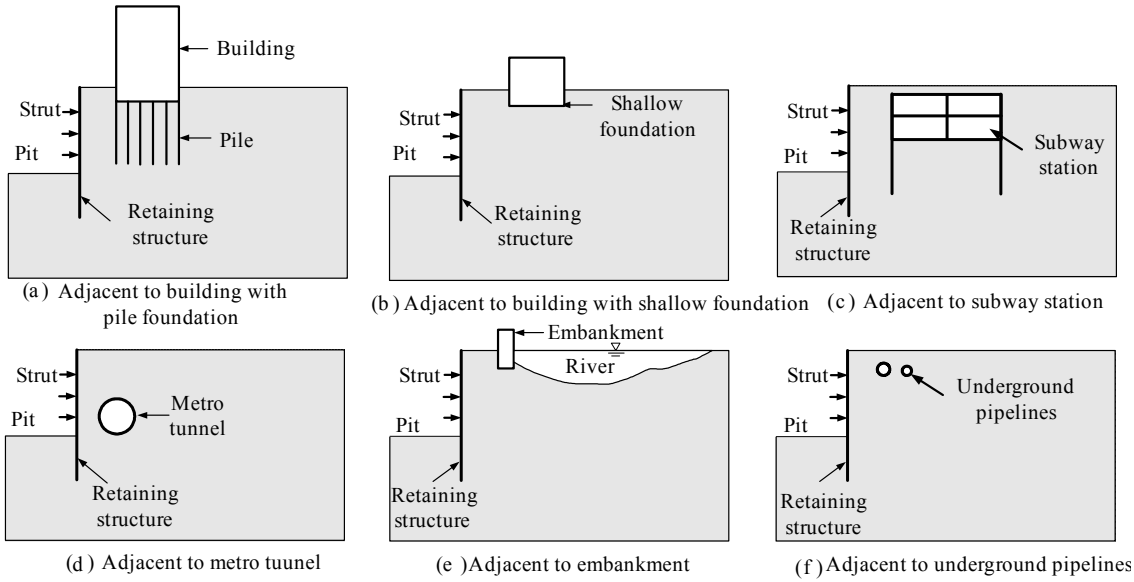

Figure 1: Sketch maps of typical situations of excavations adjacent to properties

Deep excavations in such complex urban environment have brought up many new problems to the engineers involved in designing and constructing the new project, such as how to protecting the existing

adjacent structures, how to control the additional deformation arisen from the deep excavations, etc. In many cases, the strict deformation control is required to consider in order to minimize the damage to adjacent structures during excavation. As a result, the concept of performance-based design rather than conventional strength-based design should be adopted. In a performance-based design, accurate prediction of the distortion of retaining structure and the displacement of adjacent properties becomes very important. Unfortunately, most of the present codes (e.g. ACECS 1997, CABR 1999) only suggest analysis methods for calculating deformation and internal forces of retaining walls, but the calculation on the impact to the adjacent structures is not mentioned. Quantitative accurate prediction on the deformation of adjacent properties is still the most challenging task to the geotechnical engineers.

Numerical analysis does provide an efficient way to analyze ground deformation induced by deep excavations. However, an accurate numerical prediction of the influence of the excavation on the environment contained many key aspects. This paper describes many important aspects of the prediction of the impact on adjacent properties by FEM. By adjusting parameters of the soil, reasonable lateral displacement of the retaining wall (verified by that obtained by Beam on Elastic Foundation method which has enough practical experience in Shanghai district) can be obtained. Subsequent displacement of adjacent properties can thus be reasonably obtained. Cases study showed that the calculated results by this method agreed well with the in-situ monitored data.

2 REVIEW OF CONVENTIONAL METHODS IN PREDICTING EXCAVATION INDUCED MOVEMENTS OF ADJACENT PROPERTIES

In conventional methods, ground surface settlement caused by excavation can be used to evaluate the movements of adjacent properties caused by excavation. Accurate prediction of the magnitude and distribution of ground movements adjacent to excavation is also quite difficult as it depends on many factors such as the dimensions of the excavation, the types and properties of the ground, the existing horizontal stresses in the ground, the water pressure beneath and around the excavation, the method of excavation and the support to the perimeter, the time during which the excavation remains open. Predicting ground surface settlement induced by deep excavation can use the conventional methods such as the semi-empirical method and the beam on elastic foundation method.

2.1 Semi-empirical method

Peck's (1969) state-of-the-art-report was the first comprehensive review of the performance of deep excavations in soil. Based on deformation data from excavations supported by temporary braced sheet pile and soldier pile walls, he developed plots of ground settlement, normalized by the excavation depth, against distance from the excavation. Empirical envelopes that bound observed ground settlements at sites as a function of soil conditions have been presented by Clough and O'Rourke (1990). Hsieh and Ou (1998) also developed a semi-empirical method to predict the distribution of ground movements. The semi-empirical method is useful to engineers who wish to estimate the magnitude of ground movements or to check the rationality of numerical analysis of deep excavations. However, the semi-empirical method is a rough method to predict the impact of excavation to the surround soil and the impact on adjacent properties. Moreover, the process of stages excavation can not be considered in this method.

2.2 Method based on beam on elastic foundation method (BEF)

Mana and Clough (1981), Ou (1993), and Moormann (2004) proposed some statistical relationships between the maximum ground settlement and the maximum lateral displacement of the retaining wall based on a large number of monitored data. If the maximum lateral displacement of the retaining wall is known, the maximum ground surface settlement can be obtained according to these statistical relationships. Lateral displacement of the retaining wall can be reasonably obtained by beam on elastic foundation method (BEF), which was suggested by the codes (e.g. ACECS 1997, CABR 1999). In the BEF method, Winkler elastic foundation model is used to model the brace-retaining structure. Earth pressures are modeled with a series of independent spring supports, and the struts are modeled with elastic supports. The springs represent the load of soil and water acting on the retaining structure. At each excavation phase, the spring loads change according to the changes of soil, water, and support system loads during the load and unload processes. The properties of soil,

the retaining structures and stage excavation are considered in the BEF method. However, the BEF method can only provide an approximate estimation of the retaining wall-soil interaction in a one-dimensional characteristic of the soil mass and ground movements behind the retaining structure can not be specified in this model. As a result, ground movements behind the retaining structure are not available. However, the BEF method has provided an effective way to determine the deformation and internal forces of retaining structure at each excavation stage. It should be pointed out that the method predicting ground surface settlement based on the BEF method is also a rough method.

3 ANALYSIS OF THE IMPACT ON ADJACENT PROPERTIES OF EXCAVATION BY FEM

3.1 Finite element method (FEM)

Finite element method (FEM) is a powerful method which can be used for the analysis of staged construction. With the development of hardware/software of computer and soil constitutive models, numerical methods became to be widely used and accepted in the deep excavation engineering (Clough and Wong 1971, Borja 1990, Finno 1991, Ou 1996, Roboski 2004). When using the FEM, the prediction accuracy of excavation-induced impact on adjacent properties is base on many important factors such as proper calculation model, adequate representation of constitutive responses of soil, rational calculation parameters, accurate midelling of the initial stress state, and midelling of the interaction of soil and structure. The FEM simulates the excavation with a two dimensional or three dimensional models which include the soil mass, retaining structure and adjacent structures. Movements of ground and adjacent properties can thus be directly obtained by this method.

Many finite element software programs were issued in the past. Some of them were tested in order to select the one most suitable for the analysis of deep excavations in Shanghai. Eventually Plaxis (Brinkgreve, 2006) was selected mainly because of its extensive soil mode library. Moreover, the easy to use Windows interface and many automated settings allow deep excavation problems to be analyzed efficiently and accurately with the minimum of training. All the FEM analysis in this paper was done by the Plaxis software.

3.2 Selection of soil constitutive model

A key issue in the FEM analysis is to select suitable soil constitutive models. Considering the modelling of soil behavior by means of constitutive relationships, many models have been proposed by researchers in the past, among which the Linear Elastic Model (LE), Mohr-Coulomb Model (MC), Drucker-Prager Model (DP), Duncan-Chang Model (DC), Modified Cam-Clay Model (MCC), and the Plaxis Hardening soil Model (HS) are probably the most widely used. Each constitutive model has its application scope and limitations as it represents only a particular or some aspects of the soil behavior.

The LE model is entirely inappropriate for the analysis of deep excavations because active and passive earth pressures can not be reasonably modeled as there is no restriction on the tensile stresses in the soil. The linear-elastic perfectly plastic models such as MC model and DP model usually produce unrealistically large pit bottom heave and generally give poor predictions of both of the magnitude and extent of ground surface settlement. Therefore, the MC model and DP can only be used to get a first estimate of deformations of deep excavations. The DC model, developed for non-linear elasticity, does not revolve any plastic theory. Distinction is made between primary loading stiffness and unloading stiffness in the DC model. Therefore, the DC model can be used to get an improved first estimate of deformations of deep excavations. The MCC model and HS model are strain hardening plastic constitutive models. They represent much more advanced models than the linear-elastic perfectly plastic models such as MC model and DP model. These two models can reflect many important features of soil which are important in excavation simulations. These features include plasticity, strain hardening, difference between loading and unloading stiffness, and stress dependent stiffness. After relevant research, it was found that the HS model was the most suitable model for deep excavations in Shanghai district (suitable for both clay and sand).

In the HS model, the soil stiffness is described much more accurately by using three different input stiffnesses: the oedometer loading stiffness, E_{oed}, the triaxial loading stiffness, E_{50}, and the triaxial unloading stiffness, E_{ur}. The limiting states of stress are described by means of the friction angle, φ, the cohesion, c, and the dilatancy angle, ψ. In contrast to the linear-elastic perfectly plastic Mohr-Coulomb model which uses a

stress-independency (constant) stiffness moduli, the HS model also accounts for stress-dependency of stiffness moduli. This means that all stiffnesses increase with pressure.

3.3 Determination of soil parameters

Parameters of the HS model can be obtained from high quality laboratory and field tests. Unfortunately, high quality laboratory tests such as triaxial tests are seldom carried out in normal geotechnical investigations in Shanghai district. Therefore determination of appropriate parameters of the HS model is quite difficult in most cases. Inverse analysis (Calvello 2002) has provided an efficient way to determine parameters of soil. In inverse modelling, a model is calibrated by iteratively changing the estimates of the model input parameters until the computed results match the observed data. In deep excavations, observed data such as lateral displacement of retaining wall and ground settlement are usually used for back-analysis. However, during the design stage, these observed data are not available. Beam on elastic foundation method (BEF) has been widely used in Shanghai and much experience has been gained in adopting this method. Lateral displacement of the retaining wall obtained by the BEF method is generally reasonable in Shanghai district. Therefore, during the design stage, the lateral displacement of retaining wall obtained by the BEF method can be used as an object for calibration in the inverse analysis.

The initial input parameters can be estimated according to experience in Shanghai and geotechnical investigation reports. A large number of sensitively calculations have been made to decide which parameters are the most sensitive to wall and ground displacement. The most sensitive parameters are then updated to run new set of calculations until the optimized input parameters have been obtained when calculated lateral displacement of retaining wall is closer to that obtained by BEF method. Movement of adjacent properties caused by excavation can simultaneously obtained at the last finite element (FE) run when using the optimized input parameters. Figure 2 shows the flow chart for determining soil parameters.

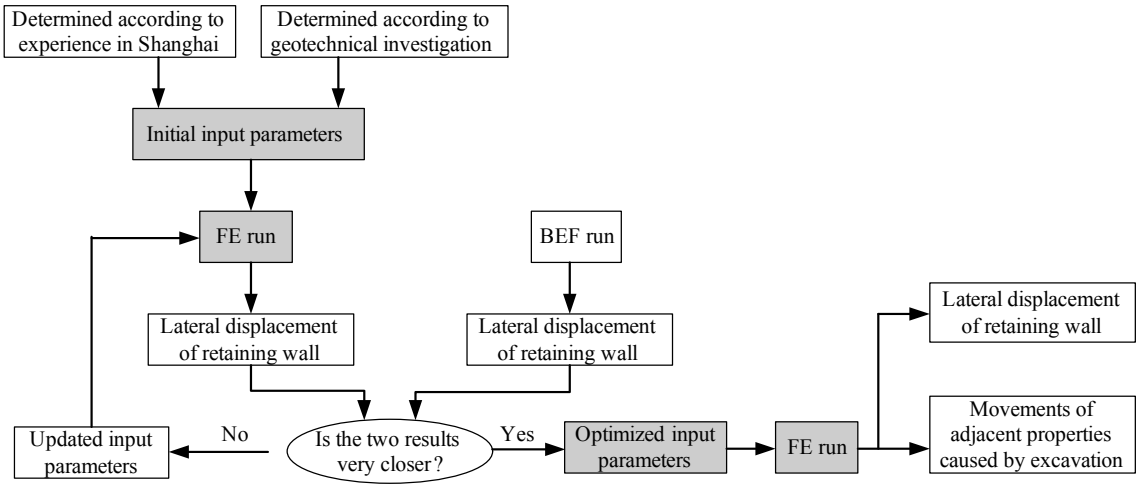

Figure 2: Flow chart for determining soil parameters

3.4 Modelling of the initial condition

For excavations in close proximity to existing properties, properly modelling the initial condition is important. Higgins et al. (1996) analyzed a 37 m deep excavation which was adjacent to tunnels. He compared the lateral displacement of the retaining wall obtained with and without the tunnels present. It was found that the presence of the tunnels obviously affected the wall displacement. This demonstrates the importance of modelling the complete construction history prior to excavations. The presence of adjacent properties such as buildings, tunnels, underground stations has modified the state of stress within the ground. In order to perform a more accurate FEM analysis, such effects should be taken into consideration. Therefore, the structure of the adjacent properties and their load condition should be obtained in the FEM models. Before performing the analysis of the excavation, the pre-construction activities should be completely modeled. Displacements of the

whole model caused by the pre-construction activities should be reset to zero before performing the excavation analysis as these displacements have already occurred before the excavation.

3.5 Other important aspects in the FEM analysis

Other important aspects in the FEM analysis include the modelling of the interaction between soil and structure, the size and boundary conditions of the models, and modelling the procedure of the excavation. Interface elements can be used to model the interaction between soil and structure. It is important to adopt interface element as it has significant effect on soil movement and subsequent movements in adjacent properties. The size of the models is determined by the soil condition, the excavation depth, the excavation width, presence of adjacent properties, and so on. Simple boundary conditions are usually used for plane strain FEM analysis. Horizontal fixity boundary condition can be applied to the side boundary the symmetric boundary. Both horizontal and vertical fixity boundary condition can be applied to the bottom side boundary. The excavation procedure can be rationally modeled by multi-stage finite element analysis. In each analysis stage, the geometry and load configuration can be changed by deactivating or reactivating relevant meshes and loads. Moreover, the properties of the soil can be changed from one step to the next to simulate the change in behavior that results from soil reinforcement. Practical construction methods such as bermed excavation or island excavation can also be modeled by stage analysis.

4 Cases study

4.1 Case of excavation adjacent to building with pile foundations

The Central Hotel Phase II project was located in the central urban area of Huangpu district in Shanghai. The area of the excavation was about 5000 m^2. The excavation depth was about 14.6 m. The size of the pit was 60 m $\times$ 81 m. Figure 3 presents the location of excavation and the surrounding environments.

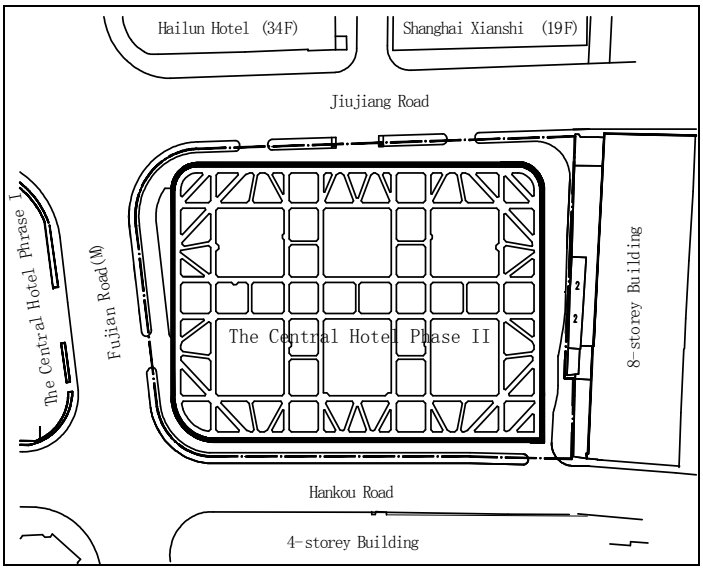

Figure 3: Location of the excavation and surrounding buildings

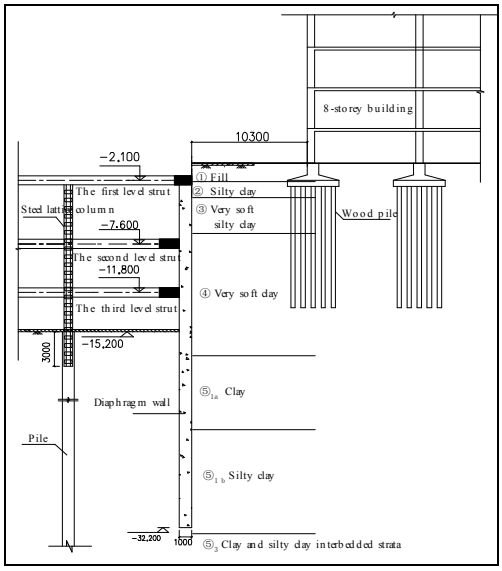

Figure 4: Sectional view of the excavation

Figure 3 shows that there were several buildings located around the excavation, such as Hailun Hotel with 34 stories, Shanghai Xianshi with 19 stories to the north, a building with 4 stories to the south et al. A 8-storey building was located bout 10.3 m east of the excavation. The building was built in the early 1920s. It is a reinforced concrete frame structure with strip foundations underpinned by wood piles. The diameter of the wood pile is 300 mm and the length of the piles is about 10 m. The pile spacing is about 1.0 m. The influence of the excavation on the adjacent 8-storey building was a significant design issue.

Diaphragm walls, which were 1.0 m thick and 30 m deep, were used both as the earth-retaining structure and the permanent wall of the basement. The walls were supported by three levels of temporary reinforced

concrete struts at the excavation stage. The bracing system plane is shown in the Fig.3. Figure 4 shows a sectional view of the excavation showing the soil profile and the supporting structure.

A two-dimension finite element model was set up using the Plaxis software to analyze the staged excavation. The clayey soils were modeled by the HS model. The initial soil parameters were obtained by experience and from geotechnical investigation report. The 8-storey building together with its foundation was also included in the model. The columns, slabs and piles of the building were simulated by beam elements. A uniform load of 15 kPa acting on each level slab was considered in the model. The BEF analysis was carried out to calculate the lateral displacement of the retaining wall. It was used to calibrate the finite element analysis. Table 1 depicts the modelling sequences conducted in the finite element analysis. Deformed mesh of the whole model at the final excavation stage is shown in Figure 4.

Table 1 Modelling sequence in the finite element analysis

Stages	Modeling construction sequences
1	Initial condition at the presence of adjacent 8-storey building(stress only)
2	Construction the diaphragm wall (stress only)
3	Excavated to the elevation of -2.4 m
4	Construction the first level strut and excavated to the elevation of -7.9 m
5	Construction the second level strut and excavated to the elevation of -12.1 m
6	Construction the third level strut and excavated to the bottom

Several settlement survey points were distributed around the building to record the displacement of the adjacent buildings. Lateral displacements of the diaphragm wall were monitored by inclinometers installed in the wall. Calculated results by finite element analysis and monitored data were compared in Figure 6. It can be seen that the predicted lateral displacement profile of the wall agreed quite well with the measured profile. The predicted maximum building settlement was 19.7 mm while the measured settlements were 15~19 mm. The predicted settlement of the building also agreed well with the monitored data.

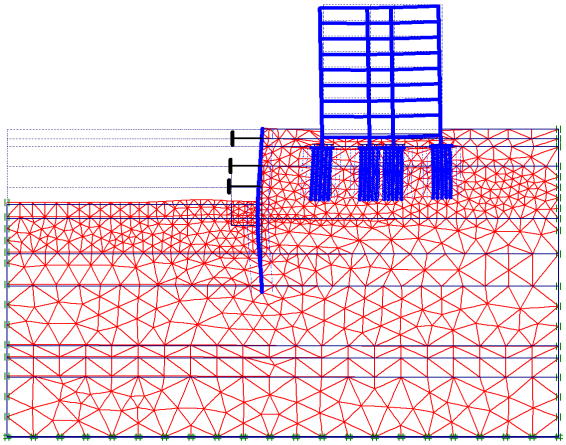

Fig.5 Deformed mesh of the whole model after the final excavation

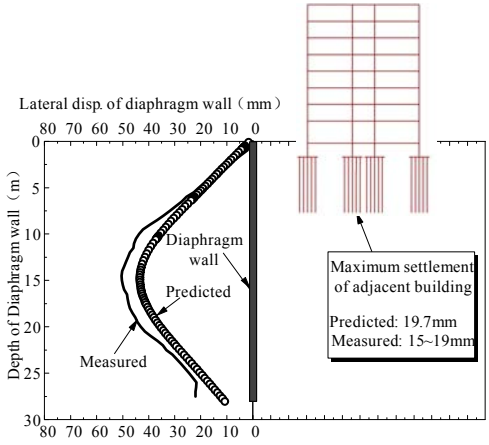

Fig.6 Comparison between calculated and measured displacement after the final excavation

4.2 Case of excavation adjacent to metro tunnel

The Daning Plaza project was located in the urban area of Zhabei district in Shanghai. The excavation area was about 44,000 m^2. The plan of the excavation was roughly square and the excavation depth was 6~8 m. The No.1 subway (in operation) was adjacent to the excavation. The minimum distance between the excavation and the metro tunnels was about 5.4 m. Figure 7 depicts a plane view of the excavation showing the location of the metro tunnels. The running subway has a strict protection standard. It was required that the additional deformation of the tunnels induced by the excavation should be less than 20 mm.

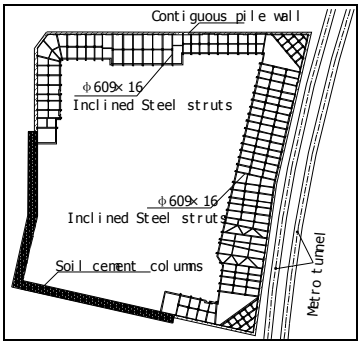

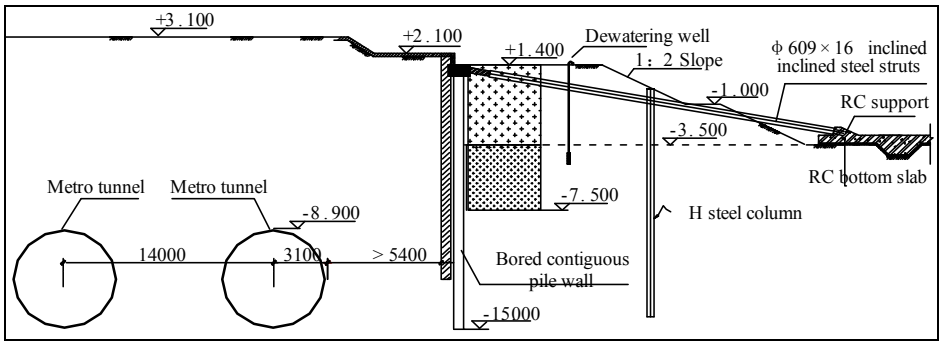

Figure 6: A plane view of excavation site

Figure 7: Sectional view of the excavation

A supporting system was used to protect the adjacent metro tunnel. The contiguous bored pile (with a diameter of 0.9 m and depth of 18 m) wall was used as retaining wall at the north side and east side. The retaining wall was supported by one level of temporary inclined steel tube strut at the excavation stage. Soil cement columns were used as retaining wall at the west and south side. Considering the large area of excavation, bermed excavation method was adopted.

The finite element method was used to predict the response of metro tunnel induced by the excavation. A two-dimension finite element model including the tunnel structures and soil mass was setup to simulate the excavation procedure. The adjacent tunnel linings were simulated by beam elements. The soil was modeled by the HS model. The influence of metro tunnel to the initial stress field was considered. The bermed excavation was also simulated in the analysis. Lateral displacement of the retaining wall obtained by the BEF analysis was also used to calibrate the finite element analysis. Figure 8 shows the deformed mesh of the whole model after the final excavation. At the final excavation stage, the calculated maximum horizontal an uplift of the tunnels are 5.15 mm and 7.62 mm, respectively.

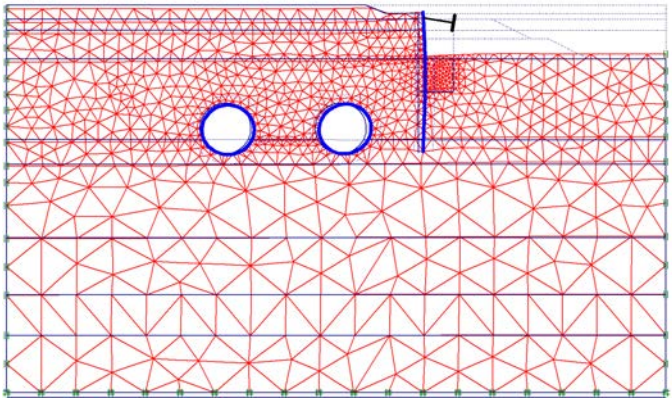

Figure 8: Deformed mesh of the whole model after final excavation

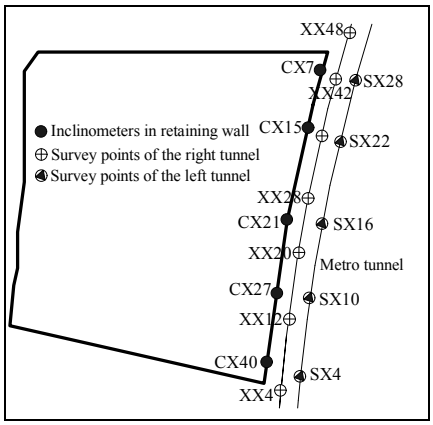

Figure 9: Locations of the monitored points

In order to monitor the performance of the excavation and it impact on the tunnels, inclinometers were installed in the contiguous bored pile wall and displacement survey points were set in the tunnels. Figure 9 shows the locations of the monitored points. Figure 10 shows the movement of the tunnel at survey points along the tunnel. The maximum observed horizontal displacement and uplift of the tunnels was 4 mm and 7 mm, respectively. The calculated displacements of the tunnels agreed quite well with the monitored data. Figure 11 shows the monitored lateral displacement of the retaining wall. Calculated lateral displacements of the retaining wall by the BEF method and finite element method are also shown in the figure. It can be seen that the calculated results also agreed well with the in-site monitored data.

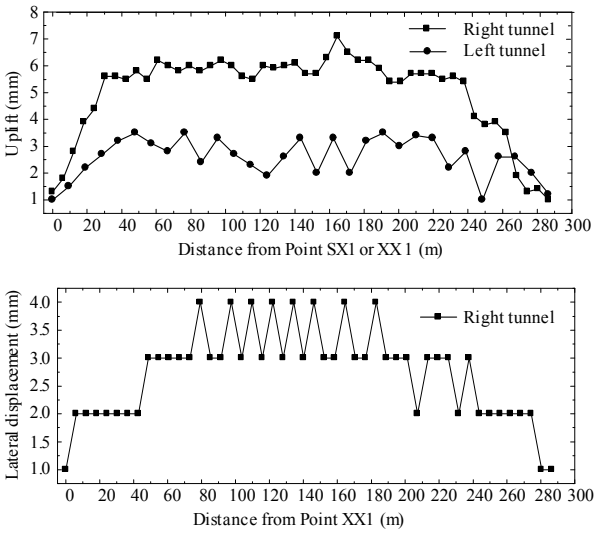

Figure 10: Monitored displacement of the tunnel

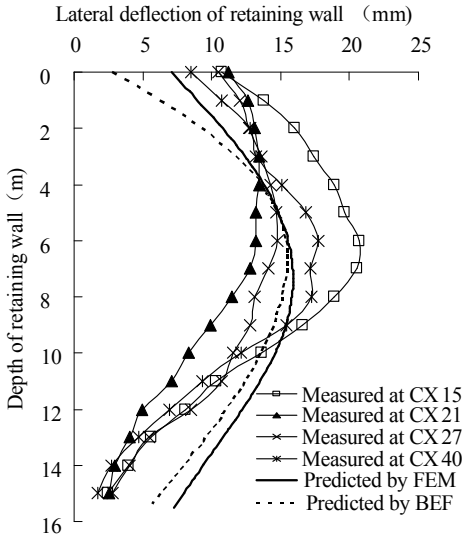

Figure 11: Predicted and monitored displacement of the wall

5 CONCLUSIONS

Prediction the displacement of the adjacent properties caused by deep excavation is a significant design issue for deep excavation adjacent to properties. Conventional methods including the semi-empirical method and the method based on beam on elastic foundation can only provide very crude estimation of the displacement of the adjacent properties. Finite element method is used to analyze the impact on adjacent properties. Many important aspects when using the finite element method was discussed. It was recommended to use the Plaxis Hardening Soil (HS) model to simulate the constitutive responses of soils in Shanghai when using the finite element method to model deep excavations. The appropriate calculation parameters of the HS models are obtained by using inverse analysis. Lateral displacement of the retaining wall calculated by the beam on elastic foundation method (BEF) is used to calibrate the inverse analysis. Appropriate modelling the initial condition, moodelling the interface between soil and structure, the size and boundary conditions of the model, and modelling the procedure of the excavation are also important aspects in the finite element analysis. Cases study shows that the calculated results using finite element method agreed well with the in-site monitored data in deep excavations adjacent to properties. This validated the capability and reliability of the method analyzing the impact of deep excavation on adjacent properties in soft soil district.

REFERENCES

Association of Civil Engineering Consultants in Shanghai (ACECS). (1997). Shanghai Standard Code for Design of Excavation Engineering-DBJ08-61-97, Shanghai. (in Chinese)

Brinkgreve R.B.J., Broere W., and Waterman D. (2006). PLAXIS version 8.2 Manual. A A Balkema, Rotterdam, the Netherlands

Borja R.I. (1990). Analysis of incremental excavation based on critical state theory. Journal of Geotechnical Engineering, ASCE, 116(6): 964-985

Calvello M. (2002). Inverse analysis of a supported excavation through chicago glacial clays. Ph.D thesis, Northwestern University, Evanston, Illinois

China Academy of Building Research (CABR). (1999). Technical Specification for Retaining and Protection of Building Foundation Excavations-JGJ-120-99, Beijing. (in Chinese)

Clough G.W., and Duncan J.M. (1971). Finite element analyses of retaining wall behavior, Journal of the Soil Mechanics and Foundations Division, ASCE, 97(12): 1657-1673

Clough G.W., and O'Rourke T.D. (1990). Construction induced movements of in situ walls. Proceedings, ASCE Conference on Design and Performance of Earth Retaining Structures, Geotechnical Special Publication No. 25, ASCE, New York, pp: 439–470

Finno R.J., Harahap I.S., and Sabatini P.J. (1991). Analysis of braced excavations with coupled finite element formulations. Computers and Geotechnics, 12(2): 91-114

Higgins K.G., Mair R.J., and Potts D. M. (1996). Numerical midelling of the influence of the Westminster Station excavation and tunneling on the Big Ben clock tower. Procedings of the International Symposium on Geotechnical Aspects of Underground Construction in Soft Ground. London, pp: 525-530

Hsieh P.G., Ou C.Y. (1998). Shape of ground surface settlement profiles caused by excavation. Canadian Geotechnical Journal, 35(6): 1004-1017

Mana A.I., and Clough G.W. (1981). Prediction of movements for braced cuts in clay. Journal of the Geotechnical Engineering Division, ASCE, 107(6): 759-777

Moormann C. (2004). Analysis of wall and ground movements due to deep excavations in soft soil based on a new worldwide database. Soils and Foundations, 44(1): 87-98

Ou C.Y., Hsieh P.G., and Chiou D.C. (1993). Characteristics of ground surface settlement during excavation. Canadian Geotechnical Journal, 30(5): 758–767

Ou C.Y., Chiou D.C., and Wu T.S. (1996). Three-dimensional finite element analysis of deep excavations. Journal of Geotechnical Engineering, ASCE, 122(5): 337-345

Peck R.B. (1969). Deep excavation and tunneling in soft ground. In Proceedings of the 7th International Conference on Soil Mechanics and Foundation Engineering, State-of-the-Art-Volume, Mexico City, pp: 225–290

Roboski J.F. (2004). Three-dimensional performance and analyses of deep excavations. PhD thesis, Northwestern University, Evanston, Illinois

Obstacles to Innovative Technologies in Geotechnical Works in Hong Kong

V. Li
Victor Li & Associates Ltd.
S.C. Lo
The University of New South Wales

ABSTRACT

This paper discusses obstacles to innovative technologies in geotechnical works in Hong Kong. It is believed that over-regulation of the approval process of geotechnical design, McDonaldization of university research and teaching, McDonaldization of consulting services, self-interest and human psychology all have a part to play in affecting the development of innovations in Hong Kong.

1 INTRODUCTION

Geotechnical works in Hong Kong can be considered very advanced in terms of construction equipments, but may be far from being so in terms of design practice. Examples of these are many, such as:

- powerful equipments are currently available in Hong Kong for constructing large diameter bored piles with pile shaft up to 3.3m and bellout exceeding 4.5m in diameter and to founding depths exceeding 100m. However, design of bored piles is still mainly based on end-bearing piles founding on strong rock and based on conservative presumed allowable bearing capacities.
- modern and efficient high capacity hydraulic hammers are used for pile driving, but final setting of piles is still often achieved using medieval drop hammers.

Geotechnical engineers tend to solve geotechnical problems by advanced and heavy construction equipments (i.e. money) and not technical innovation.

The theme of the 2008 HKIE Geotechnical Division Annual Seminar is on innovative technologies in geotechnical works in Hong Kong. In the authors' view, the promotion of innovative technologies in Hong Kong faces a number of severe challenges. The paper is written in a somewhat frank manner to arouse more debates on how one can achieve the honourable goal of being innovative in geotechnical work.

2 SOME ACHIEVEMENTS

There is no doubt that engineers in Hong Kong have contributed towards the development of innovative technologies in Hong Kong and overseas. In 2002, two pile jacking machines with perhaps the highest capacity in the world were procured by a Hong Kong foundation contractor. Pioneering research had subsequently been conducted by the first author and other researchers in developing practical techniques for installing high capacity jacked steel H-piles. This has put Hong Kong in the forefront of the research of jacked piling in the world map.

The Road and Traffic Authority, New South Wales, Australia, has "borrowed" the system from Hong Kong for assessing long-term strength of geosynethetics. This has set a level playing field for the development of a wide range of innovative soil reinforcement systems in Australia. The second author is closely involved in some of these innovative technologies.

The questions to be asked are: why jacked piles are still not accepted by most government authorities in Hong Kong; and why innovative applications of geosynethetics in soil reinforcement can blossom in Australia but not in Hong Kong. We hope to provide some answers to these questions in this paper.

3 FROM CONTROL TO OVER-CONTROL?

In his seminal paper presented in 1980, Professor Peter Lumb made the following remarks:

> "*At the present time, while still in the shadows cast by the Sau Mau Ping and Po Shan disasters, the controls imposed have become somewhat oppressive. The toehold established by soil engineering in the 1950s has become a strangle-hold, and many practitioners would say that soil mechanics has thrown civil engineering onto the mat and is breaking its arm. The engineering judgment, so characteristic of the better class projects described, appears to be discounted and an unhealthy trust in being placed on stress-accounting and immaculate bookkeeping, accepting the quaint views that structural engineers hold about soil behaviour"*. (Lumb, 1980).

The remarks made by Professor Lumb may even be truer at the present time of 2008. There is a proliferation of design guidelines, design codes, practice notes and technical documents for geotechnical and foundation design in Hong Kong published by various government authorities since the early 1980s. Design of geotechnical works in Hong Kong has become increasingly regulated by guidelines promulgated in these documents. It may be argued that the publication of guidance documents on geotechnical design can give geotechnical engineers clear and transparent guidelines on the minimum design standard required of geotechnical works in Hong Kong. Such good-to-follow guidelines, as predicted by Professor Lumb in the early 1980s in his conversations with the first author, will invariably become rigid ought-to-follow rules for geotechnical practitioners. This will no doubt suffocate the development of innovative technologies in Hong Kong.

As an example, the present design guidelines for soil nails are that the spacing, nail length and dip angle should preferably be limited to 2m, 20m and 20^{o} respectively. As a result, most soil nail designs in Hong Kong look strikingly similar and have been turned into a dull exercise to be left to junior engineers. Our points can be further illustrated by the following stories known to the authors.

In 2002, a design for upgrading a masonry wall prepared by a geotechnical engineer was submitted to relevant government authorities for approval. The masonry wall was very small in size and two soil nails of several metres in length were found to be sufficient to upgrade the wall to current design standard. The design was completed in the aftermath of a few events of suspected scandals of "short soil nails" which had surfaced a few months earlier. At that time, there was a known but unwritten government policy that non-destructive testing, such as time-domain reflectometer (TDR), should be used to verify the actual length of soil nails after installation. The engineer who designed the soil nails in this case wanted the condition of non-destructive testing to be waived. He proposed to personally measure the nail length on site and supervise the entire installation of the two soil nails full-time on site. The offer was rejected. One might have to sadly conclude that the credibility of an accurate measurement taken personally by a qualified geotechnical engineer who designed the soil nails was lower than the result obtained from an error-prone TDR test.

A similar event occurred in 1999 when the same geotechnical engineer had prepared the design for upgrading a loose fill slope. The fill slope was originally protected by stone pitching. The slope was in the shade of a building for most of the time and vegetation would not be expected to grow properly on the slope. The engineer and the residents who were responsible for maintaining the slope all considered that it would be best to retain the original stone-pitching surface cover for the slope after completion of upgrading works. At that time, the government policy was to encourage greening of slopes. Therefore, stone pitching was not considered to be acceptable. In the end, hydro-mulching was used for surface protection of the slope. As expected, the vegetation could not grow properly on the slope due to lack of sunshine and the slope was subjected to significant surface erosion. Worse still, the residents complained bitterly about the suffering of being constantly bit by mosquitoes that bred on the "greened" slope.

Careful considerations should be given in setting a right level of control of geotechnical works in Hong Kong. Clear and uniform design standard for geotechnical works are useful in giving practitioners an understanding of the minimum design requirements. But if such guidelines have been turned into rigid rules, geotechnical engineering will no longer be an attractive profession to newcomers.

4 McDONALDIZATION OF UNIVERSITY RESEARCH AND TEACHING

As discussed by Ritzer (2000), McDonaldization has become wide-spread in our modern society. Products, including university research outputs, are produced according to pre-set patterns, rules and formulas like making hamburgers.

Innovation in geotechnical works relies heavily on quality research in academia and good students who are inflicted by their teachers with a passion of wanting to become a geotechnical engineer. Unfortunately, the wave of McDonaldization has swept through the university sector.

For administrative convenience, university administrators develop rules for measuring the achievements of a university researcher and hence his/her promotion prospect by a process somewhat resembling a bean counting machine.

To meet the criteria for attaining research achievements, university researchers are often forced to focus on topics which can lead to more publications and not issues which have a higher practical significance when a research project is conceived. Being a good teacher has unfortunately become less important than being a prolific writer. Teaching staff are often recruited based on their latent ability in producing research publications for the university and not so much on their knowledge in professional engineering. Very often, the most "successful" researchers who can rise up rapidly to the echelon of professorship are those who succeed in expanding their publication list by publishing strikingly similar papers in different venues and using different languages, plagiarizing work of others at times and subletting the bulk of the work of publishing a book or paper to his/her students or other joint authors. The second author had witnessed a group discussion amongst university researchers on how one can recycle technical papers into more publications. Is it not true that only wastes are recycled?

University teaching has become increasingly business focused, with students now being treated as customers. University teachers have to be mindful of not making his/her lectures too difficult for students to avert receiving poor evaluation reports from students. Indeed, the passing rates of students have been used for some universities as one of the key performance indicators for evaluating the performance of a university faculty. The end result is that fewer and fewer fundament concepts of soil mechanics are taught in undergraduate and even postgraduate courses. The first author had once been told by his employee that all that he had been taught about slope stability analysis in the university was a brief introduction on how to use the program SLOPE/W.

If such are the qualities of graduates produced by universities at the present time, there remains a long way to go in trying to inject innovative technologies in the geotechnical profession in Hong Kong.

5 McDONALDIZATION OF CONSULTING SERVICES

While some geotechnical practitioners may have negative feelings about rigid design guidelines, the reality is that they are actually welcome by many entrepreneurial consultants. When rigid design guidelines are enforced, they can be more efficient in McDonaldizing their work process to gain maximum productivity and hence profit margin. Once the production process is McDonaldized, often with the help of tailor-made worksheets or commercial softwares, design work can be undertaken by technician grade staff without the need for the staff to fully understand the basic concepts behind the design process.

The principals of some consulting firms prefer geotechnical works to be highly regulated by government departments as this will help to reduce the professional liability of their firms. The first author have witnessed the principal of a consulting firm expressing his view openly that he relied on the government regulatory authorities to perform quality assurance of work produced by his firm.

Low-technology McDonaldizable consultancy work may actually be more profitable than innovative design work. Sometimes, consulting firms are themselves obstacles to innovative technologies in geotechnical works.

6 SELF-INTEREST

Innovative technologies may not always be welcome. As an example, many foundation engineers in Hong Kong, including the authors (Li et al, 2000), questioned the real benefit of providing a bellout in a bored pile. The first author also argued that the current practice of plate loading test should be changed to promote wider use of spread footing and raft footings founded on soils for supporting taller buildings (Li, 2007).

From discussions with major foundation contractors in Hong Kong, the authors have the impression that bellouts are actually welcome because continued use of bellouts can help maintain the competitive edge of large companies who can afford to purchase more expensive foundation equipments. Likewise, footings are not preferred by large foundation contractors for similar reasons. Of course, one may get an entirely different impression when talking to smaller contractors.

When promoting technical innovations, one must take account of the resistance from and balance the interests of various sectors of the construction industry.

7 HUMAN PSYCHOLOGY

Most people worry about changes. Government officials and engineers are often nervous about accepting a geotechnical design which has not or seldom been implemented in Hong Kong even if such a design methodology has been widely used outside Hong Kong.

The psychological barrier is not easy to overcome when one gets very little glory for approving an innovative design, but he has to get the cane for accepting a design which turns out to be a disaster later. There is no easy solution to this problem.

Anxiety arises from uncertainty. Many seemingly innovative technologies used in Hong Kong have in fact been used in other countries for many years and a wealth of experience may have already been available in the literature for a long time. Jacked piles are a good example. Although Hong Kong has jacking machines with perhaps the highest capacity in the world and that extensive experiences have been published in the literature for jacked piles in other countries for many decades, government authorities in Hong Kong are still lukewarm about this new foundation system because most engineers in Hong Kong are still not familiar with jacked piles.

Sometimes, engineers responsible for developing an innovative design are themselves to blame for failing to obtain approval for their design. They concentrate too much on the technical calculations, not realizing that the more important thing is to alleviate the checking engineer's anxieties about approving an innovative design. Civil engineering is an old profession. From the authors' experience, when sufficient historical information have been gathered for a particular innovative design, one will often find that the design is not as innovative as it may seem. The checking engineer will then be more at ease in approving a less conventional design rather than an innovative design.

8 WAY FORWARD

There is no easy formula for fostering an environment that is conductive to the development of innovative technologies in geotechnical works in Hong Kong. The following are some suggestions:

- University teaching should be back to basics and focus more on teaching of fundamental concepts. University must change it system to reward genuinely good teachers and researchers and not to allow the system to be abused by opportunists and professional writers. This sounds simple but is most difficult to implement. Ultimately, it is the society that will suffer.
- In Hong Kong, one has to accept the fact that the common people will expect the government to implement a system of geotechnical control to protect public safety. Many of the government publications on geotechnical practices are very useful technical references. However, the government should be mindful in preventing good-to-follow suggestions from turning into de-facto must-follow rules. The innovative applications of geosynthetics in soil reinforcement in Australia mentioned earlier are a good example. It is the engineering principles, not the rigid rules, developed in Hong Kong that have provided the basis for innovations in Australia. One must allow geotechnical engineers enough freedom to develop their own ideas of innovation. In return, a system should perhaps be put in place to discipline those engineers who abuse the freer system of geotechnical control.

- Professionalism is a long forgotten word in the consulting business. McDonaldization of consulting services will ultimately lead to dwindling respect from clients. If consultancy services are delivered in a factory-like manner, the client will only be willing to play the price of a hamburger for the services.
- Self-learning and continuing professional development are important in enhancing one's technical capabilities. If one is better informed about the latest technological development of geotechnical works in Hong Kong and overseas, it is more likely that he can develop his own innovative ideas by borrowing some ideas and proven techniques from others. More importantly, a better-informed design checker will be less nervous in accepting new ideas and approving innovative designs.

REFERENCES

Li, V. 2007. Use of plate load test for design of shallow foundations – a suggested alternative practice. *Bridging Research and Practice – the VLA Experience*, Centre for Research & Professional Development, 191-199.

Li, K.S., Lo, S-C.R. and Lam, J. 2000. Design of pile foundations in Hong Kong – time for change? *Proc. HKIE Geotechnical Division Annual Seminar – Foundations*, 119-126.

Lumb, P. (1980). Thirty years of soil engineering in Hong Kong, Rupert H Myers Lecture, Leura, Australia.

Ritzer, G. (2000). *The McDonaldization of Society*, Pine Forge Press.

Case Study on Slope Improvement Works to a Remote Hilly Terrain Site in Shenzhen PRC

J.Y.C. Lo & M.H.Y.Wong
Maunsell Geotechnical Services Limited
P.C.F.Chan & A.S.M.Chu
Engineering Projects Department, CLP Power Hong Kong Limited

ABSTRACT

This paper presents a case study on the slope improvement works conducted for a transmission pylon located in a remote terrain site in Shenzhen of PRC. The concerned slope was about 8m high with an average slope angle of 35º at an elevation above 240mPD. The closest access route was located at 1.5km away from the concerned site. In view of the physical site constraints, the improvement works design needed to account for constructability, materials logistic, duration of construction, environmental impact and economical factors etc. An improvement works design made use of the soil debris, a bare minimum number of soil nails, provision of surface drainages, construction of mass concrete toe wall so that the slope improvements works could end up blending very well with the natural environment effectively and efficiently. This paper will illustrate the difficulties encountered, the solutions adopted, and the experiences gained during the design and construction stage of the slope improvement works.

1 INTRODUCTION

In recent years, consultants and contractors in Hong Kong have had more opportunities than ever before to participate in the design and construction works of the slope improvement projects in Mainland China. However, it is understood that the slope work practices applied in Mainland China are different from in Hong Kong, such as the geological and working environments, labour and materials resources, skills and equipments. In order to account for the differences in work practices, a comprehensive design and implementation strategy, management and communication has to be planned ahead for a practical and smooth execution of slope improvement projects in Mainland China.

This case study explored a slope improvement project located at a remote hilly terrain in Shenzhen. During the design stage of the project, critical factors including submission procedures and requirements, site constraints, construction methods, upgrading schemes, duration of construction time, environmental impact and economical factor were considered. This project adopted an integrated design and construction strategy, direct adoption of the common slope improvement practices of Hong Kong might have become impractical given the site constraints and construction practice. This paper presents the physical site constraints, solutions and the lessons learnt during the design and construction stage of the slope improvement project in Shenzhen.

2 SITE DESCRIPTION

The project involved the slope upgrading work located at close proximity to an existing high voltage transmission pylon in Shenzhen. The objective of the project was to improve the stability of the slope area within the 60m x 60m area around the pylon to enhance the safety of the pylon against landslide.

In August 2005, a landslide was reported at the natural slope below the electricity transmission pylon at the northern ridge crest of a remote hilly terrain in Shenzhen (see Plates 1 & 2). The failure was probably attributed to the excessive infiltration of surface water resulting from a prolonged heavy rainfall. The failed slope was about 8m long and 15m wide, and the failure debris was about 120m^3 in volume. Fortunately, the existing transmission pylon was unaffected as the original foundation was seated deep on bed rock. In order to

protect the existing pylon from any further landslide, design and construction of the slope rectification works on the concerned slope were of paramount importance.

The concerned site was located within an overland at a remote hilly terrain at the level above 240mPD, surrounded by an orchard of lychee trees owned by local farmers. No direct vehicular access leading to the site was available. The closest vehicular access was about 1.5km away from the site.

Plate 1: General View of the Site

Plate 2: General View of the Landslide Extent

3 STATUTORY REQUIREMENTS IN MAINLAND CHINA

Government Submission

The design submission had to satisfy procedures and requirements set out in both the local and national standards as well as the code of practices in Shenzhen and Mainland China respectively. In general, design submissions including plans, reports and calculations, bills of quantities and method statements of the slope project were all required in processing of getting approval from local authorities, namely the town planning and land use authorities.

Unless licensed by the Chinese government, contractors from Hong Kong or overseas are not qualified to carry out design and works in China; they, if commissioned, have to form a joint venture with a local company for carrying out the construction work in Mainland China. For application of the construction consent in Mainland China, documents attached to the application include registered certificate for quality supervision, audit forms for site safety and certificate of the contractor qualification grade. In addition, the client (or developer) of the works need to hire a supervisory unit to undertake the site supervision work; the supervision unit must be a third party independent of the design institute and contractor.

Upon completion of the site works, as-built drawings and records have to be endorsed by the site supervisory engineer and submitted to the local government for record and filing all the material certificates and sample test results have to be submitted to the local quality control authority for checking.

For slope works relating to hazard mitigation or remediation of landslide hazards of failed natural terrain, the relevant national regulation in China require that the design of works of this shall be undertaken by qualified and licensed design institute; and the design approval procedure includes assessment of design by an expert panel formed agreed by the local construction authority.

Ground Investigation Works

Design and construction of the ground investigation works have to follow the code of practice and standards issued by the Ministry of Construction, People of Republic of China (MCPRC, 中华人民共和国国家标准):

- Code for Investigation of Geotechnical Engineering, GB50021-2001(岩土工程勘察规范)
- Standard for Engineering Classification of Rock Masses, GB50218-1994(工程岩体分级标准)
- Standard for Soil Classification, GBJ145-1990(土的分类标准)
- Standard for Soil Test Method, GB/T50123-1999(土工试验方法标准)
- Standard for Tests Method of Engineering Rock Masses, GB/T50266-1999(工程岩体试验方法标准)

Slope Improvement Work

Similar to the ground investigation works, design and construction of the slope improvement works have to follow the code of practice and standards issued by the Ministry of Construction, People of Republic of China (中华人民共和国国家标准):

- Technical Code for Building Slope Engineering, GB50330-2002(建筑边坡工程技术规范)
- Code for Design of Concrete Structures, GB50010-2002(混凝土结构设计规范)
- Code for Construction and Acceptance of Plant Engineering in City and Town, CJJ、J82-1999 (城市绿化工程施工及验收规范)
- Specifications for Bolt-shotcrete Support, GB50086-2001(锚杆喷射混凝土支护规范)
- Specification for Retaining and Protection in Building Excavation Engineering, DBJ/T15-20-1997 (广东省建筑基坑支护工程技术规程)
- Metallic Coatings-Hot Dip Galvanized Coatings on Fabricated Iron and Steel Articles-Specifications and Test Methods, GB/T13912-2002(金属覆盖层—钢铁制件热浸镀锌层—技术要求及试验方法)

4 SITE CONSTRAINTS AND DIFFICULTIES ENCOUNTERED

As the site was situated at a remote hilly terrain without direct vehicular and pedestrian access, the location of the site thus imposed inaccessibility to the works. During the design stage, accounts of difficulties and problems that the design had to be taken into included transportation of materials and equipments, restricted area that led to the fact that the use of conventional works equipment was almost impossible, there were also lack of works area for material and plant storage, accommodation and transportation arrangement of the workers. All these challenges had to be met within the predetermined construction schedule and budget.

Other encountered difficulties that were yet to be dealt with later on in the construction phase, and they imposed a great hindrance to the works, included complaints from farmers of the nearby orchard who planted a substantial amount of lychee trees encompassing the pylon and within the area of the failed slope, and efforts that needed to be paid in liaison with local villagers for providing an access route from the closest vehicular access to the site that seemed to be the only possible solution to resolve the problem of site accessibility; nevertheless, the access road to the site could only be a narrow and winding path zigzagging through between the lychee trees. Besides felling of trees, land issue for works area and site probably encroaching on private lands were yet to be dealt with.

5 PROPOSED SLOPE UPGRADING SCHEME

At the beginning of the design stage of the project and after the expert panel held in 2006, an option that a hand dug caisson wall to be founded on rock was considered, which was an acceptable to be the slope improvement scheme (see Figures 1 & 2). As a conventional and one of the most popular approaches, construction of hand dug caisson in Mainland China have the following advantages: comparatively short construction period-large manpower input with common skills and techniques are used; only limited working area is required and a low construction cost. However, this upgrading scheme, though technically accepted by and passed the expert panel, was not adopted eventually because of practicality problems aforementioned in preceding Section 4. The scheme that was eventually adopted was an integrated slope upgrading scheme.

In view of the site location constraints and other difficulties and concerns aforementioned in previous sections, the integrated upgrading works strategies (see Figures 3 & 4) included (1) installation of soil nails, (2) construction of mass concrete toe wall, (3) backfilling the slope by cement soil fill, (4) provision of surface drainage, and (5) hydroseeding surface. In terms of design consideration by using this method, the possibility of deep sited failure was taken care by installing soil nails, while the shallow failure and liquefaction was taken care by soil replacement using cement soil.

The compacted cement soil was to serve the purpose of avoiding water infiltration to the underlying soil stratum so as to minimize the risk slope detritions. Economically in comparison with the caisson wall scheme, there were a construction cost saving of about 30% and a supervision cost saving of having less safety supervisory staff about 30%. Transportation cost was also reduced by using the selected fill of soil debris as part of the source for the soil replacement material, hence less amount of unsuitable materials were carried off

site. Apart from the tangible benefits mentioned above there were intangible benefits. There were environmental benefits of reducing tree felling for temporary access road and reducing visual impact as no artificial structure would be left in as permanent work (in this case caisson wall); safety benefits of eliminating the relatively high risk construction activities in caisson wall construction and benefit of public relation by having a relatively simplier construction to minimize the disturbances to the nearby villagers. This upgrading scheme was also technically accepted and passed expert panel to replace the scheme of caisson wall.

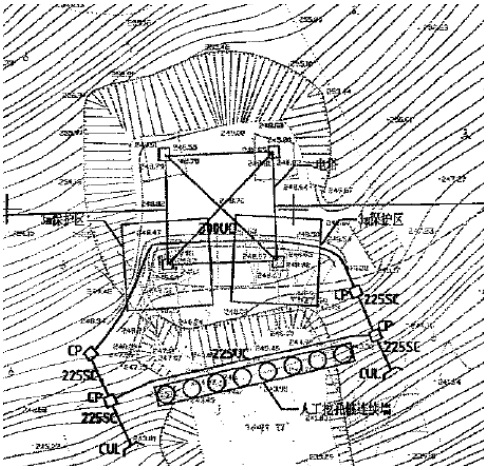

Figure 1: Proposed 1st Upgrading Scheme – Hang Dug Caisson Wall Layout Plan

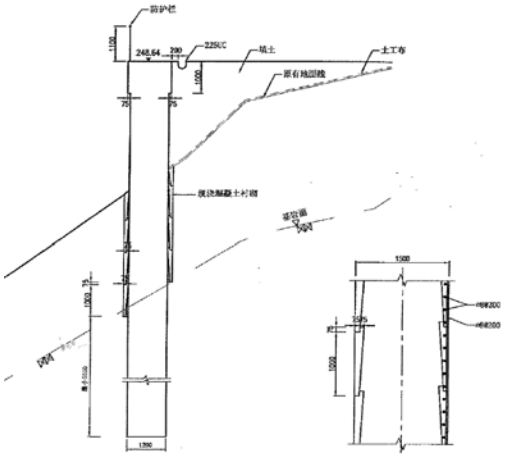

Figure 2: Proposed 1st Upgrading Scheme – Section and Detail of Proposed Hang Dug Caisson Wall

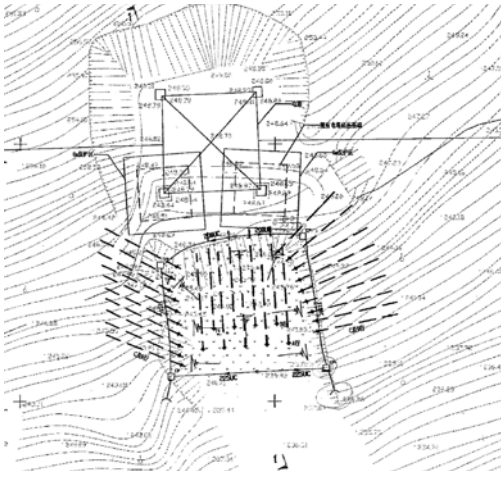

Figure 3: Proposed Alternative Upgrading Scheme - Integrated Slope Upgrading Work

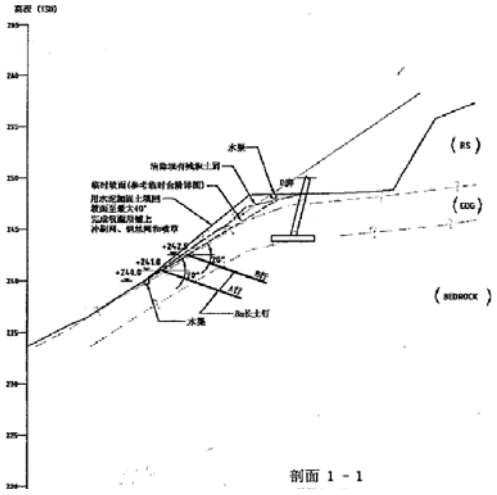

Figure 4: Proposed Alternative Upgrading Scheme – Section of the Integrated Slope Upgrading works

6 CONSTRUCTION WORKS ON SITE

The construction method and sequence of the slope improvement works were apparently different from that could be seen in general construction practice either in Hong Kong or even in Mainland China.

Before the commencement of the construction works, all the construction materials and equipments were well planned to transport to the designated storage area adjacent to the site. Mules were in use to resolve the transportation difficulties encountered in this project. They were mainly used to carry steel bars, bags of cement, components of the machineries and the working equipments from the closest vehicular access to the hilltop site (see Plate 3). Despite the long transportation time, it was the most practical way and the most effective method to transport the necessary construction materials and equipments on the bumpy roads of hilly terrain to the site. Finally, the logistic planning of materials transportation could effectively and efficiently be accomplished as scheduled and within the final construction budget.

Plate 3: Transportation Tool - Mules

Plate 4: Photo of Electric Mixer Used on Site

The machineries used in this project were obvious small scaled due to the site constraints. Small sized generators were widely used on remote sites to provide electric supply for the construction equipments. For examples, the electric mixer (see Plate 4), which was used to mix up the cement and the in-situ soil, which was selected from the soil debris, for the final backfilling works; the grouting and pumping machine, which was used to produce the cement grout and pumped to the soil nails.

When the construction materials and the machineries were ready, the slope upgrading construction works started immediately according to schedule. Since the site had experienced a landslide previously, the left on site soil debris and the loose soil on top of the slope had to be removed. After the removal of soil debris, benching were formed, soil nails were installed, a concrete wall was built at the toe of the slope and backfilling the slope to 35º maximum by cement soil were carried out to improve the overall slope stability. Site trials for cement soil re-compaction, in-situ density test for the compacted soil and the collection of samples for laboratory testing were all conducted on site easily as per the specifications. Finally, surface drainage system and hydroseeding were provided on finished slope surface to maintain the green appearance and provide a harmony environment (see Plate 5).

Plate 5: General View of Upgraded Slope

7 LESSONS LEARNT

Based on the experiences gained from this difficult slope improvement works, it was noted that a successful construction design management was the key to success. At the beginning of the project, the proposed construction of a haul road might have led to mass felling of the lychee trees and trespass through private lands from which strong complaints of the local farmers would have been unavoidable. No materials or workers would have been allowed to access the site via their lands. After several meetings and negotiations among the farmers, local contractors and relevant government departments, the disputes were finally settled with the proposal of an alternative design where no construction of haul (but a narrow winding access path)

road, no felling of trees were needed and works could be commenced as scheduled. This is a good example of good project management to show that communications and cooperative interaction among all stakeholders should come in play in the early stage of the project; thus many difficulties with works in such a remote area and with complicated land issues could be resolved in time. In addition, it set a good example of works for showing the importance of appreciation of site constraints for design of slope works in remote areas. The present case also demonstrated how to reuse the materials that should have been removed from site, in this case as valuable resources for soil replacement works- an added value to the environment and to cost effectiveness of the works.

8 CONCLUSION

The project was completed safely, on time and within budget. This paper has shared some experiences of good project management through a slope upgrading works project carried out in a remote hilly terrain in Shenzhen.

ACKNOWLEDGEMENT

The authors would like to express their gratitude to the CLP Power HK Ltd for their kind permission to publication of the project information mentioned in the present paper.

REFERENCES

GEO (1984). *Geotechnical Manual for Slopes*. Geotechnical Engineering Office, Hong Kong.
GEO (2005). *Good Practice in Design of Steel Soil Nails for Soil Cut Slopes. GEO Technical Guidance Notes No. 23 (TGN 23*). Geotechnical Engineering Office, Hong Kong.
中华人民共和国国家标准:岩土工程勘察规范(GB50021-2001)
中华人民共和国国家标准:工程岩体分级标准(GB50218-1994)
中华人民共和国国家标准:土的分类标准(GBJ145-1990)
中华人民共和国国家标准:土工试验方法标准(GB/T50123-1999)
中华人民共和国国家标准:工程岩体试验方法标准(GB/T50266-1999)
中华人民共和国国家标准:建筑边坡工程技术规范(GB50330-2002)
中华人民共和国国家标准:混凝土结构设计规范（GB50010-2002）
中华人民共和国国家标准:城市绿化工程施工及验收规范（CJJ、J82-1999）
中华人民共和国国家标准:锚杆喷射混凝土支护规范（GB50086-2001）
中华人民共和国国家标准:广东省建筑基坑支护工程技术规程（DBJ/T15-20-1997）
中华人民共和国国家标准:金属覆盖层——钢铁制件热浸镀锌层——技术要求及试 (GB/T13912-2002)
中华人民共和国国务院令(2003)，第394号，地质灾害防治条例，2003年11月19日

Innovations in the Temporary Support Design for Weak Zones encountered during the Salt-Water Reservoir Tunnel Excavation, Hong Kong University Centennial Campus

A. Mackay
Hyder Consulting Ltd.

D. Steele
Gammon Construction Ltd.

G. Toh
Lambeth Associates Ltd.

ABSTRACT

The existing leveled platform, located immediately west of the Hong Kong University, Pok Fu Lam, is presently being developed to allow extension of the Hong Kong University Centennial Campus. In order to utilize this area, the Reservoirs occupying the site belonging to the Water Supplies Department will be relocated to allow development to proceed. As part of this, the Salt Water Service Reservoirs will be incorporated within two tunnels located adjacent to steep man made cut slopes and beneath natural terrain flanking the platform to the south.

The Site Investigation within the tunnel footprint revealed the geology to be complex, comprising bedded and massive volcanics, metamorphosed ash tuff (Hornfels), eutaxites and meta-sandstone, of the Mount Davis Formation. As well as confirming the complex geology, the ground investigation also revealed that the rock head level was variable; with a reduction in rock head cover above the tunnel crown to less than half the tunnel span locally; and the geotechnical characteristics variable with notable changes in the discontinuity characteristics, groundwater information, weathering depth, soil and rock strength and the presence of localised "weak zones".

This paper discusses the use of rapid and innovative design techniques to analyze the tunnel stability across the localized "weak zones" as data becomes available in order to install suitable and cost effective temporary support solutions. The emphasis of the design is to implement rapid processing incorporating a range of data. Although the Q-System includes robust support solutions that can be assessed simply and rapidly, the support in weaker ground can be costly and time consuming and often may involve spanning weak zones that cut the tunnel obliquely. The analyses applying Løset's formula and PLAXIS modeling techniques are discussed. The paper also outlines the limitations of these design techniques and how all design techniques are dependent on the use of high quality data obtained by experienced practitioners if worthwhile solutions are to be obtained.

1 INTRODUCTION

Excavation of the two Salt Water Reservoirs (SWSRs) is currently being carried out as part of the design, reprovisioning of the Water Supplies Department (WSD) utilities and infrastructure works for the proposed Hong Kong University (HKU) Centennial Campus, due for completion September 2009 (HKIE, 2008). The tunneling works comprise a 7.2m internal diameter (ID) tunnel of approximately 53m length, connecting to two transition tunnels, increasing in ID from 7.2 to 15m over a 10m length. These transitions then connect to two 15m ID by 50m length tunnels (see Plate 1) accommodating the future SWSRs (see Figure 1). In order to ensure the effective implementation of the works a rigorous site investigation was carried out followed by detailed geological mapping and probing ahead of the excavation to verify the temporary support requirements as the excavation proceeds. Based on this data the temporary support requirements have been analyzed using a finite element analysis program (PLAXIS) and available empirical assessments, including the use of empirical formulae (Løset, 1990) to provide a rapid and effective stabilization assessment to supplement the findings of the Q system.

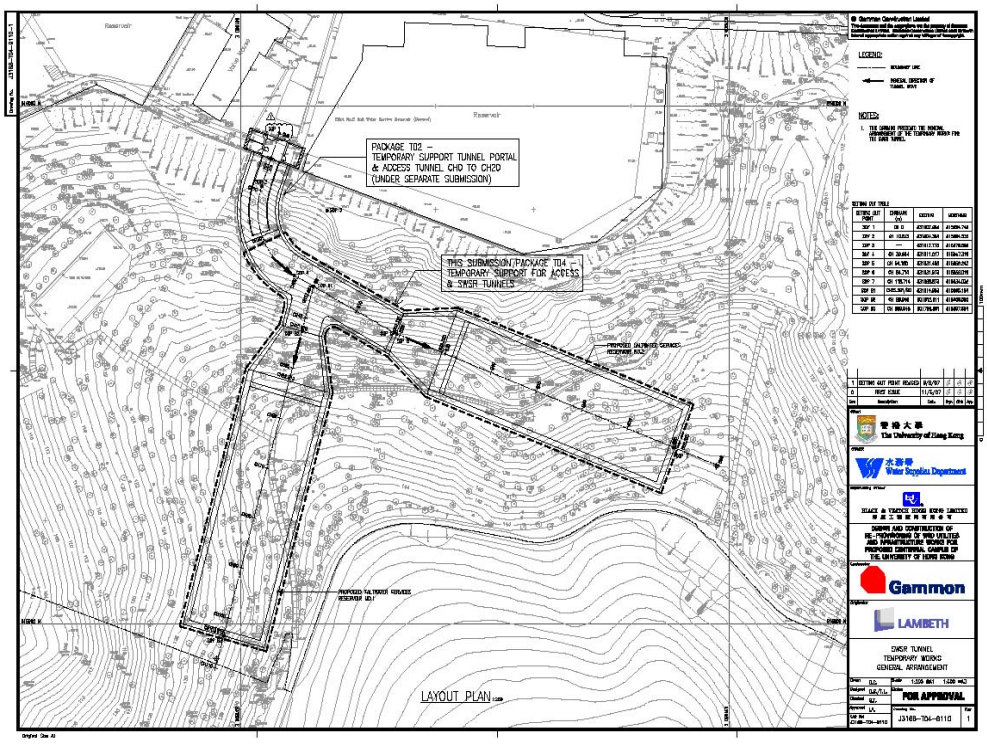

Figure 1: Salt water reservoir tunnel (SWSR) layout plan

Plate 1: SWSR tunnel No. 2 top heading excavation

2 THE WORKS

The SWSR tunnel portal is built into the existing cut slope, bounding the Centennial Campus platform to the south. Due to the potential slope instability above the tunnel footprint, excavation using blasting techniques was prohibited; mechanical excavation methods were therefore adopted. The temporary support has been assessed using the Norwegian Geotechnical Institution (NGI) "Q" system (Barton, 2002).

To date, the support installed within the portal zone comprises a roof canopy of 12m long, 114.3mm outside diameter (OD) steel pipes at 310mm c/c spacing. The pipes were perforated along their length to allow the injection of a 'grout canopy' to provide additional support for the excavation (John T et al, 2002). Within the canopy and spanning the excavation, 203mm by 203mm steel support frames have been installed at 1m c/c spacing, followed by application of a minimum 200mm thickness of steel fibre reinforced shotrete (see Plate

2). This support caters for the limited rock head profile (Geoguide 4), within the portal zone up to CH27 along the tunnel.

Plate 2 : Steel support frames and shotcrete lagging at portal access tunnel

The tunnel was excavated by backhoe mounted hydraulic point breakers with the addition of rock splitting methods adopted as the Unconfined Compressive Strength (UCS) increased above 200MPa. The sequence adopts a heading and bench method of excavation; a jumbo mounted hydraulic rock splitter was used in the relatively harder rock excavation. The excavation for the SWSR placement tunnels is presently on going.

3 GROUND CONDITIONS

The site is underlain by coarse ash tuff of the Mount Davis Formation. This has been metamorphosed and partly intruded by the adjacent Kowloon Granite Pluton, refer to the Geological Maps, Figure 2a and 2b, and by dolerite and rhyolite dykes and quartz veins. The Mount Davis Formation comprises fine ash tuff, eutaxites, banded tuffs deposited in a sedimentary environment, and locally intercalated, quartzitic sandstone. Towards the granite pluton, there are localized intrusions of fine-grained granite and localized contact metamorphism of the fine ash tuff to Hornfels, generally characterized by an increase in the UCS. The area is dominated by an ENE to WSW trending fault, referred to as the “Jordan Valley” fault, located immediately south of the site (refer to Figure 2a).

The ground investigation (GI) comprised more than 20 vertical, inclined and horizontal drillholes within the tunnel footprint area (refer to Figure 2b). Packer (lugeon) in-situ testing, acoustic televiewer down the hole surveys and UCS laboratory testing were used to assess the groundwater inflow, discontinuity regimes and rock strength respectively and the subsequent initial rock mass designation (Barton 2002). The rock head level assumed a Total Core Recovery of 85 % or better over any given 1.5m core length, which revealed the rock head level to vary between about 0 to 40m above the tunnel crown. Notwithstanding, due to the core loss (maximum 200mm thickness) below rock-head level, there remained concerns regarding the presence of weak zones.

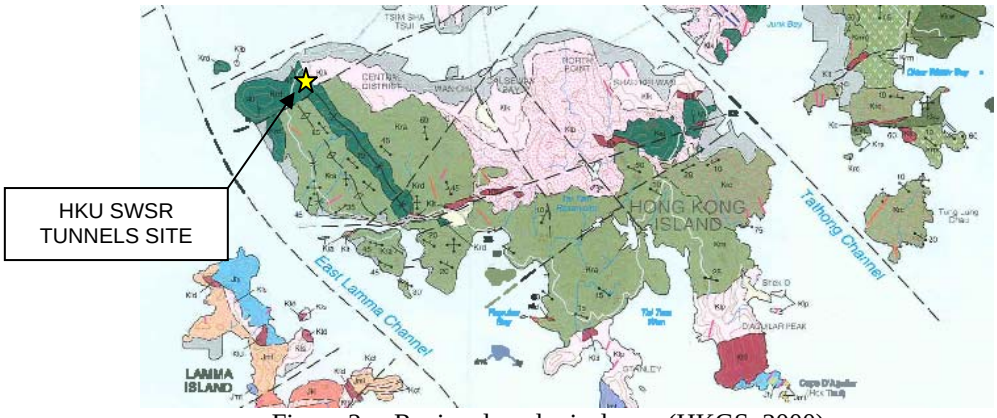

Figure 2a : Regional geological map (HKGS, 2000)

Based on the findings of the GI, the weak zones were assumed to have developed along faults and intrusions, possibly associated with the adjacent Jordan Valley Fault, This may have undergone weakening from the effects of weathering or other geological processes (GEO, 2007). In addition dyke intrusions were expected to trend sub-vertically in NW to SE and NNW to SSE directions. Both the faults and dykes were considered to have a major controlling influence on the discontinuity patterns.

Tunnel mapping data revealed the presence of 2 to 3 major joint sets, generally described as smooth to rough planar with minimal coating and infilling or signs of alteration or metamorphism, the available piezometric data revealed the groundwater level to be at or marginally below the tunnel crown and the packer (lugeon) tests that the bedrock had a low storativity with anomalously higher values potentially resulting from groundwater concentrations along or at fracture zones. The UCS values ranged from 6 to 240MPa, with the lower values considered to be influenced by micro defects. Based on previous hydro-fracture in-situ tests for stress ratios in the area (Free et al, 2000), the values were expected to range between 2 to 4 for the excavation and trend NW to SE; in a similar orientation to the dyke intrusions revealed on site. Notwithstanding, the Stress Reduction Factors (SRF) for the Q support system, were estimated to be 2.5 to 5, to ensure a degree of conservatism was incorporated into the assessment.

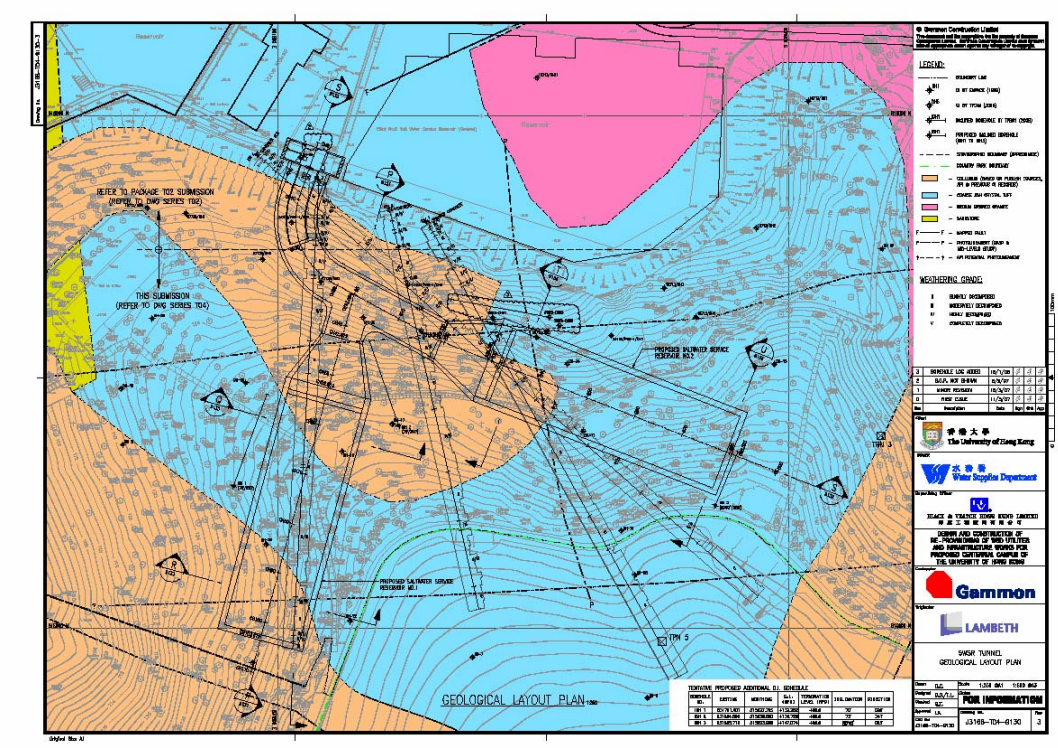

Figure 2b : Site geological map and GI layout plan (HKGS)

Probing ahead of the excavation face using a constant drill feed pressure was carried out to verify the geology and groundwater conditions. Based on the results, partial weathered zones were anticipated between CHB26 to CHB36 into the excavation. This was further verified by additional vertical and inclined drillholes, which ascertained the presence of partially weathered zones beneath rock-head level.

4 TEMPORARY SUPPORT DESIGN

The temporary design support follows the recommendations set out in the NGI Rock Mass Quality 'Q-system' (Barton et al, 1974; Grimstad and Barton, 1993, Barton 2002), which ranges from no support / spot bolting to pre-cast concrete arches. The system was further refined by adopting the excavation support ratio (ESR), ranging from 1.3 for the standard span and SWSR tunnels to 1.0 for the portal and tunnel intersection zone.

Although the Q system is an internationally adopted approach to tunnel support, it is well known that its determination is highly subjective and requires an experienced engineering geologist to effectively assess the

data. A good example of this is presented by Fookes, 1997, which presented the findings of two assessments prepared independently by experienced engineering geologists familiar with the rock mass systems. One assessment showed the required support to be 200mm of reinforced shotcrete, the other considered that the tunnel could remain unsupported for a month. The Q system is also considered to be highly dependent on the Rock Quality Designation (RQD), which has an arbitrary core recovery of 100mm length incorporated into the determination (IMS, 2000).

Due to the subjectivity of the Q system, it was decided to supplement the interpretation of the support requirements, especially where zones of weakness intersect the tunnel, by the Løset's formula. This was used to estimate the mean Q-value for support design (Løset, 1990), presented in Figure 3. This support assumes that the weak zone intersects the tunnel obliquely and that enhanced support spans across a weak zone of relatively limited thickness and was found to be particularly useful as the robust approach of installing steel ribs following the standard Q-System support is both costly and time consuming, especially as it is required over an extended tunnel length to support a weak zone of limited thickness.

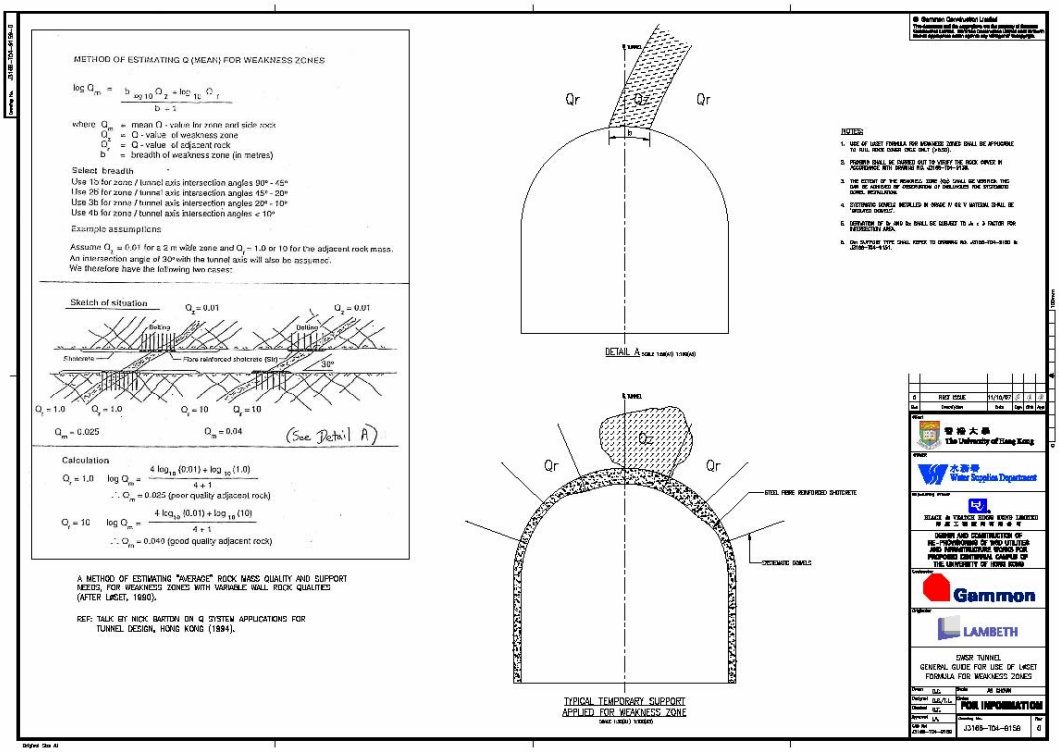

Figure 3 : Application of Løset's formula to weakness zones

In addition, to further verify the support requirements, the interaction between soil / rock and temporary support was analysed using the Finite Element computer-modelling programme, "PLAXIS". The rock head level and soil to rock boundary were modelled, see Figure 4, and soil overburden pressure assessed to verify if the support installation in accordance with the Q-System was adequate.

To incorporate a degree of conservatism within the analysis, the ground water level was taken to be 10m above the tunnel crown level, despite the monitoring data indicating the level to be considerably lower. To incorporate the potential presence of weak zones during the excavation, a grade IV/III weathered zone, partial weathered zone in accordance with Geoguide 3, was located immediately above the tunnel crown level. Further conservatism was incorporated into the geological model by assuming Grade III weathered rock to be present within the tunnel left shoulder, facing the tunnelling direction. The presence of the Grade IV/III layer was further verified by cross checking against the findings of the adjacent surface slope stripping. Grade III or better rock was also observed on the excavated faces during the tunnelling works at this section.

In the PLAXIS model, the overburden weathered rock layers were modelled using conservatively low parameters. For the Grade IV/III weathered material, the rock mass parameters were determined using the Geological Strength Index (GSI) method (Hoek and Brown, 1982). A linear elastic material was assumed for Grade III rock in the model. To ensure the stability of the PLAXIS analysis, the lateral resistance from the soil nails installed into the slope was considered in the model. Shotcrete of 150mm thickness, following the

support according from the Q-system, was also modelled. Additional support measures such as the pattern bolting were conservatively discounted in the PLAXIS model.

The results of the PLAXIS model are presented in Figure 4. The figure shows the deformation of the shotcrete lining with maximum deformation of about 7mm at the location of the deep weathering at the completion of the tunnel heading. Upon tunnel completion of the tunnel, a maximum deformation of 9mm is predicted. The axial loading and bending moment of the shotcrete lining was checked to be within the capacity of the shotcrete that is steel fibre reinforced. At the current tunnelling works, the tunnel heading was completed. The measured deformation from the convergence points is about 3mm, which is less than half of the predicted magnitude. The tunnel convergence arrays are typically installed at 10 to 15m spacing and monitored daily (Desaintpaul et al and Leung et al, 2006).

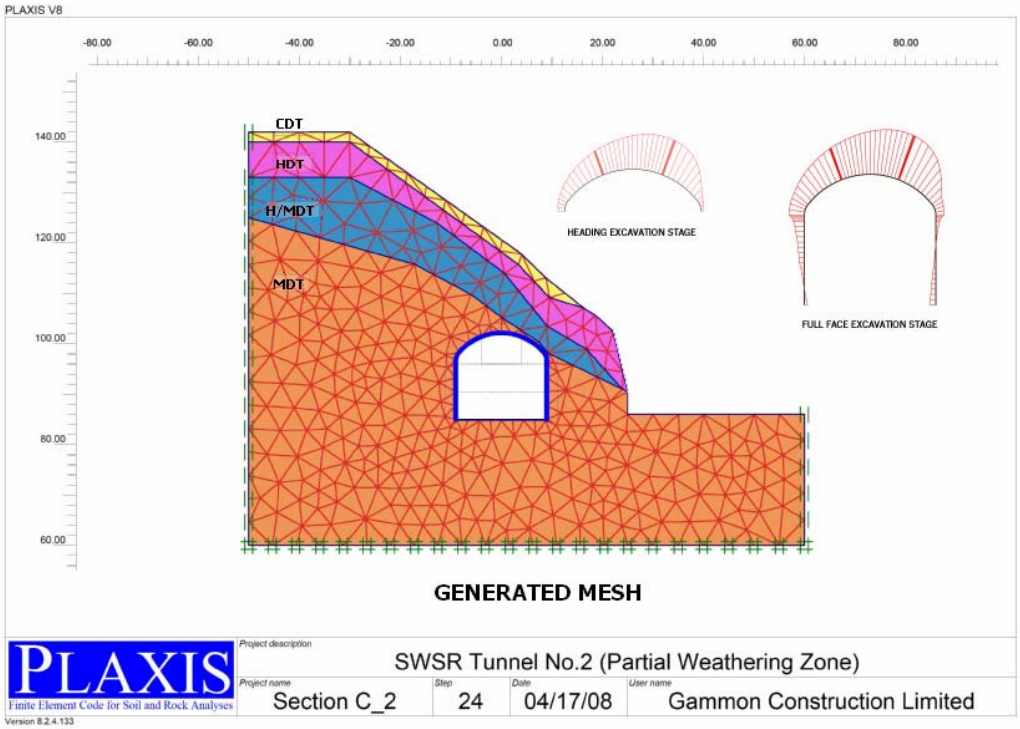

Figure 4 : Deformation of the tunnel lining

5 CONCLUSION

The paper outlines the need for a rigorous GI and ground verification as the tunnel excavation proceeds, together with close scrutiny of the findings to highlight potential instability. A range of techniques have been used to analyze the "weak zones" potentially impacting the tunnel stability and suitable cost effective temporary support solutions considered.

Although the Q-System includes robust support solutions that can be assessed simply and rapidly, the analyses, applying Løset's formula and PLAXIS modeling techniques used in combination with active tunnel convergence monitoring, suggest that decreased support could viably be adopted spanning across weak zones thereby reducing time and cost.

Although the analyses provide options for alternative support methods, more robust support techniques were considered to be more appropriate and therefore adopted. This is partly due to the degree of confidence with the input data and interpretation of the ground conditions between available boreholes.

The collection and use of high quality data obtained by experienced practitioners in the field is therefore imperative if worthwhile more cost effective solutions are to be obtained.

ACKNOWLEDGEMENTS

The authors would like to thank the University of Hong Kong and Water Supplies Department (Hong Kong Government) for their kind permission to publish this paper.

REFERENCES

Barton, N.R. & Grimstad, E. (1994). The Q system following 20 years of application in NMT support selection. Proceedings of the 43rd Geomechanics Colloquy, Salzburg.

Barton, N., Lien, I., and Lunde, J., (1974). Engineering Classification of Rock Masses for the Design of Tunnel Support, Rock Mechanics, Vol. 6, No. 4, pp. 186-236.

Barton, N., Lien, R. & Lunde, J. (1977). Estimation of support requirements for underground excavations, Proc. of 16th Symposium on Design Methods in Rock Mechanics, Minnesota, 1975. 163-177. ASCE, NY.

Barton N. (2002). Some New Q-Value Correlations to Assist in Site Characterisation and Tunnel Design. International Journal of Rock Mechanics & Mining Sciences 39 (2002) 185-216.Civil Engineering Department. (1992). General Specification for Civil Engineering Works, Volume 1,1992 Edition, Section 7 pp. 193-245.

Desaintpaul, F. & Askew, I (2006) Temporary Support Design for a Shallow Driven Tunnel on Hong Kong Island, The HKIE Geotechnical 26th Annual Seminar on Cavern and Tunnel Engineering

Fookes, P.G. (1997). Geology for Engineers. The Geological Model, prediction and performance (The 1st Glossop Lecture). Quarterly Journal of Engineering Geology. Vol. 30, No. 4, pp 293-424.

Free M. W, Haley, J, Klee, G. & Rummel. F (2000). Determination of in-situ stress in jointed rock in Hong Kong using Hydro fracture and Over Coring Methods. Proceeding of the Conference on Engineering Geology, Hong Kong 2000, Institution of Mining and Metallurgy, No. 2000.

Geotechnical Engineering Office (1998). Guide to Cavern Engineering (Geoguide 4), Geotechnical Engineering Office, Hong Kong.

Geotechnical Engineering Office (1996). Rock and Soil Logging (Geoguide 3), Geotechnical Engineering Office, Hong Kong.

Geotechnical Engineering Office (2007). GEO Publication 1/2007, Engineering Geological Practice in Hong Kong.

Geotechnical Engineering Office (2000). The Pre-Quaternary Geology of Hong Kong. The Hong Kong Geological Survey, Department of the HK SAR, Sewell, R. J., Campbell S. D. G., Fletcher C. J. N, Lai, K. W. & Kirk P. A.

Geotechnical Engineering Office. Hong Kong Geological Survey. - Memoir No. 2, Geology of Hong Kong Island and Kowloon, (GCO. 1986).

Geotechnical Engineering Office. Geoguide 1 - Guide to Retaining Wall Design, (GCO. 2000)

Grimstad, E and Barton, N. (1993). Updating of the Q-system for NMT. Proceedings of the International Symposium on Sprayed Concrete – Modern Use of Wet Mix Sprayed Concrete for Underground Support, Fagernes, 1993 (Eds. Kompen, Opsahl and Berg). Norwegian Concrete Association, Oslo Norway, 1-21 October 1996.

Grimstad E & Barton N (1993). Updating the Q system for NMT. Proceedings of the International Symposium on Sprayed Concrete. Modern Use of Wet Mix Sprayed Concrete for Underground Support, Fegemes, Norway.

Hoek E & D. Brown D. (1982). Underground Excavation, the Institution of Mining and Metallurgy.

John T. & Mattle B. (2002). Design of tube umbrellas.

Leung, T; Poon P; Cunningham B. and Lo J. Monitoring during excavation of Route 8 Eagle's Nest Tunnel, HKIE Geotechnical Division 26th Annual Seminar, 2006.

Løset, F. (1990). Use of the Q-method for securing small weakness zones and temporary support (in Norwegian), NGI internal report No. 548140-1.

McFeat Smith, I (2000). Mechanized Tunneling for Asia, IMS Consultancy.

Application of Persistent Scatter Interferometry to Monitor Tunnelling Induced Settlements in Urban Areas of Hong Kong

S.W. Millis & D. Salisbury
Ove Arup & Partners Hong Kong Limited, Hong Kong
R. Burren & A. Thomas
Fugro-NPA Satellite Mapping, UK

ABSTRACT

Tunnelling related ground movements comprise one of the largest risks to any underground construction project in an urban area. Whilst these can largely be mitigated against by competent design and careful construction, the inability to accurately predict all adverse sub-surface features means that a risk of adverse ground movement always remains. As such, an integral part of any tunnelling project comprises the monitoring of ground and structure movements in the vicinity of the excavation. Whilst this has traditionally been carried out at a local scale through the establishment of a number of surface monitoring points along the tunnel alignment, recent technological advances mean that remote sensing methods can also be undertaken to compliment the local monitoring a provide a much wider area of cover. One of the most promising remote sensing techniques for such purposes is Persistent Scatter Interferometry (PSI). This technique involves advanced interferometric processing of a collection of satellite images to identify dense networks of persistently reflecting features, such as building corners, against which precise measurements of movement can be made. PSI can map extremely wide areas (100's km^2) and when applied to urban settings will typically yield 100's of Persistent Scatter (PS) points per km^2. Such dense networks of monitoring points, coupled with regular acquisition of new satellite images, allows for the detection of on-going ground movements. Additionally, the back catalogue of existing satellite images provides a unique capability to map historical movement trends within a study area

1 INTRODUCTION

Building damage resulting from tunnelling induced ground movements comprises one of the largest risks to an underground engineering project in an urban area and it is widely recognised that notable ground movements can occur as a result of either poorly designed / managed tunnelling works or the presence of unforeseen and adverse ground conditions. Traditionally, monitoring of tunnelling induced ground movements is undertaken through the establishment of a number of surface monitoring points along the alignment, such as survey markers and building tilt meters. These stations can either be surveyed manually or monitored automatically using devices such as Robotic Total Stations. However, the development and operation of such systems within a densely populated urban area is both time consuming and often difficult to undertake. Under such conditions, the use of accurate and reliable remote sensing technologies becomes highly beneficial as a means of both complimenting the traditional monitoring techniques and providing a wider area of coverage for the monitoring.

This paper reviews the application of Persistent Scatter Interferometry (PSI) as a means of monitoring ground movements associated with tunnelling works and discusses the reasons for the adoption of the technique on the forthcoming construction of the Drainage Services Department (DSD) Hong Kong West Drainage Tunnel. The paper reviews the past and current application of the PSI technique for monitoring tunnelling induced ground movements and discusses the potential benefits for Clients, Consultants and Contractors resulting from the ability to determine long-term ground settlement trends.

2 SATELLITE INTERFEROMETRY (InSAR)

2.1 Introduction to InSAR

The ability to remotely capture and record information relating to the stability and movement of the ground surface, or that of any structures placed upon it, is of huge benefit to the planning and construction of an engineering project and can greatly enhance data obtained from more conventional surveying and monitoring methods. Whilst this can be achieved by a variety of techniques, potentially the most promising for application within an urban environment is the use of Interferometric Synthetic Aperture Radar (InSAR).

Synthetic Aperture Radar (SAR) images are obtained from satellites that transmit electromagnetic radiation signals (at microwave and radio frequency) and measures the intensity of backscatter and the time delay (phase) of the reflected signal. The advantage of radar over other remote sensing techniques is that it is generally unaffected by atmospheric conditions, such as rain, dust and cloud cover, and can be used day or night.

The brightness or intensity of the returned signal is a function of the surface roughness, dielectric constant, moisture content and the slope of the ground or structure upon which the signal is reflected (Figure 1). Any areas within an SAR image of high reflectivity (dominant scatterers) appear as bright regions within the image and these points often correspond to the location of structures and rocky outcrops. In contrast, any areas of low reflectivity, such as vegetation and water, will appear as dark regions within the image.

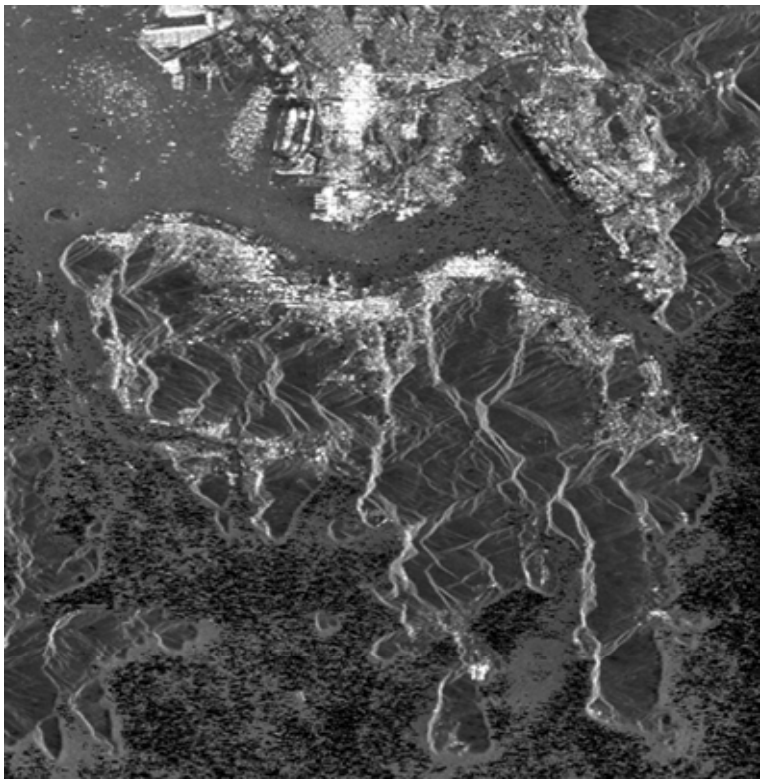

Figure 1: Envisat SAR intensity image of Hong Kong Island and the Kowloon Peninsula. Data copyright ESA 2003 – 2007. Image copyright NPA 2007.

The phase contains information about the position of the ground at the time when the image was acquired and forms the basis of InSAR. As subsequent satellite images are acquired over time it is possible, through complex processing of the phase information, to assess changes in topography i.e. surface displacements.

This complex processing, known as InSAR, is based upon comparison of the phase information contained within multiple SAR images of a study area that have been obtained at different times (Figure 2), typically between 24-35 days apart depending on the satellites orbit time (Table 1). The resulting differential signal/interference between the images, termed the differential interferogram, is a representation of the

topographic change in location of the dominant scatterer during the time period under assessment. Due to the scale at which satellite images are acquired, InSAR is capable of mapping motion phenomena for extremely large areas (up to 100km x 100km), with up to millimetric precision, and at a fraction of the cost of comparable land-based methods.

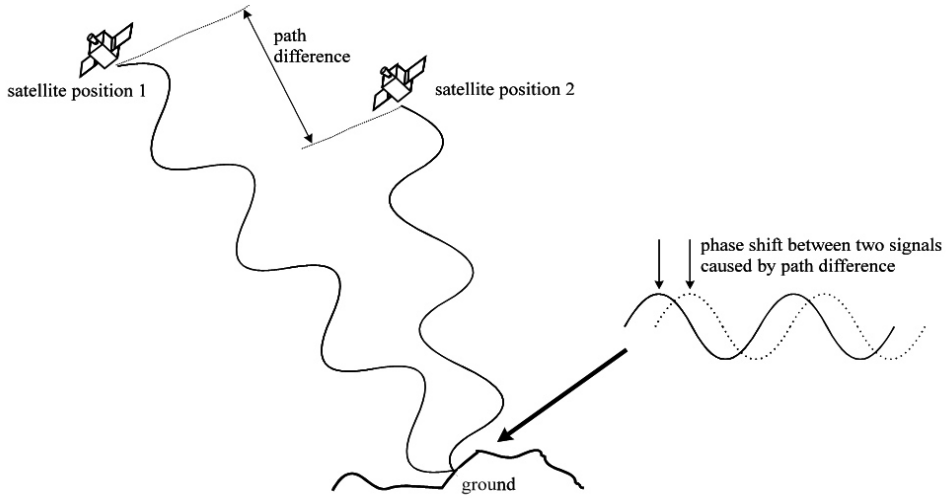

Figure 2: SAR satellite imaging geometry and configuration during successive orbit cycles. Image copyright NPA 2007.

Platform	Country	Launch	Repeat pass	Sensor incidence angle	Resolution
ERS-1	Europe	1991	35 days	23º	20m
ERS-2	Europe	1995	35 days	23º	20m
Radarsat-1	Canada	1995	24 days	20-50º	Up to 8m
Envisat	Europe	2002	35 days	15-45º	20m
ALOS	Japan	2006	46 days	10-51º	Up to 10m
TerraSar-X	Europe	2007	11 days	20-55º	Up to 1m
Radarsat-2	Canada	2007	24 days	20-50º	3 - 100m

Table 1: Current and planned SAR imaging satellites.

Since 1991 European Space Agency (ESA) SAR satellites (ERS 1 & 2 and Envisat) have been acquiring SAR imagery across the world and currently have an archive of over 1.5 million images. Through use of this archive of SAR images it is possible to measure ground motions retrospectively, which is a capability unique to InSAR. By programming new acquisitions of satellite radar images, InSAR can also be used to monitor ground movements throughout the course of a construction project.

The resolution and accuracy of InSAR measurements are generally limited by the satellite characteristics listed in Table 1, for example measurements are only possible in the line-of-sight (i.e. viewing direction) of the sensor[1] and temporal sampling depends on the orbit frequency of the satellite. For the measurement of long-term historical measurements over a given area, the data archive needs to be checked to determine the back catalogue availability of sufficient and appropriate SAR images. Modern satellites, such as TerraSAR-X (launched in June 2007) and Radarsat-2 (launched in December 2007), have high spatial resolution capabilities which will improve object detection and recognition. This will be particularly useful when discriminating between ground features and will also increase the density of identifiable dominant scatter points within an image.

[1] SAR sensors transmit and receive near-vertical 'line of sight' signals at an angle typically between 20 and 40 degrees from nadir. Any motion detected could therefore comprise an element of both vertical and horizontal motion.

2.2 Persistent Scatter Interferometry (PSI or PSInSAR)

A state-of-the-art InSAR technology is Persistent Scatter Interferometry (PSI). PSI exploits the SAR data archive, using a minimum of 15 co-registered images of the same location, to identify time persistent radar scatter (PS) points. Each scatterer corresponds to a particular feature on the ground that can be monitored (bright reflectors in Figure 1) and it is not uncommon for between 400-500 scatterers to be present within every km^2 across a dense urban environment.

Using the principles of InSAR detailed in Section 2.1 it is possible to assess the height change of individual PS points over time. Each image is assessed for PS and, provided that they are present in each image, the PS point will be retained and its changing height over time derived. The magnitude of the calculated height change is relative to an assumed stable reference point located within the study area. It should be noted that it is the motion (height change) of a persistent scatterer that is measured and not that of the ground (although in some cases there might be a component of one or the other, or both). The output of PSI processing is a GIS compatible database of 10's or even 100's of thousands of points, each with its own motion history for the time period assessed. In some cases this can stretch as far back as 1992.

Under the right conditions, PSI can provide monitoring at millimetric motion precision; The large number of SAR images allows one to screen and filter out (both temporally and spatially) atmospheric contributions to phase, reducing error budgets and ultimately providing more precise information than conventional InSAR.

PSI's ability to map wide-area relative ground motion with millimetric precision makes it more precise than most GPS in the vertical domain. The absolute spatial accuracy of SAR is typically 15m (sensor dependent), so by combing the superior spatial accuracy of GPS with PSI allows for accurate geo-locating of Persistent Scatterers (PS), whilst increasing the vertical precision of GPS.

The capabilities of PSI allows the technology to be employed in a diverse range of engineering, environmental and geohazard applications, ranging from the detection of tunnel induced settlement, flood risk assessment and even slope instability. However, given that the technique is best suited to the measurement of vertical displacement and is reliant on the presence of a high number of scatter surfaces in order to ensure meaningful interpretation, the monitoring of settlement / heave within a densely developed urban environment offers potentially its best application.

3 APPLICATION OF PSI FOR TUNNELLING WORK

3.1 Potential for Application on Tunnelling Projects

Ground movements along the alignment of a tunnel typically occur as a result of either face loss induced by the construction method or due to soil consolidation induced by construction related groundwater drawdown. Traditionally, monitoring of ground movements along the alignment of a tunnel are carried out by means of manual surveying (occasionally automated) of survey markers. This is often complimented by a variety of instruments installed on critical structures or around critical works activities such as shaft excavation. The necessity to carry out extensive installation of survey markers / instruments means that monitoring is typically only carried out for a narrow corridor situated along the tunnel alignment.

Whilst the extent of ground settlement due to face loss is typically confined to the area directly above the tunnel, with settlement occurring on a Gaussian curve profile above the tunnel crown (Peck, 1969), those resulting from groundwater drawdown can be far wider reaching, particularly in areas where linear transmissive features such as faults are encountered. The far reaching effects of uncontrolled groundwater inflows along such features were clearly demonstrated during construction of Tunnel C of the Hong Kong Strategic Sewerage Disposal Scheme, where adverse ground movements associated with the works were recorded in reclaimed land up to 2 km away (GEO, 2007). As such, the extent of conventional monitoring typically carried out may be insufficient to capture the full impact of tunnel construction. Under such circumstances, the ability to undertake wider scale regional monitoring without the need for excessive installation of additional monitoring points is highly beneficial. Given the ready availability of potential monitoring points within an urban area, the application of PSI for such purposes is considered well suited.

PSI data can be assessed in conjunction with conventionally surveyed measurements to help densify the measurement network, allow for the assessment of tunnel related settlement outside of the tunnel buffer, and reduce long term project costs. Such information may also prove extremely useful in assessing post-construction insurance claims.

3.2 Examples of Previous Overseas Application

PSI has been used to monitor tunnelling induced ground movements on a variety of European tunnelling projects, including major construction projects in London, Barcelona, Toulouse as well as many other densely populated cities. The power of PSI to detect tunnel related settlement was first demonstrated by NPA in 2002 when PSI processing was carried out for London using an archive of ERS-1 and ERS-2 SAR images acquired between 1992 and 2000. The result identified a number of linear subsidence features across central London. One such linear feature correlated to the route of the London Underground Jubilee Line Extension (JLE) project (Figures 3) and detailed interrogation of movement data from PS points revealed the magnitude to which tunnel construction had affected certain structures (Figure 4).

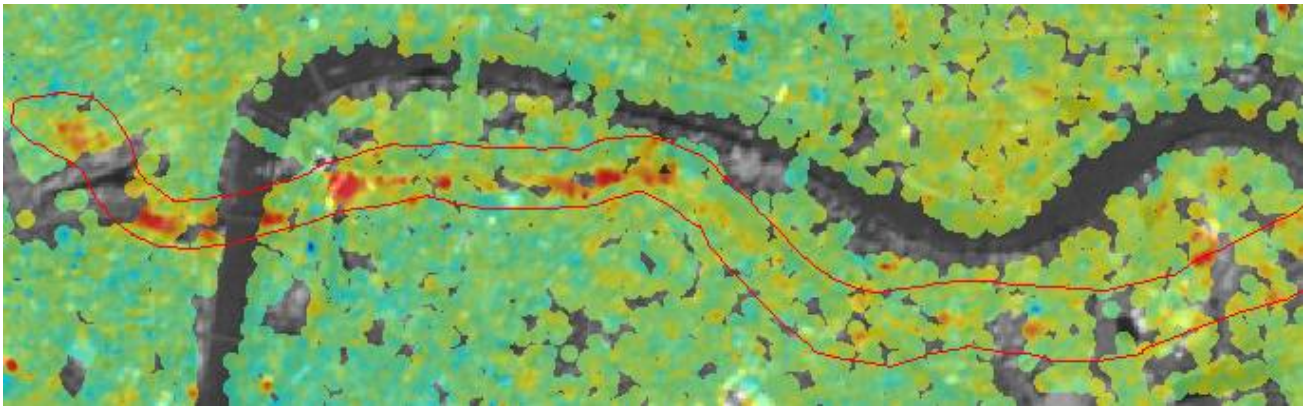

Figure 3: Spatially interpolated PSI result of London, with a clear area of settlement apparent along the alignment of the Jubilee Line Extension. Tunnel buffer superimposed. Image copyright NPA 2002.

PSI has detected similar features across other sites including St Petersburg, Russia where settlement associated with the construction of Line 4 of the Metro system was successfully detected. PSI revealed an average ground settlement of ~5mm each year between 1992 and 2004.

To take advantage of PSI's capability of long term monitoring of prime fixed assets and historical structures, the technique has been adopted to assist in mapping baseline ground and structure stability prior to the constriction of the North-South metro in Amsterdam, Netherlands. The activity has been performed as part of a large PSI validation activity funded by the European Space Agency.

3.3 Considerations and limitations

The orientation of scatterers with respect to the geometry of the SAR signal can result in a loss of persistent scatterer coverage, and some areas (e.g. rural) naturally exhibit extremely low densities of persistent scatterers. In areas where measurements are critical this can be a significant limitation. To overcome this issue NPA have developed artificial radar scatterers. Corner Reflectors (CRs) and Compact Active Transponders (CATs) can be deployed in areas yielding low scatterer densities. Once installed on the ground and/or structures of interest, SAR imagery is acquired and CR and/or CAT responses are analysed over time to map any movement that might have occurred. If used over a long period of time the artificial scatterers may end up being isolated as persistent scatterers during PSI processing, thus contributing to any long-term monitoring campaign.

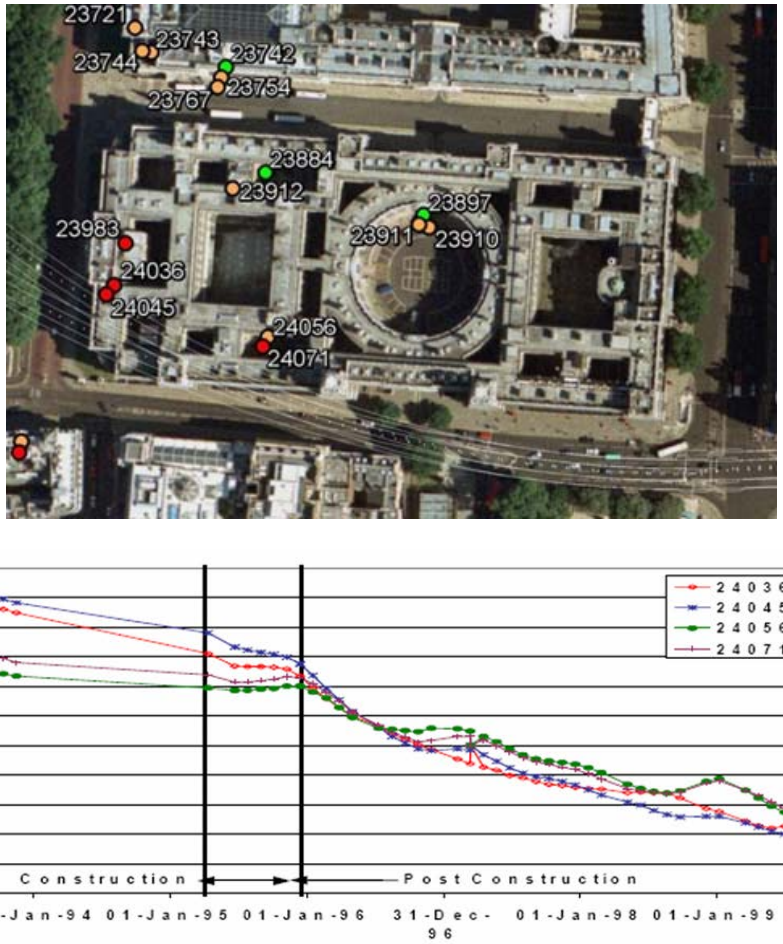

Figure 4: Time series plot of PSI monitoring data for PS points on the Treasury Building, London, which is located along the alignment of the Jubilee Line Extension. Copyright NPA 2002.

3.4 Proposed / Potential Application on Tunnelling Projects in Hong Kong

The limited available land space in Hong Kong means that future developments must either reclaim land, encroach into steep hillside areas or be formed underground. The environmentally sensitive nature of the first two options, which often result in substantial disturbance of natural landforms and habitats, means that provision of facilities below ground is often desirable. In view of the high number of proposed infrastructure projects within the territory, as outlined within the Chief Executives 2007 Policy Address (Hong Kong Government, 2007), a continuing growth in the number of underground excavation projects is anticipated within the coming decade.

Among the various projects currently planned within the territory are a number of tunnels passing through or in close proximity to densely developed areas, such as the DSD Hong Kong West Drainage Tunnel (HKWDT), HATS Stage 2 Tunnels, and various planned MTR Lines etc. The density of sensitive receivers in close proximity to the alignments of these planned tunnels means that there is a high risk of claims for damages against Clients, Consultants and Contractors in the event that ground movements or building damage occur. Whilst many of these claims may be legitimate and could be specifically correlated to one or other of the construction works, particularly for those located within the corridor subjected to detailed physical monitoring of any one project, there is always a risk of claims being filed which are less straightforward. It often becomes a subject of dispute when attempting to determine to what extent, if any, and against whom, any liability rests. This will be particularly difficult within areas beyond the scope of the physical monitoring. The ability to check ground movements outside the physical monitoring zone, and to historically investigate them, is of significant benefit in determining the outcome of ground movement related claims.

Initial works carried out for the HKWDT project, which includes requirements for preconstruction assessments of PS locations as well as bi-annual PSI interpretation reports throughout its 4-year construction

period, have identified an SAR back catalogue for Hong Kong that extends back to 2003 and includes 32 archive images taken between 2003 to 2007 (Figure 5).

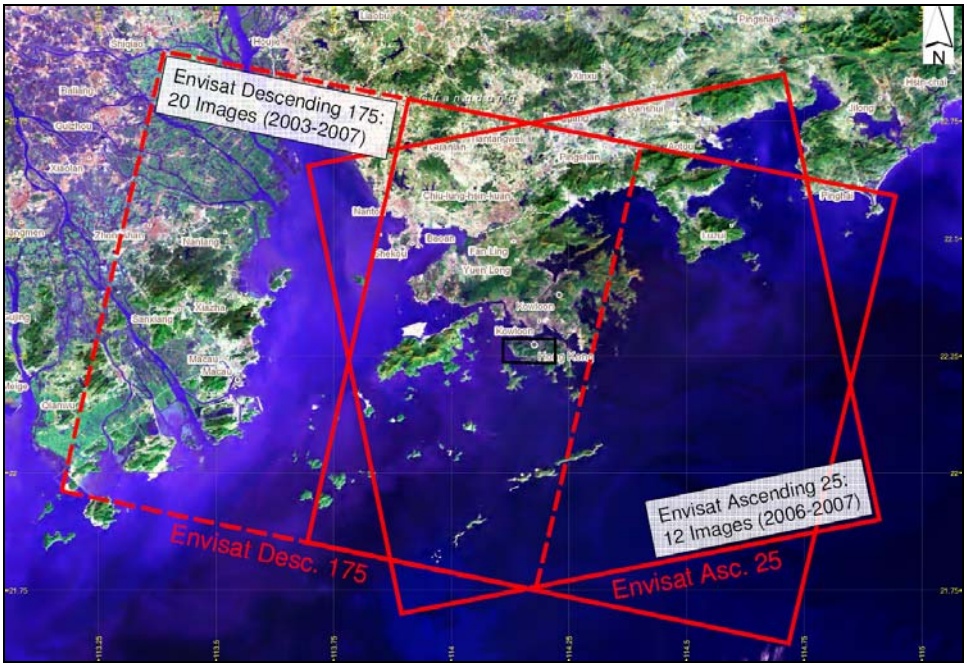

Figure 5: Summary of Archive ENVISAT SAR Images for Hong Kong.

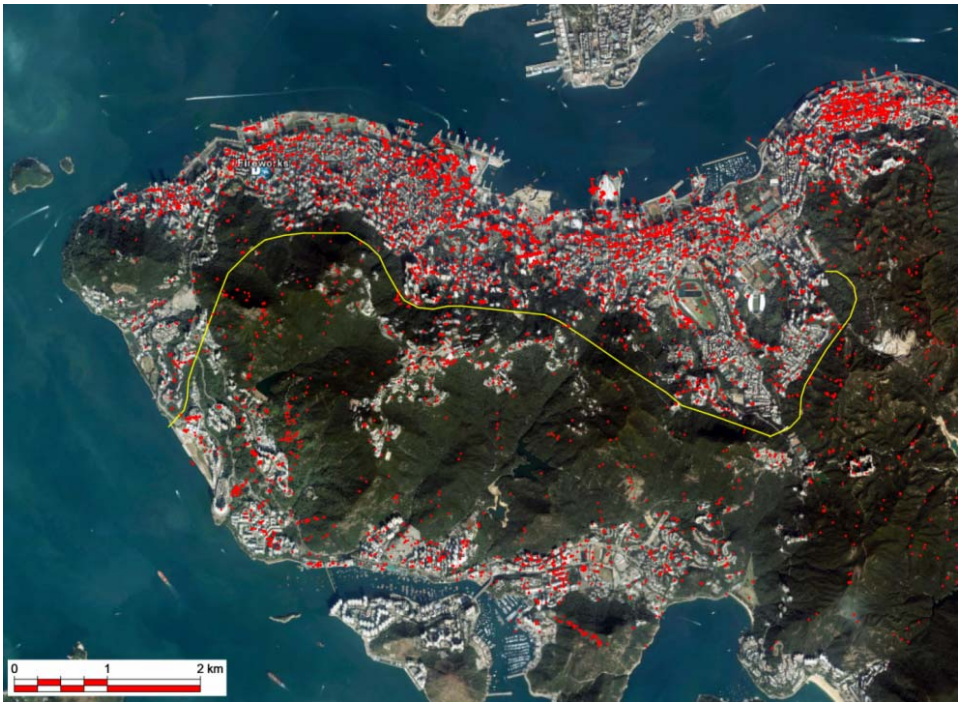

Figure 6: Location of Persistent Scatter Surfaces on North-western Hong Kong Island. Copyright NPA 2007.

Additionally, a preliminary assessment of PS locations within northwest Hong Kong Island (Figure 6), undertaken by NPA Group, has identified the presence of abundant scatter surfaces. This indicates that the area is ideal for the use of PSI as a building movement monitoring tool.

4 CONCLUSIONS

PSI should not be considered as a method to facilitate real-time monitoring of a construction project, due to the time delay between the infrequent capture and analysis of the SAR images. It is, however, considered a highly complimentary technique for conventional construction monitoring works. Its unique capability to record monitoring data without the need for any project specific mobilisation of equipment and manpower means that monitoring of a far wider area around a tunnel alignment can be conducted for comparatively little additional cost. Such monitoring will allow the detection of ground movement trends outside of the narrow corridor conventionally monitored along a tunnel alignment, providing an ability to revise and modify the detailed physical monitoring to target any identified areas of concern.

The need for detailed assessment and physical monitoring of existing buildings, structures and services along and adjacent to a tunnel alignment remains. Where PSI is to be adopted there should be appropriate clauses included in the Contract documents to allow targeted monitoring to be undertaken as and when the PSI data indicates an area of concern

The three major tunnelling projects along the northwestern end of Hong Kong Island outlined above are all due to be under construction between 2009 and 2012. While there is little physical interface between the permanent works of these projects, there remains, at some locations, a high risk of overlap between their potential ground movement and groundwater drawdown effects. The ability to interrogate historical data of a large area in a holistic way, and hence determine over what period and to what extent construction works have resulted in ground movements should provide Clients, Engineers and Contractors with a valuable tool in determining their risk exposure to, and mitigation of, the consequences of ground movements induced from tunnelling works.

As this technology becomes more widely available, and its potential more greatly understood, it seems inevitable that those responsible for underwriting major tunnelling projects will insist on such technologies being adopted as a pre-requisite to providing third party insurance cover to such high risk projects.

ACKNOWLEDGEMENTS

This paper is published with the permission of the Director of Drainage Services of the Government of the Hong Kong Special Administrative Region.

REFERENCES

Geotechnical Engineering Office. 2007. Chapter 6.7.6, Hydrogeology. *Engineering Geological Practice in Hong Kong (GEO Publication No. 1/2007).* 222-224. The Government of the Hong Kong Special Administrative Region.

Hong Kong Government, 2007. 2007-2008 Policy Address, A New Direction for Hong Kong. The Government of the Hong Kong Special Administrative Region.

Peck, R.B. 1969. Deep excavations and tunnelling in soft ground. *Proceedings of the 7th International Conference on Soil Mechanics and Foundation Engineering*, State of the Art Volume.

Pilot Airborne LiDAR Survey in Hong Kong – Application to Natural Terrain Hazard Study

K.C. Ng & K.M. Chiu
Geotechnical Engineering Office, Civil Engineering and Development Department,
Government of the Hong Kong Special Administrative Region, China

ABSTRACT

The Geotechnical Engineering Office of the Civil Engineering and Development Department conducted a pilot air-borne LiDAR (Light Detection and Ranging) survey in December 2006 for Hong Kong Island, to assess the 'virtual deforestation' capability on heavily vegetated hillsides and the ability to detect subtle and concealed topographical features on such conditions. The pilot survey results have demonstrated the capability of the LiDAR technology to generate high-resolution digital elevation models (DEM) of vegetated terrain for Hong Kong Island. This high-resolution ground data allows clear definition of ground features for terrain evaluation and the interpretation of landslide morphology. The associated LiDAR-intensity returns can also be used to produce ortho-images that have the potential of mapping the distribution of landforms, which may be related to the underlying ground and/or groundwater conditions. The experience gained from the pilot survey is being used to plan future surveys for the remaining parts of Hong Kong. It is anticipated that airborne LiDAR will bring about enhanced remote sensing capability that will greatly facilitate assessment of natural terrain hazards, by identifying features that are disguised under a thick vegetation cover.

1 INTRODUCTION

Over 60% of the 1,100 km^2 land area of Hong Kong comprises hilly natural terrain. The risk from natural terrain landslides continues to increase due to new urban development encroaching on natural hillsides (Wong 2004). However, the dense vegetation typical of the natural hillsides obscures the morphology of landslides, particularly relict features, and subtle ground features (e.g. hummocky terrain) both in the field and in aerial photography. Furthermore, topographical data, compiled largely from traditional photogrammetry, has limitations in providing accurate elevation data on heavily vegetated hillsides.

Advances in airborne LiDAR (Light Detection and Ranging) technology allow efficient measurement of topography over a large area and at competitive cost. An important recent development of the technology is the ability to measure multiple returns for each laser pulse (Figure 1) that covers circa one metre in diameter on ground. With the use of an advanced numerical algorithm, the last returns that come from the ground surface are extracted by filtering out other returns from vegetation and building structures (a technique known as 'virtual deforestation'). The technique has been used to produce fine-scale topographical maps and digital elevation models (DEM) typically with grid size of about 1 m. Hence, the system has the capability of mapping the ground surface of vegetated terrain (e.g. McKean and Roering 2004; Schulz 2007, Sturzenegger et al 2007).

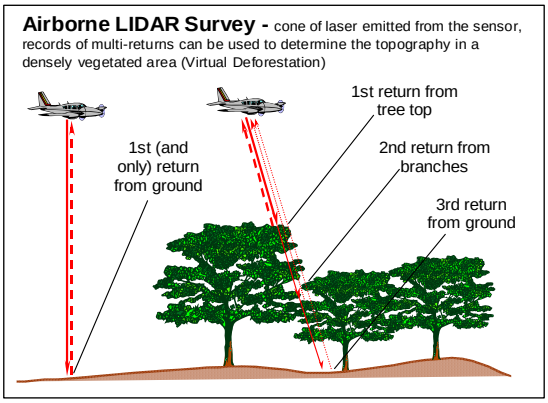

Figure 1: 'Virtual deforestation' capability of airborne LiDAR survey

The Geotechnical Engineering Office (GEO) of the Civil Engineering and Development Department (CEDD) conducted a pilot airborne LiDAR survey in December 2006 for Hong Kong Island, to assess the 'virtual deforestation' capability on heavily vegetated hillsides and the ability to detect slope features behind tall buildings. This paper describes the data acquisition including logistic arrangement,

and discusses the survey results, in particular, the potential of airborne LiDAR data for identifying ground features that are disguised under a thick vegetation cover.

2 DATA ACQUISITION

The technical requirements of the pilot survey were sampling interval at 1.3 m and horizontal and vertical data accuracies at 0.3 m and 0.13 m respectively. An aerial survey and mapping service provider, AAMHatch Pty Limited of Australia was awarded the survey contract which included deploying multi-return LiDAR equipment for the survey and processing of the data acquired.

A fixed-wing aircraft deployed for the survey was ferried 18,000 km return trip from Australia. The LiDAR system consists of a laser sensor, a laser receiver, Global Positioning System (GPS) receiver and Inertial Measuring Unit (IMU). All these components are integrated on an aircraft. The laser sensor pulses a narrow laser beam towards the earth as the aircraft flies whereas the laser receiver receives the reflection of these pulses as they bounce off the objects below back to the aircraft. The GPS and IMS record the position and orientation of the aircraft respectively while transmitting and receiving the pulses. Some key parameters of the data acquisition are as follows (AAMHatch 2007):

- Flying height: c. 1100 m
- Flying speed: c. 220 km/h
- Laser class: IV
- Scan angle: 15°
- Flight lines: 33 east-west lines and 1 north-south cross-strip (Figure 2)

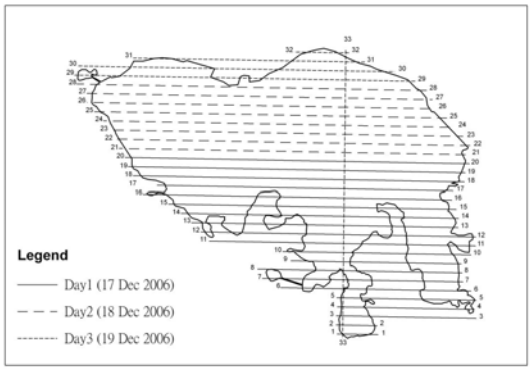

Figure 2: Flight lines

Despite the actual time taken for the data capture of Hong Kong Island (c. 80 km^2) was about eight hours, it took three consecutive days to complete the survey (Figure 2). This is largely due to the restrictions imposed by the Civil Aviation Department (CAD), which allowed data to be collected only between 6 am and 10 am, to avoid undue noise (before 6 am) and interference with regular air movements (after 10 am). The survey aircraft was on standby at the airport awaiting the actual flight time advised by the CAD. GPS data logged at the Lands Department's Continuous Operating Reference Stations (CORS) were used to compute the aircraft trajectory and orientation. An independent land surveying exercise was carried out at three selected areas, to compare with LiDAR terrain elevation data and to check for systematic error.

3 SURVEY RESULTS

The data points collected were geo-referenced and then classified into different point categories. The co-ordinates and elevation of each data point were computed based on the trajectory of the aircraft established from the data from GPS and IMU, and the details of the signals such as return time and scan angle. Automatic and manual processes were applied to classify the data points into different categories including ground, non-ground and vegetation.

Datasets for DEM and digital surface model (DSM) were required. DEM refers to digital elevation model/modelling with fixed sampling interval in single layer of the terrain (natural and artificial surface of the Earth at ground level) only. DSM refers to digital surface model/modelling with fixed sampling interval in single layer of the terrain and above ground objects including vegetations, buildings, elevated platforms/roads and any prominent free standing objects. The survey results, in Hong Kong 1980 Grid System and Hong Kong Principal Datum, were supplied in the following formats:

(a) Point cloud data of the DEM and DSM in ASCII format providing only the co-ordinates and elevation of each data point;
(b) DEM and DSM in 1-m grid raster format (Figure 3, Figure 4);
(c) Intensity images in 1 m grid raster format showing the intensity of the return signals (Figure 5);
(d) All LiDAR data in LAS format 1.0, a standard format for LiDAR data exchange introduced by the American Society for Photogrammetry & Remote Sensing; and
(e) Deduced vegetation thickness in 1-m grid raster format (Figure 6).

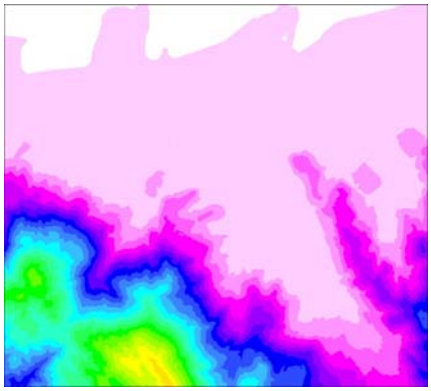

Figure 3: Example of LiDAR DEM

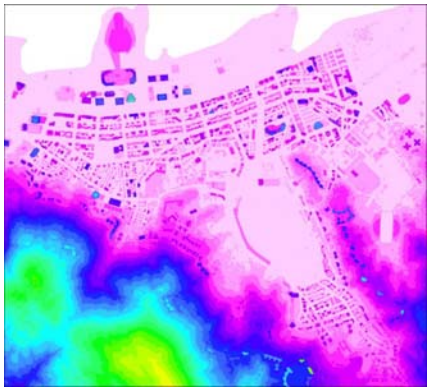

Figure 4: Example of LiDAR DSM

Figure 5: Example of LiDAR intensity image

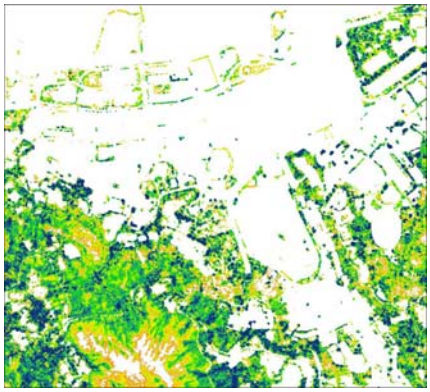

Figure 6: Example of deduced vegetation thickness

A total of about 768 million data points were provided and the overall size of the data files provided was about 31 GB.

4 REVIEW OF SURVEY RESULTS

4.1 Generation of 2-D and 3-D DEM using LiDAR data

The natural hillside behind the Queen Mary Hospital is heavily vegetated (Figure 7a). Using the point cloud LiDAR data, a 0.2-m grid DEM was generated for the hillside.

(a) Hillside in December 2006 (b) Ground points from LiDAR Survey (c) DEM generated using LiDAR data

Figure 7: Generation of DEM of the natural hillside behind Queen Mary Hospital

The closely-spaced ground points (Figure 7b) indicated a successful penetration of the laser beams through the vegetation in the area to survey the ground. Figure 7c shows the DEM overlaid with locations of landslides occurred on the hillside as identified from aerial photographs. It can be observed that the DEM generated using LiDAR data shows clearly the morphology of landslides and other ground features on the hillside. The LiDAR data provide very useful information for engineering geological and geomorphological interpretation in natural terrain hazard study.

The DEM can also be visualized in a 3-D manner (Figure 8a). In addition to natural hillside, LiDAR survey data can be used to generate 3-D urban models or cityscape (Figure 8b).

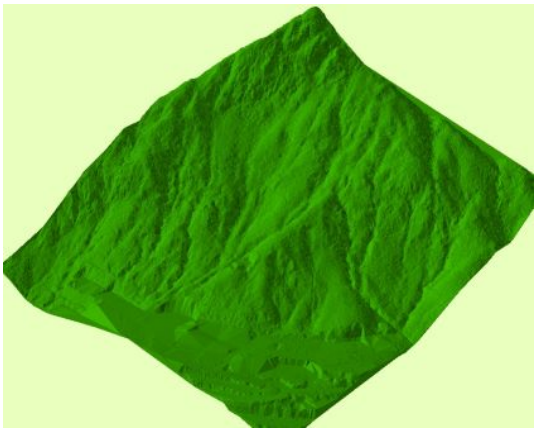

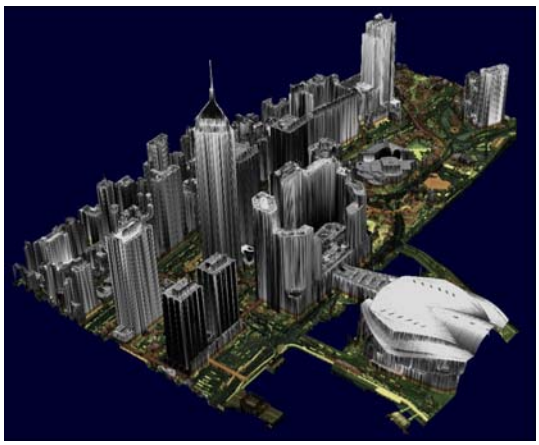

(a) Natural hillside behind the Queen Mary Hospital (b) Wan Chai North area (AAMHatch 2007)

Figure 8: 3-D models generated using LiDAR data

4.2 Comparison with land survey results

Data verification and evaluation of the pilot survey results was carried out by CEDD's Survey Division. Digital terrain models were prepared using the as-built survey results of some man-made features and compared with the DEM generated using LiDAR data. Figure 9 shows one of the comparison results. It is a retaining wall of up to 8 m high supporting a cut slope, below which is a playground. Areas where the elevation difference between the two models exceeds the tolerance were highlighted in grey in the figure. The comparison concluded that the elevation differences in majority of the area were within the tolerance. Anomalies were found along edges of features such as corner of walls and over ragged terrain. It was considered that the former anomalies were due to inefficiency of LiDAR data in defining breaklines while the latter was due to insufficient land survey points in inaccessible areas. In general, the accuracy of hard surface was about ±5 cm whereas the accuracy of vegetated surface was about ±10 cm. In areas of dense shrubland, where laser penetration was relatively low, the accuracy could be lower.

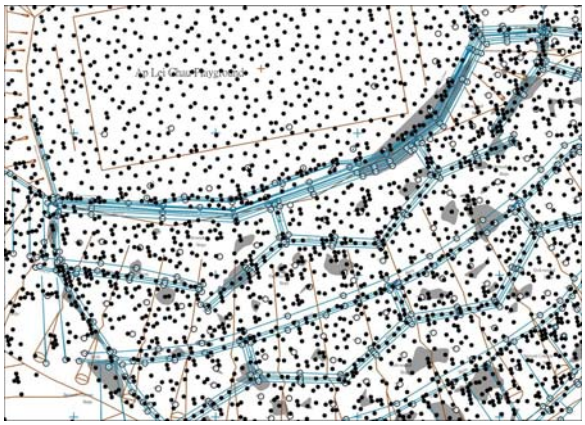

Figure 9: Comparison of LiDAR data and as-built survey (black dots are LiDAR data while hollow dots are as-built survey spot heights)

4.3 Intensity images

The intensity of the return signal depends on the reflectivity of the object or the material. Song et al (2002) noted that LiDAR intensity could be used for land-cover classification using adequate interpolation and filtering. Hasegawa (2006), based on the on-the-ground and aerial surveys, concluded that the reflected intensity decreased with distance and was angle dependent. He also noted that some materials, such as soil, gravel and grass, could be distinguished from each other.

The intensity images supplied under the pilot survey (Figure 5) show distinctive details of different objects and features. As the intensity images were constructed using geo-referenced point data, they could be used as ortho-images to assist classification of land features.

An intensity image of the natural hillside in Pokfulam area was generated using the intensity values of ground points (Figure 10). Distinctive boundaries can be observed that separate the hillside into two zones. When compared with the ortho-image prepared using aerial photographs in November and December 2006, the zones with higher intensity values generally cover exposed boulders or non-vegetated areas such as footpaths and site formation. This observation suggests the potential of using the intensity values to distinguish different surface geology. Further studies are required to confirm and establish the algorithm for such classifications.

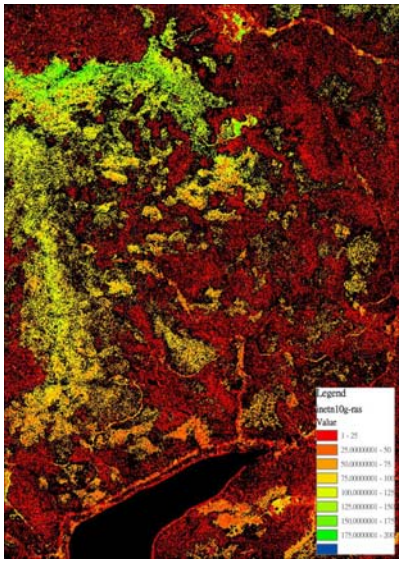

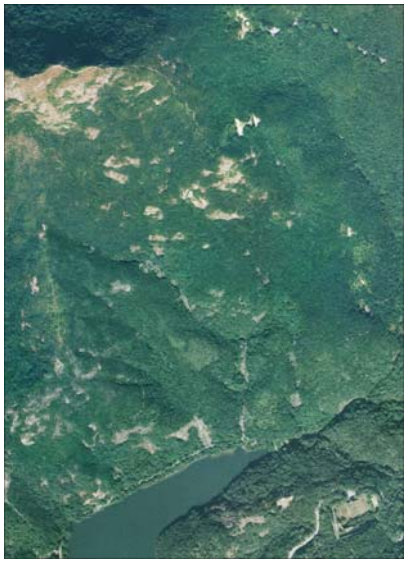

(a) Intensity image generated using intensity values of ground points (b) Ortho-image

Figure 10: Comparison of intensity image and ortho-image at Pokfulam area

4.4 Penetration of laser beams

The success of LiDAR survey depends mainly on how effective the laser beams can reach the ground. Building structures can obstruct the laser beams; however, areas under overhanging structures such as bridges can still be surveyed by laser beams with inclined angle of incidence. Vegetation may block the passage of laser beams. The blockage is not necessarily related to the size of the vegetation but to the space between the leaves available for laser beam passage. An area with few ground points was visited and it was found that the area was covered by closely-grown shrubs which prevent the laser beams from reaching the ground.

4.5 Discussions

The pilot survey for Hong Kong Island proves the capability of LiDAR to survey a large area at high accuracy within a short period of time, and to obtain the 'bare-earth' ground profile by virtual deforestation in Hong Kong conditions. With closely-spaced ground point data, high-resolution DEM can be generated showing clearly the geomorphological features on natural hillsides. The intensity images can be used as ortho-images for identification of topographical and land features. Both the high-resolution DEM and intensity images provide valuable complements to conventional aerial photograph interpretation for assessing landslide processes on natural terrain.

Complex building structures in urban areas can be re-constructed digitally from the LiDAR data. However, the laser beams could be blocked by overhanging structures such as bridges and sometimes by vegetation irrespective of their sizes. The limitations of breakline definition should also be noted when generating digital models and additional survey information should be acquired. The experience gained in the pilot survey is being used to plan a territory-wide survey.

The vast amount of data can lead to data management issues. Sufficient computer storage space should be allowed for data storage and data manipulation. Furthermore, specialist software designed for processing such a huge amount of data for digital modeling, or image generation, is required to enhance the effectiveness and efficiency in the data manipulation.

5 CONCLUSIONS

Multi-return airborne LiDAR technology possesses a 'virtual deforestation' capability. This allows efficient measurement of the 'bare-earth' profile, and the generation of high-resolution DEM of vegetated terrain. Data acquired from the pilot airborne LiDAR survey of Hong Kong Island have confirmed the potential for identifying ground features, e.g. relict landslides and subtle terrain morphology, that are disguised under a thick vegetation cover. Airborne LiDAR will bring about enhanced remote sensing capability that will greatly facilitate assessment of geomorphological processes and natural terrain hazards, thereby revolutionizing the approach to natural terrain hazard study. However, it is important to recognize the limitations of the data and significant processing effort required to reap full benefits of the data quality.

ACKNOWLEDGEMENTS

The paper is published with the permission of the Head of the Geotechnical Engineering Office and the Director of the Civil Engineering and Development Department, Government of the Hong Kong Special Administrative Region.

REFERENCES

AAMHatch Pty Limited. 2007. *Pilot Airborne Light Detection and Ranging (LiDAR) Survey in the Hong Kong SAR – Final Report*. June 2007.

Hasegawa, H. 2006. Evaluations of LiDAR reflectance amplitude sensitivity towards land cover conditions. *Bulletin of the Geographical Survey Institute*, Vol. 53, March, 2006. Geographical Survey Institute, Government of Japan.

McKean, J. & Roering, J. 2004. Objective landslide detection and surface morphology mapping using high-resolution air-borne laser altimetry. *Geomorphology*, 57: 331-351.

Parry, S. & Jonas, D.A. 2007. The use of LiDAR for landslide hazard assessments: Hong Kong case studies. *Proc. of Conference on Engineering Geology in Geotechnical Management, Hong Kong, 24 November 2007*. Hong Kong Regional Group of the Geological Society of London.

Schulz, W.H. 2007. Landslide susceptibility revealed by LIDAR imagery and historical records, Seattle, Washington. *Engineering Geology*, 89: 67-87.

Song, J.H., Han, S.H., Yu, K. & Kim, Y.I. 2002. Assessing the possibility of land-cover classification using LiDAR intensity data. *Proc. of ISPRS Commission III, Symposium 2002 "Photogrammetric Computer Vision", Graz, Austria, September 9-13, 2002.* The International Society for Photogrammetry and Remote Sensing.

Sturzenegger M., Stead D., Froese C., Moreno F. & Jaboyedoff M. 2007. Ground-based and airborne LiDAR for structural mapping of the Frank Slide. *Proc. of 1st Canada-US Rock Mechanics Symposium, Vancouver, 27-31 May 2007.*

Wong, H.N. 2004. Natural terrain management criteria – Hong Kong practice and experience (Invited paper). *Proc of International Conference on Fast Slope Movements: Prediction and Prevention for Risk Mitigation. Vol. 2, Naples, Italy, 11-13 May 2003.*

A Special Combined Deep Foundation System for a Residential Complex

J.W. Pappin, A.K.M. Lam & J.W.C. Sze
Ove Arup and Partners Hong Kong Limited

K.M. Chan
Bachy Soletanche Group Limited

ABSTRACT

Large diameter bored pile foundation with steel stanchions was proposed to facilitate a top-down construction of a 3-level basement supporting a high-rise residential complex at San Po Kong, Kowloon. The final column load in some locations were too large to be supported by a single pile and hence supplementary bored piles were required to be connected to some of these columns upon reaching the final basement excavation level to share the final structural loads. However, these supplementary piles would not be fully utilized since the central piles directly supporting the columns will be overloaded due to the lock-in stress prior to such connection. In lieu of the above option, a more cost-effective scheme as an alternative was devised. The alternative design again adopted large diameter bored piles as the central piles with allowable capacity up to 117MN. The more innovative part was to replace the supplementary bored piles by smaller pre-bored steel H-piles socketed into Grade III rock with pre-loading at the pile heads using synchronized jacks upon reaching pile head level in order to fully mobilize the capacity of the two foundation systems. With a maximum of 9 nos. supplementary pre-bored H-pile at each column, the maximum combined allowable capacity is around 167MN. These resulted in a significant cost saving as well as a higher degree of flexibility in the construction programme.

1 INTRODUCTION

The site is located near the former Kai Tak Airport with a site area of approximately 80m by 120m. The development consisted of five residential towers, 37 to 41 storeys, above a 3-level basement and a 5-level retail podium. The depth of the basement was about 13m below ground.

The ground investigation revealed that the site consists of fill overlying a layer of marine deposit and alluvium, which is then underlain by a thick layer of completely to highly decomposed (IV/V) granite. Moderately to slightly decomposed (III/II) granitic bedrock is encountered at depth varying from 40m to 80m below ground across the site. The thickness of superficial deposits varies form about 7m to 12m. A corestone layer comprising moderately to highly decomposed granite (Grade III/IV) with variable thickness is encountered immediately above the bedrock.

2 CONFORMING FOUNDATION DESIGN

In view of the site geology and loading condition, pile foundation bearing on Grade III rock or better was proposed to be the foundation system. To expedite the construction programme of the project, the basement was constructed by top-down method using diaphragm wall as both temporary and permanent retaining wall such that the basement, podium and tower structures were constructed simultaneously. Diaphragm wall panels supporting the perimeter podium columns were found on rock with allowable bearing capacity of 5000kPa while other panels supporting the basement slabs only were found on soil with standard penetration test of N-value exceeding 200 and allowable bearing capacity of 1000kPa. Prior to the construction of the pile cap at the final formation level inside the basement, steel stanchions extruding from the cut-off level of bored piles to ground level at each column were adopted to support the temporary load from the basement, podium and tower structures. Due to the significant permanent column loads from the residential towers, the full capacity

of a conventional 3.0m diameter bored pile with 4.5m bell-out diameter was not sufficient to sustain the loads at some columns and supplementary piles were therefore required to be connected to these columns via the pile cap upon reaching the final formation level to share the loads.

The conforming foundation design adopted 81 nos. of large diameter bored piles with shaft diameter of 2.5m and 3.0m and bell-out diameter up to 4.5m under each permanent column/stanchion to facilitate the top-down construction of the basement. Due to the significant column loads, another 55 nos. of large diameter supplementary bored piles were required to share the loads.

3 ALTERNATIVE FOUNDATION DESIGN

The design and build foundation contract was awarded to Bachy Soletanche Group Limited with the supports from Arup to derive the alternative designs. The Contractor's design basically adopted the conforming diaphragm wall design although further optimization had been carried out to achieve cost-effectiveness in supporting the perimeters column as well as facilitating the top-down excavation of the basement.

Comparing to the conforming foundation design, the major difference is the replacement of the large diameter supplementary bored piles by pre-bored H-piles connected to the columns via the pile cap upon reaching the final formation level to share the loads. This is due to the shortcoming of the capacity of these supplementary bored piles having very low percentage of utilization after connection at final formation level in a top-down construction of the basement. Otherwise, the central piles directly supporting the columns will be overloaded due to the lock-in stress prior to such connection.

In the alternative design, large diameter bored piles with bell-out diameter up to 4.5m and increased rock socket length up to 6m to give a higher bored pile capacity directly underneath the column/steel stanchion was adopted. Grade III rock was also specified as the founding material in deriving the pile capacity. The supplementary bored piles were proposed to be replaced by a total of 73 nos. Grade 55C 305x305x223 kg/m pre-bored steel H-piles socketed into Grade III rock. This gave a change in pile type and resulted in a combined foundation system in supporting a column. The major innovation part in respect to the foundation system is on the introducing of pre-loading to the pile heads of these rock socketed H-piles upon casting the common pile cap in order to fully utilize the capacity of the two foundation systems. These resulted in significant cost saving as well as flexibility on construction programme. The details of the foundation system are discussed in the following sections.

3.1 Combined Foundation system

The large diameter bored pile was located at the column center to sustain the temporary and permanent column loads while the supplementary pre-bored H-piles were located concentric from the center of the pile cap at equal distance to share the permanent column loads together with the center bored pile. A typical pile layout plan is shown in Figure 1.

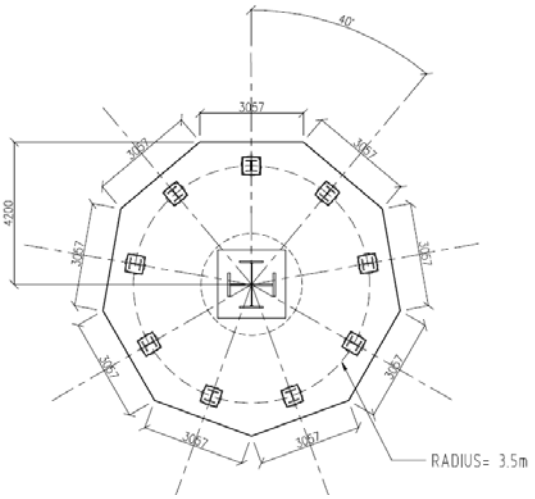

Figure 1: Typical Pile layout with 9 nos. Supplementary Socketed H-pile

The load sharing between the centre bored pile and the supplementary pre-bored H-piles is based on their corresponding axial stiffnesses after connection via a rigid pile cap at the final formation level. However, these supplementary piles cannot be fully utilized as the bored pile directly supporting the columns has been stressed up due to the temporary load during the top-down construction prior to such connection unless a process of pre-loading is carried out at the head of pre-bored H-piles to release this lock-in stress in the bored pile such that additional loads shared between bored pile and pre-bored H-piles can fully utilize the capacity of these piles.

With this connection, pre-loading was proposed to be carried out at the head of pre-bored H-piles using pressurized jacks. Two jacking systems were considered namely flat jack and hydraulic jack. Flat jack was designed to be situated at the head of pre-bored H-pile and was part of the permanent structural element. After the required pre-loading force was achieved, the jack oil inside the flat jack would be displaced and filled up by epoxy resin and the injection pressure would be monitored by pressure gauge during the displacement process. A typical pile head details using flat jack is shown in Figure 2.

An alternative to flat jack was hydraulic jack, which was used in this project. The advantage of using hydraulic jack was that it was only for temporary use and the axial pile load would be permanently transferred through the structural steel. Two brackets were constructed at the head of pre-bored H-pile and two hydraulic jacks were placed on top of the brackets. After the required pre-loading force was achieved, shim plates would be installed and welded at the head of pre-bored H-pile to lock the system, which formed part of the permanent structural element. The hydraulic jacks would then be unloaded and removed. Synchronized jacks were used to exhibit same loads and the rate of pile head settlement prior to shim plate insertion should be less than 0.05mm in 10minutes to each of the pre-bored H-pile. A typical pile head details using hydraulic jack is shown in Figure 3.

As all pre-bored H-piles are located concentric from the center of the pile cap at equal distance, the applied load can be equally shared among the pre-bored H-piles. Lateral wind shear load was designed to be taken by the passive soil resistance behind the diaphragm wall and therefore shear transfer at the head of pre-bored H-piles was minimal.

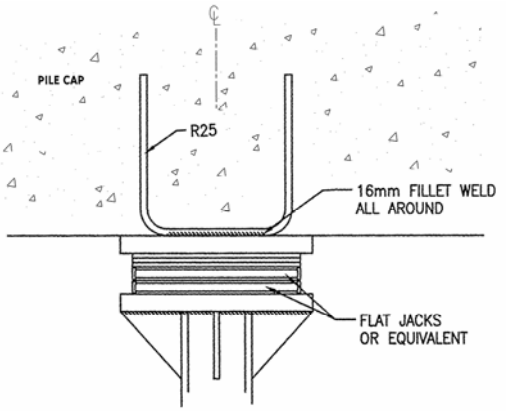

Figure 2: Typical pile head detail using flat jack

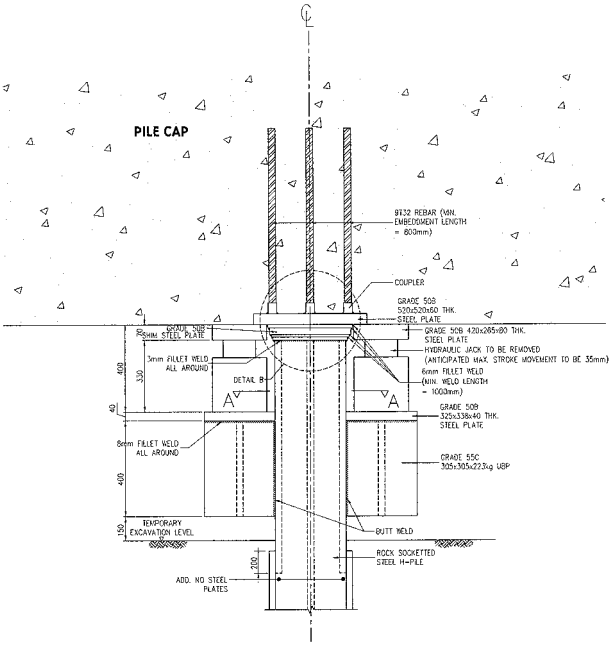

Figure 3: Typical pile head detail using hydraulic jack

3.2 Pile design

The bored pile and pre-bored H-pile were designed in accordance with the Code of Practice for Foundations (BD, 2004). The rock socket friction for Grade III rock was taken to be 700kPa under compression and transient wind load while the end bearing capacity was taken to be 5000kPa for bored pile bearing on Grade III rock. A 3m diameter bored pile with a bell-out diameter of 4.5m and rock socket length of 6m gave an

allowable working capacity of 117MN. Extra steel reinforcement is required to compensate the deficiency in Grade 45 tremie concrete in taking such high stress.

The allowable working capacity of the pre-bored H-pile with a steel section of 305x305x223kg/m UBP and a 6.5m rock socket length was 5.9MN but typical 5.6MN was utilized to offset the additional axial and bending stresses due to lateral effects and construction tolerances. With a maximum of 9 nos. supplementary pre-bored H-piles at each column, the maximum combined allowable axial capacity is around 167MN upon full mobilization.

3.3 Optimized jack force

Prior to the construction of the pile cap, the temporary vertical loading including dead, live and wind loads are transferred directly onto the bored pile, denoted by F_1. Assuming that the jack force is denoted by P, the load on bored pile after jacking is $F_1 - NP$. After the bored pile and pre-bored H-piles are connected via the rigid pile cap, the additional load, denoted by F_2, will be shared between them depending on their corresponding stiffnesses. The load on bored pile and pre-bored H-pile in permanent condition is shown in equations (1) and (2) respectively.

$$F_1 - NP + \frac{F_2 k_B}{k_B + NK_H} \tag{1}$$

$$P + \frac{F_2 k_H}{k_B + Nk_H} \tag{2}$$

where F_1 = dead, live and wind loads before jacking, F_2 = additional dead, live and wind loads after jacking, P = jack force on each pre-bored H-pile, k_B = vertical stiffness of bored pile, k_H = vertical stiffness of pre-bored H-pile and N = nos. of pre-bored H-pile within the pile cap.

An optimized jack force to fully utilize the capacity of both bored pile and pre-bored H-pile can be determined by considering the pile head movement at different stage of loading. The pile head settlement required to mobilize the full capacity for both bored pile and pre-bored H-pile are represented by equations (3) and (4) respectively. Prior to connection via the pile cap, the pile head settlement of the bored pile can be determined by equation (5). When the jack force P is applied to the head of pre-bored H-pile, the pile head of bored pile move upwards while that of pre-bored H-pile moves downward. The magnitudes of pile head movement due to jacking are represented by equations (6) and (7). After jacking, the remaining movement before the full capacity of bored pile is reached shall be (3) – (5) + (6) while that of pre-bored H-pile shall be (4) – (7), which can be represented by equation (8) as both bored pile and pre-bored H-pile shall move together with the same magnitude after connection via the cap. The optimized jack force can then be determined by rearranging equation (8) to obtain equation (9).

$$\Delta_B = \frac{P_B}{k_B} \tag{3}$$

$$\Delta_H = \frac{P_H}{k_H} \tag{4}$$

$$T_B = \frac{F_1}{k_B} \tag{5}$$

$$S_B = \frac{NP}{k_B} \tag{6}$$

$$S_H = \frac{P}{k_H} \tag{7}$$

$$\Delta_H - S_H = \Delta_B + S_B - T_B \tag{8}$$

$$P = \frac{\Delta_H - \Delta_B + T_B}{\left(\frac{N}{k_B} + \frac{1}{k_H}\right)} \tag{9}$$

where Δ_B = bored pile settlement at full load, Δ_H = pre-bored H-pile settlement at full load, T_B = bored pile settlement at temporary load, S_B = bored pile upward movement due to jacking force, S_H = pre-bored H-pile downward movement due to jacking force, P_B = bored pile allowable capacity and P_H = pre-bored H-pile allowable capacity.

In determining the optimized jack force, allowable working capacities of bored pile and pre-bored H-pile were considered. Under ultimate load condition, because of the relatively higher stiffness of the bored pile, it would share more column loads than the pre-bored H-pile and reinforcements should be designed to sustain this ultimate load.

3.4 Illustration of column load transfer mechanism

To illustrate the idea of pre-loading of the supplementary pre-bored H-piles, a column supported by one large bored pile and nine supplementary pre-bored H-piles is selected, as shown in Figure 4. The final column load is 167MN. The temporary load on the bored pile is 56MN upon reaching the time of jacking. Each of the pre-bored H-pile is pre-loaded to 3MN which helps to release the load on the center bored pile by 27MN. With the construction continued, the final loads shared by these piles are depending on the pile stiffness and the magnitude of the pre-loading is determined with an aim to fully mobilize the capacity in each system.

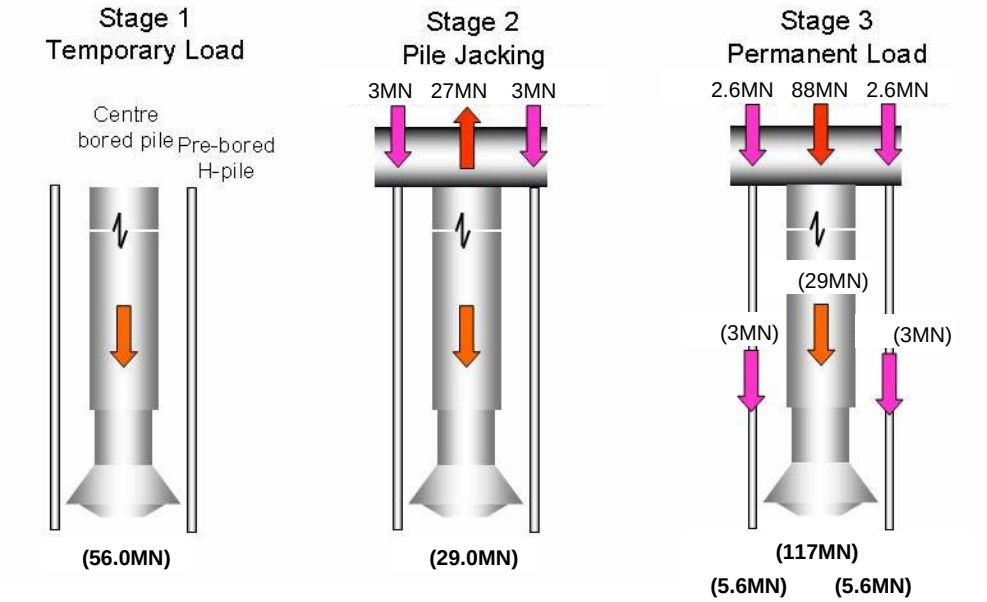

Figure 4: Illustration of load transfer with pile jacking

4 PILE INSTALLATION

4.1 Large Diameter Bored Pile

The bored piles were constructed using common pile construction technique in which a temporary steel casing was used to support the pile bore over the depth in soils. The casing was advanced using an oscillator or a casing rotator and extended by coupling or welding. Soil within the casing was excavated using hammer grab. Water was used as the flushing medium. The excavation in soil was carried out by hammer grab and the rock socket and bell-out was formed by reverse circulation drill (RCD), as shown in Plate 1. In most of the cases, the pre-drill of the bored pile also serves to determine the founding level of the supplementary pre-bored H-piles underneath the same column.

4.2 Pre-bored H-pile

The pre-bored H-piles with 550mm diameter in rock were constructed using ODEX drilling in the soil followed by down-the-hole hammer drilling in rock, powered by compressed air as shown in Plate 2. A temporary steel casing was advanced simultaneously with the ODEX drill bit and hence the entire soil section was fully cased. The steel H-pile section was lowered into the hole in the specified orientation and the void was filled up by tremie cement grout. At each pile cap, one steel H-pile section was extended close to the existing ground surface to facilitate the proof load test to be carried out at the existing ground.

Plate 1: RCD mounted on casing top

Plate 2: Pre-bored H-pile construction

At the time of preparing this paper, the basement excavation is still in progress and the jacking for pre-bored H-pile is envisaged to be carried out by summer of this year when the final excavation is reached. A mockup will be constructed on site to test the jacking procedures prior to actual pile jacking.

5 CONCLUSIONS

The innovative foundation system involving a combined use of the two conventional piling systems, one being large bored pile and the other being pre-bored rock socketed H-piles, was devised with an introduction of pile jacking/pre-loading to enable all the piles in the system to work close to their full capacity. This had provided a cost effective solution to give a high loading capacity at each column to facilitate the top-down basement construction with significant column loads. With a maximum of 9 nos. supplementary pre-bored H-piles adopted at each column, the maximum combined allowable axial capacity is around 167MN.

ACKNOWLEDGEMENT

The authors would like to express their sincere gratuity to Sun Hung Kai Architects and Engineers Ltd., the Client's representative and the architect of the project, for their permission in publishing this Paper.

REFERENCES

BD. 2004. "Code of Practice for Foundations", Buildings Department, HKSAR, 57p.

Iterative Approach to Blast Vibration Assessment for Multiple Hard Rock Tunnels beneath Hong Kong Island

D. Rule, D. Salisbury, P. Huong & M. Wallace
Ove Arup & Partners Hong Kong Ltd

ABSTRACT

Under the Hong Kong Regulations, wherever explosives are proposed for use on a construction project in Hong Kong, a detailed Blasting Assessment Report is required to be submitted to the Mines Division, Geotechnical Engineering Office of the Civil Engineering and Development Department. The requirements of a Blasting Assessment indicates that all sensitive receivers, including buildings, roads, utilities, slopes and retaining walls within the area affected by blast vibrations should be assessed to ensure they will not be damaged due to the blasting operations. This generally involves calculation of the maximum allowable peak particle velocity for each sensitive receiver within the blasting zone of influence.

During the planning of the Hong Kong West Drainage Tunnel for the Drainage Services Department an initial assessment indicated that over 7,000 sensitive receivers, including 3,000 slopes and retaining walls, were located within a 300m plan radius from the multiple blasting locations. These locations consisted of 34 adits, totalling nearly 8.0km of tunnel, one shaft and two TBM launch chambers. It became clear that a more structured approach than used previously for a typical single tunnel blasting site was required for this project to reduce the number of sensitive receivers to be analysed as part of the Blasting Assessment study.

This paper will outline the methodology used to identify and assess the critical sensitive receives, which were typically slopes and retaining walls, and the iterative process by which these sensitive receivers were filtered out using digital terrain models and peak particle velocity contouring.

1 INTRODUCTION

1.1 Purpose and Nature of Project

Rapid urbanisation, change in land use and substantial increase in paved area have resulted in a significant increase in surface run-off, affecting much of the lower catchment of Northern Hong Kong Island. Despite local improvements to the 50 years old drainage system, flooding still frequently occurs.

To alleviate this flooding and meet the community's increased expectations for a higher standard of flood protection, Drainage Services Department (DSD) commissioned a drainage master plan study for Northern Hong Kong Island to assess the existing drainage systems.

Due to the topography and size of the catchments, the quantity of stormwater flowing from the upper catchments into the lower urban areas can accumulate in a short period of time during heavy rainstorms and overload the drainage systems there. Apart from causing flooding, traffic disruption and damage to properties, the large and rapid flows from the hills may also impose potential risks to life.

In view of the above, the study recommended three key components to be implemented, one of which being the Hong Kong West Drainage Tunnel.

The Hong Kong West Drainage Tunnel project is a system of 34 catchment intakes, dropshafts, adits and a drainage tunnel from Tai Hang to Pok Fu Lam, see Figure 1. This drainage system will alleviate the risks of

flooding at the lower catchment by using the tunnel to intercept the stormwater flow from the upper catchment.

In March 2006, DSD commissioned Ove Arup and Partners Hong Kong Limited to undertake the consultancy assignment of Agreement No. CE 17/2005 (DS) Tender and Construction of Hong Kong West Drainage Tunnel – Design & Construction.

1.2 Location

The upstream Eastern Portal is located at Tai Hang Road, to the south of Lai Tak Tsuen, this is the highest point of the main tunnel at approximately +48mPD. The proposed alignment of the main tunnel runs generally south-westwards to a point beneath Wong Nai Chung Gap Road, beneath to the Hong Kong Tennis Centre. The route of the tunnel then turns west-north-west to a location below Magazine Gap. The alignment then trends westwards towards Tregunter Path near Tavistock, here the tunnel alignment turns north-westwards to near the most northerly part of Lugard Road. The tunnel then proceeds westwards to near Hatton Road where it turns south-west to discharge adjacent to the Cyberport development into the East Lamma Channel.

The level of the tunnel gradually decreases from +48mPD at the eastern portal to +3mPD at Cyberport.

A network of shafts and adits will collect and feed stormwater runoff from the upper catchments, before it enters the main urban areas, into the main tunnel for safe discharge directly into the sea at Cyberport. The shafts and adits are all on the northern side of the main tunnel and vary in surface level and depth from approximately +49mPD to +208mPD, between 14m and 182m deep and vary in length from 15m to 765m.

1.3 Tunnel

The main tunnel will be excavated by two Tunnel Boring Machines (TBMs), one excavating from the west portal at Cyberport with a diameter of approximately 8.0m, the other from the east portal at Tai Hang Road which will have a diameter of approximately 7.0m. The retrieval of the TBMs will be via adit W0 on Stubbs Road. This adit will be the only one excavated from the dropshaft towards the main tunnel, all others being excavated from the main tunnel.

1.4 Adits

There are 28 adits providing connections from the shafts to the main tunnel, some adits having more than one shaft connecting to them, these adits are shown on Figure 1. The adits will be excavated to a horseshoe profile and an excavated minimum internal diameter of approximately 3.0m. The adits will generally be constructed using mechanical means for at least 5m from the main TBM tunnel. Blast precautions, consisting mainly of a blast door, will then be installed and the remainder of the adit will be excavated using drill and blast methods. Where blasting vibration limits dictate, it may be necessary to excavate some limited sections of the adits by mechanical methods.

Given the small diameter of the adits and therefore the limited efficient pull length of each blasted round, a maximum expected instantaneous charge weight of 5 kg per delay was assumed for the Blasting Assessment. This was based on discussions with contractors blasting specialists and Arup's own staff as a reasonable maximum charge weigh per delay for this scale of work. As such it became the basis for defining the initial zone of influence of the blasting and would form a constraint if the Blasting Assessment were to be adopted by the Contractor without modification. This effectively permitted efficient blasting to excavate the maximum possible pull in one round for a 3m diameter tunnel, but also constrained the area that needed to be examined during the preparation of the Blasting Assessment Report.

1.5 Shafts

There are 32 shafts, between 1.2m and 2.3m diameter, which will provide the vertical connection from the intake structure to the adit. The shafts are positioned to maximise the collection of runoff water from various stream and channels, the locations of these shafts is shown on Figure 1. These shafts will generally be constructed using raise-bore for the rock sections and RCD piling techniques or other mechanical soft ground

techniques for the soft sections. However, it is envisaged that at least one shaft, W0, will be constructed using mechanical methods to permit the retrieval of the TBMs. The use of blasting is not envisaged for the shaft and intake structures.

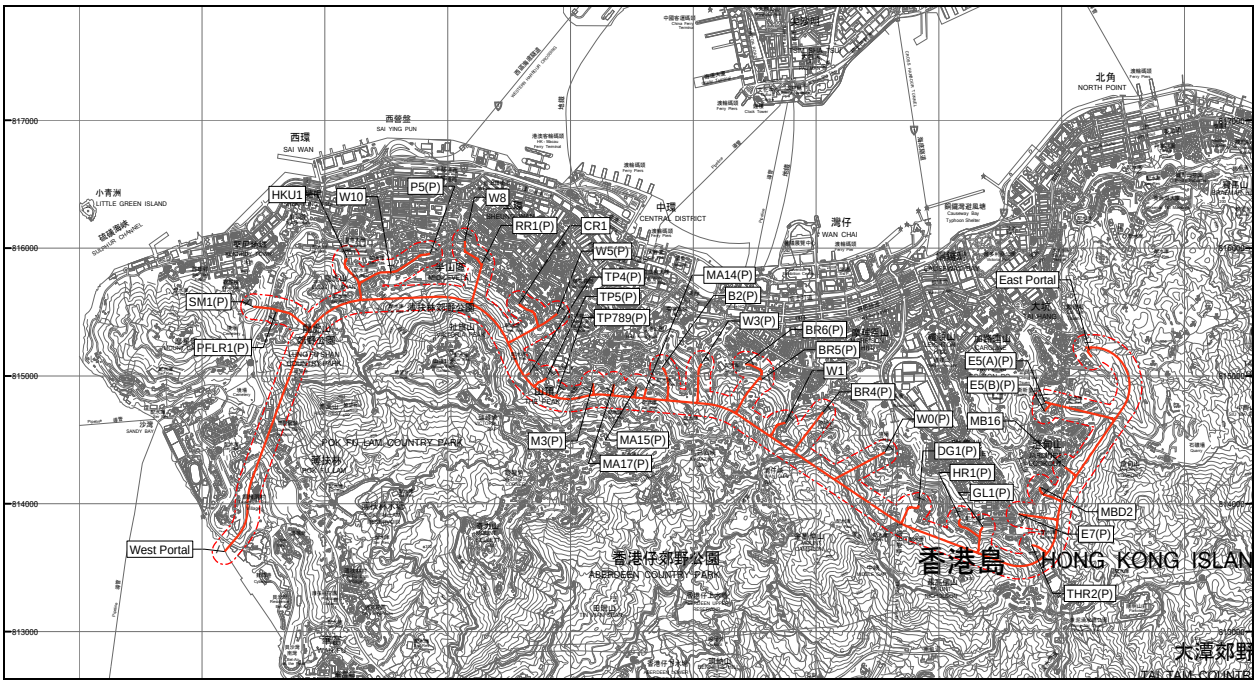

Figure 1 : Layout of Hong Kong West Drainage Tunnel, Shafts and Adits

1.6 General Topography

The alignment of the main tunnel and the shafts and adits are located beneath the north side of Hong Kong Island. The topography of this area is generally steeply sloping ground dipping towards the north. The average slope angle is approximately 20º to 30º.

The eastern portion of the tunnel route above Tai Hang and Happy Valley is below north-west facing slopes. There are significant linear lows along Tai Hang Valley, Wong Nai Chung Gap Road and Wanchai Gap Road. The general slope orientation above the tunnel section from Wong Nai Chung Gap Road to Magazine Gap is towards the north-east. The topography trends northwards for the section from Magazine Gap to Hatton Road, except for the short section from Tregunter Path to Lugard Road where the slopes face north-eastwards. To the west of Hatton Road, the ground slopes towards the west.

The complete tunnel network and a topographic map are shown on Figure 1.

1.7 Physical Site Constraints

There are numerous physical constraints affecting the construction of this project. These constraints include; restricted working space at many of the shafts and both portals; steeply sloping sites; underground structures such as the Aberdeen Road Tunnel, Braemar Hill Gas Tunnel and the Tai Tam reservoir tunnel; numerous adjacent residential buildings; ancient monuments; Water Services Department facilities etc. All of these features and structures, along with utilities, slopes and retaining walls require consideration as sensitive receivers for blast vibrations.

2 REVIEW OF ALLOWABLE PEAK PARTICLE VELOCITIES (PPVs) IN HONG KONG

2.1 General

Sensitive Receivers can be defined as anything that may be damaged by blast vibrations. The common sensitive receivers are structures such as buildings and bridges, man made slopes and retaining walls, natural slopes, roads and utilities. Maximum allowable vibration limits were allocated for these receivers and maximum allowable charge weights calculated for the distance from the blast face accordingly.

The sensitive receivers, except for man-made slopes and retaining walls, within 100m in plan of the portions of the tunnel to be blasted were assessed to determine the maximum allowable charge weight for any specific point along the tunnel.

2.2 Effective Zone of Influence

The effective zone of influence was determined by assuming a maximum expected charge weight per delay of 5kg. When using 5kg per delay, at a distance of 100m, the resulting PPV from the standard calculation in Equation 1 is 6.2mm/s. This is less than the lowest prescribed allowable peak particle velocity applicable to the project of 13mm/s which is allocated to cable joints and water retaining structures.

$$PPV = K (R/ \sqrt{W})^{-B} \qquad \text{—— Equation (1)}$$

Where PPV – peak particle velocity (mm/s)

K – rock transmission constant

R – distance between blast and measuring point (m)

W– maximum charge weight per delay interval (kg)

B – attenuation exponent.

The Mines Division of the Hong Kong Government Geotechnical Engineering Office have monitored blasting vibrations since 1965. Analysis of 520 blasting records taken since 1984 were published in 1992 (Li and Ng, 1992), giving guidance for constants appropriate for use in Hong Kong. It has been identified that the type of blasting develops different responses within the ground. The attenuation relationship for surface and underground confined blasting is known to be different.

The constants at the 84% confidence level for blasting recommended by Mines Division are:

$$K = 644$$

$$B = 1.22$$

Hence

$$PPV = 644 (100/ \sqrt{5})^{-1.22} = 6.2 \text{ mm/s}$$

Geoguide 4 Section 5.7.1 states “As a general guide, blast vibrations from sub-surface works are normally not potentially damaging at distances of more than 50m and only exceptionally at distances of more than 100m.” As this plan distance does not take account of any difference in level between the point of detonation in the tunnel and the ground surface the 100m radius was considered a suitably conservative starting point for the analysis.

2.3 Existing Man Made Slopes and Retaining Walls

There are over 1,500 man-made slopes and retaining walls within the potential zone of blasting influence from the adits. These features include cut slopes, fill slopes, retaining walls and a combination of these. The slopes are covered with all types of facing, including shotcrete, chunam, stone facing and vegetation. A methodology using an iterative approach was devised to identify the most critical features for further analysis. The methodology adopted is detailed below.

Six of the shafts, approximately 1.8km of adits and approximately 1.5 kilometres of the main tunnel, are within the Mid-Levels Scheduled Area. This area was designated following the Mid-Levels Study as an area of potential instability and as such particular attention was given to the inspection of slopes in this area. However, the process of analysis was the same.

2.4 Existing Natural Terrain Slopes

Much of the alignment of the adits is beneath natural terrain hillside. The natural terrain hillsides were allocated 25mm/s as the maximum allowable blast vibration. When the hillside would be subjected to a vibration of more than 5mm/s by a blast, with the expected maximum charge weight, an analysis of the hillside was carried out to determine whether 25mm/s was an appropriate limit.

An assessment of the presence of boulder fields on the natural terrain had been carried out at the Investigation and Preliminary Design stage of the project. Where boulder fields were likely to be influenced by blast vibrations a field inspection was carried out to determine whether the boulders would be susceptible to blast induced failure. Where failure was considered possible, remedial works to be carried out before blasting works approach the location were proposed.

2.5 Buildings and Other Structures

There are a very large number of buildings and other structures (in excess of 1,500) within the 100m zone of influence of the proposed blasting works. These building are mostly multi-storey residential buildings, however there are also low rise residential buildings, a cathedral, university buildings, fire stations, swimming pools, road bridges and elevated roads amongst others. A blast limit of 25mm/s was applied to all recently constructed reinforced concrete structures. An exception to this is water retaining structures, such as swimming pools and WSD reservoirs, a limit of 13mm/s was allocated to these in line with WSD recommendations.

A list of registered historic monuments was checked. A blast vibration limit of 5mm/s was applied to all Historic Building and Declared Monuments within 300m plan distance of the blasting zones. Following the assessment no historic monuments were located within the 5mm/s contour zone of blasting influence.

A preliminary visual inspection of buildings was carried out. To screen out buildings that were deemed to be of concern, the expected PPV was calculated based upon the minimum distance from the structure to the nearest adit using a charge weight of 5kg per delay. Any structure which had an expected PPV of greater than 12.5mm/s was inspected and a record of that inspection was prepared for inclusion in the Blasting Assessment Report. 12.5mm/s was chosen as this is the lowest allowable PPV calculated using the Swedish Code method for building damage assessment. All buildings of Cultural Heritage significance and all buildings over 50 years old within 100m plan of the tunnels or adits were also inspected.

A further review to identify any especially sensitive structures within 300m was carried out.

2.6 WSD Facilities

There are many WSD facilities that will be affected by blast vibrations on the project. These include water mains, covered reservoirs, a major water conduit and a water tunnel. In line with WSD recommendations a blast vibration limit of 25mm/s was allocated to water mains and a limit of 13mm/s was applied to water retaining structures such as reservoirs.

In accordance with WSD Instruction No.1038, excavation is not permitted within a 45º angle of WSD reservoirs unless permission is granted by WSD. Numerous portions of the adits and the main tunnel fall within this criteria.

A major water conduit runs along a contour path from Kotewall Road to Pok Fu Lam Road south of Queen Mary Hospital, WSD has stipulated a 50m wide no-blast zone to this facility. The adits for Shafts SM1, HKU1 and P5 are partially located within this no blast zone.

The Tai Tam Conduit Tunnel runs from Tai Tam Reservoir to the Eastern Treatment Works, a 60m wide plan no blasting and no excavation limit has been set around this tunnel. The adits for Shafts THR2, GL1 and HR1 are partially or totally located within this no blast zone.

A separate Impact Assessment Report was submitted to WSD to provide justification to allow excavation and blasting where appropriate. In many cases the radial distance to the adit is far greater than the plan distance. In these cases a request for relaxation of the no-blast zone was made to the Director of WSD in accordance with Instruction No.1038.

2.7 Utility Companies

Utility companies have many services near the proposed tunnels and adits, mainly buried beneath roads. These services include gas pipes, electricity cables, telephone cables, cable television services, stormwater drains and sewage pipes. Hong Kong Electric imposes a vibration limit of 13mm/s on substations and underground cable joints. A general limit of 25mm/s applies to all other services.

Hong Kong and China Gas Co Ltd own the Braemar Hill Gas Tunnel which runs from the south end of Braemar Hill Road to the corner of Tai Hang Road, east of Blue Pool Road, the portal is close to Shaft THR2 and the tunnel crosses Adit E7. The gas tunnel is at approximately 125mPD. A no blast zone of 60m from the tunnel has been set and a maximum blast vibration limit of 13mm/s on the tunnel has been allocated. The adit is more than 70m below the tunnel and therefore blasting is permitted.

2.8 Other Facilities

Aberdeen Road Tunnel runs from Happy Valley, south-west of the Royal Hong Kong Jockey Club Racecourse south to Wong Chuk Hang. This tunnel consists of twin bores with two lanes in each direction. The main tunnel will pass within 10m of the crown of the Aberdeen Tunnel.

The Civil Engineering and Development Department is constructing two tunnels at for Landslide Preventative Works at Po Shan Road. These tunnels will be completed before blasting works are ongoing, some finishing works may be ongoing. In this event there must be close coordination between the two projects to ensure that safe practice is followed at all times.

Drainage Services Department proposes to construct the HATS II project which involves the excavation of a series of sewage transfer tunnels along the western coast of Hong Kong Island. The HATS II tunnel will cross the alignment of the proposed tunnel adjacent to the western portal. Both tunnels will be under construction at the same time, close coordination between the two projects is to be maintained to minimize the interface issues.

Documentation of agreement from the stakeholders to the allocated vibration limits was collected and presented in the Blasting Assessment Report.

3 METHODOLOGY OF ANALYSIS FOR SLOPES AND RETAINING WALLS

The calculation of the allowable vibration limits of the existing slopes and retaining walls were based upon the critical peak particle velocity (PPVc) which was calculated based on the methods set out in GEO Report No. 15. These PPVc values were then utilized to assess the maximum allowable charge weight per delay for every point along the tunnel alignment.

The PPVc values of existing soil slopes were calculated from the following formulae:

$$PPVc = Kcg/(\omega Ka) \qquad \text{Equation (2)}$$

where:

Kcg = the critical acceleration at which the slope has a factor of safety of 1.0 against failure (ms^{-2})
g = the acceleration due to gravity (ms^{-2})
ω = the circular frequency of the ground motion ($2\pi f$)
Ka = the magnification factor

In order to obtain Kc, slope stability analyses were performed with varying values of g until a pseudo-static factor of safety was achieved. ω is dependent on the frequency of the vibration, which typically ranges from 20-100Hz due to blasting. A frequency of 30Hz was adopted, as recommended in GEO Report 15, in the assessment.

The peak particle velocity PPV of a rock block was calculated based on the Energy approach by assessing the stability and the downslope displacement of the rock block based on the principle of conservation of energy. The shear strength and stiffness of rock joints with various joint characteristics was also assessed in the analysis.

The vibration limits of existing retaining walls were calculated in accordance with amended EUROCODE 8, Part 5, where a total design force, both static and dynamic, acting on the existing retaining wall structure is calculated.

The stability of existing retaining walls was assessed using the partial factor approach which is recommended in Eurocode 8. The basis of the partial factor approach is that it is possible to share the margin of safety among the different parameters used in the stability analysis. A ratio of overturning and restraining moments, Mo/Mr and the active and restraining sliding forces Fa/Fr was calculated. When the dynamic force was applied to the retaining wall these ratios would be equal to or greater than 1.0. The partial factors applied to the loading and material parameters are shown in Table 1.

The maximum allowable PPV was then calculated from Equation (2).

3.1 5mm/s Contour Reference

Following a number of meetings with Mines Division and GEO, a lower PPV boundary of 5mm/s was adopted an initial baseline for the analysis. There were two reasons for this. Firstly the theoretical zone of influence from blasting is infinite as Equation 1 will always produce a positive PPV for any distance. Secondly, while it can be demonstrated using the methods set out in GEO Report No. 15 that for some retaining walls and slopes the derived allowable PPV could be less than 5mm/s, the conservative approach in the analysis and the need to limit the number of features to be analyzed at the first stage of the process required some compromise as a starting point.

Following the initial stage all potential sensitive receivers within 50m of the 5mm/s contour were reviewed to identify ancient monuments, listed buildings, very old or large retaining walls etc. which may have posed a particular concern.

Table 1: Summary of Applied Loading/Materials and Associated Partial Factors

Loading / Material Parameters	Partial Factors
Dead Load	1.0
Imposed Loads (storage, residential, etc)	1.0
Transient Loads considered as surcharge in Hong Kong (traffic, pedestrian loads, etc)	1.0
Loading / Material Parameters	Partial Factors
Water Pressure	1.0
tan ’ . where ’ is angle of shear resistance including base friction angle (tan b)	1.1
Soil apparent cohesion, c’	1.2

3.2 Generation if Initial 5mm/s Contour Using Utilities and Structures

Peak particle velocity (PPV) contour plots were produced for all areas where blasting is proposed. These plots were presented as a set of contours which were shown as a dashed line, indicating the PPV that will be received at the ground surface when the blast charge weight is calculated using all sensitive receivers except slopes and subject to a maximum 5kg per delay charge weight.

4 ITERATIVE PROCESS OF SLOPE AND RETAINING WALL ANALYSIS

An iterative process was used to arrive at the final version of "Max. PPV's Contour Based on All Sensitive Receivers", after production of the critical “Structures and Utilities” contour line, by selecting relevant slopes and retaining walls for analysis of the maximum allowable PPV. Any slopes or retaining walls that were Consequence to Life Category 3 and could affect a public road were also analysed. The calculated maximum allowable PPVs for these analysed features were then added into the calculation of the maximum allowable

charge weight and a new set of “All Sensitive Receivers” contours produced. If there remained any features inside the 5mm/s “All Sensitive Receiver” contour that had not been analysed, the process was repeated until all slopes and retaining walls within the 5mm/s “All Sensitive Receiver” contour had been analysed. By this process the allowable maximum chargeweight at any point along the length of each adit was determined to avoid exceeding the allowable vibration of any sensitive receiver.

4.1 Regeneration of 5mm/s Contour Lines

At the end of the iterative process described above a final set of contours were generated labelled "Max. PPV's Contour Based on All Sensitive Receivers". These show the contours of Peak Particle Velocity received at the surface when the blast charge weight is calculated using all sensitive receivers including all slopes and retaining walls.

The final results of all sensitive receivers plotted showing the allowable maximum chargeweight along the chainage of the adit, in 3m sections is then tabulated. The critical features are highlighted at each change in the table. Final plans of each adit were also produced indicating the predicted PPV at the surface in 5mm/s, 13mm/s and 25mm/s contours. The combination of these final plans and the allowable chargeweight tables provide a useful tool for the Contractor’s Blasting Engineer to plan the drill and blast works including programming, costs, monitoring and production logistics.

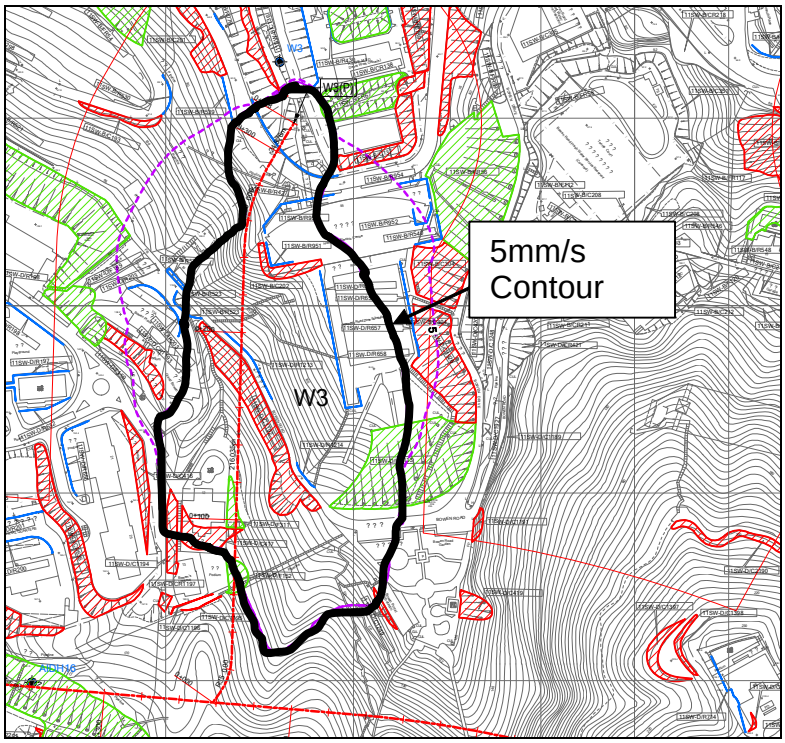

Figure 2. Surface contour for 5mm/s vibration using all Sensitive receivers

5 SELECTION OF SLOPES, RETAINING WALLS AND STRUCTURES FOR INSPECTION

All man-made slopes and retaining walls, features within the final 5mm/s contour plot were selected for visual examination. Where the stability of a feature had been analysed, the assumptions that had been made for this analysis such as groundwater levels and geometry were verified during the inspection. Any signs of distress or adverse geotechnical condition were noted and amendment of the analysis or a recommendation to do further assessment or analysis was then given as necessary. Features that were Consequence to Life Consequence 3 were only inspected briefly to determine if the Consequence to Life Category had been changed and that the feature poses no threat to public roads. This process will require repeating prior to the works commencing as some of the blasting will not take place for up to four years following the initial Blast Assessment.

6 CONCLUSION

The revised requirements for Blasting Assessment detailed in PNAP 178 Appendix A, combined with the very large number of potential sensitive receivers which could be affects by the multiple blasting locations on the Hong Kong West Drainage Tunnel project required a more holistic and sophisticated approach to blasting assessment. While the prescriptive allowable vibrations provided by some utility companies and government departments can be used to determine allowable chargeweights per delay for those sensitive receivers, there is no prescriptive vibration limits for many sensitive receivers such as private structures, historical monuments, slopes or retaining walls.

The use of an iterative approach to assess these features using a limiting chargeweight has reduced the number of features requiring assessment from over 7,000 within a 300m plan radius, to around 1,500 within a 100m plan radius. Three dimensional analysis and projected vibration contour plots further reduced the number of features requiring detailed analysis by taking the revised allowable chargeweights from each feature analysed, putting that into the chargeweight table for each adit and reproducing the projected vibration contour plots. This process usually produced a result were the allowable vibration of all sensitive receivers was satisfied within three or four iterations of the process even for adits with over a hundred potential sensitive receivers.

Despite this, the overall Blasting Assessment required the analysis and inspection of over 600 slopes and retaining walls on Hong Kong Island. The analysis, inspection and documentation required a large resource of personnel including three full time engineers and a large number of par time supporting engineers and technicians. The process of production took over eight months, submission and dealing with comments overlapped the production process by breaking the report down into separate volumes and appendices for each adit, the final report comprising a total of 14 volumes, standing over 600mm high, See Figure 3.

The Blasting Assessment produced at the reference design stage of the project only provides a basis to show that blasting is feasible for the proposed works. It can be adopted or modified by the Contractor to suit his proposed blasting methods. Much of the work will have to be repeated prior to the actual blasting being undertaken. However, it does provide a level basis for Contractors to tender the works with some certainty.

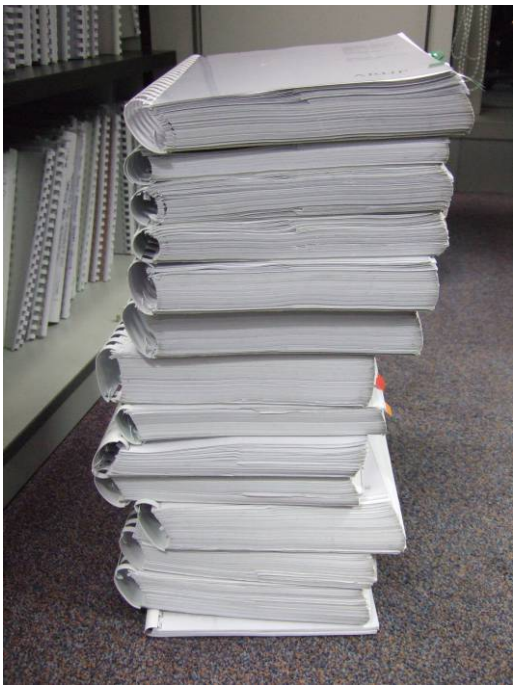

Figure 3. The complete Reference Design Blasting Assessment

REFERENCES

Practice Note for Authorised Persons and Registered Structural Engineers No. 178, Building Department, HKSAR.

Instruction No.1038, Water Services Department, HKSAR.

GEO. 1992. GEO Report No. 15: Assessment of Stability of Slopes Subjected to Blasting Vibration. Geotechnical Engineering Office, HKSAR.

Eurocode 8: Design Provisions for Earthquake Resistant Structures.

Constructional Aspect of Underwater Vacuum Preloading Technique

S.T.C. So, X.F. Han & A.K.L. Kwong
Department of Civil Engineering, The University of Hong Kong
Hong Kong Special Administrative Region, China

ABSTRACT

Vacuum preloading technique incorporating prefabricated vertical drains is one of the most widely used ground improvement methods for improving the engineering properties of soft clays. Although many successful on-shore cases using vacuum preloading technique have been reported, the effectiveness of applying the technique under water has not yet been investigated. Moreover, many technical and operation factors, that play important roles in vacuum consolidation, are also not yet fully understood. To study the feasibility of under water vacuum preloading, two large-scale field tests were conducted. Instruments such as piezometers, vacuum sensors, inclinometers, settlement plates and extensometers were installed to monitor the performance of the system. Vane shear tests and cone penetration tests were conducted before and after vacuum preloading to determine the effectiveness of the operation. This paper documents the constructional aspects of the technique and reports the major findings. The results demonstrate that the stiffness and strength of the soft clay can be effectively improved.

1 INTRODUCTION

Conventional practices of reclamation involve dredging of soft marine deposit from the seabed or deploying prefabricated vertical drains to expedite consolidation process in surcharging method. The former method, inevitably disturbing the seabed habitat, triggering contaminated marine deposit to release toxic substances and clouding up surrounding waters, has increasingly incurred objections from environmentalists. The latter improves the marine deposit in-situ. Owing to the very low undrained shear strength of the marine deposit, the dumping rate of the surcharging fill has to be carefully controlled to prevent bearing failure. The stringent technical requirement results in slow construction. A low cost but effective and efficient alternative is thus in demand.

Vacuum preloading has been an effective soil improvement technique to stiffen and strengthen soft ground without causing adverse environmental impacts. Successful cases of onshore vacuum preloading have been documented in the literature (Shang et al., 1998; Tang and Shang, 2000; Yan and Chu, 2005). The major differences between vacuum preloading and surcharging method are that a) the total stresses of the vacuum consolidated remain unchanged throughout the whole improvement process, b) lateral displacements are inward as opposed to those in surcharging and c) bearing failure will not occur as a result of suction application. The authors believe that the merits of vacuum preloading render it an environmentally friendly substitute of surcharging method and its use can be extended to an underwater environment.

Theoretically, the mechanism of underwater vacuum preloading is no difference from that of the onshore application. However, there are challenges during implementation. To testify its practicality, two field tests were carried out (So, 2007; Kwong et al., 2008). The first test has the objective in identifying practical problems during the membrane installation process. Since it was for preliminary purpose, the test site had minimum instrumentation. The monitoring data and experience gained in the first test served as a reference for the second, which was carefully planned and heavily instrumented. This paper presents the set-up of the two field tests and the analyses of the monitoring data. Effectiveness of vacuum preloading with respect to implementation and degree of improvement is also discussed.

2 PRELIMINARY FIELD TEST

2.1 Site Description

The first preliminary test was conducted on a 30 m by 30 m site located on the northern river bank of the Shenzhen River close to Deep Bay, China. The 0.9 m thick fill layer on the ground surface was underlain by a layer of 5.2 m thick dark marine deposit. A layer of fine sand and shell existed underneath the marine deposit.

2.2 Configuration of Preliminary Test

To minimize tidal influence, the test was carried out in a 2.6 m deep excavated basin which was pumped dry initially. The bottom of the basin was covered by two layers of 300 mm thick loosely compacted sand sandwiching a horizontal network of perforated pipes. The main pipe was connected to a vacuum pump on the ground surface. After filling the basin with water to a depth of 2 m, two large pieces of water-tight geo-membrane, each manufactured by joining rolls of geo-membrane together before delivery to site, were sequentially sunk onto the sand drainage layer with the assistance of four employed divers. As the practicality of the underwater vacuum preloading technique was the focus of this preliminary test, vertical drains were not installed. Single-way drainage was assumed during vacuum-assisted consolidation. A piezometer was installed about 1 m below the excavated level before laying the horizontal sand drainage layer and four surface settlement plates were placed above the geo-membrane in the four different quadrants of the vacuum-consolidated area (at about mid-distance between the centre and the edge). In the sand drainage layer, a vacuum gauge was installed to measure the vacuum attained and served as an indicator of the water-tightness of the geo-membrane.

2.3 Monitoring data and analysis

The variation in applied vacuum, measured pore pressure and settlement with time are shown in Figure 1. The measured pore water pressure and applied vacuum are represented by the solid and dotted lines, respectively. Settlements are represented by the solid curves with marks.

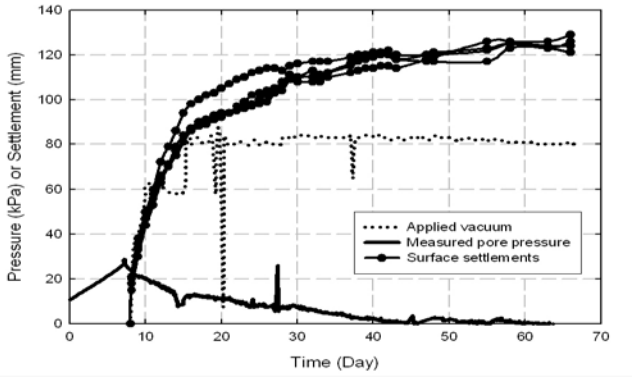

Figure 1: Monitoring data of preliminary field test

The 11 kPa initial piezometric reading indicates that the water level was approximately at the excavated level at the time of measurement. The pore pressure increased by 20 kPa after filling the basin with 2 m of water above the excavated level.

A vacuum of 80 kPa was reached in approximately a week in the sand drainage layer. The halt in the increase in vacuum at about 60 kPa 3 days after the start of pumping was suspected to be due to suction leakage through the gap between the geo-membrane and marine clay. The gap was quickly sealed by manually placing big pieces of stones along the edge of the geo-membrane. The vacuum suction continued to rise to 80 kPa within a day afterwards. Unlike conventional construction of onshore vacuum preloading, burying geo-membrane in a circumferential trench as a means of sealing was not required. Stone placed on geo-membrane sink and pressed the geo-membrane into soft marine clay. If filling work is carried out simultaneously with vacuum consolidation, the fill also helps sealing the gap. To guarantee water-tightness of the vacuum system, it is recommended that the geo-membrane should extend further to lengthen the drainage

path. The test demonstrated the trenchless construction is effective to ensure water-tightness and can facilitate faster progress in reality.

Another way to evaluate the effectiveness of the vacuum preloading is to compare monitored settlement with theoretically calculated value. Pre-consolidation pressures of the clay layer at different depths were first determined in accordance with the geological profile of the site, assuming lowest tidal level and fill unit weight, bulk unit weight of marine clay and void ratios of marine clay samples. Assuming the decrease in pore pressure as a result of vacuum application varied linearly from 80 kPa to 0 kPa from top to bottom of the marine clay layer, and with compression and recompression indices determined from laboratory consolidation test, the surface settlement at the centre of the vacuum consolidated zone was estimated to be 175 mm. If surface settlement immediately outside the geo-membrane was assumed zero and linearly varied across the site, the surface settlement measured by the settlement plates would take half of the value of the surface settlement at the centre of the site. However, from experience, significantly less surface settlement occurred only near the edge. Thus, surface settlements measured by the settlement plates should be some values between 0.5 to 1 time the settlement at the centre. The ultimate settlement of around 130 mm as shown in Figure 1 was in good agreement with the estimate. In terms of settlement, the test demonstrated that the application of vacuum could effectively consolidate soft clay in an underwater environment.

2.4 Experience gained

Water-tightness of the geo-membrane is the key to the success of vacuum preloading. The geo-membrane should be handled with care during delivery to site and installation. A puncture in the geo-membrane can result in a total failure. Geo-membrane was delivered to site in a roll. Unfolding it in water was difficult. It is better to unfold it on the ground and pull one edge into the water. Every part of the long leading edge of the geo-membrane should advance in the same pace to avoid tangling and tearing as a result of differential movement in water. Owing to the large size, geo-membrane should be positioned in water with some mechanical aid such as motorized boat. Geo-membrane with a density less than water and large air bubbles trapped underneath geo-membrane rendered the laying process difficult. Using geo-membrane with a higher density than water or attaching weights to the geo-membrane can solve the problem. Trapping of air bubbles can be prevented by allowing bubbles to escape through air vents in the geo-membrane which should be tightly sealed afterwards. Sinking one of the edges of the geo-membrane first and then getting rid of air from the underneath of the geo-membrane until the opposite edge is sunk into the water can also eliminate the problem of air bubbles.

3 COMPREHENSIVE FIELD TEST

3.1 Site Description

Figure 2: Location map of comprehensive field test

The second field test was conducted in a rectangular pond 2 km north of the Shenzhen Airport as shown in Figure 2, where the geological condition is similar to that in Hong Kong. The 2500 m^2 area modified by vacuum preloading was square in shape and 1.5 m below water. According to ground investigation prior to the field test, a 7 m thick clay layer lies at the bottom of the pond.

3.2 Field Test Procedure

1) Water was totally pumped out from the pond.
2) A 600 mm thick sand layer was placed on the bottom of the pond to serve as a working platform.
3) Prefabricated vertical drains were installed in a 1.2 m centre-to-centre in a triangular pattern to a depth of 7 m.
4) Instruments were installed.
5) Vane shear tests and cone penetration tests were also conducted to reveal initial conditions of the clay.
6) A horizontal network of perforated pipes was laid on the sand layer connecting the prefabricated vertical drains hydraulically to three vacuum pumps on the ground surface.
7) The pond was filled with water.
8) When steady hydrostatic pressure as revealed by the installed piezometers was reached in the clay, a piece of custom-made 2.0 mm thick geo-membrane was laid on the sand cushion in an underwater environment.
9) Vacuum was applied to the sand cushion for approximately three months. Monitoring was ongoing during this period.
10) The pond was dewatered again.
11) Vane shear tests and cone penetration tests were conducted to evaluate the effectiveness of the ground improvement

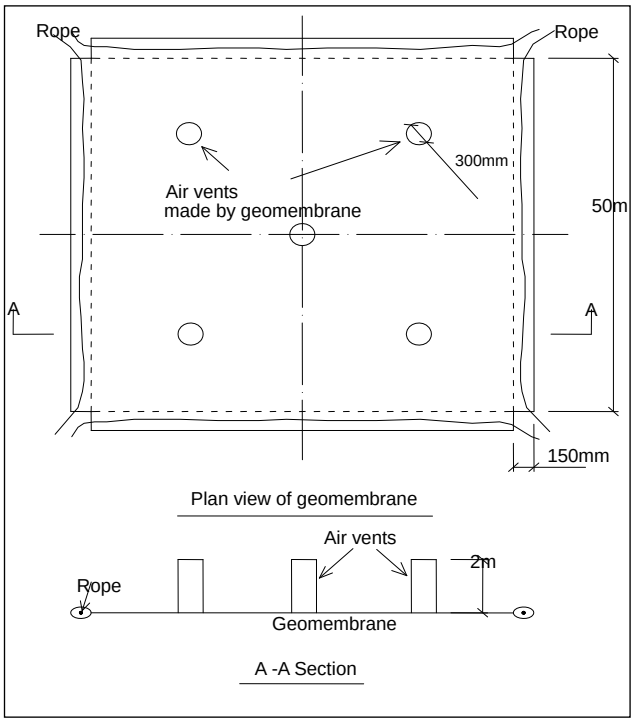

Figure 3: Custom-made geo-membrane

In accordance with the experience gained from the preliminary field test, a number of special features as illustrated in Figure 3 were incorporated into the design of the custom-made geo-membrane. Air bubbles easily trapped underneath the geo-membrane during placement were expelled through five air vents. The vertical pipe-shaped air vents were made of the same material as the geo-membrane and attached to the geo-membrane with special glue. Water-tightness was a necessary requirement for the joint between the air vents and the geo-membrane. Difficulties in steering and unfolding the large geo-membrane in water were overcome by controlling the four long ropes attached to the edge of the geo-membrane. Sinking of the geo-membrane was assisted by the weight of steel rods attached to the geo-membrane. To ensure achieving a high vacuum in the sand cushion, a tight seal between the clay and the geo-membrane was secured by placing sand bags along the edge of the geo-membrane as in the preliminary field test. The sand bags also helped fix the geo-membrane in position in water.

3.3 Instrumentation

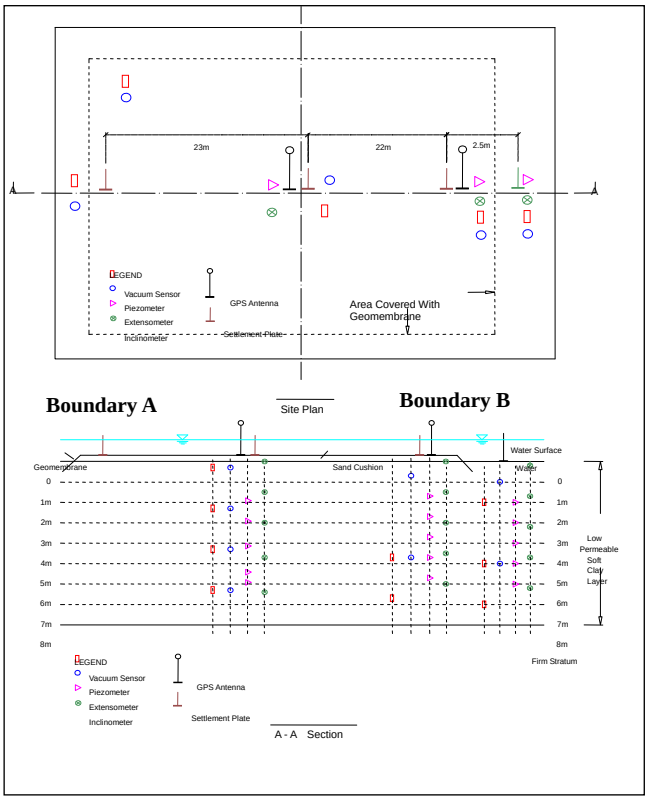

Figure 4: Instrumentation plan

To comprehensively monitor the field test performance, the site was heavily instrumented with piezometers, vacuum sensors, in-place inclinometers, extensometers, surface settlement plates, and moisture probes as shown in Figure 4. Calibration of instruments was carried out before installation. Owing to difficult site access, wireless data transmission was adopted. Except surface settlement plates, each instrument was connected to a data logger. Readings were sent to the office in The University of Hong Kong via a GSM modem. This technology not only facilitated remote but also real-time monitoring. Data sampling frequency could also be altered remotely. The whole system was powered by solar energy.

3.4 Monitoring data and analysis

Vacuum was applied to the treatment area for 96 days. The variation of measured vacuum in the sand cushion during the period is shown in Figure 5. A vacuum of approximately 80 kPa was maintained for 62 days. Vacuum was elevated from atmospheric pressure back to 70 kPa within two days after occasional suspensions of vacuum for maintenance and additional installation works. The achievement of the high vacuum and high reloading rate attributed to the excellent water-tightness of the geo-membrane and simple sealing technique mentioned before. The level of vacuum achieved in the sand cushion did not highly depend on the number of vacuum pumps. However, higher vacuum could reach deeper clay. Pore pressure at 1 m depth reached -70 kPa and became stable quickly due to the dual influence of vacuum from the sand cushion and vertical drain.

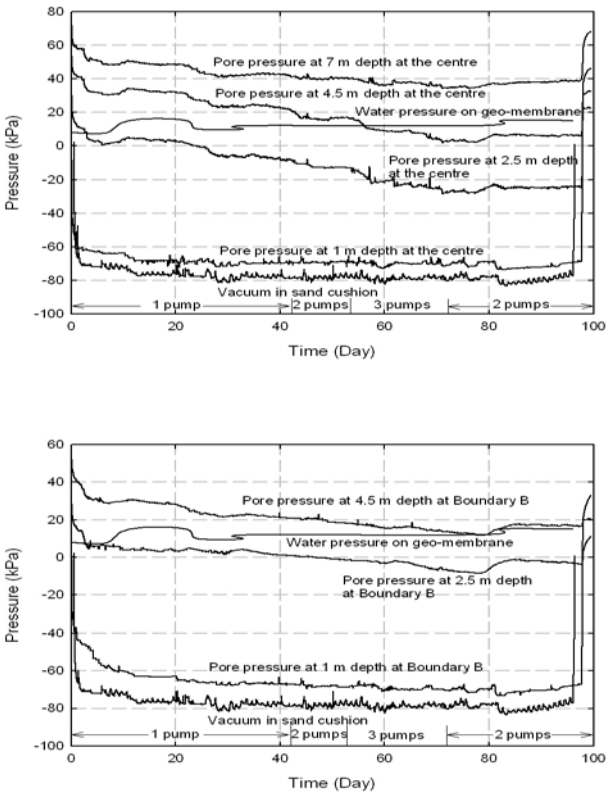

Figure 5: Pore pressure variation with time

Figure 6 shows the spatial distribution of pore pressure in the vacuum-consolidated clay 80 days after the start of pumping. Since vacuum sensors were installed at the centre and edge of the treated zone, the variation of pore pressure between the two monitoring points was assumed to be linear for ease of illustration. Uniform distribution of pore pressure was observed in the top 1 m. For depth below 1 m, the pore pressure at the centre was lower than that at the edge. The higher pore pressure at the edge was due to the inflow of water into the treatment zone, neutralizing the negative pore pressure.

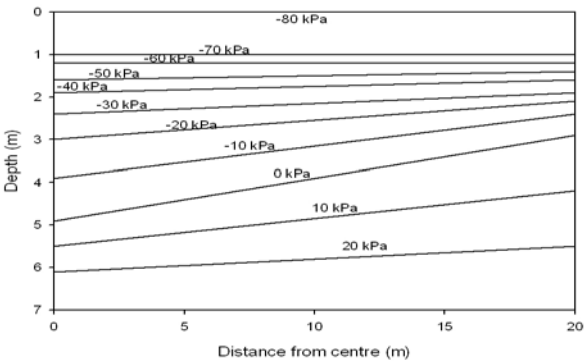

Figure 6: Pore pressure distribution after 80 days

To evaluate the effectiveness of vacuum preloading, theoretically predicted settlement and undrained shear strength are compared with the measured values after the application of vacuum. Surface settlements and settlements at different depths are shown in Figure 7. A maximum surface settlement of 890 mm, which was 13% of the initial thickness of the clay layer, was reached on the 96th days at the centre of the treatment zone.

Settlements occurring at various depths suggested that vacuum preloading was effective for the entire clay layer. When uncovering the vacuum-preloaded clay after test, a concave shape was observed in the ground.

According to laboratory tests conducted on samples taken prior to application of vacuum, the average compression index and void ratio were determined to be 0.50 and 2.06, respectively. Assuming the initial void ratio of the whole layer of marine clay was uniform and took the value of 2.06, with increases in vertical effective stress being 80 kPa, the theoretical average settlement is determined to be 990 mm. The measured settlement is almost 90% of the theoretical values, showing that underwater vacuum consolidation is very effective with respect to settlement.

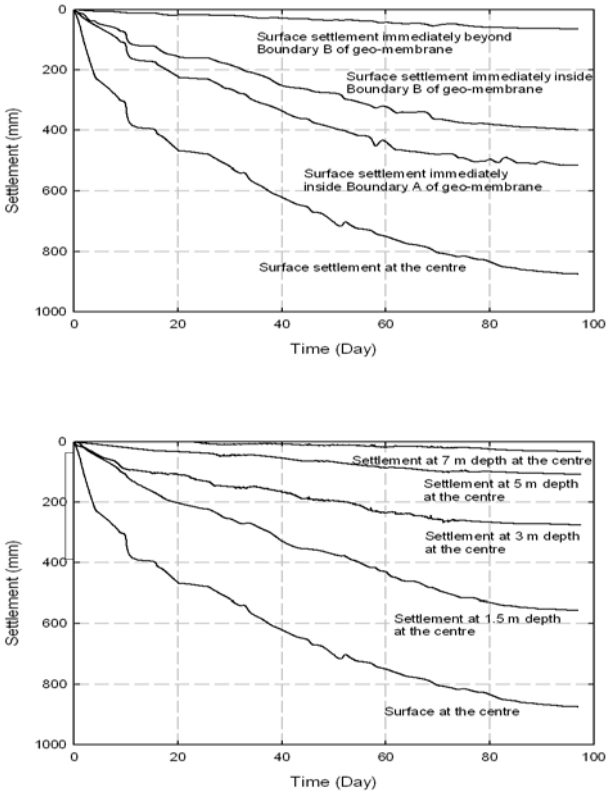

Figure 7: Settlement records

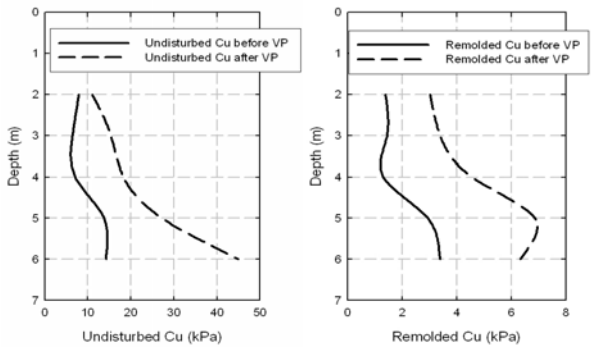

Figure 8: Undisturbed and remolded undrained shear strengths before and after vacuum preloading at the centre of the site

Figure 8 shows the undisturbed and remolded undrained shear strength before and after application of vacuum. If a linear regression line was drawn for the undisturbed undrained shear strength before application of vacuum, it would pass through the origin, suggesting the clay layer was normally consolidated initially.

There were substantial increases in undrained shear strengths after vacuum was applied. It is interesting to note that the increase in undisturbed undrained shear strength varied from less than one-fold near the surface to three-fold at the bottom of the clay layer. According to critical state soil mechanics, the theoretical increase in undrained shear strength before and after application of vacuum is a function of initial vertical effective stresses and its increase, i.e.,

$$\frac{\sigma_{v0}^{'} + \Delta u}{\sigma_{v0}^{'}}$$

where $\sigma_{v0}^{'}$ is the initial vertical effective stress and Δu is the reduction in pore pressure due to vacuum application. The ratio varies approximately from 17.1 near the surface to 3.3 near the bottom. However, the measured increases are in general smaller than the theoretical ones, especially those values for clay near the surface. The smaller increase may be due to the following reasons. Clay close to the vertical drains and those underneath the sand cushion was subjected to the largest consolidation stresses (including the effect of seepages forces). The stiffened clay shared more vertical effective stresses than the clay away from the vertical drains. Clay at mid-distance between adjacent drains was less consolidated. Vane shear tests conducted at locations in the middle of adjacent vertical drains thus measured lower values. The authors believe that different undrained shear strength would be obtained from vane shear test carried out at different horizontal position between adjacent vertical drains.

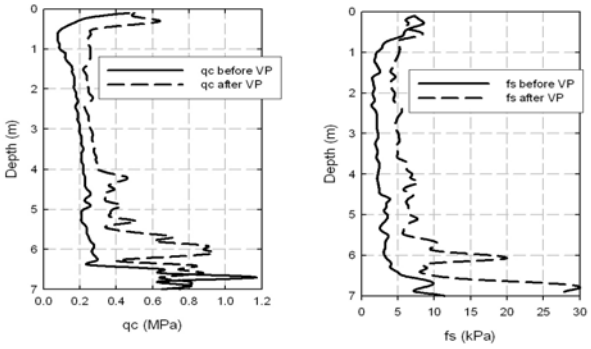

Figure 9: CPT resistance before and after vacuum preloading at the centre of the site

The increase in CPT resistance at the centre of the treatment area as shown in Figure 9 demonstrated the effectiveness of vacuum preloading.

4 CONCLUSIONS

Two field test studies on underwater vacuum preloading were reported. The second field test was designed on the basis of the experience gained from the first field test. The feasibility of the implementation of the technique was verified through successful installation of geo-membrane, maintenance of high vacuum underneath the geo-membrane by simple sealing method, propagation of the negative pore pressure deep into the improved soil, and significant gain in undrained shear strength and cone penetration resistance. In addition, automatic data collection and wireless data transmission systems were proved manpower and time saving when monitoring sites with difficult accessibility.

ACKNOWLEDGEMENT

Financial support provided by Research Grants Council Project No. HKU 1/03C "Land development by environmental vacuum preloading technique" of the Hong Kong Special Administrative Region Government for this project is gratefully acknowledged. However, the contents of this paper do not necessarily reflect the views and policies of the Hong Kong Special Administrative Region Government. The support of Nanjing Hydraulic Research Institute is also gratefully acknowledged.

REFERENCES

Kwong, A.K.L., Han, X.F., Tham, L.G., Lee, P.K.K., Zhao, W.B. 2008. A field test study on under water vacuum preloading method. The 6th International Conference on Case Histories in Geotechnical Engineering, in press.

So, T.C. 2007. Field trial of submarine vacuum preloading. In K.C. Chang, H.P. Tserng, Y.W. Chan, S.H. Hsieh, L.M. Chang (ed.), The 4th Civil Engineering conference in the Asian Region, 25-28 June 2007, The Asian Civil Engineering Coordinating Council.

Shang, J.Q., Tang, M. and Miao, Z. 1998. Vacuum preloading consolidation of reclaimed land: a case study. Canadian Geotechnical Journal, 35: 834-841.

Tang, M. and Shang, J.Q. 2000. Vacuum preloading consolidation of Yaoqiang Airport runway. Géotechnique, 50: 613-623.

Yan, S.W. and Chu, J. 2005. Soil improvement for a storage yard using the combined vacuum and fill preloading method. Canadian Geotechnical Journal, 42: 1094-1104.

Automated Wireless Groundwater Monitoring System at Po Shan Road

I.J. Solomon & W.M. Chan
Fugro Geotechnical Services Ltd, Hong Kong
A.J. Westmoreland
Maunsell Geotechnical Services Ltd, Hong Kong
E. Tang
China State – China Railway Joint Venture, Hong Kong

ABSTRACT

An automated wireless groundwater monitoring system has been installed on the hillside above Po Shan Road in the Mid-Levels region of Hong Kong as part of a project to lower the groundwater table in order to improve the stability of the hillside against large-scale slope failure. The automatic monitoring system is based on a state-of-the art, self-organising network of wireless sensor. The paper provides an overview of the monitoring system and the challenges encountered in its implementation. The paper also looks at the methods used to deliver the information generated by the system to the project stakeholders in real time, including the use of websites, PDAs and mobile phones.

1 INTRODUCTION

1.1 Project background

In Hong Kong, a combination of high population density and mountainous terrain has led to extensive development on and around the many steep slopes in the territory. Every summer, Hong Kong experiences heavy sub-tropical rainstorms that can saturate the slopes, increasing the likelihood of landslips.

The slope above Po Shan Road in Mid-Levels has been affected in the past by significant landslides, and has been the subject of extensive monitoring and geotechnical works to improve its stability.

The previous geotechnical works were constructed some 20 years ago and consisted primarily of horizontal drains drilled into the hillside. However, maintenance of these drains has proven difficult, and the implementation of an improved groundwater drainage system was recently commissioned by the Geotechnical Engineering Office of the Civil Engineering and Development Department under Contract No. GE/2005/45.

The main works under the current contract was the driving of two 3.5m diameter horizontal access tunnels about 300 metres into the hillside. On completion of the tunnels, approximately 200 small diameter sub-vertical drains (up to 104m in length) were drilled up through the tunnel roof into the overlying soil layers of the slope (Figure 1).

The new system of tunnels and sub-vertical drains is intended to control the levels of ground water that build up in the slope during the summer rains, thus reducing the risk of a large-scale, deep-seated landslip occurring at this location.

The contract also provided for other risk mitigation works at various locations on the site, intended to reduce the risk of shallow landslides and loose debris affecting the developed area.

A detailed description of the maintenance and geotechnical works is beyond the scope of this paper, and they are described in detail elsewhere (Ho et al. 2008).

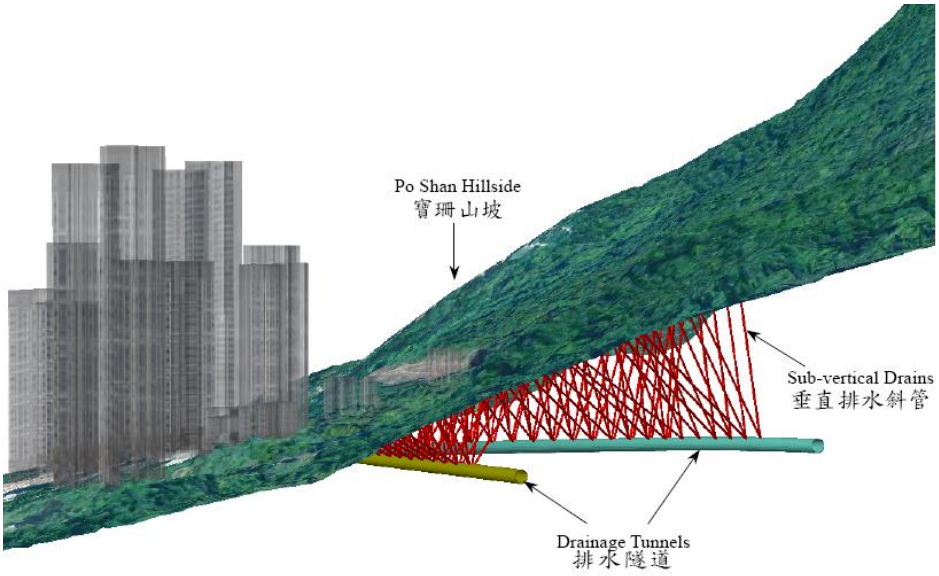

Figure 1: New groundwater drainage system

1.2 Instrumentation Requirements

In order to monitor groundwater levels in the slope above the new groundwater drainage system during and after construction, a real time groundwater monitoring system was specified in the contract, augmented by some conventional manual instrumentation to monitor settlement and deformation in the slope above the new drainage system. The instrumentation installation and monitoring was carried out by Fugro Geotechnical Services Ltd, under a sub-contract awarded by the main contractor, China State-China Railway JV. The system was installed and commissioned between late December 2006 and the end of February 2007.

The instrumentation to be installed under the contract is summarised below:

- 1 real time automated wireless groundwater monitoring system with approximately 50 sensors
- 3 extensometers (plus take over 5 extensometers installed under a previous contract)
- 3 inclinometers (plus take over 2 inclinometers installed under a previous contract)
- 64 deformation monitoring points
- 25 tilt monitoring points
- 6 vibration monitoring points

The manually read conventional instrumentation (extensometers, inclinometers, deformation, tilt and vibration monitoring points) was unexceptional, and will not be described further in this paper.

In contrast, the groundwater monitoring system installed was a state-of-the-art system using wireless networking and the Internet to deliver groundwater information directly to stakeholders in real time, without human involvement in the entire process.

The specification for the groundwater monitoring system required that it be based on self-organising wireless dataloggers sending data to a central base station without cabling or the need for line-of-sight between sensors and the base station. Data received by the base station was to be sent off-site to a remote computer system for processing, verification, storing and checking of threshold levels. The processed and verified data was then to be made available on a website accessible to authorised users, with the system automatically sending out emails and SMS text messages in the event that any reading had exceeded a threshold level.

2 AUTOMATED WIRELESS GROUNDWATER MONITORING SYSTEM

2.1 Overview

A simplified schematic diagram of the automated groundwater monitoring system implemented is shown below in Figure 2:

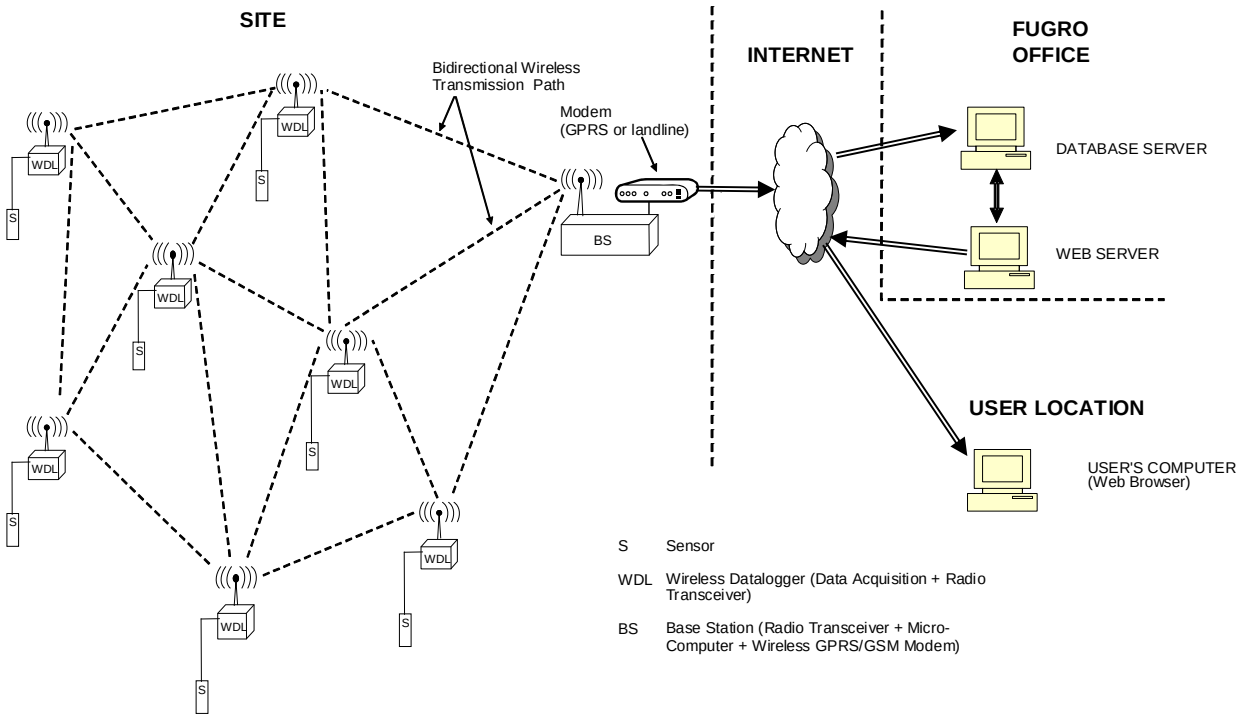

Figure 2: Simplified schematic of Automated Wireless Groundwater Monitoring System

The system may be conveniently split into major subsystems as follows:

- Instrumentation
- Data acquisition system and wireless network
- Base station (data transmission system)
- Data management system (database and web servers)

The instrumentation comprises intelligent piezometers installed in boreholes. At the top of each borehole is a datalogger that automatically reads the piezometers every five minutes and transmits the readings to a base station via a wireless network. The base station collects the readings from all the wireless dataloggers and then sends them over the Internet to an off-site data management system. The data management system allows users to view the current (and previous) readings from a website.

Each subsystem is described in further detail in the following sections.

2.2 Instrumentation

The groundwater levels in the slope are measured using a total of 52 In-Situ Inc. “LevelTROLL” Automatic Groundwater Monitoring Devices installed in 40 boreholes distributed across the site (Figure 3). Each borehole has either one or two LevelTROLLs installed.

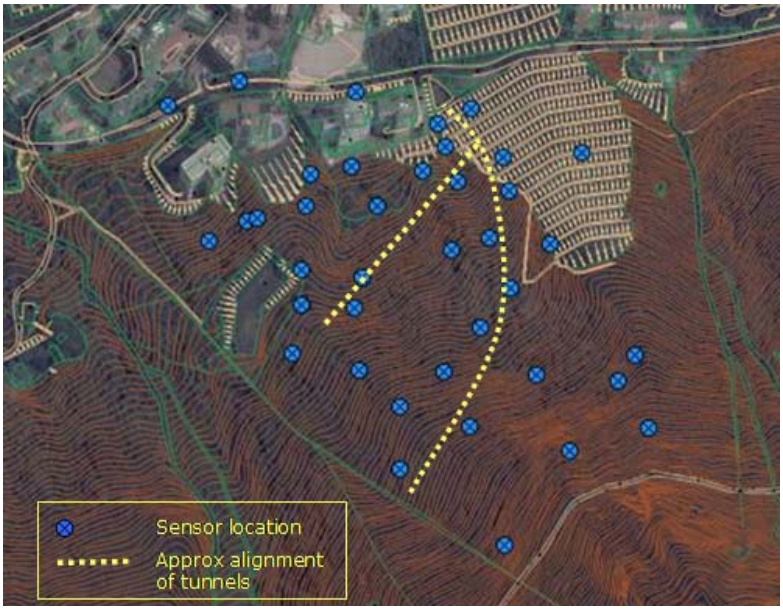

Figure 3: Site plan showing sensor locations

The LevelTROLLs are intelligent piezometers comprising a pressure sensor, datalogger and battery pack within an 18mm diameter package. The datalogger memory has a capacity of 100,000 data points and the battery pack has a maximum life of five years and/or two million readings. For this application, the LevelTROLLs were used in a real-time mode, with the current reading being sent up a cable to the top of the borehole as an analogue voltage signal, as well as being simultaneously logged and stored in the internal memory, as a redundancy measure.

The LevelTROLLs measure absolute pressure, which means that the readings are influenced by fluctuations in atmospheric pressure. A barometric pressure sensor was installed at one of the wireless datalogger locations in order to provide a real-time correction for these fluctuations.

2.3 *Data acquisition system and wireless network:*

A wireless datalogger was located at the top of each borehole to read the LevelTROLL(s) in that borehole and forward the readings to the base station. Forty wireless dataloggers were installed in all, one at each borehole. The wireless datalogger system was a proprietary system developed by Fugro for geotechnical monitoring applications, and had previously been used in other projects in Hong Kong, although not on such a large scale as this.

The wireless dataloggers were housed in lockable stainless steel enclosures installed at the top of the borehole. The dataloggers were powered by alkaline batteries installed in the same enclosure, with a nominal life of three months. When an enclosure was sealed, the only part of the system exposed was the antenna, cable and cable support pipe, giving a very secure and rugged system (Figure 4).

Up to four sensors may be connected to each wireless datalogger, and up to 32 dataloggers may be assigned to a base station, giving a maximum capacity of 128 sensors per base station. The wireless dataloggers were programmed to read the sensors every five minutes and then transmit the readings, together with battery status information, to the base station. If the datalogger was out of service, for example during battery replacement, the groundwater readings would continue to be stored in the LevelTROLL's internal memory, and could be manually downloaded if required.

Figure 4: External and internal view of wireless datalogger enclosure at top of borehole

The wireless dataloggers (together with the base station) act as nodes in a self-organising wireless network. In a self-organising wireless network, each node can act as a receiver or a transmitter, and can communicate directly with any of the other nodes, but in practice will only communicate with the nearest neighbour nodes. Data received by a node that it is intended for another node will be forwarded to a neighbour node closer to the intended destination, until that destination is reached. In the current application, the sensor readings and battery status information will hop from wireless datalogger to wireless datalogger until they reach the base station.

Self-organising wireless networks of this type are very robust, as when a node is taken out of service, the data will automatically find a different route. Similarly, if a new node is added, no reconfiguration of the network is necessary.

Because with this type of wireless network the data hops from node to node, it is not necessary to have a direct line-of-site connection between each datalogger location and the base station, as is the case with many conventional wireless data acquisition systems. Not needing a line-of-sight connection was a significant advantage for this project, where the datalogger locations were widely spaced in heavily vegetated and hilly terrain.

The radio transmitters in the wireless dataloggers are low powered, and operate in a license-free band. The maximum line-of-sight transmission range for the dataloggers used is around 100m (around 300m with the latest generation design), however the achievable range is heavily dependent on site conditions, such as the vegetation and other obstructions encountered on this project.

2.4 Base station

The base station is a small industrial computer system running the Linux operating system, fitted with a wireless transceiver similar to those in the wireless dataloggers. The base station is used to collect the readings from all of the wireless dataloggers at regular intervals. The collected readings are stored in non-volatile memory in the base station, and a backup copy is made on a removable Compact Flash memory card. The collected data is then transmitted over the Internet to the data management system, by an FTP server built into the base station.

In order to add redundancy to the system and thus increase overall reliability, two base stations were installed, each with different power and Internet connection arrangements. One base station was located at the foot of the slope in a steel enclosure (Figure 5), powered by a combination of batteries and a solar panel, and connected to the Internet over a GPRS wireless network. The other base station was installed inside a container office adjacent to the tunnel portal, powered by mains electricity, and connected to the Internet via a landline. The base stations operate in a redundant manner, with the wireless dataloggers able to communicate

with either base station. A datalogger will send data to the nearest base station, but if that base station becomes unavailable, the datalogger will automatically switch to the other base station.

Figure 5: Base Station located at foot of slope

2.5 Data management system

The data management system was located in Fugro's offices, approximately 20km from the site (although the location is not important, and could be anywhere in the world with an internet connection). The data management system was hosted on a Windows server containing the following key software sub-systems:

- An interfacing module to receive real-time readings from GEO's rainfall monitoring system via a leased line, and store them the database.
- A staging area for data received from the FTP servers in the base stations before it is loaded into the database.
- A loader module to retrieve new files from the staging area and load their readings into the database.
- A database system to process and store the readings
- A web server connected to the database to allow users with an Internet connection to check system status, to view the stored readings in text and graphical form, and to generate reports
- An FTP server for storage and downloading of generated reports

The interfacing and loader modules were already in existence and proven on previous projects, requiring only minor customisation and modification to suit the specific project requirements.

The database system was based on Fugro's mature and proven GIMS (Geotechnical Instrumentation Management System) application. This is a multi-user database system built on the Oracle platform, with a long and successful record of use on large-scale instrumentation projects (Solomon et al. 2001; Chan et al. 2003).

Readings loaded into the database are checked automatically against predetermined thresholds, and if the thresholds are exceeded, the system will issue automatic alerts via SMS text message to key personnel, who may then check the readings via the website hosted on the web server.

The web server was similarly based on work carried out for previous projects, although a reasonably significant amount of project-specific customisation was required. The web server was configured so that it could provide two user interfaces, one for a conventional desktop computer, and one with limited functionality and small page size, intended for a PDA or smartphone with internet browsing capability.

The main user interface allows two different levels of access, depending on the user login details. Users with "Observer" access can only view readings and download reports and so on. Users with "Control Access" have the additional ability to configure parameters such as the threshold levels used to trigger the SMS text messages sent to users. The PDA user interface allows only "Observer" access.

Further information on the user interface is provided in the following section.

2.6 Challenges

The major challenges encountered were due to the nature of the site. The slope covers an area of approximately 400m by 400m, is very steep, with gradients of approximately 35°, and is heavily vegetated. Many of the sensors were located in locations that were both difficult to access, and surrounded with physical obstructions that interfered with the transmission of the wireless signals (Figure 6).

Figure 6: Typical installation conditions for wireless dataloggers

Initially, problems were encountered with intermittent data transmission between wireless loggers, mainly in locations where there were physical obstructions and heavy vegetation in the upper parts of the slope, but also on occasion in lower locations where construction activities related to the surface drainage improvements were being carried out.

These difficulties were overcome by installing repeaters that provided alternative transmission routes between the wireless dataloggers in order to maintain connectivity to the base station. It was necessary to install a total of fifteen repeaters before consistent and reliable data transmission was achieved. The repeaters were essentially identical to the wireless dataloggers, but with no sensors attached.

During the initial period while these issues were being addressed, no data was lost, due to the ability of both the wireless dataloggers and the sensors themselves to store the readings in their own internal memory.

3 USER INTERFACES AND DATA DELIVERY

3.1 Overview

Three main channels are used to deliver data and information to the users. These are a conventional website, SMS text messages, and a website optimised for small display such as a PDA or smartphone with internet access.

The conventional website is the interface most commonly used by users, as it offers the most functionality. SMS text messages are used to communicate to users that a sensor reading has exceeded a predefined threshold level. The PDA website offers limited functionality, but is very convenient for allowing users to check the status of a sensor after they have received an SMS message advising that a threshold had been exceeded.

3.2 Main website

After the user login process has been completed, the main website opens with an overview page (Figure 7). The overview page lists the current summary status of the health of each sensor (time of last reading, current communications / power status and so on), and identifies any sensors whose readings currently exceed the threshold level. The overview page also contains a site plan (aerial photo overlaid with an engineering drawing) showing the sensor locations over the site.

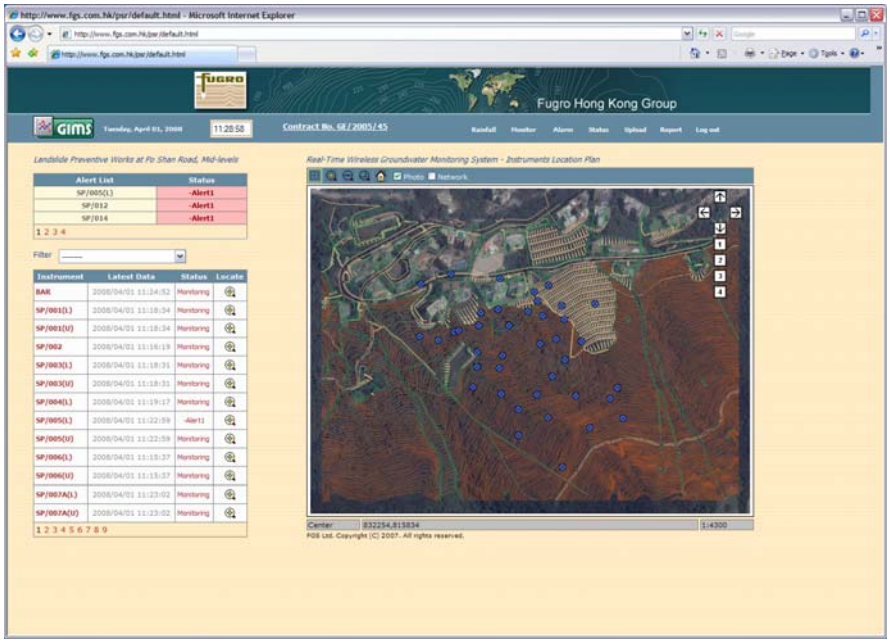

Figure 7: Website overview page

The user may zoom in and out of the site plan. Clicking on the instrument symbols allows the user to obtain further detail of the instrument, and where applicable an installation photo (Figure 8). By selecting instruments from the list, users may retrieve sensor and rainfall readings for a specified time period, either in graphical or tabular format (Figure 9). From here data may be exported as a standard Excel spreadsheet for further analysis.

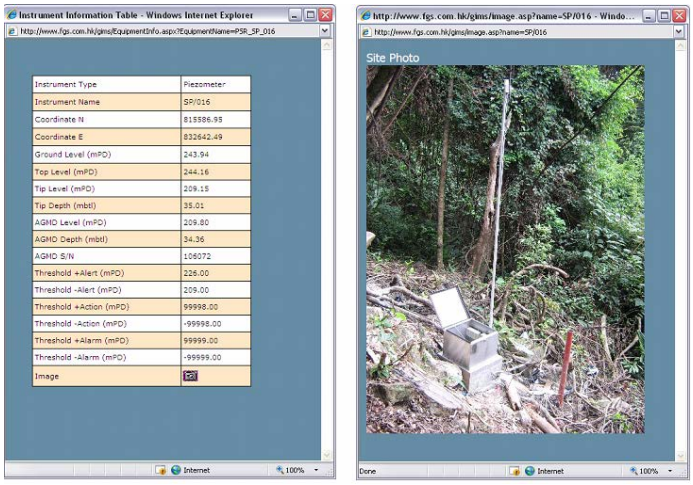

Figure 8: Clicking on the instrument symbols retrieves sensor information and installation photo

The menu bar at the top of the website provides further functionality to the user, for example the ability to retrieve rainfall data for a particular time period, check the battery status of the wireless dataloggers and base

station, manually upload data retrieved from the sensors when its datalogger was being serviced, and to generate reports. Report generation is automatic, and is done by selecting various parameters in a sensor checklist (Figure 10). Once the required sensors and parameters are set up, the system will proceed to generate the reports as PDF files and store them on the FTP server, from where they may be downloaded.

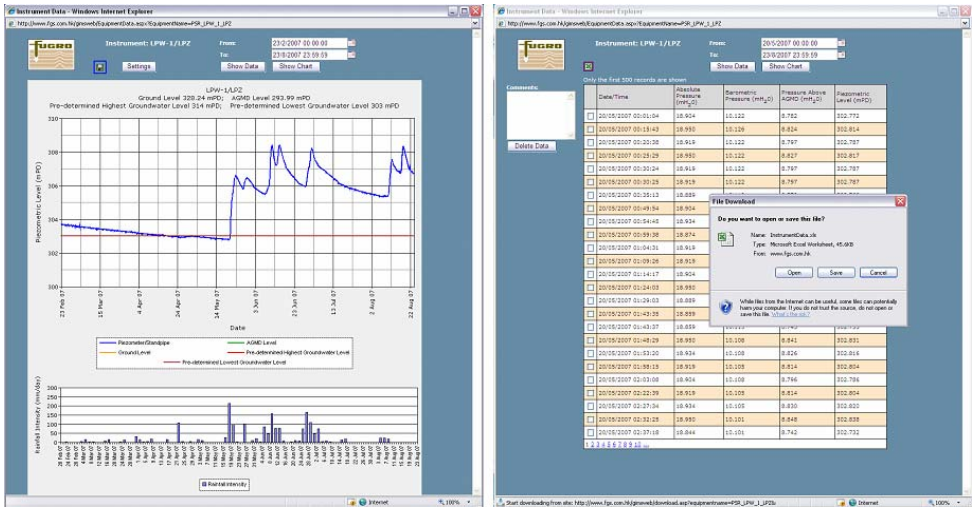

Figure 9: Retrieving data for specified time period in graphical and tabular format, then export to Excel

select instruments and reporting parameters to generate hard copy reports:

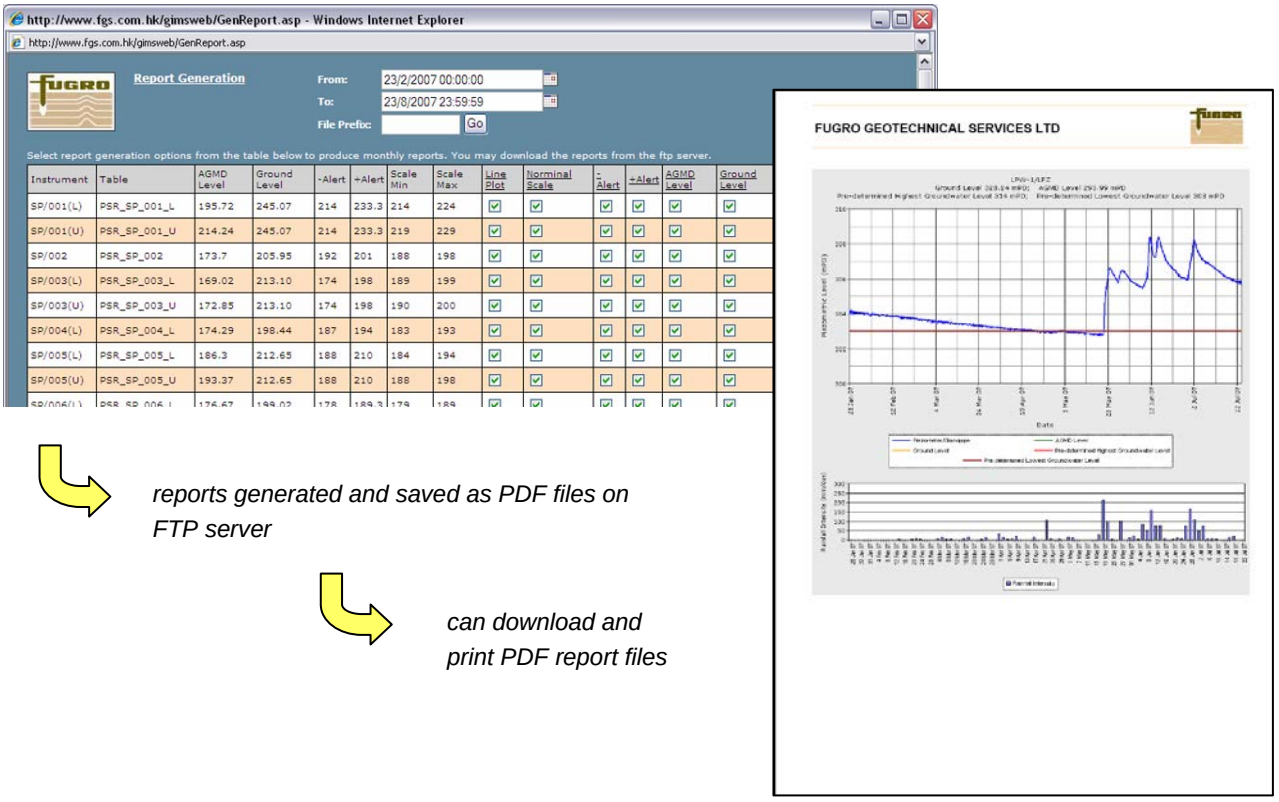

Figure 10: Automatic generation of PDF report files

3.3 SMS text messages

Because the site personnel with an interest in the instrumentation readings would not be sitting at a computer on a regular basis, but would be carrying a mobile phone, SMS messages were considered a practical method by which users of the system could quickly be notified of events requiring their attention, so that they may then know to check the website and take appropriate action.

The database system would automatically check all incoming readings and if they were found to have exceeded the predefined threshold values, an SMS message containing summary information would be sent out to a list of recipients. SMS messages were also triggered to notify power or communications failures if data had not been received within a defined period.

Initially SMS messages were sent out via a third party service using an internet-based system, a system that had previously been used by Fugro. However later in the project a direct transmission mechanism was adopted, with the SMS messages sent directly from a mobile phone connected to the database server, thus giving Fugro more control of the communications process.

3.4 PDA website

The use of smart phones and PDAs as mobile internet connection points is becoming more common. This offers the opportunity for users to gain access to the monitoring information at any time, whether or not they have access to a desktop computer.

The ability to access the system via a smartphone or PDA allows a user quickly to obtain additional information, such as trends, or readings from adjacent sensors, that cannot be included in an SMS message, which by its nature is brief and text based.

Initial trials revealed that the main website described above was difficult to use on a PDA for a number of reasons including:

- physical layout considerations; the website was designed to be used on a widescreen desktop monitor with a resolution of approximately 1400 by 800 pixels, not the typical PDA display of 240 by 320 pixels; this meant either that only a small portion of the website could be seen at one time, with lots of scrolling and panning required to see other portions, or that the items on the website were scaled down so much that they were not usable.
- slow (and possibly expensive) download and user response times due to the large amount of graphics and tabular information on each page
- difficult for a user to use the interface designed for a mouse and keyboard with a scroll button or stylus.

In order to overcome these issues, it was decided to implement a separate website optimised for use with PDAs and smartphones. The PDA website was specifically formatted for a small screen, with limited graphics and user selection of functions from simple lists. The functionality available was limited to that considered necessary to give a user a quick overview of the monitoring situation in the event of receiving an SMS message. The key elements were the ability to generate a listing of the previous three hours' readings of each sensor, plus a plot showing the trend in the readings over the past two weeks (Figure 11).

4 CURRENT STATUS

At the time of writing, the system has been in operation for just over one year, without major incident. Both access tunnels have been completed, and the drilling of the sub-vertical drains is well under way. The main contract works are scheduled for substantial completion in September 2008, however the automated wireless groundwater monitoring system will continue to be operated under the contract for a further two years, after which time it will be handed over to the client for their future use in monitoring and controlling the new drainage system.

The database is now approximately 20GB in size, and increasing at about 1.8GB per month, which represents some 110 million readings currently being held in the database, with around ten million new readings being added per month.

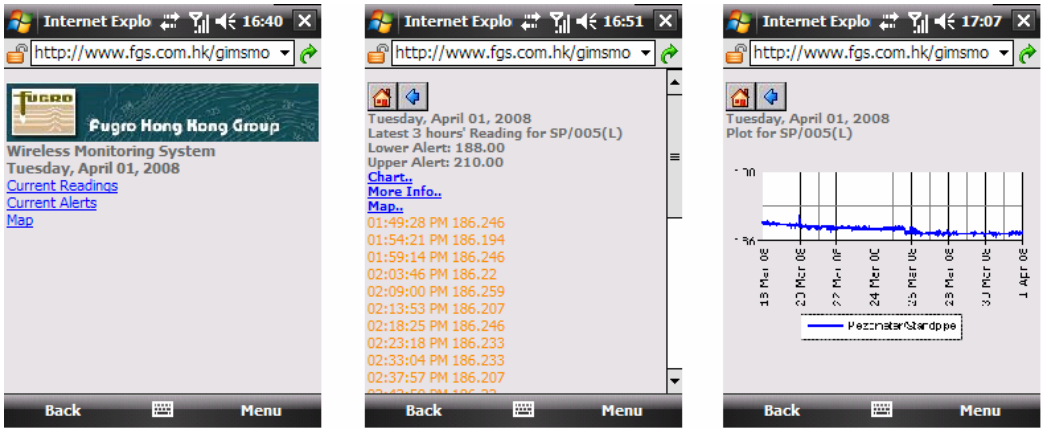

Figure 11: PDA website showing home page, list of last three hours' readings and two weeks trend plot

5 SUMMARY AND CONCLUSIONS

A sophisticated instrumentation and data management system was installed and commissioned in a relatively short time to provide real-time data on groundwater status in a site with challenging physical conditions. The high frequency of monitoring required, and the difficult terrain of the site meant that conventional monitoring solutions were impractical. Use of modern data acquisition, computing and communications technologies in the field of geotechnical instrumentation has opened up new possibilities for real-time monitoring on slopes and construction sites. The use of these techniques is not limited to groundwater monitoring, as most types of instrument that may be automated may be used with the system described, including inclinometers, strain gauges, crack gauges, tilt sensors and so on; for example Fugro and Maunsell are currently involved in another slope monitoring project in the western New Territories, where the wireless monitoring system is taking readings from in-place inclinometers and soil suction sensors.

ACKNOWLEDGEMENTS

The authors wish to thank the Head of the Geotechnical Engineering Office and the Director of Civil Engineering and Development of the Government of the Hong Kong Special Administrative Region for giving permission to publish this paper, and acknowledge that the views expressed in this paper are those of the authors and not necessarily those of their employers or of the Government of the Hong Kong Special Administrative Region. The mention of trade names and commercial products is not intended to constitute endorsement or recommendation for use.

REFERENCES

Chan, C., Saunders, J., Ma, E., So, D., Chui, A. and Solomon, I. 2003. Continuous automatic deformation monitoring for MTR tunnels adjacent to Tsim Sha Tsui Station. *Proc 7th South-East Asian Survey Congress*, Hong Kong.

Ho, J., Lam, Y.C., Lo, Y.C.J. 2008. Innovative Designs in Po Shan Tunnel Project, *Proc. 28th Annual Seminar of the HKIE Geotech. Div.*, Hong Kong: HKIE

Solomon I.J., Chan H.F.C., Ireland J.P., Lee S.C. &. Fung S.T. 2001. 'GIMS' - A client / server database system for management of geotechnical instrumentation data on West Rail, *Proc. 14th South East Asian Geotechnical Conference*, Paper 023.

Use of Geomembranes in River Bunds for Upper River Indus Training Works, Hong Kong

N.R. Wightman
Maunsell Geotechnical Services Limited, Hong Kong

L.C.L. Cheung
Formerly Maunsell Consultants Asia Limited, Hong Kong

ABSTRACT

The Upper River Indus river training works completed in 2004 involved one of Hong Kong's largest earthwork and river training projects. The purpose of the project was to alleviate the devastating floods close to the town of Sheung Shui in the northern New Territories caused by the over flowing Upper River Indus that occurred during severe rainstorms and to protect nearby villages, farmland and road users from the China border crossing at Man Kam To. The project design required the widening and straightening of the river which required raising the river banks up to 4m to contain elevated levels of storm water for up to a 1 in 200 year return period. A soil specification change from Embankment Fill to a coarser General Fill material made it necessary for an 'impervious core' to be installed in new river earthworks acting as a cutoff within the bunds to prevent internal piping seepage forces from failing the earthworks. A geomembrane was proposed for the impervious core and the quality control of soil compaction and geomembrane installation for over 6 km of bunds is described. Seepage models include comparison of the innovative geomembrane cutoff solution with that of the original Embankment Fill bunds.

1 INTRODUCTION

1.1 The project

The river training scheme involved part of the Fanling - Sheung Shui and adjacent hinterland areas which involved one of Hong Kong's largest non-reclamation earthwork projects, Figure 1. The river training project passes close to the town of Sheung Shui in the northern New Territories and many small villages and farm house dwellings. The purpose of the project was to alleviate the devastating floods caused by the Upper River Indus over flowing its banks that occurred during severe rainstorms in and around the low lying valley plains that affect dwellers, road users from the China Border crossing and farmland. The existing river was a narrow steep sided, meandering mature river passing in between hill ranges.

The purpose of the river training, by straightening and raising 4.8km of river banks above the valley floor by up to 4m, was to provide protection to the neighbouring villages from large amounts of flood water for event magnitudes up to 1 in 200 year storm return periods but overall this was limited to a storm severity of 1 in 50 year storm return period by the existing MTRC Bridge (previously KCRC), Plate 1, over the Upper River Indus (formerly KCRC) due to the height of the river embankments at the bridge not being able to support storm flows from more severe events. Water loss from the embankments under full storm conditions is not critical to flooding of the surrounding area due to the severity of rainfall for an event of this magnitude (1 in 200 year event). The river width was increased and floor deepened to contain envisaged floodwaters along with the replacement of bridges along the length of the new channel and an inflatable dam.

1.2 Geology

The geology of the Sheung Shui area comprises superficial alluvial deposits overlying tuff. The ground previously exposed during excavations was predominantly fine to coarse sand with some fine to coarse gravel sized

fragments of quartz. The upper layer of soil comprises sandy clayey silt. The tuff was exposed at the base of piles as slightly decomposed very thinly foliated slightly calcareous schistose coarse ash tuff.

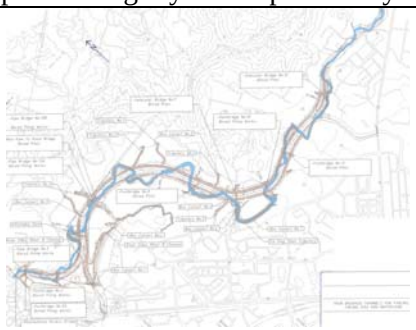

Figure 1: Plan showing the Upper River Indus at Sheung Shui

Plate 1: MTRC Bridge (KCRC) at Upper River Indus

Plate 2: Drawdown induced liquefaction failure of bank during works.

1.3 Specification Change

The project design specification for the new river bund earthworks was originally for the use of a low permeability soil comprising ‘silty fine sand’ termed ‘embankment fill’. This would provide the necessary ‘impervious core’ cutoff in the new river bunds to prevent seepage forces from damaging the earthworks in the long term. During the contract it became obvious that ‘Embankment Fill’ needed to be imported and a substitute fill material ‘General Fill’ was proposed as a replacement to speed up the works, Figure 2. The general fill was defined as being well graded including fines content and not to contain any soil particles greater than 75mm. The general fill was recognised as providing a much wider soil particle distribution envelope being up to course sized gravel and meant that an increase in bund permeability of up to 1000 times could be expected. This would allow very high seepage rates through the bunds which could result in unexpected piping failure similar to many failures of small dams and river banks. As an impervious core was essential to a sound design and successful long term performance options were explored including providing a clay core but these also proved problematic with difficulties in obtaining a suitable ‘fine fill’.

2 THE ALTERNATIVE DESIGN

2.1 Use of innovative technology and bund design requirements

In order to achieve the end aim for an impervious core, the bund design solution took a new direction towards the use of advance geotechnical innovative propriety products, a geomembrane. The design and construction measures were considered easier to manage with the potential problem of bund failure resolved. The design of the bunds takes into consideration the international design criteria for water retaining structures.

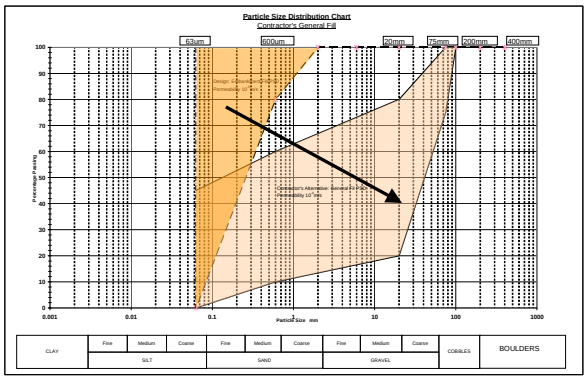

Figure 2: Change in soil fill particle size distribution from fine soils to coarse soils containing gravel.

Table 1: Soil Properties

Soil Type	Friction Angle ϕ' (◦)	Apparent Cohesion c', (kPa)	Unit Weight γ, (kN/m^3)	Permeability (m/s)
Rockfill Grade 200	40	0	21	10^{-3}
Embankment Fill	30	0	19	10^{-6}
General Fill	32	0	19	10^{-4} to 10^{-3}
Alluvium	30	0	19	10^{-5} to 10^{-4}

All earth dam embankments and river bunds/ cofferdams utilise impervious cores due to the severe consequence of internal erosion (piping failure) from seepage water flow. To this affect the river training bunds must use either a material with a low permeability or a composite of material, which has the same effect to provide an impervious core. The design of earth embankments for water retaining purposes has considerable documentation. The design of water retaining structures considers many aspects including stability, seepage, internal erosion and overtopping with allowance for sufficient freeboard including any potential settlement. For river control very similar criteria to dam embankment construction is required to control piping by erosion. The design of embankments are generally multi-zoned which requires that correctly specified soil or rock materials are correctly placed in zones to provide for an impervious core of fine materials or membrane surrounded by courser material that provides structural stability and erosion control with the use of filter zones also being considered.

2.2 Seepage control

Seepage through the embankment and foundation must be controlled to prevent excessive uplift pressures, soil piping, sloughing and removal of material by solution or erosion of material by loss into cracks, joints or cavities and was therefore important to control. Internally most water retaining embankments require some form of seepage control. For embankments with rock fill shoulders with an integral impervious core, a transition is required to control the internal piping of core material and the migration of fines through the rock fill under the hydraulic gradients. Seepage control measures require foundation cutoffs that are both adequate and form a non-brittle impervious zone. These can be formed by using grout curtains, thin concrete sections, sheet piles or slurry trench walls along with installation of drainage blankets under the bund shoulders. These protect an embankment from any undesirable or dangerous effects of seepage occurring through the embankment and reduce the risk of failure.Liquefaction soil movement from an unprotected bank had occurred in the fine sand layer at the lower slope of the channel during the works, Plate 2.

2.3 The geomembrane solution

The innovative solution allowed for a 100 percent use of ‘General Fill’ material with the use of a geomembrane cutoff in the centre of the bund extending from the bund top and keyed into the underlying existing finer fill at the base, to act as the impervious core, Figure 3. The quality control of soil compaction and the installation of a ‘cutoff’ and the performance of the bund is shown by use of seepage models showing that the allowable seepage rate is equal to or better than the original proposed embankment fill. The geomembrane toe depth was minimized depending on actual site conditions with a minimum of 1m into existing ground. The design model assumes that unsuitable weaker materials will be replaced by general fill up to a depth of 1m below ground level, i.e. should soft clays or very loose sand be found on site. The height of the overall slope of the river channel including the bund is 7m.

3 DESIGN RESULTS

3.1 Stability results

Stability analyses provide a means of evaluating the margin of safety of different embankment sections under various loading and seepage conditions. Design details covered stability of the embankment at the end of construction, as the result of sudden drawdown and steady seepage. The lateral stability of the bund with horizontal water loading on the geomembrane was found to be stable for the extreme case (1 in 200 year event water levels). For sliding checks, the factor of safety against sliding for the full river and for high level water outside the bund were 1.425 and 3.0 respectively. The results of slope stability analysis for a dry river bund gave a factor of safety between 1.205 and 1.375 and for a full river the factor of safety was over 1.4. The alternative design slope stability analysis requires a minimum factor of safety of 1.2 as in the original design completed prior to the commencement of the works. Any materials that are weaker than the strength properties stated above for the alluvium strata will need to be removed to a depth of 1m, i.e. should soft clays be found on site. The soil properties used are given in Table 1.

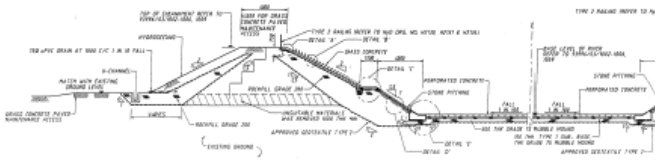

Figure 3: Position of geomembrane within the river bund

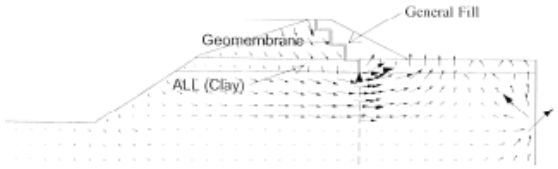

Figure 4: Seepage flow under the cutoff.

3.2 Seepage results

The key of the geomembrane into the underlying material was reduced to a minimum of 0.5m as the quantity of seepage is not an issue in flood prevention due to the negligible quantities involved compared to the flooding caused by the 1 in 200 year event. The seepage checks, Figure 4, with the geomembrane keyed into the ground by 1m was lower at 0.296m^3/hour/m run of bund compared with the value of seepage for the original embankment fill bunds at 0.63m^3/hour/m run of bund. With the potential maximum level within the River Indus at +9mPD (1m below bund top level) the seepage rate under the bund composite structure and through the natural fine sand foundation was acceptable. In the event of a 1 in 200 year storm the rainfall would result in some surface water standing in the area outside the river bunds. It has been assumed that the core of the bund is zero or very low permeability and that piping could not be induced and intermixing of the rock fill material with the core material is negated due to the positioning of a geofabric filter separator.

4 INSTALLATION OF GEOMEMBRANE

4.1 Geomembrane properties, specification and installation procedure

The geomembrane was a 0.75mm thick, black, High Density Polyethylene (HDPE) of density 0.94g/cc with a yield strength of 13N/mm and breaking strength of 21N/mm, Plate 3. The geomembrane is inert to chemical attack and biological degradation, puncture resistant, flexible and textured on both faces to provide mechanical interlock with compacted soils and protected against ultraviolet light (UV radiation) degradation by carbon black. The geomembrane manufacturer must show compliance on a national certificate for the design.

The geomembrane handling, cutting, welding and placement were carefully monitored, with the number of joints to be welded limited with the relative positions or orientation of sheets maintained with respect to each other. Prior to laying the geomembrane, the exposed surface was well compacted and free of debris especially those with sharp edges which could cause punctures. The geomembrane was installed on benches within the bund general fill, Plates 4 and 5, to give a temporary soil slope of 45 degrees maximum. The benching vertical face was at a minimum angle of 75 degrees from the horizontal and the benching horizontal surface was inclined at no more than 10 degrees but remained inclined to provide a drainage path off the benched geomembrane. The maximum benched height was between 0.3m and 1m and not laid as an inclined plane within the bund for stability reasons. The geomembrane was joined, using the manufacturers' approved method of heat welding tools and equipment, Plates 6 and 7. The geomembrane was positioned and bonded to form water tight joints with adjacent sheets and also to totally surround any obstacles, such as pipes that pass through the geomembrane to ensure the impervious cutoff is completely watertight, Plate 8. Special detailing consideration was given to curtailment of geomembrane materials at storm drains and associated manholes, graded roads interfacing with retaining walls and foundations of structures. Welded joints were quality tested at random to ensure the joined material was adequately bonded together, Plate 9. In order to maintain the designed toe level of the installed geomembrane, a concrete toe weight was first cast into the trench to provide a dead weight to minimise movement and distortion during subsequent backfilling and compaction operations. The upper 1m which is critical for storm events between 1 in 50 to 1 in 200 years return periods was formed with a special capping material comprising well graded soils with maximum particle size of 75mm with the permeability taken as 10^{-4}m/s for the calculation of the seepage rate. All river embankment bunds 1m or under in height did not require geomembrane to be installed.

Plate 3: Physical Testing Equipment

Plate 4: Trench in fine soil

Plate 5: Concrete toe pour

It was imperative for the geomembrane not to be damaged (ruptured or torn) during handling, joining, installation, compaction processes particularly by coarser sized particles. Care was taken for construction vehicles and equipment not to operate on the installed geomembranes. In cases where this was unavoidable the geomembrane was covered with fill material. The geomembrane was protected from direct exposure to daylight using tarpaulins but if this was not possible the exposure was limited to not exceeding 7 days to maintain the quality of the geomembrane. Small patch repairs to the geomembrane material which had been torn or damaged during installation were done with at least 300mm overlap beyond the edge of the damaged area.

4.2 Soil compaction control and Geomembrane installation quality control

For the geomembrane the records contained the following information: date of installation and covering with backfill; identification of structures and section of work where installed; type of joint; amount of overlap and method of any repairs to geomembrane. Sketches with dimensions showing extent and toe level of geomembrane in bund along with a description of backfill soil (with grading) were maintained.

The quality of the fill material was assessed according to the General Specification for Civil Engineering Works from CED (1992) and on site material and compaction control measures that were implemented with specialised forms developed for the process, Figures 6 to 9. Rigorous construction control was essential to ensure proper thickness distribution of fill materials and adequate compaction technique. The testing of soil grading, in-situ density and moisture contents are required for comparison with the optimum moisture content and for the calculation of the degree of compaction using the maximum dry density for each type of soil compacted on site. The length of each compacted soil layer and geomembrane sheet was nominally 30m unless obstructed. A trial compaction for the compaction plant was carried out to verify the maximum thickness of each soil layer for the general fill and the correct number of passes of compaction plant required to achieve a minimum of 95 percent of maximum dry density as derived from the standard compaction laboratory test. Layer thickness of loose soil was controlled by direct measurement. Insitu density tests were carried out to measure the density of the compacted soil for each soil layer with tests being carried out at the top, middle and bottom of the layers, Figure 5. The insitu density test results were made available as soon as the preliminary details have been determined by the soils testing laboratory that was HOKLAS accredited. Soil which is too wet or too dry may not compact to greater than 95% maximum dry density (MDD) and this soil will have lower strength and higher permeability properties which can be detrimental to stability of slopes. It is possible for the loose soil layers to be spread too thick and for the lower part of the compacted layer not to achieve the desired compaction level.

Plate 6: Heat applicator

Plate 7: Joining equipment

Plate 8: Pipes surrounded

Plate 9: test equipment

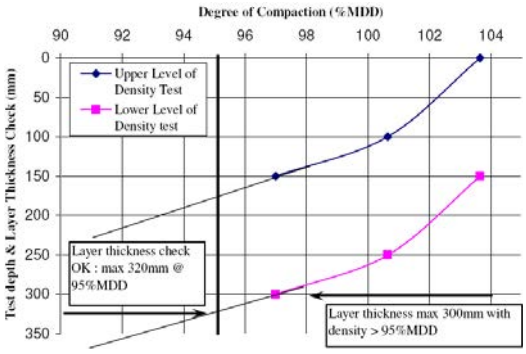

Figure 5: Degree of Compaction for 300mm layer showing dry density decrease with depth.

Plate 10 : Inflatable Dam

Plate 11 : Completed Bunds

All compacted fill was checked to verify that the minimum allowable density had been achieved throughout the compacted layer. The check form detailed failed layers that required remedial work such as further passes of the compaction plant to further densify the layer which was then retested for approval purposes. Construction control is essential with good supervision and record keeping for all stages of the bund construction process to completion. The completed river bunds are shown in Plates 10 and 11.

5 CONCLUSIONS

The design change to incorporate a geomembrane into the bunds of the river training works allowed for the safe use of general fill by providing an impervious core. The quality control measures implemented for the installation of the geomembrane and the soil compaction process were deemed essential to the process.

6 ACKNOWLEDGEMENTS

The authors wish to thank CEDD for permission to publish this paper

7 REFERENCES

CED (1992). General Specification for Civil Engineering Works – Section 6: Earthworks. Civil Engineering Department, Government of the HKSAR, pp159-194.

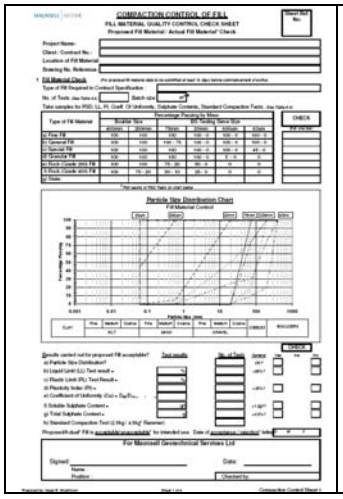

Figure 6: Control Sheet 1 Fill Material Selection

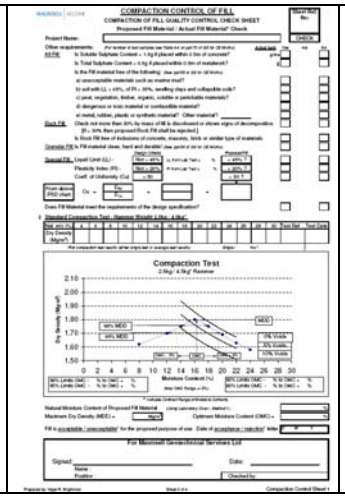

Figure 7: Control Sheet 2 Soil controlling limits

Figure 8: Control Sheet 3 Trial compaction

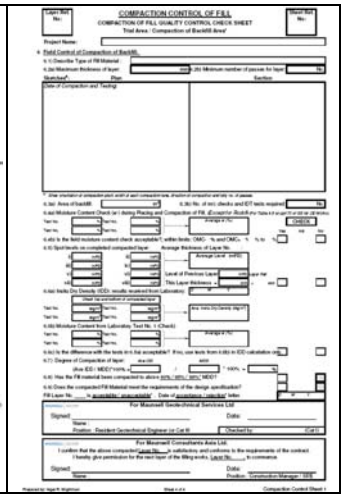

Figure 9: Control Sheet 4 On-site compaction control

Design and Construction of a Breakwater Using a Geosynthetic Raft at Tai O Bay, Hong Kong

N.R. Wightman & S. De Silva
Maunsell Geotechnical Services Limited, Hong Kong

ABSTRACT

The Tai O Breakwater was completed in 2005 to provide a sheltered boat anchorage as part of the Tai O Redevelopment Plans which included preserving the historic seawall layout that surrounds the historic Tai O salt pans. The geology at Tai O is a prime example of thick marine and terrestrial quaternary deposits comprising sands and very soft to firm clays and silts, showing evidence of multiple glacial / inter-glacial geological time periods. The original design of the breakwater envisaged the full dredging of the quaternary deposits within Tai O Bay with large volumes of excavated material needing disposal prior to the re-filling with granular materials. This operation was estimated to be expensive and would have a major impact on the marine disposal area. The breakwater design was modified to provide an innovative geosynthetic reinforced raft as the base of the breakwater after removal of only the very soft Holocene mud deposits. No vertical drainage was installed so that the deeper very sensitive clays were not disturbed. The innovative breakwater design required up to 3 layers of geosynthetic to reinforce a wide granular base raft prior to conventional construction of the breakwater structure founded on the first terrestrial sand deposit.

1 INTRODUCTION

1.1 The site

The Tai O Breakwater was completed in 2005 as part of the Tai O Redevelopment Plans which included preserving the historic seawall and the salt pans. The breakwater, with top surface at +7mPD, provides a sheltered boat anchorage in Tai O Bay, Figure 1, to the west of the town and provides a much needed protection screen from sea waves particularly with prevailing westerly storm winds.

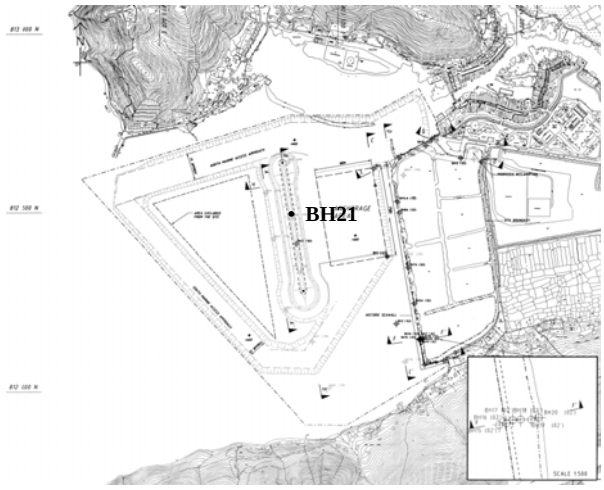

Figure 1: Site location in Tai O Bay (after Bahr *et al*, 2005).

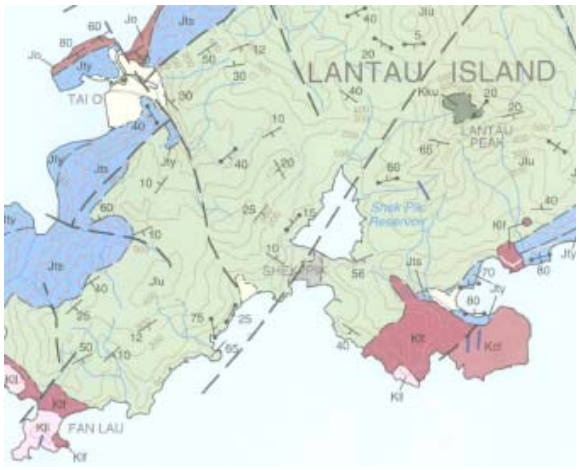

Figure 2: Geology map of Tai O Bay (CEDD, (2000))

Table 1: Absolute ages of the Quaternary marine and terrestrial units after Yim (2001) for the proposed model for the Hong Kong continental shelf after Yim & Choy (2000). Typical geological profile at the breakwater (Borehole BH21) with Lithological Units (Yim *et al*, 1988) and typical soil parameters at breakwater

Lithological Unit [Log name]	Age (ka)	Geological Period	Depth (m)	Borehole BH21 logs (Figure 1)	mc	L_L	ρ_d	φ'
(after Yim *et al* (1988))	Quater-nary		0.00	*Seabed*	%	%	Mg/m^3	Deg
M1 - [Upper Marine	<8.1	Holocene	13.00	Very soft to soft, dark grey silty CLAY with occasional shells	28-83	33-71	0.9-1.6	29 [c_u=10-15kPa]
T1 - [Upper Marine & Estuarine]	8.1-70	Last Glacial	15.60	Stiff / medium dense, brownish yellow & black SILT and CLAY with sand pockets with some fine gravels of rock fragments	23-27	47-48	1.2-1.9	25-33.7
M2 - [Upper Alluvium]	90-140	Last Inter-glacial	18.10	Firm to stiff, light grey dappled yellow or spotted yellowish brown, slightly silty CLAY.	16-34	21-75	1.3-2.0	25
T2 - [Upper Alluvium]	150-180	2nd Last Glacial	-	*Not encountered in BH21 but present elsewhere in Tai O Bay.*	21-41	21-74	1.3-1.4	16-34.6
M3 - (Lower Marine)	190-240	2nd Last Inter-glacial	30.10	Firm to stiff, grey to black, slightly silty CLAY	40-70	43-73	1.0-1.3	25 [c_u=18-38kPa]
T3 - (Lower Marine)	250-300	3rd Last Glacial	39.60	Stiff, brownish yellow silty CLAY. Yellowish brown mottled grey, silty, SAND. Light grey, sub-angular COB-BLE sized strong Tuff and siltstone..	-	-	-	-
M4 - [Lower Alluvium]	310-340	3rd Last Inter-glacial	40.10	Firm, grey mottled yellowish-brown, slightly sandy silty CLAY with occa-sional decayed plant debris. Firm, dark greenish grey, slightly sandy clayey SILT with decayed plant debris	27-48	30-56	1.0-1.6	24 [c_u=40-50kPa]
T4 – [Lower Alluvium]	350-370	4th Last Glacial	47.75	Light grey, sub-angular, GRAVEL and COBBLES of moderately weak and moderately strong rock and occasional quartz with sand / boulders.	-	-	-	-
M5	380-420	4th Last Inter-glacial	-	Not in BH21	-	-	-	-
T5	>440	5th Last Glacial	-	Not in BH21	-	-	-	-
Bedrock – Tuff (G-V)	Jurassic Age	-	-	Extremely weak, light grey, spotted white and grey, completely decom-posed, coarse ash crystal TUFF. (Firm to stiff, silty sandy CLAY)	-	-	-	-

1.2 Geological Setting: Solid and Superficial

The solid geology around Tai O Bay (Figure 2) indicates the area is part of the volcanic series comprising ash crystal Tuff of Upper Jurassic Age from the Mesozoic Era (GEO, 1989). The coarse ash crystal tuff of the Yim Tin Tsai Formation and also the Shing Mun Formation which also contained tuff breccia with intercalated siltstone; part of the Tsuen Wan Volcanic Group. To the south and east of the Tai O Bay the hillsides comprise fine ash vitric tuff and flow banded rhyolite lave with minor eutaxtic coarse ash crystal tuff part of the Lantau Volcanic Group. The superficial geology at Tai O is a prime example of deep and thick marine and terrestrial quaternary deposits comprising sands and very soft to firm clays and silts, showing evidence of

multiple glacial / inter-glacial geological time periods within Hong Kong's marine environment which is surrounded by steep hills.

1.3 Stratigraphy & Lithology

The main superficial lithological units identified in the Tai O area (Fyfe *et al*, 2000) were: Hang Hau Formation; Sham Wat Formation and Chek Lap Kok Formation. The areas surrounding high ground are covered with debris flow deposits, which comprises sand, gravel, cobbles and boulders in a silt matrix and also alluvium, which comprises silt sand and gravels occurring at the base of the hills. Estuarine deposits and beach deposits are indicated in the tidal areas which have been filled along the alignment of the South Lantau Road, the town area, areas of the fore shores of the island and the perimeter of disused salt pans that include the alignment of the historic seawall. The site of the breakwater and the historic seawall are within the marine / estuarine / alluvial deposits that comprise inter-layered mud and sand. These Quaternary era deposits include the most recent upper marine deposits (Unit M1) of Holocene age, Table 1, and the earlier slope debris, alluvial and lower marine layers identified as from the Pleistocene age. The lithology was further studied and divided into age sequenced marine environment clays (M1, M2, M3 & M4) and granular materials from terrestrial inter-glacial periods (T1, T2, T3, T4 & T5) in Table 2, as first described by Yim *et al* (1988). The lower alluvium is often recorded due to the lower marine clay (particularly M2 & M4) having been sub-aerially exposed causing discolouration to orange and due to be absence of shell fragments which dissolve over a long period of time caused by acidic ground conditions.

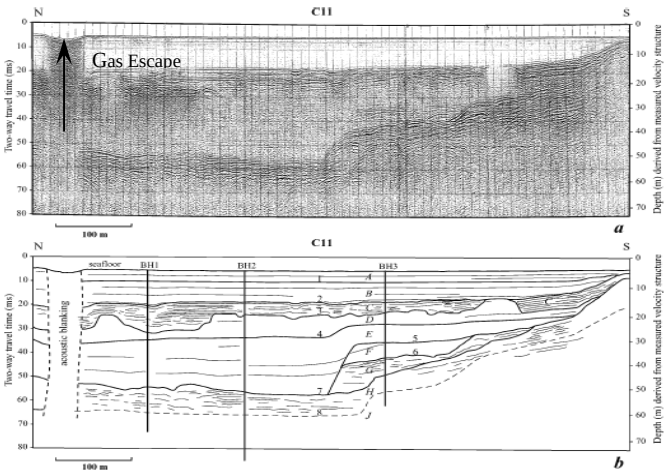

Figure 3: Seismic profile from Bahr *et al* (2005), suggests that the elongated trough in the seabed was probably formed by biogenic gas escape from the underlying deposits.

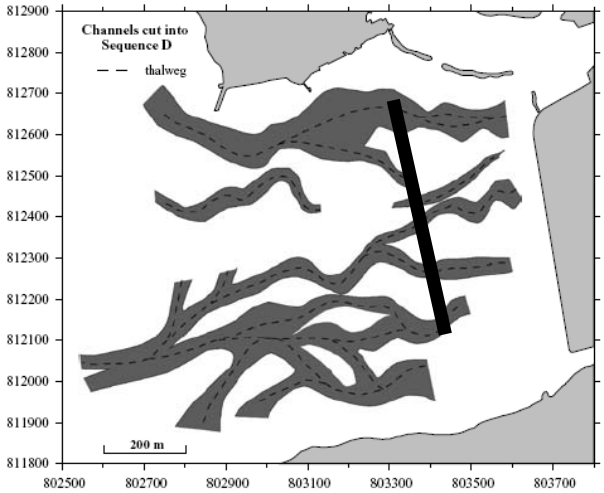

Figure 4: Channel system incised into strata D (after Bahr *et al* 2005). Position of breakwater indicated.

2 INVESTIGATION FINDINGS

2.1 Ground Investigation

The previous ground investigations carried out in Tai O Bay area with associated laboratory testing included over 80 marine drillholes and vibrocores between 1975 and 2002. Most recently one drillhole BH21 was sunk at the location of the breakwater. Geophysical surveys in 1998 were carried out for the Tai O Development including the seismic survey which was subject to analysis, Bahr *et al* (2005), with a correlation to the lithology obtained by ground truthing from borehole data. This important study confirmed the lithological model previously used for the breakwater design. The quaternary deposits consisted of numerous thick layers of alluvial sand from terrestrial periods during glaciation and inter layered marine deposits from both recent and inter-glacial periods. Evidence of biogenic gas escape seen as seismic masking of a column, Figure 3, from the

lower marine layers suggests that gas production from biogenic breakdown of shell matter within the marine layers has occurred. Gases produced at depth can remain in solution until disturbed by groundwater migration or other disturbing factors.

2.4 Ground Model and Properties

The geological profile was apparently variable with distinct channelisation in the tops of strata, Figure 3, possibly caused by surface runoff during glacial periods. Pockets or zones of weaker material occurred between stiffer clays or sand beds. Figure 4 shows the channel system obtained by seismic profiling which more accurately defines the paleochannels incised into layers. With such an irregular sub-stratum top of layer, the benefits of seismic surveys can enhance the geological profile considerably. The Paleochannel network, Figure 4, can be constructed and used to update profiles from borehole logs alone such as those shown below in Figures 5 and 6. The superficial seabed geology was confirmed to be both deep and of low strength. The lower marine clays indicated high moisture contents, with some samples higher than the liquid limit with a sensitivity of up to 12 as measured by shear vane tests. Other evidence from soils tests of weaker soils are low values of dry density at depth instead and SPT values being low. Profiles of SPT N value gave values as low as 5 at depths of over 40m within the lower marine stratum. The range of soil properties was wide indicating the variability of the different stratum present as shown by the geological profile in Table 1. The choice of parameters and properties for the analyses reflected a reasonable average or lower bound value if derived values seemed too optimistic, i.e. from desiccated crusts. The soil results at the seawall area did not show similar soil test result distribution with depth but showed the classic increased strength with depth and reduction in moisture content with depth. This may be the result of the long term seawall loading on the underlying strata.

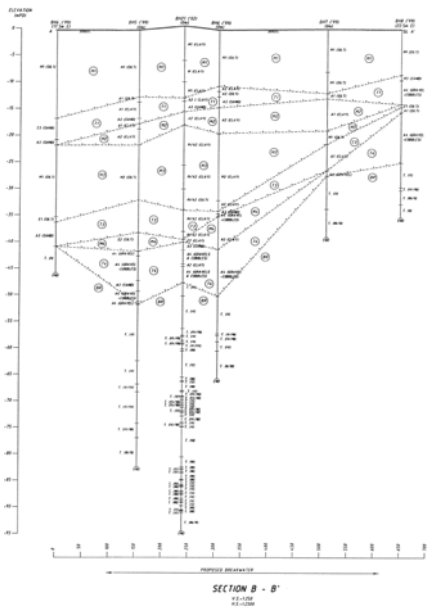

Figure 5: Geological profile along breakwater

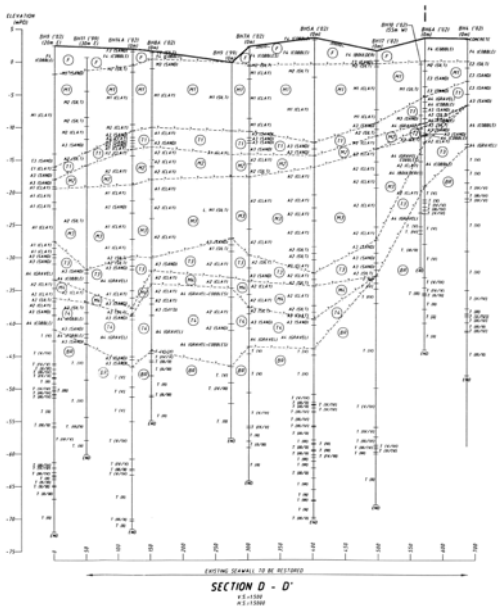

Figure 6: Geological profile along seawall (300m eastward)

3 DESIGN APPROACH

3.1 Innovative Design Approach

The original design of the breakwater envisaged the full dredging of the quaternary clay deposits within Tai O Bay to a depth of over 37m. Considerable volumes of marine clay with sands from dredging (about 5.5 million cu. m) would require disposal prior to the re-filling with granular materials. This operation was consid-

ered both expensive and having a major impact on marine mud disposal areas. The breakwater design was modified to a partial dredged solution (soft Holocene deposits) with dredge levels ranging between -14.5 mPD and -18 mPD following the top of the terrestrial sand layer T1 (alluvial sand) laid down in the last glacial period. Due to the presence of the weak and sensitive clay below this horizon, stability checks showed that fill alone would not enable the breakwater to resist failure being the usual method of providing a rubble mound as base support without surcharging the ground. In order to keep the clay undisturbed and at a higher strength, vertical wick drainage or other types of installation such as stone columns would not be installed, even though settlement was expected to be completed during the construction period. The design was modified to incorporate a geosynthetic reinforced fill raft as the sub-base for the breakwater structure. This required a reinforcement spacing of 750mm within the sand fill, Figure 8. The shoulders of the breakwater were extended beyond the seabed downward on a 1:1 slope which defined the extent of the reinforced raft.

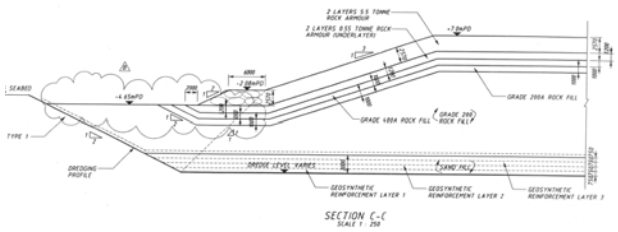

Figure 7: Arrangement of geosynthetic reinforcement at ends of breakwater within 3m thick sand raft.

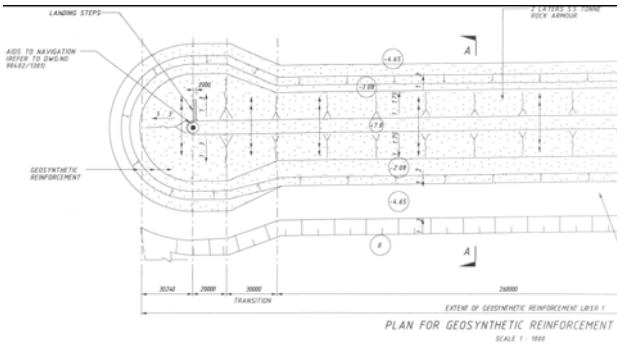

Figure 8: Arrangement of 3 layers of geosynthetic reinforcement at ends and 1 layer in central portion.

The dredged trench was sloped at 1v:2h with the fill following the arrangements shown in Figure 7. The clay was therefore not to be disturbed except by unloading and reloading the formation by the construction activities.

3.2 Stability and settlement analyses

The geosynthetic reinforced base raft (3m thick) required 3 layers placed directly under the breakwater southern and northern ends and 1 layer only for the central portion. , placed and. The reinforced shoulders extending beyond the breakwater base are essential for providing short term stability against both bearing and circular failure. The pull out bond length of the reinforcement was calculated as 12m prior to the geosynthetic rupturing at a load of 440kN/m. Plan view is shown in Figure 8. The design results are given in Table 2, indicate generally the circular or block failure of the central portion in the short term was 1.8 and would steadily improve to between 2.7 and 3.9 in the long term as the weaker clays consolidated and gain strength. The factor of safety in bearing was 1.4 in the short term and 33 in the long term. The effect of adding layers of geosynthetic to the northern head was to increase the factor of safety in the short term from 1.04 (with no reinforcement) to 1.310 for 3 layers of geosynthetic. Maximum settlement expected ranged from 552mm (central portion) to 860mm at the breakwater head. The average time to achieve 50% consolidation was 3.3 years and for 90% consolidation in 14.5 years although this could take as long as 43years due vertical drainage being through the thick clay deposits without the aid of vertical wick drainage.

4 CONSTRUCTION

4.1 Construction Material and Control

The geosynthetic reinforcement was GEOLON PET 800 woven type geotextile with a minimum longitudinal tensile strength of 800kN/m and minmum transverse tensile strength of 100kN/m.

Table 2: Design analysis results

No. of layers of Geosynthetic C= Central Section E= End of Breakwater		Factor of Safety				Consolidation	
		Circular / block stability [Min FoS = 1.3]		Bearing Stability		Settlement Max (mm)	Time to consolidate
		Short Term	Long Term	Short Term	Long Term		
None		1.04	2.7-3.9	1.4	33	C = 552 E = 860	50% in 3.3 yrs 90% in 14.5 yrs [Max of 43 yrs]
1	C =	C = 1.8	2.7-3.9	1.4	33		
	E =	E = 1.123	3.5				
2	E =	E = 1.214	3.5 – 4.7	1.2 -1.6	28		
3	E =	E = 1.310	4.7	1.2 – 1.6	28		

The geosynthetic reinforcement in the central portion was laid with the principal direction of strength aligned transversely across the breakwater. At the ends of the breakwater the layer 2 and 3 geosynthetic reinforcement were positioned with the principal direction of strength aligned longitudinally along the breakwater. The construction progressed in stages to avoid any rapid loading of the underlying weaker soils. The laying of the geosynthetic reinforcement within a sand blanket was completed prior to the staged construction and armour protection of the breakwater structure to ensure short term stresses were not exceeded. The fill comprised sand for the reinforced raft followed above by a layer of a general separator geotextile to cover the top of the raft and the dredged sides of the trench. For the protection of the breakwater, consecutive layers were used comprising Grade 200A rockfill, Grade 400 rockfill, 2 layers of 0.55 tonne rock armour (underlayer) and finally 2 layers of 5.5 tonne rock armour. No failure was detected during of the works of the breakwater base or dredged trench.

5 CONCLUSIONS

The design of the breakwater with a geosynthetic reinforced granular raft proved to be essential in providing a stable platform for construction of the breakwater structure and enabling substantial cost saving on dredging and minimising the environmental impact.

ACKNOWLEDGEMENTS

The authors wish to thank CEDD for permission to publish this paper.

REFERENCES

Bahr, A., Wong, H.K., Yim, W.W-S., Huang, G., Lüdmann, T., Chan, L.S., Ridley Thomas, W.N. (2005). Stratigraphy of Quaternary inner-shelf sediments in Tai O, Hong Kong, based on ground truthed seismic profiles. *Geo-Marine Letters*, 25: 20-33. DOI 10.2007/s00367-004-0185-y.

Fyfe, J.A., Shaw, R., Campbell, S.D.G., Lai, K.W., and Kirk, P.A. (2000). The Quaternary Geology of Hong Kong. Geotechnical Engineering Office, Civil Engineering Department, The Government of the Hong Kong SAR.

Geotechnical Engineering Office (1989). 'Hong Kong Geological Memoir No.3. – Geology of the Western New Territories', Civil Engineering Department, Hong Kong.

Geotechnical Engineering Office (1994). Hong Kong Geological Survey, 'Solid and Superficial Geology – Tung Chung', Map Sheet 9, 1:20,000, Civil Engineering Department, Hong Kong.

Yim, W.W.-S. (2001), Stratigraphy of Quaternary Offshore Sand and Gravel Deposits in the Hong Kong SAR, China. *Quaternary International*, 82 (2001), pp101-116.

Yim, W.W-S., Fan, S.Q., Wu, Z.J., Yu, K.F., He, X.X., and Jim, C.Y. (1988). Late Quaternary palaeoenvironment and sedimentation in Hong Kong. In: Whyte, P. (Ed.). The palaeoenvironment of East Asia from the Mid-Tertiary, vol I. Centre of Asian Studies, The University of Hong Kong, Hong Kong, pp117-137.

Yim, W.W-S., and Choy, A.M.S.F. (2000). Some engineering applications of Quaternary sea-level changes in Hong Kong. 10 November 2000, HKG Inst. of Mineralogy & Metallurgy Ldn, HKG Branch, pp211-218.

Analysis of Bored Piles in Saprolite with Load Transfer Method

L.W. Wong
Hong Kong Island and Islands Development Office, Civil Engineering and Development Dept., Hong Kong

ABSTRACT

The load transfer method using Winkler springs and hyperbolic relationship between the pile displacements and the shaft or the toe resistances is adopted herein for analyzing the performance of bored piles in saprolite. The hyperbolic model is verified with 2 case histories on instrumented test piles. The interpreted shaft and base resistances are consistent with the experience reported in literature.

1 INTRODUCTION

The load transfer method proposed by Coyle & Reese (1966) has been one of the consistent frameworks for considering the load transfer mechanism of piles. However, in this load transfer method the soils were modelled by linear elastic-perfectly plastic springs. Wong (2007a, 2007b) proposed that the load-displacement relationship of the interface between the pile and the supporting ground could be expressed by hyperbolic functions. The modified load transfer method was adopted to analyze case histories on instrumented driven piles and on working piles installed by the pre-boring method. Hyperbolic load-displacement parameters were assessed from these case histories.

It is considered that the load transfer characteristics of piles would be dependent on their methods of installation. Case histories on bored piles and augered piles are collected in order to back-analyze the hyperbolic load-displacement parameters for these types of piles. The results of analysis are presented in this paper for future assessment of the performance of bored piles.

2 ANALYTICAL METHOD

The load transfer method using Winkler springs, sometimes called the *t-z* curve method, that proposed by Coyle & Reese (1966) has been suggested by the Geotechnical Engineering Office (2006) as one of the methods for analyzing the performance of piles. Basically each pile is idealized as a series of elastic discrete elements supported by springs on its side and a spring at the base. These springs represent the soil-structure interaction. This method was adopted by Chang & Broms (1991) and Moh et al. (1995) for analyzing bored piles.

In the load transfer method proposed by Coyle & Reese (1966), the soils were modelled by linear elastic-perfectly plastic springs. Since the stress-displacement curves for soils would be nonlinear, linear models are deemed inappropriate. The pile shaft or pile base resistances versus displacement plots could be expressed by the hyperbolic curve approximation illustrated in Figure 1. The load-displacement curves for soil or rock could be represented by the hyperbolic function:

$$\tau = \tau_{max} / (1 + \delta_r / \delta) \quad (1)$$

where τ_{max} is the horizontal asymptote representing the ultimate shaft resistance or base resistance, δ_r is the reference displacement and τ is the mobilized resistance at the pile displacement δ.

Equation (1) shows that resistances of $0.5\tau_{max}$ and $0.9\tau_{max}$ would be mobilized at displacements of δ_r and $10\delta_r$, respectively. As defined in Figure 1, the initial tangent of the curve intersects the horizontal asymptote at δ_r. Therefore the initial stiffness or the slope of the curve *m* is defined as:

$$m = \tau_{max} / \delta_r \quad (2)$$

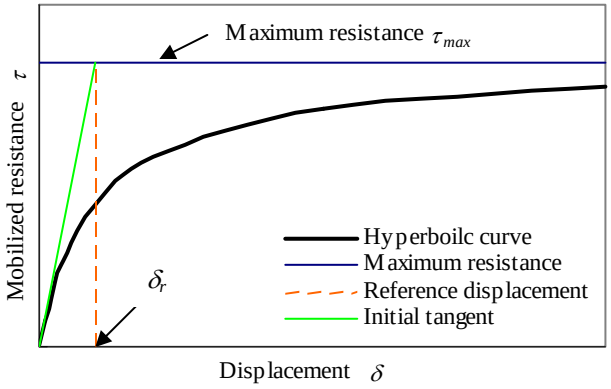

Figure 1: Hyperbolic model for resistance versus displacement relationship

Fleming (1992) adopted the hyperbolic load-displacement relationship to predict the performance of piles in clay, sand and weak rock materials. Pickles et al. (2003) reported the results of load tests on 3 bored piles. Wong & Tse (2001) presented the results for 2 instrumented piles installed by the auger-injection method. These 2 case histories on bored piles and augered piles are critically reviewed herein and the hyperbolic parameters for various soil strata are interpreted from the pile load test results.

3 HYPERBOLIC PARAMETERS

3.1 Case 1 - Bored Piles

Pickles et al. (2003) presented a well-documented case history on 3 instrumented bored piles located in one of the sites for the East Rail Extension Project in Hong Kong. As depicted in Figure 2, the fill platform was mainly underlain sequentially by the alluvium deposits of sandy clay, sandy gravel and the completely decomposed granite (CDG) of predominantly sandy silt. The groundwater level, not reported by Pickles et al. (2003), is believed locating at a depth of several metres below the ground surface.

The test piles were reinforced concrete piles of 1500 mm and 1200 mm in diameters and 40 m to 72 m in lengths. They were constructed using bentonite slurry to support the pile bores. Short temporary casings were installed at the top of the piles to provide additional support near the ground surface. The slurry level was maintained at a level at least 2 m above the groundwater table. In order to separate the shaft friction of the fill layer, sleeves of 14.5 m and 10.5 m in lengths were provided to test piles no. P117 and P125 respectively.

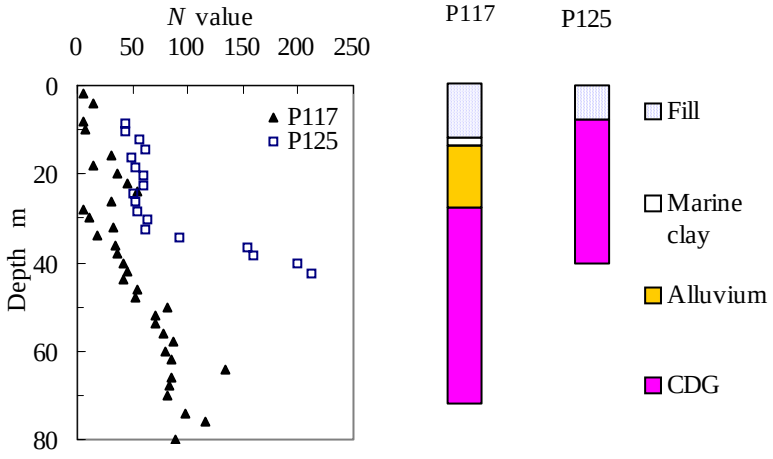

Figure 2: Subsoil conditions for pile nos. P117 & P125

Table 1: Summary of instrumented test piles

Case	Pile no.	Diameter mm	Pile length m	Maximum load MN	Pile head displacement mm	
					Maximum	Residual
1	P117	1500	72.2	15.0	12.8	4.0
	P131	1500	46.2	11.5	6.9	2.5
	P125	1200	39.7	9.5	32.0	23.0
2	TP1	610	30	6.3	45	20
	TP2	610	30	6.0	31	11

Table 1 summarizes the maximum displacements and the residual displacements observed at the pile heads. Strain gauges and extensometers were installed in the 3 test piles for measuring the strains induced in the piles. The concrete has a Young's modulus of 31 GPa.

The author conducted numerical analyses by using the Winkler springs method based on the Standard Penetration Test *N* values, pile head displacements and the load distribution data. The sets of the hyperbolic parameters for describing the t-z curves along the shafts and at the bases of test piles no. P117, P131 and P125 are back-calculated. Figure 3 depicts the results of calculated pile head displacements and load distribution curves for test pile no. P117, and Figure 4 presents those results for test pile no. P125.

The back-calculated maximum shaft resistances and their corresponding reference shaft displacements (τ_{s-max}, δ_{sr}) and the maximum base resistances and their corresponding reference base displacements (τ_{b-max}, δ_{br}) are summarized in Tables 2 and 3 respectively.

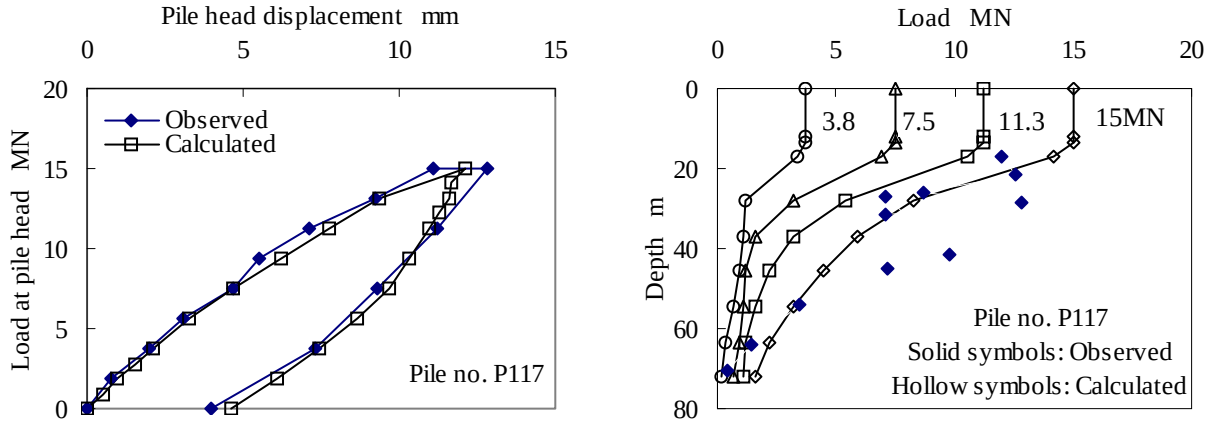

Figure 3: Pile head displacements and load distribution for pile no. P117

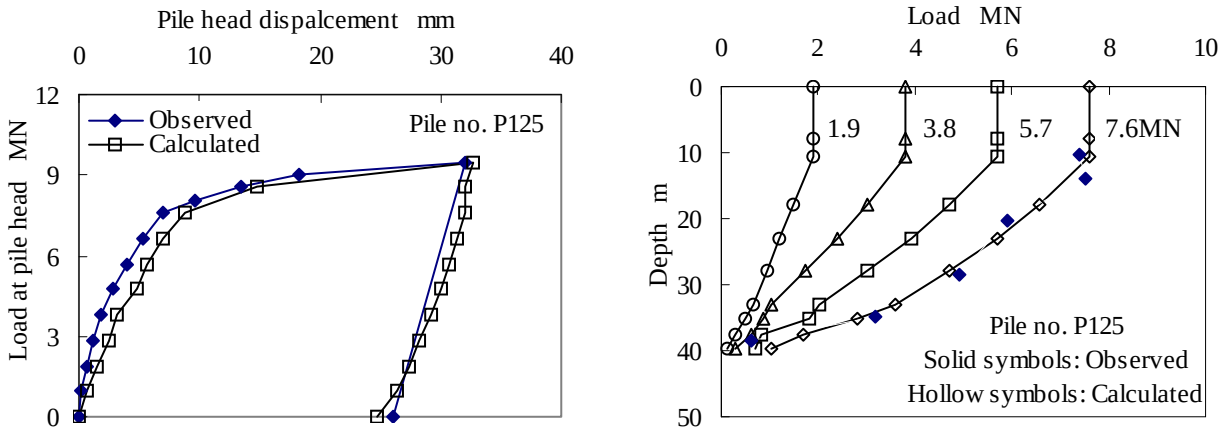

Figure 4: Pile head displacements and load distribution for pile no. P125

Table 2: Back-analyzed hyperbolic parameters for shaft resistances

Case	Soil type	*N* value	Maximum shaft resistance		Reference shaft displacement
			τ_{s-max} kPa	τ_{s-max}/N kPa	δ_{sr} mm
1	Fill	8 ~ 12	27	3	2
	Alluvium	20 ~ 50	60 ~ 150	3	1.8
	CDG	20 ~ 150	45 ~ 480	1.45 ~ 3.5	0.8
2	Alluvium	3 ~ 48	120	3.3	1
	MSS Grade V	20 ~ 120	95 ~ 400	3.3	1

Table 3: Back-analyzed hyperbolic parameters for base resistances

Case	Soil type	Average *N* value	Maximum base resistance		Reference base displacement
			τ_{b-max} MPa	τ_{b-max}/N kPa	δ_{br} mm
1	CDG	140 ~ 180	1.8 ~ 2.3	13	3 ~ 4.5
2	MSS Grade V	136	2.2	16	3

To allow for variability of the strata across the site and for comparison with other case histories, the τ_{s-max} and τ_{b-max} values are normalized with the *N* values. It is noted that the lower bound τ_{s-max}/N value of 1.45 for CDG is back-analyzed from test pile no. P125 while the upper bound value of 3.5 is interpreted from test piles no. P117 and P131. Pickles et al. (2003) noted that the Standard Penetration Test profile recorded down to the depth of 25 m at pile no. P125 is 30 % to 50 % higher than that recorded at 5 adjacent boreholes. This would probably be one of the reasons for the lower τ_{s-max}/N value back-calculated from this test pile.

3.2 Case 2 - Augered Piles

Wong & Tse (2001) presented the case histories of load tests on augered bored piles for a building site at Yuen Long in northwest Hong Kong. In a descending sequence, the subsoil comprised the fill, alluvium and the completely decomposed interbedded meta-sandstone and siltstone (MSS Grade V). Marble bedrock of Carboniferous age is located at depths between 60 m and 100 m. The groundwater level is located at a depth around 3 m below the ground surface. Table 4 depicts the subsoil conditions at this building site.

The test piles, which were instrumented with strain gauges, were installed by screwing hollow stem continuous flight augers with a diameter of 610 mm. After augering down to the depth of 37.5 m, cement grout was injected through the hollow stems and the flight augers were withdrawn simultaneously. Upon removal of the flight augers, steel H-piles of Grade 50B 305 x 305 x 110 kg/m were inserted into the grouted shafts. It is noted that the H-piles were only embedded to a depth of 14 m below the cut-off level, which is 7.5 m below the ground surface. The cement grout has a 28-day design strength of 20 MPa.

Table 1 summarizes the maximum displacements and the residual displacements observed at the pile heads of the test piles no. TP1 and TP2. The hyperbolic parameters for the shafts and the bases were analyzed by matching the pile head displacements and the loads transmitted to the pile base. It was reported that at the maximum test load of 6.3 MN, an axial load of 1 MN was transmitted to the base of pile no. TP1. The results of analysis for pile no. TP1 are shown in Figure 5, indicating a good agreement between the observed and the calculated data. The sets of back-calculated hyperbolic parameters are presented in Tables 2 and 3.

Table 4: Subsoil conditions for Case 2

Soil type	Thickness of stratum m	*N* value
Fill	1 ~ 4	< 10
Alluvium	9 ~ 15	3 ~ 48
Interbedded meta-sandstone & siltstone Grade V	44 ~ 60	20 ~ 200

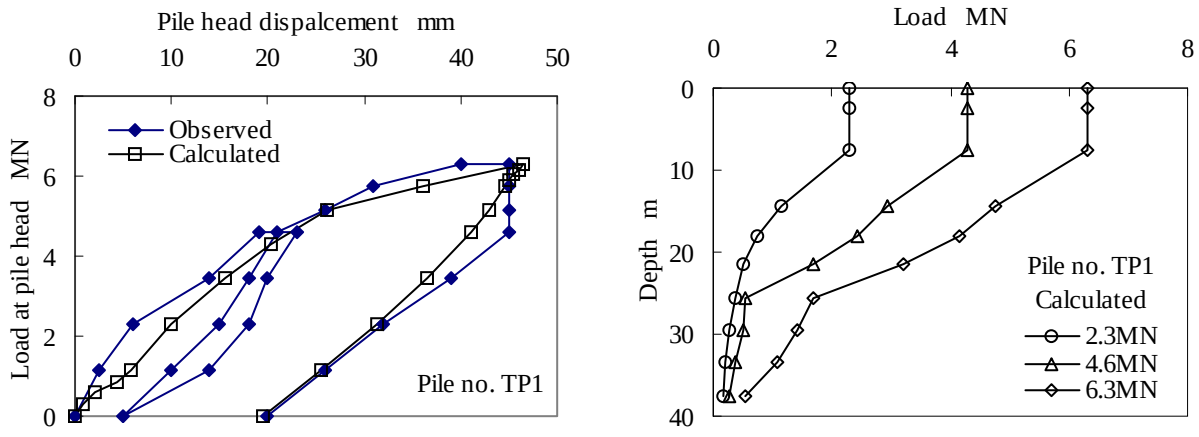

Figure 5: Pile head displacements and load distribution for pile no. TP1

4 COMPARISON OF PILE RESISTANCES

The sets of hyperbolic parameters for shaft resistances (τ_{s-max}/N, δ_{sr}) and base resistances (τ_{b-max}/N, δ_{br}) for saprolitic soils of the completely decomposed granite (CDG) and the completely decomposed interbedded meta-sandstone and siltstone (MSS Grade V) interpreted from the instrumented pile load test results of Case 1 and Case 2 in this study are summarized in Table 5. The results of studies conducted by Chang & Broms (1991) and Wong (2007a) on augered bored piles and on pre-bored piles respectively are also presented for comparison.

Chang & Broms (1991) presented the load transfer parameters of bored piles in residual soils in Singapore. In general, the piles of 600 mm to 1200 mm in diameters and 15 m to 20 m in lengths were constructed by rotary drilling rigs and short-flight augers. The piles were constructed in highly weathered sandstones, siltstones or shales of the Jurong Formation, a sedimentary rock formation of Late Triassic and Lower to Middle Jurassic age. Based on the results of 10 instrumented bored piles, Chang & Broms (1991) interpreted that for materials with N values less than 180, the τ_{s-max}/N ratios range from 1.2 to 3.4 (kPa), with an average of 2.0 (kPa). It is however noted that the 2 load transfer parameters, the ultimate resistance and the corresponding critical displacement to fully mobilize this resistance, that estimated by Chang & Broms (1991) follow the load-displacement relationships defined by Vijayvergiya (1977). The critical displacements could not be readily compared with the reference displacements adopted in this study.

The τ_{s-max}/N values reviewed in this study (Case 1 and Case 2) are consistent with the experience on bored piles reported in literature. For slurry supported and augered bored piles in saprolite, the τ_{s-max}/N ratios range from 1.45 to 3.5 (kPa), which are in a close agreement with those reported by Chang & Broms (1991) on bored piles in Singapore's weathered Jurong Formation. The reference shaft displacements (δ_{sr}) for the slurry supported bored piles and the augered piles is 0.8 mm and 1 mm respectively and vary in a narrow range.

Wong (2007a) estimated the load transfer parameters for pre-bored piles of 610 mm in diameter socketed in granite. The uncased pre-bored piles have τ_{s-max}/N ratios of 0.5 to 1 (kPa) in CDG, or about 30 % of those could be developed by bored piles or augered piles. For the cased pre-bored piles that the temporary casings

Table 5: Summary of pile resistance parameters for bored piles in saprolite

Pile type	Ground type	Shaft resistance		Base resistance		References
		τ_{s-max}/N kPa	δ_{sr} mm	τ_{b-max}/N kPa	δ_{br} mm	
Slurry supported bored pile	CDG	1.45 ~ 3.5	0.8	13	3 ~ 4.5	This study
Augered bored pile	MSS Grade V	3.3	1	16	3	This study
Augered bored pile	Residual soils	1.2 ~ 3.4	-	-	-	Chang & Broms (1991)
Uncased pre-bored pile	CDG	0.5 ~ 1	2	-	-	Wong (2007a)
Cased pre-bored pile	CDG	0.1	2	-	-	Wong (2007a)

were left in place, the τ_{s-max}/N ratio is 0.1 (kPa). Compared with other types of bored piles, the lower development of shaft resistances of the pre-bored piles could be attributable to the installation method. The Odex (Overburden Drilling Eccentric Method) type drill bits were used for sinking the temporary casings and annular voids between the temporary casings and the surrounding ground were created.

The 2 case histories reviewed in this study show that the sets of hyperbolic parameters for base resistances mobilized by the slurry supported and the augered bored piles are within a narrow range, with the τ_{b-max}/N ratios varying between 13 and 16 (kPa) and the reference base displacements varying between 3 and 4.5 mm.

CONCLUSIONS

The hyperbolic load-displacement relationships of the shaft and the base resistances of bored piles have been interpreted from case histories of instrumented piles. The following concluding remarks could be drawn:

(1) The shaft and base resistances that could be developed by the slurry supported bored piles and augered piles are similar.
(2) The shaft resistances of bored piles in saprolite interpreted from Case 1 and Case 2 of this study are consistent with the experience reported in literature.
(3) The pre-bored piles that created annular voids outside the temporary casings during boring develop less shaft resistances than the slurry supported or the augered bored piles.
(4) The load-transfer characteristics are dependent on the pile installation methods and the construction details.

This study demonstrates that the load transfer method using Winkler springs is a useful tool for assessing pile performance and for interpretation of results of pile load tests.

ACKNOWLEDGEMENTS

The author wishes to express his sincere thanks to Dr R.N. Hwang for his valuable comments on the paper.

REFERENCES

Chang, M.F. & Broms, B.B. 1991. Design of bored piles in residual soils based on field performance data. *Canadian Geotechnical J.* 28: 200-209.

Coyle, H.M. & Reese, L.C. 1966. Load transfer for axially loaded piles in clay. *J. of the Soil Mechanics and Foundation Division*, ASCE, Vol. 92, no. SM2: 1-26.

Fleming, W.G.K. 1992. A new method for single pile settlement prediction and analysis. *Geotechnique* 42: 411-425.

Geotechnical Engineering Office 2006. Foundation design and construction. *GEO Publication No. 1/2006.* Geotechnical Engineering Office, Civil Engineering and Development Department, The Government of the Hong Kong SAR.

Moh, Z.C., Chang, M.F. & Hwang, R.N. 1995. Load transfer in piles during load reversals. *Proc., 10th Asian Regional Conference on SMFE*, Beijing, China, 207-210.

Pickles, A.R., Lee, S.W. & Tosen, R. 2003. Shaft capacity of friction piles constructed in saprolite under bentonite and implications for end bearing piles. *Proc., HKIE Geotechnical Division Annual Seminar 2003*, 214-222.

Vijayvergiya, V. N. 1977. Load-settlement characteristics of piles. *Proc. of Ports '77 Conference*, Long Beach. CA, 269-284.

Wong, C.M. & Tse, Y.P. 2001. Auger-injected piles floating above karstic marble. *Proc., 14th Southeast Asian Geotechnical Conference*, Hong Kong, 1067-1070.

Wong, L.W. 2007a. Load transfer of pre-bored piles socketed in granite. *Proc., 16th Southeast Asian Geotechnical Conference*, Kuala Lumpur, Malaysia.

Wong, L.W. 2007b. Analysis of driven piles with load transfer method. *HKIE Geotechnical Division Annual Seminar 2007*, 293-297.

Use of Grid-Based Tactile Pressure Sensor in Geotechnical Engineering

A.T. Yeung, Y.Y. Liu and S.T.C. So
University of Hong Kong, Hong Kong

ABSTRACT

The distributions of normal stress underneath foundations, acting on earth retaining structures, or imposing on pipelines, tunnel linings or other buried structures are often required in the solutions of many geotechnical engineering problems. Although there are many existing solutions for the problem, the validity of these solutions may not have been verified experimentally. The most common instrumentation being used to measure normal stress in soil is the total pressure cell. However, the measurements of normal stress distributions by total pressure cells suffer from many technical limitations, in particular in laboratory-scale physical model tests when the size of the physical geotechnical model is relatively small. The use of grid-based tactile pressure sensors may provide a versatile and innovative solution for the problem. The grid-based tactile pressure sensors were originally developed by the Artificial Intelligence Laboratory of MIT for use in the sensation system of robots. The technology was later developed into medical applications to measure tooth, foot, and orthopedic pressures. A geotechnical engineering research team at the Department of Civil Engineering of The University of Hong Kong is investigating the potential uses of the technology in geotechnical engineering. Some of their experimental observations are presented in this paper.

1 THE PROBLEM

The distribution of normal stresses underneath foundations, acting on earth retaining structures, or imposing on pipelines, tunnel linings or other buried structures is an important field of study in geotechnical engineering. The subject is theoretically challenging for theorists and practically important for practicing engineers. Many theories have been developed to describe the distributions of normal stresses under different loading conditions and boundary conditions. However, it is difficult to evaluate the validity of these theories comprehensively through experiments due to the limitations of geotechnical instrumentation, in particular for the less expensive laboratory-scale physical model tests when the size of the model is relatively small.

In conventional geotechnical projects, the distribution of normal stress in soil is measured by total pressure cells. The total pressure cell is constructed from two stainless steel plates welded together around their peripheries and separated by a narrow gap filled with hydraulic fluid. A length of high-pressure stainless steel tubing connects the fluid-filled cavity to a vibrating wire pressure transducer. The external pressure acting on the cell is balanced by an equal pressure induced in the internal fluid. The internal pressure required to maintain the balance is converted by the transducer into an electrical signal that can be read by a readout device or data logger (Dunnicliff 1988; Yeung et al. 2006). Although the total pressure cell may be adequate to give an indication of the total stress in soil at a particular location, it is not suitable for detailed and accurate studies of normal stress distribution in soil for two main technical reasons: (1) the huge contrast in stiffness between the stainless steel total pressure cell and soil; and (2) the assumption of uniform stress distribution throughout the measurement area of the total pressure cell.

Due to the rigidity of the stainless steel total pressure cell, the contrast in stiffness between the cell and soil is significant. The huge contrast in stiffness may cause an increase or a decrease in the measured stress due to soil arching depending on installation details (Selig 1989). As only the internal hydraulic fluid pressure required to balance the external soil pressure is measured, the stress distribution acting on the total pressure cell has to be assumed to be uniform. The assumption of uniform stress distribution restricts the use of total pressure cells when the boundary conditions are complex. Nonetheless, as the only available alternative, the total pressure cell is widely used in geotechnical engineering projects regardless of its serious limitations. When the distribution of stress as a function of space and time is required, the distributions are obtained through the measurements made through a network of total pressure cells installed over the area of interest as

a function of time. For a better measurement of stress distribution, a large number of cells are required. However, the accuracy of the measurement decreases with the increase in the number of cells used and the extent of intrusion. It should be noted that the increase in the number of cells increases the rigidity of the system being measured and the extent of intrusion. In laboratory-scale physical model tests, there may not be enough space in the relatively small model to accommodate the required number of total pressure cells. Moreover, the handling of the connecting wires is another physical and technical problem.

Therefore, it is evident that there is a need for a sensor system that can make normal stress measurements at close spacing to quantify the stress distribution with an acceptable intrusion to the system being measured. Moreover, the sensor system has to be very flexible to minimize the errors induced by soil arching.

2 THE SOLUTION USING GRID-BASED TACTILE PRESSURE SENSORS

The development of grid-based tactile pressure sensors may provide a solution for the problem. Grid-based tactile pressure sensors were originally developed at the Artificial Intelligence Laboratory of the Massachusetts Institute of Technology of the U.S.A. as a development of the sensation system for robots so that a robot finger can recognize small objects by touch (Hillis 1981; Purbrick 1981). The technology was further developed by Tekscan, Inc. of South Boston, Massachusetts, U.S.A. in 1987 for dentistry to help dentists quantify the pressures between individual teeth generated by a patient's closure (bite) for the analysis of dental occlusion (Podoloff & Benjamin 1989). Since then, Tekscan has been improving the technology and extending its applications in a variety of industries. Grid-based tactile pressure sensors are now being used to measure tooth, foot, and orthopedic pressures in medical fields. Industrial applications of the sensors include measurements of contact stress of robot hand, tire tread, seat, and pinch roller pressures.

The standard Tekscan matrix-based sensor consists of two thin, flexible polyester sheets that have electrical strip patterns (conductors) deposited on them as shown in Figure 1. Typically, the inside surface of one sheet employs a row pattern while the inner surface of the other employs a column pattern. The spacing between the strip patterns (rows and columns) varies according to sensor application and can be as small as ~0.5 mm or as large as desired. Before assembly, a patented, semi-conductive coating (or ink) is applied as an intermediate layer between the electrical contacts.

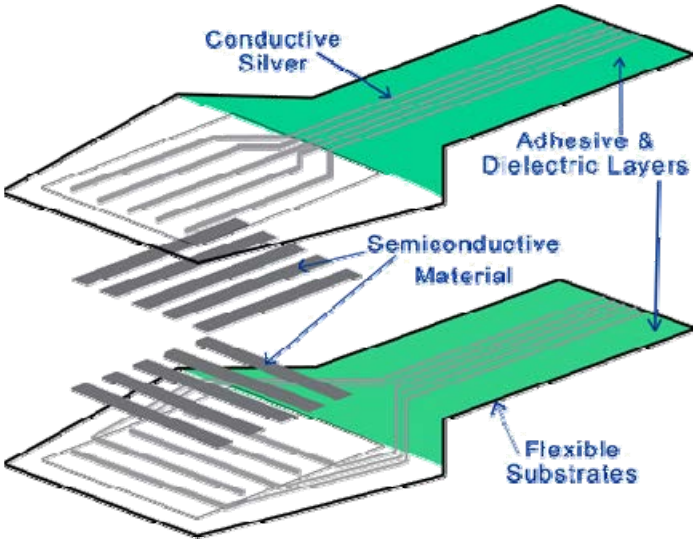

Figure 1. Tactile pressure sensor technology

When the two polyester sheets are in contact with each other, a grid pattern of electrical contacts, or sensing locations is formed at the intersection of each row and column. These intersections form the sensing cells or sensels. When a force is applied to these sensing cells, the electrical resistance in the ink changes in response to the applied normal force. Therefore, Tekscan's matrix-based systems provide an array of force sensitive cells that enable measurement of the pressure distribution between two surfaces. The total thickness of the sensor is less than 0.1 mm. The sensor is so thin and flexible that it can be easily installed between two mating surfaces and remains minimally intrusive to the true pressure pattern and fit in almost any application. Moreover, the high sensitivity and high density of sensels within a small area make it possible to measure the distribution of contact pressure precisely and practically continuously.

Sensor grids are available in a wide range of shapes and sizes. They are also available in various pressure ranges from 0-14 kPa to 0-175 MPa. For example, the details of Sensor #3150 are presented in Figure 2. Every Tekscan Industrial system uses a specially designed sensor interface electronic called a "handle" as shown in Figure 3. The handle connects to the sensor, collects the data from the sensor, and then processes and sends these data to a computer through an USB interface. The interface embodies sophisticated microprocessor based circuitry to control the scanning sequence and frequency, adjust sensitivity, and

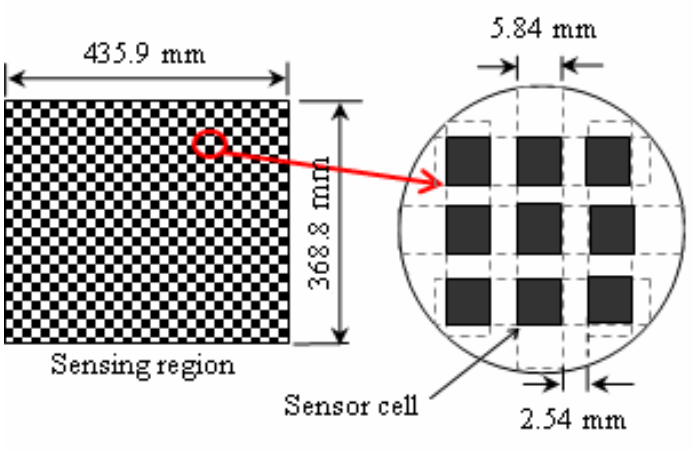

Figure 2. Details of the tactile pressure sensor #3150 (Tekscan, 2007)

Figure 3. The handle

optimize the performance of sensors. The software of the system provides advanced, yet simple to use tools to display force and pressure data in real-time. Data can also be saved, analyzed in different graphs, or exported into ASCII programs.

There are equilibration/calibration devices of different stress ranges used to calibrate the pressure measurement system. These devices apply uniform pressures covering the operating stress range of the sensor to the active area of the sensor to allow the software to compensate for variation in the output of individual sensels. The software determines and applies a gain (scale factor) to each sensel so that its digital output is equal to the average digital output of all the equally-loaded sensels. The equilibration/calibration device being used by The University of Hong Kong is shown in Figure 4. It can also be observed in Figure 4 how the sensor is connected to a laptop computer through the handle.

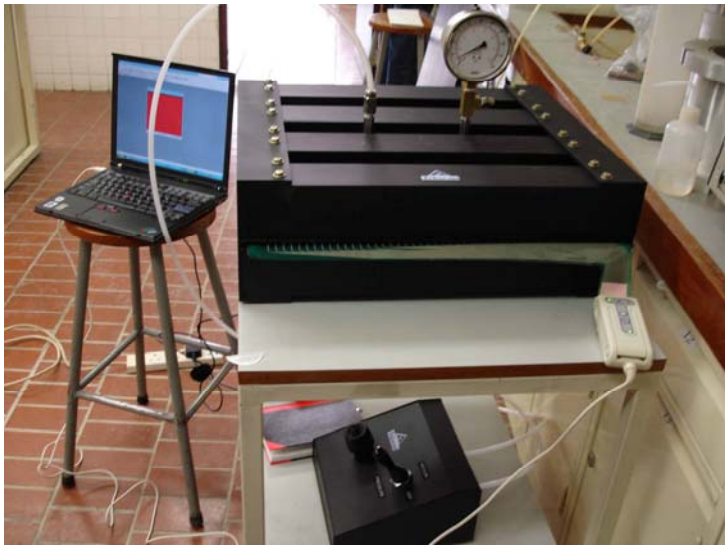

Figure 4. The equilibration/calibration device

The technology has been applied successfully to measure stress distribution in geotechnical engineering (Paikowsky & Hajduk 1997) in the measurement of classic normal stress distribution underneath a sand pile, experimental evaluation of Terzaghi's famous trap door problem (Terzaghi 1936; Paikowsky et al. 2003), measurement of stress distribution underneath a rigid strip footing (Paikowsky et al. 2000), etc.

3 Ongoing Research at The University of Hong Kong

With support from the Research Grants Council of the Government of the Hong Kong Special Administrative Region, the research team under the supervision of the first author has acquired the system from Tekscan, Inc. and performed experiments on various laboratory-scale and field-scale normal stress distribution problems in geotechnical engineering. Some of the results are presented here and they are by no means exhaustive.

3.1 Vertical stress distribution underneath confined sand columns

The vertical stress distribution underneath confined sand columns is of practical significance to many, as the design problems relating to the storage of sugar or other food grains in silos fall into this category. As early as 1895, H.A. Janssen, a German engineer, proposed the existence of a saturation value for the vertical pressure

or mean vertical stress underneath the column of granular material of increasing height ensiled in silos. In Janssen's original analysis, the mean vertical stress σ_z underneath a column of dry granular material of height z is given by (Nedderman 1992; Sperl 2006)

$$\sigma_z = \frac{\gamma D}{4K \tan\delta}\left[1 - \exp\left(-K \tan\delta \frac{4z}{D}\right)\right] \quad (1)$$

where γ = dry unit weight of the granular material; D = internal diameter of the silo; δ = friction angle between the granular material and the vertical cylindrical wall of the silo; K = Janssen constant = $(1 - \sin\varphi)/(1 + \sin\varphi)$ (= Rankine's coefficient of lateral earth pressure); and φ = internal friction angle of the granular material. However, the theory gives no distribution of vertical stress.

An experiment as shown in Figure 5 was setup to evaluate the vertical stress distribution underneath confined sand columns using the tactile pressure sensors. The results are presented in Figure 6. The measured vertical pressure is normalized by the vertical pressure determined by γz and the distance from the center of the silo is normalized by the radius of the silo, i.e., R = D/2. It can be observed that the distribution of vertical stress is highly non-uniform. In general, it attains a maximum value at approximately 0.6R from the center of the silo. The impact of friction along the sand-silo interface and soil arching on the vertical stress distribution is evident. More details can be obtained from Liu & Yeung (2008).

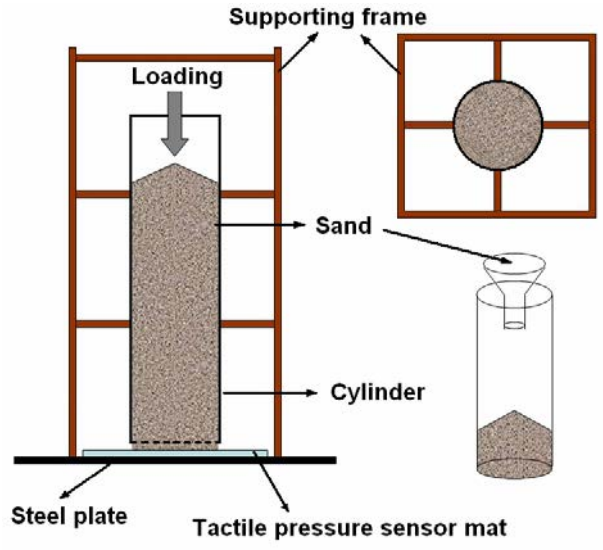

Figure 5. Experimental setup for vertical stress distribution under confined sand columns

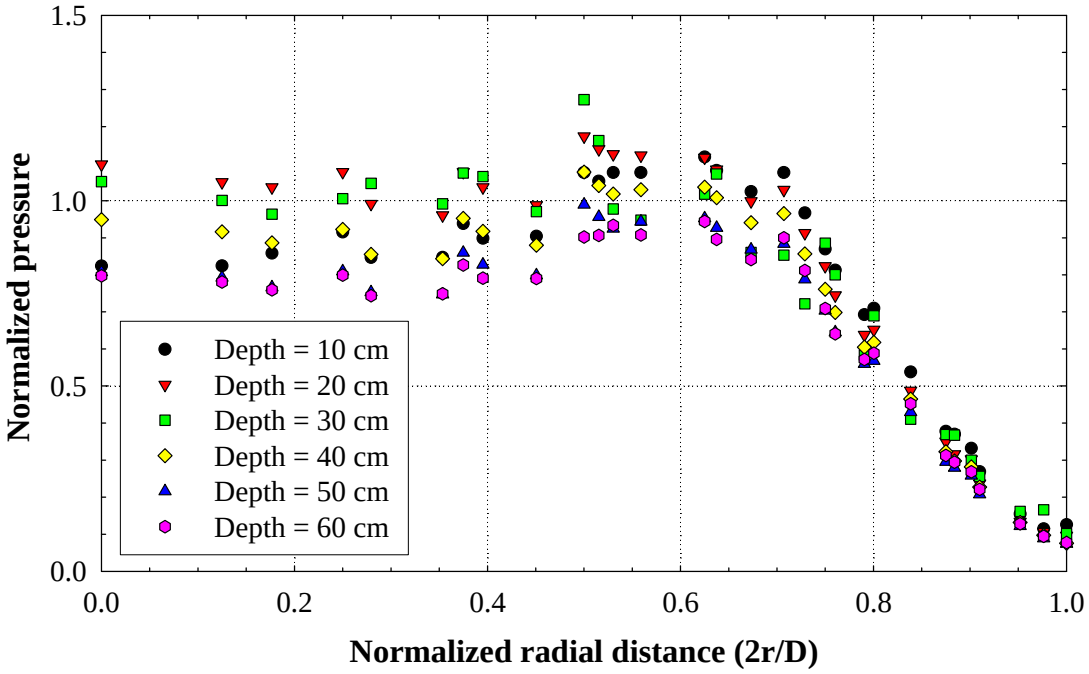

Figure 6. Normalized vertical pressure versus normalized radial distance from silo center

3.2 Distribution of bearing pressure during a plate load test

The bearing pressure distribution underneath the steel loading plate in the plate load test is often assumed to be uniform, and no measurement is made in routine tests. However, if the distribution of bearing pressure is known, the results obtained can be better understood, leading to better design of shallow foundations when the results are extrapolated to a field-scale footing or raft foundation made of concrete and of a considerably larger size, as the effects of the stiffness of foundation construction material and the scale can be properly addressed. Therefore, a field-scale experiment as shown in Figure 7 was setup.

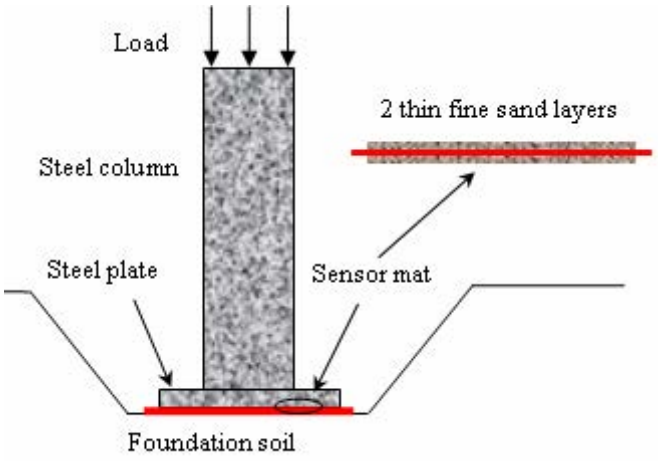

Figure 7. Setup of plate load test with vertical stress distribution measurement

The load was in the sequence of 0, 200(a), 400(b), 200(c), 0, 200(d), 400(e), 600(f), 800(g), 600(h), 400(i), 200, and 0 kPa. The letter in parentheses denotes the different loading stages. The distributions of vertical stresses at each of these loading stages are presented in Figure 8. It can be observed that the stress distribution is again highly non-uniform. However, the stress distributions under the same loading at different loading stages are similar, although the settlements are not necessarily similar.

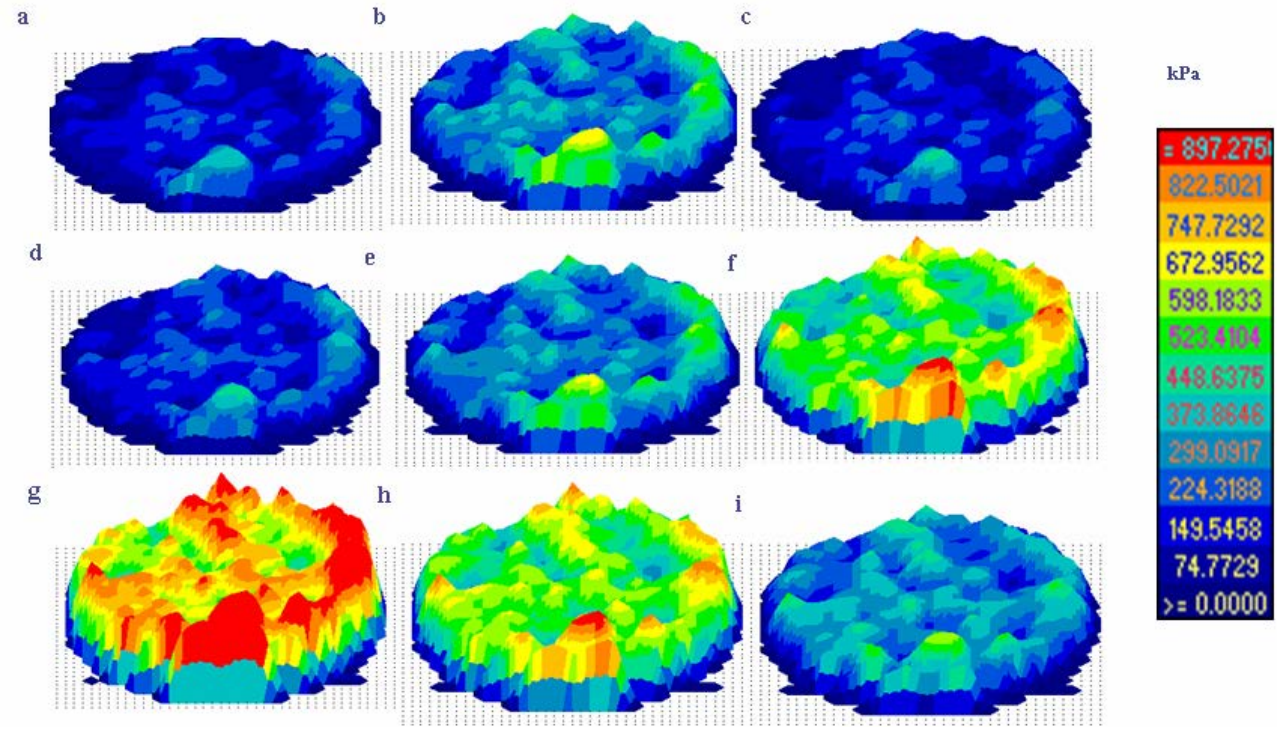

Figure 8. Vertical contact pressure distribution underneath the steel loading plate during a plate load test

4 CONCLUSIONS

In this research, a new grid-based tactile pressure sensor mat has been adopted successfully for laboratory-scale and field-scale experiments on the determination of vertical stress distribution underneath confined sand columns and bearing pressure underneath the steel loading plate during a plate load test. Our experience indicates that the grid-based tactile pressure sensor can be developed into a versatile tool in stress distribution

measurement for geotechnical engineering applications. In fact, research is on-going at The University of Hong Kong to explore other applications of the technology in geotechnical engineering.

ACKNOWLEDGEMENTS

Financial support provided by Research Grants Council Project No. HKU 7193/05E of the Hong Kong Special Administrative Region Government for this project is gratefully acknowledged. However, the contents of this paper do not necessarily reflect the views and policies of the Hong Kong Special Administrative Region Government, or does the mention of trade names and commercial products constitutes endorsement or recommendation for use.

REFERENCES

Dunnicliff, J. 1988. *Geotechnical instrumentation for monitoring field performance*. New York: Wiley.

Hillis, W.D. 1981. *Active touch sensing*. Artificial Intelligence Laboratory Memo 629, MIT, Cambridge, Massachusetts.

Liu, Y.Y., So, S.T.C. & Yeung, A.T. 2008. Use of tactile pressure sensor for plate load test. *Geotechnical and geophysical site characterization, Proc., 3rd International Conference on Site Characterization ISC'3*, Taipei, 1335-1338.

Liu, Y.Y. & Yeung, A.T. 2008. Accurate measurement of vertical stress distribution underneath sand columns. *Proc., 3rd NASA/ARO/ASCE Granular Materials in Lunar and Martian Exploration Workshop, Earth & Space Conference 2008*, ASCE, Long Beach, California.

Nedderman, R.M. 1992. *Static and kinematics of granular materials*. Cambridge University Press, New York, New York.

Podoloff, R.M. & Benjamin, M. 1989. Tactile sensor for analyzing dental occlusion. *SOMA Engineering for the Human Body*, 3(3): 1-6.

Purbrick, J.A. 1981. A force transducer employing conductive silicone rubber. *Proc., 1st Robotic Vision and Sensors Conference*, Stratford-on-Avon, United Kingdom.

Paikowsky, S.G. & Hajduk, E.L. 1997. Calibration and use of grid-based tactile pressure sensors in granular material. *Geotechnical Testing Journal*, ASTM, 20(2): 218-241.

Paikowsky, S.G., Palmer, C.J. & DiMillio, A.F. 2000. Visual observation and measurement of areal stress distribution under a rigid strip footing. *Performance verification of constructed geotechnical facilities*. Lutenegger and DeGroot, Editors, Geotech. Spec. Publ. No. 94, ASCE, Reston, Virginia, 148-169.

Paikowsky, S.G., Rolwes, L.E. & Tien H.S. 2003. Visualization and measurements of stresses around a trap door. *Soil and Rock America 2003*, Proc. 12th Panamerican Conf. Soil Mech. Geotech. Engrg. & 39th U.S. Rock Mech. Symp., MIT, Cambridge, Vol. 1, 1171-1177.

Selig, E.T. 1989. In situ stress measurements. *Proc. Symposium on State of the Art of Pavement Response Systems for Roads and Airfield*, W. Lebanon, New Hampshire.

Sperl, M. 2006. Experiments on corn pressure in silo cells - translation and com-ment of Janssen's paper from 1895. *Granular Matter*, 8(2): 59-65.

Tekscan, Inc. 2007. http://www.tekscan.com/

Terzaghi, K. 1936. Stress distribution in dry and in saturated sand above a yielding trap-door. *Proc, 1st International Conference on Soil Mechanics and Foundation Engineering*, Cambridge, Massachusetts, 307-311.

Yeung, A.T., Mok, K.Y., Tham, L.G., Lee, P.K.K. & Pei, G. 2006. Use of inert C&D materials for seawall foundation: A field-scale pilot test. *Resources, Conservation and Recycling*, 47(4): 375-393.

Innovative Optical Fiber Sensors for Monitoring Displacement of Geotechnical Structures

J.H. Yin, H.H. Zhu, and K.W. Fung

The Department of Civil and Structural Engineering, The Hong Kong Polytechnic University Hung Hom, Kowloon, Hong Kong, China

W. Jin

The Department of Electrical Engineering, The Hong Kong Polytechnic University, Hong Kong, China

L.M. Mak and K. Kuo

LMM Consulting Engineers Ltd, Suite 901, 88 Hing Fat Street, North Point, Hong Kong, China

ABSTRACT

The measurement of displacements occurred within geotechnical structures is of great importance. Existing techniques for measuring displacements inside geotechnical structures have limitations. This paper introduces innovative optical fiber sensors based on fiber Bragg grating (FBG) technology and associated devices for measuring displacements within geotechnical structures, for example, inside a slope or soil ground. The scientific principle of the sensors are presented and explained first. All optical fiber sensors are designed and made in The Hong Kong Polytechnic University. All sensors have been calibrated in laboratory. Typical calibration results are presented. Afterwards, the optical fiber sensors are used to monitor the internal displacements of a model dam. The results measured using these optical fiber sensors are compared with those obtained using conventional displacement transducers. It is found that the results from the two technologies are in good agreement. The advantages of the optical fiber sensors are presented. The innovative optical fiber sensors have great potential applications in Hong Kong, for example, measuring lateral movement of slopes, heave or settlement of ground due to trenchless tunneling, settlement of soft soil ground, lateral movement of excavations, *etc*.

1 INTRODUCTION

For geotechnical structures such as foundations, dams and retaining walls, deformation monitoring supplies information on the behavior of the structures and their interactions with the ground soil. Monitoring results may also be used in verifying design parameters and providing early warning of impending failure. There are a variety of geotechnical instruments that have been developed for deformation measurements in the past decades. For the measurement of horizontal and vertical displacement of ground surface, conventional surveying methods are commonly used. For subsurface deformation measurement, different types of extensometers, inclinometers and tilt meters can be implemented. However, these existing techniques for monitoring deformation have limitations including low accuracy, poor reliability, high cost and difficulty of installation and operation (Dunnicliff 1993).

Optical fiber sensor plays an increasingly important role in deformation monitoring of civil structures (Saouma et al. 1998; Casas et al. 2003 Chan et al. 2006; Glisic et al. 2007; Metje et al. 2008). Compared with conventional instruments, they are immune to electrical interference, have high excellent durability and accuracy, and offer multiplexed sensing array (Yin et al. 2007; Zhu et al. 2007). In this paper, two innovative optical fiber sensors based on fiber Bragg grating (FBG) technology were developed for the measurement of displacements occurred within geotechnical structures. The sensors were calibrated in laboratory and successfully applied to deformation monitoring of a model dam test, a mat foundation and a soil nailed slope. The reliability of these sensors was verified by laboratory tests and field applications.

2 WORKING PRINCIPLES

2.1 Operating principle of FBG

FBGs are intrinsic sensing elements written into optical fibers by exposure to ultraviolet light through phase masks. The grating acts as a selective spectral reflector at a characteristic wavelength λ_B. The wavelength is strain and temperature dependent and can be described by the following equation (Othonos et al. 1999):

$$\frac{\Delta\lambda_B}{\lambda_B} = c_\varepsilon \Delta\varepsilon + c_T \Delta T \tag{1}$$

where $\Delta\lambda_B$ is the change in wavelength due to strain and temperature variation; λ_B is the original wavelength under strain free and 0 ^oC condition; $\Delta\varepsilon$ is the change in axial strain; ΔT is the change in temperature; c_ε and c_T are coefficients.

2.2 FBG sensing tube for measuring displacement profile

Sensing tubes with FBGs connected in series have been developed for measuring horizontal or vertical displacement profile. Four optical fibers are designed to be adhered on the tube surface perpendicularly. Each fiber consists of several FBGs at regular intervals and forms a quasi-distributed sensing array. These sensing tubes are placed in the ground soil vertically or horizontally. When ground movement occurs, they work like an elastic beam under simultaneous axial and transverse loading, shown in Figure 1. According to the elastic beam theory, the strain distributions depend on the normal axial force $N(z)$ and distributions of the bending moments $M_x(z)$ and $M_y(z)$ along the neutral line of the beam and can be described by

$$\varepsilon = \frac{N(z)}{EA} \pm \frac{M_x(z)}{EI_x} R \pm \frac{M_y(z)}{EI_y} R = \varepsilon_A(z) \pm \varepsilon_{Bx}(z) \pm \varepsilon_{By}(z) \tag{2}$$

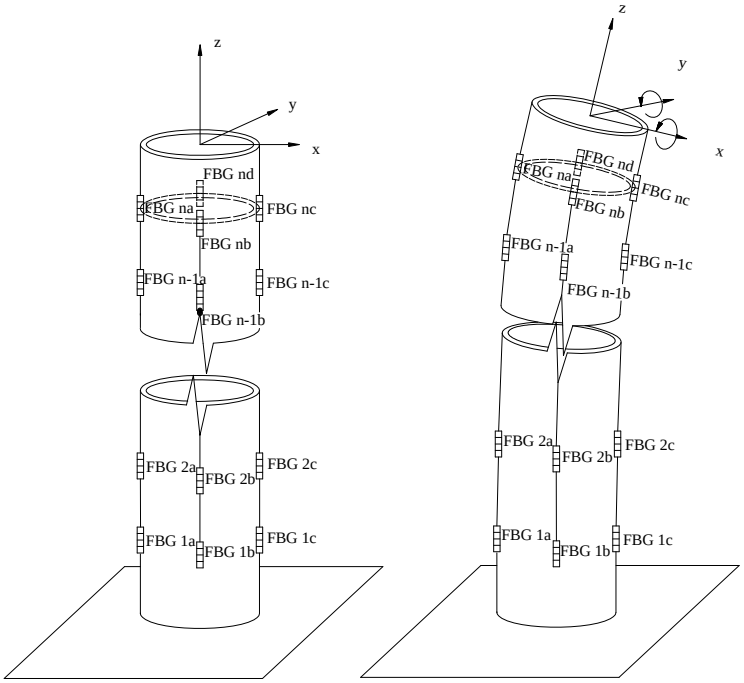

(a) Before deformation (b) After deformation

Figure 1: Schematic illustration of an FBG sensing tube for measuring displacement profile

where $\varepsilon_A(z)$ is the strain induced by axial loading; $\varepsilon_{Bx}(z)$ and $\varepsilon_{By}(z)$ are the strains induced by arbitrary transverse loading in x and y direction and dependent on the bending moments $M_x(z)$ and $M_y(z)$; R is the outer diameter of the sensing tube.

Due to deformation compatibility, the displacement profile of ground soil is equal to the displacement profile of the sensing tube. Since the surface adhered FBGs measure the strain distributions along the sensing tube perpendicularly, the tube elongation or compression in z direction due to axial loading can be calculated by

$$S_z = \int \varepsilon_A(z) dz \tag{3}$$

Similarly, the relative deflections in x and y directions due to bending can be computed by

$$S_x = \frac{1}{R}\int\int \varepsilon_{Bx}(z)\, dzdz \tag{4}$$

$$S_y = \frac{1}{R}\int\int \varepsilon_{By}(z)\, dzdz \tag{5}$$

In field, the FBG sensing tubes can be installed under dams or shallow foundations horizontally and used to measure the profile of settlement or heave in ground soil. For slopes, the FBG sensing tubes can be installed in drill holes and used to measure the lateral movements in two horizontal directions and vertical direction. Like inclinometer casings, prior to field installation, the sensing tubes are connected to each other by couplers to provide continuous displacement monitoring. The diameter and length of the tube, as well as the FBG spacing, can be adjusted to ensure accuracy and facilitate installation. For laboratory application such as deformation monitoring of small-scale model tests, the sensing tube can be even replaced by a small diameter bar.

2.3 FBG sensing tube for measuring settlement in a drill hole

For settlement measurement in a drill hole, the FBG sensing tubes can be connected in a series and placed in the hole with proper backfill. Every tube measures the vertical compression inside ground soil for each 1m (or other predefined length) vertical layer at different depth.

Illustrated in Figure 2, the sensing tube mainly consists of a stainless steel spring, a zig-zag tube and a pre-tensioned FBG adhered in a polyethylene (PE) tube. When soil settlement occurs, the zig-zag tube is loaded by friction at the interface, causing compressive force in the spring. The compressed spring applies a reaction force on the PE tube. Based on force equilibrium of the PE tube, the displacement can be calculated by the following equation:

$$kS_i = EA\varepsilon_i \text{ or } S_i = \frac{EA}{k}\varepsilon_i = c_S\varepsilon_i \tag{6}$$

where ε_i is the strain measured by FBG of the *i*th tube; A is the section area of the PE tube; E is Young's modulus of PE (600~900 MPa); S_i is the compression of the *i*th soil layer; k is the spring constant; c_S is a calibration coefficient. From equation (1) and (8), the FBG wavelength shift is proved to be proportional to the settlement.

Provided that the bottom of the deepest tube is located on the bedrock, the total settlement can be calculated by the following equation

$$S = \sum S_i = \sum c_S\varepsilon_i \tag{7}$$

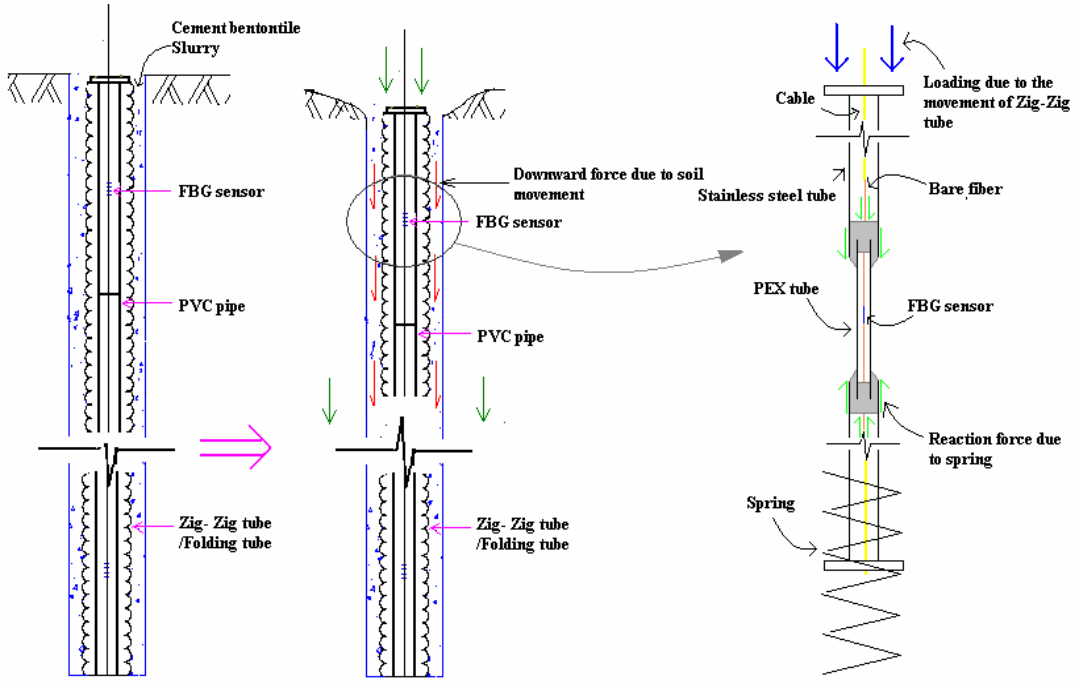

Figure 2: Mechanism of the FBG sensing tubes for measuring settlements

3 LABORATORY CALIBRATION RESULTS

3.1 Calibration of FBG sensing bars for measuring displacement profile

In order to verify the effectiveness of the new instrument for displacement profile measurement, several FBG sensing bars were prepared for calibration. The calibration consisted of two categories: elongation tests and deflection tests. For the demodulation of FBGs, a four channel interrogator sm125 was employed. It reads the reflected wavelengths of FBGs in an ascending order and interrogates up to 512 FBGs simultaneously, with 0.1 pm (10^{-12} m) resolution and 1 Hz acquisition speed (Micron Optics Inc. 2007). Therefore rapid and accurate measurements can be achieved in real time. In this system, the computer used to record the test data is connected to the interrogator through Ethernet and remote monitoring is definitely accessible.

In elongation tests, loading / unloading cycles were applied to FBG sensing bars using a universal hydraulic servo-controlled machine. The displacement was calculated by the measurement of surface adhered strain gauges. In deflection tests, sensing bars were subjected to lateral movement manually at arbitrary locations and the deflections were measured by digital displacement transducers. Typical calibration test results are shown in Figure 3. There is a linear relationship between FBG wavelength and applied elongation displacement. By comparison of the deflections measured by the FBG sensing tube and displacement transducers, a good agreement can be seen.

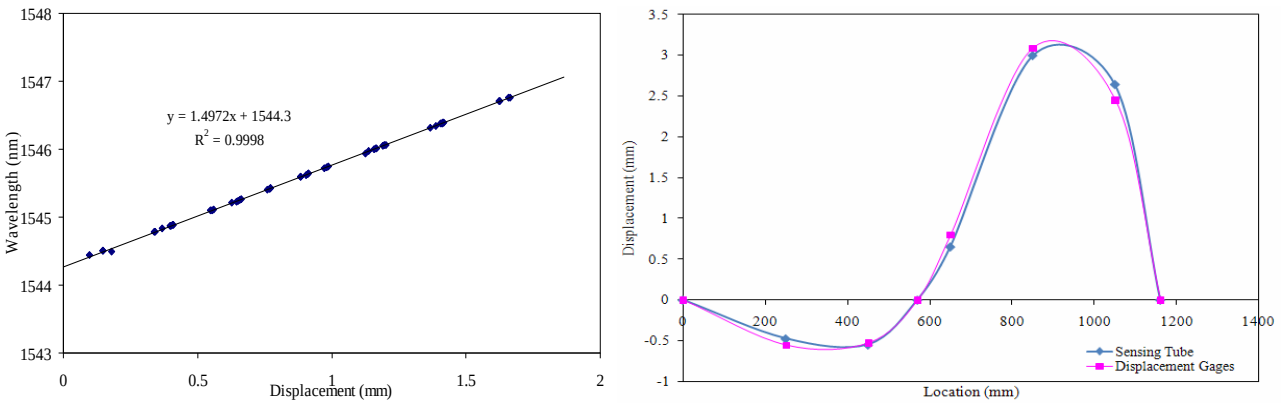

(a) Elongation test (b) Deflection test

Figure 3: Typical calibration test results of the FBG sensing bars for measuring displacement profiles

3.2 Calibration of FBG sensing tubes for measuring settlements in a drill hole

To verify the effectiveness of the FBG sensing tubes for measuring settlements, a multi-stage loading was applied on the tube. Figure 4 illustrates the relationship between the wavelength shift and the settlement. By comparison, it is found that the FBG wavelength is proportional to the applied settlement.

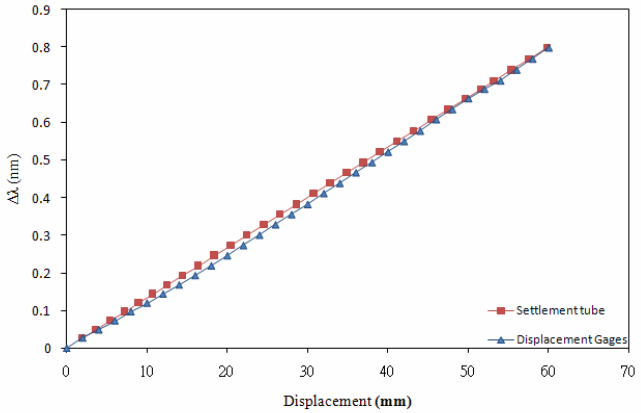

Figure 4: Typical calibration test results of FBG sensing tubes for measuring settlements

4 FIELD APPLICATIONS

These two kinds of FBG based sensors have been successfully applied the displacement monitoring of geotechnical structures in laboratory and in field.

A 1:150-scaled 2D physical model of a gravity dam was constructed in College of Hydraulic and Hydroelectric Engineering, Sichuan University. An overload test was carried out to evaluate the dam stability and simulate the failure mechanism. A step-wise loading was adopted by hydraulic jacks, from 0.5q (q is the normal water load) until dam failure.

To monitor the dam deformation, two FBG sensing bars were installed in the model dam, together with linear variable displacement transducers (LVDTs). Each bar had a diameter of 10 mm and a length of 500 mm, with ten FBGs evenly distributed on the surface. One was embedded in the dam structure monitoring the deformation profile from the dam top to the ground. The other was embedded in the downstream rock foundation near to the dam toe, monitoring the deformation profile in the dam foundation. Figure 5 shows the installation of the FBG sensing bars. During the test, significant shear sliding occurred in the dam foundation and a small amount of deflections were observed in the upstream dam surface, shown in Figure 6. In Figure 7, the horizontal displacement monitored by the FBG sensing bar and a LVDT at the 50mm depth in the dam foundation is compared. It is observed that the displacements from these two sensors are in good agreement.

Figure 5: Installation of two FBG sensing bars for measuring displacement profiles

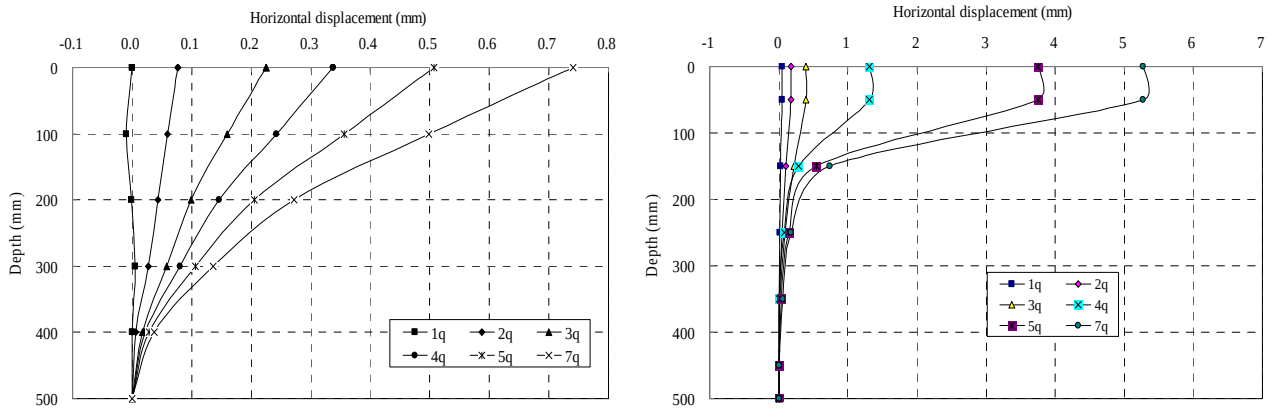

(a) Deflections of the dam structure (b) Deflections of the foundation

Figure 6: Distribution of deflections of the dam structure and the foundation monitored by the FBG sensing bars

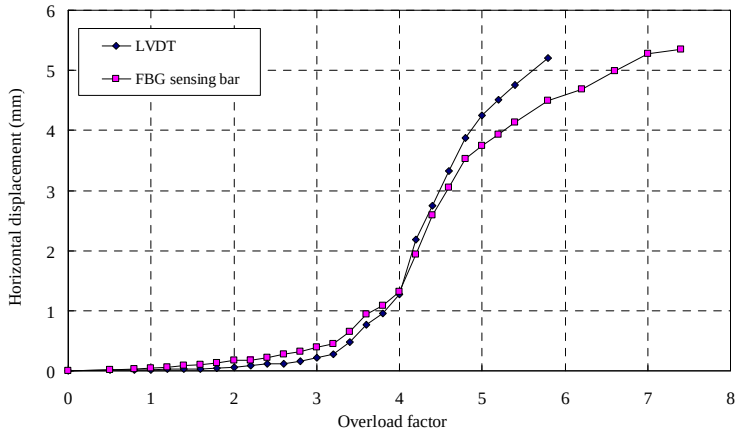

Figure 7: Comparison of monitored horizontal displacements in the dam foundation (50mm depth)

At the site of China Graduate School of Theology in Kowloon Tong, a three-storied building would be constructed on an 11.6m×11.4m mat foundation. For measuring settlement profile, two series of FBG sensing tubes were installed horizontally in the soil 100mm underneath the foundation, shown in Figure 8(a). Each series had a total length of 12 m, with 36 surface adhered FBGs. In two 4m-depth pre-drilled holes, totally eight FBG sensing tubes for measuring settlement were grouted by cement-bentonite slurry, shown in Figure 8(b). Monitoring data have been collected periodically since Feb 2007 and used to evaluate the performance of the mat foundation.

(a) FBG sensing tubes for settlement profile measurements (b) A FBG sensing tube in a drill hole

Figure 8: Installation of the FBG sensing tubes in the site of China Graduate School of Theology

In March 2008, at a slope site in Luk Keng, five FBG sensing tubes were installed vertically in a drill hole of 100mm diameter to measure potential lateral movements of the slope. The tubes had a total length of 15m and a diameter of 60mm. A total of 40 FBGs were adhered perpendicularly on the tube surface. The FBG spacing was designed to be 1.5m. Figure 9 demonstrated the detail of the FBG sensing tube and its field installation. The monitoring of slope movements will last for several years.

(a) Details of the sensing tubes (b) The sensing tubes after installation

Figure 9: Installation of the FBG sensing tubes in a slope in Luk Keng

5 CONCLUSIONS

Based on this study, the following conclusions can be drawn:

(a) The FBG based sensors can provide the measurement of ground deformation with high accuracy and sensitivity. In the calibration tests, the displacements measured using these optical fiber sensors are compared with those obtained using conventional displacement transducers. It is found that the results from the two technologies are in good agreement.

(b) In laboratory model test or field applications, these FBG based sensors are proved to be reliable for displacement measurements. These innovative optical fiber sensors have great potential applications in Hong Kong, for example, measuring lateral movement of slopes, heave or settlement of ground due to tunneling, settlement of soft soil ground, lateral movement of excavations, *etc*.

In addition to the above developments, other special optical fiber sensors can be developed for special applications, for example, measuring cracks, temperature, inclination, pore water pressures, earth pressures *etc*. The research and development (R&D) in this area is in progress at The Hong Kong Polytechnic University.

ACKNOWLEDGEMENTS

The authors gratefully acknowledge the financial support provided by cross-faculty grants of The Hong Kong Polytechnic University (G-YE14 and G-YE54). The support of LMM Consulting Engineers Ltd and Ove Arup & Partners Hong Kong Ltd in the instrumentation of the mat foundation and the slope is acknowledged. The monitoring work of the model dam is from the joint co-operation project between The Hong Kong Polytechnic University and Sichuan University. The authors wish to thank Prof. Zhang Lin for co-operation in the monitoring work.

REFERENCES

Casas, J.R. & Cruz, P.J.S. 2003. Fiber optic sensors for bridge monitoring. *Journal of Bridge Engineering*, 8(6): 362-373.

Chan, T.H.T., Yu, L., Tam, H.Y., Ni, Y.Q., Liu, S.Y., Chung, W.H. & Cheng, L.K. 2006. Fiber Bragg grating sensors for structural health monitoring of Tsing Ma Bridge: Background and experimental observation. *Engineering Structures*, 28(5): 648-659.

Dunnicliff J. 1993. *Geotechnical instrumentation for monitoring field performance.* New York: John Wiley & Sons Inc.

Glisic, B. & Inaudi, D. 2007. *Fibre optic methods for structural health monitoring.* New York: John Wiley & Sons, Ltd.

Metje, N., Chapman, D.N., Rogers, C.D.F., Henderson, P. & Beth, M. 2008. An optical fiber sensor system for remote displacement monitoring of structures–prototype tests in the laboratory. *Structural Health Monitoring*, 7(1): 51-63.

Micron Optics. 2007. Sm125 Optical sensing interrogator instruction manual.

Othonos, A. & Kalli, K. 1999. *Fiber Bragg gratings: fundamentals and applications in telecommunications and sensing*. London: Artech House.

Saouma, V.E., Anderson, D.Z., Ostrander, K., Lee, B. & Slowik, V. 1998. Application of fiber Bragg grating in local and remote infrastructure health monitoring, *Journal of Materials and Structures*, 31: 259–266.

Yin, J.H., Zhu, H.H., Jin, W., Yeung, A.T. &Mak L.M. 2007. Performance evaluation of electrical strain gauges and optical fiber sensors in field soil nail pullout tests. *Geotechnical Advancements in Hong Kong since 1970s, The HKIE Geotechnical Division 27th Annual Seminar*. Hong Kong, 249-254.

Zhu, H.H., Yin, J.H., Jin, W., Zhou, W.H. 2007. Soil nail monitoring using Fiber Bragg Grating sensors during pullout tests, *Proceedings of the Joint 60th Canadian Geotechnical and 8th IAH-CNC Conferences*. Ottawa, 821-828.

ARUP

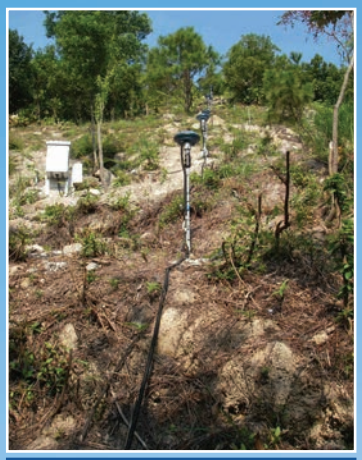

Real time landslide monitoring

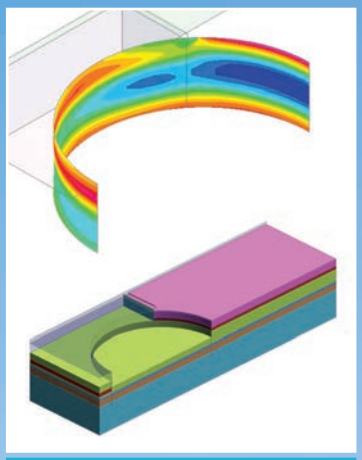

3D analysis for the Marina Bay Sands

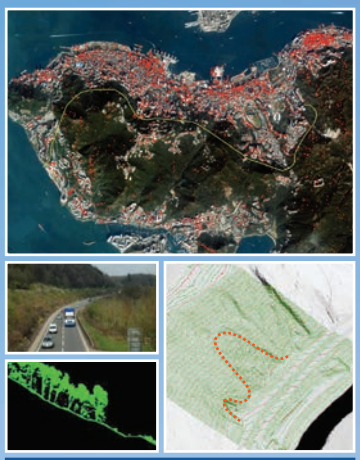

Application of remote sensing technology

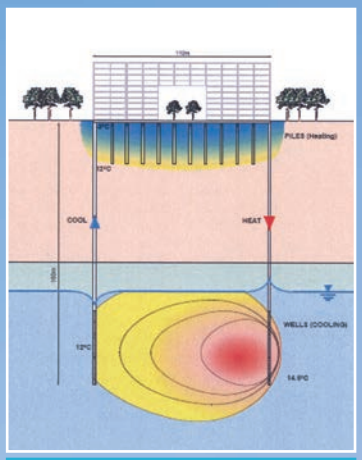

Pioneering use of ground energy systems

Main Visual:
120m diameter Diaphragm Wall excavation, Marina Bay Sands Integrated Resort, Singapore

We shape a better world

Global expertise and local resources in planning, engineering and project management meeting the needs of our clients with imagination, efficiency and economy

More than 9,000 staff working in over 90 offices around the world

www.arup.com